The Institute of Paper Chemistry

Appleton, Wisconsin

Doctor's Dissertation

An Investigation of the Vibrational Spectra of the Pentose Sugars

Steven Lawrence Edwards

January, 1976

AN INVESTIGATION OF THE VIBRATIONAL SPECTRA OF THE PENTOSE SUGARS

A thesis submitted by

Steven Lawrence Edwards

B.A. (Chem.) 1969, Luther College — Decorah, Iowa

M.S. 1972, Lawrence University

in partial fulfillment of the requirements
of The Institute of Paper Chemistry
for the degree of Doctor of Philosophy
from Lawrence University
Appleton, Wisconsin

January, 1976

TABLE OF CONTENTS

SUMMARY

The vibrational spectra of the pentoses (namely, β-arabinose, β-lyxose, and α-xylose) were investigated. The Raman and infrared spectra of these molecules were measured from the crystalline samples in the range of 4000 to approximately 150 wave numbers (cm^{-1}). The low temperature Raman spectra were also recorded for arabinose and xylose over this frequency range. Extensive vibrational coupling below 1500 cm^{-1} complicated interpretive efforts requiring the use of detailed normal coordinate analyses in this investigation.

The analyses were carried out on the pentoses using a series of computer programs which established and, in turn, solved the vibrational secular equation. The secular equation was obtained using assumed structural data and a set of assumed intramolecular force constant parameters. Solving the secular equation produced a set of vibrational frequencies which were then assigned to the observed frequencies. The difference between these observed and calculated frequencies was the basis for the refinement of the initial set of force constant parameters. A nonlinear least-squares refinement procedure was used to adjust, simultaneously, the force constant parameters until the difference between observed and calculated frequencies was minimized. The result of these refinements on arabinose, lyxose, and xylose gave an overall average error of 7.4 cm^{-1}.

The force field derived from the refinements predicted reasonable frequency distributions for the pentose molecules and also for the alpha and beta forms of methyl xylopyranoside. The normal coordinate calculations of these xylopyranosides demonstrated force field transferability to structurally similar molecules and also sensitivity to changes in the configuration at the anomeric site. In addition, the effect of the methyl group on the vibrational spectra of the pentoses was investigated.

The success of the normal coordinate analyses of the crystalline pentoses and the methyl xylopyranosides provided the basis for the extension of the force field to the alternate anomers of these pentoses and to the pyranose anomers of ribose. Calculations performed on the pentose anomers reveal that the frequency distributions for each are mainly influenced by hydroxyl group orientation around the pyranose ring. The coupling patterns in the calculated modes of each anomer are complex and cannot be readily related to trends in hydroxyl group orientation.

GENERAL INTRODUCTION

The thesis research presented here is part of a broader effort to eventually interpret the vibrational spectra of complex polysaccharide molecules. Work toward this goal was begun by Pitzner (1) with normal coordinate analyses of the 1,5-anhydropentitols (1,5-AHP's). These analyses revealed the effect of hydroxyl group orientation upon the vibrational spectra of pyranose molecules. Later, the normal coordinate analyses of the acyclic pentitols were carried out by Watson (2). These analyses revealed the sensitivity of the calculated spectra to small changes in the conformation of the acyclic molecules. The results of the above investigations provided the basis necessary to undertake similar analyses of the spectra of the pentose sugars.

The objective of the normal coordinate analyses of the pentoses was to provide a basis for interpretation of the vibrational spectra and to determine the effects of anomeric substitution upon the spectra of these molecules. This work with the pentoses has been divided into four separate parts. Part I covers the vibrational analyses of those pentose sugars which can be obtained in a pure crystalline form containing only a single anomer, namely: β-arabinose, β-lyxose, and α-xylose. The molecular structures are known and the vibrational spectra are readily obtained. The objective of Part I was to develop a suitable force field from an initial field derived from the work of Pitzner (1) and to interpret the vibrational spectra of these molecules. The work presented in Part I provides the basis for the extension of the analyses to other related molecules.

Part II deals mainly with the effect of a configurational change at the anomeric site on the vibrational spectra of the pentoses interpreted in Part I. In solution the pentoses undergo mutarotation. The effect of this $\alpha \rightleftharpoons \beta$ equilibrium on the vibrational spectrum is investigated. The normal coordinate calculations

of both anomeric forms of these pentoses have been included. Calculated bands are compared to the bands observed in the aqueous solutions of the pentoses, and the effect of anomerization on the spectra is discussed.

Part III is devoted entirely to the interpretation of the vibrational spectra of the pyranose forms of ribose. Ribose is of special importance in biological systems and exists in several forms. The work in this part is directed toward comparison of the calculated spectra of the pyranoid forms of ribose with the bands observed from the polymorphic solid.

Lastly, Part IV concerns the application of the pentose force field to the alpha and beta forms of methyl xylopyranoside. The objective of this work was to interpret the spectra of these molecules and to investigate the sensitivity of the force field to configurational changes at the anomeric site in these pyranoid molecules. The effects on the vibrational spectrum due to the addition of the methyl group are discussed.

PART I

AN INVESTIGATION OF THE VIBRATIONAL SPECTRA OF THE CRYSTALLINE PENTOSE SUGARS

INTRODUCTION

The recent advances in Raman spectroscopy and computer technology have stimulated interest in using complete vibrational analyses to interpret the vibrational spectra of polysaccharide molecules. These polysaccharides are especially interesting because of their abundance in natural systems and their importance in medicine and industrial technology. However, the vibrational spectra of polysaccharides are generally too complex to interpret directly.

Early attempts to interpret these polysaccharide spectra relied on the use of characteristic frequencies developed from investigations of simpler molecules. This group frequency approach was severely limited by both the large number of bands in the polysaccharide spectra and the coupling of the vibrational motions within these large molecules. Spectral interpretations based upon group frequency correlations have been comprehensively reviewed by Neely (3) and later by Spedding (4). Examination of the work on these complex molecules reveals that most band interpretations are limited to spectral bands above 1350 wave numbers (cm^{-1}) and in the range of 700 to 1000 cm^{-1}. Other spectral regions exhibit bands that are too highly coupled to be interpreted by the group frequency approach. Within the proper spectral regions there are many group frequency correlations known. Tipson (5) has compiled an exhaustive review of these group frequencies as they pertain to carbohydrate molecules.

Normal coordinate analyses can be used to interpret all the fundamental bands in the vibrational spectrum of large molecules. While the normal coordinate technique has long been available, it was not until the middle 1960's

that the computational difficulties encountered with large molecules were overcome. However, before realistic spectral interpretations of polysaccharide spectra can be obtained, the analyses of smaller more easily understood saccharide molecules must first be completed. The complexity of the polysaccharide spectra in combination with a poorly defined force field prohibits the direct application of normal coordinate calculations to polysaccharide molecules.

Early normal coordinate analyses proved very useful in helping to interpret the spectra of carbohydrate molecules. Must of the interpretive work carried out at the Birmingham School (6-8) on the pento- and hexopyranoses and their derivatives was based upon an earlier interpretation of the spectrum of tetrahydropyran (THP) by Burkett and Badger (9). This interpretation of THP was, in turn, based upon an earlier normal coordinate analysis of cyclohexane by Becket, et al. (10). In particular, Burkett and Badger (9) examined the infrared spectrum of THP and assigned various bands between 800 and 1060 cm^{-1} to ring stretching vibrations analogous to those in cyclohexane.

It was the work of Schachtschneider and Snyder (11,12) on the hydrocarbons and the work of Snyder and Zerbi (13) on the ethers and THP that established the possibility of using systematic normal coordinate analyses to interpret the spectra of groups of related molecules. Their work consisted of using a force constant refinement technique to develop a force field which would suitably predict the observed frequencies of all the molecules. Since the completion of their work, many spectral investigations employing the normal coordinate techniques have been undertaken; some using force constant refinement, and some merely transferring suitable force constants to the molecules in question.

Vasko (14) at Case Western Reserve University used a force field based upon that of THP (13) and other nonpyranoid molecules (15,16) to interpret the spectrum of α-glucose. Later workers at the above university used normal coordinate analyses to interpret the spectra of β-glucose (17) and cellulose (18).

The recent work begun by Pitzner (1) with the 1,5-AHP's represents the beginning of a series of investigations designed to eventually interpret the vibrational spectra of complex polysaccharides. Pitzner's work represents the first refinements attempted on a group of complex pyranose molecules using the nonlinear refinement technique developed by Fletcher and Powell (19). This technique overcomes convergence problems associated with highly correlated force constants. The interpretation of the spectra of the 1,5-AHP's revealed that a relatively simple force field, not unlike the field developed for THP (13), could adequately predict the vibrational frequencies of all the 1,5-AHP's. This meant that the differences in the vibrational spectra of the 1,5-AHP's can be related to $\underset{\sim}{G}$ matrix (kinetic energy) differences arising directly out of the differences in hydroxyl group orientations. A similar result was found for the acyclic pentitols by Watson's (2) normal coordinate analyses of these compounds. The final force field for these alditols exhibited only slight differences from the field of the 1,5-AHP's. Most of the differences could be attributed to the cyclic structure of the 1,5-AHP's. Furthermore, the analyses of the acyclic molecules revealed that vibrational frequencies are very sensitive to the conformations of the various rotational isomers of these molecules.

The pentose sugar molecules were chosen for this, the next investigation in the series of analyses of saccharide spectra. Structurally similar to the 1,5-AHP's, the pentoses are the simplest pyranose molecules exhibiting the effect of the anomeric hydroxyl group on the vibrational spectrum.

The purpose of this investigation was, then, to expand the force field developed for the 1,5-AHP's to accommodate the spectral interpretations of the crystalline pentoses: β-arabinose, β-lyxose, and α-xylose. With an initial force field based upon the field previously developed for the 1,5-AHP's (1), a series of force constant refinements were undertaken to improve the correlation between the observed and calculated bands. There were several constraints applied to the refinements to insure development of a suitable force field. First, the force field had to adequately account for the observed spectral bands of each of the pentoses. That is, the field had to be suitably general so that differences in the relative orientations of the hydroxyl groups around the pyranose rings could account for the spectral bands of each molecule. Secondly, the spectral interpretations which were based on the normal coordinate calculations were required to be consistent with prior experience concerning saccharide spectra using group frequency correlations. Finally, the force field had to be general enough to have good predictive capabilities as demonstrated by the application of the field to molecules similar to the pentoses.

EXPERIMENTAL

SAMPLE PREPARATION

The crystalline samples of β-arabinose, β-lyxose, and α-xylose were obtained from Pfanstiehl Laboratories, Inc. Purification was by recrystallization from suitable solvents. Sample purity was determined by melting points after the recrystallizations. Deuteration of the hydroxyl groups of arabinose and xylose was accomplished by repeated crystallization from D_2O followed by drying in a vacuum desiccator. The degree of deuteration was not rigorously determined. A sample of β-arabinose fully deuterated at the carbons (β-arabinose C-d_6) was obtained from Merck and Company, Inc., and was used without further purification.

SPECTRA

The Raman spectra were measured with a Spex Raman system with a Coherent Radiation Model 52A Argon ion laser source. A laser wavelength of 514.5 nm (19,435 cm^{-1}) was used. The slit widths were set for a minimum resolution of 5 cm^{-1}.

The room temperature Raman spectra were obtained using pressed powder pellets mounted in a 180° back-scattering arrangement. The low temperature Raman spectra were obtained using pressed powder pellets mounted at 45° with respect to the incident light beam. This sample holder arrangement was then placed inside a Harney-Miller temperature control cell. Cold nitrogen was passed through the cell at a rate necessary to maintain the desired temperature. Nitrogen flow was regulated by a rheostatically controlled heating element submerged in the Dewar holding the liquified nitrogen. The temperature of the sample was constantly monitored with a Bailey Cryo-Thermometer having a temperature range of 100 to -200°C. The probe was inserted into the temperature cell adjacent the sample pellet. The low temperature Raman spectra were recorded in a range of -150 to -175°C.

The deuterated samples were prepared in a dry-air bag. To minimize the loss of deuterium, the pellets were also prepared for pressing and later removed from the die in the air bag. To reduce the exchange of deuterium during the recording of the spectra, each pellet was sandwiched between two cover slides that had been conditioned with D_2O.

The room temperature infrared spectra of the powdered samples were recorded with a Perkin-Elmer 621 IR spectrometer using KBr pellets prepared in a standard manner. The low temperature infrared spectra were recorded by Wells (20) and were run as Nujol mulls near the temperature of liquid nitrogen. The infrared

spectrum of β-arabinose C-d_6 was also recorded by Wells (20) and run as Nujol and Fluorolube mulls.

COMPUTER PROGRAMS

The computer programs used to solve the secular equation and hence obtain the vibrational frequencies and distributions for the molecules were developed by Schachtschneider (21). These programs were adapted by Pitzner (1) for the IBM 360/44 operating system. The nonlinear refinement algorithm of Fletcher and Powell (19) was used for the refinement of the force constants.

RESULTS

INFRARED AND RAMAN SPECTRA

β-Arabinose

The infrared and Raman spectra of β-arabinose measured at room temperature and at low temperature are presented in Fig. 1 and 2, respectively. The frequencies of the observed bands in each spectrum are listed in Table I.

β-Lyxose

The room temperature infrared and Raman spectra of β-lyxose are shown in Fig. 3. The frequencies of the observed bands in each spectrum are listed in Table II.

α-Xylose

The infrared and Raman spectra of α-xylose measured at room temperature and at low temperature are shown in Fig. 4 and 5, respectively. The frequencies of the observed bands in each spectrum are listed in Table III.

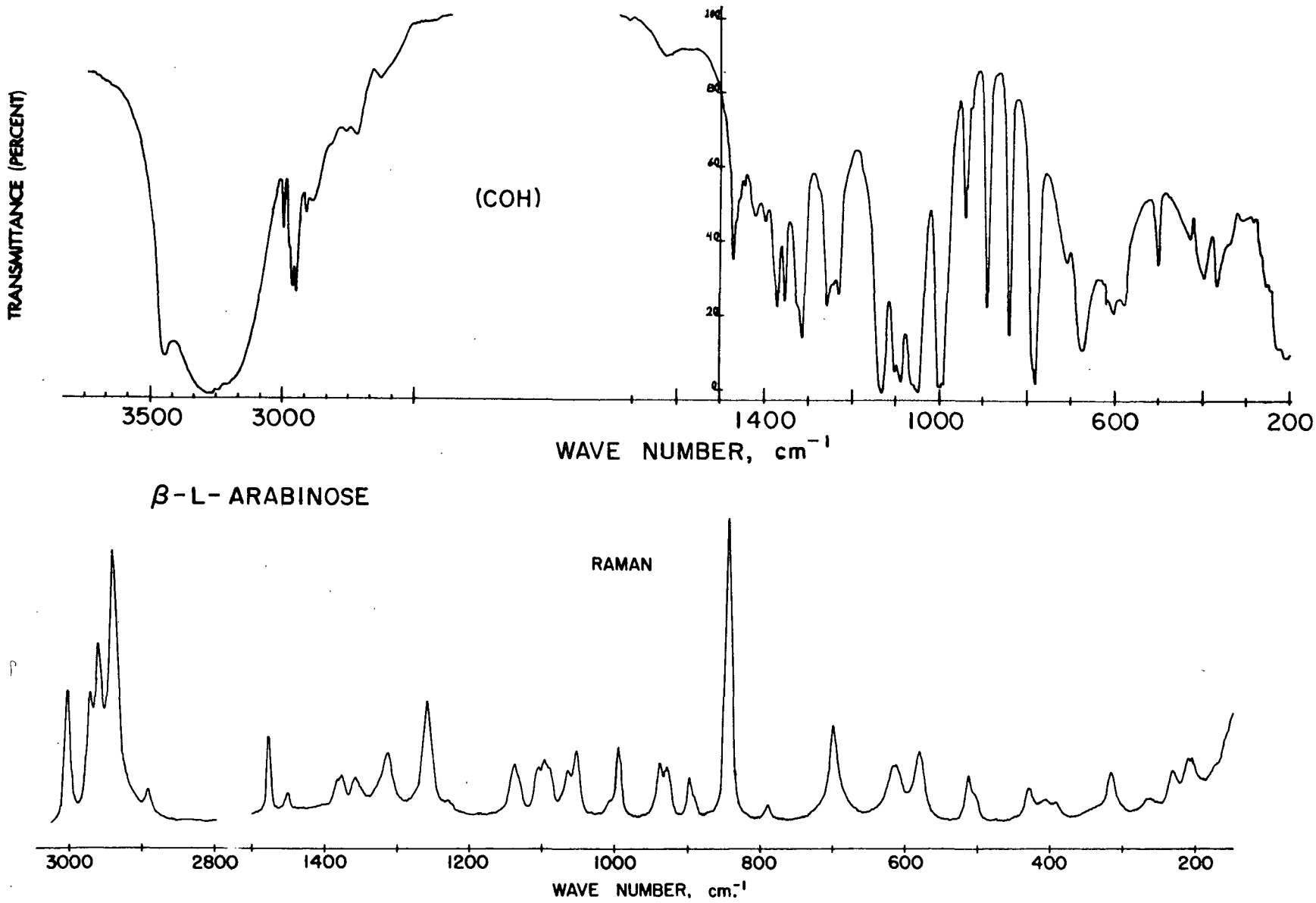

Figure 1. Infrared and Raman Spectra of Arabinose

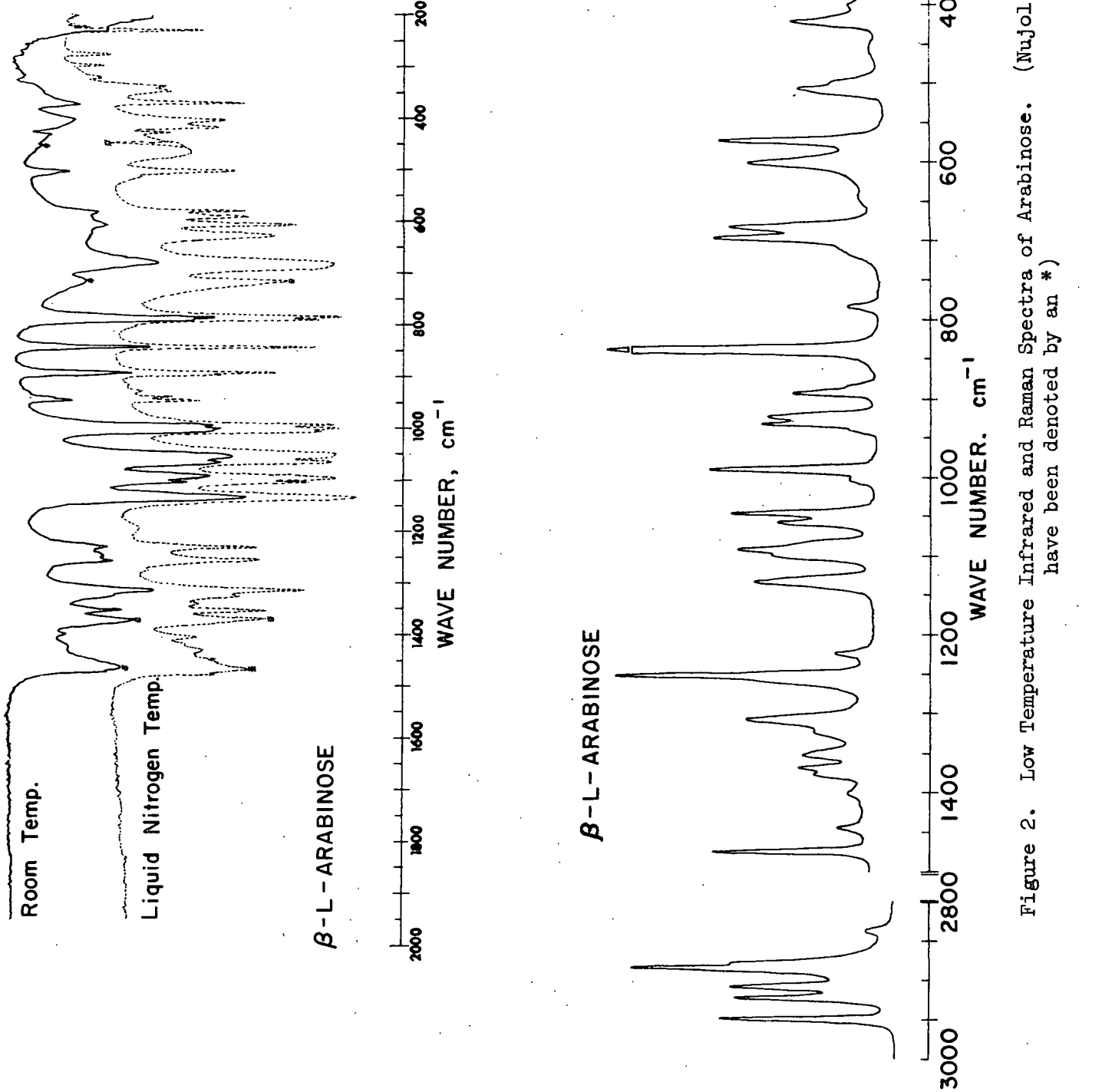

Figure 2. Low Temperature Infrared and Raman Spectra of Arabinose. (Nujol peaks have been denoted by an *)

TABLE I

VIBRATIONAL SPECTRA OF β-ARABINOSE

Raman		Infrared	
Room Temperature, cm^{-1}	Low Temperature[a], cm^{-1}	Room Temperature, cm^{-1}	Low Temperature[a], cm^{-1}
		3530 (vs,b)[b]	
		3330 (vs,b)	
3005 (s)	3002 (s)	3000 (w)	
2973 (s)	2973 (s)	2970 (m,sh)	
2962 (vs)	2961 (s)	2960 (s)	
2942 (vs)	2938 (vs)	2940 (s)	
	2931 (s,sh)		
2893 (w)	2890 (vw)	2895 (vw)	
		2870 (vw)	
1480 (m)	1475 (s)	1472 (m)	1478 (m)
1445 (w)	1445 (w)	1445 (vw)	
		1422 (w)	1430 (w)
1405 (w)	1403 (w)	1400 (w)	1405 (w)
1387 (w,sh)	1378 (w)		1375 (m,sh)
1380 (w)	1369 (m)	1370 (m)	1370 (s,sh)
1362 (w)	1354 (m)	1353 (m)	1355 (s)
1328			1342 (w)
1328 (m,sh)	1325 (w,sh)	1325 (m,sh)	1328 (m,sh)
1317 (m)	1308 (s)	1315 (s)	1314 (s)
			1275 (vw)
1262 (s)	1252 (vs)	1257 (s)	1255 (s)
		1245 (s)	
1235 (w)	1225 (w)	1230 (s)	1232 (s)
			1195 (vw)
1143 (m)	1134 (m)	1142 (vs)	1132 (vs)
1110 (m)		1105 (s)	1103 (vs)
1100 (m)	1100 (m,sh)	1090 (s)	1095 (vs)
1095 (w,sh)	1093 (s)	1085 (s,sh)	
1068 (w)	1086 (m,sh)	1065 (s)	1065 (vs)
1057 (m)	1058 (m)	1052 (s)	1050 (vs)
1010 (w,sh)	1047 (vw,sh)	1000 (vs)	1005 (vs)
1000 (m)	1004 (vw,sh)	995 (vs,sh)	1000 (vs)
	990 (s)		993 (vs)
942 (m)	940 (vw,sh)	942 (m)	946 (w)

TABLE I (Continued)

VIBRATIONAL SPECTRA OF β-ARABINOSE

Raman		Infrared	
Room Temperature, cm^{-1}	Low Temperature[a], cm^{-1}	Room Temperature, cm^{-1}	Low Temperature[a], cm^{-1}
933 (m)	933 (m)	938 (w,sh)	939 (w)
903 (w)	923 (m)		928 (vw)
893 (w,sh)	893 (m)	891 (vs)	896 (s,sh)
	885 (vw,sh)		892 (s)
848 (vs)	840 (vs)	842 (vs)	843 (vs)
795 (vw)		788 (w,sh)	790 (vs)
	785 (w)	782 (vs)	784 (vs)
705 (m)	713 (w,sh)	710 (vw)	718 (s)
	698 (s)		690 (s,sh)
	685 (s)	675 (m)	685 (vs)
	645 (vw)		628 (s)
619 (w)	603 (s)	605 (w)	607 (s)
			592 (m)
585 (m)	575 (s)	580 (w)	578 (m)
518 (w)	510 (m)		512 (vw,sh)
510 (w,sh)	500 (w,sh)	503 (m)	505 (m)
	455 (vw)		465 (m,b)
435 (w)	423 (m)	430 (w,b)	428 (w)
415 (w)	403 (w)		418 (m)
395 (vw)	388 (w)	400 (w,b)	403 (m)
	368 (vw)	370 (w)	372 (m)
	335 (w)	340 (vw,sh)	350 (w)
			340 (w)
323 (w)	313 (m)		325 (vw)
	296 (vw,sh)		300 (vw)
265 (w)	260 (w)		278 (vw)
	246 (vw)		
236 (w)	228 (w)		230 (m)
	210 (w)		
	160 (w)		

[a] Low temperature for Raman is about -150° C., for IR is about -190° C.

[b] Conventional symbolism indicating relative intensity: vs = very strong, s = strong, m = medium, w = weak, v = very, b = broad, sh = shoulder.

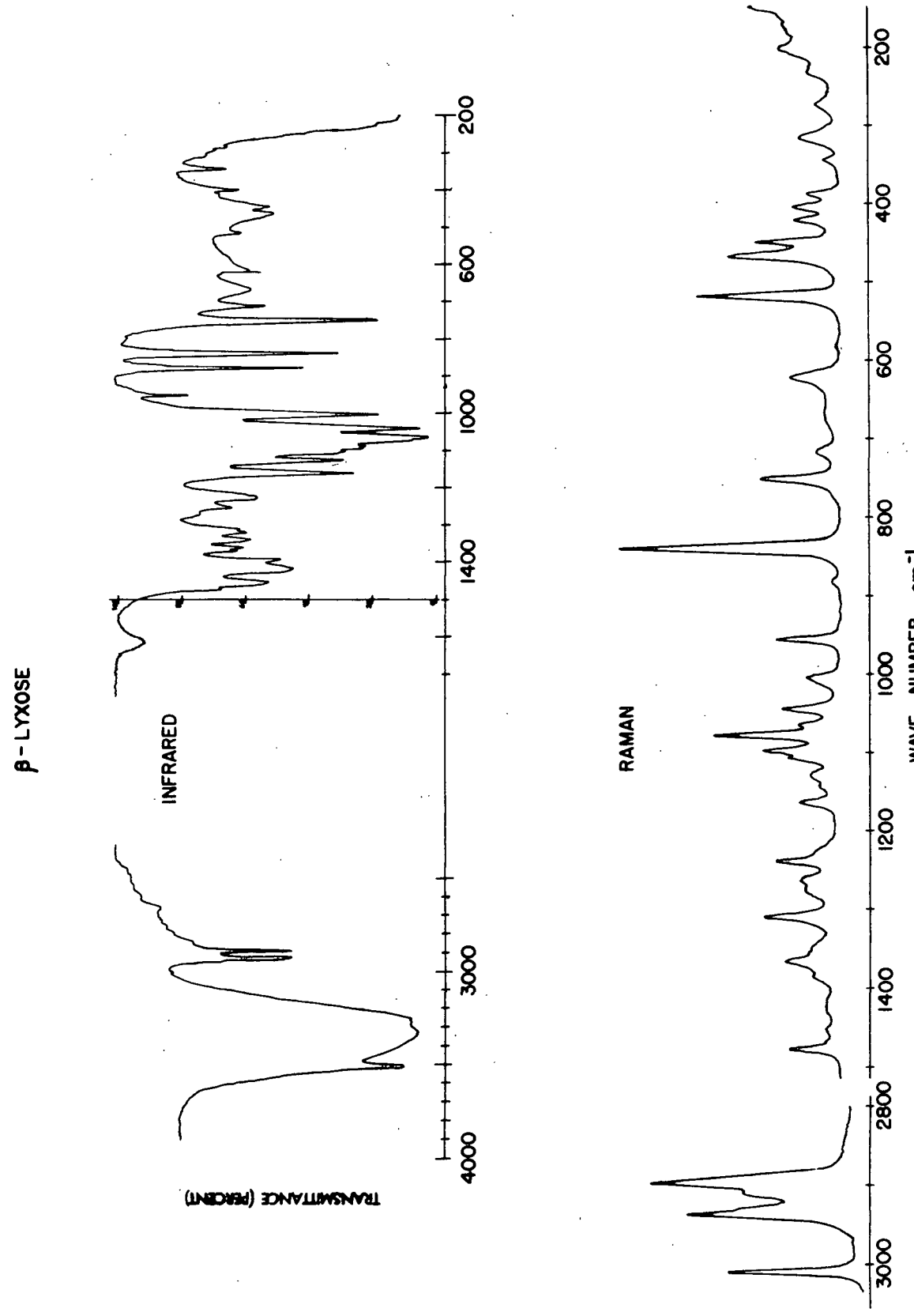

Figure 3. Infrared and Raman Spectra of Lyxose

TABLE II

VIBRATIONAL SPECTRA OF β-LYXOSE

Raman, cm^{-1}	Infrared, cm^{-1}	Raman, cm^{-1}	Infrared, cm^{-1}
3520	3520 (vs)[a]	1098 (m)	1095 (w,sh)
	3330 (vs,b)		1088 (w,sh)
	3260 (vs,b)	1079 (s)	1075 (w,sh)
3012 (s)		1066 (m)	1064 (s)
2939 (vs)	2945 (m,sh)	1047 (m)	1040 (s)
2935 (s,sh)	2932 (s)	1005 (w)	1003 (s)
2918 (s)	2925 (s)	957 (m)	952 (w)
2898 (vs)	2895 (w)	885 (vw)	878 (vs)
1479 (m)	1472 (w,sh)	845 (vs)	836 (vs)
1455 (w)	1455 (m)	754 (m)	750 (vs)
1425 (w)	1420 (m)	718 (w)	710 (w)
1385 (w)	1395 (m)	668 (w)	668 (w,b)
1375 (w,sh)	1370 (w,sh)	624 (w)	615 (vw,b)
1367 (m)	1362 (w)	520 (vs)	513 (vw)
1350 (w)	1340 (w)	469 (s)	462 (w)
	1320 (w)	451 (s)	442 (w)
1312 (m)	1310 (w,sh)	423 (m)	
1277 (w)	1270 (vw,sh)	407 (m)	410 (w)
1264 (w)	1254 (w)	391 (m)	398 (w)
1240 (m)	1225 (m)	341 (w)	342 (vw,sh)
1227 (w,sh)	1218 (w,sh)	317 (m)	305 (vw,sh)
1165 (m)	1160 (s)	276 (w)	
1145 (m,sh)		233 (vw)	
1131 (w)	1127 (m)	209 (vw)	
1108 (m)	1103 (w,sh)	203 (vw)	

[a]Conventional symbolism indicating relative intensity: vs = very strong, s = strong, m = medium, w = weak, v = very, b = broad, sh = shoulder.

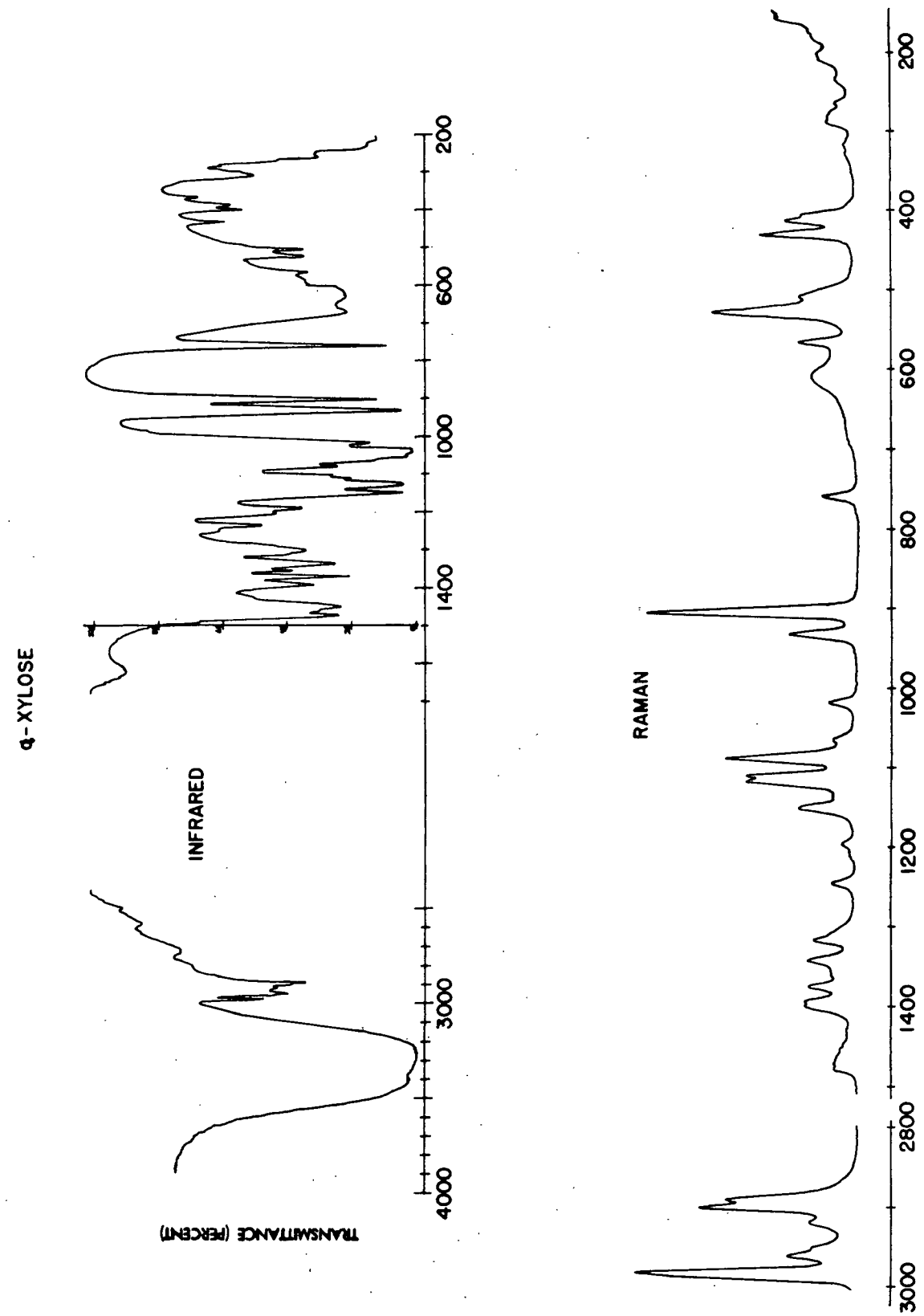

Figure 4. Infrared and Raman Spectra of Xylose

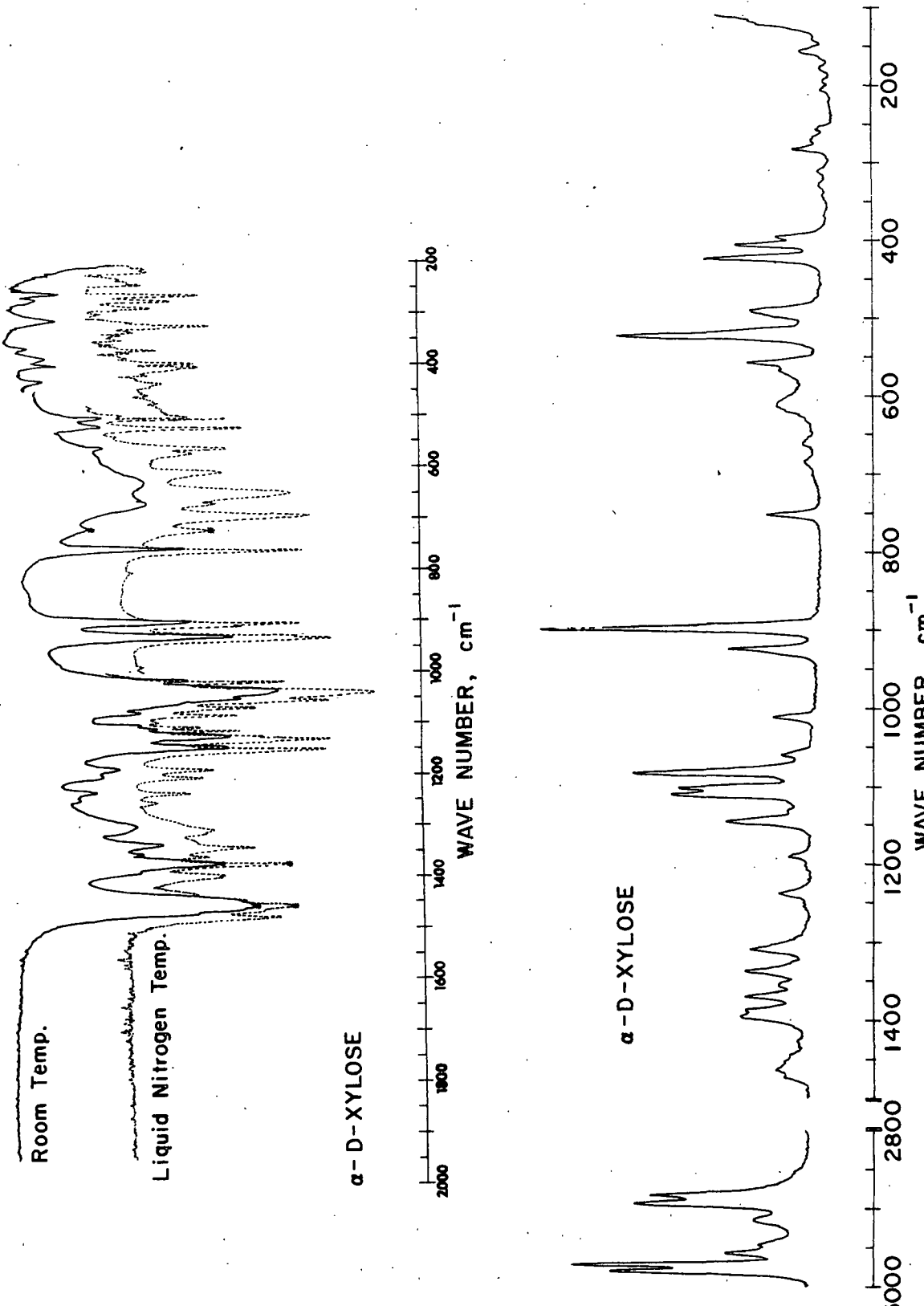

Figure 5. Low Temperature Infrared and Raman Spectra of Xylose. (Nujol peaks denoted by an *)

TABLE III

VIBRATIONAL SPECTRA OF α-XYLOSE

Raman		Infrared	
Room Temperature, cm^{-1}	Low Temperature[a], cm^{-1}	Room Temperature, cm^{-1}	Low Temperature[a], cm^{-1}
		3410 (vs,b)[b]	
		3340 (vs,b)	
		3275 (vs,b)	
2983 (vs)	2982 (vs)	2985 (m)	
2963 (m)	2973 (vs)	2960 (w,sh)	
2954 (w)	2958 (m)	2950 (m)	
	2947 (w,sh)		
2922 (m)	2915 (w)	2920 (w)	
2903 (vs)	2895 (s)	2900 (w,sh)	
2892 (s)	2884 (s)	2890 (m)	
1480 (w)	1473 (vw,sh)	1475 (s)	1478 (s)
1470 (b,w)	1463 (vw,sh)	1460 (w,sh)	1465 (m,sh)
1455 (w,b)	1453 (vw,b)	1450 (s)	1445 (m,sh)
1430 (vw)	1430 (vw,sh)	1440 (w,sh)	1435 (vw,sh)
1400 (m)	1395 (w)	1425 (vw,sh)	1400 (w)
1394 (m)	1386 (w)	1393 (w)	1395 (w)
1376 (m)	1370 (w)	1372 (m)	1375 (s,sh)
1358 (w)	1355 (vw)	1358 (w)	1358 (vw)
1343 (m)	1338 (w)	1338 (m)	1342 (m)
1318 (w)	1309 (w)	1313 (w,sh)	1314 (vw)
1307 (w,sh)	1304 (vw,sh)	1303 (m)	1308 (vw)
	1255 (vw)	1253 (vw,sh)	1253 (vw)
1246 (w)		1250 (w,sh)	
	1238 (w)	1235 (w)	1235 (w)
1212 (vw)	1205 (vw)	1205 (w,sh)	1203 (w)
1197 (vw)	1190 (vw)	1190 (w)	1188 (w)
1152 (m)	1146 (m)	1150 (s)	1152 (vs)
1137 (w)	1132 (vw,sh)	1128 (s)	1132 (vs)
			1125 (m,sh)
1118 (vs)	1110 (s)	1112 (m,sh)	1113 (m)
1111 (s)	1103 (s)	1105 (w,sh)	1107 (w)
			1095 (vw)
1089 (s)	1083 (vs)	1080 (w,sh)	1082 (w)

TABLE III (Continued)

VIBRATIONAL SPECTRA OF α-XYLOSE

Raman		Infrared	
Room Temperature, cm^{-1}	Low Temperature[a], cm^{-1}	Room Temperature, cm^{-1}	Low Temperature[a], cm^{-1}
1066 (w)	1060 (vw)	1065 (w,sh)	1068 (m)
		1055 (s)	1055 (s)
		1040 (s)	1040 (vs)
1019 (w)	1013 (w)	1017 (m)	1018 (s)
934 (m)	924 (m)	932 (vs)	933 (vs)
			928 (s,sh)
907 (vs)	898 (vs)	903 (vs)	909 (m,sh)
			904 (s)
			898 (w,sh)
760 (w)	753 (w)	762 (vs)	762 (vs)
	685 (vw)		695 (s)
	663 (vw)	670 (w)	670 (vw)
			650 (s)
613 (w)	613 (vw)	625 (w,b)	610 (w)
567 (m)	568 (vw,sh)	566 (vw)	572 (vw)
	558 (w)		562 (w)
530 (s)	522 (vs)	524 (w)	522 (s)
509 (m,sh)	494 (w)	507 (w)	503 (s)
433 (s)	424 (m)	432 (w)	440 (vw)
			435 (vw)
414 (m)			407 (w,sh)
407 (m,sh)	406 (m)	400 (m)	403 (w)
	395 (w,sh)	388 (w)	397 (w)
	343 (vw)	365 (vw)	369 (vw)
331 (vw)	318 (vw)		326 (vw,sh)
318 (vw)	312 (vw)	310 (m)	322 (m)
280 (w)	287 (vw)	285 (w,sh)	287 (w)
265 (vw)	270 (vw)	270 (vw,sh)	272 (w)
	255 (vw)	260 (vw,sh)	262 (m)
235 (vw)		230 (vw,sh)	
212 (vw)			
205 (vw)	157 (vw)		

[a] Low temperature for Raman is about -150° C., for IR is about -190° C.

[b] Conventional symbolism indicating relative intensity: vs = very strong, s = strong, m = medium, w = weak, v = very, b = broad, sh = shoulder.

Hydroxyl Group Deuterated (COD) Molecules

The infrared and Raman spectra of COD deuterated β-arabinose and α-xylose are shown in Fig. 6 and 7, respectively. The measured frequencies of each spectrum are tabulated in Table IV.

β-Arabinose C-d_6

The room temperature and low temperature Raman spectra of β-arabinose C-d_6 are shown in Fig. 8. The room temperature infrared spectrum is shown in Fig. 9. Table V lists the measured frequencies of each spectrum.

VIBRATIONAL ANALYSES

The solution of the vibrational secular equation is the basis of a normal coordinate analysis. This secular equation represents the condition under which the set of simultaneous differential equations describing the molecular motions involved in each degree of freedom have solutions. Several different forms of the secular equation can be used in a normal coordinate analysis. However, in this work the Wilson "$\underset{\sim}{GF}$" method as detailed by Wilson, et al. (22) and implemented for computer solution by Schachtschneider (21) was used. A simplified outline of the theoretical approach to the solution of the secular equation is presented in Appendix I.

The molecular structures used for β-arabinose, β-lyxose, and α-xylose were based upon the assumed structural parameters previously used for the 1,5-AHP's (1). These structural parameters, summarized in Table VI, provided a uniform basis for the construction of the $\underset{\sim}{G}$ matrices of all the molecules in this investigation. With the uniform molecular structures, the effect of hydroxyl group orientations upon the vibrational spectra could best be studied. It should also be noted that Hordvik has determined the molecular structures of β-arabinose (23), β-lyxose (24), and α-xylose (25) using x-ray diffraction

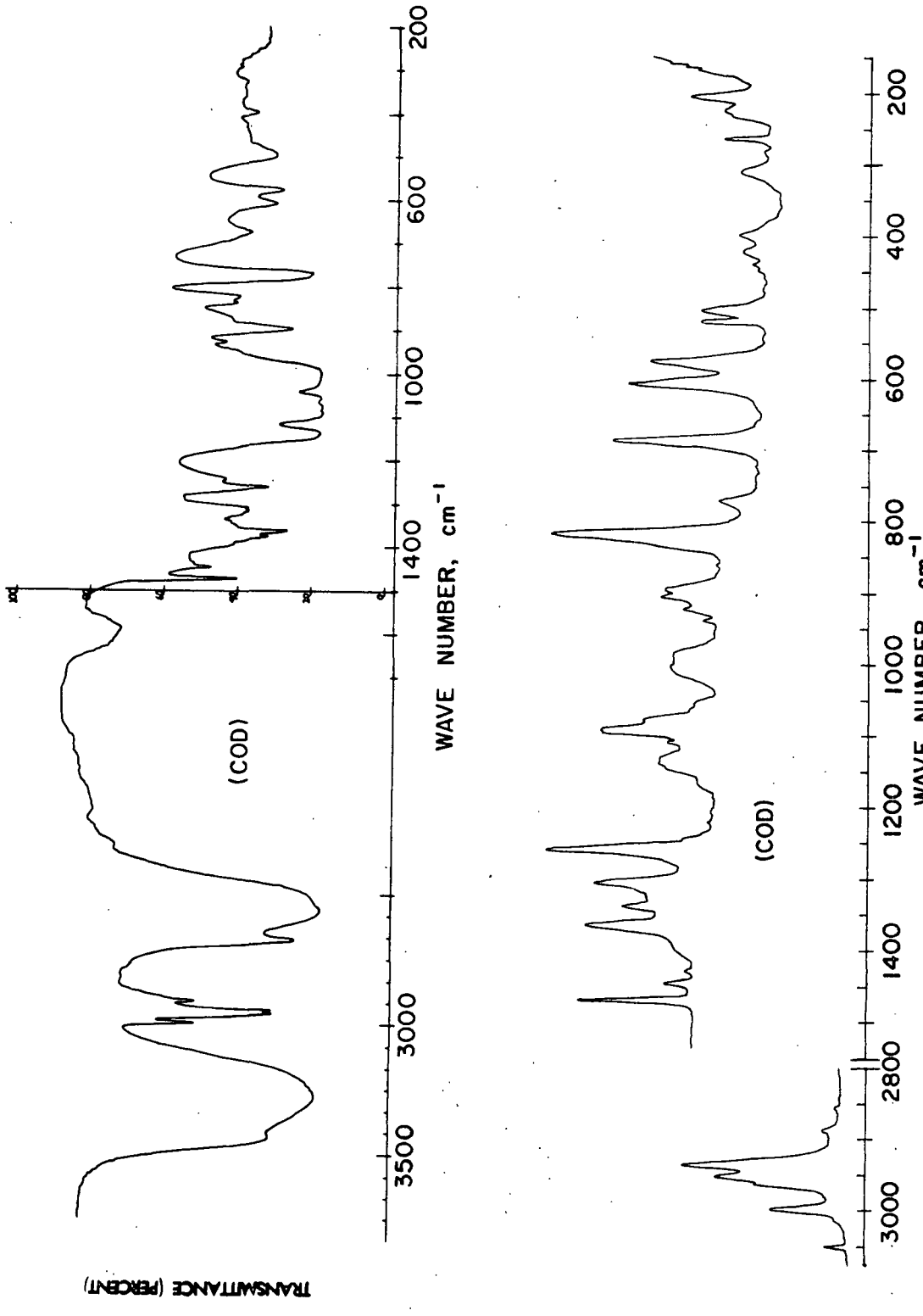

Figure 6. Infrared and Raman Spectra of O-D Deuterated Arabinose

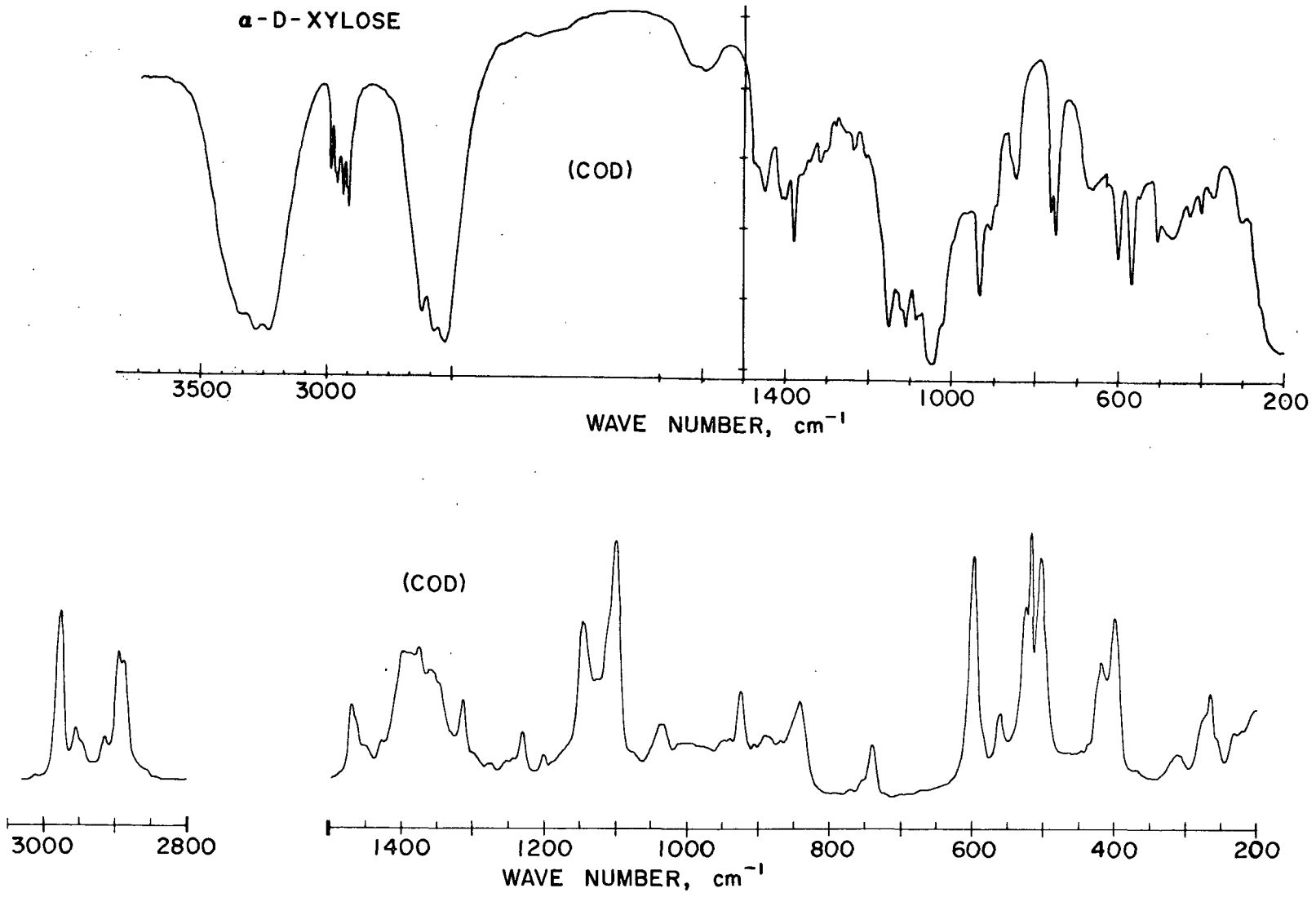

Figure 7. Infrared and Raman Spectra of O-D Deuterated Xylose

TABLE IV

TABULATED FREQUENCIES FOR THE RAMAN AND INFRARED SPECTRA OF THE CRYSTALLINE DEUTERATED (COD) PENTOSES

β-Arabinose		α-Xylose	
Raman, cm^{-1}	IR, cm^{-1}	Raman, cm^{-1}	IR, cm^{-1}
	3530 (s,b)[a]		3410 (vs,b)
	3330 (vs,b)		3340 (vs,b)
2995 (s)	2995 (m)		3270 (vs,b)
2963 (m,sh)	2960 (s,sh)	2978 (vs)	2985 (m)
2953 (s)	2950 (s)	2956 (m)	2962 (m,sh)
2937 (s)	2935 (s)	2950 (w,sh)	2955 (m)
2890 (vw)	2895 (m)	2915 (w)	2925 (m)
	2880 (w,sh)	2895 (s)	2905 (m,sh)
	2610 (s)	2887 (s)	2900 (m)
	2480 (vs,b)		2540 (vs,b)
	2420 (s,sh)		2490 (vs,b)
			2430 (vs,b)
1472 (s)	1472 (m)	1472 (m)	1475 (m,sh)
1445 (w)	1445 (w)	1453 (m,sh)	1450 (m)
1430 (vw)		1428 (w,sh)	1410 (m)
1400 (w)	1395 (w,sh)	1400 (s,b)	1400 (m)
1374 (w,sh)	1378 (m)	1378 (s,b)	1380 (s)
1367 (s)	1362 (m)	1363 (s,b)	1360 (w,sh)
	1350 (w,sh)	1350 (m,sh)	1340 (vw)
1341 (w)	1340 (w)	1310 (m)	1320 (vw)
1318 (vw,sh)	1320 (w,sh)	1300 (vw,sh)	1300 (w)
	1315 (w)	1275 (vw)	1280 (vw,sh)
1308 (m)	1308 (w)	1255 (vw,sh)	1255 (vw)
1263 (s)	1260 (m)	1245 (vw)	
	1240 (w,sh)	1233 (w)	1237 (vw)
1168 (vw,sh)		1203 (vw)	1205 (vw)
1146 (w,sh)			1152 (s)
1140 (w,sh)	1140 (vs)	1147 (s)	1145 (s,sh)

TABLE IV (Continued)

TABULATED FREQUENCIES FOR THE RAMAN AND INFRARED SPECTRA OF THE CRYSTALLINE DEUTERATED (COD) PENTOSES

β-Arabinose		α-Xylose	
Raman, cm^{-1}	IR, cm^{-1}	Raman, cm^{-1}	IR, cm^{-1}
1132 (w)		1111 (s,sh)	1120 (s,sh)
1095 (s)	1095 (vs,b)	1103 (vs)	1110 (s)
1080 (m,sh)	1075 (vs,b)		1085 (s)
1057 (vw)	1055 (vs,b)	1075 (vw,sh)	1075 (s)
1005 (m,b)	1020 (vs,b)		1050 (s,b)
990 (m,b)	1005 (vs,b)	1035 (m,b)	1025 (m,sh)
941 (vw)			1000 (w,sh)
924 (w)	928 (vw)	950 (vw,b)	933 (s)
908 (m)	895 (s)	925 (m)	910 (w)
895 (w)	870 (w,sh)	890 (vw)	895 (vw,sh)
831 (m,sh)	835 (m)		855 (vw,sh)
820 (vs)	820 (m)	843 (m,b)	845 (w)
	775 (s,sh)	753 (vw,sh)	762 (s)
772 (w)	770 (s)	742 (m)	750 (s)
688 (s)	675 (m,b)		670 (m,b)
607 (s)	607 (m)	598 (vs)	602 (m)
583 (m,sh)		563 (m)	568 (m)
577 (s)	578 (m)	527 (s,sh)	550 (vw)
519 (m)		518 (vs)	
504 (m)	495 (m,b)	505 (vs)	507 (w)
448 (vw)			470 (w,b)
440 (w)		419 (s)	440 (vw)
422 (w)		400 (s)	400 (vw)
400 (w)	400 (w)	370 (vw,sh)	370 (vw)
312 (w)		314 (vw,b)	305 (vw)
283 (vw)		272 (w,sh)	
266 (w)		266 (m)	

[a] Conventional symbolism indicating relative intensity: s = strong, m = medium, w = weak, v = very, b = broad, sh = shoulder.

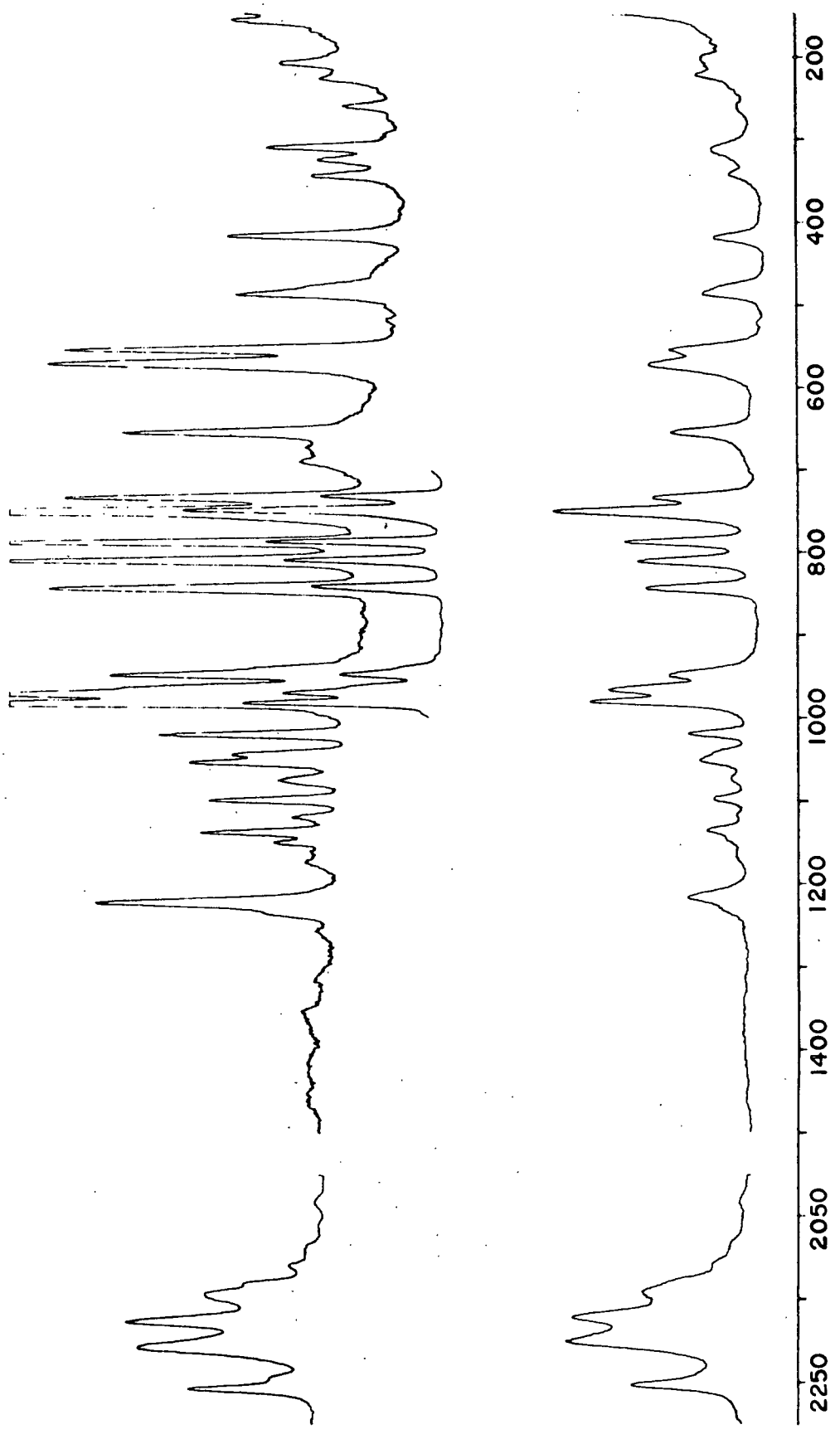

Figure 8. Raman Spectra of β-Arabinose C-d_5: (a) Low Temperature (-175°C) and (b) Room Temperature

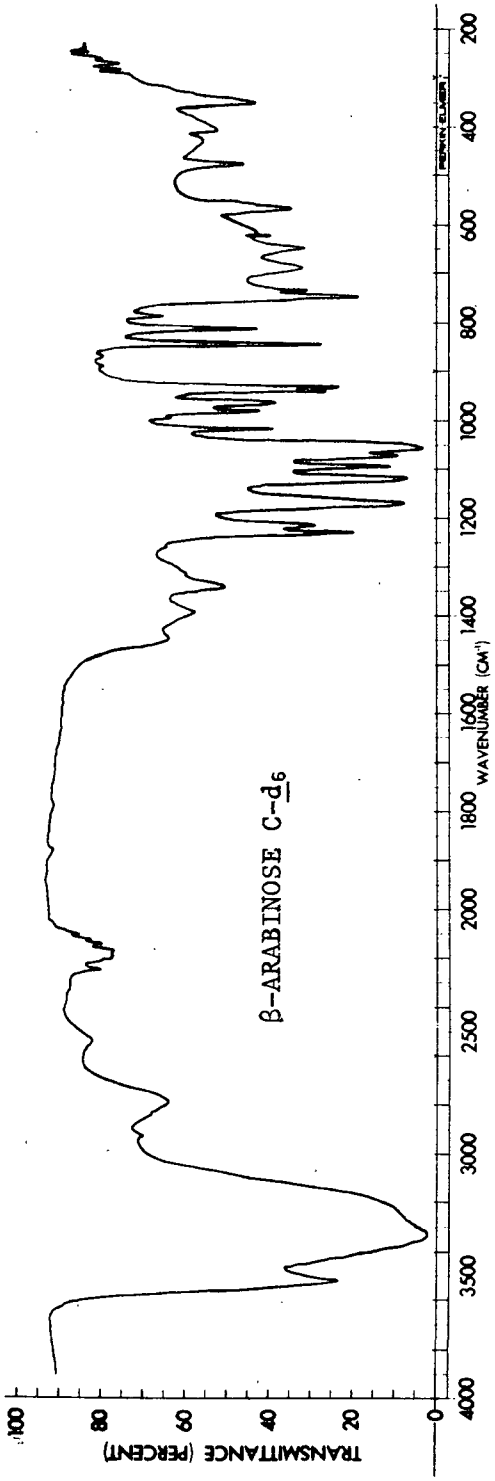

Figure 9. The Infrared Spectrum of β-Arabinose C-d_6

TABLE V

VIBRATIONAL SPECTRA OF β-ARABINOSE C-$\underline{d}_6$

IR, cm^{-1}	RT Raman, cm^{-1}	LT Raman,[a] cm^{-1}	IR, cm^{-1}	LT Raman, cm^{-1}	LT Raman,[a] cm^{-1}
3530 (vs,b)[b]			993 (vw,sh)		
3340 (vs,b)			980 (w)	981 (vs)	981 (vs)
3250 (vs,b)			964 (m)	966 (s)	970 (vs)
2250 (w)	2254 (s)	2258 (s)	960 (w,sh)		964 (w,sh)
		2245 (vw,sh)	948 (vw)	949 (m)	948 (s)
2195 (w)	2200 (s)	2209 (vs)	938 (s)		940 (w,sh)
2185 (w)	2172 (s)	2178 (vs)	932 (s)		
2140 (w)	2141 (m)	2144 (s)	845 (w,sh)		
2120 (w)		2133 (m,sh)	842 (vs)	844 (s)	844 (s)
2100 (w)	2110 (w)	2109 (vw)	811 (s)	813 (s)	812 (vs)
1450 (w)			785 (w)	789 (s)	788 (vs)
1393 (w)			755 (w,sh)		
1340 (m)			747 (s)	751 (vs)	752 (vs)
1315 (w)			733 (w)	734 (m)	734 (s)
1230 (vs)	1230 (w,sh)	1231 (w,sh)	689 (w,b)		691 (vw)
1214 (s)	1216 (m)	1222 (s)			675 (vw)
1170 (vs)	1165 (vw,b)	1174 (vw)	647 (w)	656 (s)	656 (s)
		1162 (vw,b)	566 (m)	573 (s)	573 (s)
	1145 (vw,sh)	1150 (vw)	558 (w,sh)	557 (s)	557 (s)
	1134 (w)	1138 (m)		485 (m)	490 (m)
1121 (vs)	1117 (vw)	1120 (vw)	478 (m)	479 (m,sh)	482 (vw,sh)
1095 (s)	1097 (w)	1099 (m)	425 (vw,b)	419 (m)	420 (m)
1072 (s,sh)	1072 (vw)	1075 (w)	405 (w,b)		
1056 (vs)	1053 (m)	1053 (m)	350 (m)	344 (w)	347 (w)
1050 (m,sh)	1042 (w,sh)	1045 (m,sh)			328 (w)
1018 (m)	1019 (m)	1023 (s)		313 (m)	313 (w)
				265 (vw)	263 (vw)
				225 (vw)	
				205 (vw)	

[a] LT Raman refers to the Raman spectrum obtained at about -175° C.

[b] Conventional symbolism indicating relative intensity: vs = very strong, s = strong, m = medium, w = weak, v = very, b = broad, sh = shoulder.

techniques. A comparison of the determined and assumed structural parameters, shown in Table XXVII of Appendix II, reveals that, in most cases, the differences are within the experimental errors involved in the x-ray diffraction studies. Therefore, the use of the assumed structural parameters was justified for two reasons. First, the actual molecular structures of several of the pentose anomers have not been determined, and second, the objective of this work was to study the effects of hydroxyl group orientation upon the vibrational spectra of the pentoses.

TABLE VI

STRUCTURAL PARAMETERS FOR THE PENTOSE SUGARS

Bond Length	Average Value, A	Bond Angle	Assigned Value
C-O(r)[b]	1.423	C-O(r)-C[a]	113.2°
C-C	1.523		
C-H(CH2)	1.096		
C-H	1.093		
C-O	1.415		
O-H	0.970		

[a] The bond angles were assumed to be tetrahedral (109°, 28 ft) and the dihedral angles set equal to 60° except for the two dihedral angles involving C-3 and O-10 which were set equal to 57.5°.

[b] (r) Designates the pyranose ring oxygen.

Another question to be considered is whether or not these three pentose molecules possess enough diversification in hydroxyl group orientations in order to develop a suitably general force field for all the pentose molecules. Consider the hydroxyl group orientations at each of the four carbons of the pentoses shown in Table VII. (The actual representations of the molecular

models are given in Fig. 10.) From Table VII it is obvious that except for the C-3 each of the hydroxyl group positions about the pyranose ring are represented by at least one axial and one equatorial hydroxyl group. All C-3 hydroxyl groups are equatorial due to the exclusion of ribose from these models. This exclusion does not represent a serious problem because the relative orientations of the hydroxyl groups at C-2 and C-3 of β-lyxose are merely the reverse of those of β-ribose: a force field sensitive to the lyxose configuration would be expected to also be sensitive to the ribose configuration. Even more important to this investigation is the fact that both axial and equatorial C-1 anomeric hydroxyl group orientations are present in these models. For if the force field is to have good predictive capabilities for the other forms of the pentose sugars, it must be sensitive to both axial and equatorial forms at C-1.

TABLE VII

RELATIVE HYDROXYL GROUP ORIENTATIONS OF THE PENTOSE SUGAR MODELS

	β-Arabinose	β-Lyxose	α-Xylose
C-1	Axial	Equatorial	Axial
C-2	Equatorial	Axial	Equatorial
C-3	Equatorial	Equatorial	Equatorial
C-4	Axial	Equatorial	Equatorial

The best possible force field for the pentoses was developed in four basic steps:

1. Measurement of the observed vibrational frequencies of β-arabinose, β-lyxose, and α-xylose.
2. Computation of the vibrational frequencies for each molecule using the necessary structural data and an initial force field derived basically from the field of Pitzner (1).

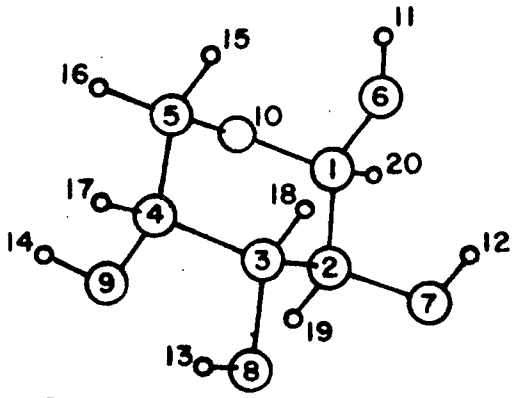

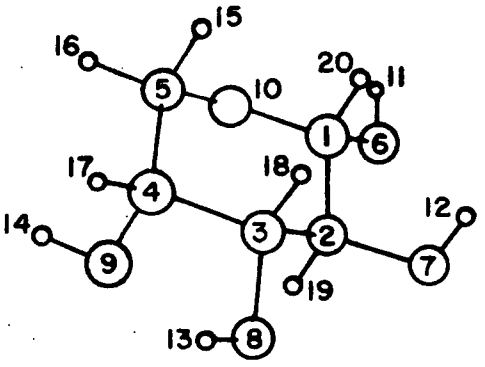

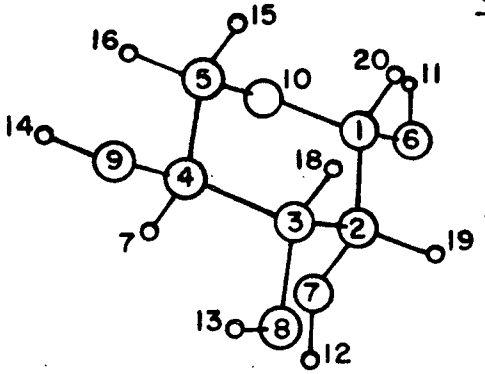

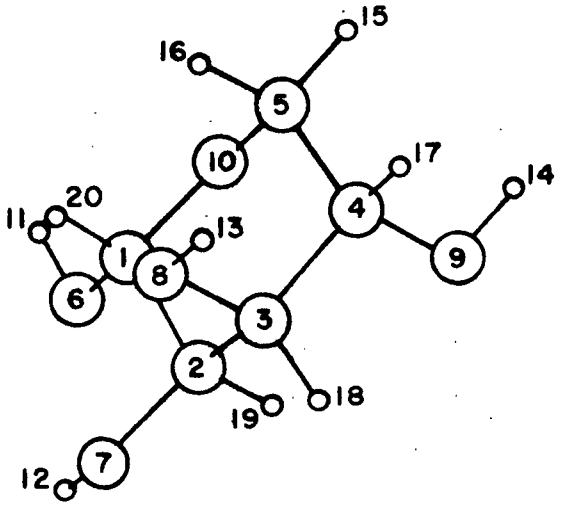

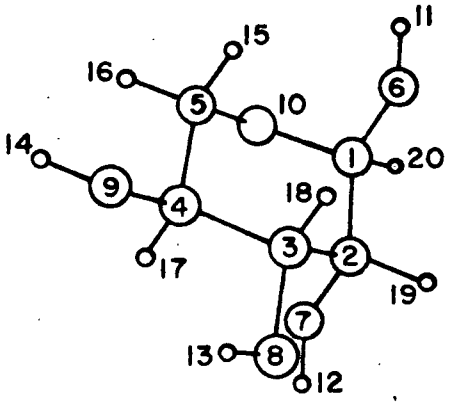

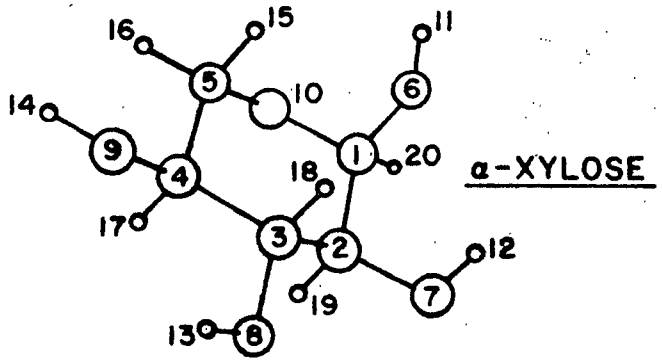

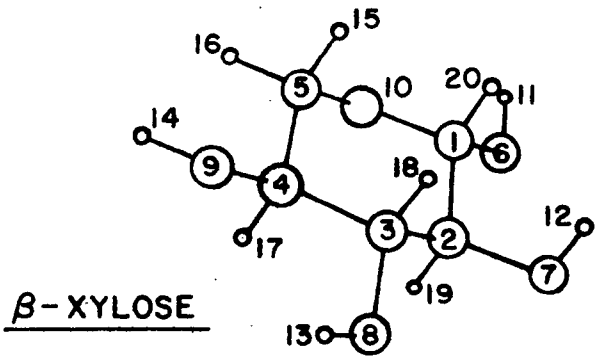

Figure 10. Representations of the Pentose Models

3. Assignment of the calculated frequencies to the observed frequencies of vibration for each molecule.

4. Refinement of the initial force field by the minimization of the least-squares deviation between the observed and calculated frequencies.

The development of this final force field was also subject to several important constraints. They were:

1. Good one to one correspondence between observed and calculated frequencies as indicated by the average error values.

2. Good agreement between the calculated band compositions and the group frequency correlations for the bands where these group frequency correlations exist.

3. Good prediction of the frequencies of molecules not included within the refinement so as to demonstrate the transferability of the force constants to similar molecular systems.

4. Maintainance of reasonable (as compared to previous normal coordinate analyses) force constant values throughout the refinements.

Normal coordinate analyses of the pentose molecules require that both the $\underset{\sim}{G}$ and $\underset{\sim}{F}$ matrices be determined or approximated for each molecule. The pentose molecules consist of 20 atoms which result in 54 vibrational degrees of freedom ($3n-6$). To describe completely the vibrational motions of these molecules required 20 stretch, 35 bend, and 10 torsion internal displacement coordinates. This description implies 11 redundancies. While 5 of these are local and removable, all were retained to facilitate construction of the force field. The descriptions of these internal displacement coordinates are given in Tables XXVIII and XXIX of Appendix II. The data used to generate the $\underset{\sim}{G}$ matrices of these pentoses are presented in Tables XXX-XXXV of Appendix II.

The $\underset{\sim}{F}$ matrices for these molecules had to be approximated since in general, there are more $\underset{\sim}{F}$ matrix elements to be determined than there are observed frequencies. Two principal assumptions can be made which will allow an $\underset{\sim}{F}$

matrix to be established. First, many off-diagonal $\underset{\sim}{F}$ matrix elements are cross terms involving internal coordinates having no common atoms or common bonds. The $\underset{\sim}{F}$ matrix elements at these interaction sites were arbitrarily set equal to zero. These cross terms often represent a large portion of the $\underset{\sim}{F}$ matrix. Setting them equal to zero greatly reduces the number of possible interaction force constants in the $\underset{\sim}{F}$ matrix. Secondly, since many of the force constants in the $\underset{\sim}{F}$ matrix describe the potential energy of very similar atomic groups, these similar force constants can be grouped together and given the same numerical value. These grouped force constants are then represented by force constant parameters. That is, instead of using four separate force constants for CC stretch, only one force constant parameter was used for all CC coordinates. For computational convenience, the $\underset{\sim}{F}$ matrix was not evaluated directly, but instead, a transformation matrix, $\underset{\sim}{Z}$, was used. Under this mathematical formalism, the $\underset{\sim}{F}$ matrix was defined by the $\underline{z}_{\underline{ijk}}$ elements and the force constant parameters. The development of this formalism is detailed in Appendix I. The introduction of these force constant parameters further reduced the number of variables present in the $\underset{\sim}{F}$ matrix. Successful application of these assumptions to the $\underset{\sim}{F}$ matrices of large molecules, structurally similar to the pentoses, has been demonstrated by several workers (1,2,13). An $\underset{\sim}{F}$ matrix determined in this manner is called a Simplified Valence Quadratic Force Field (SVQFF) after Pitzner (1).

Table VIII defined the 73 force constant parameters used to specify the SVQFF of the pentoses along with the initial and final values of these parameters. (The $\underline{z}_{\underline{ijk}}$ elements of the $\underset{\sim}{Z}$ matrices of the pentoses are listed in Table XXXVI of Appendix II. The numbering of the force constant parameters in these $\underset{\sim}{Z}$ matrices corresponds directly to the parameter numbers given in Table VIII.) For the pentoses, 23 diagonal parameters were used and up to 57

TABLE VIII

SVQFF FORCE CONSTANT PARAMETERS FOR THE PENTOSE MODELS

No.	Group	Coordinates Involved	Atoms Common to Interacting Coordinates	Final Value	Pitzner[a] (1,5-AHP's)	Watson[b] (Alditols)	Others
		STRETCH			(mdyn./A)		
1	C-C	C-C		4.183	4.247	4.227	4.261[c]
2	C-O-C	C-O		4.968	5.067		5.090[c]
3	COC-OH	C-O		5.151	(5.103)	(5.046)	(5.090[c])
4	CC-OH	C-O		5.122	5.103	5.046	5.090[c]
5	O-H	O-H		6.283[d]	6.283	6.197	6.440[e]
6	H_2COC	C-H		4.718[f]	4.597	4.591	4.626[c]
7	H-COH	C-H		4.694[f]	4.589	4.593	4.688[c]
		BEND			(mdyn.A/(rad.)^2)		
8	C-C-C	∠CCC		1.112	1.056	1.061	1.071[c]
9	C-C-OC	∠CCO		1.137	1.169		1.182[c]
10	C-C-OC	∠COC		1.316	1.318		1.313[c]
11	COC-OH	∠OCO		1.239	(1.180)		1.661[g]
12	C-C-OH	∠CCO		1.209	1.180	1.274	1.182[e]
13	C-O-H	∠HOC(bonded)[h]		0.871	0.734	0.646	0.976[e]
(73)	C-O-H	∠HOC(free)[h]		0.776	0.734	0.646	0.760[e]
14	H-C-OC	∠HCO		0.849	0.926	0.850	0.901[c]
15	H-C-OH	∠HCO		0.980	0.963	1.112	0.961[c]
16	H-C-C	∠HCC		0.698	0.725	0.730	0.718[c]
17	H_2CC	∠HCC		0.747	0.792	0.786	0.752[c]
18	H_2CO	∠HCH		0.477	0.452	0.474	0.471[c]
		TORSION			(mdyn./rad.)		
19	-C-C-	-C-C-		0.023	0.027	0.042	0.024[c]
20	C-O-C	-C-O-		0.072[i]	0.028		0.026[c]
21	C-O-H	-C-O-		0.059	0.012	0.055	0.026[c]
		STRETCH-STRETCH			(mdyn./A)		
22	C-C-C	C-C,C-C	C	0.117	0.107	0.200	0.101[c]
23	C-O-C	C-O,C-O	O	0.287	0.324		
24	COC-OH	C-O,C-O	C	0.384	(0.324)		
25	C-C-O-C	C-C,C-O	C	0.140	0.107	0.212	0.101[c]
26	C-C-OH	C-C,C-O(A)[j]	C	0.118	0.107	0.212	0.101[c]
27	C-C-OH	C-C,C-O(E)[j]	C	0.127	0.107	0.212	0.101[c]
28	H_2CO	C-H,C-H	C	-0.053[f]	-0.010	0.0	-0.046[c]
		STRETCH-BEND			(mdyn./rad.)		
29	C-C-C C-C-OC	C-C,∠CCC C-C,∠CCO	CC CC	0.271	0.485	0.539	0.417[c]
30	CC-OC	C-O,∠CCO C-O,∠COC	CO CO	0.735	0.487	0.575	0.618[c]
31	COC-OH	C-O,∠OCO	CO	0.840	(0.664)	(0.575)	
32	C-C-OH	C-O,∠CCO	CO	0.657	0.664	0.575	0.618[c]
33	C-C-OH	C-C,∠CCO	CC	0.408	0.381	0.363	0.403[c]
34	Methine	C-C,∠HCC	CC	0.518	0.481	0.344	0.478[c]
(68)	Methylene	C-C,∠HCC	CC	0.315	0.481	0.344	0.478[c]
35	Methine	C-O,∠HCO	CO	0.452	0.388	0.368	0.387[c]
(69)	Methylene	C-O,∠HCO	CO	0.396	0.388	0.368	0.387[c]
36	C-O-H	C-O,∠HOC	CO	0.342	0.357	-0.156	0.387[e]

TABLE VIII (Continued)

SVQFF FORCE CONSTANT PARAMETERS FOR THE PENTOSE MODELS

No.	Group	Coordinates Involved	Atoms Common to Interacting Coordinates	Final Value	Pitzner[a] (1,5-AHP's)	Watson[b] (Alditols)	Others
		BEND-BEND			(mdyn.A/(rad.)^2)		
37	C-C-C-C	∠CCC,∠CCC	C-C	0.031	-0.024	-0.047	0.011[c]
38	C-C-C-OH	∠CCO,∠CCC	CC-CO(g)[k]	0.018	-0.024	-0.105	0.011[c]
39	C-C-C-OH	∠CCO,∠CCC	CC-CO(t)[k]	-0.002	-0.014	-0.027	-0.011[c]
40	C-C-C-OH	∠CCO,∠CCC	C-C	0.133	0.052	-0.098	0.011[c]
41	CC(OH)C	∠CCO,∠CCO	C-O	0.074	0.052	0.063	
42	HOCCOH	∠CCO,∠CCO	OC-CO(g)	0.074	-0.024	0.070	
(74)	HOCCOH	∠CCO,∠CCO	OC-CO(t)	0.004			
43	CO-C-OH	∠CCO,∠OCO	C-O	-0.046	-0.026		
44	CO-C-OH	∠COC,∠OCO	CO-CO(g)	-0.081	-0.024		
45	CO-C-OH	∠COC,∠OCO	CO-CO(t)	-0.086	-0.014		
46	COC-COH	∠CCO,∠CCO	OC-CO(g)	-0.014	-0.024		
47	COC-COH	∠CCO,∠CCO	OC-CO(t)	0.008	-0.014		
48	CC(H)C	∠CCC,∠HCC	C-C	-0.117	-0.094	-0.238	-0.031[c]
49	CC-C-H	∠CCC,∠HCC	HC-CC(g)	-0.179	-0.106	-0.167	-0.052[c]
50	CC-C-H	∠CCC,∠HCC	HC-CC(t)	-0.155	-0.047	-0.041	0.049[c]
51	CC(H)OC	∠CCO,∠HCO	C-O	-0.237	-0.094	-0.097	-0.031[c]
52	H-C-O-C	∠COC,∠HCO	HC-OC(g)	0.028	-0.037		0.004[c]
53	H-C-O-C	∠COC,∠HCO	HC-OC(t)	-0.239	-0.094		-0.112[c]
54	C(H)COH	∠CCO,∠HCC ∠CCO,∠HCO	C-C C-O	-0.067	-0.094	-0.097	-0.031[c]
55	H-C-C-OH	∠CCO,∠HCC	HC-CO(g)	-0.164	-0.238	-0.123	-0.113[c]
56	H-C-C-OH	∠CCO,∠HCC	HC-CO(t)	-0.008	0.037		0.028[c]
57	CO-C-OH	∠OCO,∠HCO	C-O	-0.304	-0.094		
58	C-C-O-H	∠CCO,∠HOC	CC-OH(g,t)	0.151	0.010	-0.052	
59	H-CO-H	∠HCO,∠COH	HC-OH(g)	0.117		0.036	
60	H-CO-H	∠HCO,∠COH	HC-OH(t)	0.132	0.016	0.042	
61	H_2COC	∠HCC,∠HCO	C-H	0.101	0.135	0.150	0.115[c]
62	H_2COC	∠HCC,∠HCH	C-H	-0.007	0.025	0.026	0.0[c]
(72)	H_2COC	∠HCO,∠HCH	C-H	0.003	-0.026	-0.027	0.0[c]
(70)	H_2COC	∠HCC,∠HCC	C-C	0.128	0.066		0.105[c]
(71)	H_2COC	∠HCO,∠HCO	C-O	-0.019	-0.027	-0.012	-0.005[c]
63	H-COH	∠HCC,∠HCO	C-H	0.157	0.135	0.150	0.115[c]
64	COC(H)OH	∠HCO,∠HCO	C-H	0.225	(0.135)	(0.150)	
65	CC(H)C	∠HCC,∠HCC	C-H	-0.004	-0.001		0.012[c]
66	H-CC-H	∠HCC,∠CCH	HC-CH(g)	-0.004	-0.002	-0.021	0.004[c]
67	H-CC-H	∠HCC,∠CCH	HC-CH(t)	0.057	0.049	0.077	0.121[c]
68	(See force constant number 34.)						
69	(See force constant number 35.)						
70	(See force constant number 62.)						
71	(See force constant number 62.)						
72	(See force constant number 62.)						
73	(See force constant number 13.)						
74	(See force constant number 42.)						

TABLE VIII (Continued)

SVQFF FORCE CONSTANT PARAMETERS FOR THE PENTOSE MODELS

No.	Group	Coordinates Involved	Atoms Common to Interacting Coordinates	Final Value	Pitzner[a] (1,5-AHP's)	Watson[b] (Alditols)	Others
75	(dummy parameter)						
76	(dummy parameter)						
77	(dummy parameter)						
78	(dummy parameter)						
79	(dummy parameter)						
80	(dummy parameter)						

[a]Values taken from Pitzner (1).

[b]Values taken from Watson (2).

[c]Values taken from Snyder and Zerbi (13).

[d]Force constant not included in the refinements.

[e]Values taken from Vaasko (14).

[f]Force constants not directly comparable because of absence of C-H,∠HCC interaction constants.

[g]Values taken from Pickett and Strauss (26).

[h]"free" and "bonded" refer to relative strengths of the hydrogen bonds of the C-O groups within the crystal lattice.

[i]Force constant not directly comparable because of the torsion definitions in G matrix.

[j]"A" and "E" refer to axial and equatorial orientation of the C-O group.

[k]"g" and "t" refer to gauche and trans orientation across the designated bond.

off-diagonal, or interaction, parameters could have been used to complete an 80 parameter force field. However, as Table VIII shows, 7 of these parameters were not used in the final force field. The 23 diagonal elements correspond to the three types of internal coordinates describing the motions of the atoms: bond stretch, angle bond, and torsion. The 50 interaction constants couple the motions of the internal coordinates sharing a common nucleus. The four types of interactions that have been used to describe the pentose models are displayed in Fig. 11. The requirements for the presence of nonzero interaction elements in the $\underset{\sim}{F}$ matrix are that internal coordinates involved in stretch-stretch interactions must share a common atom, and that the internal coordinates involved in other interactions share a common bond. It should also be noted that the force field for the 1,5-AHP's (1) was used only as an initial force field. Later work indicated that this 1,5-AHP field did not contain enough independent parameters to adequately account for the pentose spectra.

The results of the normal coordinate calculations as applied to the pentose molecules β-arabinose, β-lyxose, and α-xylose are given in Tables IX-XI. Included in these tables are the frequencies calculated from the final set of force constants, the assigned experimental frequencies, the major contributions from the internal displacement coordinates to each of the calculated bands, and the description of the approximate motions for each band. Figure 12 illustrates some of the motions described in these tables. The key for the internal coordinate descriptions found in these tables is given in Tables XXVIII and XXIX of Appendix II. A listing of the contributions from all internal coordinates to each band is not feasible in the text, but all the contributions to each of the bands have been tabulated in Tables LX-LXII of Appendix III.

Stretch-Stretch

Stretch-Bend

Bend-Bend

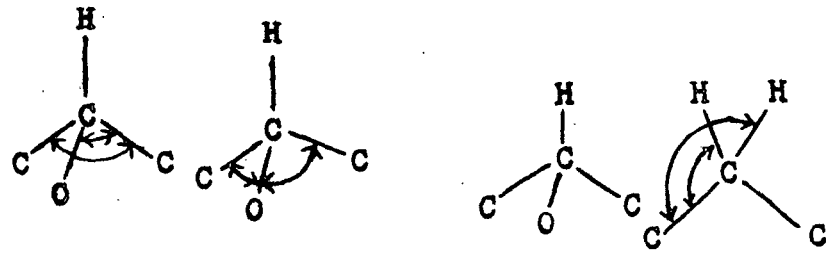

gauche

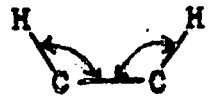

trans

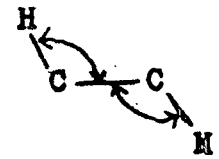

Figure 11. Some Interaction Force Constants Defined

TABLE IX

THE INTERPRETATION OF THE VIBRATIONAL SPECTRUM OF β-ARABINOSE

Band Assignment				Spectral Interpretation	
Experimental				Calculated Contributions[b],	
Raman, cm^{-1}	IR, cm^{-1}	Calc., cm^{-1}	Diff.[a], cm^{-1}	internal coordinates, %	Description of the Approximate Motions
	3530(vs)[c]	3357	d	OH11(99)	O-H stretch (str)
		3357		OH13(80) OH12(13) OH14(7)	O-H str
		3356		OH12(83) OH14(8) OH13(8)	O-H str
	3330(vs,b)	3356	d	OH14(85) OH13(12)	O-H str
3005(s)	3000(m)	3002	3	CH16(50) CH15(48)	Asymmetric methylene str
2973(s)	2970(m,sh)	2949	24	CH19(49) CH18(40) CH20(7)	Methine str
2962(vs)	2960(s)	2942	20	CH20(90) CH18(6)	Anomeric methine str
2942(vs)	2940(vs)	2939	3	CH17(95) CH19(5)	Methine str
2931[e](s,sh)	2895(vw)	2935	-4	CH18(53) CH19(45)	Methine str
2893(w)	2870(vw)	2885	8	CH15(51) CH16(50)	Symmetric methylene str
1480(m)	1472(m)	1478	2	HCH(57) H16CC(14) H15CC(11)	Methylene scissors coupled with wag
1445(w)	1445(vw)	1450	-5	HO7C(36) HC2O(19) CC3H(8) CC2H(6)	OH i.p.[f] bend coupled methine deformation (def)
	1422(w)	1428	-6	HO8C(25) CC4H(12) HC3C(8) HC2C(6) H16CO(6) H15CO(6)	OH i.p. bend coupled methine def
1405(w)	1400(w)	1405	0	H15CO(14) H16CO(13) HO8C(11) HO6C(10) H15CC(6) HC4C(5)	Methylene wag coupled with OH i.p. bend
1387(w,sh)		1402	-15	HO6C(38) HC1O(14) H16CO(8) HC1O1O(6)	Anomeric OH i.p. bend and methine def
1380(w)	1370(m)	1377	3	HC3C(19) HC2C(16) HO7C(12) HC4O(5) HC3O(5)	Methine def coupled with OH i.p. bend
1362(w)		1355	7	HC1O1O(36) HC1C(17) CC2H(11) CC3H(5) HC2C(5)	Anomeric methine def coupled with methine def
	1353(m)	1335	18	HC1O1O(21) CC2H(14) HC1O(10) HC2C(8) HO9C(7) HO8C(7) C3C4(5)	Anomeric methine def coupled with methine def
1328(m,sh)	1325(m)	1322	6	HO9C(19) HC3O(15) CC4H(12) HO8C(7) CC3H(7) C3C4(5)	OH i.p. bend coupled with methine def
1317(m)	1315(s)	1304	13	HC1O(35) HO6C(33) HC1C(11) HO9C(9)	Anomeric methine def coupled with OH i.p. bend
	1275[e](w)	1286	-11	HC4C(21) HO9C(16) H16CO(15) H16CC(15) HC4O(11) HO6C(5)	Methine def coupled with methylene wag
1262(s)	1257(s)	1262	0	HC3O(24) HC4O(22) HO8C(21) CC4H(14) CC3H(13)	Methine def coupled with OH i.p. bend
	1245(s)	1239	6	H15CO(24) HO9C(18) H15CC(14) H16CO(11) HC4O(10) C4O9(8) HC4C(5)	Methylene twist coupled with OH i.p. bend and methine def
1235(w)	1230(s)	1231	4	HC3O(27) H15CO(13) HC4O(12) H16CO(11) HO9C(9) HO8C(8) HC3C(7) HC1O(5) CC3H(5)	Methylene twist coupled with methine def and OH i.p. bend
	1195[e](w)	1199	-4	HC2O(35) HO7C(29) HC2C(10) CC2H(9) HC3O(8) HC4O(5)	Methine def coupled with OH i.p. bend

TABLE IX (Continued)

THE INTERPRETATION OF THE VIBRATIONAL SPECTRUM OF β-ARABINOSE

Band Assignment				Spectral Interpretation	
Experimental				Calculated Contributions[b],	
Raman, cm^{-1}	IR, cm^{-1}	Calc., cm^{-1}	Diff.[a], cm^{-1}	internal coordinates, %	Description of the Approximate Motions
1143(m)	1142(vs)	1156	-13	C409(17) C3C4(14) HC40(14) HC3O(13) C4C5(10) H16CC(9) HC3C(9) C5010(7) H15CO(6)	CO and CC str coupled methylene rock and methine def
1110(m)	1105(s)	1121	-11	C5010(19) C308(16) C2C3(15) H16CO(12) C4C5(11) C207(10) O10C1(10) HC2C(5)	CO and CC str coupled with methylene def
1100(m)	1090(s)	1103	-3	C308(57) O10C1(5)	CO str
1095(w,sh)	1085(s,sh)	1100	-5	C207(63) C4C5(9) CC3C(7) CC2C(6) CC4H(5)	CO str coupled with ring def
1068(w)	1065(s)	1062	6	C4C5(21) O10C1(12) H15CC(9) C207(9) C1C2(8) C2C3(6) H16CC(6) C409(5) HC40(5)	CC and CO str coupled with methylene rock
1057(m)	1052(s)	1048	9	C106(33) C1C2(16) HC20(15) HC10(13) HC1C(11) C4C5(11) C308(9) H07C(6) HC3C(5)	CO and CC str coupled with methine def
1010(w,sh) 1000(m)	1000(vs) 995(vs,sh)	998	2	O10C1(27) C1C2(25) HC10(22) C2C3(19) C5010(11) C3C4(9) C409(9) O6CC(6) HC1C(6)	Asymmetric COC str coupled with CC and CO str and methine def
942(m)	942(m)	964	-22	C3C4(41) HC4C(15) CC50(8) C2C3(8) C5010(8) H09C(6) C1C2(6) C409(5) CC09(5) C4C5(5)	CC str coupled with methine def and CO str and def
933(m)	938(w,sh)	938	-5	C106(36) HC1C(10) O10C1(10) C4C5(9) C308(8) C1C2(6) C3C4(6) C409(6) OCO(5) C2C3(5) CC2H(5)	CO str coupled with CC str and methine def
903(w)[g] 893(w,sh)	891(vs)	913	-10	C409(32) C106(19) O10C1(16) C1C2(14) C5010(7) C2C3(5)	CO str coupled with CC str
848(vs)	842(vs)	852	-4	C5010(43) O10C1(17) C409(17) C4C5(11) C1C2(5)	Symmetric COC str coupled with CO and CC str
795(vw)	788(s,sh)[g] 782(vs)	769	26	O10C1(18) COC(15) CC07(8) C5010(7) CC50(6) C106(5)	COC str and bend coupled with CO def
705(m)	710(vw) 675(m)	697	8	C2C3(32) CC50(13) CC4H(6) HC4C(6) O9CC(5)	CC str coupled with ring def
619(w)	605(w)	615	4	OCO(24) TC5010(9) C1C2(8) C2C3(5) COC(5) O9CC(5) O10C1(5)	OCO bend coupled with ring bonding
585(m)	580(w)	592	-7	CC09(21) O6CC(16) O8CC(10) COC(7) CC50(5) CCO(7)	CO def coupled with ring bending
518(w)[g] 510(w,sh)	503(m)	493	21	O7CC(22) O10C1C(16) CC08(14) O9CC(13) OCO(10) C3C4(6)	CO def coupled with ring CO str
	465[e](m)	463	2	CC4C(18) TC5010(11) O10C1C(10) C1C2(9) O9CC(6) CC08(5) CC07(5)	ring bending
435(w) 415(vw)	430(w,b)	411	24	CC07(18) O8CC(14) TC106(11) CC3C(9) CC2C(9) TC409(7) TC207(6)	CO def coupled with OH o.p. bend
395(vw)	400(w,b)	392	3	COC(20) O9CC(11) TC106(10) O7CC(9) CC50(8) CC08(8) CC2C(7) CC3C(6) TC409(6) OCO(6)	COC bend coupled with CO def and OH o.p. bend
368[e](vw)	370(w)	363	5	TC106(26) TC409(26) TC308(17)	OH o.p. bending
	350[e](w)	354	-4	TC308(46) TC409(19) TC106(8)	OH o.p. bending

TABLE IX (Continued)

THE INTERPRETATION OF THE VIBRATIONAL SPECTRUM OF β-ARABINOSE

Band Assignment				Spectral Interpretation	
Experimental				Calculated Contributions[b],	
Raman, cm^{-1}	IR, cm^{-1}	Calc., cm^{-1}	Diff.[a], cm^{-1}	internal coordinates, %	Description of the Approximate Motions
335[e](w)	340(vw,sh)	338	-3	TC207(66) TC106(8) HC2C(7) TC308(5)	OH o.p. bending
323(w)	325[e](w)	315	8	TC409(26) TC106(15) O9CC(14) O7CC(11) OCO(9) HC1C(8)	OH o.p. bend coupled CO def
296[e](vw)	300[e](w)	297	-1	CC08(22) CC09(20) O6CC(11) O7CC(10) CC4C(10) O8CC(7)	CO def
265(w)	278(w)	257	8	O8CC(17) O6CC(14) CC07(13) CC09(11) O7CC(11) CC4C(7) CC08(6) TC207(6) O10C1C(6)	CO def
236(w)	230[e]	237	-1	CC09(15) O6CC(14) O10C1C(10) O8CC(8) CC3H(6) TC1O1O(6) CC2C(6) CC2H(5) O9CC(5)	CO def coupled with ring bend
210[e](vw)		209	1	COC(29) OCO(27) HC1O1O(15) O6CC(13) O9CC(12) HC1C(10) O10C1(10) TC1O1O(8)	COC bend and anomeric CO def and methine def
160[e](w)		143	d	TC3C4(16) TC4C5(16) TC1O1O(13) TC1C2(13) HC1O(18) O10C1C(7) COC(6) CC4C(6) CC5O(5)	Ring torsional bending
		128		TC2C3(30) TC1C2(14) CC2C(14) TC3C4(13) CC3C(11)	Ring torsional bending

Average Error = 7.7 cm^{-1}

[a]Diff. = difference = observed frequency (Raman) − calculated frequency.

[b]Contributions are relative and may add to more than 100% due to contributions from negative interaction parameters in the SUQFF. Only contributions of 5% or more have been included.

[c]Conventional symbolism indicating relative intensity, vs = very strong, s = strong, m = medium, w = weak, sh = shoulder, b = broad, v = very.

[d]These frequencies are not included in average error calculations since they were not included in any refinements.

[e]These frequencies obtained from the low temperature spectrum.

[f]i.p. and o.p. refer to in-plane and out-of-plane, respectively.

[g]Apparent correlation field splitting.

TABLE X

THE INTERPRETATION OF THE VIBRATIONAL SPECTRUM OF β-LYXOSE

Band Assignment				Spectral Interpretation	
Experimental				Calculated Contributions[b],	
Raman, cm^{-1}	IR, cm^{-1}	Calc., cm^{-1}	Diff.[a], cm^{-1}	internal coordinates, %	Description of the Approximate Motions
	3520(vs)[c]	3357	d	OH11(96)	O-H stretch str
		3357		OH13(81) OH12(12) OH14(7)	O-H str
	3330(vs)	3357	d	OH14(92) OH13(6)	O-H str
	3260(b,vs)	3357	d	OH12(83) OH13(12)	O-H str
3012(s)		3000	12	CH16(49) CH15(48)	Asymmetric methylene str
	2945(m,sh)	2948	-3	CH17(50) CH18(46)	Methine str
2939(s)		2941	-2	CH20(85) CH19(13)	Methine str
2935(s,sh)	2932(s)	2939	-4	CH19(83) CH20(14)	Methine str
2918(s)	2925(s)	2935	-17	CH18(53) CH17(45)	Methine str
2898(vs)	2895(w)	2888	10	CH15(51) CH16(50)	Symmetric methylene str
1479(m)	1472(w,sh)	1478	1	HCH(46) H15CC(18) H16CC(15)	Methylene scissors coupled with wag
1455(w)	1455(m)	1440	15	HC3C(18) HO9C(15) HO8C(12) HC2C(9) CC3H(9) CC2H(5)	Methine deformation (def) coupled with OH i.p. bend
1425(w)	1420(m)	1416	9	HO8C(23) HC1C(11) C2O7(7) CC3H(6) C1C2(6) HO6C(6) HO7C(5) HC1O(5)	OH i.p. bend coupled with anomeric methine def
	1395(m)	1400	-5	HO9C(30) HC2C(10) HO6C(7) HC1O1O(7) HO7C(7) CC2H(5) HC1O(5) HC4O(5)	OH i.p. bend coupled with methine def
1385(w)		1387	-2	H15CO(21) H16CO(18) HO7C(13) HCH(10) CC4H(8) HC4C(7)	Methylene wag coupled with methine def
1375(w,sh)	1370(w,sh)	1380	-5	HO7C(34) HC1O(8) HO8C(8) HC1O1O(6) HC2O(5)	OH i.p. bend coupled with methine def
1367(m)	1362(w)	1361	6	HC4C(17) HC1O1O(16) HO9C(13) CC4H(8) H15CC(8) HO8C(8) HC1O(7) H15CO(6)	Methine def coupled with OH i.p. bend
1350(w)	1340(w)	1349	1	HC1O1O(21) CC4H(17) HC1O(17) HC4C(10) HO7C(7) H16CO(6)	Anomeric methine bend coupled with methine def
	1320(w)	1327	-7	CC2H(27) HC1O(16) HO8C(13) HC1C(10) HC2C(7) HC2O(6)	Methine def coupled with OH i.p. bend
1312(m)	1310(w,sh)	1300	12	HC4O(17) HC1O1O(13) HC1C(11) HC3C(11) CC3H(10) HO8C(8) H16CO(7) H16CC(5) HO6C(5)	Anomeric methine def coupled with methine def and OH i.p. bend
1277(w)	1270(w,sh)	1278	-1	HC2O(32) HC3O(20) HO7C(16) HO6C(13) HC2C(12)	Methine def coupled with OH i.p. bend
1264(w)	1254(w)	1253	11	HC4O(43) HO9C(20) HC4C(11) HC3C(7) H16CO(6) CC4H(6) H15CO(5)	Methine def coupled with OH i.p. bend and methylene twist
1240(m)		1235	5	HC3O(53) HO8C(20) CC3H(11) HC2C(7) HO6C(6) HC3C(5)	Methine def coupled OH i.p. bend
1227(w)	1225(m)	1229	-2	H16CO(18) H15CO(18) HC2O(16) HO6C(15) H16CC(10) H15CC(9) HC1O(8) HO9C(5)	Methylene twist coupled with methine def and OH i.p. bend

TABLE X (Continued)

THE INTERPRETATION OF THE VIBRATIONAL SPECTRUM OF β-LYXOSE

Band Assignment				Spectral Interpretation	
Experimental				Calculated Contributions[b],	
Raman, cm^{-1}	IR, cm^{-1}	Calc., cm^{-1}	Diff.[a], cm^{-1}	internal coordinates, %	Description of the Approximate Motions
	1218(w,sh)	1220	-2	H06C(25) HC20(14) H15C0(13) HC40(12) H16C0(8) CC2H(7) HC1C(5)	OH i.p. bend coupled with methine def and methylene twist
1165(m) 1145(m,sh)[f]	1160(s)	1146	19	C4C5(16) H16CC(15) C3C4(11) HC40(11) C409(11) CC4C(7) HC30(6) H15CC(6) C207(5)	CC and CO str coupled with methylene rock and methine def
1131(w)	1127(m)	1130	1	C308(48) C106(29) C2C3(8)	CO str
1108(m)	1103(w,sh)	1102	6	C409(57) HC20(11) CC50(7) C207(7) 09CC(6)	CO str coupled with CO def
1098(m)	1095(w,sh)	1093	5	C5010(50) 010C1(17) C409(11) HC1010(7) C1C2(6) H16C0(5)	Asymmetric COC str coupled with CC and CO str
1079(s)	1088(w,sh)[f] 1075(w,sh)	1075	4	C106(39) C308(26) C2C3(18) C1C2(11) C4C5(10) HC10(9) 010C1C(6) HC30(6) CC3H(5)	CO str coupled with CC ring str and methine def
1066(m)	1064(s)	1066	0	C4C5(29) C3C4(11) C2C3(10) C409(8) C106(7) H15CC(6) H16CC(6) TC5010(5) HC1010(5)	CC ring str coupled with CO str and methylene rock
1047(m)	1040(s)	1029	18	C4C5(26) C207(13) 010C1(10) C1C2(8) C5010(7) 09CC(7) C308(7)	CC and CO str
1005(w)	1003(s)	1002	3	C2C3(32) C3C4(18) C106(14) CC2H(9) 07CC(7) CC4H(5)	CC ring str coupled with CO str and bend
957(m)	952(w)	949	8	C1C2(42) 010C1(15) HC1C(10) C308(9) C2C3(9) HC2C(8) CC07(7) C3C4(6) H16CC(5)	CC ring str coupled with CO str and methine def
885(vw)	878(vs)	898	-13	C207(20) C3C4(19) C1C2(11) 010C1(9) C5010(9) CC09(6) HC1C(6) OC0(5) HC4C(5)	CO str coupled with CC and CO ring str
845(vs)	836(vs)	877	-32	C207(37) 010C1(20) HC1C(12) OC0(7) COC(5)	CO str coupled with CO ring str and bend
754(m)	750(vs)	750	4	010C1(38) CC07(9) C5010(8) 010C1C(6) CC2H(5) C106(5)	Symmetric COC str coupled with CO str and def
718(w) 668(w)	710(w) 668(w,b)	680	-12	C3C4(23) 07CC(15) CC08(10) HC2C(9) C409(7) 010C1C(6) 06CC(6) CC3C(5) HC3C(5)	CC ring str coupled with CO def
624(w)	615(vw,b)	633	-9	CC50(18) COC(16) OC0(11) 07CC(6) C3C4(5)	CO ring def
520(vs)	513(vw)	511	9	09CC(15) OC0(13) C4C5(10) 08CC(7) HC4C(6) CC4C(6)	CO def coupled with ring bending
469(s)	462(w)	492	-23	OC0(16) CC09(12) C1C2(9) TC106(9) 08CC(8) 06CC(7)	CO def
451(s)[f] 423(m)	442(w)	437	5	08CC(18) COC(16) CC2C(11) CC09(11) HC3C(7)	CO def coupled with ring bending
407(m)	410(w)	398	9	TC207(15) CC4C(13) COC(13) 010C1C(10) 06CC(9) CC3C(7) 07CC(7) 09CC(5)	Ring bending coupled with CO def and OH o.p. bend
391(m)		383	8	TC308(12) TC1010(9) 09CC(8) TC106(8) CC4C(8) COC(7) TC5010(6) CC08(6) C5010(6)	Ring def coupled with OH o.p. bend and CO def

TABLE X (Continued)

THE INTERPRETATION OF THE VIBRATIONAL SPECTRUM OF β-LYXOSE

Band Assignment				Spectral Interpretation	
Experimental				Calculated Contributions[b],	
Raman, cm^{-1}	IR, cm^{-1}	Calc., cm^{-1}	Diff.[a], cm^{-1}	internal coordinates, %	Description of the Approximate Motions
		366		TC308(30) TC409(22) COC(9)	OH o.p. bend
		360		TC106(30) TC207(16) TC409(10) CC09(8) C2C3(8)	OH o.p. bend
341(w)	342(vw,sh)	347	6	TC207(44) COC(10) CC09(8) TC106(5) CC3C(5)	OH o.p. bend coupled with CO def
317(m)	305(vw,sh)	287	d	O6CC(35) OCO(25) TC106(16) HC1O10(12) CC08(10) HC1C(8) C2C3(5)	Ring def coupled with OH o.p. bend
276(w)		278	-2	CC07(50) O7CC(9) TC207(5) CC2C(5) CC08(5) TC106(5)	CO def
		266		O8CC(26) O9CC(23) CC09(22) CC08(15) TC308(9) TC409(8)	CO def coupled with OH o.p. bend
233(vw) 209(vw) 203(vw)		234	-1	O7CC(33) CC2C(21) HC1C(7) CC2H(7) C1C2(7) CC08(6) CC3H(6) CC07(6) TC207(5) TC3C4(5)	CO def coupled with ring bending
		140		TC4C5(18) TC1C2(16) TC1O10(15) TC3C4(11) CC4C(6) CC5O(6) O1OC1C(5) CC2C(5)	Ring torsional bending
		131		TC2C3(28) TC3C4(18) CC3C(16) TC1C2(9) CC2C(5)	Ring torsional bending

Average Error = 7.7 cm^{-1}

[a]Diff. = difference = observed frequency (Raman) − calculated frequency.

[b]Contributions are relative and may add to more than 100% due to contributions from negative interaction parameters in the SUQFF. Only contributions of 5% or more have been included.

[c]Conventional symbolism indicating relative intensity, vs = very strong, s = strong, m = medium, w = weak, sh = shoulder, b = broad, v = very.

[d]These frequencies are not included in average error calculations since they were not included in any of the refinements.

[e]i.p. and o.p. refer to in-plane and out-of-plane, respectively.

[f]Apparent correlation field splitting.

TABLE XI

THE INTERPRETATION OF THE VIBRATIONAL SPECTRUM OF α-XYLOSE

Band Assignment				Spectral Interpretation	
Experimental				Calculated Contributions[b],	
Raman, cm^{-1}	IR, cm^{-1}	Calc., cm^{-1}	Diff.[a], cm^{-1}	internal coordinates, %	Description of the Approximate Motions
	3410(vs,b)[c]	3357	d	OH13(81) OH12(16)	O-H stretch (str)
		3357		OH11(99)	O-H str
	3340(vs,b)	3357	d	OH14(97)	O-H str
	3275(vs,b)	3357	d	OH12(82) OH13(17)	O-H str
2983(vs)	2985(m)	3000	-17	CH16(49) CH15(48)	Asymmetric methylene str
2963(m)	2960(w,sh)	2953	10	CH18(50) CH19(25) CH17(22)	Methine str
2954(w)	2950(m)	2943	11	CH20(63) CH17(20) CH19(14)	Methine str
2922(m)	2920(w)	2941	-19	CH19(35) CH20(34) CH17(29)	Methine str
2903(vs)	2900(w,sh)	2934	-31	CH18(48) CH17(28) CH19(25)	Methine str
2892(s)	2890(m)	2888	4	CH15(51) CH16(50)	Symmetric methylene str
1480(w)[e] 1470(w)	1475(s)[e] 1460(w,sh)	1480	0	HCH(42) H15CC(18) H16CC(13)	Methylene scissors coupled with wag
1455(w)	1450(s)	1448	7	HO7C(37) HC2O(20) CC3H(8) CC2H(6)	OH i.p.[f] bend coupled with methine deformation (def)
1430(vw)	1440(w,sh)	1440	-10	HO9C(19) HO8C(17) HC3C(11) HC2C(9) HCH(7)	OH i.p. bend coupled with methine def
1400(m)	1425(vw,sh)	1403	-3	HO6C(43) HC1O(18) HC1C(7) C1O2(6) HO7C(5)	Anomeric OH i.p. bend and methine def
1394(m)	1393(w)	1393	1	HO9C(19) HC4C(14) H16CO(11) H15CO(9) HCH(7) HO6C(5) CC4H(5)	OH i.p. bend coupled methylene wag and methine def
1376(m)	1372(m)	1383	-7	H16CO(18) H15CO(17) H15CC(10) HO9C(9) HC2C(8) HO7C(5) HC2O(5)	Methylene wag coupled with OH i.p. bend and methine def
1358(w)	1358(w)	1365	-7	HO8C(32) CC4H(13) HO9C(10) HC4O(8) HC3C(7) HC3O(7)	OH i.p. bend coupled methine def
1343(m)	1342[g](m)	1355	-12	HC1O1O(34) HC1C(14) CC2H(9) CC3H(9) HC3O(9) HO8C(5)	Anomeric methine def coupled with methine def
1338[g](w)	1338(m)	1339	-1	HC4C(19) HC3C(10) CC3H(10) CC4H(8) H15CO(8) HC2C(7) H15CC(6) H16CO(5)	Methine def coupled with methylene wag
1318(w)	1313(w,sh)	1319	-1	CC2H(20) HC1O1O(18) HC1O(10) CC3H(9) CC4H(8) HC2C(6)	Anomeric methine def coupled with methine def
1307(w,sh)	1303(m)	1302	5	HO6C(38) HC1O(34) HC1C(14) C1O6(6)	Anomeric methine def coupled with OH i.p. bend
1255[g](vw)	1253(vw,sh)	1257	-2	HC4O(46) H16CO(13) H15CO(9) HC4C(8) CC4H(7) H16CC(5)	Methine def coupled with methylene wag and twist
1246(w)	1250(w,sh)	1248	-2	HC3O(49) HO9C(17) HO8C(15) HC3C(13) HC4O(8) CC3H(6)	Methine def coupled with OH i.p. bend
1212(vw)	1235(w)[e] 1205(w,sh)	1220	-8	H15CO(23) H16CO(22) HC3O(16) HC4O(15) H15CC(11) H16CC(9)	Methylene twist coupled with methine def

TABLE XI (Continued)

THE INTERPRETATION OF THE VIBRATIONAL SPECTRUM OF α-XYLOSE

Band Assignment				Spectral Interpretation	
Experimental				Calculated Contributions[b],	
Raman, cm^{-1}	IR, cm^{-1}	Calc., cm^{-1}	Diff.[a], cm^{-1}	internal coordinates, %	Description of the Approximate Motions
1197(vw)	1190(w)	1204	-7	HC2O(37) HO7C(31) HC2C(10) CC2H(10) HO8C(5)	Methine def coupled with OH i.p. bend
1153(m)	1150(s)	1148	5	C4O9(26) C3C4(16) C4C5(13) HC4O(8) H16CC(8) CC4C(8) H15CO(6) HC3O(5) C2O7(5)	CO and CC ring str coupled with methylene rock
1137(w)	1128(s)	1128	9	C2O7(28) C5O1O(10) HC1O(9) C4O9(9) C3O8(7) HC4O(7) C2C3(6) O1OC1C(6)	CO str coupled with CC and CO ring str
1118(vs)	1112(m,sh)	1104	14	C5O1O(28) O1OC1(21) C2O7(8) H16CO(7) C1C2(6) CC2H(5)	Asymmetric COC str
1111(s)	1105(w,sh)	1097	14	C3O8(71) CC3C(10) C3C2(10) C3C4(5)	CO str coupled with CC ring str
1089(s)	1080(w,sh)	1078	11	C4O9(32) C2O7(25) HC2O(15) C2C3(13) C3C4(9) C1O6(8) HO7C(7) CC2C(7)	CO str coupled with CC str and methine def
1066(w)	1065(w,sh)[e] 1055(s)	1057	9	C4C5(53) H15CC(10) C3C4(9) H16CC(6) C4O9(6) TC5O1O(5)	CC ring str coupled with methylene rock
	1040(s)	1037	3	C1O6(26) C1C2(23) HC1C(14) HC1O(10) C5O1O(7) HC2O(7) C3O8(7) C4O9(5) TC5O1O(5)	CO str coupled with methine def and CO ring str
1019(w)	1017(vs)	1000	19	C1C2(20) HC1O1O(20) C2O7(17) C2C3(11) C5O1O(10) O1OC1(9) C1O6(8) O6CC(7) C4C5(6)	CC and CO ring str coupled with methine def
934(m)	932(vs)	935	-1	C1O6(39) C3C4(13) HC1C(7) C3O8(6) C4C5(6) H16CC(6)	CO and CC str coupled with methine def
	928[g](s)	921	7	C3C4(33) C2C3(23) CCO8(9) C1C2(9) C1O6(8) C4O9(5)	CC ring str coupled with CO str and def
907(vs)	903(vs)	906	1	O1OC1(55) C5O1O(35) C1C2(17) HC1C(6) C1O6(5) HC1O1O(5)	Symmetric COC str coupled with CC ring str
760(w)	762(vs) 670(w)	761	-1	O1OC1(16) COC(15) C2C3(15) CCO7(8) C1O6(6) O6CC(6) C1C2(5) HC2C(5) C3O8(5)	CO ring str and bend coupled with CC ring str and CO str and bend
613(w)	625(w,b)	620	-7	OCO(19) O6CC(14) COC(13) TC5O1O(6) CCO7(6) O1OC1(5)	CO def coupled with CO ring bend
567(m)	566(vw)	570	-3	OCO(14) O7CC(14) CCO8(8) HC4C(6) CC3H(6) O1OC1C(6) H15CC(5) CC5O(5) CC4C(5)	CO def coupled with methine def
530(s)	524(w)	542	-12	CC5O(21) O8CC(10) CCO9(10) O7CC(6) C4O9(6) C2C3(5) O6CC(5)	CO def coupled with ring bend
509(m,sh)	507(w)	506	3	C3C4(14) O8CC(11) O7CC(9) CCO9(9) C4C5(8) O1OC1C(7)	Ring bend coupled with CO def
433(s)	432(w)	438	-5	O9CC(17) CCO7(14) CC2C(8) TC4O9(6) OCO(6) TC1O6(6)	CO def
414(m)		425	-11	CC4C(27) TC5O1O(12) O1OC1C(10) CC3C(9) HC3C(7) O6CC(6)	Ring bend
407(m,sh)	400(m) 388(w)	389	18	CC3C(14) TC4O9(13) CC2C(10) O8CC(9) CCO8(9) CC5O(8) O9CC(8) COC(8) HC4C(5) TC3O8(5)	Ring bend coupled with OH o.p. bend

TABLE XI (Continued)

THE INTERPRETATION OF THE VIBRATIONAL SPECTRUM OF α-XYLOSE

Band Assignment					
Experimental				Calculated Contributions[b],	
Raman, cm^{-1}	IR, cm^{-1}	Calc., cm^{-1}	Diff.[a], cm^{-1}	internal coordinates, %	Description of the Approximate Motions
	365(vw)	360	5	TC106(46) TC409(11) TC207(10) COC(7)	OH o.p. bend
		359		TC308(46) TC207(15) CC08(10) 06CC(6) CC09(5)	OH o.p. bend coupled with CO def
		349		TC207(38) TC106(19) TC308(13)	OH o.p. bend
331(vw)		331	0	TC409(45) CC08(14) TC207(10) TC308(8) CC4H(5) 09CC(5)	OH o.p. bend coupled with CO def
318(vw)	310(w)				
280(w)	285(vw,sh)	275	5	CC09(24) 07CC(22) TC207(12) CC07(9) 09CC(9)	CO def
270[g](vw	270(vw,sh)	270	0	08CC(20) OC0(17) COC(12) 010C1C(11) 07CC(11) HC1C(9) TC308(8) TC106(7) C1C2(5)	CO def coupled with ring bend
265(vw)	260(vw,sh)	260	5	CC08(21) 08CC(14) 010C1C(9) 09CC(8) COC(8) OC0(6) CC0(6)	CO def
235(vw)	230(vw,sh)	231	4	06CC(42) HC1010(24) OC0(19) 010C1(14) COC(12) CC07(10) HC1C(10) 010C1C(6) TC4C5(5)	CO def coupled with methine def
		135		TC1C2(24) TO10C1(12) CC2C(12) TC4C5(11) HC1010(7) TC2C3(7) COC(6) CC4C(5)	Ring torsional bend
		127		TC3C4(26) TC2C3(23) CC3C(11) CC2C(6) CC4C(5) COC(5)	Ring torsional bend

Average Error = 6.9 cm^{-1}

[a]Diff. = difference = observed frequency (Raman) – calculated frequency.

[b]Contributions are relative and may add to more than 100% due to contributions from negative interaction parameters in the SUQFF. Only contributions of 5% or more have been included.

[c]Conventional symbolism indicating relative intensity, vs = very strong, s = strong, m = medium, w = weak, sh = shoulder, b = broad, v = very.

[d]These frequencies are not included in average error calculations since they were not included in any refinements.

[e]Apparent correlation field splitting.

[f]i.p. and o.p. refer to in-plane and out-of-plane, respectively.

[g]These frequencies obtained from the low temperature spectrum.

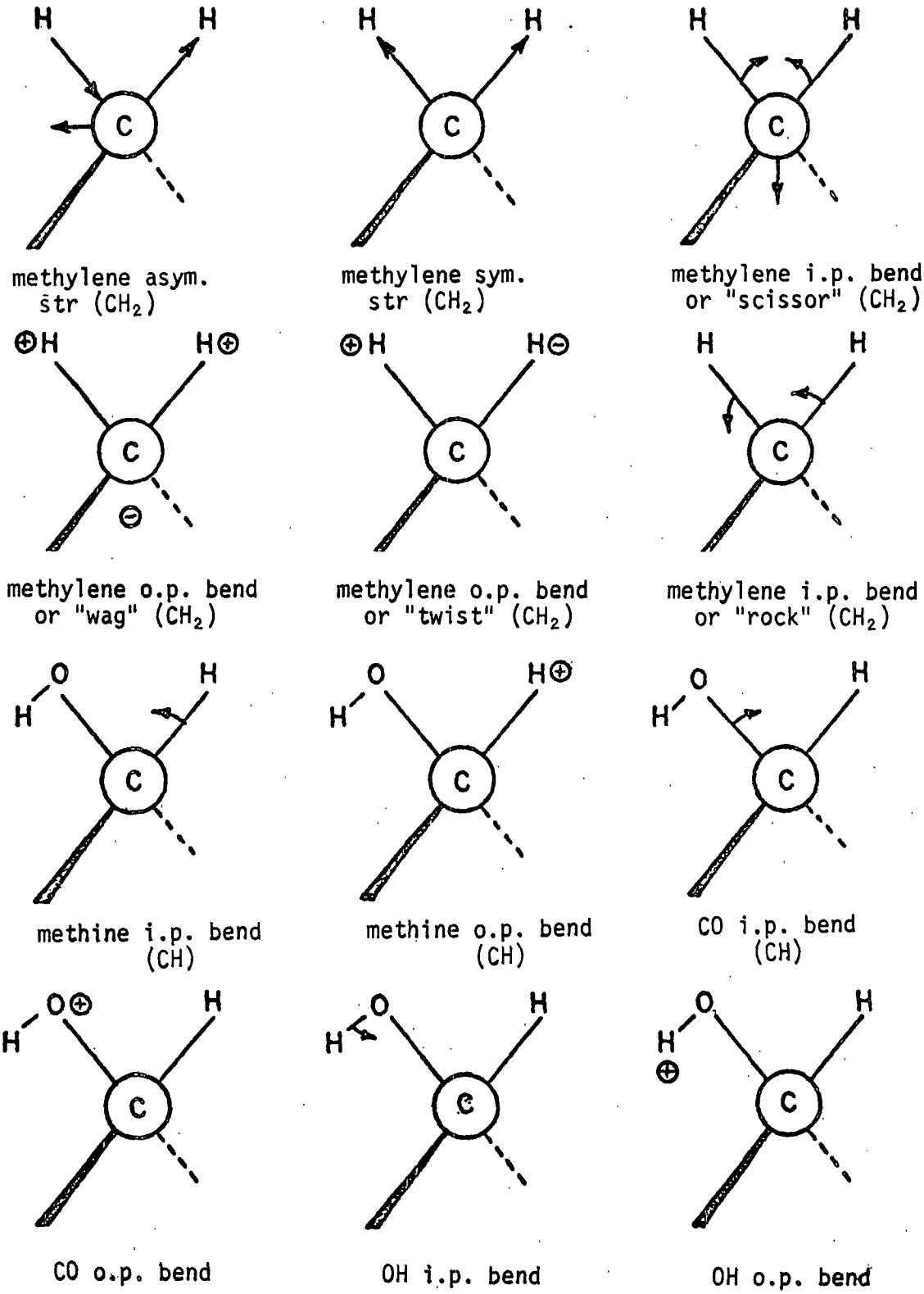

Figure 12. The Descriptions of Several of the Atomic Group Vibrations. ⊕ and ⊖ indicate movement perpendicular to the plane of the page)

Several deuterated species of the pentose molecules were also included in these normal coordinate calculations. These isotopically substituted models were very useful in developing the SVQFF for the normal molecules since they could be used to help determine the approximate energy of bands associated with particular hydrogen atom deformations. The calculations of these species were identical to the normal molecules. The $\underset{\sim}{G}$ matrices were altered only by the different mass values of the atoms.

Calculated frequencies and band distributions for the β-arabinose C-$\underline{d}_6$ model are presented in Table LXIII of Appendix III.

The Cl-D isotopically substituted molecular models of arabinose and xylose were also calculated. The frequencies and band distributions are presented in Tables LXIV and LXV of Appendix III.

The COD substituted models of arabinose and xylose were also calculated. The frequencies and band distributions are presented in Tables LXVI and LXVII of Appendix III.

DISCUSSION OF RESULTS

GENERAL COMMENTS

In general the normal coordinate calculations and SVQFF refinements performed on the pentose sugars were successful. The average error values of 7.7 cm^{-1} for β-arabinose, 7.7 cm^{-1} for β-lyxose, and 6.9 cm^{-1} for α-xylose are very good considering the complexity of these molecules. An overall average error of 7.4 cm^{-1} is only slightly greater than the 6.3 cm^{-1} reported for the 1,5-AHP's (1) and is significantly better than the 12.5 cm^{-1} reported by Snyder and Zerbi for THP (13). In addition, these normal coordinate calculations give very reasonable approximations to the motions of these molecules during

each vibrational mode. These results were obtained with only small changes in the SVQFF that had been successfully applied to the 1,5-AHP's. The close similarity of the force constant parameters in the two fields lends support to the concept of SVQFF transferability among structurally similar molecules.

CORRELATION OF OBSERVED AND CALCULATED BANDS

Average error values alone have been shown to be a rather poor indication of the fit of calculated frequencies to the experimental frequencies. The nature of the fit can only be determined after all experimental bands have been taken into consideration. For example, while Vasko (14) reported an average error of 10 cm^{-1} for the normal coordinate analysis of the spectrum of α-glucose, closer examination reveals that only six of twelve bands observed in the region spanning 1400 to 1250 cm^{-1} were assigned. Also, the region between 800 and 600 cm^{-1} contains only three assigned bands while seven were actually observed. Therefore, the fit to the experimental frequencies must be judged by actual band assignments in conjunction with average error values.

Figure 13 illustrates the distributions of the observed vibrational frequencies of β-arabinose, β-lyxose, and α-xylose and compares these assigned frequencies to the frequencies calculated for these molecules. Below 1500 cm^{-1}, the observed spectra can be divided into four regions: 1) 1500 to 1200 cm^{-1}, 2) 1160 to 900 cm^{-1}, 3) 900 to 500 cm^{-1}, and 4) 500 to 100 cm^{-1}. In three of these regions the differences between the spectra of the three pentoses are not nearly as significant as those in the region of 900 to 500 cm^{-1}. Bands in this region are very sensitive to hydroxyl group orientation about the pyranose ring, especially at the anomeric site in the molecules. Notice in Fig. 13 that these important bands are quite accurately reproduced in the calculated spectra. It is important to note that spectral gaps in the observed bands are also accurately reproduced.

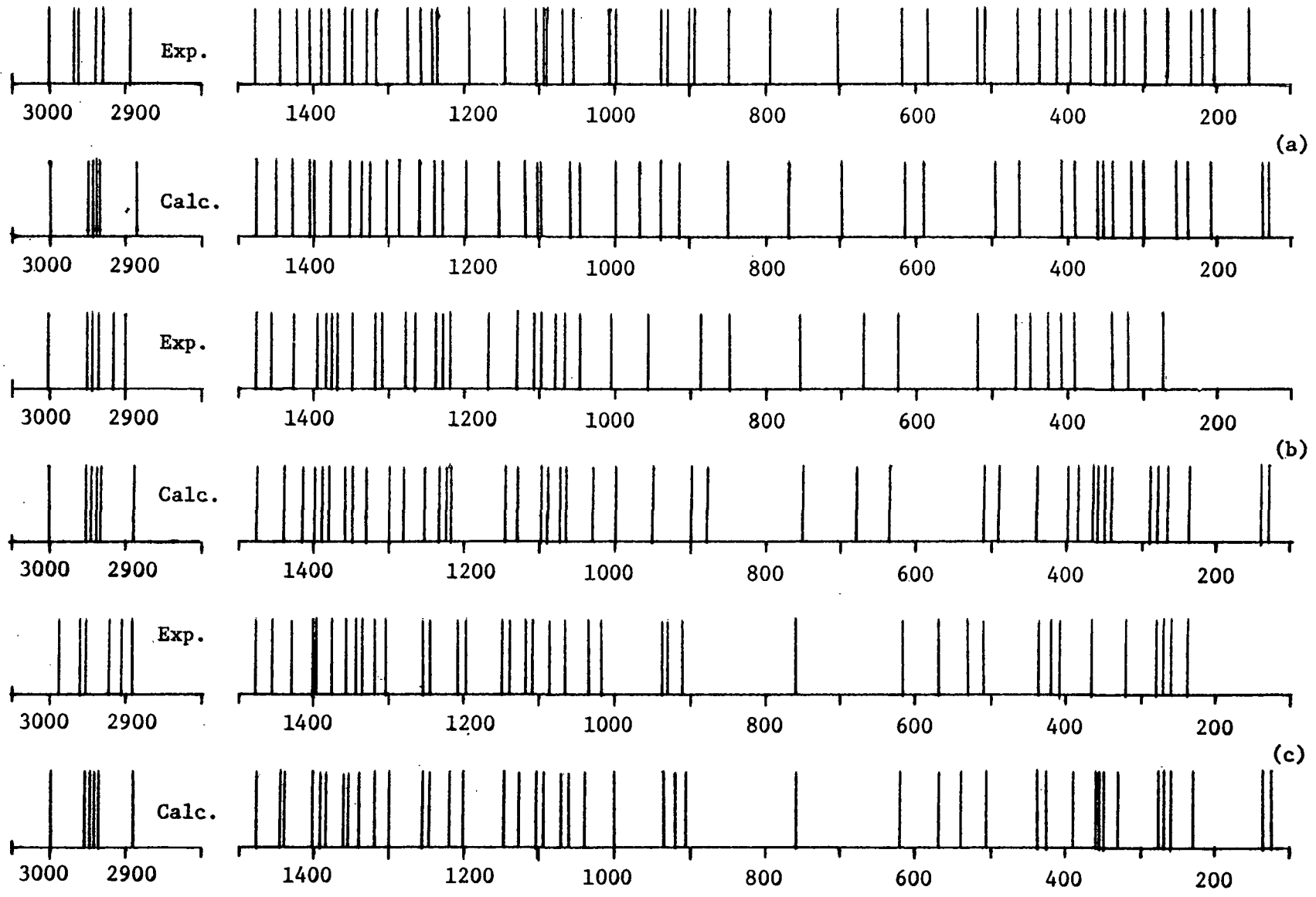

Figure 13. A Comparison of the Assigned and Calculated Frequencies of the Pentose Molecules: (a) Arabinose, (b) Lyxose, and (c) Xylose

In each of the pentoses there were several observed bands that have no calculated counterparts. It is suggested that these bands do not represent fundamental modes. These bands are included in the assignments presented in Tables IX-XI. Arabinose exhibited seven unassigned observed bands at (cm^{-1}): 1010 (R), 995 (IR), 893 (R), 788 (IR), 675 (IR), 510 (R), and 415 (IR). However, since all but the band at 675 cm^{-1} are very close to assigned observed bands and are weak in intensity compared to their neighboring band, these bands are probably a result of correlation field splitting of the fundamental vibration. (Correlation field splitting is an effect produced by the intermolecular coupling of molecules in the unit cell.) In the spectra of lyxose and xylose there are also several examples of apparent correlation field splitting which have been noted in the spectral assignments in Tables X and XI. Figure 13 also reveals that calculated bands having no observed bands assigned to them occur only in the region below 300 cm^{-1}. In this low energy region of the spectrum, resolution in both the Raman and infrared decreases considerably. As a result, bands below 300 cm^{-1} were not assigned during many of the refinements.

The infrared spectrum of each of these pentoses reveals a rather strong band at about 670 cm^{-1}: 675 cm^{-1} in arabinose, 668 cm^{-1} in lyxose and 670 cm^{-1} in xylose. Only in lyxose is this band observed in the Raman spectrum (668 cm^{-1}). It is suggested that these bands do not represent fundamental vibrations, but their exact cause is not immediately apparent. No obvious combination or overtone bands can be used to account for these bands. The difference in relative intensity in the Raman (very weak) and infrared (strong) spectrum could indicate a mode associated with OH out-of-plane bending motions. A comparison of the normal and deuterated spectra of arabinose (see Fig. 1 and 6) and xylose (see Fig. 4 and 7) reveals some distinct changes in this spectral region upon deuteration. These changes do not, however, permit any general

conclusions to be made. While several authors have assigned bands in this spectral region to OH out-of-plane bending modes, work by Patil and Bose (27) using β-arabinose and its 1,2:3,4-di-O-propylidene acetal has shown that a band at 683 cm^{-1} is in the spectrum of each even though no free hydroxyl groups are in the acetal. This finding casts doubt upon the bands associated primarily with OH out-of-plane bending motions. All attempts to calculate a frequency of vibration for this observed band while maintaining reasonable results throughout the rest of the spectrum failed, even when drastic force constant changes were introduced into the SVQFF. The band could be a lattice related mode although little evidence exists to support this hypothesis.

As a matter of interest, the Raman spectrum of β-arabinose exhibited some peculiarities with changes in the temperature at which the spectrum is obtained. Figure 14 depicts the splitting of the Raman band observed at 705 cm^{-1} (room temperature) at several temperatures. The band at 705 cm^{-1} appeared at room temperature to be a single, somewhat broadened band. As the temperature was decreased it became evident that two closely spaced bands were present. Both bands shifted in energy and showed opposite changes in intensity until at -170°C the intensities were nearly equal. The results of the shifts were two bands at 698 and 685 cm^{-1}. The effect was entirely reversible and reproducible. As the temperature increased, the changes were merely the reverse of those observed upon cooling. Repeated cooling and warming of the sample did not alter these results. Though not as dramatic, changes in the Raman spectrum of the DL mixed crystal of arabinose also occurred in this region of the spectrum upon cooling. Similar effects were not observed for lyxose or for xylose. Since these changes occur with only one band in the arabinose spectrum, one possibility is that a lattice effect relating to a change in the intermolecular hydrogen bonding may be causing these changes; no specific explanation is offered at this time.

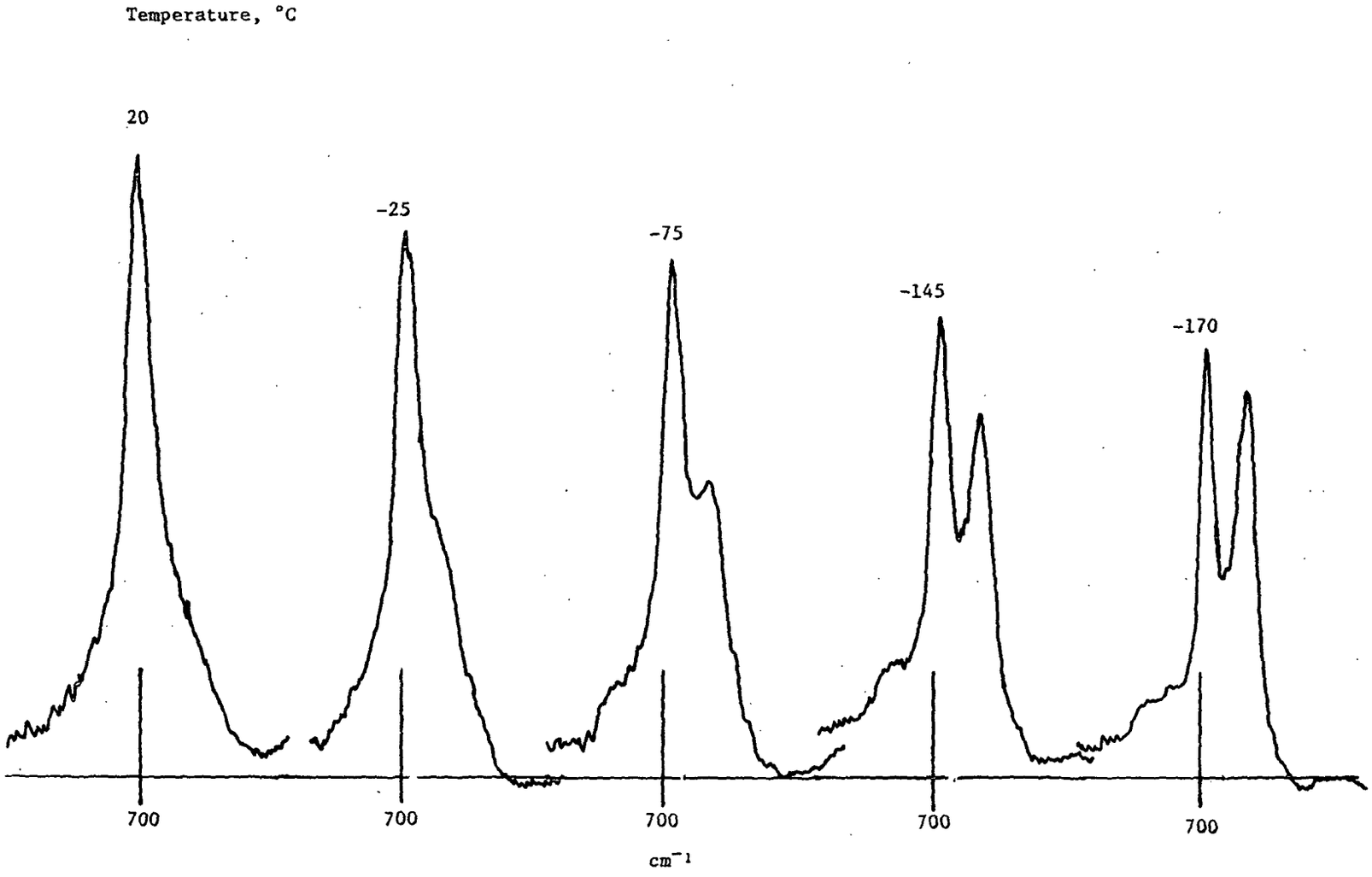

Figure 14. The Effect of Cooling on the "700" Band in β-Arabinose

INTERPRETATION OF THE PENTOSE SPECTRA

One of the most important constraints applied to the normal coordinate analyses was that the spectral interpretations based upon the calculated normal coordinates be in agreement with established group frequency charts. The limited usefulness of the group frequency approach becomes evident when normal coordinate calculations have repeatedly shown the great extent to which the vibrational motions of complex molecules couple. Successful group frequency correlations can be made only if there is relatively little coupling of motions occurring in a particular fundamental vibration. Rather than discuss the results of the NC analyses entirely in group frequency terms, I will use some newer classifications. Fuhrer, et al. (28) quantified the motions of these calculated distributions as group frequency, zone frequency, and delocalized frequency. A group frequency would be designated when 66% or more contribution to the calculated distribution is from one internal coordinate. Likewise, a zone frequency arises when two or more internal coordinates located at the same site in the molecule contribute at least 66% of the motion in the calculated mode. When neither of these two conditions exists, the mode is highly coupled and is termed a delocalized frequency. Examination of the calculated distributions below 1500 cm^{-1} presented in Tables IX-XI reveal that there are very few calculated bands that would correspond to a group frequency. Therefore any discussion relating calculated band distributions to observed frequencies must necessarily be made in terms of zone frequencies rather than group frequencies.

Before discussing the band compositions calculated for the pentose molecules, it should be noted that the motions of these molecules can be placed into five different categories, each somewhat isolated from the others. It is obvious that both OH and CH stretching modes are separated from all other types of motions. OH stretch contributes solely to the four bands above 3300 cm^{-1}.

CH stretch motions are confined to the bands between 3000 and 2850 cm^{-1}. Below 1500 cm^{-1} the first major spectral gap (see Fig. 13) occurs at about 1200 to 1160 cm^{-1}. Above this gap, modes are primarily comprised of bending motions involving at least one hydrogen atom. Below 1160 cm^{-1} to approximately 800 cm^{-1} the motions are primarily those involving the stretching of the bonds between heavy atoms. While some bands in this region have considerable contributions from hydrogen atom bending motions, these contributions are restricted to hydrogen atoms attached to heavy atoms which are involved in sizable stretching contributions to the particular mode. That is, hydrogen atom deformations occur primarily as part of zone frequencies in this region.

The last separate spectral region extending downward from about 700 cm^{-1} contains two types of motion; the heavy atom bending motions and the torsional motions. With the exception of the OH out-of-plane modes, most of the motions in this region are highly coupled. This is to be expected since a deformation of a CCC angle is likely to affect most other angles within the ring structure. Bands that fall between 700 and 800 cm^{-1} represent transition bands. That is, heavy atom stretching, bending, or both motions may constitute a large part of the modes. Table XII illustrates, in group frequency terms, the areas of the vibrational spectrum of the pentoses where the various types of motion were found. From this table it can be seen that the pentoses are quite similiar to the 1,5-AHP's, THP, and the alditols in the distribution of motions throughout the spectrum.

OH and CH Stretching

The OH stretching modes of the pentoses extend from about 3550 to 3250 cm^{-1}. In the infrared spectrum these bands are both strong and broad. Since OH stretching modes are greatly affected by hydrogen bonding within the crystal lattice, no attempt to fit these bands has been made. Only one force constant

TABLE XII

COMPARISON OF THE CALCULATED GROUP VIBRATIONAL MOTIONS

Group Vibrational Motion	Pentose Freq. Region	1,5-AHP's Freq. Region	THP (13) Freq. Region	Alditols Freq. Region
OH stretch	3357	3356		3350-3330
CH_2 asymmetric stretch	3002-3000	2982-2978	2970	2985-2950
Methine CH stretch	2953-2933	2946-2910		2940-2910
CH_2 symmetric stretch	2888-2885	2882-2880	2862	2900-2865
CH_2 scissors	1481-1474	1470-1460	1463-1448	1485-1435
CH_2 wag	~1478 1418-1339	1470-1410 1388-1347	1380-1322	1485-1300
Methine HCO bend	1450-1199	1435-1200		1450-1216
Methine HCC bend	1450-1204	1435-1200		1450-1200
CH_2 twist	1300-1220	1330-1220	1281-1170	1330-1200
CH_2 rock	1156-950	1163-850	1141-560	1148-830
OH i.p. bend	1450-1199	1410-1200		1428-850
CO stretch	1156-852	1155-850		1140-850
CC ring stretch	1156-680	1163-460	1105-806	
CO ring stretch	1156-750	1130-850	1105-806	
CCO bend	680-209	980-250		775-220
CCC skeletal bend	770-128	750-250		700-200
OH o.p. bend	411-275	285-220		430-250
CC torsion	140-127	300-130	388-232	430-50
COC bend	769-209	743-302	560-242	

was used for all OH stretches and was not included in any of the force constant refinements.

The CH stretching modes occur between 3010 and 2850 cm^{-1}. The observed bands are generally very strong and sharp in the Raman spectrum. Six bands are calculated, two are methylene stretching bands and four are methine stretching bands. The two methylene bands, asymmetric and symmetric stretching, lie at the top and bottom of this range, respectively. The methine bands lie generally between 2875 and 2900 cm^{-1}. Tables IX-XI reveal that methine stretching motions couple with each other but not with the methylene stretching motions.

These CH stretching modes are separated from the CH bending modes by at least 1400 cm^{-1}. Little coupling between stretching and bending modes would be expected under these circumstances. Calculations carried out during this work have shown that satisfactory fitting of the observed CH stretching bands can be accomplished with only a methylene CH,CH stretch-stretch interaction parameter present in the SVQFF. Both Pitzner (1) and Watson (2) included other interaction parameters involving CH stretch, but it was found that the effect of these parameters was primarily observed in the CH stretching region of the spectrum. This SVQFF change (from Pitzner and Watson) must be taken into account during any comparisons with other calculations or when these constants are transferred to other molecular models.

CH Bending

The CH bending modes can be classified into the two categories of methylene and methine bending. The four types of methylene bending motions are exhibited in Fig. 12. However, since these methylene motions can couple, bands exhibiting any of these methylene motions in a pure form would not be expected. The distributions presented in Tables IX-XI do verify that these methylene motions couple

with each other and with other motions of the molecule. As an example, the methylene scissors modes of the 1,5-AHP's, the alditols, and the calculated bands at 1478 cm^{-1} in arabinose and lyxose and at 1480 cm^{-1} in xylose are not pure scissors motions but instead represent a coupling of the scissors and wag motions. Figure 15 illustrates the composite of these motions for each of the pentoses. It is also clear that motions involving twist and wag combinations occur between 1420 and 1200 cm^{-1} and are usually highly coupled with other hydrogen deformations about the ring. The methylene rocking motions occur primarily between 1200 and 800 cm^{-1} and are extensively coupled with the stretching of the carbon-carbon and carbon-oxygen bonds. This extensive coupling of the methylene bending modes prevents the establishment of any useful (from a group frequency approach) correlations between pentose structure and the position of the methylene bending modes in the spectrum. In addition, without the use of molecules deuterated at the methylene site, no absolute verification of the accuracy of these calculated methylene modes can be accomplished. They are, however, in line with the results of other normal coordinate analyses and are, therefore, presumed to be reasonable approximations to the actual modes of vibration.

Patterns of methine motion are even more complicated in nature than the methylene modes. Examination of the calculated distributions reveals that significant contributions from methine bending motions occur throughout the entire spectrum below 1450 cm^{-1}. For example, quite unexpectedly significant contributions from the anomeric methine bending motions occur below 300 cm^{-1} (209 cm^{-1} for arabinose, 287 cm^{-1} for lyxose, and 231 cm^{-1} for xylose). In this case it is also important to note the contributions from other internal coordinates. A major portion of these coordinates contain the atom, C-1, which qualifies this mode as a zone frequency. Close examination will reveal that in

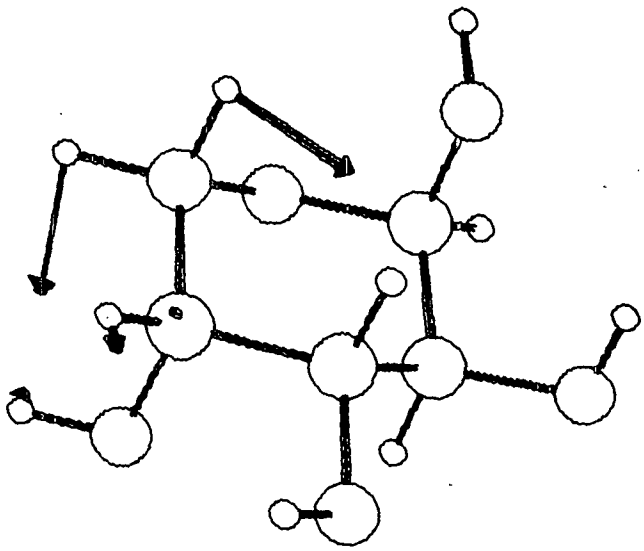

β-Arabinose, 1478 cm^{-1}

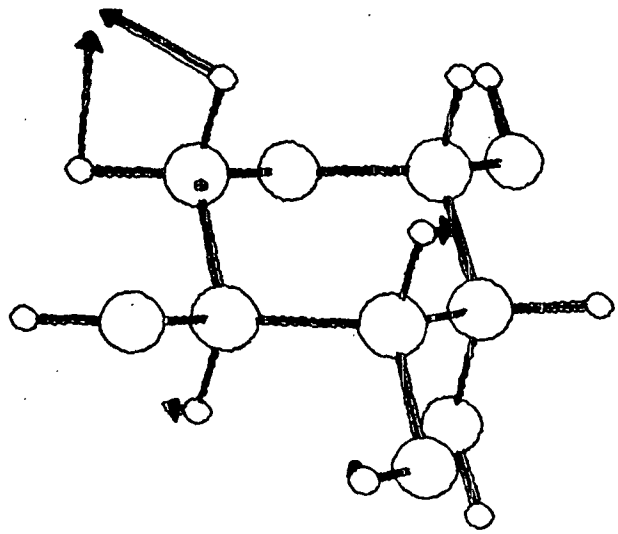

β-Lyxose, 1478 cm^{-1}

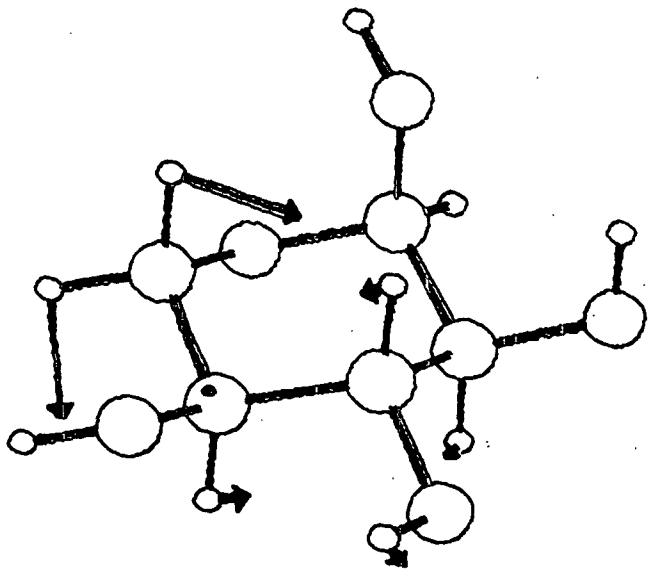

α-Xylose, 1480 cm^{-1}

Figure 15. Representations of the HCH Bending Modes of the Pentoses. (The arrows indicate relative displacements of the atoms)

the lower regions of the spectrum contributions from methine bending motions are nearly always part of a zone frequency.

Some validation of the accuracy of the calculated normal modes involving methine bending motions is possible with the use of deuterium labeling at C-1. Stacey, et al. (29) prepared the C1-D labeled arabinose and xylose molecules and published a portion of the infrared spectrum of each. Their data along with NC calculations for the isotopically substituted forms of arabinose and xylose are reproduced in Table XIII. These authors indicated the bands they felt were composed of significant contributions from anomeric methine deformations in both the normal and isotopically substituted spectra. These bands are indicated in Table LXVIII of Appendix III. Comparison of these bands with the calculated modes having significant anomeric contributions (indicated in Table XIII) reveals a remarkedly good agreement between the observed and calculated locations of anomeric methine bending motions. The changes resulting from isotopic substitution in arabinose reveals the strong influence on bands (in the normal arabinose) at 1357 and 1318 cm^{-1} from the deuterium at C-1. Table XIII indicates that calculated bands having significant contributions from C1-H bending motions include 1355, 1335, and 1304 cm^{-1} which is in good agreement with observed data. Similar comparisons made from normal and C1-D labeled xylose reveal that observed bands showing significant effects from the label at C-1 include 1398, 1340, and 1305 cm^{-1}. Bands calculated for normal xylose which have significant anomeric methine contributions fall at 1403, 1355, and 1317 cm^{-1}, again showing good agreement with observed data.

The comparison of the observed and calculated frequencies for these isotopically substituted molecules shown in Table XIII reveals that not all the frequencies are correlated. The calculated bands that are left unassigned may well be the result of insufficient resolution of the experimental bands.

TABLE XIII

COMPARISON OF THE OBSERVED AND CALCULATED FREQUENCIES OF TWO NORMAL AND C1-D SUBSTITUTED PENTOSES

β-Arabinose				α-Xylose			
Calc. C1-H	IR[a] C1-H	IR[a] C1-D	Calc. C1-D	Calc. C1-H	IR[a] C1-H	IR[a] C1-D	Calc. C1-D
1478	1472	1476	1477	1480	1480	1478	1480
1450	1450	1450	1448		1465	1460	
1428	1425	1425	1426	1448	1455	1450	1447
1405	1402	1397	1403	1440	1455	1425	1440
1402[c]			1385	1403[c]	1425	1405	1393
1377	1375	1375	1379	1393	1386		1380
1355[c]	1357[b]		1363	1383	1375	1375	1367
1335		1332	1340	1365	1360	1360	1358
1322	1329		1321	1355[c]			
1304[c]	1318[b]			1339	1340	1340	1340
1286			1290	1319[c]	1315	1322	1328
1262	1260	1266	1264	1302	1305[b]		
1239	1247	1255	1240	1257	1255	1275 1260	1259
1231	1234	1227	1238	1248	1240	1240	1249
1199			1203	1220	1205	1218	1223
1156		1162	1167	1205	1195	1200	1208
1121	1135	1115[d]	1135	1148	1150	1188	1156
1103	1103	1108	1105	1128	1130	1125	1142
1100	1093	1088	1101	1104	1110	1110	1120
1062	1065	1076	1093	1097	1080	1095	1099
1048[c]	1053	1047[d]	1053	1078	1070	1082	1088
998[c]	1001	1035	1040	1057	1055	1065[d]	1076
	998	985	981[e]	1037[c]	1035	1050	1057
964	943	974	965	1000[c]	1020	1033 1022	1022
938	925	920	925[e]	935	935	975	977[e]
913	893	893	891[e]	921			934[e]
852	865[b] 843	864[d] 858		906	905	900	916
769	785	824	839	761	762	881	891[e]
		777	758			865	886[e]
						742	741[e]

[a]IR frequencies obtained from Stacey, Moore, Barker, Weigel, Bourne and Whiffen (29)
[b]Frequencies as thought to contain significant contributions from C1-H coordinates.
[c]Frequencies calculated to contain significant contributions from C1-H coordinates.
[d]Frequencies as thought to contain significant contributions from C1-D coordinates.
[e]Frequencies calculated to contain significant contributions from C1-D coordinates.

Since neither Raman spectra nor low temperature spectra were published or recorded during this work for these isotopically substituted molecules, the lack of a sufficient number of observed bands can be expected, especially in the region above 1200 cm^{-1}. For example, consider the bands in arabinose Cl-D. The observed frequency at 1375 cm^{-1} could also be concealing the bands associated with the calculated frequencies at 1385 and 1363 cm^{-1}. Likewise each of the observed bands at 1332, 1266, and 1227 cm^{-1} may well be concealing another fundamental frequency that would correspond to the unassigned calculated bands. A similar consideration of the bands of xylose Cl-D will also reveal that bands observed at 1375 and 900 cm^{-1} may be composed of two closely spaced fundamentals. Certainly for the 900 cm^{-1} band this is possible because of the similar problem encountered with the normal coordinate analysis of normal xylose.

The observed bands that remain unassigned may well be due to other spectral anomalies such as lattice effects, combination, or overtone bands that are often found in infrared spectra. The use of the Raman spectra could help clarify this point. In any case, Table LXVIII of Appendix II taken from the work of Stacey, et al. (29) reveals that for arabinose the bands at 858 and 893 cm^{-1} are classified as very weak bands while the band at 864 cm^{-1} is strong. By assigning the calculated band at 891 cm^{-1} to the band at 864 cm^{-1}, both the bands observed at 893 and 858 cm^{-1} can be considered not to be fundamental vibrations.

COH In-Plane Bending

The COH in-plane bending modes of the pentoses fall primarily between 1200 and 1450 cm^{-1}. These modes exhibit extensive coupling with most other motions present in this region. Similar results have been observed for the alditols (2) and the 1,5-AHP's (1) and for the calculations of alpha and beta

glucose (14,17). The accuracy of these calculated COH in-plane bending modes could be determined were it not for the fact that the spectra of O-D substituted arabinose and xylose (Fig. 6 and 7) were not as useful as would be desired. No bands in these spectra were found to disappear completely with deuteration nor were any entirely new bands observed. However, intensity changes and frequency shifts were observed throughout the spectra including some dramatic intensity changes in the vicinity of 600 cm^{-1}. Resolution of these bands is complicated by several factors, but probably the most obvious factor is the lack of complete O-D exchange. It becomes impossible to distinguish between bands arising from motions of deuterium atoms and motions of undeuterated impurities. Furthermore, new bands appearing in the lower energy regions of the spectrum often interfere with bands already located in the area. New coupling patterns and band shifts caused by deuteration often affect band intensity as well as frequency. This complicates correlations of the bands from the normal sample with those from the isotopically substituted molecule.

In spite of all the difficulties involved with hydroxyl group deuteration, these O-D spectra can help validate the NC calculations and the SVQFF. Table XIV reveals reasonably good correlation between observed and calculated frequencies of the O-D species of arabinose and xylose. The liberties with which assignments were made, however, must be considered when the average errors of 10.4 cm^{-1} for arabinose and 12.4 cm^{-1} for xylose are noted. In general, many more bands can be seen in these observed spectra than can be calculated, and only the more intense bands have been assigned. Better correlations have been hindered by these complicated spectra.

CC and CO Stretching

Two important aspects of the NC analyses are encountered in the spectral region spanning 700 to 1160 cm^{-1}. First, Tables IX-XI show that the correlation

TABLE XIV

COMPARISON OF THE OBSERVED AND CALCULATED FREQUENCIES FOR THE COD SUBSTITUTED PENTOSES

β-Arabinose				α-Xylose			
Raman, cm^{-1}	IR, cm^{-1}	Calc.	Diff.[a]	Raman, cm^{-1}	IR, cm^{-1}	Calc.	Diff.[a]
2995 (s)[b]	2995 (m)	3002	-7	2978 (vs)	2985 (m)	3000	-22
2963 (m,sh)	2960 (s,sh)	2949	14	2956 (m)	2962 (m,sh)	2953	3
2953 (s)	2950 (s)	2942	11	2950 (w,sh)	2955 (m)	2943	7
2937 (s)	2935 (s)	2939	-2	2915 (w)	2925 (m)	2941	-26
2890 (vw)	2895 (m)	2935	-45	2895 (s)	2905 (m,sh)	2933	-38
	2880 (w,sh)	2885	-5	2887 (s)	2900 (m)	2888	-1
	2610 (s)	2447	c		2540 (vs,b)	2447	c
	2480 (vs,b)	2447	c		2490 (vs,b)	2447	c
		2447			2430 (vs,b)	2447	c
	2420 (s,sh)	2446	c			2446	
1472 (s)	1472 (m)	1476	-4	1472 (m)	1475 (m,sh)	1479	-7
1445 (w) 1430 (vw)	1445 (w)	1414	31	1453 (m,sh)	1450 (m)	1408	45
1400 (w)	1395 (w,sh)	1405	-5	1428 (w,sh)	1410 (m)	1395	33
1374 (w,sh)	1378 (m)	1373	1	1400 (s,b)	1400 (m)	1383	17
1367 (s)	1362 (m) 1350 (w,sh)	1351	16	1378 (s,b)	1380 (s)	1348	30
1341 (w)	1340 (w)	1347	-6	1363 (s,b)	1360 (w,sh)	1347	16
1318 (vw,sh)	1320 (w,sh)	1313	5	1350 (m,sh)	1340 (vw)	1339	11
	1315 (w)	1310	5	1310 (m)	1320 (vw)	1307	3
1308 (m)	1308 (w)	1296	12	1300 (vw,sh)	1300 (w)	1297	3
1263 (s)	1260 (m)	1258	5	1275 (vw)	1280 (vw,sh)	1272	3
	1240 (w,sh)	1234	6	1255 (vw,sh) 1243 (vw)	1255 (vw)		
1168 (vw,sh)		1174	-6	1233 (w) 1203 (vw)	1237 (vw) 1205 (vw)	1234 1182	-1 21
1146 (w,sh)		1152	-6	1147 (s)	1152 (s) 1145 (s,sh)	1141	6
1140 (w,sh)	1040 (vs)	1138	2			1131	
1132 (w)		1130	2	1111 (s,sh)	1120 (s,sh)	1130	-19
1095 (s)	1095 (vs,b)	1100	-5	1103 (vs)	1110 (s)	1125	-22
1080 (m,sh)	1075 (vs,b)	1089	-9		1085 (s)	1090	-5
1057 (vw)	1055 (vs,b)	1076	-19	1078 (vw,sh)	1075 (s)	1078	0
1005 (m,b)	1020 (vs,b)	1029	-24		1050 (s,b)	1043	7
990 (m,b)	1005 (vs,b)	994	-4	1035 (m,b)	1025 (m,sh)	1019	16
941 (vw)		955	-14		1000 (w,sh)	980	20
924 (w)	928 (vw)	934	-10	950 (vw,b)	933 (s)	951	-1

TABLE XIV (Continued)

COMPARISON OF THE OBSERVED AND CALCULATED FREQUENCIES FOR THE COD SUBSTITUTED PENTOSES

β-Arabinose				α-Xylose			
Raman, cm^{-1}	IR, cm^{-1}	Calc.	Diff.[a]	Raman, cm^{-1}	IR, cm^{-1}	Calc.	Diff.[a]
908 (m) 895 (w)	895 (s)	912	-4	890 (vw)	895 (vw,sh)	895	-5
	870 (w,sh)	867	3	925 (m)	910 (w)	931	-6
831 (m,sh)	835 (m)	847	-16		855 (vw,sh)	878	-23
820 (vs)	820 (m)	828	-8	843 (m,b)	845 (w)	834	9
772 (w)	775 (s,sh) 770 (s)	766	6	753 (vw,sh)	762 (s)	752	1
688 (s)	675 (m,b)	687	1	598 (vs)	670 (m,b) 602 (m)	600	-2
607 (s)	607 (m)	599	8	563 (m)	568 (m)	562	1
583 (m,sh) 577 (s)	578 (m)	574	3	527 (s,sh)	550 (vw)	537	-10
519 (m)		478	41	505 (vs)	507 (w) 470 (w,b)	492	13
504 (m)	495 (m,b)	460	44	419 (s)	440 (vw)	428	-9
400 (w)	400 (w)	396	4	400 (s)	400 (vw)	416	-16
		377		370 (vw,sh)	370 (vw)	378	-8
312 (w)		313	-1	314 (vw,b)		319	-5
		298			305 (vw)	304	1
283 (vw)		272	11	272 (w,sh)		298	-26
266 (w)		260	6	266 (m)		252	14
		245				244	
		219				225	
		212				217	
		185				206	
		138				129	
		122				121	
		Average Error = 10.4 cm^{-1}				Average Error = 12.4 cm^{-1}	

[a]Diff. = difference = observed frequency (Raman) - calculated frequency.

[b]Conventional symbolism indicating relative intensity: vs = very strong, s = strong, m = medium, w = weak, v = very, b = broad, sh = shoulder.

[c]Frequencies not used in the average error determinations.

of calculated frequencies with observed frequencies is somewhat less accurate than in the region above 1160 cm^{-1}. The deviations between the observed and calculated bands tend to be confined to particular bands rather than distributed over all bands in this region. For example, the calculated bands at 964 cm^{-1} in arabinose, 877 cm^{-1} in lyxose, and 1000 cm^{-1} in xylose show deviations from observed Raman bands of 22, 32, and 19 cm^{-1}, respectively. With the exception of the very weak Raman band in arabinose at 795 cm^{-1} (782 IR) calculated to be 769 cm^{-1}, the other observed bands in this region of the pentose spectra are correlated very well with calculated bands. Examination of the motions comprising these particular bands reveals that they are primarily CC and CO stretching motions. Further development of the SVQFF of complex pyranose ring structures may reduce errors encountered in this spectral region.

The second aspect of the results of the normal coordinate analyses in the region between 700 and 1160 cm^{-1} concerns the coupling of the motions making up the normal modes calculated for this region. Coupling is to be expected in these modes because of the nearly equal masses of the carbon and oxygen atoms, the ring structures of these molecules, and the similarity of the energy levels of the CC and CO stretching motions. A high degree of coupling between the CC and CO stretching motions occurs in all parts of the molecule. While zone frequencies can be identified in some cases, most modes can be labeled as delocalized frequencies. Further study of these motions reveals that while the phases of the motions of these modes could in some cases be paralleled to motions of more symmetric molecules [see a similar treatment of the motions of THP by Burkett and Badger (9)], the relative contributions from each of the internal coordinates differed enough to make any such correlations essentially useless. For example, the calculated band for lyxose at 1093 cm^{-1} parallels the "A1u" mode of cyclohexane shown in Fig. 16. That

is, each of the CC and CO ring stretching motions are in the proper phase so as to produce the ring motion illustrated by Fig. 16. However, examination of the calculated distribution for this band reveals that four of the ring bonds contribute 6% or less, one bond contributes 17%, and the C_5-O_{10} bond stretch constitutes 50% of the motions in the mode. With the relative contributions differing by this large an amount, the net ring motion is not that illustrated in Fig. 16 and, therefore, it is not practical to label the modes in this manner.

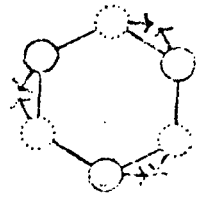

Figure 16. The "A1u" Mode of Cyclohexane as Taken from Burkett and Badger (9)

One exception has been taken, however, and it pertains to the C-O-C ring stretching motions. Two types of stretches are possible:

1. Symmetric C→O←C
2. Antisymmetric C→O—C→

These stretching modes have been identified in Tables XVIII-XX (p. must also be noted that the label of symmetric or antisymmetric stretch does not imply equal contributions from both the ring CO bonds. There were no specific patterns discovered for the location of these C-O-C stretching motions in the pentose molecules.

Low Energy Bands

Below 700 cm^{-1} three types of internal coordinates dominate the motions calculated for these normal modes. Principal contributions come from the heavy atom bending motions involving both ring CCC and CCO coordinates and hydroxyl

group CCO coordinates. The hydroxyl group torsional motions, or more commonly the OH out-of-plane bending motions, also occur along with the ring torsional motions or ring twists. Of the seventeen bands calculated for this region, two are primarily ring twisting motions and are of lowest energy, four are predominantly OH out-of-plane bending motions, and the remaining eleven are heavy atom bending motions. The ring twist modes are calculated to lie below 200 cm^{-1} and have been left unassigned. No experimental bands could be located in this region in the Raman spectrum due to their proximity to the exciting line, grating effects, and their apparent weak intensities. Generally, the assignments for the four OH out-of-plane bending modes are dubious because of the sensitivity of these modes to hydrogen bonding and the expected weak intensities of these modes.

Bands of greatest importance are the heavy atom bending motions which lie in the 400 to 700 cm^{-1} region of the vibrational spectrum. This region happens to be a well defined region, as Fig. 1-5 reveal that some of the strongest and sharpest Raman bands fall in this region. In addition, recent work with cellulose (30) has revealed that bands in this area of the spectrum may be conformation sensitive. These bands may turn out to be the most informative bands with respect to the four possible structures of cellulose. Good understanding of this spectral region could be very informative in interpreting spectra of other carbohydrate systems. However, assignment of these bands is hampered by the lack of interpretive guidelines for bands falling in this low energy region of the spectrum.

Tables IX-XI indicate that the CCC and CCO ring bending modes are generally very highly coupled, although some bands do show localization at different areas about the pyranose ring. Generally, however, this localization is much less specific than can be found in the region from 700 to 1160 cm^{-1}. The

localization that does occur is generally in the very lowest energy modes. These modes are just above the ring twisting modes. For example, each pentose exhibits a bending mode localized primarily at the anomeric site in the ring: 209 cm^{-1} in arabinose (axial OCO), 287 cm^{-1} in lyxose (equatorial OCO), and 231 cm^{-1} in xylose (axial OCO). Though no specific trend is implied, it would appear that this localized band is quite sensitive to axial versus equatorial orientation of the anomeric hydroxyl group by the 56 cm^{-1} energy gap between lyxose and xylose. Likewise, the band at 234 cm^{-1} in lyxose is localized at the C-2 site of the molecule, the location of the only axial hydroxyl group.

TRANSFERABILITY OF THE SVQFF

Factors Affecting SVQFF Transferability

The structural input used to construct the $\underset{\sim}{G}$ matrix can have a pronounced effect upon the transferability of any SVQFF. The structural input, including the definitions of the internal displacement coordinates describing the motions of the molecule, should coincide as much as possible with that of the molecules from which the SVQFF was obtained. Small changes in bond lengths are especially influential on the calculated frequencies of the bending modes. Although bond angle differences have less influence on the calculated frequencies, they can affect the composition of each mode. That is, they affect the coupling pattern within each mode.

Definition of the internal displacement coordinates involving the torsions can also influence the results of the normal coordinate calculations. The previously mentioned Wilson S-vector technique as adapted by Schachtschneider (21) employs a summation process whereby atoms in a trans-configuration across a given bond are summed to form one torsional internal coordinate. In the pentose molecules there are two situations where this rule cannot be strictly applied.

First are the C-O torsions involving the hydroxyl groups and second are the C-O ring torsions. In both cases only one additional bond extends outward from the oxygen atom and three from the adjoining carbon atom. Pitzner (1) and Watson (2) elected to define these torsions as only the one trans-configuration, ignoring the other atoms attached to the carbon. Hilderbrandt (31) notes that such definitions of the torsional coordinates may be acceptable but will not result in the true torsional force constant for that particular bond, since in reality, all atoms at each site are active in the torsional motion. In this investigation, the C-O(H) torsions were defined as the one trans-configuration across the C-O bond, but the C-O ring torsions were defined as the sum of all possible torsional orientations whether trans or gauche.

Factors affecting force constant transferability must also be considered when establishing the $\underset{\sim}{F}$ matrix for a molecule. The most important aspect concerns the extent of the grouping of similar types of motion or interactions under a single force constant parameter. For example, Pitzner (1) grouped all carbon and oxygen bend-bend interaction constants under two parameters, one for trans-orientation and one for gauche-orientation. Work with the acyclic pentitols (2) and the pentoses has indicated that these two groups were not sufficiently general to give the best calculated results. Comparisons of these trans and gauche bend-bend parameters for the acyclic pentitols and for the pentoses in Table VIII show that while Pitzner's parameters were -0.024 and -0.014 for gauche and trans-orientation, respectively, the corresponding parameters for the pentitols ranged from -0.105 to 0.070 for the gauche-interactions and from -0.027 to 0.004 for the trans-interactions. For the pentoses, the ranges are nearly as diverse though they are not exactly the same: gauche is -0.081 to 0.074 and trans is -0.086 to 0.008. When interaction parameters vary as much as these do, care must be taken so as to define interaction parameters in a way analogous with the definitions used to produce the SVQFF.

Comparison of SVQFF's

In order to achieve satisfactory frequency correlations with the refinements, 73 force constant parameters were used. This number represents a marked increase from the 56 and 59 reported for the 1,5-AHP's (1) and the alditols (2), respectively, but two diagonal and five interaction elements can be attributed directly to the anomeric site in the molecule. The remaining additional parameters are due primarily to the increased independence given the interaction parameters through more limited groupings. No C-H and O-H stretch-bend interaction parameters have been included in this SVQFF. Satisfactory fit of the C-H stretch region was obtained using only the C-H stretch-stretch parameter for the methylene group.

Included in the diagonal force constants are two constants for COH in-plane bending motion, one for the hydrogen bonded O-H groups and one for the "free" O-H groups. Work with methanol (32) revealed that crystalline methanol, which represents a highly structured system of hydrogen bonds, has a COH in-plane bending constant of 0.976* while the value for gaseous methanol, which should exhibit no hydrogen bonding, is 0.764. Clearly, reasonable values of COH in-plane bending constants ought to lie within this range. Examination of the crystal structure data reveals that only arabinose (22) and lyxose (24) have intermolecular oxygen-oxygen distances great enough to merit the label of nonbonded hydroxyl groups. In arabinose the hydroxyl group on C-4 qualifies, and in lyxose it is the hydroxyl group on C-2. Furthermore, the O-H stretching regions of the infrared spectra of these molecules shown in Fig. 1 and 3 support the existence of these "free" hydroxyl groups. The use of separate COH in-plane bending constants was decided upon when the insertion of the two separate constants into the SVQFF allowed for a much improved fit of the spectral region spanning 1200 to 1500 cm^{-1}. The final value determined by the refinements for

*The angle bending constants are expressed as $mdyn.A/(rad)^2$.

the "bonded" COH in-plane bending constant is 0.871 and for the "free" COH constant the value is 0.776, both within the range of the values of methanol.

The final values for the three torsional force constant parameters in Table VIII differ significantly from the values obtained by Pitzner with the 1,5-AHP's (1). Comparison of the C-O ring torsions is not possible since these torsional internal coordinates were defined in a different manner. The C-C torsion parameter, though lower than the value for the 1,5-AHP's, is very near the value determined for THP (9). Likewise, while the hydroxyl group C-O(H) torsion parameter is much greater than the value for the 1,5-AHP's, the value is in accord with that for the alditols (2). The differences in these torsional parameters arose as a result of a series of refinements designed to minimize assignment errors in the spectral region below 500 cm^{-1}. These refinements were constrained by the need for reasonable potential energy distributions in terms of previous normal coordinate calculations for these low energy bands and in terms of the nature of the observed band itself. That is, bands calculated to be primarily composed of OH out-of-plane bending motion were not assigned to bands that were strong and well defined in the Raman spectrum.

Direct comparison of all SVQFF parameters from other molecules is not practical because of the ways in which all the interaction parameters have been defined. However, as Table VIII shows, the differences among diagonal elements are small, which indicates the relative insensitivity of the diagonal SVQFF elements to the differences in $\underset{\sim}{F}$ and $\underset{\sim}{G}$ matrix construction. The interaction parameters, as a whole, are reasonably similar to those of the 1,5-AHP's. Even with the differences in the definitions of these parameters, a comparison of the values reveals that most are of the same sign, and several have very nearly the same values.

Transferability Demonstrated

Methyl-α-xylopyranoside and Methyl-β-xylopyranoside

Normal coordinate calculations of the alpha (MAX) and beta (MBX) anomers of methyl xylopyranoside, based on the pentose SVQFF, demonstrated the good transferability of this force field. With only minor SVQFF changes to accommodate the methyl group, the calculations based on this pentose SVQFF resulted in average error values of 7.5 and 8.5 cm^{-1}, respectively, for MAX and MBX. The correlation of the observed and calculated bands was very good. Furthermore, spectral interpretations based on these normal coordinate calculations were in excellent agreement with previous spectral interpretations. An important aspect of these calculations is the manner in which the anomeric region spanning 600 to 1000 cm^{-1} is reproduced for each anomer. Bands in this region correlated very well with observed bands, a good indication of the sensitivity of the pentose SVQFF to changes in anomeric site configuration. The fact that the pentose SVQFF transferred very satisfactorily to the methyl xylopyranosides assured that the transfer of the SVQFF to the other pentose anomers should also be satisfactory. The normal coordinate calculations presented in Parts II and III of this work are based upon the satisfactory transfer of the SVQFF to the methyl xylopyranoside which is presented in detail in Part IV of this work.

β-Arabinose C-$\underline{d}_6$

The calculation of the normal modes of β-arabinose C-$\underline{d}_6$ and subsequent correlations with observed bands have been included in this report. The purpose of this calculation was to demonstrate the transferability of the pentose SVQFF to deuterated species. The good correlations between the observed and calculated frequencies given in Table XV show that the pentose SVQFF transfer reasonably well to this carbon deuterated molecule. The frequency correlations reveal that the calculated bands differing most from observed bands fall in the spectral

TABLE XV

CORRELATION OF THE OBSERVED AND CALCULATED FREQUENCIES OF β-ARABINOSE C-$\underline{d}_6$

Experimental		Calc.,	Diff.[a],	Experimental		Calc.,	Diff.[a],
IR, cm^{-1}	Raman, cm^{-1}	cm^{-1}	cm^{-1}	IR, cm^{-1}	Raman, cm^{-1}	cm^{-1}	cm^{-1}
3530 (vs,b)[b]		3357	c	938 (s)		924	14
3340 (vs,b)		3357	c	932 (s)		919	13
3250 (vs,b)		3356	c			906	
		3356				891	
2250 (w)	2254 (s)	2247	7	845 (w,sh)		872	-27
		2210		842 (vs)	844 (s)	850	-6
2195 (w)	2200 (s)	2190	10			818	
2185 (w)	2172 (s)	2179	-7	811 (s)	813 (s)	813	0
2140 (w)	2141 (m)	2169	-28	785 (w)	789 (s)	786	3
2120 (w) 2100 (w)	2110 (w)	2106	4	755 (w,sh) 747 (s)	751 (vs)		
1450 (w)		1384	c	733 (w)	734 (m)	732	2
1393 (w)		1364	c	689 (w,b)			
1340 (m)		1354	c	647 (w)	656 (s)	651	5
1315 (w)		1290	c	566 (m)	573 (s)	587	-14
1230 (vs) 1214 (s)	1230 (w,sh) 1216 (m)	1190	26	558 (m,sh)	557 (s)	556	1
1170 (vs)	1165 (vw,b)	1171	-6		485 (m)		
	1145 (vw,sh)	1152	-7	478 (m)	479 (m,sh)	471	8
	1134 (w)	1118	16	425 (vw,b)	419 (m)	401	18
1122 (vs)	1117 (vw)	1116	1	405 (w,b)		374	31
1095 (s)	1097 (w)	1099	-2			360	
1072 (s,sh)	1072 (vw)	1097	25			351	
1056 (vs)	1053 (m)	1059	-6	350 (m)	344 (w)	335	9
1050 (m,sh)	1042 (w,sh)	1054	-12		313 (m)	307	-6
1018 (m)	1019 (m)	1044	-25			290	
993 (vw,sh)					265 (vw)	256	9
980 (w)	981 (vs)	1002	-21		225 (vw)	232	-7
964 (m)	966 (s)	976	-10		205 (vw)	206	-1
960 (w,sh) 948 (vw)	949 (m)	945	4			138	
						125	

Average Error = 10.6 cm^{-1}

[a]Diff. = difference = observed frequency (Raman) - calculated frequency.

[b]Conventional symbolism indicating relative intensity: vs = very strong, s = strong m = medium, w = weak, v = very, b = broad, sh = shoulder.

[c]Frequencies not included in average error calculation.

regions dominated by O-H and C-D bending motions; namely, from 1150 to 1450 cm^{-1} and from 850 to 1000 cm^{-1}. In other areas of the spectrum the correlations are very good, including the C-D stretch region.

In the region from 1300 to 1450 cm^{-1}, the band assignments have not been included in the calculation of the average error because of the poor frequency correlations. There are four bands observed in the infrared spectrum at 1450, 1393, 1340, and 1315 cm^{-1}. These bands are presumed to be entirely OH in-plane bending modes. Calculated bands consisting almost entirely of these motions are at 1384, 1364, 1353, and 1290 cm^{-1}. This correlation of the OH in-plane bending modes is good, especially since the pentose SVQFF has not been conditioned to effects arising from hydrogen bonding in the crystal lattice.

In regions below 1300 cm^{-1}, it is obvious that large frequency shifts can occur from new coupling patterns of the C-D bending motions with other motions of the molecule. Consider the strong bands observed at 1230 and 1214 cm^{-1} in the infrared spectrum and at 1230 and 1216 cm^{-1} in the Raman spectrum. These bands, probably arising from CC and CO stretching motions, represent shifts to higher energy levels of at least 50 cm^{-1} from the CC and CO stretching modes of normal arabinose. Calculated shifts for these bands are on the order of only 10 to 15 cm^{-1}. Though not of the proper magnitude, these calculated shifts are representative of the observed shifts for these bands. The fact that the shifts are less than those observed could be related to the effect of hydrogen bonding on the coupling patterns. Similarly large shifts of these CC and CO stretching modes have been observed for the carbon deuterated ethylene glycol molecule (33). Normal coordinate calculations performed on perdeutero ethylene glycol using a SVQFF adapted to the normal molecules also did not account completely for these large frequency shifts. More detailed investigation

using perdeutero molecules may reveal that the $\underset{\sim}{G}$ matrix changes made to account for the change in mass on deuteration are not sufficient to account for the changes in the vibrational spectra.

The interpretation of the spectral bands of perdeutero arabinose, based on these normal coordinate calculations, are given in Table LXIII of Appendix III. OH stretching modes show no effect from the deuteration in terms of frequency shifts, but band distributions do change slightly, indicating that some kinetic energy ($\underset{\sim}{G}$ matrix) effects influence these modes in the calculations. CH stretching modes shift to lower energy values, and although the CD potential energy distributions are somewhat different than the CH distributions for each calculated band, they are similar enough to allow direct band comparisons.

The spectral region below 1500 cm^{-1} can be divided into five somewhat distinct regions based on band interpretations. From 1500 to about 1300 cm^{-1} are the four, nearly pure COH bending modes. From about 1200 to 1000 cm^{-1} the bands are composed primarily of CC and CO stretch motions. It is worthy to note that the frequencies in this region correlated quite well with experimental bands. Contributions from C-D bending modes are present but are primarily as part of zone frequencies within the modes. The C-D bending modes contribute primarily to bands falling below 1000 cm^{-1} down to about 750 cm^{-1}. Some bands in this region also show substantial CC and CO stretch contributions, similar to the anomeric bands present in normal arabinose.

The spectral region below 750 cm^{-1} is composed primarily of the ring bending and torsional modes. From 750 to about 400 cm^{-1} the main contributions to the bands come from the CC and CO bending motions. Below 400 cm^{-1}, torsional modes begin to predominate along with contributions from the low energy CC and CO bending motions.

Close examination of these spectral regions will confirm that the best frequency correlations occur in regions where band distributions are less influenced by the C-D bending modes. The lower energy bands appear to be least affected by deuteration; the frequency correlations are generally very good below 700 cm^{-1}.

CONCLUSIONS

The results of the normal coordinate analyses performed on the pentose sugar molecules show that the vibrational spectra of these molecules can be adequately accounted for by a relatively simple force field that is quite similar to the force fields used in the analyses of less complex molecules. All but one of the major observed spectral bands are assigned to calculated bands, and the correspondence of these assignments is very good. In addition, the calculated potential energy distributions seem to give a reasonable description of the motions of these molecules in each of the fundamental vibrations.

These normal coordinate calculations have shown that the motions of the pentose molecules occurring below 1500 cm^{-1} are too highly coupled to be classified as group frequencies. While some bands show nearly complete delocalization of the vibrational motions, many bands exhibit localization of motion at particular sites in the molecules. Hydrogen atom deformations, shown to occur throughout the spectrum below 1200 cm^{-1}, generally occur as part of the localized motions of the skeletal bending modes. The high degree of coupling has also prevented the formation of any specific relationships between hydroxyl group orientation and frequency distribution even in the "anomeric" region of the spectrum. It was found that bands in this "anomeric" region were sensitive to the relative orientations of all the hydroxyl groups. Furthermore, the frequency changes occurring in this region with a configurational change at

the anomeric site also depends a great deal upon the relative orientation of the other hydroxyl groups about the pyranose ring.

The SVQFF developed for these molecules is relatively simple and quite similar to the fields developed from previous normal coordinate analyses. All of the observed frequencies of the pentoses were correlated with calculated bands determined solely by the relative orientations of atoms on the pyranose ring. The use of only one SVQFF and the use of the same assumed structural parameters for each of the molecules assures this fact. The SVQFF has also demonstrated good transferability to structurally similar molecules, including several deuterated species.

The results of these normal coordinate analyses provide a sound basis from which to continue the investigation of the spectra of complex saccharide molecules. It should be possible to study the effects of configurational changes at the anomeric site in these pentose molecules. Additionally, it should be possible to apply these results to a study of the pentopyranose polymers and other pentopyranose compounds.

PART II

AN INVESTIGATION OF THE EFFECT OF ANOMERIC CONFIGURATION UPON THE VIBRATIONAL SPECTRA OF THE PENTOSE SUGARS

INTRODUCTION

Pyranose molecules exhibiting mutarotation have at least two molecular configurations in aqueous solutions: the alpha and beta anomers in a given chair conformation. Aqueous solutions of pentose sugars are not restricted to pyranose forms and often these solutions contain significant amounts of other nonpyranose molecular structures. The presence of a significant proportion of nonpyranose forms in solution complicates the interpretation of the spectral bands arising in the Raman spectrum of these solutions. As a result, very little is known directly about the vibrational spectra of those pyranose forms of the pentose sugars which have not yet been crystallized.

The recent advances in the normal coordinate analysis technique provide a means to study the vibrational spectra of some of these other molecular forms that are present in an aqueous solution. The purpose of this work is to investigate the vibrational spectra of some of the alternate anomeric forms of the pentopyranoses: arabinose, lyxose, and xylose, using the normal coordinate calculations and the force field developed for the crystalline pentose sugars. These normal coordinate calculations of the alternate pentose anomers can be very useful in determining the effect of anomeric hydroxyl group orientation on the vibrational spectra.

BACKGROUND

The frequency differences between the spectra of various pyranose anomers are best observed in the 600 to 1000 cm^{-1} range of the vibrational spectrum.

Kuhn (34) first used bands in this region to distinguish between the alpha and beta anomers of some hexopyranoses. Later, extensive work was carried out developing group frequency correlations to help interpret the spectral bands in this region (6-8). Certain bands were assigned to either axial or equatorial anomeric proton deformations. While these assignments proved fairly consistent, Isbell (35) discovered certain exceptions to these assignments. Later work (29) also altered the earlier assignments of these bands. Certain bands appeared related directly to configuration at the anomeric site, but no specific assignments could be made for these bands.

The group frequency approach to assigning these anomeric bands is greatly hindered by the extensive coupling of motions within these complex saccharide molecules. The problems encountered with early group frequency correlations indicated the possibility of this extensive coupling present in the anomeric modes. But not until the work of Vasko (14) with the normal coordinate calculations of α-glucose was the extent of this coupling really examined. The normal coordinate calculations carried out on the pentose molecules also demonstrate the extensive coupling in these anomeric modes. In addition, the motions of several of these bands tend to be localized at C-1 in the molecule. Most likely, this localization of motion is the reason that the early group frequency correlations could be made but not specifically assigned within the anomeric region.

EXPERIMENTAL

The only experimental data obtained during this investigation were the Raman spectra of the aqueous solutions of the pentoses: arabinose, lyxose, and xylose. These spectra were obtained from aqueous solutions of approximately 40% sugar (wt/wt) using a standard capillary tube sampling holder.

The instrumental and computational details have been presented in Part I with the crystalline pentoses.

RESULTS

SPECTRA

The aqueous solution spectra of arabinose, lyxose, and xylose are shown in Fig. 17. The frequencies for each spectrum are tabulated in Table XVI.

VIBRATIONAL ANALYSES

Figure 10 (see Part I) depicts the structural models used for these pentose alternate anomers which cannot be crystallized from solution. The vibrational secular equation was developed exactly as it was for the normal pentoses. The only differences are reflected in the orientations of the anomeric hydroxyl groups. The data necessary to establish the $\underset{\sim}{G}$ matrices for these molecules are presented in Tables XXVIII, XXIX, and XXXVII-XLIV of Appendix II. The $\underset{\sim}{Z}$ matrix elements of these anomers are shown in Table XXXVI of Appendix II. Force constants have been transferred directly from the force field for the normal pentoses.

It should be noted that both pyranose chair forms of α-lyxose (1C-D and C1-D) have been calculated. In the alpha configuration, lyxose has two axial and two equatorial hydroxyl groups in either ring conformation. This orientation should make both forms likely to occur in solution in sizable amounts. It was therefore felt that both conformations of α-lyxose should be calculated.

The results of the normal coordinate calculations applied to the alternate anomers of the pentoses are given in Tables LXIX-LXXII of Appendix III. Included in these tables are the calculated frequencies and potential energy distributions

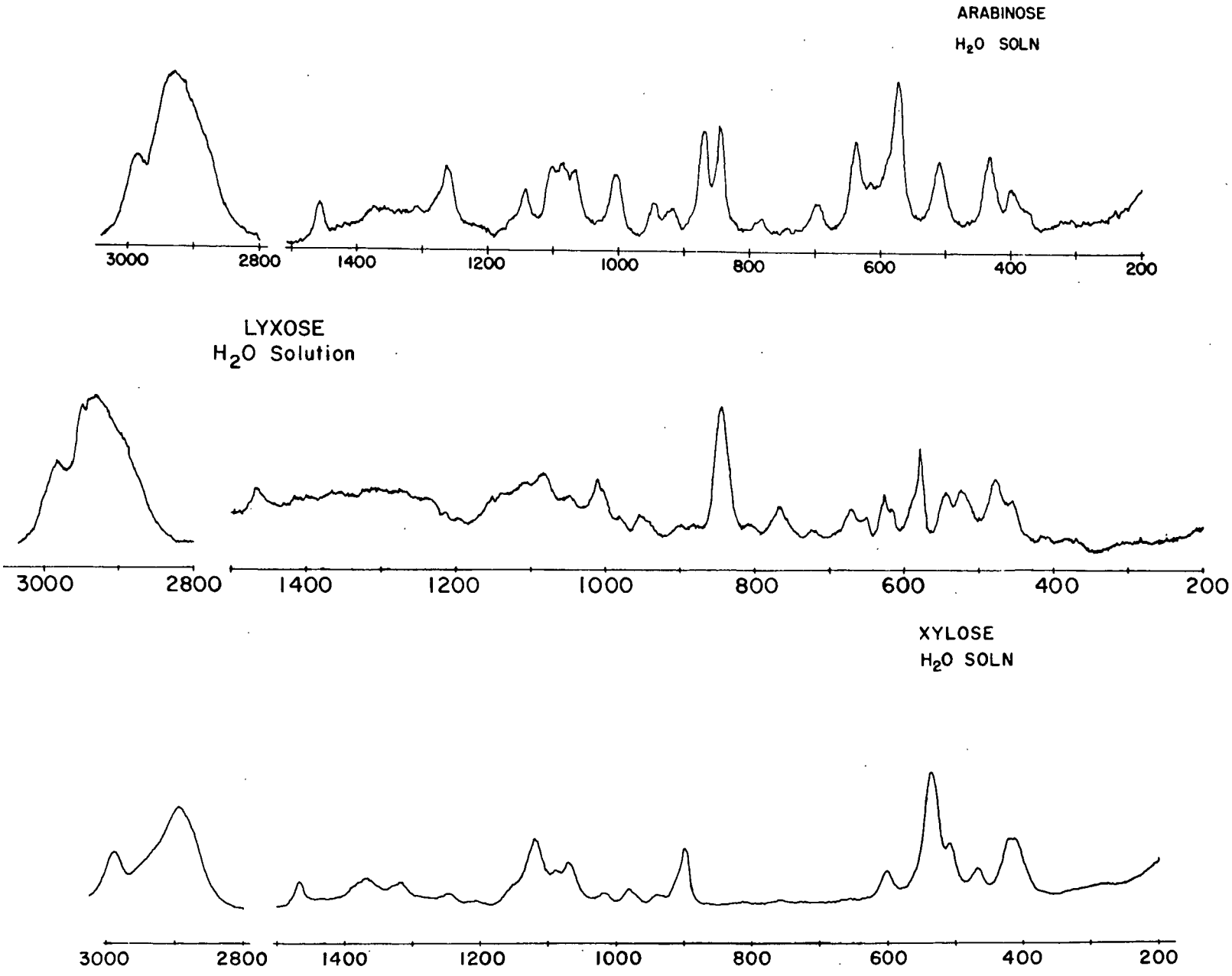

Figure 17. Raman Spectra of the Aqueous Solutions of the Pentoses

TABLE XVI

THE TABULATED FREQUENCIES FOR THE RAMAN SPECTRA OF THE WATER SOLUTIONS OF THE PENTOSES

Arabinose Raman, cm^{-1}	Lyxose Raman, cm^{-1}	Xylose Raman, cm^{-1}
1458 (m)	1465 (w,b)	1467 (m)
1375 (vw)		1365 (w,b)
1310 (vw)		1320 (w,b)
1275 (w,sh)		1250 (vw,b)
1265 (s)		1210 (vw,b)
1165 (vw,sh)		1150 (w,sh)
1142 (m)		1120 (s)
1104 (s)		
1087 (s)		1090 (vw)
1080 (s)	1080 (w)	1070 (w)
1065 (s)	1050 (w,sh)	
1005 (s,b)	1000 (m)	1020 (w)
	980 (vw)	980 (w)
945 (m,b)	950 (w,b)	940 (w)
920 (m,b)	897 (vw)	910 (m,sh)
870 (vs)	880 (vw)	900 (s)
846 (vs)	842 (vs)	
	805 (w)	
780 (w)	765 (m,b)	
740 (vw)	720 (w)	
700 (m)	670 (m)	
	650 (m,sh)	
638 (s)	620 (m)	
	610 (m,sh)	600 (m)
575 (vs)	580 (s)	
	543 (m)	535 (vs)
510 (s)	528 (m)	508 (s,sh)
	478 (s)	467 (m)
435 (s)	454 (m,sh)	
400 (m)	415 (vw)	415 (s,b)
375 (w,sh)	375 (vw)	

for each anomer. The key for the internal displacement coordinate descriptions used in these tables can be found in Table XXVIII of Appendix II.

DISCUSSION OF RESULTS

GENERAL COMMENTS

The normal coordinate calculations of the alternate anomers of arabinose, lyxose, and xylose reveal that the frequency distributions of these anomers are similar to those of the normal pentoses. There are some noticeable frequency shifts, especially in the 600 to 1000 cm^{-1} region. In general, the change in configuration at the anomeric site affects coupling patterns in most of the calculated bands, which demonstrates the extent to which these molecular motions couple.

COMPARISON WITH SOLUTION SPECTRA

No vibrational spectra are available to directly check the validity of the frequencies calculated for the alternate anomers presented in Tables LXIX-LXXII (Appendix III), but the comparison of these calculated bands with the aqueous solution spectra of arabinose, lyxose, and xylose can help verify a few of the frequency shifts that occur with a change in the configuration at the anomeric site. Recent work by Angyal and Pickles (36), where equilibrium aqueous solutions of the pentose sugars were studied using NMR spectroscopy, reveals that solutions of the pentoses generally contain a large proportion of the anomer less readily crystallized. For example, while α-xylose readily crystallizes, β-xylose comprises about 63% of the anomers in solution. Table XVII taken from their work, lists the relative amounts of the various anomeric forms which exist in the aqueous solutions of the pentoses. Because of the large amounts of these alternate anomers in solution, any bands present in

these spectra that cannot be attributed directly to the normal pentose may be taken as arising from the alternate anomer species that may be present. This technique is limited to a great extent by the fact that the calculated frequency distributions for the various pyranose anomers of these molecules are quite similar. For instance, comparison of the observed and calculated frequencies for β-arabinose, β-lyxose, and α-xylose (see Part I) revealed that the frequency distributions are quite similar with the exception of the region between 600 and 1000 cm^{-1}. Therefore, it should be reasonable to also expect the alternate anomer spectra to be quite similar to these normal spectra. They are in fact similar, and bar graphs of Fig. 18 and 19 depict this similarity. Only in the region of 600 to 1000 cm^{-1} are these differences that are easily recognized. Even then, as Fig. 18 reveals, the spectra of α- and β-arabinose are very similar throughout the spectrum. The anomers of xylose are more easily distinguished because of the disappearance of the prominant band at 760 cm^{-1} in going to the beta anomer.

TABLE XVII

PROPORTION (%) OF PYRANOSE AND FURANOSE FORMS OF ALDOSES AT EQUILIBRIUM IN DEUTERIUM OXIDE SOLUTION[a]

Aldose	Temp., °C	α-Pyranose	β-Pyranose	α-Furanose	β-Furanose
D-Arabinose	31	60	35.5[b]	2.5	2
D-Lyxose	31	70[b]	28	1.5	0.5
	44	69	27	3.5	
D-Ribose	31	21.5[b]	58.5[b]	6.5	13.5
	44	17	59	9	15
D-Xylose	31	36.5	63	<1	
	44	37	62.5	<1	

[a]Data taken from Angyal and Pickles (35).

[b]Poor correspondence of peaks in the NMR spectrum with calculated shifts for these pentose forms was taken as evidence that significant amounts of both pyranose chair forms for these anomers were present in solution.

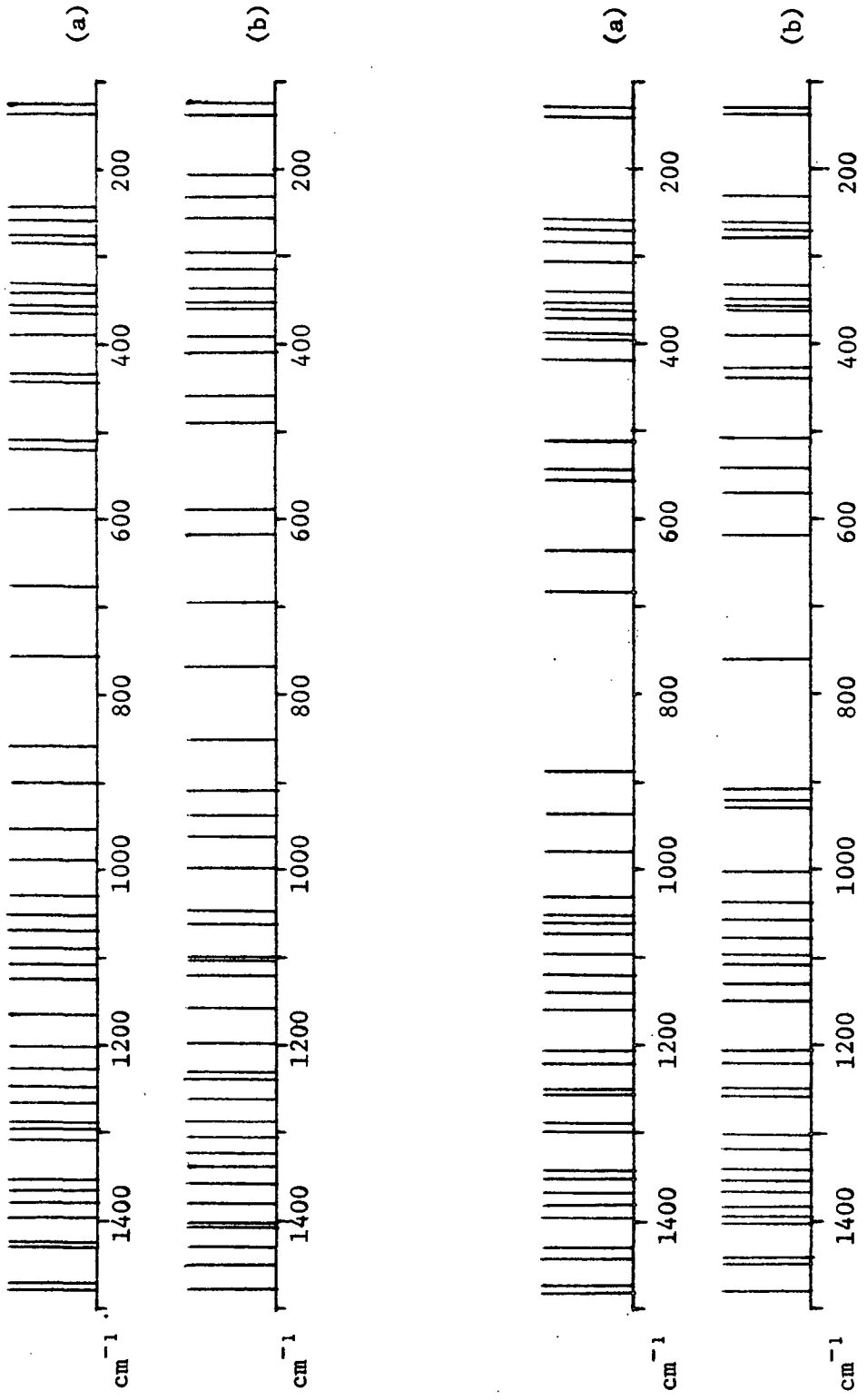

Figure 18. Calculated Frequencies of the Anomers of Arabinose and Xylose. [(a) α-Arabinose, (b) β-Arabinose, (c) β-Xylose, and (d) α-Xylose]

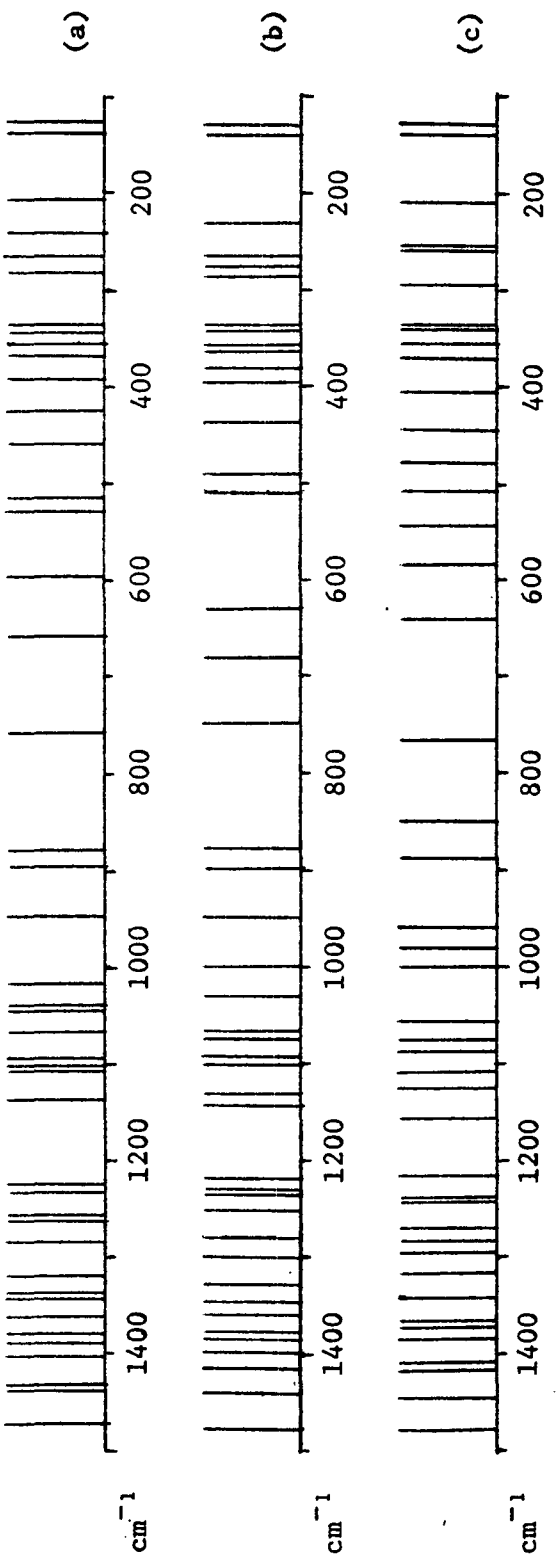

Figure 19. Comparison of the Calculated Frequencies of the Anomers of Lyxose. [(a) α-Lyxose (1C-D); (b) β-Lyxose, and (c) α-Lyxose (C1-D)]

Comparisons of the aqueous solution spectra with the calculated bands for the pyranose anomers reveal that the observed spectral bands can be accounted for very well by the calculated frequencies. Table XVIII compares the principal bands observed for arabinose and xylose with the bands calculated for the dominant anomers that are present in solution. Likewise, the solution spectrum of lyxose is compared with the calculated bands of the two dominant anomers (α-lyxose was calculated in both chair conformations) in Table XIX. A comparison of the arabinose anomers reveals little difference between the calculated bands of the alpha and beta anomers, but there are two strong bands in the arabinose solution spectrum at 870 and 846 cm^{-1}. Since β-arabinose exhibits bands at 848 and 903 cm^{-1} with no band in between, the band at 870 must result from the large amount of α-arabinose present in solution. Calculations for β-arabinose exhibit a band at 852 cm^{-1}, while for α-arabinose there is a band calculated at 859 cm^{-1}. Though the calculated shift of 7 cm^{-1} is not as large as the observed shift of 24 cm^{-1}, the shift is in the proper direction to account for the observed band. A similar comparison of the calculated frequencies for the alpha and beta anomers of xylose reveals that the beta anomer does not exhibit a band between 700 and 800 cm^{-1}. The solution spectrum of xylose does not indicate any band in this region, which is in agreement with the calculations, considering the high proportion of β-xylose present in solution.

Comparison of the anomers of lyxose is more complicated because two pyranose chair forms of α-lyxose probably exist in solution in similar proportions. In either of these alpha forms, two hydroxyl groups are axial and two equatorial around the ring. Table XIX illustrates the comparison of the observed bands of lyxose in aqueous solution with the calculated bands of the three pyranose anomers. From this comparison it is apparent that no particular calculated anomer can be distinguished. In fact, the presence of the observed band at 805 cm^{-1}, which is

TABLE XVIII

COMPARISON OF CALCULATED FREQUENCIES OF PENTOSE ANOMERS WITH OBSERVED FREQUENCIES FROM SOLUTION (H_2O) SPECTRA

Arabinose			Xylose		
Calc'd. Beta	Observed Solution	Calc'd. Alpha	Calc'd. Alpha	Observed Solution	Calc'd. Beta
1478		1476	1480		1481
1450	1458 (m)[a]	1470	1448	1467 (m)	1472
1428		1428	1440		1440
1405		1423	1403		1424
1402		1397	1393		1394
1377	1375 (vw)	1378	1383		1379
1355		1365	1365	1365 (w,b)	1366
1335		1352	1355		1350
1322	1310 (vw)	1306	1339		1340
1304		1295	1319	1320 (w,b)	1297
1286	1275 (w,sh)	1286	1302		1285
1262	1265 (s)	1263	1257	1250 (vw,b)	1254
1239		1245	1248		1249
1231		1226	1220		1220
1191		1201	1204	1210 (vw,b)	1205
1156	1165 (vw,sh)	1164	1148	1150 (w,sh)	1155
1121	1142 (m)	1134	1128	1120 (s)	1137
1103	1104 (s)	1109	1104		1115
1100	1087 (s)		1097	1090 (vw)	1097
	1080 (s)	1090	1078	1070 (w)	1072
1062	1065 (s)	1067	1057		1060
1048		1052	1037		1049
998	1005 (s,b)	1030		1020 (w)	1028
964		988	1000	980 (w)	977
938	945 (m,b)	952	935	940 (w)	933
913	920 (m,b)	902	921		
	870 (vs)	859	906	910 (m,sh)	

TABLE XVIII (Continued)

COMPARISON OF CALCULATED FREQUENCIES OF PENTOSE ANOMERS WITH OBSERVED FREQUENCIES FROM SOLUTION (H_2O) SPECTRA

Arabinose			Xylose		
Calc'd. Beta	Observed Solution	Calc'd. Alpha	Calc'd. Alpha	Observed Solution	Calc'd. Beta
852	846 (vs)			900 (s)	883
769	780 (w)		761		682
	740 (vw)	751	620	600 (m)	634
697	700 (s)	677	570		553
615	638 (s)	589	541	535 (vs)	543
592	575 (vs)		506	508 (s,sh)	510
492	510 (s)	520	438	467 (m)	416
463		507	425	415 (s,b)	416
	435 (s)	444	389		394
411		436	360		386
391		390			370
363	375 (w,sh)	365			

[a]Conventional symbolism indicating relative intensity: vs = very strong, s = strong, w = weak, m = medium, b = broad, sh = shoulder.

TABLE XIX

COMPARISON OF CALCULATED FREQUENCIES OF PENTOSE ANOMERS WITH OBSERVED FREQUENCIES FROM SOLUTION (H_2O) SPECTRA

Lyxose			
Calc'd. Beta	Calc'd. Alpha	Calc'd. Alpha (Cl-D)[a]	Observed Solution
1478	1474	1479	1465 (w,b)[b]
1440	1440	1450	
1416	1433	1418	
1400	1403	1412	
1387	1389	1386	
1380	1379	1375	
1361	1361	1366	
1348	1339	1343	
1327	1335	1314	
1300	1319	1297	
1278	1283	1286	
1253	1262	1273	
1235	1257	1243	
1229	1233	1240	
1220	1223	1216	
1146	1134	1162	
1130	1106	1125	
1102	1102	1109	
1093	1094	1087	
1075	1068	1075	1080 (w)
1066	1047	1060	1050 (w,sh)
1029	1037	1001	1000 (m)
1002	1019	982	980 (vw)
949	948	961	950 (w,b)
898	896	887	897 (vw)
877	879		880 (vw)
		850	842 (vs)

TABLE XIX (Continued)

COMPARISON OF CALCULATED FREQUENCIES OF PENTOSE ANOMERS WITH OBSERVED FREQUENCIES FROM SOLUTION (H_2O) SPECTRA

Lyxose			
Calc'd. Beta	Calc'd. Alpha	Calc'd. Alpha (C1-D)[a]	Observed Solution
			805 (w)[b]
	757	765	765 (m,b)
750			720 (w)
680			670 (m)
	658	640	650 (m,sh)
633			620 (m)
	596		610 (m,sh)
		587	580 (s)
		547	543 (m)
511	529		528 (m)
492	514	511	
	461	480	478 (s)
437	423	445	454 (m,sh)
398	393	404	415 (vw)
383	368	372	375 (vw)
366			

[a] C1-D refers to the alternate ring conformation from the other molecules listed, i.e., C1-D versus 1C-D.

[b] Convention symbolism indicating relative intensity: vs = very strong, s = strong, m = medium, w = weak, v = very, b = broad, sh = shoulder.

not correlated with any calculated frequency, indicates that other molecular forms may also be present in a significant amount in aqueous solution.

Though the comparisons of the solution spectra of these pentoses with the calculated frequencies of the various anomers indicate a reasonable SVQFF transfer, they are not very conclusive. Without the demonstration of SVQFF transferability arising from the normal coordinate calculations of the methyl xylopyranosides, the calculations of these alternate pentose anomers would not be as useful as they are now. But with the good SVQFF transferability demonstrated by the xylopyranosides in Part IV of this work, the calculated normal modes for these anomers provide the very best opportunity to date to study the effect of alpha and beta configurations upon the vibrational spectrum of a pentose molecule.

ANOMER COMPARISONS

The changes in the coupling patterns of the vibrational motions that occur with changes in anomeric configuration generally inhibit any direct band by band comparisons of the potential energy distributions of the different anomers. Examination of the calculated potential energy distributions in Tables LXIX-LXXII (Appendix III) reveals that the compositions of many bands change with changes in configuration at the anomeric site. However, the distribution of the various types of molecular motion, e.g., HCC bend, and CC and CO stretch, etc., is very similar in all the molecular forms studied.

The frequency distributions calculated for the anomeric region of the spectrum (600 to 1000 cm^{-1}) appear to be closely related to the orientations of all the hydroxyl groups about the pyranose ring. Figure 20 depicts the calculated frequencies of the bands in the anomeric regions of several pentoses and displays them along with the axial/equatorial hydroxyl group orientations.

Compound	OH Group Orientation	Frequency Distribution
β-Xylose	E-E-E-E	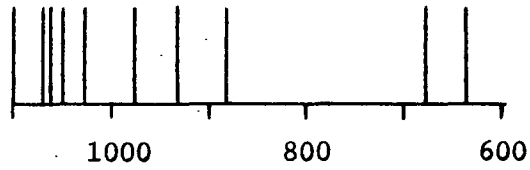
α-Xylose	A-E-E-E	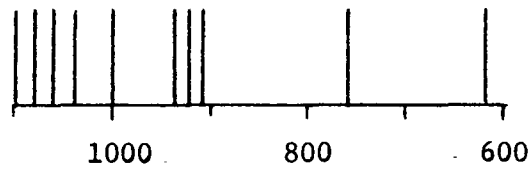
α-Arabinose	E-E-E-A	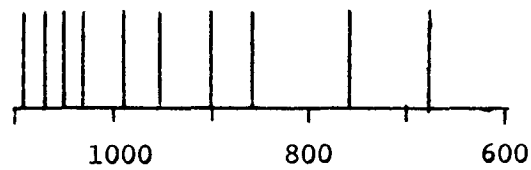
β-Arabinose	A-E-E-A	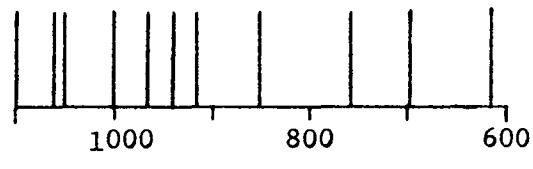
β-Lyxose	E-A-E-E	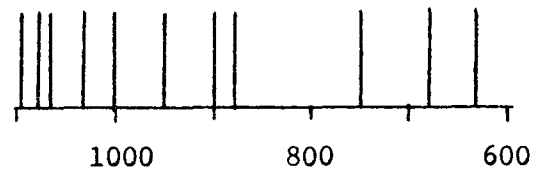
α-Lyxose	A-A-E-E	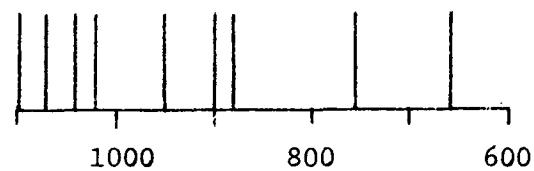

Figure 20. Comparison of the Anomeric Regions of Several of the Pentose Anomers

These bar graphs illustrate the effect of not only the anomeric hydroxyl group orientation but also the effect of the orientation of all the hydroxyl groups upon the bands in this region of the spectrum. For example, β-arabinose and α-xylose are C-4 epimers, but there are significant differences in the bands in this region. Likewise, α-arabinose and β-xylose are C-4 epimers and again there are many differences in this spectral region. In addition, the effect of anomeric change upon the spectrum is different for arabinose and xylose even though the identical change has been made in each. Therefore it can be seen that the relative orientations of the hydroxyl groups about the pyranose ring affect not only the frequency distributions of molecules but also the way in which frequency distributions change with anomeric substitution.

ALTERNATE CHAIR FORMS

The alternate pyranose ring conformation of α-lyxose in the C1-D form has been calculated. The effect of this conformational change upon the calculated spectrum of α-lyxose can be seen in Fig. 19. In general, this change produces small band shifts throughout the spectrum and also affects the calculated potential energy distributions of many of the bands.

CONCLUSIONS

The normal coordinate calculations performed on the alternate anomeric forms of the pentoses are a means of interpreting the vibrational spectra of these molecules. As might be expected from the demonstrated transferability of the pentose force field developed in Part I, the field satisfactorily predicts the bands observed in the aqueous solution spectra and provides reasonable potential energy distributions for the bands of these molecules. These normal coordinate calculations show that no simple correlations between frequency distributions and molecular structure can be made, a fact indicated by earlier attempts to correlate group frequencies with frequency distributions.

PART III

AN INVESTIGATION OF THE VIBRATIONAL SPECTRA OF THE PYRANOSE FORMS OF RIBOSE

INTRODUCTION

Of the pentose sugars, ribose is the only one which, as yet, has not been crystallized as a single molecular form. The solid phase of ribose probably consists of several different molecular forms. In an aqueous solution of ribose, significant amounts of the furanose and pyranose forms have been shown to be present. In addition, lesser amounts of the acyclic forms have also been implicated (36). This unusual behavior, in contrast to the other pentose sugars, has prevented any direct investigations of the vibrational spectra of a particular form of the ribose sugar. However, the availability of the normal coordinate analysis technique and a force field developed specifically for the pentose sugars now allow a thorough investigation of the vibrational spectra of the pyranose forms of ribose.

The objective of this work was to investigate the vibrational spectra of both chair conformations of the two pyranose anomers of ribose. This investigation was accomplished through normal coordinate calculations on both conformations of each of these anomers using the force field refined for the crystalline pentoses. The goal in these investigations was to observe the effect that the orientation of the anomeric hydroxyl group has upon the vibrational spectrum of ribose. In addition, since the vibrational spectrum of solid ribose results from a mixture of several structures, a comparison of these spectral bands with the bands calculated for the various pyranose anomers may reveal at least part of the composition of the ribose solid.

EXPERIMENTAL

The sample of solid ribose was obtained from Pfanstiehl Laboratories, Inc. and was used in the form received. The Raman and infrared spectra were obtained in the same manner as described for the normal pentoses in Part I. The solution spectrum was obtained in the standard capillary cell. Relatively high levels of background interference were observed for these ribose samples.

The computational details have been presented in Part I for the crystalline pentose sugars.

RESULTS

SPECTRA

The infrared spectrum of solid ribose is shown in Fig. 21. Figure 22 contains the Raman spectra of ribose at (a) room temperature as a solid, at (b) -175°C as a solid, and at (c) room temperature as a saturated aqueous solution. Table XX has the bands tabulated for each of the solid-state spectra.

VIBRATIONAL ANALYSES

Four possible ribose anomers exist in the two pyranose chair ring conformations:

1. β-ribose 1C-D (E-E-A-E)
2. α-ribose 1C-D (A-E-A-E)
3. α-ribose C1-D (E-A-E-A)
4. β-ribose C1-D (A-A-E-A)

where "A" and "E" refer to axial and equatorial hydroxyl group orientations around the pyranose ring. Based upon the stability factors established by

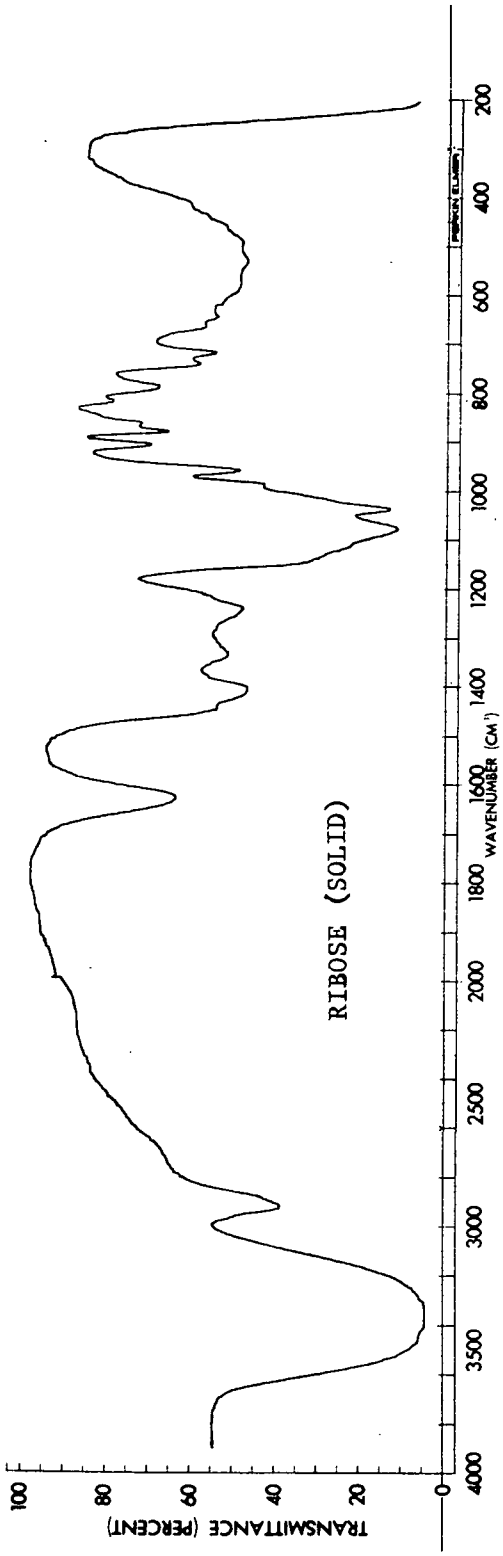

Figure 21. The Room Temperature Infrared Spectrum of Solid Ribose

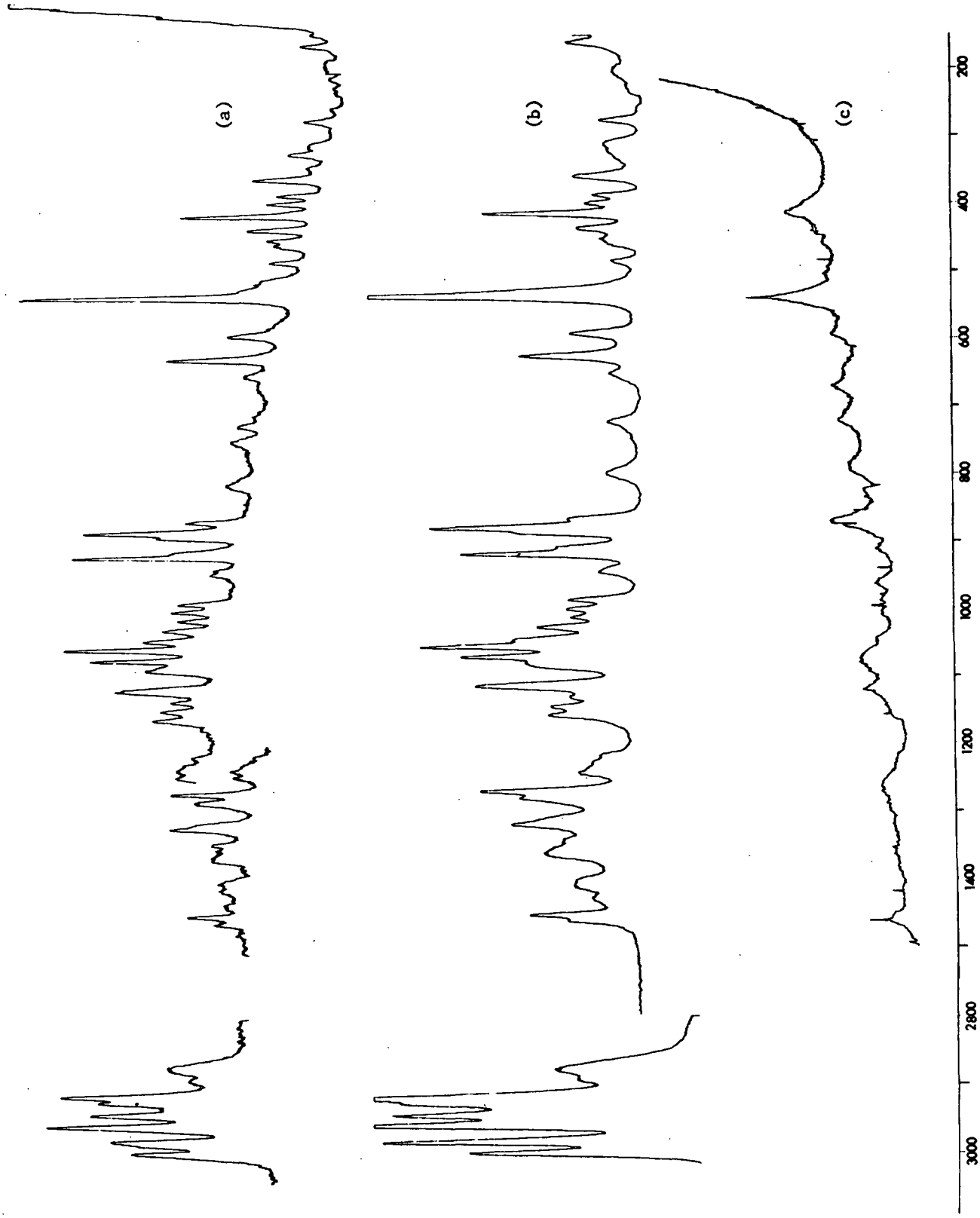

Figure 22. Raman Spectra of Ribose: (a) at -175°C, (b) at Room Temperature, and (c) as an Aqueous Solution

TABLE XX

THE TABULATED FREQUENCIES OF RIBOSE[a]

IR, cm^{-1}	Raman, cm^{-1}	LT Raman, cm^{-1}
3350 (vs,b)[b]		
	2996 (s)	2996 (s)
		2982 (m,sh)
	2979 (vs)	2979 (s)
	2956 (vs)	2957 (vs)
	2942 (vs)	2941 (s)
2920 (w,sh)	2921 (s,sh)	2922 (s,sh)
	2915 (vs)	2914 (vs)
2890 (w,sh)	2886 (m,sh)	2889 (m)
	2875 (m)	2875 (m,b)
	1458 (w,sh)	1459 (w)
1450 (w,sh)	1448 (m)	1447 (m)
	1425 (vw,b)	1431 (w,b)
1410 (m,b)	1405 (w,b)	1410 (w,b)
		1400 (w)
	1360 (m)	1366 (w,b)
	1352 (w,sh)	1350 (w,b)
1334 (w,b)		1342 (w)
	1316 (m)	1320 (m)
	1310 (w,sh)	1314 (w,sh)
	1276 (m)	1280 (m)
	1265 (s)	1269 (m)
1245 (m,b)	1240 (w,b)	1244 (w)
		1234 (w)
	1225 (vw,b)	1225 (vw,sh)
1215 (w,sh)	1216 (vw,b)	1215 (vw)
	1155 (m)	1158 (m)
	1142 (m)	1145 (m)
	1126 (w)	1130 (w)
	1112 (s)	1116 (m)
1080 (vs,b)	1079 (m,sh)	1085 (m)
	1069 (s)	1071 (s)

TABLE XX (Continued)

THE TABULATED FREQUENCIES OF RIBOSE[a]

IR, cm^{-1}	Raman, cm^{-1}	LT Raman, cm^{-1}
	1054 (s)	1054 (s)
1040 (vs)	1044 (m,sh)	1042 (w)
	1025 (m)	1026 (w)
	1010 (w)	1011 (w)
	998 (w)	998 (w)
990 (w,sh)	985 (w)	985 (w)
960 (s)	944 (w)	944 (vw)
		937 (vw,sh)
	917 (s)	918 (s)
910 (m)	908 (w,sh)	911 (m,sh)
885 (m)	885 (m,sh)	888 (m,sh)
	879 (s)	882 (s)
870 (w,sh)	866 (w,sh)	867 (w)
820 (w)		812 (w,b)
790 (m)	796 (w)	
745 (m)	735 (vw,sh)	748 (w,b)
720 (m)	722 (w)	727 (vw)
670 (vw,b)		670 (vw,b)
650 (vw,b)	650 (w)	655 (vw)
	625 (m)	627 (m)
	591 (w)	592 (w)
	536 (vs)	536 (vs)
		516 (w,sh)
	483 (w)	485 (w)
	456 (vw,sh)	460 (w)
	436 (w)	438 (m)
	413 (s)	417 (m)
	397 (w)	397 (w)
	385 (w)	386 (w)
	358 (w)	363 (m)
		345 (vw)

TABLE XX (Continued)

THE TABULATED FREQUENCIES OF RIBOSE[a]

IR, cm^{-1}	Raman, cm^{-1}	LT Raman, cm^{-1}
	325 (w,b)	327 (w)
	311 (w,b)	312 (vw,b)
	275 (w)	276 (w)
		260 (vw,b)
	235 (vw,b)	
	225 (vw,b)	
	204 (vw,b)	
	160 (w)	

[a]No tabulated frequencies have been included for the water solution spectrum of ribose because of the weak and broad nature of the spectral bands.

[b]Conventional symbolism indicating relative intensity: s = strong, m = medium, w = weak, v = very, b = broad, sh = shoulder.

Reeves (37), the first three of these ribose anomers would appear most likely to be present in significant amounts in a solid sample of ribose. However, the fourth anomer, which exhibits three axially oriented hydroxyl groups, has also been included in these calculations for three principal reasons. First, the axial anomeric hydroxyl group is stabilized by the anomeric effect, second, there is no real evidence that this anomer is not present, and third, recent structural investigations of methyl-β-ribopyranoside (38) reveal that this molecule crystallizes in the pyranose chair form exhibiting three axially oriented hydroxyl groups. The reason for the stability of this anomer apparently is a relatively strong intramolecular hydrogen bond between the two axially oriented hydroxyl groups at C-2 and C-4. Certainly, such a bond could also be possible in the ribose sugar.

Figure 23 illustrates the molecular configurations of the anomers of ribose and the atom numbering scheme used to describe the internal displacement coordinates. The structural parameters are the same as those previously discussed with the crystalline pentoses in Part I. The data necessary to construct the $\underset{\sim}{G}$ matrices for these molecules is included in Tables XLV-LIII of Appendix II. The 65 internal coordinates used to describe the motions of these molecules are presented in Tables XXVIII and XXIX. These coordinates are the same as those used for the previous pentose calculations. Only the definitions of the torsional coordinates differ to accommodate the trans-orientations of the atoms. The SVQFF developed for the pentoses in Part I is applied directly to these molecules with no alterations.

Therefore, to complete the normal coordinate calculations of ribose, the $\underset{\sim}{G}$ and $\underset{\sim}{F}$ matrices were determined and the secular equation solved for the frequencies and potential energy distributions. The results of these calculations are presented in Tables LXIII-LXXVI of Appendix III. The key to the

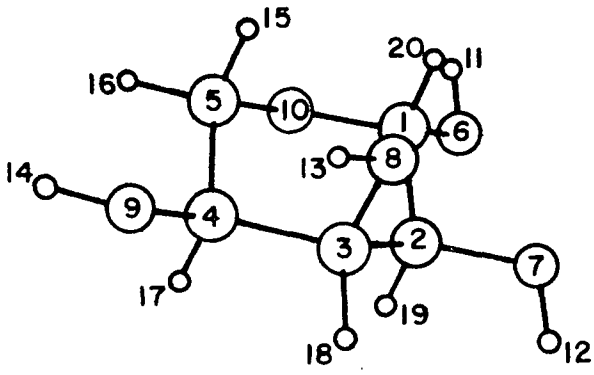

β-RIBOSE 1C-D

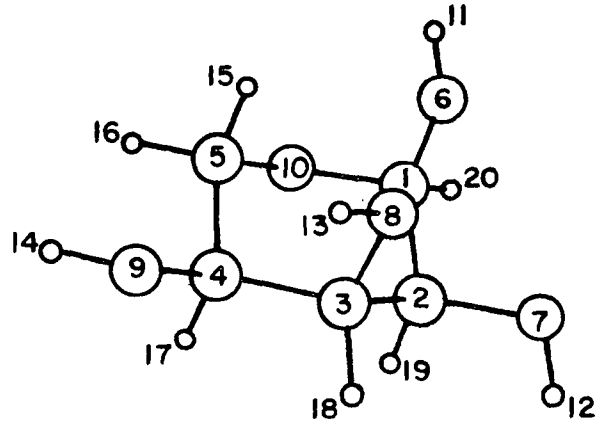

α-RIBOSE 1C-D

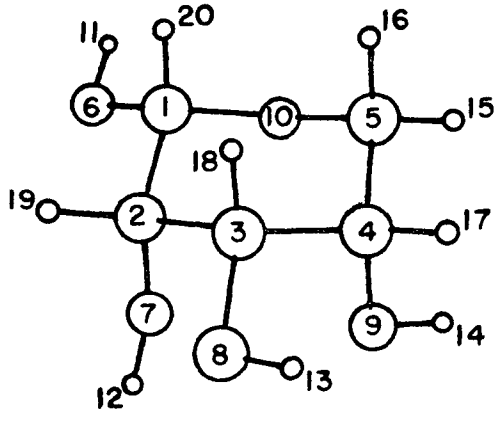

α-RIBOSE C1-D

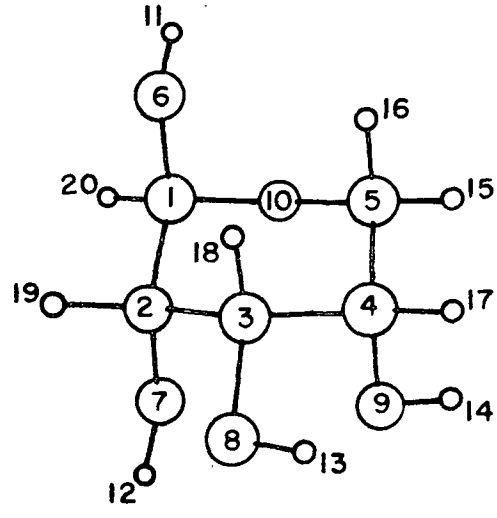

β-RIBOSE C1-D

Figure 23. Representations of the Ribose Models

internal coordinate description codes used in these tables is given in Table XXVIII of Appendix II.

DISCUSSION OF RESULTS

In general, the potential energy distributions calculated for the ribose anomers are very similar to the distributions calculated for the other pentose molecules in Parts I and II of this work. Like the other pentoses, each ribose anomer is calculated to have five somewhat distinct regions of motion generally indicated by significant gaps in the spectral bands. These regions are:

1. OH stretch
2. CH stretch
3. CH and OH bend
4. CC and CO stretch
5. CC and CO bend, and other low energy modes

The spectral gaps are obvious for the OH and CH stretching modes. CH and OH deformations are most prominent in the region from 1500 to about 1200 cm^{-1}. Below 1200 cm^{-1} to the transitional area around 700 cm^{-1} are the heavy atom stretch motions. Near 700 cm^{-1} is the transition from heavy atom stretching to bending motions. Below 700 cm^{-1} are the highly coupled low energy torsional and ring bending modes.

As with previous normal coordinate calculations involving the pentose molecules, the calculated frequency distributions for the pyranose forms of ribose are sensitive to changes in both the configuration at the anomeric site and the conformation of the pyranose ring. The bar graphs of Fig. 24 compare the calculated frequencies for the four anomers of ribose. As can be seen, between 900 and 1500 cm^{-1} and again, below 400 cm^{-1}, the four ribose

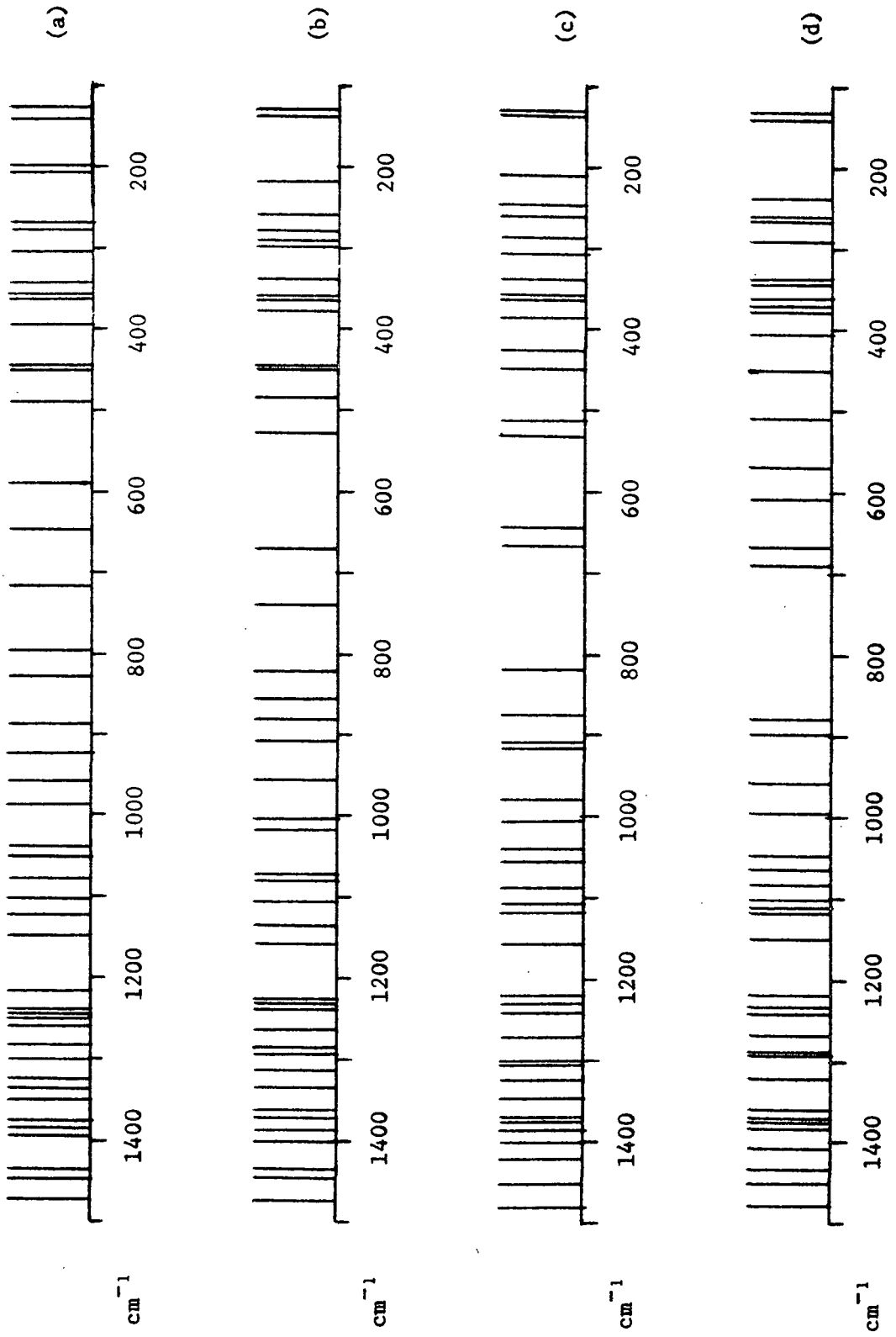

Figure 24. A Comparison of the Calculated Frequencies of the Pyranose Anomers of Ribose: (a) β-Ribose C1-D, (b) α-Ribose C1-D, (c) α-Ribose 1C-D, and (d) β-Ribose 1C-D

anomers have very similar calculated spectra. The greatest band shifts occur between 400 and 900 cm^{-1}. The most significant shift occurs with the 818 cm^{-1} band in β-ribose (1C-D) upon anomerization to α-ribose (1C-D). A simple pairing of bands calculated for these two anomers reveals a shift in energy of 129 cm^{-1} for the 818 band down to 689 cm^{-1}. Though not as pronounced as this particular example, many other bands shift in going from one anomer to another within a given chair conformation. It is also important to consider the band shifts that occur with a change in the chair conformation of the pyranose ring. Thy greatest shift of vibrational frequencies occurs with the beta anomers. For with β-ribose, a change in the pyranose ring chair conformation means a change in hydroxyl group orientation from three equatorial to three axial groups.

Careful study of the calculated potential energy distributions presented in Tables LXXIII-LXXVI of Appendix III reveals that the effect that configuration at the anomeric site has upon the coupling within these individual bands is very complex and not readily adaptable to simplified relationships. The complexity of this coupling within individual bands can also be realized by comparing the potential energy distributions for ribose anomers with distributions for pentose molecules which differ, configurationally, only by the orientation of one hydroxyl group, i.e., β-ribose and β-xylose, or α-ribose and α-xylose. Such configurational changes have a pronounced effect upon the compositions of the calculated bands and upon the calculated frequency distributions. This effect is especially noticeable in the anomeric region of the spectrum.

The comparison of the calculated frequencies of the anomers of ribose with the vibrational frequencies obtained from the solid sample of ribose is also informative. Figures 21 and 22 reveal that there are many more bands

present in these spectra than would result from the fundamental frequencies of only one molecular form. The question of which anomeric forms are present in the solid is very difficult to answer since not only pyranose but also furanose and acyclic forms may be present. Angyal and Pickles (36) have shown that while several forms of ribose are present in aqueous solution, the pyranose forms are in the greatest abundance. They represent about 80% of the forms present. It was then assumed that the pyranose of ribose comprise most of the solid phase. For if this is the case, then it is possible to assume that the pyranose forms of ribose comprise most of the solid phase. In addition, if this is the case, then a comparison of the calculated frequencies of the pyranose forms of ribose with the spectral bands observed in the solid state ought to account for all the observed spectral bands.

Since observed bands above 1200 and below 400 cm^{-1} are generally broad and less well defined, the comparison of bands will be confined to the region from 400 to 1200 cm^{-1}. Table XXI presents this band comparison for the four species of ribose. As can be seen from this comparison, all of the bands observed in the solid phase of ribose can be accounted for by the bands calculated for the four pyranose forms of ribose. The errors encountered in these band assignments are generally no greater than those observed for the assignments presented in Part I for β-arabinose, β-lyxose, and α-xylose.

CONCLUSIONS

The normal coordinate calculations of the pyranose anomers of ribose support the assumption that the four pyranose anomers dominate the solid phase of ribose.

TABLE XXI

COMPARISON OF CALCULATED FREQUENCIES OF RIBOSE ANOMERS WITH OBSERVED FREQUENCIES

Raman, cm^{-1}	β (1C-D)	α (1C-D)	α (C1-D)	β (C1-D)
1155 (m)	1150	1154	1157	1152
1142 (m)			1136	
1126 (w)	1113	1119		1125
1112 (s)	1110 1101	1110	1104	1104
1079 (m,sh)	1082	1089	1079	1080
1069 (s)	1064		1072	
1054 (s)		1056		1053
1044 (m,sh)	1047	1040		1041
1025 (m)			1018	
1010 (w)		1007	1005	
998 (w)	993			
985 (w)		980		989
944 (w)	958		954	962
917 (s)		913		926
908 (w,sh)	897	907	907	
885 (m,sh)			882	891
879 (s)	879	874		
866 (w,sh)			856	
796 (w)		818	823	799
735 (vw,sh)			740	
722 (w)				720
670 (vw,b)	689	668	672	
650 (w)	665	645		651
625 (m)	606			
591 (w)				591
536 (vs)	567	531	531	
516 (w,sh)	510	513		
483 (w)			485	491
456 (vw,sh)			447	453
450 (w)	450	449	445	445
436 (w)		429		
413 (s)	405			
397 (w)			377	396

The potential energy distributions calculated for these pyranose forms reveal a close similarity with the distributions of other pentoses. These distributions reveal that the motions of these molecules tend to couple in complex ways, which again states the need to use normal coordinate analyses to interpret the spectra of large saccharide molecules.

PART IV

AN INVESTIGATION OF THE VIBRATIONAL SPECTRA OF THE ALPHA AND BETA ANOMERS OF METHYL XYLOPYRANOSIDE

INTRODUCTION

The methyl xylopyranoside molecules were useful in the development of a SVQFF for the pentose sugars. Since both anomeric configurations of these xylopyranoside molecules are readily crystallized, the sensitivity of the pentose SVQFF to changes in anomeric site configuration can be readily evaluated. Furthermore, these xylopyranoside molecules can be used to determine the overall transferability of the pentose SVQFF to similar molecular structures. The affirmation of good SVQFF transferability and of sensitivity to changes in anomeric site configuration lends great support for the validity of the frequency distributions calculated for the alternate anomers of the pentose and the pyranose forms of ribose. The normal coordinate analyses of the methyl xylopyranosides can also be a means of determining the effects that the addition of a methyl group has upon the calculated frequencies and band distributions of the pentose sugars.

The objective of this work was to apply the SVQFF developed for the pentose sugar molecules in the normal coordinate analyses of the methyl xylopyranoside molecules. The intent of these calculations was threefold: 1) to determine the overall transferability of this pentose SVQFF to similar molecular systems, 2) to determine the sensitivity of the SVQFF to changes in configuration at the anomeric site, and 3) to provide a basis for the interpretation of the vibrational spectra of these xylopyranosides. The interpretation of the xylopyranoside spectra should provide insight into the effects of the addition

of the methyl group to a pyranose molecule as well as the effects of configuration at the anomeric site in these molecules.

EXPERIMENTAL

Samples of methyl-α-xylopyranoside (MAX) and methyl-β-xylopyranoside (MBX) in the crystalline state were obtained from Pfanstiehl Laboratories, Inc. and were used without further purification.

Raman spectra were obtained at both room temperature and about -175°C from powdered samples pressed into pellets in the same manner as previously described for the pentoses (see Part I). Likewise, infrared spectra were obtained from powdered samples examined as Nujol mulls.

RESULTS

SPECTRA

The infrared and Raman spectra of MAX and MBX are shown in Fig. 25 and 26. These spectra were obtained at room temperatures. Raman spectra obtained at low temperature (-150°C) for both MAX and MBX are shown in Fig. 27. Table XXII lists the tabulated frequencies for each of the spectra.

VIBRATIONAL ANALYSES

The molecular models used to complete the normal coordinate analyses of MAX and MBX are shown in Fig. 28. The Cartesian coordinates of the atoms in these molecules were calculated in a manner exactly the same as for the anomers of xylose, except for the addition of the methyl group attached to the anomeric hydroxyl group. Tables LIII and LIV of Appendix II show the data used to calculate the molecular structures and the Cartesian coordinates calculated for the atoms of each molecule.

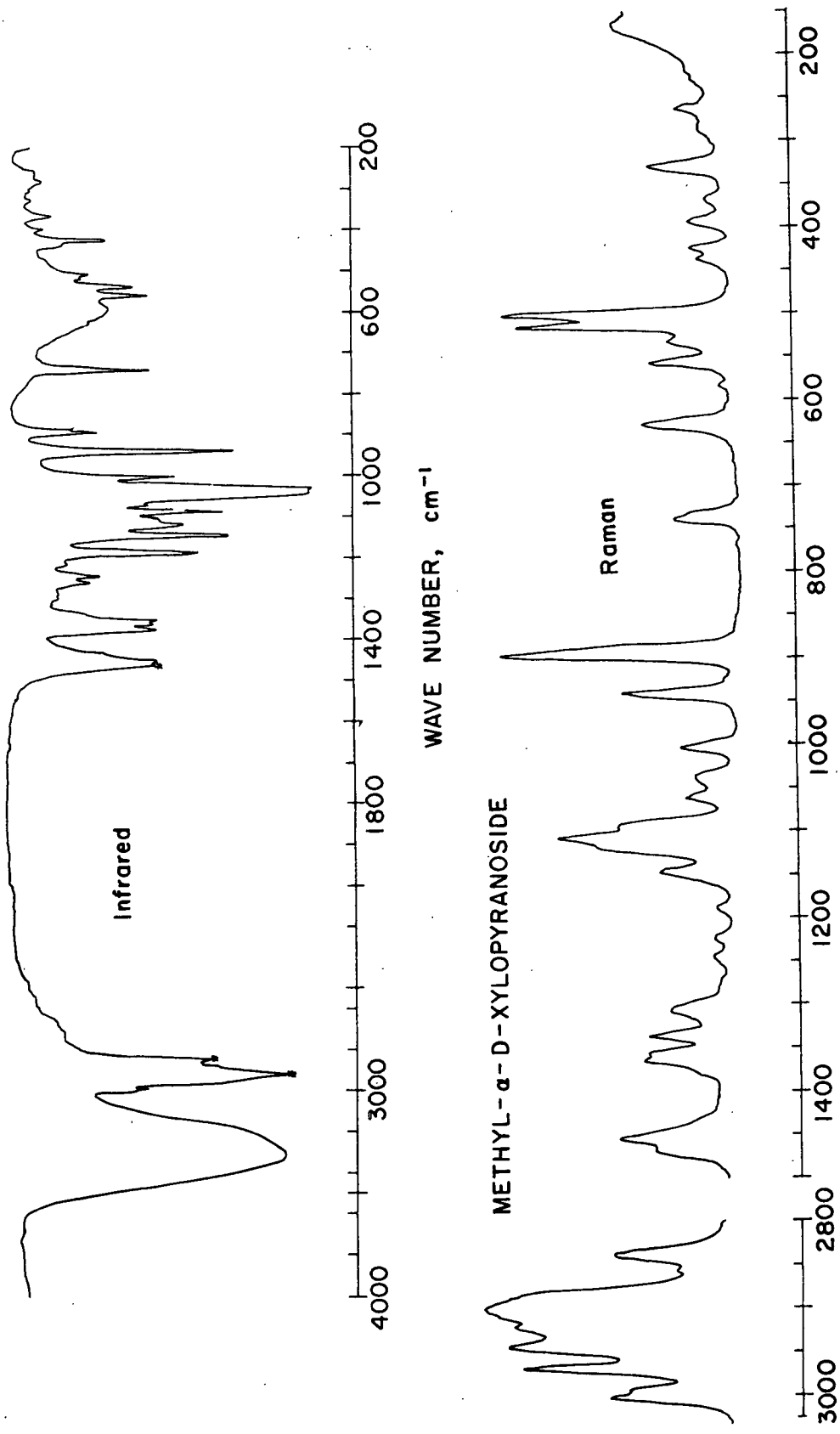

Figure 25. Infrared and Raman Spectra of Methyl-α-xylopyranoside. (Nujol peaks denoted by an *)

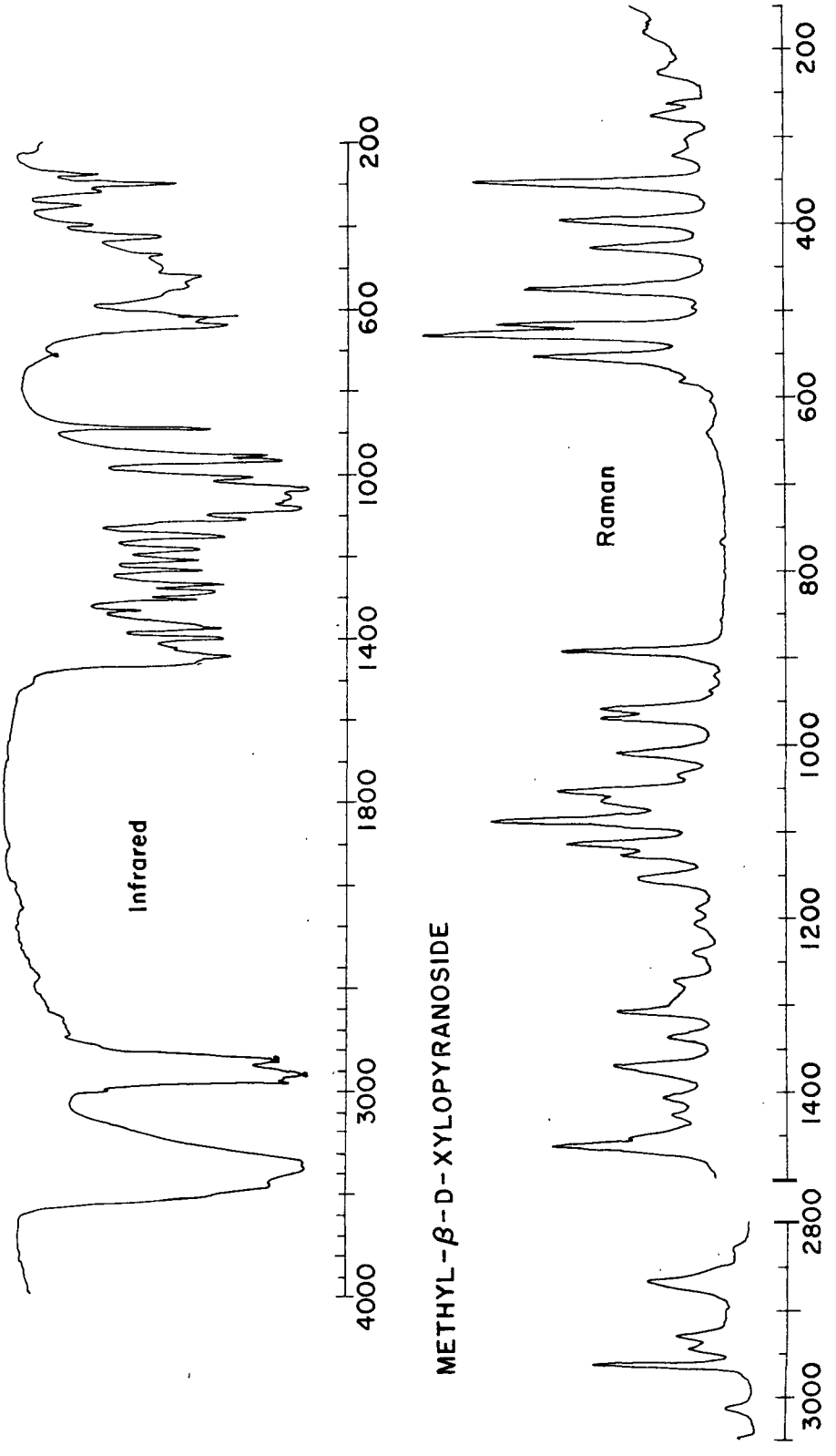

Figure 26. Infrared and Raman Spectra of Methyl-β-xylopyranoside.
(Nujol peaks denoted by an *)

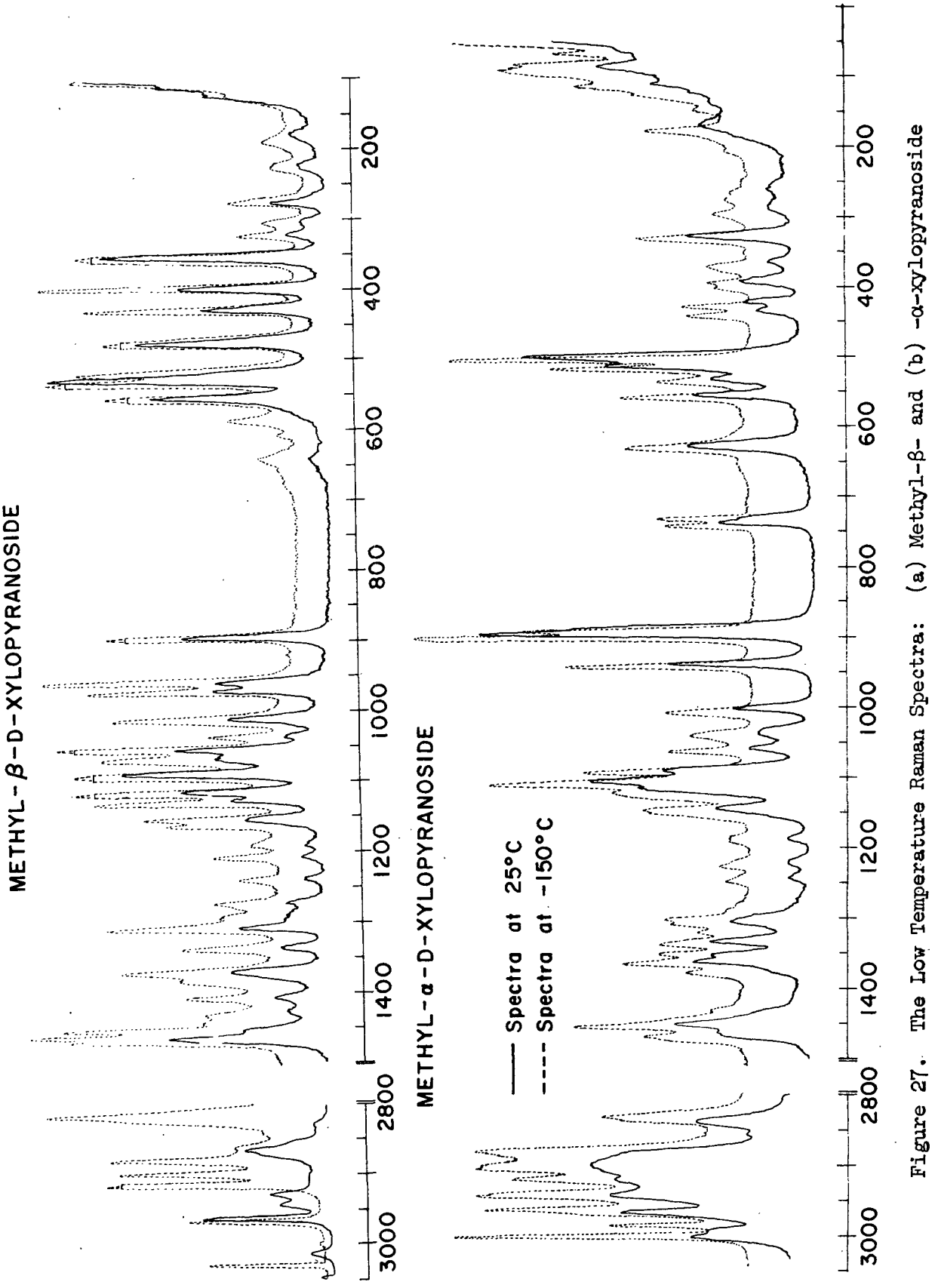

Figure 27. The Low Temperature Raman Spectra: (a) Methyl-β- and (b) -α-xylopyranoside

TABLE XXII

VIBRATIONAL SPECTRA OF THE XYLOPYRANOSIDES

Methyl-α-xylopyranoside			Methyl-β-xylopyranoside		
RT Raman, cm^{-1}	LT Raman[a], cm^{-1}	IR, cm^{-1}	RT Raman, cm^{-1}	LT Raman[a], cm^{-1}	IR, cm^{-1}
		3310 (vs,b)[b]			3460 (vs,sh)
		3250 (vs,b)			3380 (vs,b)
					3350 (vs,b)
3005 (s)	3002 (vs)	3000 (vw)	3015 (m)	3015 (m)	3010 (w)
2985 (s)	2985 (m)	2985 (w)	2965 (vs)	2965 (s)	2965 (s)
2968 (vs)	2963 (vs)	2960 (s)	2947 (s)	2949 (vs)	2945 (s)
2943 (vs)	2944 (vs)		2932 (s)	2930 (s)	
2920 (vs,sh)	2920 (s)		2910 (s,sh)	2912 (s)	
	2905 (vs)				
2900 (vs)	2900 (s,sh)	2880 (vw)	2875 (vs,sh)	2870 (s)	
2857 (m)	2880 (vs)		2868 (vs)	2865 (vw,sh)	2865 (w)
2840 (s)	2832 (m)		2857 (s,sh)		
			2835 (m)	2830 (vs)	
1467 (m,sh)	1468 (m)		1465 (s)	1470 (s)	
1455 (s)	1452 (s)	1450 (m,sh)	1455 (m)	1462 (s)	1447 (s)
				1454 (s)	
	1430 (vw,sh)		1427 (w)	1430 (w,sh)	1430 (w,sh)
			1407 (w)	1407 (w)	1407 (m)
1375 (w,sh)	1376 (w)	1377 (s)	1377 (m,sh)	1380 (w,sh)	1380 (m)
1366 (m)	1363 (m)	1363 (s)	1373 (m)	1372 (m)	1375 (m,sh)
1357 (m)	1350 (w)	1353 (s)			
1338 (m)	1337 (m)	1340 (w,sh)	1338 (w)	1340 (m)	1339 (w)
	1318 (vw)				
1309 (m)	1307 (w,sh)	1300 (vw)	1310 (m)	1310 (s)	1312 (m)
				1292 (vw,sh)	1290 (m)
1275 (vw)	1300 (w)	1285 (vw)	1273 (w)	1272 (vw)	1273 (m)
	1246 (vw)	1260 (w)	1242 (w)	1242 (vw)	1238 (m)
1246 (vw)	1226 (vw)	1243 (w)	1209 (w)	1210 (w)	1213 (m)
1225 (vw)	1220 (vw,sh)	1218 (w)	1190 (w)	1193 (vw)	1188 (m)
1190 (vw)	1175 (vw)	1188 (s)	1155	1164 (m)	
1147 (m)	1145 (m)	1147 (s)	1155 (m)	1155 (m)	1158 (s)
1117 (s,sh)	1120 (m,sh)	1120 (m)	1129 (m)	1130 (s)	1125 (w,sh)
1108 (vs)	1107 (vs)	1110 (w,sh)	1115 (s)	1117 (vs)	1115 (s)
1095 (s,sh)	1092 (s)	1090 (m)	1090 (vs)	1093 (vs)	1087 (vs)

TABLE XXII (Continued)

VIBRATIONAL SPECTRA OF THE XYLOPYRANOSIDES

Methyl-α-xylopyranoside			Methyl-β-xylopyranoside		
RT Raman, cm^{-1}	LT Raman[a], cm^{-1}	IR, cm^{-1}	RT Raman, cm^{-1}	LT Raman[a], cm^{-1}	IR, cm^{-1}
1063 (m)	1062 (w)	1072 (w,sh)	1067 (m)	1069 (s)	1070 (vs)
1038 (w)	1038 (w)	1043 (vs)	1055 (s)	1053 (vs)	1060 (vs)
		1030 (vs)	1035 (w)	1035 (vw)	1040 (vs)
1005 (w)	1006 (w)	1003 (m)	1013 (m)	1012 (s)	1011 (s)
942 (s)	940 (s)	940 (vs)	973 (m)	972 (s)	973 (vs)
925 (vw,sh)	898 (vs)	896 (w)	962 (m)	958 (s)	960 (vs)
896 (vs)	890 (s,sh)	889 (w,sh)	903 (w,sh)		
740 (m)	741 (w)	740 (s)	895 (vs)	895 (vs)	895 (vs)
734 (w,sh)	732 (w)	735 (m,sh)	670 (vw)	675 (vw)	668 (w)
630 (m)	630 (m)	630 (w,b)	645 (vw)	642 (vw)	642 (s)
585 (vw)		597 (w)	607 (vw)	610 (vw)	625 (m,sh)
558 (m)	558 (m)	558 (w)	584 (w)	587 (w)	570 (w,sh)
535 (m)	535 (w)	537 (vw)	555 (s)	555 (s)	550 (m)
517 (vs)	517 (s)	537 (vw)	530 (vs)	538 (vs)	527 (m)
503 (vs)	505 (vs)	508 (vw)	517 (vs)	519 (s)	505 (w)
440 (w)	440 (w)	435 (vw,sh)	497 (w)	477 (vs)	
426 (w)	426 (w)	425 (w)	471 (vs)		
	400 (vw,sh)		429 (s)	430 (s)	428 (m)
395 (w)	390 (vw)	400 (vw)	397 (s)	397 (s)	403 (w)
370 (vw)	368 (vw)	367 (vw)	354 (vs)	356 (vs)	358 (m)
	350 (vw)		323 (w)	325 (vw)	323 (m)
332 (m)	330 (m)	338 (vw)	305 (w)	312 (vw)	303 (s)
	295 (vw)		278 (m)		278 (m)
	275 (vw)		263 (w)	257 (w)	
	265 (vw,sh)		227 (w)	230 (vw)	220 (vw)
	250 (vw)		180 (m)	180 (vw)	
	205 (vw)				
	175 (m)				

[a]LT Raman refers to Raman spectrum obtained at about -150° C.

[b]Conventional symbolism indicating relative intensity: vs = very strong, s = strong, m = medium, w = weak, v = very, b = broad, sh = shoulder.

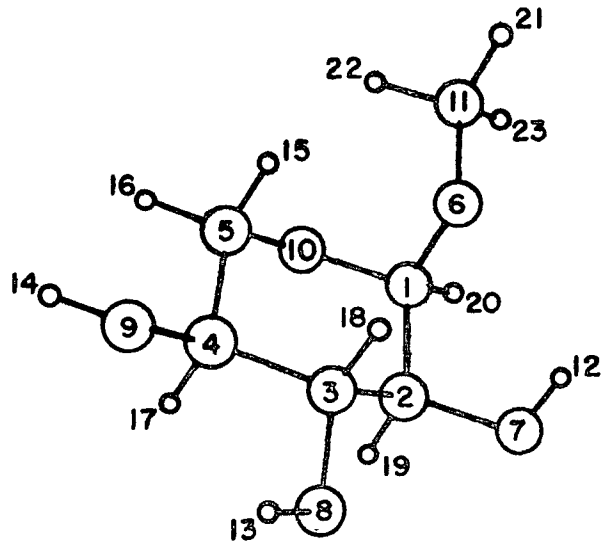

METHYL-α-XYLOPYRANOSIDE

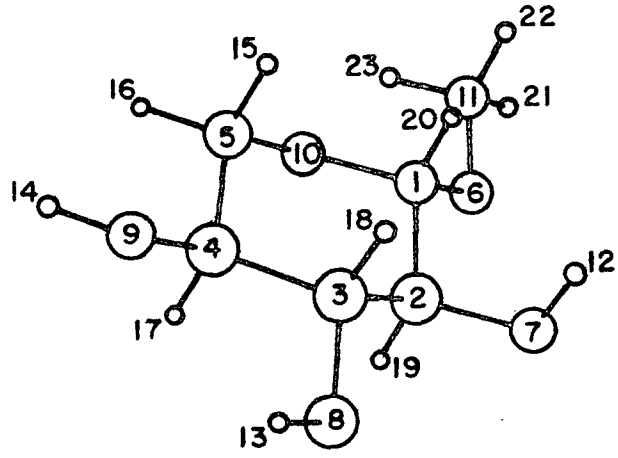

METHYL-α-XYLOPYRANOSIDE

Figure 28. Representations of the Xylopyranoside Models

To completely describe the vibrational motions of the xylopyranosides required the definition of 75 internal displacement coordinates: 23 stretch, 41 bend, and 11 torsion coordinates. These internal coordinates and their description codes are presented in Table LV of Appendix II. Tables LVI and LVII of Appendix II show the input data necessary to calculate the $\underset{\sim}{G}$ matrices of the molecules using program GMAT (21).

The $\underset{\sim}{F}$ matrices for these molecules were developed as directly as possible from the SVQFF developed for the pentoses. Table XXIII shows the only SVQFF parameters which were adjusted to give better frequency correlations for these pyranoside molecules. Interaction parameters involving proton deformations of the methyl group were taken from similar interactions involving the methylene deformations. As a result, a 78 parameter force field was used for these xylopyranosides. The $\underset{\sim}{Z}$ matrices for these molecules are listed in Tables LVIII and LIX of Appendix II.

TABLE XXIII

NEW FORCE CONSTANTS INTRODUCED FOR THE METHYL GROUP OF THE XYLOPYRANOSIDES

Coordinate	Pentose Value	Xylopyranoside Value
HCO	0.849[a]	0.880
HCH	0.477	0.508
C_1-O_6, $C_1O_6C_{11}$	0.735	0.483
O_6-C_{11}, $C_1O_6C_{11}$	0.840	0.483

[a] Force constants expressed as mdyn.A/(rad)^2.

The results of the normal coordinate calculations of MAX and MBX are presented in Tables XXIV and XXV (and LXXVII and LXXVIII of Appendix III). Tables XXIV and XXV show the frequency assignments and list the dominant contributions from the internal coordinates to the motions of the modes. Also listed is a description of each of the modes in the appropriate group frequency terms. Contributions from all the internal coordinates to each normal mode are listed in Tables LXXVII and LXXVIII. These tables facilitate the easy identification of the bands which are affected by particular internal displacement coordinates.

DISCUSSION OF RESULTS

BAND CORRELATIONS

The frequency correlations presented in Tables XXIV and XXV, resulting in average error values of 7.5 and 8.5 cm^{-1}, respectively, for MAX and MBX, indicate good transferability of the pentose SVQFF to these pyranoside molecules. Examination of MAX and MBX band correlations reveals that, generally, in the spectral region above 800 cm^{-1} more bands have been calculated than are observed. In this region, calculated bands composed of motions directly associated with the methyl group do not correlate very well with the observed spectra, which could, in part, be caused by the lack of spectral resolution of these bands. Consider the methyl scissors modes of MAX. All three of these calculated modes, spanning 1447 to 1457 cm^{-1}, have been assigned to the single band observed at 1455 cm^{-1}. Perhaps with better resolution in the Raman instrumentation (presently about 5 cm^{-1}), more precise band assignments could possibly be made, because examination of the Raman spectra in Fig. 27 reveals that there is a good possibility that these methyl bands are concealed within the band contours around 1450 cm^{-1}.

TABLE XXIV

THE INTERPRETATION OF THE VIBRATIONAL SPECTRUM OF METHYL-α-XYLOPYRANOSIDE

Band Assignments				Spectral Interpretation	
Experimental				Calculated Contributions[b],	
Raman, cm^{-1}	IR, cm^{-1}	Calc., cm^{-1}	Diff.[a], cm^{-1}	internal coordinates, %	Description of the Approximate Motions
		3357		OH13(71) OH12(24) OH14(5)	O-H stretch (str)
	3310(vs,b)[c]	3357	d	OH14(95)	O-H str
	3250(vs,b)	3356	d	OH12(73) OH13(27)	O-H str
3000(s)	3000(w,sh)	3000	d	CH16(49) CH15(48)	Asymmetric methylene str
2985(s)	2985(w)	2997	d	CH21(66) CH23(17) CH22(16)	Asymmetric methyl str
		2997		CH22(50) CH23(49)	Asymmetric methyl str
2968(vs)	2960(s,sh)	2953	d	CH18(49) CH19(24) CH17(22)	Methine str
2943(vs)		2944	d	CH20(70) CH17(17) CH19(10)	Methine str
2920(vs,sh)		2941	d	CH19(39) CH17(33) CH20(26)	Methine str
2900(vs)		2934	d	CH18(48) CH17(26) CH19(25)	Methine str
2857(m)	2880(vw,sh)	2888	d	CH15(51) CH16(49)	Symmetric methylene str
2840(s)		2831	d	CH22(34) CH23(34) CH21(34)	Symmetric methyl str
1467(m,sh)		1480	-13	HC5H(45) H15CC(16) H16CC(12)	Methylene scissors and wag
1455(s)	1450(m,sh)	1457	-2	H21CH23(26) H21CO(25) H21CH22(14) H23CO(9) HO7C(5) H22CO(5)	Methyl deformation (def)
1455(s)	1455(m,sh)	1448	7	H21CH22(41) H23CO(17) H22CH23(32) H21CH23(10)	Methyl def
1455(s)	1455(m,sh)	1447	8	H22CH23(43) H22CO(32) H21CH23(13) H21CH22(10)	Methyl def
1455(s)	1455(m,sh)	1443	12	HO7C(22) H22CH23(15) HC2O(9) HO8C(9) H23CO(8) CC2H(6) H21CO(5)	OH i.p.[e] bend coupled with methyl and methine def
1430[g]		1437	-7	HO9C(17) HO7C(16) HC2O(14) HO8C(10) HC3C(9) HC2C(9)	OH i.p. bend coupled with methine def
1375(w,sh)	1377(s)	1385	-10	HO9C(33) H15CO(10) H16CO(10) HC5H(8) HO8C(8) HC4C(6)	OH i.p. bend coupled with methylene wag and scissors
1366(m)	1363(s)	1373	-7	H15CO(21) H16CO(19) H15CC(12) HC5H(7) HO9C(7) HC2C(5) HO7C(5)	Methylene twist and wag
1357(m)	1353(s)	1356	1	HO8C(35) HC3O(13) CC4H(11) HC2C(9) CC2H(7) HC3C(6)	OH i.p. bend coupled with methine def
1338(m)	1340(w)	1333	5	HC1O(46) HC1O1O(12) CC2H(5)	Anomeric methine def
1318[g]		1318	0	CC3H(24) HC1O(15) HC4O(14) HC3C(11) HC1C(7) CC2H(6)	Methine def
1309(m)	1300(vw)	1313	-4	HC4C(25) CC4H(24) CC2H(15) HC2C(9)	Methine def
1275(vw)	1285(vw)	1278	-3	C1C2(19) HC1O1O(14) HC1C(10) HC3O(9) HC4O(8)	Anomeric methine def coupled with CC str
	1260(w)	1263	-3	HC4O(26) H16CO(21) H15CO(10) CC3H(6) H15CC(6) HC4C(5)	Methine def coupled with methylene twist
1246(vw)	1243(w)	1245	1	HC3O(36) HO9C(20) HC3C(15) HO8C(12) HC4O(12)	Methine def coupled with OH i.p. bend

TABLE XXIV (Continued)

THE INTERPRETATION OF THE VIBRATIONAL SPECTRUM OF METHYL-α-XYLOPYRANOSIDE

Band Assignments				Spectral Interpretation	
Experimental				Calculated Contributions[b],	
Raman, cm^{-1}	IR, cm^{-1}	Calc., cm^{-1}	Diff.[a], cm^{-1}	internal coordinates, %	Description of the Approximate Motions
1225(vw)	1218(w)	1220	5	HC40(19) HC30(17) H16CO(17) H15CO(17) HO8C(8) H15CC(8) H16CC(7) HC2C(5)	Methine def coupled with methylene twist and wag
1190(vw)	1188(s)	1192	-2	HC20(33) HO7C(27) CC2H(12) HC30(10) HC1C(7) C2C3(6) HC2C(5)	Methine def coupled with OH i.p. bend
		1168		H22CO(34) H23CO(17) H21CH23(10) H21CH22(5)	Methyl def
		1150		H21CO(32) H23CO(13) C207(9) C106(9) H22CH23(8) O6C11(8) C409(5)	Methyl def coupled with CO str
1147(m)	1147(s)	1138	9	C409(24) H23CO(11) C3C4(11) C207(7) H15CO(5)	CO str coupled with CC str and methyl def
1117(s,sh)	1120(m)	1128	-11	C5O10(15) O10C1(13) H16CC(11) C3C4(9) H22CO(7) HC1O(6) O6C11(6) CC3H(5) O10C1C(5)	CO ring str coupled with CC str and methylene rock
1108(vs)	1110(w,sh)	1111	-3	C207(19) C308(14) C409(10)	CO str
1095(s,sh)	1090(m)	1098	-3	C308(65) CC3C(10) C2C3(10) C5O10(6) C207(5)	CO str coupled with ring str
1063(m)	1072(w,sh)	1076	-13	C409(35) C207(24) HC20(14) C2C3(11) C106(8) HO7C(6)	CO str coupled with methine def
1038(w)	1043(vs)	1050	-12	O6C11(65) C1C2(8) H21CO(8)	Methyl CO str
	1030(vs)	1038	-8	C4C5(39) H15CC(23) H15CO(9) TC5O10(8) C409(6) HC3C(5)	CC str coupled with methylene rock
1005(w)	1003(m)	998	7	C4C5(32) HC1C(17) C5O10(16) C1C2(14) HC1O10(11) C106(8) H16CC(8) HC4C(7) C3C4(7) C308(6)	CC and CO ring str coupled with methine def
942(s)	940(vs)	962	-20	HC1O10(20) C5O10(17) C4C5(16) C207(15) C106(11) CC5O(8) O9CC(8) O6CC(5)	Ring str coupled with anomeric methine def
925(vw,sh)		920	5	C3C4(48) C2C3(23) C5O10(10) CC4H(6) CCO8(6) H16CC(5)	Ring str
896(vs)	896(w)	901	-5	HC1C(45) O10C1(42) C1C2(37) HC1O10(31) OCO(9) C4C5(8) CC2H(7) C106(7) C2C3(6)	Anomeric methine def coupled with CC and CO ring str
	889(w,sh)	889	0	C106(53) O10C1(27) HC1O10(18) C5O10(11) C2C3(10) HC1O(10) O6CC(9) CO6C(8) O6C11(7) COC(5)	Symmetric COC str coupled with CO str and methine str
740(m)[h] 734(w,sh)	740(s)[h] 735(m,sh)	749	-9	O10C1(13) C2C3(12) COC(11) C106(11) CCO7(8) C1C2(6)	Ring str coupled with CO str and def
630(m)	630(w,b)	671	-41	OCO(20) CO6C(13) O10C1(13) TC5O10(8) COC(6) CCO7(5) O6CC(5)	CO def
585(vw)	597(w)	583	2	O7CC(21) CCO9(13) CC3H(8) HC4C(7) CCO8(7) CC4H(5) HC2C(5)	CO def coupled with methine def
558(m)	558(w)	563	-5	TO6C11(52) COC(11) CC5O(11) CC4C(5)	Methyl rock coupled with ring bend

TABLE XXIV (Continued)

THE INTERPRETATION OF THE VIBRATIONAL SPECTRUM OF METHYL-α-XYLOPYRANOSIDE

Band Assignments				Spectral Interpretation	
Experimental				Calculated Contributions[b],	
Raman, cm^{-1}	IR, cm^{-1}	Calc., cm^{-1}	Diff.[a], cm^{-1}	internal coordinates, %	Description of the Approximate Motions
535(m)[h] 517(vs)	537(vw) 518(vw,sh)	515	2	O8CC(19) T06C11(15) CC50(14) CC09(11) O7CC(7) HC1C(7)	CO def coupled with ring bend
503(vs)	508(vw)	508	-5	C4C5(9) C3C4(9) T06C11(8) O10C1C(7) C2C3(6) O9CC(6) C4O9(6) OCO(5)	ring bend coupled with CO def
440(w)	435(vw,sh)	434	6	CCO7(20) O9CC(20) CC2C(7) C1C2(6) O10C1C(5) COC(5)	CO def coupled with ring bend
426(w)	425(w)	413	13	CC4C(24) CC3C(23) TC5O10(7) O10C1C(6) CC2C(5) O6CC(5)	Ring bend
395(w)	400(vw)	382	13	TC4O9(20) CCO8(11) TC3O8(11) O9CC(10) CC5O(7) O8CC(7) CCO7(5)	OH o.p. bend coupled with CO def
370(vw)	367(vw)	359	11	TC3O8(48) TC4O9(31) TC2O7(9)	OH o.p. bend
350[g]		353	-3	TC2O7(45) TC3O8(26) CCO9(6)	OH o.p. bend
332(m)	338(vw)	341	-9	TC4O9(40) CCO8(19) TC2O7(14) CCO7(6) O9CC(5)	OH o.p. bend coupled with CO def
295[g]		319	-24	CO6C(57) COC(17) HC1O(13) TC1O6(9)TC2O7(6) O10C1C(5)	Methyl COC bend coupled with OH o.p. bend
275[g]		278	-3	O8CC(37) CCO8(21) O7CC(15) O9CC(11) C1C2(6) CCO9(6)	CO def
265[g]		275	-10	CCO9(28) O7CC(19) O9CC(10) TC2O7(9) CCO7(7) C2C3(5)	CO def
250[g]		247	3	COC(25) OCO(24) O10C1C(21) TC1O1O(11) HC1C(8) CO6C(7) O6CC(6)	Ring bend
205[g] 175[g]		182	-7	O6CC(56) HC1O1O(32) OCO(25) O10C1(21) HC1C(18) COC(14) CCO7(11) TC1C2(9) O10C1C(8) TC2C3(5) CC3C(5)	Ring bend coupled with CO def
		121		TC3C4(34) TC2C3(12) CC3C(12) CC4C(9) O6CC(6) TC1O6(6) CCO9(6)	Ring torsional bending
		112		TC1C2(19) CC2C(18) TC2C3(13) HC1O(8) CO6C(8) OCO(6) TC1O6(6)	Ring torsional bending
		62		TC1O6(87)	Methyl wag

Average Error = 7.5 cm^{-1}

[a]Diff. = difference = observed frequency (Raman) – calculated frequency.

[b]Contributions are relative and may add to more than 100% due to contributions from negative interaction parameters in the SUQFF. Only contributions of 5% or more have been included.

[c]Conventional symbolism indicating relative intensity: vs = very strong, s = strong, m = medium, w = weak, sh = shoulder, b = broad, v = very.

[d]These frequencies have not been included in the calculation of the average error.

[e]i.p. and o.p. refer to in-plane and out-of-plane, respectively.

[f]Apparent correlation field splitting.

[g]These frequencies obtained from the low temperature spectrum.

TABLE XXV

THE INTERPRETATION OF THE VIBRATIONAL SPECTRUM OF METHYL-β-XYLOPYRANOSIDE

Band Assignments				Spectral Interpretation	
Experimental				Calculated Contributions[b],	
Raman, cm^{-1}	IR, cm^{-1}	Calc., cm^{-1}	Diff.[a], cm^{-1}	internal coordinates, %	Description of the Approximate Motions
	3460(vs,sh)[c]	3357	d	OH13(64) OH14(18) OH12(18)	O-H stretch(str)
	3380(vs,b)	3357	d	OH14(81) OH13(13) OH12(6)	O-H str
	3350(vs,b)	3356	d	OH12(76) OH13(23)	O-H str
3015(m)	3010(w)	3000	d	CH16(49) CH15(48)	Asymmetric methylene str
2965(vs)	2965(s)	2997	d	CH21(66) CH22(17) CH23(16)	Methyl str
2947(s)	2945(s)	2997	d	CH23(50) CH22(49)	Methyl str
2932(vs)		2956	d	CH19(41) CH18(30) CH20(17) CH17(9)	Methine str
2910(s,sh)		2947	d	CH17(36) CH20(31) CH18(21) CH19(10)	Methine str
2875(vs,sh)		2938	d	CH17(37) CH20(36) CH19(15) CH18(12)	Methine str
2868(vs)	2865(w)	2933	d	CH18(36) CH19(33) CH17(16)	Methine str
2857(s,sh)		2888	d	CH15(51) CH16(49)	Symmetric methylene str
2835(m)		2831	d	CH22(34) CH23(34) CH21(34)	Symmetric methyl str
1465(s)		1480	-15	HC5H(45) H15CC(16) H16CC(13)	Methylene scissors coupled with wag
1462[e](w)		1458	4	H21CO(22) H21CH22(22) H21CH23(13) HO7C(10) H22CO(8) H23CO(5)	Methyl deformation (def)
1455(m)	1447(s)	1449	6	HO7C(31) HC2O(13) H21CO(9) H21CH23(7) H21CH22(7) H22CH23(6) HC3C(5)	OH i.p.[f] bend coupled with methine and methyl def
1455(m)	1447(s)	1448	7	H21CH23(32) H22CO(24) H22CH23(20) H21CH22(19)	Methyl def
1455(m)	1447(s)	1447	8	H22CH23(39) H23CO(32) H21CH22(13) H21CH23(12)	Methyl def
1427(w)	1430(w,sh)	1439	-12	HO8C(18) HO9C(19) HC2C(11) HC3C(7)	OH i.p. bend coupled with methine def
1407(w)	1407(m)	1338	19	HO9C(32) H15CO(8) H16CO(8) HC2C(8) CC2H(8) HC5H(6) HC4C(6)	OH i.p. bend coupled with methylene and methine def
1377(m,sh)	1380(m)	1377	0	CC2H(20) HO8C(18) HC2O(15) HO7C(8) HO9C(5)	Methine def coupled with OH i.p. bend
1373(m)	1375(m,sh)	1372	1	H15CO(22) H16CO(21) H15CC(11) HC5H(9) HC2C(7) CC2H(6) H16CC(5)	Methylene wag coupled with twist and scissors
1338(w)	1339(w)	1348	-10	HO8C(23) CC4C(16) HC3C(7) HC4O(7) CC3H(6)	OH i.p. bend coupled with methine def
1310(m)	1312(m)	1325	-15	HC1O(53) HC1O1O(17) HC4C(10) CC4H(8) HC1C(5)	Anomeric methine def coupled with methine def
1292[e]	1290(m)	1313	-21	HC4C(20) CC3H(12) HC3C(12) HC4O(9) HC1O(9) CC4H(5)	Methine def
1273(w)	1273(m)	1263	10	HC4O(38) H16CO(13) CC4H(12) H15CO(11) H15CC(6) HC2C(5)	Methylene def coupled methine def
1242(w)		1251	-9	HC3O(61) HO8C(14) CC3H(12) HC3C(9) HO9C(8)	Methine def coupled with OH i.p. bend

TABLE XXV (Continued)

THE INTERPRETATION OF THE VIBRATIONAL SPECTRUM OF METHYL-β-XYLOPYRANOSIDE

Band Assignments				Spectral Interpretation	
Experimental				Calculated Contributions[b],	
Raman, cm^{-1}	IR, cm^{-1}	Calc., cm^{-1}	Diff.[a], cm^{-1}	internal coordinates, %	Description of the Approximate Motions
	1238(m)	1233	5	HO9C(20) HC4O(18) HC4C(14) CC3H(11) HC3O(7) HC2C(6) HC3C(6)	Methine def coupled with OH i.p. bend
1209(w)	1213(m)	1220	-11	H16CO(25) H15CO(19) HC4O(11) HO8C(10) H15CC(8)	Methylene twist coupled with rock
1190(w)	1188(m)	1175	15	HC1O1O(19) HO7C(17) HC2O(16) C1O6(11) H22CO(11) CC2H(8) HC1C(7) O6C11(6) H21CO(5)	Methine def coupled with OH i.p. bend and methyl def and CO str
		1165		H23CO(38) H21CO(14) H21CH22(11) C1O6(11) H22CO(6)	Methyl def
		1156		H22CO(18) HC2O(17) HO7C(16) C2O7(7) HC1C(7) H21CO(5) H21CH23(5) C3O8(5)	Methyl def coupled with OH i.p. bend and CO str
1155(m)	1158(s)	1143	12	C3C4(16) H16CC(15) C4O9(14) HC3O(10) O1OC1(7) HC4O(7) C4C5(6) C2C3(5)	CC and CO str coupled with methine and methylene def
1129(m)	1125(w,sh)	1127	2	C2O7(30) C4O9(21) H22CO(8)	CO str
1115(s)	1115(s)	1108	7	C3O8(40) H21CO(13) C4O9(9) C2C3(8) CC3C(5) CC4C(5) C1O6(5)	CO str coupled with methyl def and CC str
1090(vs)	1087(vs)	1097	-7	C5O1O(43) O1OC1(21) C4O9(13) C3O8(9) C3C4(8) O6C11(6)	Asymmetric COC str coupled with CO str
1067(m)	1070(vs)	1064	3	O6C11(30) C4O9(17) C1O6(13) C3O8(12) C2C3(10) H23CO(8) C2O7(8) HC2C(5)	Methyl CO str coupled with CC and CO str
1055(s)	1060(vs)	1051	4	C5O1O(23) C4C5(16) C4O9(14) C2O7(14) H15CC(8) C1O6(6)	Ring CC and CO str coupled with CO str
1035(w)	1040(vs)	1045	-10	C2O7(21) HC1O1O(12) HC2O(12) C1C2(11) C3O8(8) O6C11(7) HC1C(7) O1OC1(5)	CO str coupled with methine def and CC str
1013(m)	1011(s)	1019	-6	C2C3(29) C1C2(20) O6C11(19) C1O6(15) HC1O(15) O1OC1(8) O1OC1C(8) CCO7(7) C3C4(6)	CC and CO str coupled with methine def
973(m)	973(vs)	995	-22	C4C5(57) C1O6(14) H15CO(8) COC(6) CC5O(6) HC1O1O(5) H15CC(5) O9CC(5) H16CC(5)	CC str coupled with methylene rock
962(m)	960(vs)	955	7	C2C3(24) HC1O1O(19) C1C2(19) O6C11(16) C1O6(16) O1OC1(12) C2O7(7) CC2H(6) C3O8(5)	CC str coupled with CO str and methine def
903(w,sh)		925	-22	C3C4(51) H16CC(12) HC4C(11) CC4H(10) C4C5(8) H15CC(6) TC5O1O(5) C1C2(5)	CC str coupled with methylene twist and rock and methine def
895(vs)	895(vs)	879	16	O1OC1(42) HC1C(32) HC1O1O(20) OCO(19) C1C2(18) C5O1O(13) C2C3(11) COC(5) O6CC(5)	Symmetric COC str coupled with methine def and CC str
670(vw)	668(w)	685	-15	CCO8(13) TC11O6(12) HC1C(10) C1C2(8) O7CC(6) O1OC1(5)	CO def coupled with methyl rock
645(vw)	642(s)	657	-12	CO6C(15) OCO(10) CC5O(9) C1O6(9) O1OC1C(5)	Anomeric CO str and def coupled with ring bend
607(vw) 584(w)	625(m,sh) 570(w,sh)	596	-12	TC11O6(23) COC(12) CCO9(12) CC5O(8) O7CC(7) O8CC(6) O1OC1(6) O6CC(5)	Methyl rock coupled with ring and CO def

TABLE XXV (Continued)

THE INTERPRETATION OF THE VIBRATIONAL SPECTRUM OF METHYL-β-XYLOPYRANOSIDE

Band Assignments				Spectral Interpretation	
Experimental				Calculated Contributions[b],	
Raman, cm^{-1}	IR, cm^{-1}	Calc., cm^{-1}	Diff.[a], cm^{-1}	internal coordinates, %	Description of the Approximate Motions
555(s) 530(vs)	550(m) 527(m)	557	-2	TC106(16) COC(8) CC07(8) C06C(7) CC4C(6) HC4C(6)	Methyl rock coupled with ring and CO bend
517(vs)		514	3	TC1106(19) O8CC(12) CC09(10) HC3C(8) O7CC(7) COC(7) OCO(7)	Methyl rock coupled with CO def and ring bend
497(w) 471(vs)	505(w) 472(w)	507	-10	TC1106(11) C4C5(9) C3C4(8) O10C1C(7) C1C2(6) C2C3(5)	Methyl rock coupled with ring bending
429(s)	428(m)	436	-7	CC2C(18) C06C(15) CC07(12) CC50(9) O9CC(8) C1C2(5)	Ring and CO def
397(s)	403(w)	403	-6	CC3C(22) COC(14) CC4C(13) TC409(7) O9CC(6) TC308(5) CC08(5) CC2C(5)	Ring and CO def
		369		TC308(45) COC(10) TC409(6) TC1010(5) O8CC(5)	OH o.p. bend coupled with ring bend
		363		TC409(49) TC308(7) CC07(6) TC207(6) O9CC(5) CC4C(5)	OH o.p. bend
354(vs)	358(m)	352	2	TC207(38) TC308(17) COC(13) TC1010(5)	OH o.p. bend coupled with ring bend
		344		TC207(31) TC409(17) TC308(10) O7CC(7) O6CC(5) O9CC(5)	OH o.p. bend
323(w)	323(m)	324	-1	CC08(16) CC07(13) TC409(12) C06C(10) C1C2(8) O9CC(8) C2C3(5)	CO def
305(w)	303(s)	310	-5	O8CC(15) C06C(12) O10C1C(11) O6CC(8) TC308(7) CC09(6) C2C3(5) HC2C(5)	CO def
278(m)	278(m)	273	5	CC08(29) CC09(26) O9CC(18) O8CC(17) HC2C(5)	CO def
263(w)		267	-4	O7CC(28) CC07(17) TC207(13) C06C(7) O10C1C(5) O8CC(5)	CO def
227(w) 180(m)	220(vw)	190	-10	OCO(42) O6CC(28) C06C(26) HC1C(16) HC1O10(10) O7CC(5)	Anomeric CO def
		131		TC3C4(29) TC2C3(17) CC3C(12) TC4C5(8) CC4C(8) TC106(6)	Ring torsional bend
		125		TC1C2(21) CC2C(12) TC2C3(11) O6CC(11) TC106(9) TC5O10(8)	Ring torsional bend
		67		TC106(88)	Methyl wag

Average error = 8.5 cm^{-1}

[a]Diff. = difference = observed frequency (Raman) – calculated frequency.

[b]Contributions are relative and may add to more than 100% due to contributions from negative interaction parameters in the SUQFF. Only contributions of 5% or more have been included.

[c]Conventional symbolism indicating relative intensity: vs = very strong, s = strong, m = medium, w = weak, sh = shoulder, b = broad, v = very.

[d]These frequencies have not been included in the calculation of the average error.

[e]These frequencies obtained from the low temperature spectrum.

[f]i.p. and o.p. refer to in-plane and out-of-plane, respectively.

[g]Apparent correlation field splitting.

Only two other unassigned calculated bands lie above 800 cm^{-1}; 1168 and 1150 cm^{-1} in MAX, and 1165 and 1156 cm^{-1} in MBX. Both of these bands are composed mainly of methyl group deformations. Although these bands were not assigned, they probably do correspond to unresolved spectral bands in the vicinity of 1100 cm^{-1}. Support for assigning these methyl modes to this spectral region can be found in the work of Snyder and Zerbi (13) on aliphatic ethers. The normal coordinate calculations performed on dimethyl ether revealed the presence of significant contributions from methyl group deformations at 870, 1013, 1027, 1089, 1136, 1140, 1186, 1198, and 1243 cm^{-1}. The precise location of these methyl deformation modes in the spectra of MAX and MBX has not been determined but frequencies around 1150 cm^{-1} are in agreement with the distributions found in dimethyl ether. Changes in SVQFF parameters related to methyl group motions can influence the location of these bands. A more thorough spectral investigation of these pyranosides could result in better assignments for these bands.

In the spectral region below 800 cm^{-1} of both MAX and MBX are several observed frequencies that have been left unassigned. In MAX there is only one of these bands that can be associated with a correlation field splitting effect: 734 cm^{-1} (IR,R). This band lies very near the strong band at 740 cm^{-1}. The other unassigned spectral bands in both pyranosides must be accounted for in different ways. In MAX, the only other unassigned band is at 535 cm^{-1} in the Raman spectrum (537 cm^{-1} in IR). The unassigned spectral bands of MBX are at (cm^{-1}): 1) 607 (R), 625 (IR); 2) 530 (R), 527 (IR); and 3) 471 (R), 472 (IR). A probable cause for the unassigned bands in this spectral region is the use of unrefined SVQFF parameters relating to the C-O torsions of the methyl group. From Tables LXXVII and LXXVIII it is apparent that contributions from these torsions extend up to almost 600 cm^{-1}. On the other hand, the calculations of

Snyder and Zerbi (13) restrict these torsional motions to energy levels below 300 cm^{-1}. Further calculations using refined SVQFF torsion parameters were not carried out, but such refinements of SVQFF parameters relating to the methyl group would be expected to greatly improve the band assignments in this region of the spectrum.

Overall, the frequency correlations of MAX and MBX are very good. Comparing these correlations in Fig. 29 reveals that the frequency distributions for each molecule are accurately reproduced by the calculated bands. This is especially true of the anomeric region spanning 600 to 1000 cm^{-1}. The very good band correlations support the transferability of the pentose SVQFF to the xylopyranoside molecules and demonstrates the sensitivity of this SVQFF to changes in configuration at the anomeric site.

SPECTRAL INTERPRETATIONS

The spectra of the xylopyranosides are very similar to those of the pentoses in that they can be divided into five, somewhat isolated, regions:

1. OH and CH stretch
2. CH bend
3. COH bend
4. CC and CO stretch
5. Low energy bands consisting of torsional motions and CC and CO bending motions

The presence of the methyl group does, however, produce some changes in the calculated bands throughout the spectrum.

Consider the OH and CH stretch regions. Comparing the calculated bands reveals that no coupling of methyl stretches occurs with any of either the methylene or methine stretches. Therefore, the methyl stretches occur at the

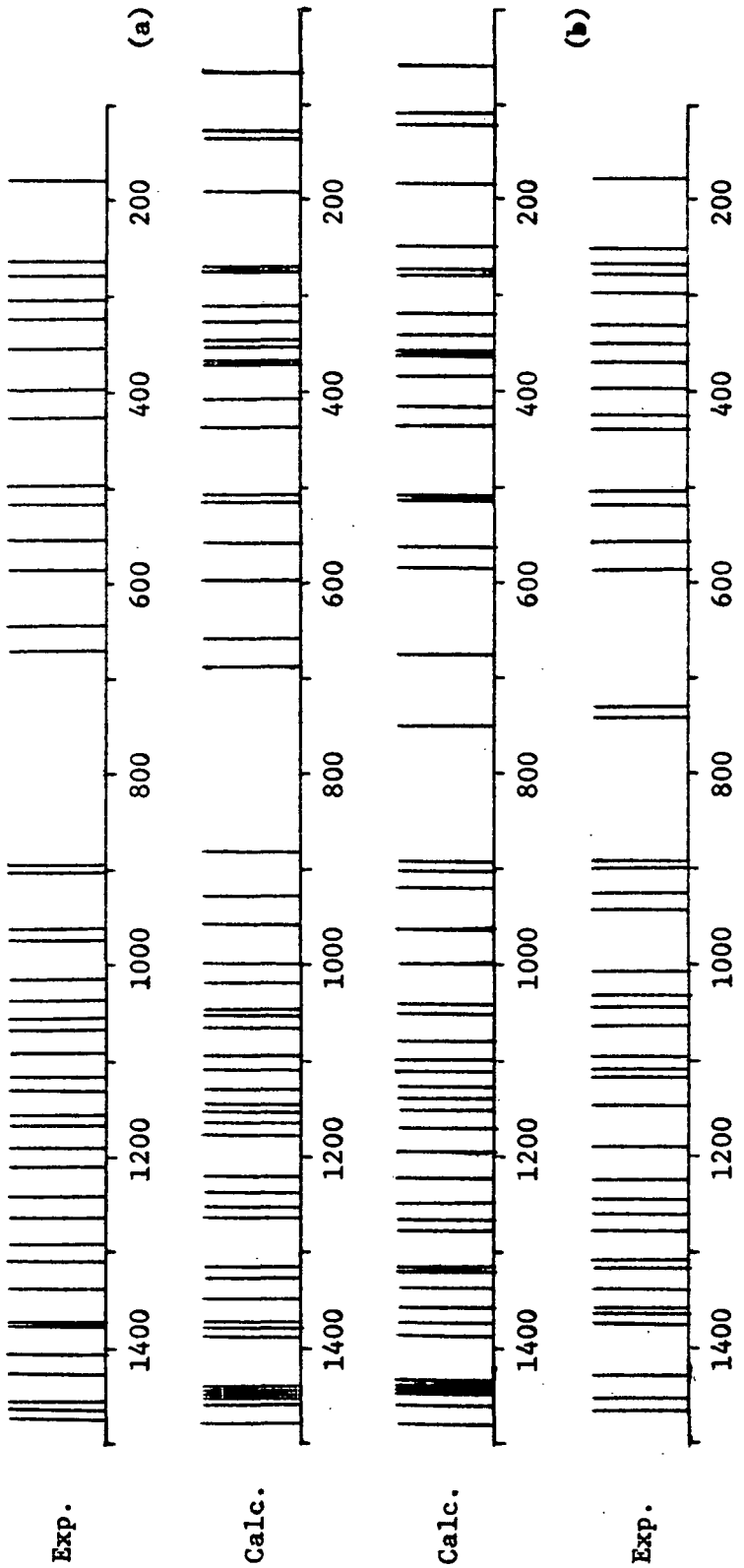

Figure 29. A Comparison of Calculated and Assigned Experimental Frequencies: (a) Methyl-β-xylopyranoside and (b) Methyl-α-xylopyranoside

same frequencies in both MAX and MBX. Furthermore, the presence of the methyl group does not alter the methine and methylene frequencies — they are the same as for the anomers of xylose. The methine stretching bands of MBX are different from those of MAX indicating that these motions are affected by the coupling patterns arising from the different anomeric site configurations.

The CH bending region extends from 1480 down to about 1150 cm^{-1}. Modes of highest energy are the methylene deformation modes — scissors coupled with wag. These modes are generally left unaffected by changes in anomeric site configuration. The analogous scissors motions of the methyl group are also not significantly affected by anomeric site configuration, which indicates that these methyl group motions are not coupled with other motions of the molecule. This lack of coupling is probably a result of the C-O-C linkage at the methyl group which separates the methyl hydrogens from close interactions with other hydrogen atoms. Other CH bending modes throughout the region are affected by anomeric site configuration as evidenced by the differences in the potential energy distributions of MAX and MBX.

The coupling patterns of the methine CH deformations appear to be influenced by the mass of the methyl group. Comparison of the methine CH bending modes of α-xylose with those of MAX reveals that most of the methine bands of α-xylose have been significantly altered in frequency, composition, or both by the addition of the methyl group. Since most of the methine deformation modes have been affected, it can be concluded that the methyl group influences some of the long range coupling that occurs within this spectral region.

Within the CH bending region occur most of the COH in-plane bending motions. As with the pentoses, these COH motions are highly coupled with the methine CH bending motions present in this region. Comparison of the bands of xylose, MAX, and MBX which contain significant contributions from

COH in-plane bending motions reveals that, in general, frequencies are shifted and band compositions altered by both methyl substitution and by changes in the configuration at the anomeric site.

The addition of the methyl group is most noticeable in the bands predominated by CC and CO stretch and bend motions. The additional mass of the methyl group strongly affects the coupling of the heavy atom motions as is indicated by a comparison of the potential energy distributions of bands in xylose, MAX, and MBX in the spectrum below 1150 cm^{-1}. These comparisons also reveal that while many of the calculated frequencies of MAX are very similar to those of α-xylose, the potential energy distributions calculated for these bands can involve some very different coupling patterns. Consider the two examples shown in Table XXVI. In each case, the calculated frequencies are quite similar, but it is obvious that the coupling patterns of the motions involved in these bands have been altered by the addition of the methyl group. Comparisons such as these illustrate the difficulties encountered when the group frequency approach is used to interpret the spectra of complex saccharide molecules.

TABLE XXVI

A COMPARISON OF CALCULATED MODES OF
α-XYLOSE AND METHYL-α-XYLOPYRANOSIDE

α-Xylose		Methyl-α-xylopyranoside	
cm^{-1}	Composition	cm^{-1}	Composition
1000	C1C2(20) HC1O1O(20) C2O7(17) C2C3(11) C5O1O(10) O1OC1(9) C1O6(8) O6CC(7)	998	C4C5(32) HC1C(17) C5O1O(16) C1C2(14) HC1O1O(11) C1O6(8) H16CC(8) HC4C(7)
761	O1OC1(16) COC(15) C2C3(15) CCO7(8) C1O6(6) O6CC(6) C1C2(5) HC2C(5)	749	O1OC1(13) C2C3(12) COC(11) C1O6(11) CCO7(8) C1C2(6)

The close similarities between the calculated frequencies of α-xylose and MAX, and β-xylose and MBX are shown in Fig. 30. Clearly, the response of the spectra to configurational changes at the anomeric site is very similar. Frequency comparisons of this type can be useful when attempting to correlate the frequency response in the pyranoside spectra to spectral changes resulting from anomeric changes with the other pentose molecules.

CONCLUSIONS

The SVQFF developed for the pentose sugars transfers reasonably well to the xylopyranoside molecules. It is quite sensitive to configuration at the anomeric site and is capable of reproducing the bands of either xylopyranoside quite well. Improvements in overall fit could be obtained with force constants refined specifically for the methyl xylopyranosides, especially for the motions involving the methyl group.

The addition of the methyl group to the anomeric hydroxyl oxygen of a pentose molecule affects the heavy atom deformations and the CH and COH deformations. Changes in the configuration of the anomeric site also affects these CH and COH deformations as well as the heavy atom deformations throughout the molecule. Overall, the band distributions are quite similar to the distributions calculated for the pentose and for other pyranose molecules.

The most important aspect of these calculations is the fact that the pentose SVQFF can be used as the basis for the normal coordinate analyses of other pentose derivatives. SVQFF refinements performed on these derivatives should only require adjustments to force constants directly related to substituent groups.

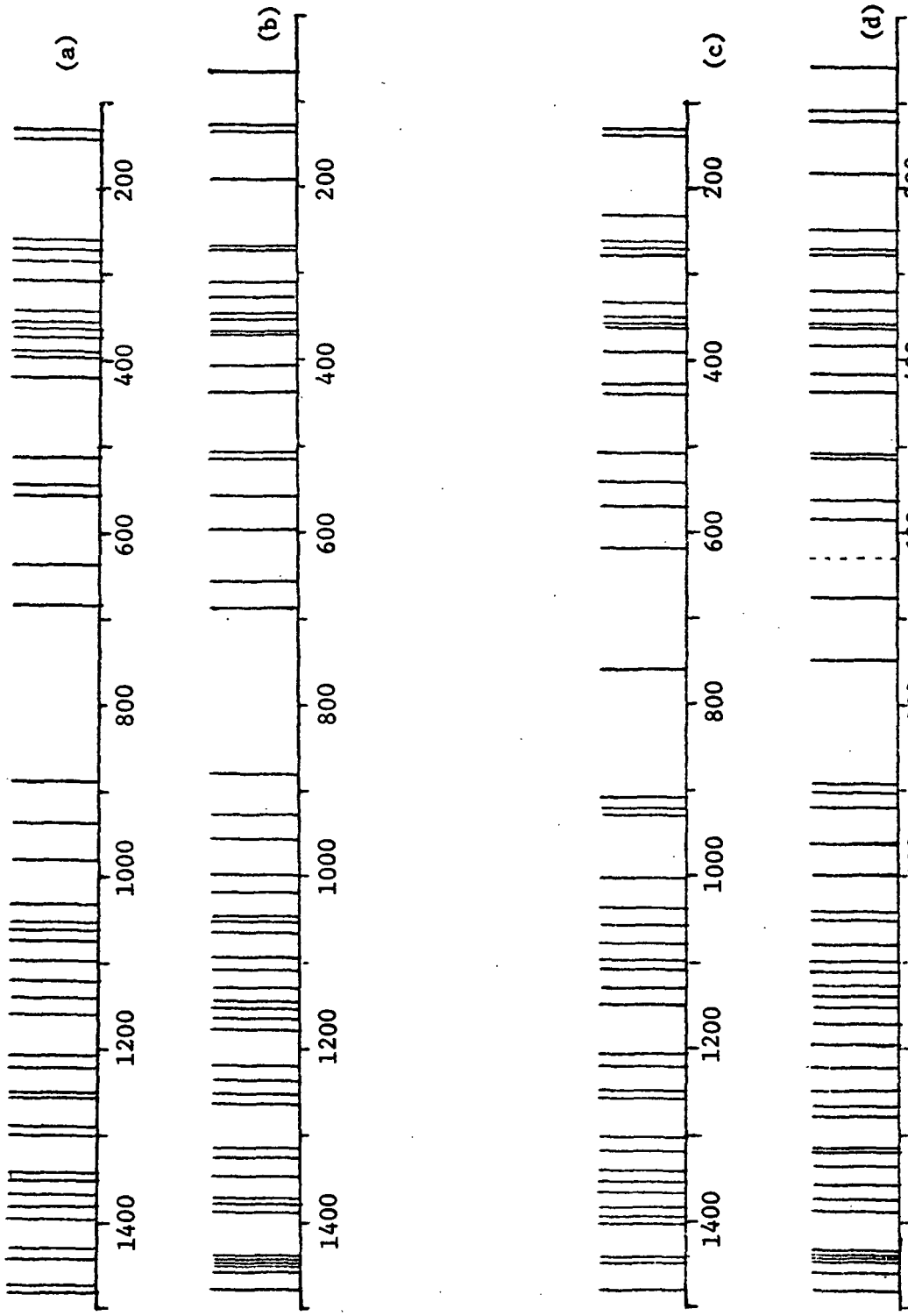

Figure 30. A Comparison of Calculated Frequencies: (a) β-Xylose, (b) Methyl-β-xylopyranoside, (c) α-Xylose, and (d) Methyl-α-xylopyranoside

NOMENCLATURE

A	Angstrom
1,5-AHP	1,5-anhydropentitol
asym.	asymmetric
$\underset{\sim}{B}$	internal coordinate transformation matrix $\underset{\sim}{S} = \underset{\sim}{B}\underset{\sim}{X}$
calc.	calculated
cm^{-1}	wave numbers
$\underset{\sim}{D}$	Hessian matrix
diff.	difference
dist.	distribution
Exp.	experimental
$\underset{\sim}{F}$	force constant matrix
F_{ij}	element of the force constant matrix $\underset{\sim}{F}$
freq.	frequency
$\underset{\sim}{G}$	inverse kinetic energy matrix
Φ_i	ith force constant parameter
i.p.	in-plane
IR	infrared
KBr	potassium bromide
$\underset{\sim}{L}$	eigenvector matrix
LT	low temperature
MAX	methyl-α-xylopyranoside
MBX	methyl-β-xylopyranoside
mdyn	millidyne
nm	nanometer
NC	normal coordinate
obs	observed
o.p.	out-of-plane

PE	potential energy
$\underline{Q}$	sum of the squared residuals
$\underline{Q}_{\underline{r}}$	sum of squared residuals after $\underline{r}$ iterations
rad.	radian
RT	room temperature
S	internal coordinates expressed as a vector
$\underline{S}_{\underline{k}}$	$\underline{k}$th internal displacement coordinate
SVQFF	Simplified Valence Quadratic Force Field
sym.	symmetric
THP	tetrahydropyran
$\underline{V}$	potential energy
X	Cartesian displacement coordinates expressed as a vector
Z	transformation matrix $F = Z\Phi$
$\lambda_{\underline{i}}$	$\underline{i}$th eigenvalue or frequency parameter
Λ	eigenvalue matrix
υ	frequency

ACKNOWLEDGMENTS

I wish to sincerely thank Dr. Rajai Atalla, Chairman of my Thesis Advisory Committee, for his personal interest in me and for his support and guidance throughout the course of this thesis. And most of all, I want to thank him for his undaunted faith in me and my intentions to complete this work.

I also wish to gratefully acknowledge Drs. G. A. Baum and R. D. McKelvey, who served on my Advisory Committee, for their guidance and critical discussions throughout the course of this thesis.

I wish to thank Messrs. J. J. Bachhuber and J. O. Church for their unending help in the manipulation of the computer programs necessary to complete this investigation.

I am deeply indebted to The Institute of Paper Chemistry for the financial support and fine academic program which have made this thesis possible.

Finally, my most sincere appreciation goes to my wife, Beth, who has endured the sacrifices and offered the support necessary to make this thesis a reality.

LITERATURE CITED

1. Pitzner, J. L. An investigation of the vibrational spectra of the 1,5-anhydropentitols. Doctoral Dissertation. Appleton, Wisconsin, The Institute of Paper Chemistry, 1973. 402 p. Spectrochim. Acta 31A:911(1975).

2. Watson, G. M. An investigation of the vibrational spectra of the pentitols and erythritol. Doctoral Dissertation. Appleton, Wisconsin, The Institute of Paper Chemistry, 1974. 202 p.

3. Neely, W. B., Advan. Carbohyd. Chem. 12:13(1957).

4. Spedding, H., Advan. Carbohyd. Chem. 19:23(1964).

5. Tipson, R. S., NBS Monograph No. 110, June, 1968.

6. Barker, S. A., Bourne, E. J., Stacey, M., and Whiffen, D. H., J. Chem. Soc. 1954:4211.

7. Barker, S. A., Bourne, E. J., Stephens, R., and Whiffen, D. H., J. Chem. Soc. 1954:3468.

8. Barker, S. A., Bourne, E. J., Stephens, R., and Whiffen, D. H., J. Chem. Soc. 1954:171.

9. Burkett, S. C., and Badger, R. M., J. Am. Chem. Soc. 72:4397(1950).

10. Becket, C. W., Pitzer, K. S., and Spitzer, R., J. Am. Chem. Soc. 69:2488(1947).

11. Schachtschneider, J. H., and Snyder, R. G., Spectrochim. Acta 19:117(1963).

12. Snyder, R. G., and Schachtschneider, J. H., Spectrochim. Acta 19:85(1963).

13. Snyder, R. G., and Zerbi, G., Spectrochim. Acta 23A:391(1967).

14. Vasko, P. D. Spectroscopic and vibrational studies of carbohydrates. Doctoral Dissertation. Cleveland, Ohio, Case Western Reserve University, Jan., 1971. 127 p.

15. Brooks, W. V. F., and Haas, C. M., J. Phys. Chem. 71:3, 656(1967).

16. Mikawa, Y., Basch, J. W., and Jakobsen, R. J., J. Molecular Spectroscopy 24:314(1967).

17. Cael, J. J., Koenig, J. L., and Blackwell, J., Carbohyd. Res. 32:79(1974).

18. Cael, J. J., Gardner, K. H., Koenig, J. L., and Blackwell, J., J. Chem. Phys. 62:1145(1975).

19. Fletcher, R., and Powell, M. J. D., Computer J. 6:163(1963).

20. Wells, H. A. Private communication, The Institute of Paper Chemistry, Appleton, Wisconsin, 1975.

21. Schachtschneider, J. H. Vibrational analysis of polyatomic molecules. Tech. Rept. No. 231-264 and No. 57-65. Emeryville, California, Shell Development Co., 1964.

22. Wilson, E. B., Jr., Decius, J. C., and Cross, P. C. Molecular vibrations. New York, McGraw-Hill Book Co., 1955. 388 p.

23. Hordvik, A., Acta Chem. Scand. 15:16(1961).

24. Hordvik, A., Acta Chem. Scand. 20:1943(1966).

25. Hordvik, A., Acta Chem. Scand. 25:2175(1971).

26. Pickett, H., and Strauss, H. J., J. Chem. Phys. 53:376(1970).

27. Patil, J. R., and Bose, J. L., Carbohyd. Res. 7:405(1968).

28. Fuhrer, H., Kartha, V. B., Krueger, P. J., Mantsch, H. H., and Jones, R. N., Chem. Rev. 72:439(1972).

29. Stacey, M., Moore, R. H., Barker, S. A., Weigel, H., Bourne, E. J., and Whiffen, D. H., Proc. 2nd United Nations Intern. Conf. on Peaceful Uses of Atomic Energy (Geneva), 1958:251-6.

30. Atalla, R. H. Unpublished work, The Institute of Paper Chemistry, Appleton, Wisconsin.

31. Hilderbrandt, R. L., J. Molecular Spectroscopy 44:599(1972).

32. Dempster, A. B., and Zerbi, G., J. Chem. Phys. 54:3600(1971).

33. Williams, R. W. Unpublished work, The Institute of Paper Chemistry, Appleton, Wisconsin.

34. Kuhn, L. P., Anal. Chem. 22:276(1950).

35. Isbell, H. S., Stewart, J. E., Frush, H. L., Moyer, J. D., and Smith, F. A., J. Res. NBS 57:179(1956).

36. Angyal, S. J., and Pickles, V. A., Aust. J. Chem. 25:1695(1972).

37. Reeves, R. E., Advan. Carbohyd. Chem. 6:107(1951).

38. James, V. J., and Stevens, J. D., Carbohyd. Res. 21:334(1972).

APPENDIX I

THEORETICAL BASIS FOR THE NORMAL COORDINATE CALCULATIONS

THEORETICAL BASIS FOR THE CALCULATIONS

The molecular model used to establish the vibrational secular equation consists of 1) point masses representing the atoms and 2) force constants representing the intramolecular forces which hold the atoms in their equilibrium configuration. To further simplify the computational procedures, the assumption is made that during a given vibrational mode the displacements of the atoms from their equilibrium positions are small. This assumption allows the use of the equations of motion for a harmonic oscillator.

By defining a set of mass weighted Cartesian displacement coordinates, $\underline{q_i}$, as: $\underline{q_1} = \underline{m_1}\Delta\underline{x_2}$, $\underline{q_2} = \underline{m_1}\Delta\underline{y_1}$, $\underline{q_3} = \underline{m_1}\Delta\underline{z_1}$, $\underline{q_4} = \underline{m_2}\Delta\underline{x_2}$, ...; the kinetic energy of a molecular system can be given by

$$2T = \sum_{i=1}^{3n} \dot{q}_i^2 \qquad (1)$$

where $\underline{n}$ is the number of atoms in the molecule. Similarly, the potential energy will be a function of atomic displacements which can be expressed as a power series in terms of the displacement coordinates, $\underline{q_i}$:

$$2V = 2V_\phi + 2 \sum_{i=1}^{3n} (\partial V/\partial q_i)_\phi q_i + \sum_{i,j=1}^{3n} (\partial^2 V/\partial q_i \partial q_j)_\phi q_i q_j + \text{higher terms.} \qquad (2)$$

Assuming small displacements and defining the zero of energy as zero leaves only two terms in Equation (2). Since at equilibrium, $(\partial \underline{V}/\partial \underline{q_i})_\phi = 0$ and the potential energy must be at a minimum, Equation (2) reduces to

$$2V = \sum_{i,j=1}^{3n} f_{ij} q_i q_j , \qquad (3)$$

where $$f_{ij} = (\partial^2 V/\partial q_i \partial q_j)_\phi$$

and the f_{ij} are referred to as the force constants.

Substituting the forms for the kinetic and potential energy of Equations (1) and (3) in Newton's equations of motion yields

$$\ddot{q}_j + \sum_{i=1}^{3n} f_{ij} q_i = 0 \qquad j = 1,2,3,\ldots,3n. \tag{4}$$

A solution to this set of $3n$ simultaneous second order differential equations is given by

$$q_i = A_i \cos(\lambda^{\frac{1}{2}} t + e). \tag{5}$$

Substituting Equation (5) in Equation (4) yields a set of $3n$ simultaneous algebraic equations given by

$$\sum_{i=1}^{3n} (f_{ij} - \delta_{ij}\lambda) A_i = 0 \qquad j = 1,2,3,\ldots,3n, \tag{6}$$

where δ_{ij} equals unity if $i = j$ and is zero otherwise. Excluding the trivial solution where $A_i = 0$ requires that Equation (6) be satisfied for only special values of λ.

Accordingly, by selecting a proper set of internal displacement coordinates instead of the Cartesian displacement coordinates, the equivalent of Equation (6), in matrix notation, becomes

$$(\underset{\sim}{G}\underset{\sim}{F} - \Lambda\underset{\sim}{E})\underset{\sim}{L} = 0, \tag{7}$$

which is commonly referred to as the vibrational secular equation. The elements of Equation (7) are the $\underset{\sim}{G}$ matrix, or the inverse kinetic energy matrix; the $\underset{\sim}{F}$ matrix, or force constant matrix; the identity matrix, $\underset{\sim}{E}$; the diagonal matrix,

$\underset{\sim}{\Lambda}$, of the frequencies of vibration; and the $\underset{\sim}{L}$ matix, or the matrix of amplitudes of the various displacements of the coordinates for each of the calculated frequencies.

For nontrivial solutions, the secular determinant,

$$|\underset{\sim}{GF} - \underset{\sim}{\Lambda E}| = 0. \tag{8}$$

In general, NC analyses consist of construction of the $\underset{\sim}{G}$ matrix from known or assumed structural parameters, estimation of the $\underset{\sim}{F}$ matrix and subsequent solution of the secular equation. These steps will now be considered in greater detail.

THE CONSTRUCTION OF THE $\underset{\sim}{G}$ MATRIX

Because of their chemical significance and their independence from translation and rotation of the molecule as a whole, internal displacement coordinates are used to replace mass weighted Cartesian displacement coordinates. The three types of internal displacement coordinates used to define the molecular models of the pentose sugars are (1) bond stretching, (2) angle bending, and (3) torsional bending. The S-vector technique described by Wilson, et al. (22) is used to calculate the transformation from Cartesian displacement to internal displacement coordinates. This transformation is given by

$$S_t = \sum_{i=1}^{3n} B_{ti}\varepsilon_i \qquad t = 1,2,3,\ldots,3n-6, \tag{9}$$

where $\underline{S_t}$ represents an internal displacement coordinate, ε_i one of the Cartesian displacement coordinates, and $\underline{B_{ti}}$ an element of the transformation. $\underset{\sim}{G}$ matrix elements, $\underline{G_{tt}}$, are then defined as

$$G_{st} = \sum_{i=1}^{3n} (1/m_i)B_{si}B_{ti} \qquad s,t = 1,2,3,\ldots,3n-6, \tag{10}$$

in which m_i is the mass of the atom to which the subscript 'i' refers. In actual practice, the program GMAT written by Schachtschneider (21) calls for the atomic masses, the equilibrium Cartesian coordinates of the atoms of the molecule, and the definitions of the internal displacement coordinates of the molecule. With this input information, then, the $\underset{\sim}{B}$ matrix is calculated. From this $\underset{\sim}{B}$ matrix and the masses of the atoms, the $\underset{\sim}{G}$ matrix is calculated by

$$\underset{\sim}{G} = \underset{\sim}{B}\underset{\sim}{M}^{-1}\underset{\sim}{B}', \tag{11}$$

where . $\underset{\sim}{M}^{-1}$ = a diagonal matrix of order $3n$ whose elements are the inverses of the atomic masses

$\underset{\sim}{B}'$ = the transpose of the $\underset{\sim}{B}$ matrix

THE CONSTRUCTION OF THE $\underset{\sim}{F}$ MATRIX

The construction of the $\underset{\sim}{F}$ matrix is simplified by the formation of a constraint matrix, $\underset{\sim}{Z}$:

$$f_{ij} = \sum_{k=1} z_{ijk}\Phi_k,$$

where f_{ij} = the elements of the $\underset{\sim}{F}$ matrix or force constants

Φ_k = the independent force constant parameters

Introduction of the $\underset{\sim}{Z}$ matrix into the calculations eliminates the need to enter zero elements of the $\underset{\sim}{F}$ matrix as data and also facilitates quick changes of parameters in the $\underset{\sim}{F}$ matrix since the adjustment of one parameter in the column matrix of Φ_k effectively changes many elements within the $\underset{\sim}{F}$ matrix. This latter fact becomes more important when the refinement procedures are discussed.

SOLUTION OF THE SECULAR EQUATION

After the computation of the $\underset{\sim}{G}$ and $\underset{\sim}{F}$ matrices, the vibrational secular equation can be solved. Separating the matrix products of Equation (7) yields

$$\underset{\sim}{GF}\underset{\sim}{L} = \underset{\sim}{L}\underset{\sim}{\Lambda}. \tag{12}$$

In reality, solution of Equation (12) implies that a matrix $\underset{\sim}{L}$ must be found which will diagonalize the matrix of the $\underset{\sim}{GF}$ product. The matrix $\underset{\sim}{L}$ is, then, the transformation from normal coordinates to internal coordinates gives as,

$$\underset{\sim}{S} = \underset{\sim}{L}^{-1}\underset{\sim}{Q}. \tag{13}$$

In addition, the $\underline{k}$th column of the matrix $\underset{\sim}{L}$ will give the eigenvectors of the $\underline{k}$th eigenvalue or calculated frequency parameter. These $\underset{\sim}{L}$ column elements represent the relative amplitudes of the internal displacement coordinates during each normal mode.

Actual solution of Equation (12) is accomplished by successive orthogonalization of the $\underset{\sim}{G}$ and $\underset{\sim}{F}$ matrices followed by Jacobi diagonalization. An advantage of using the Jacobi technique is that in addition to diagonalizing a symmetric matrix, it will simultaneously calculate the eigenvectors associated with the eigenvalues. However, while both $\underset{\sim}{G}$ and $\underset{\sim}{F}$ are symmetric matrices, their product, $\underset{\sim}{GF}$, is not generally symmetric. So in order to use the Jacobi technique, $\underset{\sim}{GF}$ is made symmetric by applying an orthogonal transformation to $\underset{\sim}{G}$ which makes $\underset{\sim}{G}$ diagonal as:

$$\underset{\sim}{A}^{t}\underset{\sim}{GA} = \underset{\sim}{DD} \tag{14}$$

or

$$\underset{\sim}{G} = \underset{\sim}{ADDA}^{t}, \tag{15}$$

where $\underset{\sim}{A}$ is the orthogonal eigenvector matrix of $\underset{\sim}{G}$, and $\underset{\sim}{D}$ is a diagonal matrix of the square roots of the eigenvalues of $\underset{\sim}{G}$. This diagonalized form of $\underset{\sim}{G}$ is not in general a unitary matrix, so a transformation matrix, $\underset{\sim}{W}$, is defined so that

$$\underset{\sim}{W} = \underset{\sim}{A}\underset{\sim}{D}. \tag{16}$$

Inserting Equation (16) in Equation (15) yields

$$\underset{\sim}{W}^{t}\underset{\sim}{G}\underset{\sim}{W} = \underset{\sim}{E}, \tag{17}$$

which transforms $\underset{\sim}{G}$ into an identity matrix. Since the $\underset{\sim}{F}$ matrix transforms as $\underset{\sim}{G}^{-1}$ (this is evident from the matrix forms of the equations for the kinetic and potential energy: $2\underset{\sim}{T} = \dot{\underset{\sim}{S}}^{t}\underset{\sim}{G}^{-1}\dot{\underset{\sim}{S}}$ and $2\underset{\sim}{V} = \underset{\sim}{S}^{t}\underset{\sim}{F}\underset{\sim}{S}$),

$$\underset{\sim}{W}\underset{\sim}{F}\underset{\sim}{W}^{t} = \underset{\sim}{H}, \tag{18}$$

and the original $\underset{\sim}{G}\underset{\sim}{F}$ product is now reduced to a symmetric matrix, $\underset{\sim}{H}$. Diagonalization of the matrix $\underset{\sim}{H}$ yields the solution to the secular equation given in Equation (12). This diagonalization is accomplished by a matrix, $\underset{\sim}{C}$:

$$\underset{\sim}{C}^{-1}\underset{\sim}{H}\underset{\sim}{C} = \underset{\sim}{C}^{-1}\underset{\sim}{W}\underset{\sim}{F}\underset{\sim}{W}^{t}\underset{\sim}{C} = \underset{\sim}{\Lambda} \tag{19}$$

where $\underset{\sim}{\Lambda}$ is the diagonal matrix of frequency parameters related to vibrational frequencies by

$$\lambda_i = 4\pi^2\nu_i^2. \tag{20}$$

The λ_i are elements of the diagonal matrix $\underset{\sim}{\Lambda}$.

The $\underset{\sim}{L}$ matrix of Equation (12) must be calculated so that the normal coordinate associated with each normal mode can be evaluated. Multiplying Equation (19) by first the matrix $\underset{\sim}{C}$ and then by the matrix $\underset{\sim}{W}$ yields

$$\underset{\sim}{WW}^{t}\underset{\sim}{FWC} = \underset{\sim}{WC}. \qquad (21)$$

Comparison of Equation (21) with Equation (12) indicates that the matrix $\underset{\sim}{L}$ can be defined as

$$\underset{\sim}{L} = \underset{\sim}{WC}. \qquad (22)$$

OPTIMIZATION OF THE FORCE CONSTANT PARAMETERS

INITIAL FORCE CONSTANTS

A procedure for the systematic optimization of the initial force constants is necessary to obtain the best fit between the observed and calculated vibrational frequencies. The selection of initial force constants is best accomplished when the force field is based upon molecules most similar to the molecules in question. The best force constants to select as initial constants for the pentose molecules come from the force field for the 1,5-AHP's by Pitzner (1), since the 1,5-AHP constants ought to apply directly to the pentoses with some modifications for the anomeric site.

Modifications to the force field of the 1,5-AHP's to accommodate the anomeric site were made along with subsequent changes in the definitions of several interaction parameters and the COH bending constant. These changes increased the size of the original force field from 56 parameters to 80 parameters. Six of these were dummy parameters to allow ample possibilities for changes during the subsequent force constant refinement stages.

FORCE CONSTANT REFINEMENT

In the refinements carried out in this work the force constant parameters were optimized using the programs of Schachtschneider (21) modified to accommodate the Fletcher-Powell minimization algorithm (19). The interested reader

should refer to the detailed presentation of this method of force constant optimization given by Pitzner (1). Briefly, the Fletcher-Powell minimization algorithm involves three main steps:

1. Compute the gradient vector $\underline{g}^r$ whose elements are given by

$$g_i^r = (\delta Q/\delta \Phi_i)^r$$

   where g_i^r represents the ith element of the gradient vector after the rth iteration and Q represents the sum of the squared residuals.

2. Determine the direction along which to move.

3. Compute a stepwise, T_m, and move in the desired direction.

The changes to be made in the force constant parameters after each iteration are then indirectly determined from

$$\Delta \Phi^r = -(\underset{\sim}{D}^r)^{-1} g^r \tag{23}$$

where $\underset{\sim}{D}^r$ is a Hessian matrix defined by

$$\underset{\sim}{D} = \sum_{ij} \underset{\sim}{D}_{ij} = \sum_{ij} \delta^2 Q/\delta \Phi_i \delta \Phi_j .$$

This matrix, $\underset{\sim}{D}^r$, is not calculated directly but rather is approximated after each iteration as the matrix, $\underset{\sim}{R}$, beginning as an identity matrix. If $\underset{\sim}{R}$ is an identity matrix as in Equation (24),

$$\Delta \Phi^r = -(\underset{\sim}{R})^{-1} g^r , \tag{24}$$

then Equation (23) becomes

$$\Delta \Phi^1 = -g_i^1 , \tag{25}$$

and the initial adjustments made to the force constants result from movement along the gradient vector in the direction of steepest descent. However, if $\underset{\sim}{R}$ is to approach $\underset{\sim}{D}$, then some means of finding a direction vector and step size must be utilized after subsequent iterations. These latter two steps have been accomplished by a method of successive linear searches in $\underset{\sim}{R}$ conjugate directions after each iteration. The theoretical basis for this method insures that as Φ^{r} approaches Φ_{min}, $\underset{\sim}{R}$ approaches $\underset{\sim}{D}$. In addition, this nonlinear search technique requires the calculation of a local minimum with each iteration. This calculation can be summarized by three steps. The first estimates the magnitude of the step size, T_m, the second determines an interval containing T_m and the third step interpolates cubically the value of T_m.

TERMINATION OF THE FORCE CONSTANT REFINEMENT

Termination of the refinement takes place when either of two of the following conditions are met. The first condition requires that all corrections to the force constant parameters, $\Delta\Phi_i$, for a particular iteration be less than or equal to an arbitrary constant supplied by the user; i.e., 0.001. The second condition requires that the ratio of the successive weighted sums of squares be greater than 0.995. However, to prevent premature termination the user can require that this condition be met several times.

APPENDIX II

DATA NECESSARY TO CONSTRUCT THE $\underset{\sim}{G}$ AND $\underset{\sim}{F}$ MATRICES FOR THE NORMAL COORDINATE ANALYSES

The information reported in this appendix is as follows:

TABLE XXVII

COMPARISON OF THE BOND LENGTHS AND BOND ANGLES OF THE PENTOSE SUGARS

Internal Coordinate	Arabinose[a]	Lyxose[b]	Xylose[c]	Average[d]	Assumed[e]
C1-C2	1.524[f]	1.538	1.531	1.531	1.523
C2-C3	1.523	1.528	1.529	1.527	1.523
C3-C4	1.554	1.509	1.515	1.526	1.523
C4-C5	1.537	1.525	1.503	1.522	1.523
C5-O10	1.440	1.422	1.449	1.437	1.423
C1-O10	1.421	1.435	1.428	1.428	1.423
C1-O6	1.382	1.364	1.393	1.380	1.380
C2-O7	1.454	1.399	1.415	1.423	1.415
C3-O8	1.426	1.430	1.418	1.425	1.415
C4-O9	1.431	1.404	1.411	1.415	1.415
C1C2C3	109.2[g]	109.9	111.3	110.1	109.5
C2C3C4	109.7	112.2	109.2	110.4	109.5
C3C4C5	107.1	109.4	110.2	108.9	109.5
C4C5O10	111.9	110.9	111.2	111.3	109.5
C5O10C1	112.7	113.8	112.4	113.0	113.2
O10C1C2	109.5	108.9	109.3	109.2	109.5
O10C1O6	113.0	108.1	111.5	110.9	109.5
O6C1C2	108.9	113.4	109.9	110.7	109.5
C1C2O7	107.3	105.9	110.2	107.8	109.5
O7C2C3	110.8	112.2	114.2	112.4	109.5
C2C3O8	109.3	109.8	106.1	108.4	109.5
O8C3C4	110.1	109.4	111.9	110.5	109.5
C3C4O9	111.7	112.3	109.3	111.1	109.5
O9C4C5	108.3	107.0	109.9	108.4	109.5

[a,b,c] Structure parameters taken from Hordvik (23-25).

[d] Average determined as A+B+C/3 .

[e] Assumed structure based on the 1,5-AHP's of Pitzner (1).

[f] Bond lengths given in Angstroms.

[g] Bond angles given in degrees.

TABLE XXVIII

DESCRIPTION OF THE 55 VALENCE BOND AND VALENCE BOND ANGLE COORDINATES OF THE MOLECULAR MODELS OF THE PENTOSES

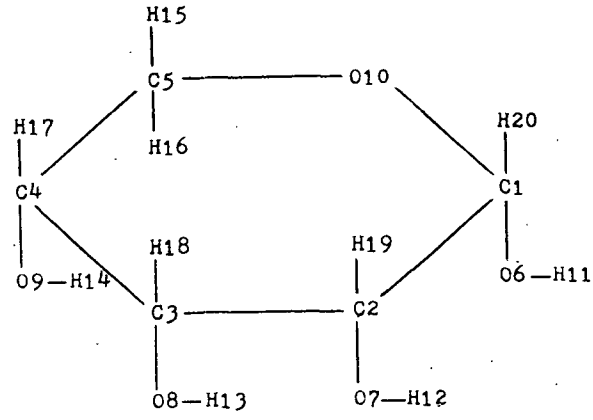

VALENCE BOND COORDINATES

		Description Code			Description Code			Description Code
1.	C1-C2	C1C2	8.	C2-O7	C2O7	15.	C2-H19	CH19
2.	C2-C3	C2C3	9.	C3-O8	C3O8	16.	C1-H20	CH20
3.	C3-C4	C3C4	10.	C4-O9	C4O9	17.	O6-H11	OH11
4.	C4-C5	C4C5	11.	C5-H15	CH15	18.	O7-H12	OH12
5.	C5-O10	C5O10	12.	C5-H16	CH16	19.	O8-H13	OH13
6.	O10-C1	O10C1	13.	C4-H17	CH17	20.	O9-H14	OH14
7.	C1-O6	C1O6	14.	C3-H18	CH18			

VALENCE BOND ANGLE COORDINATES

		Description Code			Description Code			Description Code
21.	C1-C2-C3	CC2C	33.	O9-C4-C3	CC4O	45.	H20-C1-O10	HC1O10
22.	C2-C3-C4	CC3C	34.	O9-C4-C5	OC4C	46.	H20-C1-C2	HC1C
23.	C3-C4-C5	CC4C	35.	H11-O6-C1	HO6C	47.	H19-C2-C1	CC2H
24.	C4-C5-O10	CC5O10	36.	H12-O7-C2	HO7C	48.	H19-C2-C3	HC2C
25.	C5-O10-C1	COC	37.	H13-O8-C3	HO8C	49.	H18-C3-C2	CC3H
26.	O10-C1-C2	O10C1C	38.	H14-O9-C3	HO9C	50.	H18-C3-C4	HC3C
27.	O10-C1-O6	OCO	39.	H15-C5-O10	H15CO	51.	H17-C4-C3	CC4H
28.	O6-C1-C2	OC1C	40.	H16-C5-O10	H16CO	52.	H17-C4-C5	HC4C
29.	O7-C2-C1	CC2O	41.	H17-C4-O9	HC4O	53.	H15-C5-C4	H15CC
30.	O7-C2-C3	OC2C	42.	H18-C3-O8	HC3O	54.	H16-C5-C4	H16CC
31.	O8-C3-C2	CC3O	43.	H19-C2-O7	HC2O	55.	H15-C5-H16	HCH
32.	O8-C3-C4	OC3C	44.	H20-C1-O6	HC1O			

TABLE XXIX

DESCRIPTION OF THE 10 TORSIONAL COORDINATES OF EACH OF THE MOLECULAR MODELS OF THE PENTOSES

	β-Arabinose	α-Arabinose	α-Xylose	β-Xylose
56	O10-C1C2-O7 H20-C1C2-C3 O6-C1C2-H19	O10-C1C2-O7 O6-C1C2-C3 H20-C1C2-H19	O10-C1C2-O7 O6-C1C2-H19 H20-C1C2-C3	O10-C1C2-O7 H20-C1C2-H19 O6-C1C2-C3
57	C1-C2C3-O8 H19-C2C3-H18 O7-C2C3-C4	C1-C2C3-O8 H19-C2C3-H18 O7-C2C3-C4	C1-C2C3-O8 O7-C2C3-C4 H19-C2C3-H18	C1-C2C3-O8 O7-C2C3-C4 H19-C2C3-H18
58	C2-C3C4-H17 O8-C3C4-C5 H18-C3C4-O9	C2-C3C4-H17 O8-C3C4-C5 H18-C3C4-O9	C2-C3C4-O9 O8-C3C4-C5 H18-C3C4-H17	C2-C3C4-O9 O8-C3C4-C5 H18-C3C4-H17
59	C3-C4C5-H16 O9-C4C5-H15 H17-C4C5-O10	C3-C4C5-H16 O9-C4C5-H15 H17-C4C5-O10	C3-C4C5-H16 O9-C4C5-O10 H17-C4C5-H15	C3-C4C5-H16 O9-C4C5-O10 H17-C4C5-H15

	β-Ribose	α-Ribose	β-Ribose (C1)[a]	α-Ribose (C1)
56	O10-C1C2-O7 H20-C1C2-H19 O6-C1C2-C3	O10-C1C2-O7 O6-C1C2-H19 H20-C1C2-C3	O10-C1C2-H19 H20-C1C2-C3 O6-C1C2-O7	O10-C1C2-H19 O6-C1C2-C3 H20-C1C2-O7
57	C1-C2C3-H18 H19-C2C3-O8 O7-C2C3-C4	C1-C2C3-H18 H19-C2C3-O8 O7-C2C3-C4	C1-C2C3-O8 H19-C2C3-C4 O7-C2C3-H18	C1-C2C3-O8 H19-C2C3-C4 O7-C2C3-H18
58	C2-C3C4-O9 O8-C3C4-H17 H18-C3C4-C5	C2-C3C4-O9 O8-C3C4-H17 H18-C3C4-C5	C2-C3C4-H17 H18-C3C4-O9 O8-C3C4-C5	C2-C3C4-H17 H18-C3C4-O9 O8-C3C4-C5
59	C3-C4C5-H16 O9-C4C5-O10 H17-C4C5-H15	C3-C4C5-H16 O9-C4C5-O10 H17-C4C5-H15	C3-C4C5-H15 O9-C4C5-H16 H17-C4C5-O10	C3-C4C5-H15 O9-C4C5-H16 H17-C4C5-O10

	β-Lyxose	α-Lyxose	α-Lyxose (C1)	All Models
56	O10-C1C2-H19 O6-C1C2-C3 H20-C1C2-O7	O10-C1C2-H19 H20-C1C2-C3 O6-C1C2-O7	O10-C1C2-O7 O6-C1C2-C3 H20-C1C2-H19	60 H15-C5O10-C1 H16-C5O10-C1
57	C1-C2C3-O8 O7-C2C3-H18 H19-C2C3-C4	C1-C2C3-O8 O7-C2C3-H18 H19-C2C3-C4	O7-C2C3-C4 C1-C2C3-H18 H19-C2C3-O8	61 C5-O1OC1-H20 C5-O1OC1-O6
58	C2-C3C4-O9 H18-C3C4-H17 O8-C3C4-C5	C2-C3C4-O9 H18-C3C4-H17 O8-C3C4-C5	C2-C3C4-H17 H18-C3C4-C5 O8-C3C4-O9	62 H20-C1O6-H11 63 H19-C2O7-H12 64 H18-C3O8-H13
59	C3-C4C5-H16 O9-C4C5-O10 H17-C4C5-H15	C3-C4C5-H16 O9-C4C5-O10 H17-C4C5-H15	C3-C4C5-H15 H17-C4C5-O10 O9-C4C5-H16	65 H17-C4O9-H14

[a]All molecules are set up as the 1C ring conformation of the D anomer unless otherwise noted. C1 notations are also for the D anomer.

TABLE XXX

COMPUTER INPUT AND CALCULATED CARTESIAN COORDINATES

CARTESIAN COORDINATES

BETA ARABINOSE				BOND	BOND	DIHEDRAL	ATOMIC
I	J	K	L	LENGTH	ANGLE	ANGLE	MASS
1	0	0	0	0.0	0.0	0.0	12.011149
2	1	0	0	1.523000	0.0	0.0	12.011149
3	2	1	0	1.523000	0.0	0.0	12.011149
4	3	2	1	1.523000	0.0	-56.000000	12.011149
5	4	3	2	1.523000	0.0	56.000000	12.011149
6	1	2	3	1.379999	0.0	-60.000000	15.999399
7	2	3	1	1.415000	0.0	-120.000000	15.999399
8	3	4	2	1.415000	0.0	120.000000	15.999399
9	4	5	3	1.415000	0.0	120.000000	15.999399
10	5	4	3	1.422999	0.0	-57.049988	15.999399
11	6	1	2	0.970000	0.0	180.000000	1.007970
12	7	2	1	0.970000	0.0	-60.000000	1.007970
13	8	3	2	0.970000	0.0	180.000000	1.007970
14	9	4	3	0.970000	0.0	180.000000	1.007970
15	5	4	3	1.096000	0.0	60.000000	1.007970
16	5	4	15	1.096000	0.0	120.000000	1.007970
17	4	5	3	1.092999	0.0	-120.000000	1.007970
18	3	4	2	1.092999	0.0	-120.000000	1.007970
19	2	3	1	1.092999	0.0	120.000000	1.007970
20	1	2	3	1.092999	0.0	180.000000	1.007970

ATOM NO.	X	Y	Z	MASS
1	0.0	0.0	0.0	12.011149
2	1.523000	0.0	0.0	12.011149
3	2.030665	1.435898	0.0	12.011149
4	1.442863	2.182178	1.190413	12.011149
5	-0.076976	2.096063	1.143435	12.011149
6	-0.460000	0.650538	-1.126763	15.999399
7	1.994664	-0.667037	-1.155342	15.999399
8	3.442600	1.436980	0.093061	15.999399
9	1.911469	1.598437	2.391196	15.999399
10	-0.474338	0.729781	1.125847	15.999399
11	-1.429999	0.650538	-1.126760	1.007970
12	1.671328	-0.209774	-1.947343	1.007970
13	3.765933	2.351504	0.093062	1.007970
14	1.537096	2.073741	3.149371	1.007970
15	-0.439939	2.548201	0.213358	1.007970
16	-0.499978	2.633110	2.000093	1.007970
17	1.749779	3.230455	1.150909	1.007970
18	1.726206	1.929973	-0.926199	1.007970
19	1.887331	-0.515244	0.892430	1.007970
20	-0.364333	-1.030489	0.000001	1.007970

TABLE XXXI

COMPUTER INPUT AND CALCULATED CARTESIAN COORDINATES

CARTESIAN COORDINATES

BETA LYXOSE

I	J	K	L	BOND LENGTH	BOND ANGLE	DIHEDRAL ANGLE	ATOMIC MASS
1	0	0	0	0.0	0.0	0.0	12.011149
2	1	0	0	1.523000	0.0	0.0	12.011149
3	2	1	0	1.523000	0.0	0.0	12.011149
4	3	2	1	1.523000	0.0	-56.000000	12.011149
5	4	3	2	1.523000	0.0	56.000000	12.011149
6	1	2	3	1.379999	0.0	180.000000	15.999399
7	2	3	1	1.415000	0.0	120.000000	15.999399
8	3	4	2	1.415000	0.0	120.000000	15.999399
9	4	5	3	1.415000	0.0	-120.000000	15.999399
10	5	4	3	1.422999	0.0	-57.049988	15.999399
11	6	1	2	0.970000	0.0	180.000000	1.007970
12	7	2	1	0.970000	0.0	180.000000	1.007970
13	8	3	2	0.970000	0.0	180.000000	1.007970
14	9	4	3	0.970000	0.0	180.000000	1.007970
15	5	4	3	1.096000	0.0	60.000000	1.007970
16	5	4	15	1.096000	0.0	120.000000	1.007970
17	4	5	3	1.092999	0.0	120.000000	1.007970
18	3	4	2	1.092999	0.0	-120.000000	1.007970
19	2	3	1	1.092999	0.0	-120.000000	1.007970
20	1	2	3	1.092999	0.0	-60.000000	1.007970

ATOM NO.	X	Y	Z	MASS
1	0.0	0.0	0.0	12.011149
2	1.523000	0.0	0.0	12.011149
3	2.030665	1.435898	0.0	12.011149
4	1.442863	2.182178	1.190413	12.011149
5	-0.076976	2.096063	1.143435	12.011149
6	-0.460000	-1.301075	0.000001	15.999399
7	1.994664	-0.667037	1.155342	15.999399
8	3.442600	1.436980	0.093061	15.999399
9	1.840197	3.539282	1.139271	15.999399
10	-0.474338	0.729781	1.125847	15.999399
11	-1.430000	-1.301075	0.000000	1.007970
12	2.964664	-0.667037	1.155341	1.007970
13	3.765933	2.351504	0.093062	1.007970
14	1.465824	4.014587	1.897446	1.007970
15	-0.439939	2.548201	0.213358	1.007970
16	-0.499978	2.633110	2.000093	1.007970
17	1.804832	1.731275	2.117944	1.007970
18	1.726206	1.929973	-0.926199	1.007970
19	1.887331	-0.515244	-0.892430	1.007970
20	-0.364333	0.515245	-0.892430	1.007970

TABLE XXXII

COMPUTER INPUT AND CALCULATED CARTESIAN COORDINATES

CARTESIAN COORDINATES

ALPHA XYLOSE

I	J	K	L	BOND LENGTH	BOND ANGLE	DIHEDRAL ANGLE	ATOMIC MASS
1	0	0	0	0.0	0.0	0.0	12.011149
2	1	0	0	1.523000	0.0	0.0	12.011149
3	2	1	0	1.523000	0.0	0.0	12.011149
4	3	2	1	1.523000	0.0	-56.000000	12.011149
5	4	3	2	1.523000	0.0	56.000000	12.011149
6	1	2	3	1.379999	0.0	-60.000000	15.999399
7	2	3	1	1.415000	0.0	-120.000000	15.999399
8	3	4	2	1.415000	0.0	120.000000	15.999399
9	4	5	3	1.415000	0.0	-120.000000	15.999399
10	5	4	3	1.422999	0.0	-57.049988	15.999399
11	6	1	2	0.970000	0.0	180.000000	1.007970
12	7	2	1	0.970000	0.0	-60.000000	1.007970
13	8	3	2	0.970000	0.0	180.000000	1.007970
14	9	4	3	0.970000	0.0	180.000000	1.007970
15	5	4	3	1.096000	0.0	60.000000	1.007970
16	5	4	15	1.096000	0.0	120.000000	1.007970
17	4	5	3	1.092999	0.0	120.000000	1.007970
18	3	4	2	1.092999	0.0	-120.000000	1.007970
19	2	3	1	1.092999	0.0	120.000000	1.007970
20	1	2	3	1.092999	0.0	180.000000	1.007970

ATOM NO.	X	Y	Z	MASS
1	0.0	0.0	0.0	12.011149
2	1.523000	0.0	0.0	12.011149
3	2.030665	1.435898	0.0	12.011149
4	1.442863	2.182178	1.190413	12.011149
5	-0.076976	2.096063	1.143435	12.011149
6	-0.460000	0.650538	-1.126763	15.999399
7	1.994664	-0.667037	-1.155342	15.999399
8	3.442600	1.436980	0.093061	15.999399
9	1.840197	3.539282	1.139271	15.999399
10	-0.474338	0.729781	1.125847	15.999399
11	-1.429999	0.650538	-1.126760	1.007970
12	1.671328	-0.209774	-1.947343	1.007970
13	3.765933	2.351504	0.093062	1.007970
14	1.465824	4.014587	1.897446	1.007970
15	-0.439939	2.548201	0.213358	1.007970
16	-0.499978	2.633110	2.000093	1.007970
17	1.804832	1.731275	2.117944	1.007970
18	1.726206	1.929973	-0.926199	1.007970
19	1.887331	-0.515244	0.892430	1.007970
20	-0.364333	-1.030489	0.000001	1.007970

TABLE XXXIII

COMPUTER INPUT FOR THE G MATRIX CALCULATION

```
-09
-09 1       20  65    1    0    1
   BETA ARABINOSE 1C-D RING CONFORMATION   1-2-3-4 = A-E-E-A

  1  2     1.523000  1  3    2.030665  2  3    1.435898  1  4    1.442863
  2  4     2.182178  3  4    1.190413  1  5   -0.076976  2  5    2.096063
  3  5     1.143435  1  6   -0.460000  2  6    0.650538  3  6   -1.126763
  1  7     1.994664  2  7   -0.667037  3  7   -1.155342  1  8    3.442600
  2  8     1.436980  3  8    0.093061  1  9    1.911469  2  9    1.598437
  3  9     2.391196  1 10   -0.474338  2 10    0.729781  3 10    1.125847
  1 11    -1.429999  2 11    0.650538  3 11   -1.126760  1 12    1.671328
  2 12    -0.209774  3 12   -1.947343  1 13    3.765933  2 13    2.351504
  3 13     0.093062  1 14    1.537096  2 14    2.073741  3 14    3.149371
  1 15    -0.439939  2 15    2.548201  3 15    0.213358  1 16   -0.449978
  2 16     2.633110  3 16    2.000093  1 17    1.749779  2 17    3.230455
  3 17     1.150909  1 18    1.726206  2 18    1.929973  3 18   -0.926199
  1 19     1.887331  2 19   -0.515244  3 19    0.892430  1 20   -0.364333
  2 20    -1.030489 -1  0    0.0
  1  1  1  2              2  1  2  3              3  1  3  4
  4  1  4  5              5  1  5 10              6  1 10  1
  7  1  1  6              8  1  2  7              9  1  3  8
 10  1  4  9             11  1  5 15             12  1  5 16
 13  1  4 17             14  1  3 18             15  1  2 19
 16  1  1 20             17  1  6 11             18  1  7 12
 19  1  8 13             20  1  9 14             21  2  1  2  3
 22  2  2  3  4          23  2  3  4 -5          24  2  4  5 10
 25  2  5 10  1          26  2 10  1  2          27  2 10  1  6
 28  2  6  1  2          29  2  7  2  1          30  2  7  2  3
 31  2  8  3  2          32  2  8  3  4          33  2  9  4  3
 34  2  9  4  5          35  2 11  6  1          36  2 12  7  2
 37  2 13  8  3          38  2 14  9  4          39  2 15  5 10
 40  2 16  5 10          41  2 17  4  9          42  2 18  3  8
 43  2 19  2  7          44  2 20  1  6          45  2 10  1 20
 46  2 20  1  2          47  2 19  2  1          48  2 19  2  3
 49  2 18  3  2          50  2 18  3  4          51  2 17  4  3
 52  2 17  4  5          53  2 15  5  4          54  2 16  5  4
 55  2 15  5 16          56  4 10  1  2  7         0  4 20  1  2  3
  0  4  6  1  2 19       57  4  1  2  3  8         0  4 19  2  3 18
  0  4  7  2  3  4       58  4  2  3  4 17         0  4  8  3  4  5
  0  4 18  3  4  9       59  4  3  4  5 16         0  4  9  4  5 15
  0  4 17  4  5 10       60  4 15  5 10  1         0  4 16  5 10  1
 61  4  5 10  1  6        0  4  5 10  1 20        62  4 20  1  6 11
 63  4 19  2  7 12       64  4 18  3  8 13        65  4 17  4  9 14
-02
-06              BETA ARABINOSE
   12.011149   12.011149   12.011149   12.011149   12.011149   15.999399
   15.999399   15.999399   15.999399   15.999399    1.0079700   1.0079700
    1.0079700   1.0079700   1.0079700   1.0079700   1.0079700   1.0079700
    1.0079700   1.0079700
```

TABLE XXXIV

COMPUTER INPUT FOR THE $\underset{\sim}{G}$ MATRIX CALCULATION

```
-09
-09  2      20  65   1    0    1
  BETA LYXOSE  1C-D RING CONFORMATION    1-2-3-4 = E-A-E-E

  1  2     1.523000   1  3     2.030665   2  3     1.435898   1  4     1.442863
  2  4     2.182178   3  4     1.190413   1  5    -0.076976   2  5     2.096063
  3  5     1.143435   1  6    -0.460000   2  6    -1.301075   1  7     1.994664
  2  7    -0.667037   3  7     1.155342   1  8     3.442600   2  8     1.436980
  3  8     0.093061   1  9     1.840197   2  9     3.539282   3  9     1.139271
  1 10    -0.474338   2 10     0.729781   3 10     1.125847   1 11    -1.430000
  2 11    -1.301075   1 12     2.964664   2 12    -0.667037   3 12     1.155341
  1 13     3.765933   2 13     2.351504   3 13     0.093062   1 14     1.465824
  2 14     4.014587   3 14     1.897446   1 15    -0.439939   2 15     2.548201
  3 15     0.213358   1 16    -0.499978   2 16     2.633110   3 16     2.000093
  1 17     1.804832   2 17     1.731275   3 17     2.117944   1 18     1.726206
  2 18     1.929973   3 18    -0.926199   1 19     1.887331   2 19    -0.515244
  3 19    -0.892430   1 20    -0.364333   2 20     0.515245   3 20    -0.892430
 -1  0     0.0
  1  1  1  2                  2  1  2  3                  3  1  3  4
  4  1  4  5                  5  1  5 10                  6  1 10  1
  7  1  1  6                  8  1  2  7                  9  1  3  8
 10  1  4  9                 11  1  5 15                 12  1  5 16
 13  1  4 17                 14  1  3 18                 15  1  2 19
 16  1  1 20                 17  1  6 11                 18  1  7 12
 19  1  8 13                 20  1  9 14                 21  2  1  2  3
 22  2  2  3  4              23  2  3  4  5              24  2  4  5 10
 25  2  5 10  1              26  2 10  1  2              27  2 10  1  6
 28  2  6  1  2              29  2  7  2  1              30  2  7  2  3
 31  2  8  3  2              32  2  8  3  4              33  2  9  4  3
 34  2  9  4  5              35  2 11  6  1              36  2 12  7  2
 37  2 13  8  3              38  2 14  9  4              39  2 15  5 10
 40  2 16  5 10              41  2 17  4  9              42  2 18  3  8
 43  2 19  2  7              44  2 20  1  6              45  2 10  1 20
 46  2 20  1  2              47  2 19  2  1              48  2 19  2  3
 49  2 18  3  2              50  2 18  3  4              51  2 17  4  3
 52  2 17  4  5              53  2 15  5  4              54  2 16  5  4
 55  2 15  5 16              56  4 10  1  2 19            0  4  6  1  2  3
  0  4 20  1  2  7           57  4  1  2  3  8            0  4  7  2  3 18
  0  4 19  2  3  4           58  4  2  3  4  9            0  4 18  3  4 17
  0  4  8  3  4  5           59  4  3  4  5 16            0  4  9  4  5 10
  0  4 17  4  5 15           60  4 15  5 10  1            0  4 16  5 10  1
 61  4  5 10  1  6            0  4  5 10  1 20           62  4 20  1  6 11
 63  4 19  2  7 12           64  4 18  3  8 13           65  4 17  4  9 14
-02
-06                BETA LYXOSE
    12.011149   12.011149   12.011149   12.011149   12.011149   15.999399
    15.999399   15.999399   15.999399   15.999399    1.0079700   1.0079700
     1.0079700   1.0079700   1.0079700   1.0079700   1.0079700   1.0079700
     1.0079700   1.0079700
```

TABLE XXXV

COMPUTER INPUT FOR THE G MATRIX CALCULATION

```
-09
-09  3     20  65   1   0   1
  ALPHA XYLOSE  1C-D RING CONFORMATION    1-2-3-4 = A-E-E-E

  1  2    1.523000  1  3    2.030665  2  3    1.435898  1  4    1.442863
  2  4    2.182178  3  4    1.190413  1  5   -0.076976  2  5    2.096063
  3  5    1.143435  1  6   -0.460000  2  6    0.650538  3  6   -1.126763
  1  7    1.994664  2  7   -0.667037  3  7   -1.155342  1  8    3.442600
  2  8    1.436980  3  8    0.093061  1  9    1.840197  2  9    3.539282
  3  9    1.139271  1 10   -0.474338  2 10    0.729781  3 10    1.125847
  1 11   -1.429999  2 11    0.650538  3 11   -1.126760  1 12    1.671328
  2 12   -0.209774  3 12   -1.947343  1 13    3.765933  2 13    2.351504
  3 13    0.093062  1 14    1.465824  2 14    4.014587  3 14    1.897446
  1 15   -0.439939  2 15    2.548201  3 15    0.213358  1 16   -0.499978
  2 16    2.633110  3 16    2.000093  1 17    1.804832  2 17    1.731275
  3 17    2.117944  1 18    1.726206  2 18    1.929973  3 18   -0.926199
  1 19    1.887331  2 19   -0.515244  3 19    0.892430  1 20   -0.364333
  2 20   -1.030489 -1  0    0.0
  1  1  1  2              2  1  2  3              3  1  3  4
  4  1  4  5              5  1  5 10              6  1 10  1
  7  1  1  6              8  1  2  7              9  1  3  8
 10  1  4  9             11  1  5 15             12  1  5 16
 13  1  4 17             14  1  3 18             15  1  2 19
 16  1  1 20             17  1  6 11             18  1  7 12
 19  1  8 13             20  1  9 14             21  2  1  2  3
 22  2  2  3  4          23  2  3  4  5          24  2  4  5 10
 25  2  5 10  1          26  2 10  1  2          27  2 10  1  6
 28  2  6  1  2          29  2  7  2  1          30  2  7  2  3
 31  2  8  3  2          32  2  8  3  4          33  2  9  4  3
 34  2  9  4  5          35  2 11  6  1          36  2 12  7  2
 37  2 13  8  3          38  2 14  9  4          39  2 15  5 10
 40  2 16  5 10          41  2 17  4  9          42  2 18  3  8
 43  2 19  2  7          44  2 20  1  6          45  2 10  1 20
 46  2 20  1  2          47  2 19  2  1          48  2 19  2  3
 49  2 18  3  2          50  2 18  3  4          51  2 17  4  3
 52  2 17  4  5          53  2 15  5  4          54  2 16  5  4
 55  2 15  5 16          56  4 10  1  2  7        0  4  6  1  2 19
  0  4 20  1  2  3       57  4  1  2  3  8        0  4  7  2  3  4
  0  4 19  2  3 18       58  4  2  3  4  9        0  4 18  3  4 17
  0  4  8  3  4  5       59  4  3  4  5 16        0  4  9  4  5 10
  0  4 17  4  5 15       60  4 16  5 10  1        0  4 15  5 10  1
 61  4  5 10  1  6        0  4  5 10  1 20       62  4 20  1  6 11
 63  4 19  2  7 12       64  4 18  3  8 13       65  4 17  4  9 14
-02
-06            ALPHA XYLOSE
   12.011149   12.011149   12.011149   12.011149   12.011149   15.999399
   15.999399   15.999399   15.999399   15.999399    1.0079700   1.0079700
    1.0079700   1.0079700   1.0079700   1.0079700   1.0079700   1.0079700
    1.0079700   1.0079700
```

TABLE XXXVI

$\underset{\sim}{Z}$ MATRIX ELEMENTS OF THE PENTOSES

ELEMENTS		FORCE CONSTANT NUMBER										
ROW	COL	B-A*	B-L	A-X	A-A	A-L	A-L	B-X	B-R	A-R	A-R	B-R
1	1	1	1	1	1	1	1	1	1	1	1	1
1	2	22	22	22	22	22	22	22	22	22	22	22
1	6	25	25	25	25	25	25	25	25	25	25	25
1	7	26	27	26	27	26	27	27	26	27	26	27
1	8	27	26	27	27	26	27	27	26	26	27	27
1	15	79	80	80	80	80	80	80	80	80	80	80
1	16	79	80	80	80	80	80	80	80	80	80	80
1	21	29	29	29	29	29	29	29	29	29	29	29
1	28	33	33	33	33	33	33	33	33	33	33	33
1	29	33	33	33	33	33	33	33	33	33	33	33
1	46	34	34	34	34	34	34	34	34	34	34	34
1	47	34	34	34	34	34	34	34	34	34	34	34
2	2	1	1	1	1	1	1	1	1	1	1	1
2	3	22	22	22	22	22	22	22	22	22	22	22
2	8	27	26	27	27	26	27	27	26	26	27	27
2	9	27	27	27	27	27	26	27	27	27	26	26
2	14	79	80	80	80	80	80	80	80	80	80	80
2	15	79	80	80	80	80	80	80	80	80	80	80
2	21	29	29	29	29	29	29	29	29	29	29	29
2	22	29	29	29	29	29	29	29	29	29	29	29
2	30	33	33	33	33	33	33	33	33	33	33	33
2	31	33	33	33	33	33	33	33	33	33	33	33
2	48	34	34	34	34	34	34	34	34	34	34	34
2	49	34	34	34	34	34	34	34	34	34	34	34
3	3	1	1	1	1	1	1	1	1	1	1	1
3	4	22	22	22	22	22	22	22	22	22	22	22
3	10	26	27	27	26	27	26	27	26	26	27	27
3	13	79	80	80	80	80	80	80	80	80	80	80
3	14	79	80	80	80	80	80	80	80	80	80	80
3	22	29	29	29	29	29	29	29	29	29	29	29
3	23	29	29	29	29	29	29	29	29	29	29	29
3	32	33	33	33	33	33	33	33	33	33	33	33
3	33	33	33	33	33	33	33	33	33	33	33	33
3	50	34	34	34	34	34	34	34	34	34	34	34
3	51	34	34	34	34	34	34	34	34	34	34	34
4	4	1	1	1	1	1	1	1	1	1	1	1
4	5	25	25	25	25	25	25	25	25	25	25	25
4	10	26	27	27	26	27	26	27	26	26	27	27
4	11	80	80	80	80	80	80	80	80	80	80	80
4	12	79	80	80	80	80	80	80	80	80	80	80
4	13	79	80	80	80	80	80	80	80	80	80	80
4	23	29	29	29	29	29	29	29	29	29	29	29
4	24	29	29	29	29	29	29	29	29	29	29	29
4	34	33	33	33	33	33	33	33	33	33	33	33
4	52	34	34	34	34	34	34	34	34	34	34	34
4	53	68	68	68	68	68	68	68	68	68	68	68
4	54	68	68	68	68	68	68	68	68	68	68	68
5	5	2	2	2	2	2	2	2	2	2	2	2
5	6	23	23	23	23	23	23	23	23	23	23	23
5	11	79	80	80	80	80	80	80	80	80	80	80
5	12	79	80	80	80	80	80	80	80	80	80	80
5	24	30	30	30	30	30	30	30	30	30	30	30
5	25	30	30	30	30	30	30	30	30	30	30	30
5	39	69	69	69	69	69	69	69	69	69	69	69
5	40	69	69	69	69	69	69	69	69	69	69	69
6	6	2	2	2	2	2	2	2	2	2	2	2
6	7	24	24	24	24	24	24	24	24	24	24	24
6	16	79	80	80	80	80	80	80	80	80	80	80

TABLE XXXVI (Continued)

$\underset{\sim}{Z}$ MATRIX ELEMENTS OF THE PENTOSES

ELEMENTS		FORCE CONSTANT NUMBER										
ROW	COL	B-A*	B-L	A-X	A-A	A-L	A-L	B-X	B-R	A-R	A-R	B-R
6	25	30	30	30	30	30	30	30	30	30	30	30
6	26	30	30	30	30	30	30	30	30	30	30	30
6	27	31	31	31	31	31	31	31	31	31	31	31
6	45	35	35	35	35	35	35	35	35	35	35	35
7	7	3	3	3	3	3	3	3	3	3	3	3
7	16	78	80	80	80	80	80	80	80	80	80	80
7	27	31	31	31	31	31	31	31	31	31	31	31
7	28	32	32	32	32	32	32	32	32	32	32	32
7	35	36	36	36	36	36	36	36	36	36	36	36
7	44	35	35	35	35	35	35	35	35	35	35	35
8	8	4	4	4	4	4	4	4	4	4	4	4
8	15	78	80	80	80	80	80	80	80	80	80	80
8	29	32	32	32	32	32	32	32	32	32	32	32
8	30	32	32	32	32	32	32	32	32	32	32	32
8	36	36	36	36	36	36	36	36	36	36	36	36
8	43	35	35	35	35	35	35	35	35	35	35	35
9	9	4	4	4	4	4	4	4	4	4	4	4
9	14	78	80	80	80	80	80	80	80	80	80	80
9	31	32	32	32	32	32	32	32	32	32	32	32
9	32	32	32	32	32	32	32	32	32	32	32	32
9	37	36	36	36	36	36	36	36	36	36	36	36
9	42	35	35	35	35	35	35	35	35	35	35	35
10	10	4	4	4	4	4	4	4	4	4	4	4
10	13	78	80	80	80	80	80	80	80	80	80	80
10	33	32	32	32	32	32	32	32	32	32	32	32
10	34	32	32	32	32	32	32	32	32	32	32	32
10	38	36	36	36	36	36	36	36	36	36	36	36
10	41	35	35	35	35	35	35	35	35	35	35	35
11	11	6	6	6	6	6	6	6	6	6	6	6
11	12	28	28	28	28	28	28	28	28	28	28	28
11	39	80	80	80	80	80	80	80	80	80	80	80
11	53	80	80	80	80	80	80	80	80	80	80	80
11	55	80	80	80	80	80	80	80	80	80	80	80
12	12	6	6	6	6	6	6	6	6	6	6	6
12	40	80	80	80	80	80	80	80	80	80	80	80
12	54	80	80	80	80	80	80	80	80	80	80	80
12	55	80	80	80	80	80	80	80	80	80	80	80
13	13	7	7	7	7	7	7	7	7	7	7	7
13	41	80	80	80	80	80	80	80	80	80	80	80
13	51	80	80	80	80	80	80	80	80	80	80	80
13	52	80	80	80	80	80	80	80	80	80	80	80
14	14	7	7	7	7	7	7	7	7	7	7	7
14	42	80	80	80	80	80	80	80	80	80	80	80
14	49	80	80	80	80	80	80	80	80	80	80	80
14	50	80	80	80	80	80	80	80	80	80	80	80
15	15	7	7	7	7	7	7	7	7	7	7	7
15	43	80	80	80	80	80	80	80	80	80	80	80
15	47	80	80	80	80	80	80	80	80	80	80	80
15	48	80	80	80	80	80	80	80	80	80	80	80
16	16	7	7	7	7	7	7	7	7	7	7	7
16	44	80	80	80	80	80	80	80	80	80	80	80
16	45	80	80	80	80	80	80	80	80	80	80	80
16	46	80	80	80	80	80	80	80	80	80	80	80
17	17	5	5	5	5	5	5	5	5	5	5	5
18	18	5	5	5	5	5	5	5	5	5	5	5
19	19	5	5	5	5	5	5	5	5	5	5	5
20	20	5	5	5	5	5	5	5	5	5	5	5
21	21	8	8	8	8	8	8	8	8	8	8	8

TABLE XXXVI (Continued)

$\underset{\sim}{L}$ MATRIX ELEMENTS OF THE PENTOSES

ELEMENTS		FORCE CONSTANT NUMBER										
ROW	COL	B-A*	B-L	A-X	A-A	A-L	A-L	B-X	B-R	A-R	A-R	B-R
21	22	37	37	37	37	37	37	37	37	37	37	37
21	26	37	37	37	37	37	37	37	37	37	37	37
21	28	38	39	38	39	38	39	39	38	39	38	39
21	29	40	40	40	40	40	40	40	40	40	40	40
21	30	40	40	40	40	40	40	40	40	40	40	40
21	31	39	39	39	39	39	38	39	39	39	38	38
21	46	50	49	50	49	50	49	49	50	49	50	49
21	47	48	48	48	48	48	48	48	48	48	48	48
21	48	48	48	48	48	48	48	48	48	48	48	48
21	49	49	49	49	49	49	50	49	49	49	50	50
22	22	8	8	8	8	8	8	8	8	8	8	8
22	23	37	37	37	37	37	37	37	37	37	37	37
22	30	39	38	39	39	38	39	39	38	38	39	39
22	31	40	40	40	40	40	40	40	40	40	40	40
22	32	40	40	40	40	40	40	40	40	40	40	40
22	33	38	39	39	38	39	38	39	38	38	39	39
22	48	49	50	49	49	50	49	49	50	50	49	49
22	49	48	48	48	48	48	48	48	48	48	48	48
22	50	48	48	48	48	48	48	48	48	48	48	48
22	51	50	49	49	50	49	50	49	50	50	49	49
23	23	8	8	8	8	8	8	8	8	8	9	8
23	24	37	37	37	37	37	37	37	37	37	37	37
23	32	39	39	39	39	39	38	39	39	39	38	38
23	33	40	40	40	40	40	40	40	40	40	40	40
23	34	40	40	40	40	40	40	40	40	40	40	40
23	50	49	49	49	49	49	50	49	49	49	50	50
23	51	48	48	48	48	48	48	48	48	48	48	48
23	52	48	48	48	48	48	48	48	48	48	48	48
23	53	49	49	49	49	59	50	49	50	50	49	49
23	54	50	50	50	50	50	49	50	49	49	50	50
24	24	9	9	9	9	9	9	9	9	9	9	9
24	25	37	37	37	37	37	37	37	37	37	37	37
24	34	46	47	47	46	47	46	47	46	46	47	47
24	39	51	51	51	51	51	51	51	51	51	51	51
24	40	51	51	51	51	51	51	51	51	51	51	51
24	52	50	49	49	50	49	50	49	50	50	49	49
24	53	48	48	48	48	48	48	48	48	48	48	48
24	54	48	48	48	48	48	48	48	48	48	48	48
25	25	10	10	10	10	10	10	10	10	10	10	10
25	26	37	37	37	37	37	37	37	37	37	37	37
25	27	45	45	44	45	44	45	45	44	45	44	45
25	39	52	52	52	52	52	53	52	53	53	52	52
25	40	53	53	53	53	53	52	53	52	52	53	53
25	45	53	52	53	52	53	52	52	53	52	53	52
26	26	9	9	9	9	9	9	9	9	9	9	9
26	27	43	43	43	43	43	43	43	43	43	43	43
26	28	41	41	41	41	41	41	41	43	43	41	41
26	29	47	46	47	47	46	47	47	46	46	47	47
26	45	57	57	57	57	57	57	57	57	57	57	57
26	46	57	57	57	57	57	57	57	57	57	57	57
27	27	11	11	11	11	11	11	11	11	11	11	11
27	28	43	43	43	43	43	43	43	43	43	43	43
27	35	58	58	58	58	58	58	58	58	58	58	58
27	44	57	57	57	57	57	57	57	57	57	57	57
27	45	57	57	57	57	57	57	57	57	57	57	57
28	28	12	12	12	12	12	12	12	12	12	12	12
28	29	42	42	42	42	74	42	42	74	42	42	42
28	35	58	58	58	58	58	58	58	58	58	58	58

TABLE XXXVI (Continued)

$\underset{\sim}{Z}$ MATRIX ELEMENTS OF THE PENTOSES

ELEMENTS		FORCE CONSTANT NUMBER										
ROW	COL	B-A*	B-L	A-X	A-A	A-L	A-L	B-X	B-R	A-R	A-R	B-R
28	44	57	57	57	57	57	57	57	57	57	57	57
28	46	57	57	57	57	57	57	57	57	57	57	57
28	47	56	55	56	55	55	55	55	55	55	56	55
29	29	12	12	12	12	12	12	12	12	12	12	12
29	30	41	41	41	41	41	41	41	41	41	41	41
29	36	58	58	58	58	58	58	58	58	58	58	58
29	43	54	54	54	54	54	54	54	54	54	54	54
29	46	55	56	55	55	55	55	55	55	56	55	55
29	47	54	54	54	54	54	54	54	54	54	54	54
30	30	12	12	12	12	12	12	12	12	12	12	12
30	31	42	42	42	42	42	42	42	42	42	42	42
30	36	58	58	58	58	58	58	58	58	58	58	58
30	43	54	54	54	54	54	54	54	54	54	54	54
30	48	54	54	54	54	54	54	54	54	54	54	54
30	49	55	56	55	55	56	55	55	56	56	55	55
31	31	12	12	12	12	12	12	12	12	12	12	12
31	32	41	41	41	41	41	41	41	41	41	41	41
31	37	58	58	58	58	58	58	58	58	58	58	58
31	42	54	54	54	54	54	54	54	54	54	54	54
31	48	55	55	55	55	55	56	55	55	55	55	56
31	49	54	54	54	54	54	54	54	54	54	54	54
32	32	12	12	12	12	12	12	12	12	12	12	12
32	33	42	42	42	42	42	74	42	42	42	42	42
32	37	58	58	58	58	58	58	58	58	58	58	58
32	42	54	54	54	54	54	54	54	54	54	54	54
32	50	54	54	54	54	54	54	54	54	54	54	54
32	51	55	55	55	55	55	55	55	55	55	56	56
33	33	12	12	12	12	12	12	12	12	12	12	12
33	34	41	41	41	41	41	41	41	41	41	41	41
33	38	58	58	58	58	58	58	58	58	58	58	58
33	41	54	54	54	54	54	54	54	54	54	54	54
33	50	56	55	55	56	55	55	55	56	56	55	55
33	51	54	54	54	54	54	54	54	54	54	54	54
34	34	12	12	12	12	12	12	12	12	12	12	12
34	38	58	58	58	58	58	58	58	58	58	58	58
34	41	54	54	54	54	54	54	54	54	54	54	54
34	52	54	54	54	54	54	54	54	54	54	54	54
34	53	56	55	55	56	55	55	55	55	55	55	55
34	54	55	55	55	55	55	56	55	56	56	55	55
35	35	13	73	13	13	13	13	13	13	13	13	13
35	44	59	59	59	59	59	59	59	59	59	59	59
36	36	13	13	13	13	13	13	13	13	13	13	13
36	43	60	59	60	60	59	60	60	60	60	60	60
37	37	13	13	13	13	13	13	13	13	13	13	13
37	42	59	59	59	59	59	59	59	59	59	59	59
38	38	73	13	13	13	13	13	13	13	13	13	13
38	41	59	59	59	59	59	59	59	59	59	59	59
39	39	14	14	14	14	14	14	14	14	14	14	14
39	40	71	71	71	71	71	71	71	71	71	71	71
39	53	61	61	61	61	61	61	61	61	61	61	61
39	55	72	72	72	72	72	72	72	72	72	72	72
40	40	14	14	14	14	14	14	14	14	14	14	14
40	54	61	61	61	61	61	61	61	61	61	61	61
40	55	72	72	72	72	72	72	72	72	72	72	72
41	41	15	15	15	15	15	15	15	15	15	15	15
41	51	63	63	63	63	63	63	63	63	63	63	63
41	52	63	63	63	63	63	63	63	63	63	63	63
42	42	15	15	15	15	15	15	15	15	15	15	15

TABLE XXXVI (Continued)

L MATRIX ELEMENTS OF THE PENTOSES

ELEMENTS		FORCE CONSTANT NUMBER										
ROW	COL	B-A*	B-L	A-X	A-A	A-L	A-L	B-X	B-R	A-R	A-R	B-R
42	49	63	63	63	63	63	63	63	63	63	63	63
42	50	63	63	63	63	63	63	63	63	63	63	63
43	43	15	15	15	15	15	15	15	15	15	15	15
43	47	63	63	63	63	63	63	63	63	63	63	63
43	48	63	63	63	63	63	63	63	63	63	63	63
44	44	15	15	15	15	15	15	15	15	15	15	15
44	45	64	64	64	64	64	64	64	64	64	64	64
44	46	63	63	63	63	63	63	63	63	63	63	63
45	45	15	15	15	15	15	15	15	15	15	15	15
45	46	63	63	63	63	63	63	63	63	63	63	63
46	46	16	16	16	16	16	16	16	16	16	16	16
46	47	66	66	66	67	66	67	67	66	66	66	67
47	47	16	16	16	16	16	16	16	16	16	16	16
47	48	65	65	65	65	65	65	65	65	65	65	65
48	48	16	16	16	16	16	16	16	16	16	16	16
48	49	67	66	67	67	66	66	67	66	66	66	66
49	49	16	16	16	16	16	16	16	16	16	16	16
49	50	65	65	65	65	65	65	65	65	65	65	65
50	50	16	16	16	16	16	16	16	16	16	16	16
50	51	66	67	67	66	67	66	67	66	66	66	66
51	51	16	16	16	16	16	16	16	16	16	16	16
51	52	65	65	65	65	65	65	65	65	65	65	65
52	52	16	16	16	16	16	16	16	16	16	16	16
52	53	66	67	67	66	67	66	67	66	66	67	67
52	54	66	66	66	66	66	66	66	66	66	66	66
53	53	17	17	17	17	17	17	17	17	17	17	17
53	54	70	70	70	70	70	70	70	70	70	70	70
53	55	62	62	62	62	62	62	62	62	62	62	62
54	54	17	17	17	17	17	17	17	17	17	17	17
54	55	62	62	62	62	62	62	62	62	62	62	62
55	55	18	18	18	18	18	18	18	18	18	18	18
56	56	19	19	19	19	19	19	19	19	19	19	19
57	57	19	19	19	19	19	19	19	19	19	19	19
58	58	19	19	19	19	19	19	19	19	19	19	19
59	59	19	19	19	19	19	19	19	19	19	19	19
60	60	20	20	20	20	20	20	20	20	20	20	20
61	61	20	20	20	20	20	20	20	20	20	20	20
62	62	21	21	21	21	21	21	21	21	21	21	21
63	63	21	21	21	21	21	21	21	21	21	21	21
64	64	21	21	21	21	21	21	21	21	21	21	21
65	65	21	21	21	21	21	21	21	21	21	21	21
3	9	27	27	27	27	27	27	27	27	27	27	27
1	26	29	29	29	29	29	29	29	29	29	29	29
26	47	49	50	49	49	50	49	49	50	50	49	49

*Pentose labels: A = arabinose, X = Xylose, L = lyxose, R = ribose, A- = alpha anomer, and B- = beta anomer.

TABLE XXXVII

COMPUTER INPUT AND CALCULATED CARTESIAN COORDINATES

CARTESIAN COORDINATES
ALPHA ARABINOSE

I	J	K	L	BOND LENGTH	BOND ANGLE	DIHEDRAL ANGLE	ATOMIC MASS
1	0	0	0	0.0	0.0	0.0	12.011149
2	1	0	0	1.523000	0.0	0.0	12.011149
3	2	1	0	1.523000	0.0	0.0	12.011149
4	3	2	1	1.523000	0.0	-56.000000	12.011149
5	4	3	2	1.523000	0.0	56.000000	12.011149
6	1	2	3	1.379999	0.0	180.000000	15.999399
7	2	3	1	1.415000	0.0	-120.000000	15.999399
8	3	4	2	1.415000	0.0	120.000000	15.999399
9	4	5	3	1.415000	0.0	120.000000	15.999399
10	5	4	3	1.422999	0.0	-57.049988	15.999399
11	6	1	2	0.970000	0.0	180.000000	1.007970
12	7	2	1	0.970000	0.0	-60.000000	1.007970
13	8	3	2	0.970000	0.0	180.000000	1.007970
14	9	4	3	0.970000	0.0	180.000000	1.007970
15	5	4	3	1.096000	0.0	60.000000	1.007970
16	5	4	15	1.096000	0.0	120.000000	1.007970
17	4	5	3	1.092999	0.0	-120.000000	1.007970
18	3	4	2	1.092999	0.0	-120.000000	1.007970
19	2	3	1	1.092999	0.0	120.000000	1.007970
20	1	2	3	1.092999	0.0	-60.000000	1.007970

ATOM NO.	X	Y	Z	MASS
1	0.0	0.0	0.0	12.011149
2	1.523000	0.0	0.0	12.011149
3	2.030665	1.435898	0.0	12.011149
4	1.442863	2.182178	1.190413	12.011149
5	-0.076976	2.096063	1.143435	12.011149
6	-0.460000	-1.301075	0.000001	15.999399
7	1.994664	-0.667037	-1.155342	15.999399
8	3.442600	1.436980	0.093061	15.999399
9	1.911469	1.598437	2.391196	15.999399
10	-0.474338	0.729781	1.125847	15.999399
11	-1.430000	-1.301075	0.000000	1.007970
12	1.671328	-0.209774	-1.947343	1.007970
13	3.765933	2.351504	0.093062	1.007970
14	1.537096	2.073741	3.149371	1.007970
15	-0.439939	2.548201	0.213358	1.007970
16	-0.499978	2.633110	2.000093	1.007970
17	1.749779	3.230455	1.150909	1.007970
18	1.726206	1.929973	-0.926199	1.007970
19	1.887331	-0.515244	0.892430	1.007970
20	-0.364333	0.515245	-0.892430	1.007970

TABLE XXXVIII

COMPUTER INPUT AND CALCULATED CARTESIAN COORDINATES

CARTESIAN COORDINATES

ALPHA LYXOSE C1-D

I	J	K	L	BOND LENGTH	BOND ANGLE	DIHEDRAL ANGLE	ATOMIC MASS
1	0	0	0	0.0	0.0	0.0	12.011149
2	1	0	0	1.523000	0.0	0.0	12.011149
3	2	1	0	1.523000	0.0	0.0	12.011149
4	3	2	1	1.523000	0.0	56.000000	12.011149
5	4	3	2	1.523000	0.0	-56.000000	12.011149
6	1	2	3	1.379999	0.0	180.000000	15.999399
7	2	3	1	1.415000	0.0	120.000000	15.999399
8	3	4	2	1.415000	0.0	120.000000	15.999399
9	4	5	3	1.415000	0.0	-120.000000	15.999399
10	5	4	3	1.422999	0.0	57.049988	15.999399
11	6	1	2	0.970000	0.0	180.000000	1.007970
12	7	2	3	0.970000	0.0	180.000000	1.007970
13	8	3	2	0.970000	0.0	180.000000	1.007970
14	9	4	3	0.970000	0.0	180.000000	1.007970
15	5	4	3	1.096000	0.0	180.000000	1.007970
16	5	4	15	1.096000	0.0	120.000000	1.007970
17	4	5	3	1.092999	0.0	120.000000	1.007970
18	3	4	2	1.092999	0.0	-120.000000	1.007970
19	2	3	1	1.092999	0.0	-120.000000	1.007970
20	1	2	3	1.092999	0.0	60.000000	1.007970

ATOM NO.	X	Y	Z	MASS
1	0.0	0.0	0.0	12.011149
2	1.523000	0.0	0.0	12.011149
3	2.030665	1.435898	0.0	12.011149
4	1.442863	2.182178	-1.190413	12.011149
5	-0.076976	2.096063	-1.143435	12.011149
6	-0.460000	-1.301075	0.000001	15.999399
7	1.994664	-0.667037	1.155342	15.999399
8	1.636512	2.075528	1.199059	15.999399
9	1.911469	1.598437	-2.391196	15.999399
10	-0.474338	0.729781	-1.125847	15.999399
11	-1.430000	-1.301075	0.000000	1.007970
12	1.671329	-1.581562	1.155339	1.007970
13	1.959843	2.990052	1.199059	1.007970
14	1.537097	2.073742	-3.149371	1.007970
15	-0.499977	2.633107	-2.000093	1.007970
16	-0.439939	2.548202	-0.213359	1.007970
17	1.749779	3.230455	-1.150909	1.007970
18	3.121297	1.436733	-0.071884	1.007970
19	1.887331	-0.515244	-0.892430	1.007970
20	-0.364333	0.515245	0.892430	1.007970

TABLE XXXIX

COMPUTER INPUT AND CALCULATED CARTESIAN COORDINATES

CARTESIAN COORDINATES

ALPHA LYXOSE 1C-D

I	J	K	L	BOND LENGTH	BOND ANGLE	DIHEDRAL ANGLE	ATOMIC MASS
1	0	0	0	0.0	0.0	0.0	12.011149
2	1	0	0	1.523000	0.0	0.0	12.011149
3	2	1	0	1.523000	0.0	0.0	12.011149
4	3	2	1	1.523000	0.0	-56.000000	12.011149
5	4	3	2	1.523000	0.0	56.000000	12.011149
6	1	2	3	1.379999	0.0	-60.000000	15.999399
7	2	3	1	1.415000	0.0	120.000000	15.999399
8	3	4	2	1.415000	0.0	120.000000	15.999399
9	4	5	3	1.415000	0.0	-120.000000	15.999399
10	5	4	3	1.422999	0.0	-57.049988	15.999399
11	6	1	2	0.970000	0.0	180.000000	1.007970
12	7	2	1	0.970000	0.0	180.000000	1.007970
13	8	3	2	0.970000	0.0	180.000000	1.007970
14	9	4	3	0.970000	0.0	180.000000	1.007970
15	5	4	3	1.096000	0.0	60.000000	1.007970
16	5	4	15	1.096000	0.0	120.000000	1.007970
17	4	5	3	1.092999	0.0	120.000000	1.007970
18	3	4	2	1.092999	0.0	-120.000000	1.007970
19	2	3	1	1.092999	0.0	-120.000000	1.007970
20	1	2	3	1.092999	0.0	180.000000	1.007970

ATOM NO.	X	Y	Z	MASS
1	0.0	0.0	0.0	12.011149
2	1.523000	0.0	0.0	12.011149
3	2.030665	1.435898	0.0	12.011149
4	1.442863	2.182178	1.190413	12.011149
5	-0.076976	2.096063	1.143435	12.011149
6	-0.460000	0.650538	-1.126763	15.999399
7	1.994664	-0.667037	1.155342	15.999399
8	3.442600	1.436980	0.093061	15.999399
9	1.840197	3.539282	1.139271	15.999399
10	-0.474338	0.729781	1.125847	15.999399
11	-1.429999	0.650538	-1.126760	1.007970
12	2.964664	-0.667037	1.155341	1.007970
13	3.765933	2.351504	0.093062	1.007970
14	1.465824	4.014587	1.897446	1.007970
15	-0.439939	2.548201	0.213358	1.007970
16	-0.499978	2.633110	2.000093	1.007970
17	1.804832	1.731275	2.117944	1.007970
18	1.726206	1.929973	-0.926199	1.007970
19	1.887331	-0.515244	-0.892430	1.007970
20	-0.364333	-1.030489	0.000001	1.007970

TABLE XL

COMPUTER INPUT AND CALCULATED CARTESIAN COORDINATES

CARTESIAN COORDINATES

BETA XYLOSE I	J	K	L	BOND LENGTH	BOND ANGLE	DIHEDRAL ANGLE	ATOMIC MASS
1	0	0	0	0.0	0.0	0.0	12.011149
2	1	0	0	1.523000	0.0	0.0	12.011149
3	2	1	0	1.523000	0.0	0.0	12.011149
4	3	2	1	1.523000	0.0	-56.000000	12.011149
5	4	3	2	1.523000	0.0	56.000000	12.011149
6	1	2	3	1.379999	0.0	180.000000	15.999399
7	2	3	1	1.415000	0.0	-120.000000	15.999399
8	3	4	2	1.415000	0.0	120.000000	15.999399
9	4	5	3	1.415000	0.0	-120.000000	15.999399
10	5	4	3	1.422999	0.0	-57.049988	15.999399
11	6	1	2	0.970000	0.0	180.000000	1.007970
12	7	2	1	0.970000	0.0	-60.000000	1.007970
13	8	3	2	0.970000	0.0	180.000000	1.007970
14	9	4	3	0.970000	0.0	180.000000	1.007970
15	5	4	3	1.096000	0.0	60.000000	1.007970
16	5	4	15	1.096000	0.0	120.000000	1.007970
17	4	5	3	1.092999	0.0	120.000000	1.007970
18	3	4	2	1.092999	0.0	-120.000000	1.007970
19	2	3	1	1.092999	0.0	120.000000	1.007970
20	1	2	3	1.092999	0.0	-60.000000	1.007970

ATOM NO.	X	Y	Z	MASS
1	0.0	0.0	0.0	12.011149
2	1.523000	0.0	0.0	12.011149
3	2.030665	1.435898	0.0	12.011149
4	1.442863	2.182178	1.190413	12.011149
5	-0.076976	2.096063	1.143435	12.011149
6	-0.460000	-1.301075	0.000001	15.999399
7	1.994664	-0.667037	-1.155342	15.999399
8	3.442600	1.436980	0.093061	15.999399
9	1.840197	3.539282	1.139271	15.999399
10	-0.474338	0.729781	1.125847	15.999399
11	-1.430000	-1.301075	0.000000	1.007970
12	1.671328	-0.209774	-1.947343	1.007970
13	3.765933	2.351504	0.093062	1.007970
14	1.465824	4.014587	1.897446	1.007970
15	-0.439939	2.548201	0.213358	1.007970
16	-0.499978	2.633110	2.000093	1.007970
17	1.804832	1.731275	2.117944	1.007970
18	1.726206	1.929973	-0.926199	1.007970
19	1.887331	-0.515244	0.892430	1.007970
20	-0.364333	0.515245	-0.892430	1.007970

TABLE XLI

COMPUTER INPUT FOR THE G MATRIX CALCULATION

```
-09
-09 4       20  65   1   0   1
   ALPHA ARABINOSE 1C-D RING CONFORMATION    1-2-3-4 = E-E-E-A

  1  2     1.523000  1  3     2.030665  2  3     1.435898  1  4     1.442863
  2  4     2.182178  3  4     1.190413  1  5    -0.076976  2  5     2.096063
  3  5     1.143435  1  6    -0.460000  2  6    -1.301075  1  7     1.994664
  2  7    -0.667037  3  7    -1.155342  1  8     3.442600  2  8     1.436980
  3  8     0.093061  1  9     1.911469  2  9     1.598437  3  9     2.391196
  1 10    -0.474338  2 10     0.729781  3 10     1.125847  1 11    -1.430000
  2 11    -1.301075  1 12     1.671328  2 12    -0.209774  3 12    -1.947343
  1 13     3.765933  2 13     2.351504  3 13     0.093062  1 14     1.537096
  2 14     2.073741  3 14     3.149371  1 15    -0.439939  2 15     2.548201
  3 15     0.213358  1 16    -0.499978  2 16     2.633110  3 16     2.000093
  1 17     1.749779  2 17     3.230455  3 17     1.150909  1 18     1.726206
  2 18     1.929973  3 18    -0.926199  1 19     1.887331  2 19    -0.515244
  3 19     0.892430  1 20    -0.364333  2 20     0.515245  3 20    -0.892430
 -1  0     0.0
  1  1  1  2                2  1  2  3                3  1  3  4
  4  1  4  5                5  1  5 10                6  1 10  1
  7  1  1  6                8  1  2  7                9  1  3  8
 10  1  4  9               11  1  5 15               12  1  5 16
 13  1  4 17               14  1  3 18               15  1  2 19
 16  1  1 20               17  1  6 11               18  1  7 12
 19  1  8 13               20  1  9 14               21  2  1  2  3
 22  2  2  3  4            23  2  3  4  5            24  2  4  5 10
 25  2  5 10  1            26  2 10  1  2            27  2 10  1  6
 28  2  6  1  2            29  2  7  2  1            30  2  7  2  3
 31  2  8  3  2            32  2  8  3  4            33  2  9  4  3
 34  2  9  4  5            35  2 11  6  1            36  2 12  7  2
 37  2 13  8  3            38  2 14  9  4            39  2 15  5 10
 40  2 16  5 10            41  2 17  4  9            42  2 18  3  8
 43  2 19  2  7            44  2 20  1  6            45  2 10  1 20
 46  2 20  1  2            47  2 19  2  1            48  2 19  2  3
 49  2 18  3  2            50  2 18  3  4            51  2 17  4  3
 52  2 17  4  5            53  2 15  5  4            54  2 16  5  4
 55  2 15  5 16            56  4 10  1  2  7          0  4 20  1  2 19
  0  4  6  1  2  3         57  4  1  2  3  8          0  4 19  2  3 18
  0  4  7  2  3  4         58  4  2  3  4 17          0  4  8  3  4  5
  0  4 18  3  4  9         59  4  3  4  5 16          0  4  9  4  5 15
  0  4 17  4  5 10         60  4 15  5 10  1          0  4 16  5 10  1
 61  4  5 10  1  6          0  4  5 10  1 20         62  4 20  1  6 11
 63  4 19  2  7 12         64  4 18  3  8 13         65  4 17  4  9 14
-02
-06              ALPHA ARABINOSE
   12.011149   12.011149   12.011149   12.011149   12.011149   15.999399
   15.999399   15.999399   15.999399   15.999399    1.0079700   1.0079700
    1.0079700   1.0079700   1.0079700   1.0079700   1.0079700   1.0079700
    1.0079700   1.0079700
```

TABLE XLII

COMPUTER INPUT FOR THE G MATRIX CALCULATION

```
-09
-09  6     20  65   1   0   1
   ALPHA LYXOSE  1C-D RING CONFORMATION        1-2-3-4 = A-A-E-E

  1  2     1.523000  1  3    2.030665  2  3    1.435898  1  4    1.442863
  2  4     2.182178  3  4    1.190413  1  5   -0.076976  2  5    2.096063
  3  5     1.143435  1  6   -0.460000  2  6    0.650538  3  6   -1.126763
  1  7     1.994664  2  7   -0.667037  3  7    1.155342  1  8    3.442600
  2  8     1.436980  3  8    0.093061  1  9    1.840197  2  9    3.539282
  3  9     1.139271  1 10   -0.474338  2 10    0.729781  3 10    1.125847
  1 11    -1.429999  2 11    0.650538  3 11   -1.126760  1 12    2.964664
  2 12    -0.667037  3 12    1.155341  1 13    3.765933  2 13    2.351504
  3 13     0.093062  1 14    1.465824  2 14    4.014587  3 14    1.897446
  1 15    -0.439939  2 15    2.548201  3 15    0.213358  1 16   -0.499978
  2 16     2.633110  3 16    2.000093  1 17    1.804832  2 17    1.731275
  3 17     2.117944  1 18    1.726206  2 18    1.929973  3 18   -0.926199
  1 19     1.887331  2 19   -0.515244  3 19   -0.892430  1 20   -0.364333
  2 20    -1.030489 -1  0    0.0
  1  1  1  2                2  1  2  3                3  1  3  4
  4  1  4  5                5  1  5 10                6  1 10  1
  7  1  1  6                8  1  2  7                9  1  3  8
 10  1  4  9               11  1  5 15               12  1  5 16
 13  1  4 17               14  1  3 18               15  1  2 19
 16  1  1 20               17  1  6 11               18  1  7 12
 19  1  8 13               20  1  9 14               21  2  1  2  3
 22  2  2  3  4            23  2  3  4  5            24  2  4  5 10
 25  2  5 10  1            26  2 10  1  2            27  2 10  1  6
 28  2  6  1  2            29  2  7  2  1            30  2  7  2  3
 31  2  8  3  2            32  2  8  3  4            33  2  9  4  3
 34  2  9  4  5            35  2 11  6  1            36  2 12  7  2
 37  2 13  8  3            38  2 14  9  4            39  2 15  5 10
 40  2 16  5 10            41  2 17  4  9            42  2 18  3  8
 43  2 19  2  7            44  2 20  1  6            45  2 10  1 20
 46  2 20  1  2            47  2 19  2  1            48  2 19  2  3
 49  2 18  3  2            50  2 18  3  4            51  2 17  4  3
 52  2 17  4  5            53  2 15  5  4            54  2 16  5  4
 55  2 15  5 16            56  4 10  1  2 19          0  4 20  1  2  3
  0  4  6  1  2  7         57  4  1  2  3  8          0  4  7  2  3 18
  0  4 19  2  3  4         58  4  2  3  4  9          0  4 18  3  4 17
  0  4  8  3  4  5         59  4  3  4  5 16          0  4  9  4  5 10
  0  4 17  4  5 15         60  4 15  5 10  1          0  4 16  5 10  1
 61  4  5 10  1  6          0  4  5 10  1 20         62  4 20  1  6 11
 63  4 19  2  7 12         64  4 18  3  8 13         65  4 17  4  9 14
-02
-06            ALPHA LYXOSE
   12.011149   12.011149   12.011149   12.011149   12.011149   15.999399
   15.999399   15.999399   15.999399   15.999399    1.0079700   1.0079700
    1.0079700   1.0079700   1.0079700   1.0079700   1.0079700   1.0079700
    1.0079700   1.0079700
```

TABLE XLIII

COMPUTER INPUT FOR THE $\underset{\sim}{G}$ MATRIX CALCULATION

```
-09
-09  5      20  65    1    0    1
   ALPHA LYXOSE C1-D RING CONFORMATION      1-2-3-4 = E-E-A-A

  1  2     1.523000   1  3     2.030665   2  3     1.435898   1  4     1.442863
  2  4     2.182178   3  4    -1.190413   1  5    -0.076976   2  5     2.096063
  3  5    -1.143435   1  6    -0.460000   2  6    -1.301075   1  7     1.994664
  2  7    -0.667037   3  7     1.155342   1  8     1.636512   2  8     2.075528
  3  8     1.199059   1  9     1.911469   2  9     1.598437   3  9    -2.391196
  1 10    -0.474338   2 10     0.729781   3 10    -1.125847   1 11    -1.430000
  2 11    -1.301075   1 12     1.671329   2 12    -1.581562   3 12     1.155339
  1 13     1.959843   2 13     2.990052   3 13     1.199059   1 14     1.537097
  2 14     2.073742   3 14    -3.149371   1 15    -0.499977   2 15     2.633107
  3 15    -2.000093   1 16    -0.439939   2 16     2.548202   3 16    -0.213359
  1 17     1.749779   2 17     3.230455   3 17    -1.150909   1 18     3.121297
  2 18     1.436733   3 18    -0.071884   1 19     1.887331   2 19    -0.515244
  3 19    -0.892430   1 20    -0.364333   2 20     0.515245   3 20    -0.892430
 -1  0     0.0
  1  1  1  2                2  1  2  3                3  1  3  4
  4  1  4  5                5  1  5 10                6  1 10  1
  7  1  1  6                8  1  2  7                9  1  3  8
 10  1  4  9               11  1  5 15               12  1  5 16
 13  1  4 17               14  1  3 18               15  1  2 19
 16  1  1 20               17  1  6 11               18  1  7 12
 19  1  8 13               20  1  9 14               21  2  1  2  3
 22  2  2  3  4            23  2  3  4  5            24  2  4  5 10
 25  2  5 10  1            26  2 10  1  2            27  2 10  1  6
 28  2  6  1  2            29  2  7  2  1            30  2  7  2  3
 31  2  8  3  2            32  2  8  3  4            33  2  9  4  3
 34  2  9  4  5            35  2 11  6  1            36  2 12  7  2
 37  2 13  8  3            38  2 14  9  4            39  2 15  5 10
 40  2 16  5 10            41  2 17  4  9            42  2 18  3  8
 43  2 19  2  7            44  2 20  1  6            45  2 10  1 20
 46  2 20  1  2            47  2 19  2  1            48  2 19  2  3
 49  2 18  3  2            50  2 18  3  4            51  2 17  4  3
 52  2 17  4  5            53  2 15  5  4            54  2 16  5  4
 55  2 15  5 16            56  4 10  1  2  7             0  4  6  1  2  3
  0  4 20  1  2 19         57  4  1  2  3 18             0  4  7  2  3  4
  0  4 19  2  3  8         58  4  2  3  4 17             0  4 18  3  4  5
  0  4  8  3  4  9         59  4  3  4  5 15             0  4 17  4  5 10
  0  4  9  4  5 16         60  4 15  5 10  1             0  4 16  5 10  1
 61  4  5 10  1  6          0  4  5 10  1 20            62  4 20  1  6 11
 63  4 19  2  7 12         64  4 18  3  8 13            65  4 17  4  9 14
-02
-06              ALPHA LYXOSE
    12.011149   12.011149   12.011149   12.011149   12.011149   15.999399
    15.999399   15.999399   15.999399   15.999399   1.0079700   1.0079700
    1.0079700   1.0079700   1.0079700   1.0079700   1.0079700   1.0079700
    1.0079700   1.0079700
```

TABLE XLIV

COMPUTER INPUT FOR THE G MATRIX CALCULATION

```
-09
-09  7     20  65    1    0    1
   BETA XYLOSE 1C-D RING CONFORMATION    1-2-3-4 = E-E-E-E

  1  2     1.523000  1  3     2.030665  2  3     1.435898  1  4     1.442863
  2  4     2.182178  3  4     1.190413  1  5    -0.076976  2  5     2.096063
  3  5     1.143435  1  6    -0.460000  2  6    -1.301075  1  7     1.994664
  2  7    -0.667037  3  7    -1.155342  1  8     3.442600  2  8     1.436980
  3  8     0.093061  1  9     1.840197  2  9     3.539282  3  9     1.139271
  1 10    -0.474338  2 10     0.729781  3 10     1.125847  1 11    -1.430000
  2 11    -1.301075  1 12     1.671328  2 12    -0.209774  3 12    -1.947343
  1 13     3.765933  2 13     2.351504  3 13     0.093062  1 14     1.465824
  2 14     4.014587  3 14     1.897446  1 15    -0.439939  2 15     2.548201
  3 15     0.213358  1 16    -0.499978  2 16     2.633110  3 16     2.000093
  1 17     1.804832  2 17     1.731275  3 17     2.117944  1 18     1.726206
  2 18     1.929973  3 18    -0.926199  1 19     1.887331  2 19    -0.515244
  3 19     0.892430  1 20    -0.364333  2 20     0.515245  3 20    -0.892430
 -1  0     0.0
  1  1  1  2              2  1  2  3              3  1  3  4
  4  1  4  5              5  1  5 10              6  1 10  1
  7  1  1  6              8  1  2  7              9  1  3  8
 10  1  4  9             11  1  5 15             12  1  5 16
 13  1  4 17             14  1  3 18             15  1  2 19
 16  1  1 20             17  1  6 11             18  1  7 12
 19  1  8 13             20  1  9 14             21  2  1  2  3
 22  2  2  3  4          23  2  3  4  5          24  2  4  5 10
 25  2  5 10  1          26  2 10  1  2          27  2 10  1  6
 28  2  6  1  2          29  2  7  2  1          30  2  7  2  3
 31  2  8  3  2          32  2  8  3  4          33  2  9  4  3
 34  2  9  4  5          35  2 11  6  1          36  2 12  7  2
 37  2 13  8  3          38  2 14  9  4          39  2 15  5 10
 40  2 16  5 10          41  2 17  4  9          42  2 18  3  8
 43  2 19  2  7          44  2 20  1  6          45  2 10  1 20
 46  2 20  1  2          47  2 19  2  1          48  2 19  2  3
 49  2 18  3  2          50  2 18  3  4          51  2 17  4  3
 52  2 17  4  5          53  2 15  5  4          54  2 16  5  4
 55  2 15  5 16          56  4 10  1  2  7        0  4  6  1  2  3
  0  4 20  1  2 19       57  4  1  2  3  8        0  4  7  2  3  4
  0  4 19  2  3 18       58  4  2  3  4  9        0  4 18  3  4 17
  0  4  8  3  4  5       59  4  3  4  5 16        0  4  9  4  5 10
  0  4 17  4  5 15       60  4 16  5 10  1        0  4 15  5 10  1
 61  4  5 10  1  6        0  4  5 10  1 20       62  4 20  1  6 11
 63  4 19  2  7 12       64  4 18  3  8 13       65  4 17  4  9 14
-02
-06              BETA XYLOSE
    12.011149   12.011149   12.011149   12.011149   12.011149   15.999399
    15.999399   15.999399   15.999399   15.999399    1.0079700   1.0079700
     1.0079700   1.0079700   1.0079700   1.0079700   1.0079700   1.0079700
     1.0079700   1.0079700
```

TABLE XLV

COMPUTER INPUT AND CALCULATED CARTESIAN COORDINATES

CARTESIAN COORDINATES

BETA RIBOSE 1C-D

I	J	K	L	BOND LENGTH	BOND ANGLE	DIHEDRAL ANGLE	ATOMIC MASS
1	0	0	0	0.0	0.0	0.0	12.011149
2	1	0	0	1.523000	0.0	0.0	12.011149
3	2	1	0	1.523000	0.0	0.0	12.011149
4	3	2	1	1.523000	0.0	-56.000000	12.011149
5	4	3	2	1.523000	0.0	56.000000	12.011149
6	1	2	3	1.379999	0.0	-60.000000	15.999399
7	2	3	1	1.415000	0.0	-120.000000	15.999399
8	3	4	2	1.415000	0.0	-120.000000	15.999399
9	4	5	3	1.415000	0.0	-120.000000	15.999399
10	5	4	3	1.422999	0.0	-57.049988	15.999399
11	6	1	2	0.970000	0.0	180.000000	1.007970
12	7	2	1	0.970000	0.0	180.000000	1.007970
13	8	3	2	0.970000	0.0	180.000000	1.007970
14	9	4	3	0.970000	0.0	180.000000	1.007970
15	5	4	3	1.096000	0.0	60.000000	1.007970
16	5	4	15	1.096000	0.0	120.000000	1.007970
17	4	5	3	1.092999	0.0	120.000000	1.007970
18	3	4	2	1.092999	0.0	120.000000	1.007970
19	2	3	1	1.092999	0.0	120.000000	1.007970
20	1	2	3	1.092999	0.0	180.000000	1.007970

ATOM NO.	X	Y	Z	MASS
1	0.0	0.0	0.0	12.011149
2	1.523000	0.0	0.0	12.011149
3	2.030665	1.435898	0.0	12.011149
4	1.442863	2.182178	1.190413	12.011149
5	-0.076976	2.096063	1.143435	12.011149
6	-0.460000	0.650538	-1.126763	15.999399
7	1.994664	-0.667037	-1.155342	15.999399
8	1.636512	2.075528	-1.199059	15.999399
9	1.840197	3.539282	1.139271	15.999399
10	-0.474338	0.729781	1.125847	15.999399
11	-1.429999	0.650538	-1.126760	1.007970
12	2.964664	-0.667038	-1.155340	1.007970
13	1.959844	2.990051	-1.199059	1.007970
14	1.465824	4.014587	1.897446	1.007970
15	-0.439939	2.548201	0.213358	1.007970
16	-0.499978	2.633110	2.000093	1.007970
17	1.804832	1.731275	2.117944	1.007970
18	3.121297	1.436733	0.071884	1.007970
19	1.887331	-0.515244	0.892430	1.007970
20	-0.364333	-1.030489	0.000001	1.007970

TABLE XLVI

COMPUTER INPUT AND CALCULATED CARTESIAN COORDINATES

CARTESIAN COORDINATES

ALPHA RIBOSE 1C-D

I	J	K	L	BOND LENGTH	BOND ANGLE	DIHEDRAL ANGLE	ATOMIC MASS
1	0	0	0	0.0	0.0	0.0	12.011149
2	1	0	0	1.523000	0.0	0.0	12.011149
3	2	1	0	1.523000	0.0	0.0	12.011149
4	3	2	1	1.523000	0.0	-56.000000	12.011149
5	4	3	2	1.523000	0.0	56.000000	12.011149
6	1	2	3	1.379999	0.0	180.000000	15.999399
7	2	3	1	1.415000	0.0	-120.000000	15.999399
8	3	4	2	1.415000	0.0	-120.000000	15.999399
9	4	5	3	1.415000	0.0	-120.000000	15.999399
10	5	4	3	1.422999	0.0	-57.049988	15.999399
11	6	1	2	0.970000	0.0	180.000000	1.007970
12	7	2	1	0.970000	0.0	180.000000	1.007970
13	8	3	2	0.970000	0.0	180.000000	1.007970
14	9	4	3	0.970000	0.0	180.000000	1.007970
15	5	4	3	1.096000	0.0	60.000000	1.007970
16	5	4	15	1.096000	0.0	120.000000	1.007970
17	4	5	3	1.092999	0.0	120.000000	1.007970
18	3	4	2	1.092999	0.0	120.000000	1.007970
19	2	3	1	1.092999	0.0	120.000000	1.007970
20	1	2	3	1.092999	0.0	-60.000000	1.007970

ATOM NO.	X	Y	Z	MASS
1	0.0	0.0	0.0	12.011149
2	1.523000	0.0	0.0	12.011149
3	2.030665	1.435898	0.0	12.011149
4	1.442863	2.182178	1.190413	12.011149
5	-0.076976	2.096063	1.143435	12.011149
6	-0.460000	-1.301075	0.000001	15.999399
7	1.994664	-0.667037	-1.155342	15.999399
8	1.636512	2.075528	-1.199059	15.999399
9	1.840197	3.539282	1.139271	15.999399
10	-0.474338	0.729781	1.125847	15.999399
11	-1.430000	-1.301075	0.000000	1.007970
12	2.964664	-0.667038	-1.155340	1.007970
13	1.959844	2.990051	-1.199059	1.007970
14	1.465824	4.014587	1.897446	1.007970
15	-0.439939	2.548201	0.213358	1.007970
16	-0.499978	2.633110	2.000093	1.007970
17	1.804832	1.731275	2.117944	1.007970
18	3.121297	1.436733	0.071884	1.007970
19	1.887331	-0.515244	0.892430	1.007970
20	-0.364333	0.515245	-0.892430	1.007970

TABLE XLVII

COMPUTER INPUT AND CALCULATED CARTESIAN COORDINATES

CARTESIAN COORDINATES

ALPHA RIBOSE C1-D

I	J	K	L	BOND LENGTH	BOND ANGLE	DIHEDRAL ANGLE	ATOMIC MASS
1	0	0	0	0.0	0.0	0.0	12.011149
2	1	0	0	1.523000	0.0	0.0	12.011149
3	2	1	0	1.523000	0.0	0.0	12.011149
4	3	2	1	1.523000	0.0	56.000000	12.011149
5	4	3	2	1.523000	0.0	-56.000000	12.011149
6	1	2	3	1.379999	0.0	60.000000	15.999399
7	2	3	1	1.415000	0.0	-120.000000	15.999399
8	3	4	2	1.415000	0.0	-120.000000	15.999399
9	4	5	3	1.415000	0.0	-120.000000	15.999399
10	5	4	3	1.422999	0.0	57.049988	15.999399
11	6	1	2	0.970000	0.0	180.000000	1.007970
12	7	2	1	0.970000	0.0	180.000000	1.007970
13	8	3	2	0.970000	0.0	180.000000	1.007970
14	9	4	3	0.970000	0.0	180.000000	1.007970
15	5	4	3	1.096000	0.0	180.000000	1.007970
16	5	4	15	1.096000	0.0	120.000000	1.007970
17	4	5	3	1.092999	0.0	120.000000	1.007970
18	3	4	2	1.092999	0.0	120.000000	1.007970
19	2	3	1	1.092999	0.0	120.000000	1.007970
20	1	2	3	1.092999	0.0	180.000000	1.007970

ATOM NO.	X	Y	Z	MASS
1	0.0	0.0	0.0	12.011149
2	1.523000	0.0	0.0	12.011149
3	2.030665	1.435898	0.0	12.011149
4	1.442863	2.182178	-1.190413	12.011149
5	-0.076976	2.096063	-1.143435	12.011149
6	-0.460000	0.650538	1.126763	15.999399
7	1.994664	-0.667037	-1.155342	15.999399
8	3.442600	1.436980	-0.093061	15.999399
9	1.911469	1.598437	-2.391196	15.999399
10	-0.474338	0.729781	-1.125847	15.999399
11	-1.429999	0.650537	1.126761	1.007970
12	2.964664	-0.667038	-1.155340	1.007970
13	3.765933	2.351504	-0.093061	1.007970
14	1.537097	2.073742	-3.149371	1.007970
15	-0.499977	2.633107	-2.000093	1.007970
16	-0.439939	2.548202	-0.213359	1.007970
17	1.749779	3.230455	-1.150909	1.007970
18	1.726206	1.929973	0.926199	1.007970
19	1.887331	-0.515244	0.892430	1.007970
20	-0.364333	-1.030489	0.000001	1.007970

TABLE XLVIII

COMPUTER INPUT AND CALCULATED CARTESIAN COORDINATES

CARTESIAN COORDINATES

BETA RIBOSE C1-D

I	J	K	L	BOND LENGTH	BOND ANGLE	DIHEDRAL ANGLE	ATOMIC MASS
1	0	0	0	0.0	0.0	0.0	12.011149
2	1	0	0	1.523000	0.0	0.0	12.011149
3	2	1	0	1.523000	0.0	0.0	12.011149
4	3	2	1	1.523000	0.0	56.000000	12.011149
5	4	3	2	1.523000	0.0	-56.000000	12.011149
6	1	2	3	1.379999	0.0	180.000000	15.999399
7	2	3	1	1.415000	0.0	-120.000000	15.999399
8	3	4	2	1.415000	0.0	-120.000000	15.999399
9	4	5	3	1.415000	0.0	-120.000000	15.999399
10	5	4	3	1.422999	0.0	57.049988	15.999399
11	6	1	2	0.970000	0.0	180.000000	1.007970
12	7	2	1	0.970000	0.0	180.000000	1.007970
13	8	3	2	0.970000	0.0	180.000000	1.007970
14	9	4	3	0.970000	0.0	180.000000	1.007970
15	5	4	3	1.096000	0.0	180.000000	1.007970
16	5	4	15	1.096000	0.0	120.000000	1.007970
17	4	5	3	1.092999	0.0	120.000000	1.007970
18	3	4	2	1.092999	0.0	120.000000	1.007970
19	2	3	1	1.092999	0.0	120.000000	1.007970
20	1	2	3	1.092999	0.0	60.000000	1.007970

ATOM NO.	X	Y	Z	MASS
1	0.0	0.0	0.0	12.011149
2	1.523000	0.0	0.0	12.011149
3	2.030665	1.435898	0.0	12.011149
4	1.442863	2.182178	-1.190413	12.011149
5	-0.076976	2.096063	-1.143435	12.011149
6	-0.460000	-1.301075	0.000001	15.999399
7	1.994664	-0.667037	-1.155342	15.999399
8	3.442600	1.436980	-0.093061	15.999399
9	1.911469	1.598437	-2.391196	15.999399
10	-0.474338	0.729781	-1.125847	15.999399
11	-1.430000	-1.301075	0.000000	1.007970
12	2.964664	-0.667038	-1.155340	1.007970
13	3.765933	2.351504	-0.093061	1.007970
14	1.537097	2.073742	-3.149371	1.007970
15	-0.499977	2.633107	-2.000093	1.007970
16	-0.439939	2.548202	-0.213359	1.007970
17	1.749779	3.230455	-1.150909	1.007970
18	1.726206	1.929973	0.926199	1.007970
19	1.887331	-0.515244	0.892430	1.007970
20	-0.364333	0.515245	0.892430	1.007970

TABLE XLIX

COMPUTER INPUT FOR THE $\mathcal{L}$ MATRIX CALCULATION

```
-09
-09 4       20  65   1   0   1
   BETA RIBOSE  1C-D RING CONFORMATION          1-2-3-4 = E-E-A-E

  1  2     1.523000  1  3     2.030665  2  3     1.435898  1  4     1.442863
  2  4     2.182178  3  4     1.190413  1  5    -0.076976  2  5     2.096063
  3  5     1.143435  1  6    -0.460000  2  6    -1.301075  1  7     1.994664
  2  7    -0.667037  3  7    -1.155342  1  8     1.636512  2  8     2.075528
  3  8    -1.199059  1  9     1.840197  2  9     3.539282  3  9     1.139271
  1 10    -0.474338  2 10     0.729781  3 10     1.125847  1 11    -1.430000
  2 11    -1.301075  1 12     2.964664  2 12    -0.667038  3 12    -1.155340
  1 13     1.959844  2 13     2.990051  3 13    -1.199059  1 14     1.465824
  2 14     4.014587  3 14     1.897446  1 15    -0.439939  2 15     2.548201
  3 15     0.213358  1 16    -0.499978  2 16     2.633110  3 16     2.000093
  1 17     1.804832  2 17     1.731275  3 17     2.117944  1 18     3.121297
  2 18     1.436733  3 18     0.071884  1 19     1.887331  2 19    -0.515244
  3 19     0.892430  1 20    -0.364333  2 20     0.515245  3 20    -0.892430
 -1  0     0.0
  1  1  1  2                2  1  2  3                3  1  3  4
  4  1  4  5                5  1  5 10                6  1 10  1
  7  1  1  6                8  1  2  7                9  1  3  8
 10  1  4  9               11  1  5 15               12  1  5 16
 13  1  4 17               14  1  3 18               15  1  2 19
 16  1  1 20               17  1  6 11               18  1  7 12
 19  1  8 13               20  1  9 14               21  2  1  2  3
 22  2  2  3  4            23  2  3  4  5            24  2  4  5 10
 25  2  5 10  1            26  2 10  1  2            27  2 10  1  6
 28  2  6  1  2            29  2  7  2  1            30  2  7  2  3
 31  2  8  3  2            32  2  8  3  4            33  2  9  4  3
 34  2  9  4  5            35  2 11  6  1            36  2 12  7  2
 37  2 13  8  3            38  2 14  9  4            39  2 15  5 10
 40  2 16  5 10            41  2 17  4  9            42  2 18  3  8
 43  2 19  2  7            44  2 20  1  6            45  2 10  1 20
 46  2 20  1  2            47  2 19  2  1            48  2 19  2  3
 49  2 18  3  2            50  2 18  3  4            51  2 17  4  3
 52  2 17  4  5            53  2 15  5  4            54  2 16  5  4
 55  2 15  5 16            56  4 10  1  2  7          0  4 20  1  2 19
  0  4  6  1  2  3         57  4  1  2  3 18          0  4 19  2  3  8
  0  4  7  2  3  4         58  4  2  3  4  9          0  4  8  3  4 17
  0  4 18  3  4  5         59  4  3  4  5 16          0  4  9  4  5 10
  0  4 17  4  5 15         60  4 15  5 10  1          0  4 16  5 10  1
 61  4  5 10  1  6          0  4  5 10  1 20         62  4 20  1  6 11
 63  4 19  2  7 12         64  4 18  3  8 13         65  4 17  4  9 14
-02
-06            BETA RIBOSE  1C-D       1-2-3-4 =E-E-A-E
   12.011149   12.011149   12.011149   12.011149   12.011149   15.999399
   15.999399   15.999399   15.999399   15.999399    1.0079700   1.0079700
    1.0079700   1.0079700   1.0079700   1.0079700   1.0079700   1.0079700
    1.0079700   1.0079700
```

TABLE L

COMPUTER INPUT FOR THE G MATRIX CALCULATION

```
-09
-09  3      20  65   1   0   1
       ALPHA RIBOSE 1C-D RING CONFORMATION   1-2-3-4 = A-E-A-E

  1  2    1.523000  1  3    2.030665  2  3    1.435898  1  4    1.442863
  2  4    2.182178  3  4    1.190413  1  5   -0.076976  2  5    2.096063
  3  5    1.143435  1  6   -0.460000  2  6    0.650538  3  6   -1.126763
  1  7    1.994664  2  7   -0.667037  3  7   -1.155342  1  8    1.636512
  2  8    2.075528  3  8   -1.199059  1  9    1.840197  2  9    3.539282
  3  9    1.139271  1 10   -0.474338  2 10    0.729781  3 10    1.125847
  1 11   -1.429999  2 11    0.650538  3 11   -1.126760  1 12    2.964664
  2 12   -0.667038  3 12   -1.155340  1 13    1.959844  2 13    2.990051
  3 13   -1.199059  1 14    1.465824  2 14    4.014587  3 14    1.897446
  1 15   -0.439939  2 15    2.548201  3 15    0.213358  1 16   -0.499978
  2 16    2.633110  3 16    2.000093  1 17    1.804832  2 17    1.731275
  3 17    2.117944  1 18    3.121297  2 18    1.436733  3 18    0.071884
  1 19    1.887331  2 19   -0.515244  3 19    0.892430  1 20   -0.364333
  2 20   -1.030489 -1  0    0.0
  1  1  1  2          2  1  2  3          3  1  3  4
  4  1  4  5          5  1  5 10          6  1 10  1
  7  1  1  6          8  1  2  7          9  1  3  8
 10  1  4  9         11  1  5 15         12  1  5 16
 13  1  4 17         14  1  3 18         15  1  2 19
 16  1  1 20         17  1  6 11         18  1  7 12
 19  1  8 13         20  1  9 14         21  2  1  2  3
 22  2  2  3  4      23  2  3  4  5      24  2  4  5 10
 25  2  5 10  1      26  2 10  1  2      27  2 10  1  6
 28  2  6  1  2      29  2  7  2  1      30  2  7  2  3
 31  2  8  3  2      32  2  8  3  4      33  2  9  4  3
 34  2  9  4  5      35  2 11  6  1      36  2 12  7  2
 37  2 13  8  3      38  2 14  9  4      39  2 15  5 10
 40  2 16  5 10      41  2 17  4  9      42  2 18  3  8
 43  2 19  2  7      44  2 20  1  6      45  2 10  1 20
 46  2 20  1  2      47  2 19  2  1      48  2 19  2  3
 49  2 18  3  2      50  2 18  3  4      51  2 17  4  3
 52  2 17  4  5      53  2 15  5  4      54  2 16  5  4
 55  2 15  5 16      56  4 10  1  2  7       0  4  6  1  2 19
  0  4 20  1  2  3   57  4  1  2  3 18       0  4  7  2  3  4
  0  4 19  2  3  8   58  4  2  3  4  9       0  4 18  3  4  5
  0  4  8  3  4 17   59  4  3  4  5 16       0  4  9  4  5 10
  0  4 17  4  5 15   60  4 16  5 10  1       0  4 15  5 10  1
 61  4  5 10  1  6    0  4  5 10  1 20      62  4 20  1  6 11
 63  4 19  2  7 12   64  4 18  3  8 13      65  4 17  4  9 14
-02
-06            ALPHA RIBOSE 1C-D    1-2-3-4=A-E-A-E
   12.011149   12.011149   12.011149   12.011149   12.011149   15.999399
   15.999399   15.999399   15.999399   15.999399    1.0079700   1.0079700
    1.0079700   1.0079700   1.0079700   1.0079700   1.0079700   1.0079700
    1.0079700   1.0079700
```

TABLE LI

COMPUTER INPUT FOR THE $\mathcal{L}$ MATRIX CALCULATION

```
-09
-09  2      20  65    1    0    1
     ALPHA RIBOSE C1-D RING CONFORMATION          1-2-3-4 = E-A-E-A

  1  2     1.523000   1  3     2.030665   2  3     1.435898   1  4     1.442863
  2  4     2.182178   3  4    -1.190413   1  5    -0.076976   2  5     2.096063
  3  5    -1.143435   1  6    -0.460000   2  6    -1.301075   1  7     1.994664
  2  7    -0.667037   3  7    -1.155342   1  8     3.442600   2  8     1.436980
  3  8    -0.093061   1  9     1.911469   2  9     1.598437   3  9    -2.391196
  1 10    -0.474338   2 10     0.729781   3 10    -1.125847   1 11    -1.430000
  2 11    -1.301075   1 12     2.964664   2 12    -0.667038   3 12    -1.155340
  1 13     3.765933   2 13     2.351504   3 13    -0.093061   1 14     1.537097
  2 14     2.073742   3 14    -3.149371   1 15    -0.499977   2 15     2.633107
  3 15    -2.000093   1 16    -0.439939   2 16     2.548202   3 16    -0.213359
  1 17     1.749779   2 17     3.230455   3 17    -1.150909   1 18     1.726206
  2 18     1.929973   3 18     0.926199   1 19     1.887331   2 19    -0.515244
  3 19     0.892430   1 20    -0.364333   2 20     0.515245   3 20     0.892430
 -1  0     0.0
  1  1  1  2              2  1  2  3              3  1  3  4
  4  1  4  5              5  1  5 10              6  1 10  1
  7  1  1  6              8  1  2  7              9  1  3  8
 10  1  4  9             11  1  5 15             12  1  5 16
 13  1  4 17             14  1  3 18             15  1  2 19
 16  1  1 20             17  1  6 11             18  1  7 12
 19  1  8 13             20  1  9 14             21  2  1  2  3
 22  2  2  3  4          23  2  3  4  5          24  2  4  5 10
 25  2  5 10  1          26  2 10  1  2          27  2 10  1  6
 28  2  6  1  2          29  2  7  2  1          30  2  7  2  3
 31  2  8  3  2          32  2  8  3  4          33  2  9  4  3
 34  2  9  4  5          35  2 11  6  1          36  2 12  7  2
 37  2 13  8  3          38  2 14  9  4          39  2 15  5 10
 40  2 16  5 10          41  2 17  4  9          42  2 18  3  8
 43  2 19  2  7          44  2 20  1  6          45  2 10  1 20
 46  2 20  1  2          47  2 19  2  1          48  2 19  2  3
 49  2 18  3  2          50  2 18  3  4          51  2 17  4  3
 52  2 17  4  5          53  2 15  5  4          54  2 16  5  4
 55  2 15  5 16          56  4 10  1  2 19        0  4  6  1  2  3
  0  4 20  1  2  7       57  4  1  2  3  8        0  4  7  2  3 18
  0  4 19  2  3  4       58  4  2  3  4 17        0  4 18  3  4  9
  0  4  8  3  4  5       59  4  3  4  5 15        0  4  9  4  5 16
  0  4 17  4  5 10       60  4 15  5 10  1        0  4 16  5 10  1
 61  4  5 10  1  6        0  4  5 10  1 20       62  4 20  1  6 11
 63  4 19  2  7 12       64  4 18  3  8 13       65  4 17  4  9 14
-02
-06              ALPHA RIBOSE C1-D    1-2-3-4 = E-A-E-A
    12.011149   12.011149   12.011149   12.011149   12.011149   15.999399
    15.999399   15.999399   15.999399   15.999399    1.0079700   1.0079700
     1.0079700   1.0079700   1.0079700   1.0079700   1.0079700   1.0079700
     1.0079700   1.0079700
```

TABLE LII

COMPUTER INPUT FOR THE $\underset{\sim}{G}$ MATRIX CALCULATION

```
-09
-09 1       20  65    1    0    1
    BETA RIBOSE  C1-D RING CONFORMATION    1-2-3-4 = A-A-E-A

  1  2     1.523000  1  3     2.030665  2  3     1.435898  1  4     1.442863
  2  4     2.182178  3  4    -1.190413  1  5    -0.076976  2  5     2.096063
  3  5    -1.143435  1  6    -0.460000  2  6     0.650538  3  6     1.126763
  1  7     1.994664  2  7    -0.667037  3  7    -1.155342  1  8     3.442600
  2  8     1.436980  3  8    -0.093061  1  9     1.911469  2  9     1.598437
  3  9    -2.391196  1 10    -0.474338  2 10     0.729781  3 10    -1.125847
  1 11    -1.429999  2 11     0.650537  3 11     1.126761  1 12     2.964664
  2 12    -0.667038  3 12    -1.155340  1 13     3.765933  2 13     2.351504
  3 13    -0.093061  1 14     1.537097  2 14     2.073742  3 14    -3.149371
  1 15    -0.499977  2 15     2.633107  3 15    -2.000093  1 16    -0.439939
  2 16     2.548202  3 16    -0.213359  1 17     1.749779  2 17     3.230455
  3 17    -1.150909  1 18     1.726206  2 18     1.929973  3 18     0.926199
  1 19     1.887331  2 19    -0.515244  3 19     0.892430  1 20    -0.364333
  2 20    -1.030489 -1  0     0.0
  1  1  1  2              2  1  2  3              3  1  3  4
  4  1  4  5              5  1  5 10              6  1 10  1
  7  1  1  6              8  1  2  7              9  1  3  8
 10  1  4  9             11  1  5 15             12  1  5 16
 13  1  4 17             14  1  3 18             15  1  2 19
 16  1  1 20             17  1  6 11             18  1  7 12
 19  1  8 13             20  1  9 14             21  2  1  2  3
 22  2  2  3  4          23  2  3  4  5          24  2  4  5 10
 25  2  5 10  1          26  2 10  1  2          27  2 10  1  6
 28  2  6  1  2          29  2  7  2  1          30  2  7  2  3
 31  2  8  3  2          32  2  8  3  4          33  2  9  4  3
 34  2  9  4  5          35  2 11  6  1          36  2 12  7  2
 37  2 13  8  3          38  2 14  9  4          39  2 15  5 10
 40  2 16  5 10          41  2 17  4  9          42  2 18  3  8
 43  2 19  2  7          44  2 20  1  6          45  2 10  1 20
 46  2 20  1  2          47  2 19  2  1          48  2 19  2  3
 49  2 18  3  2          50  2 18  3  4          51  2 17  4  3
 52  2 17  4  5          53  2 15  5  4          54  2 16  5  4
 55  2 15  5 16          56  4 10  1  2 19        0  4 20  1  2  3
  0  4  6  1  2  7       57  4  1  2  3  8        0  4 19  2  3  4
  0  4  7  2  3 18       58  4  2  3  4 17        0  4 18  3  4  9
  0  4  8  3  4  5       59  4  3  4  5 15        0  4  9  4  5 16
  0  4 17  4  5 10       60  4 15  5 10  1        0  4 16  5 10  1
 61  4  5 10  1  6        0  4  5 10  1 20       62  4 20  1  6 11
 63  4 19  2  7 12       64  4 18  3  8 13       65  4 17  4  9 14
-02
-06          BETA RIBOSE C1-D          1-2-3-4=A-A-E-A
   12.011149   12.011149   12.011149   12.011149   12.011149   15.999399
   15.999399   15.999399   15.999399   15.999399    1.0079700   1.0079700
    1.0079700   1.0079700   1.0079700   1.0079700   1.0079700   1.0079700
    1.0079700   1.0079700
```

TABLE LIII

COMPUTER INPUT AND CALCULATED CARTESIAN COORDINATES

CARTESIAN COORDINATES

ALPHA XYLOPYRANOSIDE

I	J	K	L	BOND LENGTH	BOND ANGLE	DIHEDRAL ANGLE	ATOMIC MASS
1	0	0	0	0.0	0.0	0.0	12.011149
2	1	0	0	1.523000	0.0	0.0	12.011149
3	2	1	0	1.523000	0.0	0.0	12.011149
4	3	2	1	1.523000	0.0	-56.000000	12.011149
5	4	3	2	1.523000	0.0	56.000000	12.011149
6	1	2	3	1.379999	0.0	-60.000000	15.999399
7	2	3	1	1.415000	0.0	-120.000000	15.999399
8	3	4	2	1.415000	0.0	120.000000	15.999399
9	4	5	3	1.415000	0.0	-120.000000	15.999399
10	5	4	3	1.422999	0.0	-57.049988	15.999399
11	6	1	2	1.426999	0.0	180.000000	12.011149
12	7	2	1	0.970000	0.0	-60.000000	1.007970
13	8	3	2	0.970000	0.0	180.000000	1.007970
14	9	4	3	0.970000	0.0	180.000000	1.007970
15	5	4	3	1.096000	0.0	60.000000	1.007970
16	5	4	15	1.096000	0.0	120.000000	1.007970
17	4	5	3	1.092999	0.0	120.000000	1.007970
18	3	4	2	1.092999	0.0	-120.000000	1.007970
19	2	3	1	1.092999	0.0	120.000000	1.007970
20	1	2	3	1.092999	0.0	180.000000	1.007970
21	11	6	1	1.099999	0.0	180.000000	1.007970
22	11	6	1	1.099999	0.0	-60.000000	1.007970
23	11	6	1	1.099999	0.0	60.000000	1.007970

ATOM NO.	X	Y	Z	MASS
1	0.0	0.0	0.0	12.011149
2	1.523000	0.0	0.0	12.011149
3	2.030665	1.435898	0.0	12.011149
4	1.442863	2.182178	1.190413	12.011149
5	-0.076976	2.096063	1.143435	12.011149
6	-0.460000	0.650538	-1.126763	15.999399
7	1.994664	-0.667037	-1.155342	15.999399
8	3.442600	1.436980	0.093061	15.999399
9	1.840197	3.539282	1.139271	15.999399
10	-0.474338	0.729781	1.125847	15.999399
11	-1.886998	0.650538	-1.126760	12.011149
12	1.671328	-0.209774	-1.947343	1.007970
13	3.765933	2.351504	0.093062	1.007970
14	1.465824	4.014587	1.897446	1.007970
15	-0.439939	2.548201	0.213358	1.007970
16	-0.499978	2.633110	2.000093	1.007970
17	1.804832	1.731275	2.117944	1.007970
18	1.726206	1.929973	-0.926199	1.007970
19	1.887331	-0.515244	0.892430	1.007970
20	-0.364333	-1.030489	0.000001	1.007970
21	-2.253667	1.169082	-2.024904	1.007970
22	-2.253660	1.169083	-0.228612	1.007970
23	-2.253663	-0.386553	-1.126758	1.007970

TABLE LIV

COMPUTER INPUT AND CALCULATED CARTESIAN COORDINATES

CARTESIAN COORDINATES

BETA XYLOPYRANOSIDE

I	J	K	L	BOND LENGTH	BOND ANGLE	DIHEDRAL ANGLE	ATOMIC MASS
1	0	0	0	0.0	0.0	0.0	12.011149
2	1	0	0	1.523000	0.0	0.0	12.011149
3	2	1	0	1.523000	0.0	0.0	12.011149
4	3	2	1	1.523000	0.0	-56.000000	12.011149
5	4	3	2	1.523000	0.0	56.000000	12.011149
6	1	2	3	1.379999	0.0	180.000000	15.999399
7	2	3	1	1.415000	0.0	-120.000000	15.999399
8	3	4	2	1.415000	0.0	120.000000	15.999399
9	4	5	3	1.415000	0.0	-120.000000	15.999399
10	5	4	3	1.422999	0.0	-57.049988	15.999399
11	6	1	2	1.426999	0.0	180.000000	12.011149
12	7	2	1	0.970000	0.0	-60.000000	1.007970
13	8	3	2	0.970000	0.0	180.000000	1.007970
14	9	4	3	0.970000	0.0	180.000000	1.007970
15	5	4	3	1.096000	0.0	60.000000	1.007970
16	5	4	15	1.096000	0.0	120.000000	1.007970
17	4	5	3	1.092999	0.0	120.000000	1.007970
18	3	4	2	1.092999	0.0	-120.000000	1.007970
19	2	3	1	1.092999	0.0	120.000000	1.007970
20	1	2	3	1.092999	0.0	-60.000000	1.007970
21	11	6	1	1.099999	0.0	180.000000	1.007970
22	11	6	1	1.099999	0.0	-60.000000	1.007970
23	11	6	1	1.099999	0.0	60.000000	1.007970

ATOM NO.	X	Y	Z	MASS
1	0.0	0.0	0.0	12.011149
2	1.523000	0.0	0.0	12.011149
3	2.030665	1.435898	0.0	12.011149
4	1.442863	2.182178	1.190413	12.011149
5	-0.076976	2.096063	1.143435	12.011149
6	-0.460000	-1.301075	0.000001	15.999399
7	1.994664	-0.667037	-1.155342	15.999399
8	3.442600	1.436980	0.093061	15.999399
9	1.840197	3.539282	1.139271	15.999399
10	-0.474338	0.729781	1.125847	15.999399
11	-1.886999	-1.301076	-0.000000	12.011149
12	1.671328	-0.209774	-1.947343	1.007970
13	3.765933	2.351504	0.093062	1.007970
14	1.465824	4.014587	1.897446	1.007970
15	-0.439939	2.548201	0.213358	1.007970
16	-0.499978	2.633110	2.000093	1.007970
17	1.804832	1.731275	2.117944	1.007970
18	1.726206	1.929973	-0.926199	1.007970
19	1.887331	-0.515244	0.892430	1.007970
20	-0.364333	0.515245	-0.892430	1.007970
21	-2.253665	-2.338165	0.000001	1.007970
22	-2.253664	-0.782532	-0.898146	1.007970
23	-2.253665	-0.782530	0.898145	1.007970

TABLE LV

DESCRIPTION OF THE 75 INTERNAL COORDINATES OF THE METHYL XYLOPYRANOSIDES

Valence Bond Coordinates

		Code			Code			Code			Code
1	C1-C2	C1C2	7	C1-06	C106	13	C5H16	CH16	19	C11H22	CH22
2	C2-C3	C2C3	8	C2-07	C207	14	C4H17	CH17	20	C11H23	CH23
3	C3-C4	C3C4	9	C3-08	C308	15	C3H18	CH18	21	07H12	OH12
4	C4-C5	C4C5	10	C4-09	C409	16	C2H19	CH19	22	08H13	OH13
5	C5-010	C5010	11	06-C11	C110	17	C1H20	CH20	23	09H14	OH14
6	010-C1	010C1	12	C5-H15	CH15	18	C11H21	CH21			

Valence Bond Angle Coordinates

		Code			Code			Code
24	C1-C2-C3	CC2C	37	09-C4-C3	CC09	50	H15-C5-C4	H15CC
25	C2-C3-C4	CC3C	38	09-C4-C5	09CC	51	H16-C5-C4	H16CC
26	C3-C4-C5	CC4C	39	H23-C11-06	H23C0	52	H17-C4-C5	HC4C
27	C4-C5-010	CC50	40	H22-C11-06	H22C0	53	H17-C4-C3	CC4H
28	C5-010-C1	C0C	41	H21-C11-06	H21C0	54	H18-C3-C4	HC3C
29	010-C1-C2	010C1C	42	H20-C1-06	HC10	55	H18-C3-C2	CC3H
30	C1-06-C11	C06C	43	H20-C1-010	HC1010	56	H19-C2-C3	HC2C
31	06-C1-C2	06CC	44	H19-C2-07	HC20	57	H19-C2-C1	CC2H
32	06-C1-010	0C0	45	H18-C3-08	HC30(	58	H20-C1-C2	HC1C
33	07-C2-C1	CC07	46	H17-C4-09	HC40	59	H21-C11-H22	H21CH22
34	07-C2-C3	07CC	47	H16-C5-010	H16C0	60	H22-C11-H23	H22CH23
35	08-C3-C2	CC08	48	H15-C5-010	H15C0	61	H21-C11-H23	H21CH23
36	08-C3-C4	08CC	49	H15-C5-H16	HCH	62	H12-07-C2	H07C
						63	H13-08-C3	H08C
						64	H14-09-C4	H09C

Torsional Coordinates

65	C5-010C1-H20 C5-010C1-06	69	H19-C2C3-H18 07-C2C3-C4 C1-C2C3-08	71	H14-09C4-C3
66	H15-C5010-C1 H16-C5010-C1	70	H20-C1C2-H19 010-C1C2-07 (β) 06-C1C2-C3	72	H13-08C3-C2
67	09-C4C5-010 H17-C4C5-H15 C3-C4C5-H16	70	H20-C1C2-C3 010-C1C2-07 (α) 06-C1C2-H19	73	H12-07C2-H19
68	C5-C4C3-08 09-C4C3-C2 H17-C4C3-H18			74	C11-06C1-C2
				75	H21-C11-06-C1 H22-C11-06-C1 H23-C11-06-C1

TABLE LVI

COMPUTER INPUT FOR THE G MATRIX CALCULATION

```
-09
-09          23  75   1
   METHYL ALPHA XYLOPYRANOSIDE

  1  2     1.523000   1  3     2.030665   2  3     1.435898   1  4     1.442863
  2  4     2.182178   3  4     1.190413   1  5    -0.076976   2  5     2.096063
  3  5     1.143435   1  6    -0.460000   2  6     0.650538   3  6    -1.126763
  1  7     1.994664   2  7    -0.667037   3  7    -1.155342   1  8     3.442600
  2  8     1.436980   3  8     0.093061   1  9     1.840197   2  9     3.539282
  3  9     1.139271   1 10    -0.474338   2 10     0.729781   3 10     1.125847
  1 11    -1.886998   2 11     0.650538   3 11    -1.126760   1 12     1.671328
  2 12    -0.209774   3 12    -1.947343   1 13     3.765933   2 13     2.351504
  3 13     0.093062   1 14     1.465824   2 14     4.014587   3 14     1.897446
  1 15    -0.439939   2 15     2.548201   3 15     0.213358   1 16    -0.499978
  2 16     2.633110   3 16     2.000093   1 17     1.804832   2 17     1.731275
  3 17     2.117944   1 18     1.726206   2 18     1.929973   3 18    -0.926199
  1 19     1.887331   2 19    -0.515244   3 19     0.892430   1 20    -0.364333
  2 20    -1.030489   1 21    -2.253667   2 21     1.169082   3 21    -2.024904
  1 22    -2.253660   2 22     1.169083.  3 22    -0.228612   1 23    -2.253663
  2 23    -0.386553   3 23    -1.126758  -1  0     0.0
  1  1  1  2                  2  1  2  3                  3  1  3  4
  4  1  4  5                  5  1  5 10                  6  1  1 10
  7  1  1  6                  8  1  2  7                  9  1  3  8
 10  1  4  9                 11  1 11  6                 12  1  5 15
 13  1  5 16                 14  1  4 17                 15  1  3 18
 16  1  2 19                 17  1  1 20                 18  1 11 21
 19  1 11 22                 20  1 11 23                 21  1  7 12
 22  1  8 13                 23  1  9 14                 24  2  1  2  3
 25  2  2  3  4              26  2  3  4  5              27  2  4  5 10
 28  2  5 10  1              29  2 10  1  2              30  2 11  6  1
 31  2  6  1  2              32  2  6  1 10              33  2  7  2  1
 34  2  7  2  3              35  2  8  3  2              36  2  8  3  4
 37  2  9  4  3              38  2  9  4  5              39  2 23 11  6
 40  2 22 11  6              41  2 21 11  6              42  2 20  1  6
 43  2 20  1 10              44  2 19  2  7              45  2 18  3  8
 46  2 17  4  9              47  2 16  5 10              48  2 15  5 10
 49  2 15  5 16              50  2 15  5  4              51  2 16  5  4
 52  2 17  4  5              53  2 17  4  3              54  2 18  3  4
 55  2 18  3  2              56  2 19  2  3              57  2 19  2  1
 58  2 20  1  2              59  2 21 11 23              60  2 22 11 23
 61  2 21 11 22              62  2 12  7  2              63  2 13  8  3
 64  2 14  9  4              65  4  5 10  1 20           00  4  5 10  1  6
 66  4  1 10  5 16           00  4  1 10  5 15           67  4  9  5  4 10
 00  4 15  5  4 17           00  4 16  5  4  3           68  4  5  4  3  8
 00  4  9  4  3  2           00  4 17  4  3 18           69  4 19  2  3 18
 00  4  7  2  3  4           00  4  1  2  3  8           70  4  6  1  2 19
 00  4 10  1  2  7           00  4 20  1  2  3           71  4 14  9  4  3
 72  4 13  8  3  2           73  4 12  7  2 19           74  4 11  6  1  2
 75  4 21 11  6  1           00  4 22 11  6  1           00  4 23 11  6  1
-02
-06                    METHYL ALPHA XYLOPYRANOSIDE
12.011149   12.011149   12.011149   12.011149   12.011149   15.999399
15.999399   15.999399   15.999399   15.999399   12.011149   1.0079700
1.0079700   1.0079700   1.0079700   1.0079700   1.0079700   1.0079700
1.0079700   1.0079700   1.0079700   1.0079700   1.0079700
```

TABLE LVII

COMPUTER INPUT FOR THE G MATRIX CALCULATION

```
-09
-09          23  75   1
   METHYL BETA XYLOPYRANOSIDE
  1  2     1.523000  1  3     2.030665  2  3     1.435898  1  4     1.442863
  2  4     2.182178  3  4     1.190413  1  5    -0.076976  2  5     2.096063
  3  5     1.143435  1  6    -0.460000  2  6    -1.301075  1  7     1.994664
  2  7    -0.667037  3  7    -1.155342  1  8     3.442600  2  8     1.436980
  3  8     0.093061  1  9     1.840197  2  9     3.539282  3  9     1.139271
  1 10    -0.474338  2 10     0.729781  3 10     1.125847  1 11    -1.886999
  2 11    -1.301076  1 12     1.671328  2 12    -0.209774  3 12    -1.947343
  1 13     3.765933  2 13     2.351504  3 13     0.093062  1 14     1.465824
  2 14     4.014587  3 14     1.897446  1 15    -0.439939  2 15     2.548201
  3 15     0.213358  1 16    -0.499978  2 16     2.633110  3 16     2.000093
  1 17     1.804832  2 17     1.731275  3 17     2.117944  1 18     1.726206
  2 18     1.929973  3 18    -0.926199  1 19     1.887331  2 19    -0.515244
  3 19     0.892430  1 20    -0.364333  2 20     0.515245  3 20    -0.892430
  1 21    -2.253665  2 21    -2.338165  1 22    -2.253664  2 22    -0.782531
  3 22    -0.898147  1 23    -2.253665  2 23    -0.782531  3 23     0.898144
 -1  0     0.0
  1  1  1  2          2  1  2  3          3  1  3  4
  4  1  4  5          5  1  5 10          6  1  1 10
  7  1  1  6          8  1  2  7          9  1  3  8
 10  1  4  9         11  1 11  6         12  1  5 15
 13  1  5 16         14  1  4 17         15  1  3 18
 16  1  2 19         17  1  1 20         18  1 11 21
 19  1 11 22         20  1 11 23         21  1  7 12
 22  1  8 13         23  1  9 14         24  2  1  2  3
 25  2  2  3  4      26  2  3  4  5      27  2  4  5 10
 28  2  5 10  1      29  2 10  1  2      30  2 11  6  1
 31  2  6  1  2      32  2  6  1 10      33  2  7  2  1
 34  2  7  2  3      35  2  8  3  2      36  2  8  3  4
 37  2  9  4  3      38  2  9  4  5      39  2 23 11  6
 40  2 22 11  6      41  2 21 11  6      42  2 20  1  6
 43  2 20  1 10      44  2 19  2  7      45  2 18  3  8
 46  2 17  4  9      47  2 16  5 10      48  2 15  5 10
 49  2 15  5 16      50  2 15  5  4      51  2 16  5  4
 52  2 17  4  5      53  2 17  4  3      54  2 18  3  4
 55  2 18  3  2      56  2 19  2  3      57  2 19  2  1
 58  2 20  1  2      59  2 21 11 23      60  2 22 11 23
 61  2 21 11 22      62  2 12  7  2      63  2 13  8  3
 64  2 14  9  4      65  4  5 10  1  6    00  4  5 10  1 20
 66  4  1 10  5 16   00  4  1 10  5 15    67  4  9  4  5 10
 00  4 15  5  4 17   00  4 16  5  4  3    68  4  5  4  3  8
 00  4  9  4  3  2   00  4 17  4  3 18    69  4 19  2  3 18
 00  4  7  2  3  4   00  4  1  2  3  8    70  4 20  1  2 19
 00  4 10  1  2  7   00  4  6  1  2  3    71  4 14  9  4  3
 72  4 13  8  3  2   73  4 12  7  2 19    74  4 11  6  1  2
 75  4 21 11  6  1   00  4 22 11  6  1    00  4 23 11  6  1
-02
-06
                      METHYL BETA XYLOPYRANOSIDE
12.011149   12.011149   12.011149   12.011149   12.011149   15.999399
15.999399   15.999399   15.999399   15.999399   12.011149   1.0079700
1.0079700   1.0079700   1.0079700   1.0079700   1.0079700   1.0079700
1.0079700   1.0079700   1.0079700   1.0079700   1.0079700
```

TABLE LVIII

$\underset{\sim}{Z}$ MATRIX

METHYL ALPHA XYLOPYRANOSIDE

1	1	1	1.000000	1	2	22	1.000000	1	6	25	1.000000	1	7	26	1.000000
1	16	74	1.000000	1	17	74	1.000000	1	24	29	1.000000	1	29	29	1.000000
1	31	33	1.000000	1	33	33	1.000000	1	57	34	1.000000	1	58	34	1.000000
2	2	1	1.000000	2	3	22	1.000000	2	8	27	1.000000	2	9	27	1.000000
2	15	74	1.000000	2	16	74	1.000000	2	24	29	1.000000	2	25	29	1.000000
2	34	33	1.000000	2	35	33	1.000000	2	55	34	1.000000	2	56	34	1.000000
3	3	1	1.000000	3	4	22	1.000000	3	9	27	1.000000	3	10	27	1.000000
3	14	74	1.000000	3	15	74	1.000000	3	25	29	1.000000	3	26	29	1.000000
3	36	33	1.000000	3	37	33	1.000000	3	53	34	1.000000	3	54	34	1.000000
4	4	1	1.000000	4	5	25	1.000000	4	10	27	1.000000	4	12	74	1.000000
4	13	74	1.000000	4	14	74	1.000000	4	26	29	1.000000	4	27	29	1.000000
4	38	33	1.000000	4	50	34	1.000000	4	51	34	1.000000	4	52	34	1.000000
5	5	2	1.000000	5	6	23	1.000000	5	12	74	1.000000	5	13	74	1.000000
5	27	30	1.000000	5	28	30	1.000000	5	47	35	1.000000	5	48	35	1.000000
6	6	2	1.000000	6	7	24	1.000000	6	17	74	1.000000	6	28	30	1.000000
6	29	30	1.000000	6	32	31	1.000000	6	43	35	1.000000	7	7	3	1.000000
07	11	24	1.000000	07	17	74	1.000000	07	30	30	0.657100	07	31	32	1.000000
7	32	31	1.000000	7	42	35	1.000000	8	8	4	1.000000	8	16	74	1.000000
8	33	32	1.000000	8	34	32	1.000000	8	44	35	1.000000	8	62	36	1.000000
9	9	4	1.000000	9	15	74	1.000000	9	35	32	1.000000	9	36	32	1.000000
9	45	35	1.000000	9	63	36	1.000000	10	10	4	1.000000	10	14	74	1.000000
10	37	32	1.000000	10	38	32	1.000000	10	46	35	1.000000	10	64	36	1.000000
11	11	4	1.000000	11	18	74	1.000000	11	19	74	1.000000	11	20	74	1.000000
11	30	31	0.575000	11	39	69	1.000000	11	40	69	1.000000	11	41	69	1.000000
12	12	6	1.000000	12	13	28	1.000000	12	48	75	1.000000	12	49	75	1.000000
12	50	75	1.000000	13	13	6	1.000000	13	47	75	1.000000	13	49	75	1.000000
13	51	75	1.000000	13	52	75	1.000000	14	14	7	1.000000	14	46	75	1.000000
14	53	75	1.000000	15	15	7	1.000000	15	45	75	1.000000	15	54	75	1.000000
15	55	75	1.000000	16	16	7	1.000000	16	44	75	1.000000	16	56	75	1.000000
16	57	75	1.000000	17	17	7	1.000000	17	42	75	1.000000	17	43	75	1.000000
17	58	75	1.000000	18	18	6	1.000000	18	19	28	1.000000	18	20	28	1.000000
18	41	75	1.000000	18	59	75	1.000000	18	61	75	1.000000	19	19	6	1.000000
19	20	28	1.000000	19	40	75	1.000000	19	60	75	1.000000	19	61	75	1.000000
20	20	6	1.000000	20	39	75	1.000000	20	59	75	1.000000	20	60	75	1.000000
21	21	5	1.000000	22	22	5	1.000000	23	23	5	1.000000	24	24	8	1.000000
24	25	37	1.000000	24	29	37	1.000000	24	31	38	1.000000	24	33	40	1.000000
24	34	40	1.000000	24	35	39	1.000000	24	55	49	1.000000	24	56	48	1.000000
24	57	48	1.000000	24	58	50	1.000000	25	25	8	1.000000	25	26	37	1.000000
25	34	39	1.000000	25	35	40	1.000000	25	36	40	1.000000	25	37	39	1.000000
25	53	49	1.000000	25	54	48	1.000000	25	55	48	1.000000	25	56	49	1.000000
26	26	8	1.000000	26	27	37	1.000000	26	36	39	1.000000	26	37	40	1.000000
26	38	40	1.000000	26	50	49	1.000000	26	51	50	1.000000	26	52	48	1.000000
26	53	48	1.000000	26	54	49	1.000000	27	27	9	1.000000	27	28	37	1.000000
27	38	47	1.000000	27	47	54	1.000000	27	48	54	1.000000	27	50	54	1.000000
27	51	54	1.000000	27	52	49	1.000000	28	28	10	1.000000	28	29	37	1.000000
28	32	44	1.000000	28	43	53	1.000000	28	47	53	1.000000	28	48	52	1.000000
29	29	9	1.000000	29	31	40	1.000000	29	32	43	1.000000	29	33	47	1.000000
29	43	57	1.000000	29	57	55	1.000000	29	58	57	1.000000	30	30	10	1.000000
30	31	45	1.000000	30	32	44	1.000000	30	39	52	1.000000	30	40	52	1.000000
30	41	53	1.000000	30	42	55	1.000000	31	31	12	1.000000	31	32	43	1.000000
31	42	57	1.000000	31	57	56	1.000000	31	58	57	1.000000	32	32	11	1.000000
32	42	57	1.000000	32	43	57	1.000000	33	33	12	1.000000	33	34	41	1.000000
33	44	54	1.000000	33	57	54	1.000000	33	58	55	1.000000	33	62	58	1.000000
34	34	12	1.000000	34	35	42	1.000000	34	44	54	1.000000	34	55	55	1.000000
34	56	54	1.000000	34	62	58	1.000000	35	35	12	1.000000	35	36	41	1.000000
35	45	54	1.000000	35	55	54	1.000000	35	56	55	1.000000	35	63	58	1.000000
36	36	12	1.000000	36	37	42	1.000000	36	45	54	1.000000	36	53	55	1.000000
36	54	54	1.000000	36	63	58	1.000000	37	37	12	1.000000	37	38	41	1.000000
37	46	54	1.000000	37	53	54	1.000000	37	54	55	1.000000	37	64	58	1.000000
38	38	12	1.000000	38	46	54	1.000000	38	50	55	1.000000	38	51	55	1.000000
38	52	54	1.000000	38	64	58	1.000000	39	39	14	1.037000	39	40	71	1.000000
39	41	71	1.000000	39	59	72	1.000000	39	60	72	1.000000	40	40	14	1.037000
40	41	71	1.000000	40	60	72	1.000000	40	61	72	1.000000	41	41	14	1.037000
41	59	72	1.000000	41	61	72	1.000000	42	42	15	1.000000	42	58	64	1.000000
42	43	64	1.000000	43	43	14	1.000000	43	58	64	1.000000	44	44	15	1.000000
44	56	63	1.000000	44	57	63	1.000000	44	62	60	1.000000	45	45	15	1.000000
45	54	63	1.000000	45	55	63	1.000000	45	63	59	1.000000	46	46	15	1.000000
46	64	59	1.000000	46	53	63	1.000000	46	52	63	1.000000	47	47	14	1.000000
47	48	71	1.000000	47	49	72	1.000000	47	51	61	1.000000	48	48	14	1.000000
48	49	72	1.000000	48	50	61	1.000000	49	49	18	1.000000	49	50	62	1.000000
49	51	62	1.000000	50	50	17	1.000000	50	51	70	1.000000	50	52	67	1.000000
51	51	17	1.000000	51	52	66	1.000000	52	52	16	1.000000	52	53	65	1.000000
53	53	16	1.000000	53	54	67	1.000000	54	54	16	1.000000	54	55	65	1.000000
55	55	16	1.000000	55	56	67	1.000000	56	56	16	1.000000	56	57	65	1.000000
57	57	16	1.000000	57	58	66	1.000000	58	58	16	1.000000	59	59	18	1.065000
59	60	62	1.000000	59	61	62	1.000000	60	60	18	1.065000	60	61	62	1.000000
61	61	18	1.065000	62	62	13	1.000000	63	63	13	1.000000	64	64	13	1.000000
65	65	20	1.000000	66	66	20	1.000000	67	67	19	1.000000	68	68	19	1.000000
69	69	19	1.000000	70	70	19	1.000000	71	71	21	1.000000	72	72	21	1.000000
73	73	21	1.000000	74	74	21	1.000000	75	75	21	1.000000	01	08	27	1.000000
31	33	42	1.000000	-2											

TABLE LIX

Z MATRIX

METHYL BETA XYLOPYRANOSIDE

01	01	01	1.000000	01	02	22	1.000000	01	06	25	1.000000	01	07	27	1.000000
1	16	74	1.000000	1	17	74	1.000000	1	24	29	1.000000	1	29	29	1.000000
1	31	33	1.000000	1	33	33	1.000000	1	57	34	1.000000	1	58	34	1.000000
2	2	1	1.000000	2	3	22	1.000000	2	8	27	1.000000	2	9	27	1.000000
2	15	74	1.000000	2	16	74	1.000000	2	24	29	1.000000	2	25	29	1.000000
2	34	33	1.000000	2	35	33	1.000000	2	55	34	1.000000	2	56	34	1.000000
3	3	1	1.000000	3	4	22	1.000000	3	9	27	1.000000	3	10	27	1.000000
3	14	74	1.000000	3	15	74	1.000000	3	25	29	1.000000	3	26	29	1.000000
3	36	33	1.000000	3	37	33	1.000000	3	53	34	1.000000	3	54	34	1.000000
4	4	1	1.000000	4	5	25	1.000000	4	10	27	1.000000	4	12	74	1.000000
4	13	74	1.000000	4	14	74	1.000000	4	26	29	1.000000	4	27	29	1.000000
4	38	33	1.000000	4	50	34	1.000000	4	51	34	1.000000	4	52	34	1.000000
5	5	2	1.000000	5	6	23	1.000000	5	12	74	1.000000	5	13	74	1.000000
5	27	30	1.000000	5	28	30	1.000000	5	47	35	1.000000	5	48	35	1.000000
6	6	2	1.000000	6	7	24	1.000000	6	17	74	1.000000	6	28	30	1.000000
6	29	30	1.000000	6	32	31	1.000000	6	43	35	1.000000	7	7	3	1.000000
07	11	24	1.000000	07	17	74	1.000000	07	30	30	0.657100	07	31	32	1.000000
7	32	31	1.000000	7	42	35	1.000000	8	8	4	1.000000	8	16	74	1.000000
8	33	32	1.000000	8	34	32	1.000000	8	44	35	1.000000	8	62	36	1.000000
9	9	4	1.000000	9	15	74	1.000000	9	35	32	1.000000	9	36	32	1.000000
9	45	35	1.000000	9	63	36	1.000000	10	10	4	1.000000	10	14	74	1.000000
10	37	32	1.000000	10	38	32	1.000000	10	46	35	1.000000	10	64	36	1.000000
11	11	4	1.000000	11	18	74	1.000000	11	19	74	1.000000	11	20	74	1.000000
11	30	31	0.575000	11	39	69	1.000000	11	40	69	1.000000	11	41	69	1.000000
12	12	6	1.000000	12	13	28	1.000000	12	48	75	1.000000	12	49	75	1.000000
12	50	75	1.000000	13	13	6	1.000000	13	47	75	1.000000	13	49	75	1.000000
13	51	75	1.000000	13	52	75	1.000000	14	14	7	1.000000	14	46	75	1.000000
14	53	75	1.000000	15	15	7	1.000000	15	45	75	1.000000	15	54	75	1.000000
15	55	75	1.000000	16	16	7	1.000000	16	44	75	1.000000	16	56	75	1.000000
16	57	75	1.000000	17	17	7	1.000000	17	42	75	1.000000	17	43	75	1.000000
17	58	75	1.000000	18	18	6	1.000000	18	19	28	1.000000	18	20	28	1.000000
18	41	75	1.000000	18	59	75	1.000000	18	61	75	1.000000	19	19	6	1.000000
19	20	28	1.000000	19	40	75	1.000000	19	60	75	1.000000	19	61	75	1.000000
20	20	6	1.000000	20	39	75	1.000000	20	59	75	1.000000	20	60	75	1.000000
21	21	5	1.000000	22	22	5	1.000000	23	23	5	1.000000	24	24	8	1.000000
24	25	37	1.000000	24	29	37	1.000000	24	31	39	1.000000	24	33	40	1.000000
24	34	40	1.000000	24	35	39	1.000000	24	55	49	1.000000	24	56	48	1.000000
24	57	48	1.000000	24	58	49	1.000000	25	25	8	1.000000	25	26	37	1.000000
25	34	39	1.000000	25	35	40	1.000000	25	36	40	1.000000	25	37	39	1.000000
25	53	49	1.000000	25	54	48	1.000000	25	55	48	1.000000	25	56	49	1.000000
26	26	8	1.000000	26	27	37	1.000000	26	36	39	1.000000	26	37	40	1.000000
26	38	40	1.000000	26	50	49	1.000000	26	51	50	1.000000	26	52	48	1.000000
26	53	48	1.000000	26	54	49	1.000000	27	27	9	1.000000	27	28	37	1.000000
27	38	47	1.000000	27	47	54	1.000000	27	48	54	1.000000	27	50	54	1.000000
27	51	54	1.000000	27	52	49	1.000000	28	28	10	1.000000	28	29	37	1.000000
28	32	45	1.000000	28	43	52	1.000000	28	47	53	1.000000	28	48	52	1.000000
29	29	9	1.000000	29	31	40	1.000000	29	32	43	1.000000	29	33	47	1.000000
29	43	57	1.000000	29	57	55	1.000000	29	58	57	1.000000	30	30	10	1.000000
30	31	45	1.000000	30	32	44	1.000000	30	39	52	1.000000	30	40	52	1.000000
30	41	53	1.000000	30	42	55	1.000000	31	31	12	1.000000	31	32	43	1.000000
31	42	57	1.000000	31	57	55	1.000000	31	58	57	1.000000	32	32	11	1.000000
32	42	57	1.000000	32	43	57	1.000000	33	33	12	1.000000	33	34	41	1.000000
33	44	54	1.000000	33	57	54	1.000000	33	58	55	1.000000	33	62	58	1.000000
34	34	12	1.000000	34	35	42	1.000000	34	44	54	1.000000	34	55	55	1.000000
34	56	54	1.000000	34	62	58	1.000000	35	35	12	1.000000	35	36	41	1.000000
35	45	54	1.000000	35	55	54	1.000000	35	56	55	1.000000	35	63	58	1.000000
36	36	12	1.000000	36	37	42	1.000000	36	45	54	1.000000	36	53	55	1.000000
36	54	54	1.000000	36	63	58	1.000000	37	37	12	1.000000	37	38	41	1.000000
37	46	54	1.000000	37	53	54	1.000000	37	54	55	1.000000	37	64	58	1.000000
38	38	12	1.000000	38	46	54	1.000000	38	50	55	1.000000	38	51	55	1.000000
38	52	54	1.000000	38	64	58	1.000000	39	39	14	1.037000	39	40	71	1.000000
39	41	71	1.000000	39	59	72	1.000000	39	60	72	1.000000	40	40	14	1.037000
40	41	71	1.000000	40	60	72	1.000000	40	61	72	1.000000	41	41	14	1.037000
41	59	72	1.000000	41	61	72	1.000000	42	42	15	1.000000	42	58	64	1.000000
42	43	64	1.000000	43	43	14	1.000000	43	58	64	1.000000	44	44	15	1.000000
44	56	63	1.000000	44	57	63	1.000000	44	62	60	1.000000	45	45	15	1.000000
45	54	63	1.000000	45	55	63	1.000000	45	63	59	1.000000	46	46	15	1.000000
46	64	59	1.000000	46	53	63	1.000000	46	52	63	1.000000	47	47	14	1.000000
47	48	71	1.000000	47	49	72	1.000000	47	51	61	1.000000	48	48	14	1.000000
48	49	72	1.000000	48	50	61	1.000000	49	49	18	1.000000	49	50	62	1.000000
49	51	62	1.000000	50	50	17	1.000000	50	51	70	1.000000	50	52	67	1.000000
51	51	17	1.000000	51	52	66	1.000000	52	52	16	1.000000	52	53	65	1.000000
53	53	16	1.000000	53	54	67	1.000000	54	54	16	1.000000	54	55	65	1.000000
55	55	16	1.000000	55	56	67	1.000000	56	56	16	1.000000	56	57	65	1.000000
57	57	16	1.000000	57	58	67	1.000000	58	58	16	1.000000	59	59	18	1.065000
59	60	62	1.000000	59	61	62	1.000000	60	60	18	1.065000	60	61	62	1.000000
61	61	18	1.065000	62	62	13	1.000000	63	63	13	1.000000	64	64	13	1.000000
65	65	20	1.000000	66	66	20	1.000000	67	67	19	1.000000	68	68	19	1.000000
69	69	19	1.000000	70	70	19	1.000000	71	71	21	1.000000	72	72	21	1.000000
73	73	21	1.000000	74	74	21	1.000000	75	75	21	1.000000	01	08	27	1.000000
31	33	42	1.000000	-2											

APPENDIX III

RESULTS OF THE ANALYSES

The information reported in this appendix is as follows:

TABLE LX

CALCULATED INTERNAL COORDINATE DISTRIBUTIONS
BETA ARABINOSE

CONTRIBUTIONS FROM CH AND OH STR.

	CH15	CH16	CH17	CH18	CH19	CH20	OH11	OH12	OH13	OH14
3357.	0.	0.	0.	0.	0.	0.	99.	1.	0.	0.
3356.	0.	0.	0.	0.	0.	0.	1.	13.	80.	7.
3356.	0.	0.	0.	0.	0.	0.	0.	83.	8.	8.
3356.	0.	0.	0.	0.	0.	0.	0.	3.	12.	85.
3002.	48.	50.	0.	0.	0.	0.	0.	0.	0.	0.
2949.	0.	0.	2.	40.	49.	7.	0.	0.	0.	0.
2942.	0.	0.	1.	6.	1.	90.	0.	0.	0.	0.
2939.	0.	0.	95.	0.	4.	1.	0.	0.	0.	0.
2935.	0.	0.	2.	53.	44.	1.	0.	0.	0.	0.
2885.	51.	50.	0.	0.	0.	0.	0.	0.	0.	0.

CONTRIBUTIONS FROM TORSIONS

	TC12	TC23	TC34	TC45	TC50	TOC1	TCO6	TCO7	TCO8	TCO9
913.	0.	0.	0.	0.	1.	0.	0.	0.	1.	0.
852.	0.	0.	0.	0.	0.	1.	0.	0.	0.	0.
769.	0.	0.	0.	0.	0.	3.	0.	0.	0.	0.
697.	0.	0.	0.	0.	0.	0.	0.	0.	0.	0.
615.	0.	0.	0.	2.	9.	3.	1.	0.	0.	0.
592.	1.	0.	0.	0.	0.	0.	0.	0.	2.	0.
492.	0.	0.	1.	1.	0.	0.	0.	4.	1.	0.
463.	0.	0.	0.	3.	11.	2.	0.	0.	1.	0.
411.	0.	0.	0.	0.	0.	0.	11.	6.	4.	7.
391.	0.	0.	0.	1.	1.	0.	10.	1.	2.	6.
363.	0.	0.	0.	0.	1.	1.	26.	3.	17.	26.
354.	0.	0.	0.	0.	1.	0.	8.	1.	46.	19.
338.	0.	0.	0.	0.	0.	0.	8.	66.	5.	2.
315.	1.	0.	1.	1.	0.	0.	15.	5.	1.	26.
297.	0.	2.	0.	0.	3.	0.	4.	1.	7.	0.
257.	0.	4.	0.	0.	1.	1.	1.	6.	5.	0.
237.	0.	0.	2.	0.	0.	6.	0.	0.	3.	1.
209.	3.	1.	0.	6.	2.	8.	4.	0.	0.	2.
143.	13.	0.	16.	16.	0.	13.	0.	0.	0.	1.
128.	14.	30.	13.	0.	4.	0.	0.	0.	0.	0.

TABLE LX (Continued)

CALCULATED INTERNAL COORDINATE DISTRIBUTIONS
BETA ARABINOSE

CONTRIBUTIONS FROM HCC,HCO,HCH BEND

	HO6C	HO7C	HO8C	HO9C	HC5O	HC5O	HC4O	HC3O	HC2O	HC1O	HCO'	HC1C	HC2C	HC2C	HC3C	HC3C	HC4C	HC4C	HC5C	HC5C	HC5H
1478.	0.	0.	0.	1.	3.	1.	1.	0.	0.	0.	0.	0.	0.	0.	0.	0.	1.	2.	11.	14.	57.
1450.	3.	36.	4.	0.	0.	0.	0.	0.	19.	1.	0.	0.	6.	0.	8.	3.	0.	0.	0.	0.	0.
1428.	0.	2.	25.	0.	6.	6.	0.	1.	3.	0.	1.	1.	1.	6.	2.	8.	12.	8.	1.	4.	1.
1405.	10.	4.	11.	2.	14.	13.	3.	1.	3.	5.	0.	3.	0.	4.	0.	2.	0.	5.	6.	4.	4.
1402.	38.	1.	4.	1.	4.	8.	1.	0.	0.	14.	6.	3.	1.	1.	0.	1.	0.	2.	2.	2.	2.
1377.	1.	12.	0.	1.	1.	1.	5.	5.	9.	1.	0.	1.	1.	16.	11.	19.	4.	0.	2.	0.	0.
1355.	0.	1.	3.	0.	3.	0.	0.	2.	1.	2.	36.	17.	11.	5.	5.	1.	1.	1.	1.	0.	1.
1335.	0.	0.	7.	7.	0.	0.	2.	2.	0.	10.	21.	1.	14.	8.	3.	1.	0.	1.	2.	1.	0.
1322.	0.	0.	7.	19.	1.	3.	4.	15.	1.	1.	1.	1.	4.	0.	7.	1.	12.	1.	1.	3.	0.
1304.	33.	1.	1.	9.	1.	0.	3.	0.	0.	35.	1.	11.	1.	0.	0.	1.	0.	2.	1.	0.	1.
1286.	5.	0.	0.	16.	2.	15.	11.	2.	0.	1.	2.	3.	1.	0.	0.	2.	3.	21.	2.	15.	0.
1262.	1.	1.	21.	4.	3.	0.	22.	24.	1.	1.	1.	0.	0.	1.	13.	0.	18.	1.	4.	0.	0.
1239.	0.	1.	2.	18.	24.	11.	10.	1.	2.	0.	0.	0.	4.	0.	0.	0.	0.	5.	14.	4.	0.
1231.	0.	1.	8.	9.	13.	11.	12.	27.	1.	5.	2.	0.	0.	2.	5.	7.	3.	1.	4.	2.	0.
1199.	0.	29.	2.	3.	2.	0.	5.	8.	35.	2.	0.	2.	9.	10.	2.	0.	0.	3.	0.	0.	0.
1156.	0.	4.	1.	0.	6.	2.	14.	12.	4.	4.	3.	0.	0.	1.	3.	9.	3.	0.	3.	9.	0.
1121.	0.	1.	0.	2.	1.	12.	4.	3.	2.	4.	1.	0.	1.	5.	3.	0.	1.	1.	2.	0.	0.
1103.	1.	0.	0.	0.	2.	3.	0.	0.	2.	0.	0.	1.	1.	0.	0.	0.	0.	1.	3.	4.	0.
1100.	0.	1.	1.	0.	0.	2.	0.	1.	2.	1.	0.	1.	3.	0.	0.	1.	5.	0.	1.	0.	0.
1062.	2.	0.	0.	3.	0.	0.	5.	2.	0.	1.	1.	1.	4.	0.	1.	2.	0.	1.	9.	6.	2.
1048.	0.	6.	1.	0.	0.	0.	0.	0.	15.	13.	0.	11.	1.	1.	0.	5.	1.	0.	1.	1.	0.
998.	3.	0.	0.	0.	0.	0.	2.	0.	0.	0.	22.	6.	4.	1.	4.	3.	2.	1.	2.	2.	0.
964.	1.	1.	2.	6.	0.	0.	0.	1.	3.	0.	3.	0.	0.	1.	0.	3.	1.	15.	3.	1.	2.
938.	0.	0.	0.	0.	0.	1.	1.	0.	0.	4.	0.	10.	5.	3.	0.	1.	4.	0.	4.	4.	0.
913.	0.	1.	1.	0.	0.	0.	1.	0.	3.	0.	4.	1.	1.	0.	1.	4.	2.	1.	0.	2.	0.
852.	0.	0.	0.	0.	0.	1.	0.	0.	0.	0.	1.	1.	0.	0.	0.	0.	0.	1.	2.	0.	1.
769.	1.	0.	0.	0.	0.	0.	0.	0.	0.	0.	2.	2.	0.	3.	0.	0.	1.	1.	1.	0.	0.
697.	1.	0.	0.	2.	0.	0.	0.	0.	0.	0.	1.	4.	0.	1.	2.	0.	6.	6.	1.	2.	1.
615.	0.	0.	0.	0.	0.	0.	0.	0.	0.	2.	0.	4.	2.	0.	1.	1.	0.	0.	1.	0.	0.
592.	1.	0.	0.	1.	0.	0.	0.	0.	0.	0.	0.	1.	1.	3.	4.	3.	2.	0.	0.	1.	0.
492.	0.	0.	1.	0.	0.	0.	0.	0.	1.	3.	0.	1.	0.	5.	3.	0.	1.	1.	1.	1.	0.
463.	0.	0.	0.	0.	0.	0.	0.	0.	0.	4.	0.	0.	0.	0.	1.	0.	0.	0.	0.	0.	0.
411.	0.	0.	0.	0.	0.	0.	0.	0.	0.	0.	0.	0.	0.	0.	1.	0.	0.	0.	0.	0.	0.
391.	0.	0.	0.	0.	0.	1.	0.	0.	0.	0.	0.	2.	1.	0.	0.	1.	0.	1.	1.	0.	0.
363.	0.	0.	0.	0.	0.	0.	0.	0.	0.	0.	0.	0.	0.	1.	1.	1.	1.	1.	0.	0.	0.
354.	0.	0.	0.	0.	0.	0.	0.	0.	0.	0.	0.	1.	1.	0.	2.	1.	1.	1.	0.	0.	0.
338.	0.	0.	0.	0.	0.	0.	0.	0.	0.	0.	1.	3.	4.	7.	0.	1.	0.	0.	0.	0.	0.
315.	0.	0.	0.	0.	0.	0.	0.	0.	0.	1.	1.	8.	1.	2.	0.	0.	4.	1.	0.	1.	0.
297.	0.	0.	0.	1.	0.	0.	1.	0.	0.	0.	3.	0.	1.	0.	0.	7.	3.	0.	0.	1.	0.
257.	0.	0.	0.	0.	0.	0.	0.	0.	0.	0.	5.	3.	0.	0.	2.	0.	0.	1.	0.	1.	0.
237.	1.	0.	0.	0.	0.	0.	0.	0.	0.	0.	3.	0.	5.	3.	6.	2.	0.	2.	0.	0.	0.
209.	0.	0.	0.	0.	0.	3.	0.	0.	0.	1.	15.	10.	0.	2.	0.	1.	1.	0.	4.	0.	2.
143.	0.	0.	0.	0.	1.	0.	3.	0.	0.	8.	3.	0.	0.	1.	1.	0.	0.	0.	0.	0.	1.
128.	0.	0.	0.	0.	0.	0.	1.	0.	0.	1.	0.	0.	0.	0.	0.	0.	0.	0.	1.	0.	0.

TABLE LX (Continued)

CALCULATED INTERNAL COORDINATE DISTRIBUTIONS
BETA ARABINOSE

CONTRIBUTIONS FROM CC STRETCH

	C1C2	C2C3	C3C4	C4C5	C5O*	O*C1	C1O6	C2O7	C3O8	C4O9
1478.	0.	0.	0.	0.	0.	0.	0.	0.	0.	1.
1450.	0.	4.	0.	0.	0.	0.	0.	1.	0.	0.
1428.	0.	2.	1.	1.	1.	0.	0.	0.	0.	0.
1405.	2.	1.	0.	0.	1.	0.	0.	0.	0.	1.
1402.	4.	0.	0.	0.	0.	0.	0.	0.	0.	0.
1377.	0.	0.	0.	0.	0.	0.	0.	1.	0.	3.
1355.	1.	3.	1.	0.	3.	1.	0.	0.	0.	1.
1335.	2.	0.	5.	0.	1.	0.	3.	0.	0.	2.
1322.	0.	1.	5.	0.	0.	0.	1.	1.	1.	0.
1304.	0.	1.	0.	1.	0.	1.	4.	1.	0.	1.
1286.	1.	0.	0.	1.	0.	1.	2.	0.	0.	2.
1262.	0.	0.	1.	2.	0.	1.	0.	0.	0.	0.
1239.	0.	0.	0.	1.	0.	0.	1.	0.	0.	8.
1231.	0.	1.	0.	3.	2.	1.	0.	0.	0.	3.
1199.	3.	2.	1.	0.	0.	0.	4.	2.	0.	0.
1156.	1.	0.	14.	10.	7.	5.	1.	0.	0.	17.
1121.	0.	15.	3.	11.	19.	7.	0.	10.	16.	1.
1103.	2.	4.	2.	2.	3.	5.	2.	0.	57.	0.
1100.	1.	2.	3.	9.	4.	1.	3.	63.	4.	0.
1062.	8.	6.	0.	21.	2.	12.	0.	9.	0.	5.
1048.	16.	0.	1.	11.	1.	1.	33.	1.	9.	0.
998.	25.	19.	9.	1.	11.	27.	3.	4.	0.	8.
964.	6.	8.	41.	5.	8.	0.	1.	0.	0.	5.
938.	6.	5.	6.	9.	0.	10.	36.	5.	8.	6.
913.	14.	5.	0.	2.	7.	16.	19.	0.	1.	32.
852.	5.	0.	3.	11.	43.	17.	1.	0.	0.	17.
769.	5.	4.	4.	0.	7.	18.	5.	4.	4.	2.
697.	0.	32.	0.	1.	0.	1.	0.	2.	0.	1.
615.	8.	5.	3.	1.	1.	5.	0.	1.	1.	0.
592.	0.	0.	2.	1.	0.	1.	0.	0.	0.	0.
492.	0.	0.	6.	2.	0.	0.	0.	2.	0.	0.
463.	9.	1.	3.	2.	0.	0.	0.	2.	3.	0.
411.	0.	0.	2.	2.	0.	1.	0.	1.	1.	0.
391.	0.	0.	0.	4.	0.	0.	0.	0.	0.	0.
363.	0.	1.	1.	0.	1.	0.	0.	0.	0.	0.
354.	3.	1.	0.	0.	0.	0.	0.	0.	0.	0.
338.	3.	1.	0.	0.	0.	0.	0.	0.	0.	0.
315.	1.	0.	0.	0.	0.	1.	1.	0.	1.	0.
297.	1.	0.	5.	0.	0.	1.	0.	0.	0.	0.
257.	0.	0.	0.	1.	0.	4.	0.	0.	0.	0.
237.	2.	0.	1.	0.	0.	1.	1.	1.	1.	0.
209.	1.	0.	1.	1.	3.	10.	0.	0.	0.	0.
143.	1.	0.	0.	0.	0.	2.	0.	0.	0.	0.
128.	0.	0.	0.	0.	0.	0.	0.	1.	1.	0.

CALCULATED INTERNAL COORDINATE DISTRIBUTIONS
BETA ARABINOSE

CONTRIBUTIONS FROM CCC AND CCO BEND

	CC2C	CC3C	CC4C	CC5O	COC	OC1C	OCO6	O6CC	CCO7	O7CC	CCO8	O8CC	CCO9	O9CC
1478.	0.	0.	0.	0.	0.	0.	0.	0.	0.	0.	0.	0.	0.	0.
1450.	2.	0.	0.	0.	0.	0.	0.	1.	0.	1.	1.	0.	0.	0.
1428.	0.	0.	0.	0.	0.	0.	0.	0.	0.	0.	2.	1.	0.	0.
1405.	0.	0.	0.	0.	0.	0.	0.	0.	0.	0.	0.	0.	0.	0.
1402.	0.	0.	0.	0.	0.	0.	0.	1.	0.	0.	1.	0.	0.	0.
1377.	0.	0.	1.	0.	0.	0.	0.	0.	0.	0.	0.	0.	0.	0.
1355.	0.	0.	0.	0.	0.	0.	0.	0.	0.	1.	0.	0.	0.	0.
1335.	0.	1.	0.	0.	0.	0.	0.	0.	0.	0.	0.	0.	0.	1.
1322.	0.	0.	1.	0.	0.	0.	0.	0.	0.	0.	0.	0.	0.	0.
1304.	0.	0.	0.	0.	0.	0.	0.	1.	0.	0.	0.	0.	0.	0.
1286.	0.	0.	0.	0.	0.	0.	0.	0.	0.	0.	0.	0.	0.	0.
1262.	0.	0.	0.	0.	0.	0.	0.	0.	0.	0.	0.	0.	1.	0.
1239.	0.	1.	0.	0.	0.	0.	0.	0.	0.	0.	0.	0.	2.	0.
1231.	0.	0.	1.	0.	0.	0.	0.	0.	0.	0.	0.	1.	1.	0.
1199.	0.	1.	0.	0.	0.	1.	0.	0.	0.	0.	0.	0.	0.	0.
1156.	0.	0.	5.	0.	0.	0.	0.	0.	0.	1.	0.	3.	0.	1.
1121.	1.	2.	1.	0.	4.	4.	2.	0.	4.	0.	0.	2.	0.	3.
1103.	2.	2.	3.	0.	2.	2.	0.	0.	1.	0.	1.	1.	0.	0.
1100.	6.	7.	1.	0.	0.	3.	0.	0.	3.	3.	1.	1.	0.	2.
1062.	1.	1.	1.	1.	0.	1.	2.	1.	1.	4.	0.	2.	2.	1.
1048.	3.	0.	0.	0.	0.	3.	1.	1.	3.	0.	3.	0.	0.	1.
998.	0.	1.	1.	1.	3.	0.	1.	6.	0.	2.	0.	2.	0.	0.
964.	0.	0.	1.	8.	1.	1.	0.	1.	0.	2.	4.	2.	5.	1.
938.	0.	1.	0.	0.	1.	0.	5.	0.	0.	1.	1.	0.	0.	1.
913.	2.	0.	0.	1.	1.	0.	0.	1.	0.	1.	3.	0.	0.	2.
852.	1.	0.	0.	3.	0.	1.	2.	1.	1.	1.	0.	4.	0.	1.
769.	2.	3.	0.	6.	15.	1.	0.	4.	8.	3.	2.	0.	0.	2.
697.	0.	3.	3.	13.	1.	0.	2.	2.	1.	0.	0.	1.	4.	5.
615.	0.	0.	0.	2.	5.	2.	24.	4.	4.	0.	0.	3.	4.	5.
592.	3.	3.	1.	5.	7.	0.	3.	16.	5.	0.	0.	10.	21.	4.
492.	0.	0.	2.	0.	0.	16.	10.	2.	0.	22.	14.	1.	0.	13.
463.	0.	1.	18.	0.	3.	10.	2.	1.	5.	2.	5.	1.	0.	6.
411.	9.	9.	1.	1.	0.	1.	4.	0.	17.	3.	1.	14.	0.	4.
391.	7.	6.	1.	8.	20.	0.	6.	0.	2.	9.	8.	2.	0.	11.
363.	0.	0.	0.	1.	2.	0.	0.	0.	4.	0.	3.	2.	2.	1.
354.	0.	1.	1.	0.	2.	0.	0.	2.	3.	2.	5.	0.	0.	0.
338.	1.	1.	0.	1.	0.	0.	2.	0.	0.	0.	3.	2.	0.	1.
315.	0.	0.	1.	0.	1.	6.	3.	1.	2.	11.	3.	1.	3.	14.
297.	0.	0.	10.	0.	0.	2.	2.	11.	2.	10.	22.	7.	20.	1.
257.	2.	1.	7.	1.	0.	6.	2.	14.	13.	11.	6.	17.	11.	0.
237.	6.	2.	1.	1.	2.	10.	1.	14.	3.	1.	1.	8.	10.	2.
209.	0.	4.	5.	5.	29.	0.	27.	13.	4.	0.	0.	0.	2.	12.
143.	3.	4.	6.	5.	6.	7.	0.	4.	1.	0.	0.	1.	0.	0.
128.	14.	11.	0.	0.	0.	0.	0.	1.	3.	3.	3.	3.	1.	0.

TABLE LXI

CALCULATED INTERNAL COORDINATE DISTRIBUTIONS
BETA LYXOSE

CONTRIBUTIONS FROM CH AND OH STR.

	CH15	CH16	CH17	CH18	CH19	CH20	OH11	OH12	OH13	OH14
3357.	0.	0.	0.	0.	0.	0.	96.	4.	0.	0.
3356.	0.	0.	0.	0.	0.	0.	0.	12.	81.	7.
3356.	0.	0.	0.	0.	0.	0.	0.	1.	6.	92.
3356.	0.	0.	0.	0.	0.	0.	4.	83.	12.	0.
3000.	48.	49.	1.	0.	0.	0.	0.	0.	0.	0.
2948.	0.	0.	50.	46.	2.	0.	0.	0.	0.	0.
2941.	0.	0.	1.	0.	13.	85.	0.	0.	0.	0.
2939.	0.	0.	2.	0.	83.	14.	0.	0.	0.	0.
2935.	0.	0.	45.	53.	1.	0.	0.	0.	0.	0.
2888.	51.	50.	0.	0.	0.	0.	0.	0.	0.	0.

CONTRIBUTIONS FROM TORSIONS

	TC12	TC23	TC34	TC45	TC50	TOC1	TCO6	TCO7	TCO8	TCO9
898.	0.	0.	0.	1.	4.	0.	1.	0.	1.	1.
877.	0.	0.	0.	0.	0.	1.	2.	0.	0.	0.
750.	0.	0.	0.	0.	0.	0.	0.	0.	0.	0.
680.	0.	0.	0.	0.	0.	0.	0.	0.	0.	0.
633.	0.	0.	0.	0.	0.	3.	0.	0.	0.	1.
511.	0.	0.	0.	1.	3.	0.	2.	0.	1.	2.
492.	0.	1.	0.	0.	4.	1.	9.	2.	0.	1.
437.	0.	0.	0.	0.	3.	0.	1.	0.	1.	2.
398.	0.	0.	0.	1.	0.	0.	0.	15.	3.	3.
383.	1.	0.	1.	3.	6.	9.	8.	1.	12.	1.
366.	0.	0.	0.	2.	3.	2.	3.	2.	30.	22.
360.	0.	0.	0.	0.	2.	1.	30.	16.	0.	10.
347.	2.	1.	0.	4.	1.	4.	5.	44.	0.	2.
337.	0.	0.	0.	0.	0.	1.	10.	0.	33.	38.
287.	0.	0.	0.	0.	1.	2.	16.	1.	0.	1.
278.	0.	2.	0.	0.	0.	2.	5.	5.	0.	0.
266.	0.	0.	0.	0.	0.	0.	0.	0.	9.	8.
234.	2.	0.	5.	0.	0.	1.	2.	5.	1.	0.
140.	16.	1.	11.	18.	1.	15.	0.	0.	0.	0.
130.	9.	28.	18.	1.	3.	0.	0.	0.	0.	0.

TABLE LXI (Continued)

CALCULATED INTERNAL COORDINATE DISTRIBUTIONS
BETA LYXOSE

CONTRIBUTIONS FROM HCC,HCO,HCH BEND

	HO6C	HO7C	HO8C	HO9C	HC5D	HC5O	HC4O	HC3O	HC2O	HC1O	HCO'	HC1C	HC2C	HC2C	HC3C	HC3C	HC4C	HC4C	HC5C	HC5C	HC5H
1478.	0.	0.	1.	0.	0.	0.	0.	0.	0.	0.	0.	0.	0.	0.	0.	2.	2.	0.	18.	15.	46.
1440.	3.	1.	12.	15.	0.	0.	0.	1.	1.	1.	1.	0.	4.	9.	9.	18.	0.	1.	0.	2.	2.
1416.	6.	5.	23.	0.	0.	0.	0.	4.	0.	5.	0.	11.	1.	1.	6.	0.	0.	0.	0.	0.	0.
1400.	7.	7.	0.	30.	2.	2.	5.	1.	0.	5.	7.	0.	5.	10.	1.	1.	1.	3.	0.	3.	0.
1387.	0.	13.	1.	0.	21.	18.	0.	0.	2.	0.	3.	1.	0.	4.	1.	0.	8.	7.	4.	4.	10.
1380.	4.	34.	6.	0.	4.	5.	0.	3.	5.	8.	6.	0.	3.	0.	3.	0.	1.	1.	1.	1.	3.
1361.	1.	3.	8.	13.	6.	3.	2.	1.	1.	7.	16.	1.	0.	0.	3.	3.	8.	17.	8.	1.	0.
1348.	1.	7.	0.	1.	3.	6.	2.	2.	1.	17.	21.	0.	1.	0.	0.	1.	17.	10.	3.	1.	1.
1327.	1.	1.	13.	4.	0.	0.	3.	3.	6.	16.	0.	10.	27.	7.	0.	3.	3.	0.	0.	0.	0.
1300.	5.	2.	8.	2.	0.	7.	17.	0.	4.	0.	13.	11.	0.	0.	10.	11.	4.	1.	0.	5.	0.
1278.	13.	16.	0.	0.	1.	0.	0.	20.	32.	4.	0.	0.	0.	12.	4.	2.	0.	0.	0.	1.	0.
1253.	1.	0.	1.	20.	5.	6.	43.	2.	0.	0.	4.	2.	0.	0.	1.	7.	6.	11.	1.	0.	1.
1235.	6.	0.	20.	0.	0.	1.	1.	52.	3.	4.	2.	3.	1.	7.	11.	5.	0.	2.	0.	0.	0.
1229.	15.	1.	1.	5.	18.	18.	4.	2.	16.	8.	1.	1.	3.	1.	2.	0.	1.	1.	9.	10.	0.
1220.	25.	2.	1.	2.	13.	8.	12.	2.	14.	4.	1.	5.	7.	0.	0.	1.	3.	1.	4.	2.	0.
1146.	0.	1.	1.	1.	4.	1.	11.	6.	1.	2.	1.	1.	2.	0.	3.	2.	1.	0.	6.	15.	0.
1130.	0.	0.	0.	2.	1.	1.	1.	0.	1.	2.	0.	1.	0.	2.	1.	0.	0.	1.	0.	1.	0.
1102.	1.	1.	1.	0.	0.	0.	0.	1.	11.	2.	3.	2.	1.	3.	0.	3.	2.	1.	0.	0.	4.
1093.	4.	0.	0.	1.	1.	5.	0.	0.	2.	0.	7.	1.	2.	0.	0.	0.	0.	1.	0.	1.	1.
1075.	1.	1.	0.	1.	0.	4.	2.	6.	0.	9.	1.	3.	3.	2.	5.	0.	0.	1.	1.	0.	0.
1066.	3.	0.	2.	2.	4.	4.	0.	0.	3.	0.	5.	0.	0.	0.	4.	4.	1.	2.	6.	6.	0.
1029.	1.	0.	0.	0.	0.	0.	4.	0.	4.	6.	2.	2.	0.	0.	4.	1.	1.	0.	2.	0.	4.
1002.	0.	0.	2.	0.	1.	0.	0.	0.	0.	1.	0.	1.	9.	0.	2.	1.	5.	1.	2.	4.	0.
949.	0.	5.	0.	1.	0.	0.	0.	1.	0.	0.	3.	10.	1.	8.	0.	1.	2.	4.	5.	5.	0.
898.	0.	0.	1.	1.	0.	1.	0.	1.	0.	0.	1.	6.	0.	2.	4.	0.	2.	5.	3.	3.	1.
877.	3.	0.	0.	0.	0.	0.	0.	0.	1.	1.	0.	12.	0.	1.	0.	0.	1.	0.	1.	1.	0.
750.	1.	2.	0.	0.	0.	0.	0.	0.	0.	1.	2.	0.	5.	1.	0.	0.	0.	1.	1.	0.	0.
680.	1.	0.	1.	0.	0.	0.	0.	0.	0.	1.	1.	0.	1.	9.	1.	4.	0.	0.	0.	0.	0.
633.	0.	0.	0.	0.	0.	0.	0.	0.	0.	0.	0.	1.	0.	2.	1.	2.	0.	1.	3.	0.	1.
511.	0.	0.	0.	0.	0.	1.	0.	0.	0.	0.	0.	2.	0.	1.	0.	0.	1.	6.	2.	1.	0.
492.	0.	0.	0.	1.	0.	0.	0.	0.	0.	0.	1.	4.	3.	1.	0.	4.	5.	1.	0.	0.	1.
437.	0.	0.	1.	0.	0.	0.	0.	0.	0.	0.	1.	0.	1.	1.	0.	7.	4.	3.	0.	0.	0.
398.	1.	0.	0.	0.	0.	1.	0.	0.	0.	1.	1.	0.	0.	0.	0.	0.	1.	0.	0.	1.	1.
383.	0.	0.	0.	0.	0.	1.	0.	0.	0.	0.	1.	0.	0.	1.	0.	1.	0.	2.	2.	0.	1.
366.	0.	0.	0.	0.	0.	2.	0.	0.	0.	0.	0.	0.	0.	0.	1.	1.	0.	3.	3.	0.	1.
360.	0.	0.	0.	0.	0.	0.	0.	0.	0.	0.	0.	1.	1.	1.	0.	0.	1.	0.	0.	1.	0.
347.	0.	0.	0.	0.	0.	1.	0.	0.	0.	0.	0.	0.	1.	2.	1.	1.	3.	1.	1.	0.	0.
337.	0.	0.	0.	0.	0.	0.	0.	0.	0.	0.	1.	2.	0.	1.	2.	2.	3.	0.	0.	0.	0.
287.	0.	0.	0.	0.	0.	0.	0.	0.	0.	0.	12.	8.	2.	0.	1.	0.	0.	0.	0.	0.	0.
278.	0.	1.	0.	0.	0.	0.	0.	0.	0.	1.	0.	4.	0.	4.	0.	1.	0.	0.	0.	0.	0.
266.	0.	0.	0.	0.	1.	1.	0.	0.	0.	0.	0.	0.	0.	2.	3.	1.	3.	1.	1.	1.	0.
234.	0.	1.	0.	0.	0.	0.	0.	0.	0.	0.	2.	7.	7.	0.	6.	2.	2.	1.	0.	0.	0.
140.	0.	0.	0.	0.	1.	0.	0.	0.	1.	0.	0.	0.	0.	0.	1.	0.	0.	0.	1.	0.	1.
130.	0.	0.	0.	0.	0.	0.	0.	0.	3.	0.	0.	1.	0.	0.	0.	0.	0.	0.	1.	0.	0.

TABLE LXI (Continued)

CALCULATED INTERNAL COORDINATE DISTRIBUTIONS
BETA LYXOSE

CONTRIBUTIONS FROM CC STRETCH

	C1C2	C2C3	C3C4	C4C5	C50'	O'C1	C1O6	C2O7	C3O8	C4O9
1478.	0.	0.	0.	0.	0.	0.	0.	0.	0.	1.
1440.	0.	0.	0.	0.	0.	1.	0.	1.	0.	0.
1416.	6.	3.	2.	0.	0.	1.	0.	7.	1.	0.
1400.	0.	0.	5.	0.	0.	1.	1.	1.	0.	1.
1387.	0.	1.	1.	0.	0.	0.	0.	1.	0.	0.
1380.	3.	3.	1.	0.	0.	0.	0.	1.	0.	0.
1361.	0.	0.	0.	1.	1.	0.	0.	0.	0.	1.
1348.	0.	0.	1.	0.	0.	0.	0.	0.	0.	0.
1327.	0.	0.	0.	0.	0.	2.	0.	1.	0.	1.
1300.	0.	0.	1.	0.	0.	1.	0.	0.	0.	1.
1278.	0.	2.	1.	0.	1.	0.	0.	1.	0.	1.
1253.	0.	0.	1.	2.	2.	0.	0.	0.	1.	0.
1235.	0.	0.	0.	1.	0.	0.	2.	0.	0.	0.
1229.	1.	0.	0.	0.	0.	1.	0.	1.	0.	0.
1220.	0.	0.	0.	0.	2.	1.	3.	3.	0.	0.
1146.	0.	2.	11.	16.	5.	5.	0.	5.	1.	11.
1130.	3.	8.	3.	0.	2.	2.	29.	4.	48.	0.
1102.	3.	2.	4.	0.	1.	0.	0.	7.	2.	57.
1093.	6.	0.	3.	2.	50.	17.	2.	5.	1.	11.
1075.	11.	18.	0.	10.	0.	4.	39.	0.	26.	2.
1066.	0.	10.	11.	29.	3.	1.	7.	2.	0.	8.
1029.	8.	2.	0.	26.	7.	10.	1.	13.	7.	1.
1002.	3.	32.	18.	1.	5.	1.	14.	4.	4.	0.
949.	42.	9.	6.	3.	4.	15.	0.	0.	9.	1.
898.	10.	2.	19.	3.	9.	9.	1.	20.	1.	0.
877.	2.	0.	1.	0.	4.	20.	0.	37.	1.	0.
750.	1.	1.	0.	0.	8.	38.	5.	0.	1.	1.
680.	1.	1.	23.	2.	0.	0.	1.	0.	0.	7.
633.	1.	0.	5.	1.	0.	0.	4.	0.	2.	2.
511.	0.	2.	5.	10.	2.	0.	1.	0.	2.	1.
492.	9.	4.	0.	2.	2.	0.	1.	0.	2.	1.
437.	4.	1.	0.	3.	2.	1.	0.	0.	1.	1.
398.	0.	0.	0.	0.	0.	0.	1.	0.	0.	2.
383.	4.	0.	0.	0.	6.	1.	1.	0.	1.	0.
366.	0.	0.	2.	0.	4.	1.	0.	0.	0.	0.
360.	0.	8.	0.	0.	0.	0.	0.	0.	0.	0.
347.	1.	0.	0.	0.	0.	0.	0.	0.	0.	1.
337.	1.	1.	0.	0.	1.	1.	0.	0.	0.	0.
287.	0.	5.	0.	1.	2.	3.	0.	0.	0.	0.
278.	2.	0.	0.	0.	0.	0.	0.	0.	0.	0.
266.	0.	4.	0.	2.	2.	0.	0.	0.	0.	0.
234.	7.	2.	0.	0.	0.	2.	0.	1.	1.	0.
140.	0.	0.	0.	0.	0.	0.	1.	0.	0.	1.
130.	0.	0.	0.	0.	0.	0.	0.	0.	1.	1.

CALCULATED INTERNAL COORDINATE DISTRIBUTIONS
BETA LYXOSE

CONTRIBUTIONS FROM CCC AND CCO BEND

	CC2C	CC3C	CC4C	CC5O	COC	OC1C	OC06	O6CC	CCO7	O7CC	CCO8	O8CC	CCO9	O9CC
1478.	0.	0.	0.	0.	0.	0.	0.	0.	0.	0.	0.	0.	0.	1.
1440.	0.	0.	0.	0.	0.	0.	0.	1.	0.	0.	1.	0.	2.	0.
1416.	3.	0.	0.	0.	0.	0.	0.	1.	0.	0.	3.	0.	0.	0.
1400.	0.	1.	0.	0.	0.	0.	0.	1.	1.	0.	0.	0.	1.	0.
1387.	0.	0.	0.	0.	0.	0.	0.	0.	0.	0.	0.	1.	0.	0.
1380.	0.	0.	0.	0.	0.	0.	0.	0.	1.	0.	0.	0.	0.	0.
1361.	0.	0.	0.	0.	0.	0.	0.	0.	0.	0.	0.	0.	0.	0.
1348.	0.	0.	0.	0.	0.	0.	0.	0.	0.	0.	0.	0.	0.	0.
1327.	0.	0.	0.	0.	0.	0.	0.	1.	0.	0.	0.	0.	0.	0.
1300.	0.	0.	0.	0.	0.	0.	0.	0.	0.	0.	0.	0.	0.	0.
1278.	0.	1.	0.	0.	0.	0.	0.	1.	1.	0.	0.	0.	0.	0.
1253.	0.	0.	0.	0.	0.	0.	0.	0.	0.	0.	0.	0.	0.	0.
1235.	0.	0.	0.	0.	0.	0.	0.	0.	0.	0.	0.	0.	0.	0.
1229.	0.	0.	0.	0.	0.	0.	0.	0.	0.	0.	0.	0.	0.	0.
1220.	0.	0.	0.	0.	0.	0.	0.	0.	0.	0.	0.	0.	0.	0.
1146.	0.	0.	7.	0.	1.	0.	0.	0.	1.	1.	0.	3.	0.	0.
1130.	3.	4.	3.	0.	2.	2.	1.	0.	0.	0.	1.	2.	1.	0.
1102.	2.	3.	1.	7.	0.	1.	0.	1.	0.	1.	2.	0.	2.	6.
1093.	2.	0.	0.	0.	1.	0.	1.	1.	0.	1.	1.	0.	0.	0.
1075.	0.	3.	2.	0.	3.	6.	1.	2.	1.	2.	0.	4.	2.	0.
1066.	3.	1.	0.	0.	0.	0.	0.	2.	0.	1.	1.	0.	1.	0.
1029.	3.	1.	0.	7.	1.	1.	0.	1.	0.	0.	3.	2.	0.	7.
1002.	1.	1.	0.	0.	0.	3.	1.	0.	0.	7.	2.	1.	0.	1.
949.	0.	3.	0.	0.	0.	0.	4.	0.	7.	0.	0.	1.	1.	0.
898.	1.	1.	1.	1.	3.	0.	5.	1.	4.	0.	2.	1.	6.	2.
877.	0.	0.	0.	0.	5.	3.	7.	2.	1.	1.	0.	0.	0.	1.
750.	2.	2.	0.	0.	4.	6.	2.	3.	9.	0.	3.	0.	0.	3.
680.	1.	5.	2.	0.	2.	6.	2.	6.	0.	15.	10.	2.	2.	0.
633.	0.	0.	3.	18.	16.	3.	11.	1.	0.	6.	2.	3.	1.	1.
511.	0.	0.	5.	1.	2.	0.	13.	4.	0.	2.	2.	7.	2.	15.
492.	0.	1.	2.	3.	1.	0.	16.	7.	1.	1.	2.	8.	12.	0.
437.	11.	2.	2.	5.	16.	0.	1.	0.	0.	2.	3.	18.	11.	0.
398.	1.	7.	13.	4.	13.	10.	1.	9.	2.	6.	2.	2.	0.	5.
383.	2.	4.	8.	3.	7.	2.	3.	0.	0.	3.	6.	1.	3.	8.
366.	1.	0.	0.	3.	9.	0.	0.	0.	4.	0.	4.	1.	1.	5.
360.	1.	1.	4.	1.	1.	4.	0.	4.	3.	1.	0.	1.	8.	0.
347.	0.	5.	1.	1.	10.	0.	0.	1.	1.	0.	0.	1.	8.	0.
337.	0.	0.	0.	0.	0.	0.	1.	0.	0.	1.	2.	0.	0.	4.
287.	0.	0.	0.	0.	1.	1.	25.	35.	0.	1.	10.	2.	1.	2.
278.	5.	0.	1.	1.	1.	4.	1.	0.	50.	9.	5.	0.	0.	0.
266.	0.	0.	1.	0.	0.	0.	0.	0.	0.	0.	15.	26.	22.	23.
234.	21.	4.	1.	0.	1.	4.	3.	3.	6.	33.	6.	1.	1.	0.
140.	5.	1.	6.	6.	2.	5.	2.	1.	0.	2.	0.	0.	3.	4.
130.	5.	16.	3.	1.	1.	2.	2.	0.	0.	0.	3.	4.	1.	1.

TABLE LXII

CALCULATED INTERNAL COORDINATE DISTRIBUTIONS
ALPHA XYLOSE

CONTRIBUTIONS FROM CH AND OH STR.

	CH15	CH16	CH17	CH18	CH19	CH20	OH11	OH12	OH13	OH14
3356.	0.	0.	0.	0.	0.	0.	1.	16.	81.	2.
3357.	0.	0.	0.	0.	0.	0.	99.	1.	0.	0.
3356.	0.	0.	0.	0.	0.	0.	0.	1.	1.	97.
3356.	0.	0.	0.	0.	0.	0.	0.	82.	17.	0.
3000.	48.	49.	1.	0.	0.	0.	0.	0.	0.	0.
2953.	0.	0.	22.	50.	25.	2.	0.	0.	0.	0.
2943.	0.	0.	20.	1.	14.	63.	0.	0.	0.	0.
2941.	0.	0.	29.	0.	35.	34.	0.	0.	0.	0.
2933.	0.	0.	27.	48.	25.	0.	0.	0.	0.	0.
2888.	51.	50.	0.	0.	0.	0.	0.	0.	0.	0.

CONTRIBUTIONS FROM TORSIONS

	TC12	TC23	TC34	TC45	TC50	TOC1	TC06	TC07	TC08	TC09
921.	0.	0.	0.	0.	2.	0.	0.	0.	1.	0.
906.	0.	0.	0.	0.	0.	0.	1.	0.	0.	0.
761.	0.	0.	0.	0.	0.	2.	0.	0.	0.	0.
620.	0.	0.	0.	2.	6.	0.	2.	0.	1.	0.
570.	0.	0.	1.	0.	0.	2.	1.	2.	2.	0.
541.	0.	0.	0.	0.	2.	0.	0.	0.	0.	1.
506.	0.	0.	0.	1.	1.	0.	0.	0.	0.	0.
438.	1.	0.	0.	0.	0.	0.	6.	2.	0.	6.
425.	0.	1.	0.	0.	12.	2.	3.	1.	1.	2.
389.	0.	0.	0.	0.	0.	2.	0.	0.	5.	13.
360.	1.	0.	0.	1.	0.	0.	46.	10.	3.	11.
359.	0.	0.	0.	1.	0.	1.	0.	15.	46.	3.
349.	0.	0.	0.	1.	1.	1.	19.	38.	13.	2.
331.	0.	1.	0.	0.	0.	1.	1.	10.	8.	45.
275.	1.	1.	0.	1.	0.	0.	0.	12.	0.	2.
270.	0.	0.	2.	4.	1.	4.	7.	0.	8.	4.
260.	0.	2.	3.	2.	0.	4.	2.	2.	4.	2.
232.	2.	0.	0.	5.	3.	0.	4.	0.	0.	0.
135.	24.	7.	3.	11.	1.	12.	1.	0.	0.	0.
127.	3.	23.	26.	3.	3.	4.	0.	0.	0.	0.

TABLE LXII (Continued)

CALCULATED INTERNAL COORDINATE DISTRIBUTIONS
ALPHA XYLOSE

CONTRIBUTIONS FROM HCC,HCO,HCH BEND

	HO6C	HO7C	HO8C	HO9C	H15O	H16O	HC4O	HC3O	HC2O	HC1O	HCO'	HC1C	HC2C	HC2C	HC3C	HC3C	HC4C	HC4C	H15C	H16C	HC5H
1480.	0.	0.	2.	0.	0.	0.	0.	0.	0.	0.	0.	0.	0.	2.	0.	2.	4.	0.	18.	13.	42.
1448.	3.	37.	3.	0.	0.	0.	0.	0.	20.	0.	0.	0.	6.	0.	8.	2.	0.	0.	0.	0.	0.
1440.	0.	2.	17.	19.	0.	0.	1.	1.	3.	0.	0.	0.	2.	9.	1.	11.	2.	0.	0.	4.	7.
1403.	43.	5.	0.	1.	1.	0.	0.	0.	2.	18.	4.	7.	0.	0.	0.	0.	0.	1.	0.	0.	0.
1393.	6.	2.	2.	19.	9.	11.	2.	1.	2.	1.	3.	0.	1.	4.	1.	1.	6.	14.	0.	4.	7.
1383.	0.	5.	4.	9.	17.	18.	0.	0.	5.	0.	4.	4.	1.	8.	2.	2.	0.	1.	10.	3.	4.
1365.	0.	1.	32.	10.	1.	0.	8.	7.	0.	2.	2.	0.	1.	2.	2.	7.	13.	2.	1.	0.	0.
1355.	0.	2.	5.	0.	3.	0.	2.	6.	2.	3.	34.	14.	9.	2.	9.	1.	0.	2.	0.	0.	1.
1339.	0.	3.	1.	3.	8.	5.	3.	0.	2.	0.	3.	2.	2.	7.	10.	10.	8.	19.	6.	3.	1.
1319.	1.	0.	2.	4.	1.	0.	3.	4.	1.	10.	18.	1.	20.	6.	9.	1.	8.	3.	0.	1.	0.
1302.	38.	1.	0.	1.	0.	2.	0.	1.	0.	34.	0.	14.	2.	0.	0.	1.	0.	0.	0.	0.	1.
1257.	0.	1.	3.	5.	9.	13.	46.	4.	0.	3.	0.	0.	0.	0.	4.	0.	7.	8.	4.	5.	0.
1248.	2.	0.	15.	17.	0.	0.	8.	49.	0.	0.	1.	0.	0.	1.	6.	13.	2.	2.	1.	2.	0.
1220.	0.	0.	4.	5.	23.	22.	15.	16.	0.	0.	1.	0.	1.	1.	2.	1.	3.	3.	11.	9.	0.
1204.	0.	31.	5.	1.	0.	0.	1.	4.	37.	2.	0.	2.	10.	10.	1.	0.	1.	1.	0.	0.	0.
1148.	0.	3.	0.	1.	6.	3.	8.	5.	2.	1.	2.	0.	0.	1.	1.	2.	1.	0.	2.	8.	0.
1128.	0.	0.	0.	0.	1.	1.	7.	0.	1.	9.	0.	0.	0.	0.	5.	0.	0.	0.	0.	5.	0.
1104.	1.	0.	0.	1.	3.	7.	0.	4.	0.	2.	0.	1.	5.	2.	0.	0.	0.	1.	0.	0.	3.
1097.	0.	1.	0.	2.	0.	0.	0.	4.	2.	0.	0.	0.	0.	1.	1.	0.	0.	2.	0.	1.	0.
1078.	1.	7.	2.	0.	0.	0.	1.	0.	15.	0.	1.	2.	0.	4.	1.	3.	3.	0.	0.	0.	1.
1057.	0.	0.	1.	2.	2.	3.	2.	0.	0.	1.	0.	0.	0.	0.	0.	2.	1.	2.	10.	6.	1.
1037.	0.	3.	0.	1.	0.	0.	0.	0.	7.	10.	3.	14.	3.	3.	0.	2.	3.	2.	5.	5.	0.
1000.	4.	0.	0.	0.	0.	0.	1.	1.	0.	0.	20.	2.	4.	0.	4.	1.	2.	0.	0.	1.	2.
935.	0.	0.	0.	1.	1.	1.	0.	1.	0.	4.	0.	7.	5.	3.	0.	0.	3.	4.	4.	6.	1.
921.	0.	2.	3.	0.	0.	0.	1.	0.	3.	0.	3.	0.	0.	1.	2.	4.	2.	2.	3.	3.	0.
906.	0.	1.	0.	0.	0.	0.	0.	1.	1.	0.	5.	6.	0.	0.	0.	0.	1.	0.	0.	0.	1.
761.	2.	0.	0.	0.	0.	0.	0.	0.	0.	0.	4.	4.	1.	5.	0.	0.	0.	0.	0.	0.	0.
620.	0.	0.	0.	0.	0.	0.	0.	0.	0.	1.	0.	1.	3.	3.	1.	1.	2.	2.	0.	0.	0.
570.	0.	0.	1.	0.	0.	0.	0.	0.	0.	2.	0.	4.	0.	3.	6.	0.	2.	6.	5.	0.	0.
541.	1.	0.	0.	1.	0.	0.	0.	0.	0.	1.	0.	4.	0.	0.	0.	2.	2.	0.	2.	0.	2.
506.	0.	0.	0.	0.	0.	0.	0.	0.	1.	1.	0.	0.	0.	0.	0.	5.	0.	0.	0.	1.	0.
438.	0.	0.	0.	0.	0.	2.	0.	0.	0.	1.	0.	0.	0.	0.	3.	0.	0.	3.	1.	0.	0.
425.	0.	0.	0.	0.	0.	0.	0.	0.	0.	3.	0.	0.	0.	2.	2.	7.	2.	1.	0.	1.	0.
389.	0.	0.	1.	0.	0.	0.	0.	0.	0.	0.	0.	1.	0.	0.	0.	2.	0.	5.	2.	0.	1.
360.	0.	0.	0.	0.	0.	1.	0.	0.	0.	0.	1.	0.	0.	1.	0.	0.	1.	1.	1.	0.	0.
359.	0.	0.	0.	0.	0.	0.	0.	0.	0.	0.	1.	0.	0.	0.	3.	0.	0.	0.	0.	0.	0.
349.	0.	0.	0.	0.	0.	0.	0.	0.	0.	1.	1.	3.	3.	3.	1.	1.	1.	0.	1.	0.	0.
331.	0.	0.	0.	0.	0.	0.	0.	0.	0.	0.	0.	0.	1.	2.	0.	4.	5.	0.	0.	0.	0.
275.	0.	0.	0.	0.	0.	0.	0.	0.	0.	0.	0.	1.	0.	3.	1.	1.	1.	1.	0.	0.	0.
270.	1.	0.	0.	0.	0.	0.	0.	0.	0.	1.	1.	9.	5.	0.	5.	0.	3.	1.	0.	0.	1.
260.	0.	0.	0.	0.	0.	1.	0.	0.	0.	0.	0.	1.	1.	1.	0.	1.	2.	0.	1.	1.	0.
232.	0.	0.	0.	0.	0.	2.	0.	0.	0.	2.	24.	10.	3.	4.	2.	1.	1.	1.	2.	0.	0.
135.	0.	0.	0.	0.	0.	0.	0.	0.	0.	7.	3.	0.	0.	1.	1.	0.	0.	0.	0.	0.	0.
127.	0.	0.	0.	0.	0.	0.	0.	0.	0.	0.	1.	0.	0.	0.	0.	0.	0.	0.	1.	0.	0.

TABLE LXII (Continued)

CALCULATED INTERNAL COORDINATE DISTRIBUTIONS
ALPHA XYLOSE

CONTRIBUTIONS FROM CC STRETCH

	C1C2	C2C3	C3C4	C4C5	C5O'	O'C1	C1O6	C2O7	C3O8	C4O9
1480.	0.	0.	0.	0.	0.	0.	0.	0.	1.	1.
1448.	0.	3.	0.	0.	0.	0.	0.	1.	0.	0.
1440.	0.	1.	2.	0.	0.	0.	0.	0.	0.	0.
1403.	6.	1.	0.	0.	0.	0.	0.	0.	0.	0.
1393.	0.	0.	1.	0.	0.	0.	0.	0.	0.	1.
1383.	0.	0.	1.	1.	0.	1.	0.	0.	0.	0.
1365.	0.	1.	4.	0.	0.	0.	0.	1.	1.	0.
1355.	1.	2.	0.	0.	2.	1.	0.	1.	0.	0.
1339.	0.	0.	0.	1.	3.	0.	0.	0.	0.	1.
1319.	2.	0.	0.	0.	1.	0.	4.	0.	0.	0.
1302.	0.	2.	0.	0.	0.	1.	6.	1.	1.	0.
1257.	0.	0.	3.	1.	1.	2.	0.	0.	0.	0.
1248.	0.	1.	0.	0.	0.	1.	1.	0.	0.	0.
1220.	0.	0.	0.	0.	0.	1.	0.	0.	0.	0.
1204.	3.	2.	0.	0.	1.	0.	4.	1.	0.	1.
1148.	0.	2.	16.	13.	1.	1.	1.	5.	0.	26.
1128.	0.	6.	0.	6.	10.	6.	0.	28.	7.	9.
1104.	6.	1.	0.	2.	28.	21.	2.	8.	4.	4.
1097.	0.	10.	5.	0.	1.	0.	1.	3.	71.	4.
1078.	1.	13.	9.	0.	1.	1.	8.	25.	2.	32.
1057.	3.	3.	9.	53.	0.	3.	9.	1.	0.	6.
1037.	23.	2.	4.	4.	7.	1.	26.	2.	6.	5.
1000.	20.	11.	1.	6.	11.	9.	8.	17.	0.	4.
935.	4.	5.	13.	6.	0.	4.	39.	4.	6.	0.
921.	9.	23.	33.	0.	2.	0.	8.	2.	0.	5.
906.	17.	0.	1.	0.	35.	55.	5.	0.	1.	0.
761.	5.	15.	1.	1.	3.	16.	6.	1.	4.	1.
620.	5.	2.	0.	1.	0.	5.	0.	1.	0.	0.
570.	5.	2.	2.	2.	1.	1.	0.	0.	2.	0.
541.	0.	5.	0.	3.	2.	0.	0.	1.	0.	6.
506.	2.	1.	14.	8.	2.	0.	0.	3.	1.	3.
438.	3.	2.	0.	3.	4.	1.	0.	3.	0.	0.
425.	2.	1.	1.	0.	1.	0.	0.	0.	2.	2.
389.	1.	0.	0.	1.	1.	0.	0.	0.	1.	0.
360.	0.	1.	1.	0.	2.	0.	0.	0.	0.	0.
359.	1.	1.	1.	0.	0.	0.	0.	0.	0.	0.
349.	3.	0.	0.	0.	0.	0.	0.	0.	0.	0.
331.	2.	0.	0.	0.	1.	0.	0.	0.	0.	0.
275.	0.	4.	3.	0.	1.	2.	0.	0.	1.	0.
270.	5.	1.	1.	0.	0.	1.	1.	0.	0.	0.
260.	0.	0.	0.	2.	2.	0.	1.	0.	0.	0.
232.	0.	0.	0.	0.	2.	14.	0.	0.	0.	1.
135.	1.	0.	0.	0.	0.	2.	0.	0.	0.	0.
127.	0.	0.	0.	0.	0.	1.	0.	1.	1.	1.

CALCULATED INTERNAL COORDINATE DISTRIBUTIONS
ALPHA XYLOSE

CONTRIBUTIONS FROM CCC AND CCO BEND

	CC2C	CC3C	CC4C	CC5O	COC	OC1C	OC06	O6CC	CCO7	O7CC	CCO8	O8CC	CCO9	O9CC
1480.	0.	0.	0.	0.	0.	0.	0.	0.	0.	0.	0.	0.	0.	1.
1448.	2.	0.	0.	0.	0.	0.	0.	1.	0.	1.	1.	0.	0.	0.
1440.	0.	1.	0.	0.	0.	0.	0.	0.	0.	0.	1.	0.	3.	0.
1403.	0.	0.	0.	0.	0.	0.	0.	1.	0.	0.	0.	0.	0.	0.
1393.	0.	0.	0.	0.	0.	0.	0.	0.	0.	0.	0.	0.	0.	0.
1383.	0.	0.	0.	0.	0.	0.	0.	0.	0.	0.	0.	0.	0.	0.
1365.	0.	1.	0.	0.	0.	0.	0.	0.	0.	1.	1.	1.	0.	0.
1355.	0.	0.	0.	0.	0.	0.	0.	0.	0.	1.	0.	0.	0.	0.
1339.	0.	0.	0.	0.	0.	0.	0.	0.	0.	0.	0.	0.	0.	0.
1319.	0.	0.	0.	0.	0.	1.	1.	0.	0.	0.	0.	0.	0.	0.
1302.	0.	0.	0.	0.	0.	0.	0.	2.	1.	0.	0.	0.	0.	0.
1257.	0.	0.	0.	0.	0.	0.	0.	0.	0.	0.	0.	0.	0.	0.
1248.	0.	0.	0.	0.	0.	0.	0.	0.	0.	0.	0.	0.	0.	0.
1220.	0.	0.	0.	0.	0.	0.	0.	0.	0.	0.	0.	0.	0.	0.
1204.	0.	1.	0.	0.	0.	1.	0.	0.	0.	0.	1.	0.	1.	0.
1148.	1.	0.	8.	1.	1.	0.	0.	0.	0.	0.	0.	4.	0.	0.
1128.	1.	1.	1.	1.	1.	6.	1.	0.	4.	1.	0.	2.	0.	1.
1104.	0.	2.	0.	2.	2.	2.	2.	0.	2.	2.	0.	0.	1.	2.
1097.	2.	10.	4.	1.	0.	1.	0.	0.	0.	4.	1.	2.	4.	1.
1078.	7.	0.	0.	1.	0.	1.	0.	1.	1.	0.	3.	0.	1.	2.
1057.	0.	0.	0.	3.	2.	0.	0.	0.	1.	0.	0.	1.	2.	3.
1037.	1.	0.	0.	0.	0.	3.	2.	0.	3.	0.	1.	1.	0.	0.
1000.	0.	1.	0.	6.	3.	0.	0.	7.	0.	2.	0.	2.	0.	5.
935.	0.	1.	0.	0.	2.	0.	4.	0.	0.	2.	1.	1.	2.	1.
921.	1.	0.	0.	0.	0.	1.	1.	0.	1.	1.	9.	5.	0.	0.
906.	2.	0.	1.	2.	2.	1.	3.	2.	1.	0.	0.	0.	0.	4.
761.	3.	1.	0.	1.	15.	1.	1.	6.	8.	1.	1.	1.	2.	1.
620.	0.	0.	1.	0.	13.	0.	19.	14.	6.	3.	0.	0.	4.	0.
570.	0.	0.	5.	5.	0.	6.	14.	0.	1.	14.	8.	1.	5.	1.
541.	1.	0.	2.	21.	2.	2.	3.	5.	3.	6.	1.	10.	10.	1.
506.	0.	1.	0.	0.	1.	7.	4.	0.	0.	9.	2.	11.	9.	7.
438.	8.	5.	0.	0.	3.	4.	6.	0.	14.	0.	2.	1.	2.	17.
425.	0.	9.	27.	1.	3.	10.	0.	6.	4.	0.	0.	1.	1.	3.
389.	10.	14.	1.	8.	6.	0.	2.	0.	5.	3.	9.	9.	2.	8.
360.	0.	1.	1.	1.	7.	0.	1.	0.	3.	2.	1.	1.	2.	1.
359.	1.	0.	0.	1.	0.	2.	0.	6.	2.	0.	10.	0.	5.	0.
349.	0.	0.	1.	1.	4.	0.	0.	0.	3.	2.	2.	0.	1.	0.
331.	0.	0.	1.	0.	0.	0.	0.	1.	1.	1.	14.	0.	0.	5.
275.	0.	2.	0.	0.	0.	0.	1.	0.	9.	22.	1.	0.	24.	9.
270.	0.	0.	1.	1.	12.	11.	17.	2.	0.	11.	2.	20.	3.	4.
260.	3.	0.	1.	3.	8.	9.	6.	3.	4.	2.	21.	14.	6.	8.
232.	4.	3.	0.	1.	12.	6.	19.	42.	10.	0.	0.	1.	2.	2.
135.	12.	0.	5.	3.	6.	4.	0.	2.	2.	1.	0.	0.	1.	3.
127.	6.	11.	5.	0.	5.	0.	1.	2.	1.	2.	3.	3.	2.	2.

TABLE LXIII

CALCULATED INTERNAL COORDINATE DISTRIBUTIONS
BETA ARABINOSE CD6, OH4

CONTRIBUTIONS FROM CH AND OH STR.

	CD15	CD16	CD17	CD18	CD19	CD20	OH11	OH12	OH13	OH14
3357.	0.	0.	0.	0.	0.	0.	99.	0.	0.	0.
3356.	0.	0.	0.	0.	0.	0.	0.	2.	7.	91.
3356.	0.	0.	0.	0.	0.	0.	0.	5.	86.	8.
3356.	0.	0.	0.	0.	0.	0.	0.	93.	7.	0.
2247.	46.	49.	0.	0.	0.	0.	0.	0.	0.	0.
2210.	0.	0.	1.	37.	47.	7.	0.	0.	0.	0.
2190.	0.	0.	2.	6.	2.	86.	0.	0.	0.	0.
2179.	0.	0.	92.	0.	4.	1.	0.	0.	0.	0.
2169.	0.	0.	2.	52.	43.	1.	0.	0.	0.	0.
2106.	51.	48.	0.	1.	1.	0.	0.	0.	0.	0.

CONTRIBUTIONS FROM TORSIONS

	TC12	TC23	TC34	TC45	TC50	TOC1	TC06	TC07	TC08	TC09
813.	0.	0.	0.	0.	8.	0.	0.	0.	0.	1.
786.	0.	0.	0.	0.	3.	1.	0.	0.	0.	0.
732.	0.	0.	0.	0.	0.	3.	1.	0.	0.	0.
651.	0.	0.	0.	0.	0.	1.	1.	0.	0.	1.
587.	0.	0.	0.	2.	6.	2.	2.	1.	0.	0.
556.	1.	0.	0.	0.	1.	0.	0.	1.	2.	0.
471.	0.	0.	1.	0.	0.	0.	1.	4.	1.	0.
437.	0.	0.	0.	3.	11.	2.	0.	2.	3.	0.
401.	0.	0.	0.	0.	0.	0.	11.	10.	3.	6.
374.	0.	0.	0.	1.	2.	0.	7.	0.	0.	22.
360.	1.	0.	0.	1.	2.	1.	33.	1.	20.	16.
351.	0.	0.	0.	0.	1.	0.	11.	0.	44.	16.
335.	0.	0.	0.	0.	0.	0.	7.	62.	3.	3.
307.	1.	0.	0.	1.	0.	0.	6.	5.	0.	19.
290.	0.	1.	0.	0.	4.	0.	5.	0.	8.	3.
256.	0.	4.	0.	0.	1.	1.	1.	6.	4.	0.
232.	0.	0.	2.	0.	0.	6.	1.	0.	2.	1.
206.	3.	1.	0.	7.	2.	8.	4.	0.	0.	2.
138.	11.	0.	17.	16.	0.	13.	0.	0.	0.	0.
125.	15.	30.	11.	0.	4.	0.	0.	0.	0.	0.

TABLE LXIII (Continued)

CALCULATED INTERNAL COORDINATE DISTRIBUTIONS
BETA ARABINOSE CD6, OH4

CONTRIBUTIONS FROM HCC,HCO,HCH BEND

	HO6C	HO7C	HO8C	HO9C	D15O	D16O	DC4O	DC3O	DC2O	DC1O	DCO'	DC1C	DC2C	DC2C	DC3C	DC3C	DC4C	DC4C	D15C	D16C	DC5D
1384.	7.	37.	36.	0.	0.	0.	0.	0.	4.	0.	0.	0.	0.	0.	0.	0.	0.	0.	0.	0.	1.
1364.	70.	0.	19.	0.	0.	0.	0.	0.	0.	0.	1.	0.	0.	0.	0.	0.	0.	0.	0.	0.	0.
1354.	12.	48.	30.	1.	0.	0.	0.	0.	4.	0.	0.	0.	0.	0.	0.	1.	0.	0.	0.	0.	0.
1290.	0.	0.	4.	84.	0.	0.	0.	0.	0.	0.	0.	0.	0.	0.	0.	0.	1.	2.	0.	1.	0.
1190.	0.	0.	0.	0.	2.	0.	7.	0.	0.	0.	0.	0.	0.	0.	0.	5.	1.	1.	3.	4.	1.
1171.	0.	0.	0.	0.	11.	6.	1.	0.	0.	0.	0.	0.	0.	1.	1.	0.	1.	5.	17.	8.	2.
1152.	2.	0.	1.	1.	0.	0.	0.	5.	1.	0.	1.	2.	1.	0.	2.	0.	3.	0.	0.	1.	0.
1118.	0.	0.	0.	0.	1.	1.	3.	1.	2.	4.	2.	1.	0.	8.	8.	2.	1.	0.	1.	0.	0.
1111.	0.	1.	0.	1.	0.	0.	0.	6.	0.	1.	2.	0.	1.	1.	1.	2.	1.	0.	0.	0.	1.
1099.	1.	0.	0.	0.	0.	5.	0.	0.	0.	1.	3.	8.	9.	5.	4.	2.	2.	1.	2.	4.	1.
1097.	2.	4.	2.	1.	6.	8.	0.	2.	1.	3.	1.	1.	0.	0.	3.	0.	0.	0.	0.	1.	7.
1059.	0.	1.	3.	0.	1.	6.	0.	2.	1.	1.	0.	1.	15.	16.	1.	0.	1.	0.	0.	1.	1.
1054.	0.	0.	1.	2.	3.	1.	0.	2.	1.	0.	0.	0.	0.	1.	5.	1.	2.	0.	4.	13.	41.
1044.	0.	0.	2.	1.	1.	2.	0.	5.	2.	0.	1.	1.	4.	0.	2.	11.	18.	6.	2.	1.	2.
1002.	0.	0.	2.	5.	13.	0.	0.	0.	2.	12.	2.	1.	3.	0.	1.	3.	0.	4.	0.	2.	11.
976.	0.	0.	0.	1.	1.	7.	10.	0.	1.	46.	4.	4.	1.	0.	2.	0.	0.	5.	0.	1.	5.
944.	0.	1.	1.	0.	0.	1.	41.	12.	2.	9.	6.	0.	0.	1.	8.	0.	8.	0.	0.	0.	1.
924.	0.	3.	0.	0.	0.	2.	16.	27.	15.	1.	0.	1.	0.	6.	10.	0.	0.	2.	1.	2.	0.
919.	3.	1.	0.	0.	0.	0.	1.	1.	11.	1.	55.	16.	1.	1.	2.	0.	0.	0.	0.	0.	0.
906.	0.	1.	0.	0.	31.	22.	0.	6.	11.	2.	7.	1.	3.	2.	1.	3.	2.	7.	3.	0.	1.
891.	0.	2.	0.	0.	7.	13.	3.	30.	17.	2.	0.	2.	0.	10.	2.	5.	7.	1.	0.	0.	0.
872.	0.	1.	0.	1.	1.	12.	5.	1.	13.	0.	16.	3.	2.	1.	1.	5.	1.	20.	2.	3.	0.
850.	0.	1.	0.	0.	2.	3.	8.	3.	14.	10.	1.	17.	14.	1.	4.	12.	5.	1.	3.	2.	0.
818.	0.	0.	0.	0.	1.	1.	3.	0.	1.	3.	1.	5.	14.	7.	7.	16.	3.	0.	0.	0.	0.
813.	0.	0.	0.	0.	0.	0.	0.	1.	0.	2.	1.	0.	0.	0.	0.	1.	7.	8.	17.	27.	0.
786.	0.	0.	0.	0.	1.	0.	3.	1.	0.	0.	1.	0.	0.	0.	0.	1.	0.	3.	20.	5.	0.
732.	1.	0.	0.	0.	0.	0.	1.	0.	3.	1.	0.	7.	1.	4.	0.	0.	1.	4.	1.	0.	0.
651.	1.	0.	0.	2.	1.	0.	3.	0.	0.	1.	1.	7.	0.	0.	1.	1.	11.	7.	0.	2.	1.
587.	0.	0.	0.	0.	2.	0.	0.	0.	0.	2.	0.	2.	4.	0.	0.	0.	0.	0.	1.	0.	0.
556.	1.	0.	0.	1.	0.	0.	0.	0.	0.	1.	0.	3.	0.	5.	6.	4.	4.	0.	1.	2.	0.
471.	1.	0.	0.	0.	0.	0.	0.	0.	1.	5.	1.	1.	0.	5.	3.	0.	1.	2.	2.	3.	0.
437.	0.	0.	1.	0.	0.	0.	0.	0.	0.	2.	0.	1.	0.	0.	2.	0.	1.	0.	0.	0.	1.
401.	0.	0.	0.	0.	0.	0.	0.	0.	0.	0.	0.	0.	0.	0.	3.	1.	0.	0.	0.	0.	0.
374.	0.	0.	0.	0.	0.	0.	0.	0.	0.	0.	0.	1.	0.	0.	0.	0.	0.	3.	2.	1.	0.
360.	0.	0.	0.	0.	0.	0.	0.	0.	0.	0.	1.	0.	0.	1.	2.	1.	1.	0.	0.	0.	0.
351.	0.	0.	0.	0.	0.	0.	0.	0.	0.	1.	0.	2.	1.	0.	2.	1.	1.	1.	0.	0.	0.
335.	0.	0.	0.	0.	0.	0.	0.	0.	0.	1.	1.	3.	5.	9.	0.	0.	0.	0.	1.	0.	0.
307.	1.	0.	0.	0.	0.	0.	0.	0.	0.	1.	0.	6.	2.	2.	1.	0.	2.	1.	1.	2.	0.
290.	0.	0.	0.	1.	0.	0.	1.	0.	0.	0.	3.	2.	1.	0.	1.	7.	6.	0.	0.	0.	0.
256.	0.	0.	0.	0.	0.	0.	0.	0.	0.	0.	7.	4.	1.	0.	2.	0.	0.	1.	0.	1.	0.
232.	1.	0.	0.	0.	0.	0.	0.	0.	0.	1.	2.	0.	6.	4.	8.	2.	0.	2.	0.	0.	0.
206.	0.	0.	0.	0.	0.	3.	0.	0.	0.	2.	15.	11.	0.	2.	0.	1.	1.	0.	3.	0.	2.
138.	0.	0.	0.	0.	1.	0.	3.	0.	0.	7.	3.	0.	0.	1.	1.	0.	0.	0.	0.	0.	1.
125.	0.	0.	0.	0.	0.	0.	0.	0.	0.	1.	0.	0.	0.	0.	0.	0.	0.	0.	1.	0.	0.

TABLE LXIII (Continued)

CALCULATED INTERNAL COORDINATE DISTRIBUTIONS
BETA ARABINOSE CD6, OH4

CONTRIBUTIONS FROM CC STRETCH

	C1C2	C2C3	C3C4	C4C5	C5O'	O'C1	C1O6	C2O7	C3O8	C4O9
1384.	0.	6.	0.	1.	1.	0.	0.	3.	0.	0.
1364.	4.	0.	1.	0.	0.	1.	1.	0.	0.	0.
1354.	2.	0.	1.	0.	0.	0.	0.	2.	0.	0.
1290.	0.	0.	6.	2.	0.	0.	0.	0.	0.	1.
1190.	0.	2.	11.	14.	7.	1.	0.	1.	0.	50.
1171.	0.	2.	3.	15.	32.	8.	1.	1.	3.	2.
1152.	12.	26.	6.	0.	1.	2.	14.	2.	29.	3.
1118.	5.	1.	1.	0.	1.	0.	4.	57.	0.	1.
1111.	21.	1.	10.	1.	3.	0.	32.	0.	16.	1.
1099.	3.	5.	0.	0.	6.	16.	9.	0.	0.	0.
1097.	0.	4.	2.	5.	0.	10.	1.	5.	14.	0.
1059.	5.	1.	0.	1.	3.	8.	3.	8.	6.	0.
1054.	0.	3.	7.	1.	1.	0.	0.	2.	9.	0.
1044.	1.	4.	1.	19.	1.	0.	6.	6.	5.	1.
1002.	0.	9.	18.	19.	4.	1.	1.	2.	1.	4.
976.	0.	0.	5.	8.	1.	2.	0.	1.	8.	0.
944.	1.	0.	2.	0.	2.	0.	1.	4.	1.	2.
924.	3.	0.	4.	0.	0.	0.	6.	0.	1.	7.
919.	23.	0.	0.	0.	1.	40.	6.	2.	0.	0.
906.	1.	1.	1.	1.	6.	4.	0.	0.	0.	0.
891.	3.	1.	1.	0.	4.	1.	1.	2.	2.	0.
872.	3.	2.	3.	0.	6.	3.	0.	0.	2.	1.
850.	7.	0.	0.	0.	2.	7.	11.	2.	1.	4.
818.	0.	11.	1.	0.	5.	0.	17.	0.	0.	10.
813.	3.	0.	14.	0.	9.	1.	0.	1.	2.	0.
786.	0.	0.	0.	11.	19.	3.	1.	0.	0.	23.
732.	6.	5.	2.	0.	8.	14.	4.	3.	2.	1.
651.	0.	28.	0.	0.	1.	0.	0.	1.	0.	0.
587.	8.	4.	2.	0.	0.	5.	0.	1.	1.	0.
556.	0.	1.	2.	1.	0.	0.	0.	1.	0.	0.
471.	1.	1.	8.	3.	0.	0.	0.	3.	1.	0.
437.	6.	0.	0.	2.	0.	0.	0.	1.	2.	0.
401.	1.	0.	2.	2.	0.	1.	0.	1.	1.	0.
374.	0.	0.	1.	3.	0.	0.	0.	0.	0.	0.
360.	0.	1.	1.	0.	1.	0.	0.	0.	0.	0.
351.	2.	1.	0.	0.	0.	0.	0.	0.	0.	0.
335.	3.	1.	0.	0.	0.	0.	0.	0.	0.	0.
307.	2.	1.	1.	0.	0.	1.	1.	0.	0.	0.
290.	1.	0.	4.	0.	0.	1.	0.	0.	0.	0.
256.	0.	0.	0.	1.	0.	5.	0.	0.	0.	0.
232.	2.	0.	1.	0.	0.	1.	1.	1.	1.	0.
206.	1.	0.	1.	1.	3.	10.	0.	0.	0.	0.
138.	1.	0.	0.	0.	0.	2.	0.	0.	0.	0.
125.	0.	0.	0.	0.	0.	0.	0.	1.	1.	0.

CALCULATED INTERNAL COORDINATE DISTRIBUTIONS
BETA ARABINOSE CD6, OH4

CONTRIBUTIONS FROM CCC AND CCO BEND

	CC2C	CC3C	CC4C	CC5O	COC	OC1C	OCO6	O6CC	CCO7	O7CC	CCO8	O8CC	CCO9	O9CC
1384.	2.	0.	0.	1.	0.	0.	0.	0.	0.	0.	2.	0.	0.	0.
1364.	0.	0.	0.	0.	0.	0.	0.	2.	0.	0.	1.	0.	0.	0.
1354.	0.	0.	0.	0.	0.	0.	0.	0.	0.	0.	0.	0.	0.	0.
1290.	0.	0.	0.	0.	0.	0.	0.	0.	0.	0.	0.	0.	3.	1.
1190.	0.	0.	9.	0.	0.	0.	0.	0.	0.	0.	0.	4.	1.	1.
1171.	0.	0.	0.	0.	1.	1.	0.	0.	0.	0.	0.	1.	0.	1.
1152.	0.	4.	1.	0.	0.	4.	0.	0.	5.	3.	1.	1.	0.	1.
1118.	1.	5.	0.	0.	0.	1.	0.	1.	1.	6.	0.	0.	0.	0.
1111.	0.	3.	1.	0.	0.	2.	3.	1.	2.	1.	0.	0.	0.	1.
1099.	0.	0.	0.	2.	1.	0.	0.	2.	0.	3.	0.	1.	0.	0.
1097.	8.	1.	1.	0.	1.	3.	3.	1.	3.	0.	1.	1.	1.	0.
1059.	2.	0.	0.	0.	0.	0.	2.	0.	1.	1.	6.	0.	1.	0.
1054.	1.	1.	1.	0.	0.	1.	0.	0.	0.	0.	0.	2.	0.	0.
1044.	1.	1.	0.	0.	1.	0.	1.	1.	0.	0.	1.	3.	0.	5.
1002.	0.	0.	0.	3.	2.	0.	0.	0.	0.	0.	1.	0.	5.	1.
976.	0.	0.	0.	0.	1.	1.	1.	0.	0.	0.	0.	0.	0.	1.
944.	0.	0.	1.	2.	0.	0.	0.	0.	1.	0.	0.	0.	1.	1.
924.	0.	0.	1.	2.	1.	0.	0.	0.	0.	0.	0.	1.	0.	1.
919.	0.	0.	0.	0.	5.	0.	1.	7.	1.	0.	0.	0.	0.	0.
906.	0.	0.	0.	1.	3.	0.	0.	0.	0.	0.	0.	0.	0.	1.
891.	0.	0.	1.	0.	0.	0.	0.	0.	0.	0.	0.	0.	0.	1.
872.	0.	0.	1.	2.	1.	1.	1.	0.	1.	0.	2.	0.	0.	0.
850.	1.	0.	0.	1.	0.	0.	2.	0.	0.	0.	0.	0.	0.	0.
818.	1.	1.	0.	1.	1.	0.	0.	0.	0.	2.	2.	0.	0.	1.
813.	1.	0.	0.	1.	1.	0.	0.	0.	0.	1.	1.	2.	0.	1.
786.	1.	0.	0.	2.	0.	0.	1.	0.	0.	0.	0.	1.	0.	0.
732.	1.	2.	0.	5.	14.	0.	1.	2.	6.	2.	2.	0.	0.	3.
651.	1.	3.	3.	12.	1.	0.	2.	3.	1.	0.	0.	1.	5.	4.
587.	0.	0.	0.	1.	4.	1.	29.	11.	8.	0.	1.	0.	0.	1.
556.	2.	2.	1.	6.	3.	1.	0.	11.	2.	0.	0.	12.	24.	5.
471.	1.	0.	0.	0.	0.	22.	11.	2.	2.	15.	7.	0.	0.	7.
437.	1.	4.	14.	2.	0.	4.	2.	0.	1.	12.	14.	1.	0.	6.
401.	8.	9.	0.	1.	1.	0.	2.	0.	18.	3.	1.	13.	0.	1.
374.	5.	3.	3.	7.	15.	0.	2.	0.	3.	3.	3.	1.	1.	15.
360.	0.	0.	1.	0.	5.	0.	0.	0.	2.	0.	3.	3.	2.	0.
351.	1.	1.	0.	0.	3.	1.	0.	2.	4.	2.	5.	0.	0.	0.
335.	1.	1.	1.	1.	0.	0.	2.	0.	0.	0.	5.	3.	0.	2.
307.	0.	0.	0.	0.	2.	6.	6.	4.	3.	18.	0.	0.	10.	16.
290.	0.	0.	11.	0.	1.	1.	4.	7.	1.	5.	26.	11.	11.	8.
256.	2.	1.	8.	1.	0.	6.	2.	16.	13.	11.	4.	14.	12.	0.
232.	6.	3.	1.	1.	3.	10.	2.	13.	3.	2.	1.	7.	15.	3.
206.	0.	4.	4.	5.	32.	0.	28.	12.	4.	0.	0.	0.	2.	10.
138.	3.	5.	7.	5.	6.	7.	0.	4.	0.	0.	1.	1.	0.	0.
125.	14.	11.	0.	0.	1.	1.	1.	0.	3.	3.	3.	3.	1.	0.

TABLE LXIV

CALCULATED INTERNAL COORDINATE DISTRIBUTIONS
BETA ARABINOSE C1D,CH5,OH4

CONTRIBUTIONS FROM CH AND OH STR.

	CH15	CH16	CH17	CH18	CH19	CD20	OH11	OH12	OH13	OH14
3357.	0.	0.	0.	0.	0.	0.	99.	1.	0.	0.
3356.	0.	0.	0.	0.	0.	0.	1.	15.	77.	8.
3356.	0.	0.	0.	0.	0.	0.	0.	80.	8.	12.
3356.	0.	0.	0.	0.	0.	0.	0.	5.	15.	80.
3002.	48.	50.	0.	0.	0.	0.	0.	0.	0.	0.
2948.	0.	0.	2.	45.	52.	0.	0.	0.	0.	0.
2939.	0.	0.	95.	0.	4.	0.	0.	0.	0.	0.
2935.	0.	0.	2.	54.	43.	0.	0.	0.	0.	0.
2885.	51.	50.	0.	0.	0.	0.	0.	0.	0.	0.
2191.	0.	0.	0.	0.	0.	95.	0.	0.	0.	0.

CONTRIBUTIONS FROM TORSIONS

	TC12	TC23	TC34	TC45	TC50	TOC1	TC06	TC07	TC08	TC09
891.	0.	0.	0.	0.	0.	1.	5.	1.	0.	0.
839.	0.	0.	0.	0.	0.	1.	0.	0.	0.	0.
758.	0.	0.	0.	0.	0.	3.	1.	0.	0.	0.
680.	0.	0.	0.	0.	0.	1.	1.	0.	0.	0.
613.	0.	0.	0.	2.	9.	3.	1.	0.	0.	0.
591.	1.	0.	0.	0.	0.	0.	0.	0.	2.	0.
492.	0.	0.	1.	1.	0.	0.	0.	3.	1.	0.
462.	0.	0.	0.	3.	11.	2.	0.	0.	1.	0.
410.	0.	0.	0.	0.	0.	1.	11.	6.	4.	6.
391.	0.	0.	0.	1.	1.	0.	11.	1.	1.	7.
363.	0.	0.	0.	0.	1.	1.	25.	3.	19.	26.
354.	0.	0.	0.	0.	1.	0.	9.	1.	44.	20.
338.	0.	0.	0.	0.	0.	0.	8.	66.	5.	2.
314.	1.	0.	1.	1.	0.	0.	15.	5.	0.	25.
297.	0.	2.	0.	0.	3.	0.	4.	1.	7.	0.
257.	0.	4.	0.	0.	1.	1.	1.	6.	5.	0.
237.	0.	0.	2.	0.	0.	6.	0.	0.	3.	1.
209.	3.	1.	0.	6.	2.	8.	4.	0.	0.	2.
142.	12.	0.	16.	16.	0.	13.	0.	0.	0.	1.
128.	15.	30.	12.	0.	4.	0.	0.	0.	0.	0.

TABLE LXIV (Continued)

CALCULATED INTERNAL COORDINATE DISTRIBUTIONS
BETA ARABINOSE C1D,CH5,OH4

CONTRIBUTIONS FROM HCC,HCO,HCH BEND

	H06C	H07C	H08C	H09C	H15O	H16O	HC4O	HC3O	HC2O	DC1O	DCO'	DC1C	HC2C	HC2C	HC3C	HC3C	HC4C	HC4C	H15C	H16C	HC5H
1477.	0.	0.	0.	1.	2.	0.	0.	0.	0.	0.	0.	0.	0.	0.	0.	0.	2	0.	12.	14.	57.
1448.	2.	37.	4.	0.	0.	0.	0.	0.	20.	0.	0.	0.	6.	0.	8.	3.	0.	0.	0.	0.	0.
1426.	0.	2.	28.	0.	5.	5.	0.	1.	3.	0.	0.	0.	1.	6.	2.	9.	13.	7.	1.	3.	1.
1403.	0.	2.	12.	2.	20.	22.	4.	1.	2.	0.	0.	0.	1.	6.	0.	2.	0.	8.	7.	6.	7.
1379.	7.	16.	1.	0.	1.	1.	5.	4.	9.	0.	0.	0.	0.	12.	10.	17.	3.	0.	2.	0.	0.
1361.	75.	0.	1.	1.	1.	0.	1.	1.	0.	0.	1.	0.	0.	1.	3.	4.	0.	0.	1.	0.	0.
1340.	3.	0.	9.	3.	0.	0.	1.	8.	1.	1.	0.	1.	29.	15.	7.	1.	0.	0.	2.	1.	0.
1321.	1.	0.	6.	26.	0.	3.	7.	12.	1.	0.	0.	0.	2.	0.	6.	1.	11.	0.	1.	3.	0.
1290.	0.	0.	0.	21.	2.	15.	11.	1.	0.	0.	0.	0.	0.	0.	0.	2.	5.	26.	3.	14.	0.
1264.	2.	1.	21.	2.	1.	0.	24.	26.	0.	0.	0.	0.	0.	1.	13.	0.	15.	0.	3.	1.	0.
1240.	0.	0.	0.	1.	41.	23.	0.	11.	0.	0.	0.	0.	3.	1.	1.	3.	3.	1.	16.	4.	0.
1238.	0.	2.	9.	26.	0.	0.	19.	9.	3.	0.	0.	0.	2.	1.	4.	4.	0.	5.	1.	1.	1.
1203.	1.	27.	2.	4.	2.	1.	5.	4.	35.	0.	0.	0.	7.	13.	1.	0.	0.	2.	0.	0.	0.
1167.	0.	2.	1.	0.	5.	1.	16.	22.	2.	0.	1.	0.	1.	1.	1.	9.	3.	1.	4.	11.	0.
1135.	1.	1.	0.	1.	0.	2.	4.	2.	1.	0.	0.	5.	2.	4.	5.	0.	0.	0.	0.	1.	0.
1105.	0.	0.	0.	1.	3.	13.	2.	1.	0.	2.	0.	0.	1.	0.	0.	0.	3.	2.	7.	1.	0.
1101.	0.	4.	0.	0.	1.	1.	0.	1.	8.	0.	4.	0.	4.	0.	0.	0.	1.	0.	0.	0.	0.
1093.	1.	4.	0.	0.	0.	0.	0.	0.	10.	1.	2.	1.	2.	0.	0.	0.	3.	0.	1.	5.	0.
1053.	1.	1.	1.	3.	0.	0.	4.	2.	0.	2.	0.	1.	3.	1.	1.	3.	0.	1.	8.	6.	2.
1040.	1.	2.	1.	0.	0.	0.	2.	0.	6.	1.	2.	3.	0.	0.	4.	8.	0.	0.	0.	0.	1.
981.	1.	0.	0.	0.	0.	0.	1.	0.	1.	47.	4.	4.	0.	0.	1.	0.	4.	1.	3.	2.	0.
965.	0.	1.	2.	6.	0.	0.	0.	1.	2.	8.	4.	0.	0.	1.	1.	3.	1.	14.	4.	3.	1.
925.	3.	1.	1.	0.	0.	1.	0.	0.	2.	19.	50.	1.	0.	1.	0.	1.	1.	1.	1.	1.	0.
910.	0.	1.	1.	0.	0.	0.	1.	0.	2.	5.	0.	2.	1.	0.	1.	4.	3.	1.	1.	3.	0.
891.	1.	0.	0.	0.	0.	0.	0.	0.	0.	10.	32.	44.	7.	1.	0.	0.	0.	0.	0.	1.	0.
839.	0.	0.	0.	0.	0.	0.	0.	0.	0.	1.	5.	0.	0.	0.	0.	0.	0.	0.	2.	0.	2.
758.	1.	0.	0.	1.	0.	0.	0.	0.	0.	1.	0.	6.	0.	3.	0.	0.	2.	2.	1.	0.	0.
680.	1.	0.	0.	2.	0.	0.	0.	0.	0.	2.	1.	10.	0.	1.	1.	0.	6.	5.	0.	1.	1.
613.	0.	0.	0.	0.	0.	0.	0.	0.	0.	3.	1.	4.	2.	0.	1.	1.	0.	0.	1.	0.	0.
591.	1.	0.	0.	1.	0.	0.	0.	0.	0.	0.	0.	2.	1.	4.	4.	3.	2.	0.	0.	1.	0.
492.	0.	0.	1.	0.	0.	0.	0.	0.	1.	3.	0.	1.	0.	4.	3.	0.	1.	1.	1.	1.	0.
462.	0.	0.	0.	0.	0.	0.	0.	0.	0.	4.	0.	0.	0.	0.	1.	0.	0.	0.	0.	0.	0.
410.	0.	0.	0.	0.	0.	0.	0.	0.	0.	0.	0.	0.	0.	0.	2.	0.	0.	0.	0.	0.	0.
391.	0.	0.	0.	0.	0.	1.	0.	0.	0.	0.	0.	2.	1.	0.	0.	1.	0.	1.	1.	0.	0.
363.	0.	0.	0.	0.	0.	0.	0.	0.	0.	0.	0.	0.	0.	1.	1.	1.	1.	1.	0.	0.	0.
354.	0.	0.	0.	0.	0.	0.	0.	0.	0.	0.	0.	2.	1.	0.	2.	1.	1.	1.	0.	0.	0.
338.	0.	0.	0.	0.	0.	0.	0.	0.	0.	0.	1.	3.	4.	7.	0.	1.	0.	0.	0.	0.	0.
314.	0.	0.	0.	0.	0.	0.	0.	0.	0.	2.	1.	9.	1.	2.	0.	0.	3.	1.	0.	1.	0.
297.	0.	0.	0.	1.	0.	0.	1.	0.	0.	0.	3.	0.	1.	0.	0.	7.	3.	0.	0.	1.	0.
257.	0.	0.	0.	0.	0.	0.	0.	0.	0.	0.	6.	3.	0.	0.	2.	0.	0.	1.	0.	1.	0.
237.	1.	0.	0.	0.	0.	0.	0.	0.	0.	0.	3.	0.	5.	3.	6.	2.	0.	2.	0.	0.	0.
209.	0.	0.	0.	0.	0.	3.	0.	0.	0.	1.	15.	11.	0.	2.	0.	1.	1.	0.	4.	0.	1.
142.	0.	0.	0.	0.	1.	0.	3.	0.	0.	7.	3.	0.	0.	1.	1.	0.	0.	0.	0.	0.	1.
126.	0.	0.	0.	0.	0.	0.	0.	0.	0.	1.	0.	0.	0.	0.	0.	0.	0.	0.	1.	0.	0.

TABLE LXIV (Continued)

CALCULATED INTERNAL COORDINATE DISTRIBUTIONS
BETA ARABINOSE C1D,CH5,OH4

CONTRIBUTIONS FROM CC STRETCH

	C1C2	C2C3	C3C4	C4C5	C5O*	O*C1	C1O6	C2O7	C3O8	C4O9
1477.	0.	0.	0.	0.	0.	0.	0.	0.	0.	0.
1448.	0.	4.	0.	0.	0.	0.	0.	1.	0.	0.
1426.	0.	3.	1.	1.	1.	0.	0.	0.	0.	1.
1403.	0.	0.	0.	0.	1.	0.	0.	0.	1.	1.
1379.	1.	0.	0.	0.	0.	0.	0.	2.	0.	2.
1361.	5.	0.	1.	0.	0.	1.	1.	0.	0.	1.
1340.	0.	1.	3.	0.	0.	1.	5.	0.	0.	1.
1321.	0.	0.	6.	1.	0.	0.	0.	0.	0.	0.
1290.	0.	0.	0.	2.	1.	1.	0.	0.	0.	2.
1264.	0.	0.	2.	1.	0.	1.	1.	0.	1.	0.
1240.	0.	1.	0.	1.	2.	2.	1.	0.	0.	0.
1238.	0.	0.	0.	4.	3.	0.	0.	1.	0.	12.
1203.	6.	0.	1.	0.	0.	0.	6.	1.	0.	0.
1167.	0.	1.	14.	7.	9.	5.	1.	0.	1.	13.
1135.	8.	28.	1.	3.	2.	0.	3.	11.	34.	0.
1105.	0.	1.	2.	24.	26.	10.	0.	8.	2.	0.
1101.	11.	0.	9.	0.	2.	0.	5.	61.	6.	1.
1093.	18.	0.	7.	1.	3.	0.	14.	1.	31.	2.
1053.	4.	8.	0.	17.	7.	17.	0.	3.	2.	7.
1040.	1.	12.	1.	12.	3.	10.	21.	0.	4.	7.
981.	0.	0.	10.	7.	0.	5.	1.	0.	13.	3.
965.	0.	12.	43.	4.	3.	4.	0.	1.	0.	2.
925.	13.	1.	0.	1.	0.	7.	35.	6.	2.	3.
910.	9.	4.	0.	4.	5.	11.	6.	1.	1.	41.
891.	17.	2.	2.	1.	0.	23.	19.	0.	0.	0.
839.	2.	0.	3.	10.	44.	11.	1.	1.	1.	12.
758.	7.	2.	4.	0.	9.	13.	3.	5.	3.	2.
680.	1.	34.	0.	1.	0.	1.	0.	1.	1.	0.
613.	8.	5.	3.	1.	1.	5.	0.	1.	1.	0.
591.	0.	0.	2.	1.	0.	1.	0.	0.	0.	0.
492.	3.	0.	6.	2.	0.	0.	0.	2.	0.	0.
462.	8.	1.	3.	2.	0.	0.	0.	2.	3.	0.
410.	0.	0.	1.	2.	0.	1.	0.	1.	1.	0.
391.	0.	0.	1.	4.	0.	0.	1.	0.	0.	0.
363.	0.	1.	1.	0.	1.	0.	0.	0.	0.	0.
354.	3.	1.	0.	0.	0.	0.	0.	0.	0.	0.
338.	3.	1.	0.	0.	0.	0.	0.	0.	0.	0.
314.	1.	0.	0.	0.	0.	1.	1.	0.	0.	0.
297.	1.	0.	5.	0.	0.	1.	0.	0.	0.	0.
257.	0.	0.	0.	1.	0.	4.	0.	0.	0.	0.
237.	2.	0.	1.	0.	0.	1.	1.	1.	1.	0.
209.	1.	0.	1.	1.	3.	10.	0.	0.	0.	0.
142.	1.	0.	0.	0.	0.	2.	0.	0.	0.	0.
128.	0.	0.	0.	0.	0.	0.	0.	1.	1.	0.

CALCULATED INTERNAL COORDINATE DISTRIBUTIONS
BETA ARABINOSE C1D,CH5,OH4

CONTRIBUTIONS FROM CCC AND CCO BEND

	CC2C	CC3C	CC4C	CC5O	COC	OC1C	OC06	O6CC	CC07	O7CC	CC08	O8CC	CC09	O9CC
1477.	0.	0.	0.	0.	0.	0.	0.	0.	0.	0.	0.	0.	0.	0.
1448.	2.	0.	0.	0.	0.	0.	0.	1.	0.	1.	1.	0.	0.	0.
1426.	0.	0.	0.	0.	0.	0.	0.	0.	0.	0.	2.	1.	0.	0.
1403.	0.	0.	0.	0.	0.	0.	0.	0.	0.	0.	1.	0.	1.	0.
1379.	0.	1.	1.	0.	0.	0.	0.	0.	0.	0.	0.	0.	0.	0.
1361.	0.	0.	0.	0.	0.	0.	0.	1.	0.	0.	0.	0.	0.	0.
1340.	0.	0.	0.	0.	0.	0.	0.	1.	0.	0.	0.	0.	0.	0.
1321.	0.	0.	1.	0.	0.	0.	0.	0.	0.	0.	0.	0.	0.	1.
1290.	0.	0.	0.	0.	0.	0.	0.	0.	0.	0.	0.	0.	0.	0.
1264.	0.	0.	0.	0.	0.	0.	0.	0.	0.	0.	0.	0.	1.	0.
1240.	0.	0.	0.	0.	0.	0.	0.	0.	0.	0.	0.	0.	0.	0.
1238.	0.	0.	1.	0.	0.	0.	0.	0.	0.	0.	0.	1.	3.	0.
1203.	0.	0.	0.	0.	0.	1.	1.	0.	1.	0.	1.	0.	0.	0.
1167.	0.	1.	4.	0.	0.	0.	0.	0.	0.	2.	0.	2.	0.	1.
1135.	0.	3.	3.	0.	0.	3.	0.	0.	5.	1.	1.	3.	0.	1.
1105.	0.	1.	0.	0.	3.	0.	2.	0.	0.	0.	0.	0.	0.	5.
1101.	8.	6.	1.	0.	1.	3.	1.	0.	1.	4.	2.	1.	0.	0.
1093.	0.	3.	1.	0.	0.	3.	1.	0.	4.	0.	0.	0.	0.	0.
1053.	2.	0.	1.	2.	0.	2.	2.	1.	2.	3.	0.	2.	3.	1.
1040.	3.	1.	0.	1.	2.	0.	0.	4.	0.	1.	2.	1.	0.	0.
981.	0.	1.	0.	0.	1.	1.	2.	0.	0.	1.	0.	2.	0.	1.
965.	0.	0.	1.	5.	0.	1.	1.	0.	1.	1.	3.	3.	5.	0.
925.	1.	0.	0.	1.	4.	0.	0.	3.	0.	0.	3.	0.	1.	1.
910.	1.	0.	0.	1.	1.	0.	0.	0.	0.	1.	1.	0.	0.	3.
891.	0.	1.	0.	0.	1.	0.	3.	3.	1.	1.	0.	0.	0.	0.
839.	1.	0.	0.	5.	0.	1.	1.	0.	1.	1.	0.	3.	0.	0.
758.	1.	5.	1.	9.	13.	0.	0.	2.	5.	2.	2.	0.	1.	4.
680.	1.	2.	3.	8.	3.	0.	3.	2.	1.	0.	0.	1.	5.	3.
613.	0.	0.	0.	3.	5.	2.	24.	4.	4.	0.	0.	3.	4.	5.
591.	3.	3.	1.	5.	7.	0.	3.	17.	5.	0.	0.	10.	20.	4.
492.	0.	0.	2.	0.	0.	16.	10.	2.	0.	22.	14.	1.	0.	12.
462.	0.	2.	18.	0.	3.	10.	1.	1.	4.	2.	5.	1.	0.	7.
410.	9.	9.	1.	1.	1.	1.	3.	0.	19.	3.	1.	14.	0.	3.
391.	6.	6.	1.	8.	20.	1.	6.	0.	2.	9.	8.	1.	0.	11.
363.	0.	0.	0.	1.	2.	0.	0.	0.	4.	0.	3.	2.	2.	1.
354.	0.	1.	1.	0.	2.	0.	0.	2.	3.	2.	5.	0.	0.	0.
338.	1.	1.	0.	1.	0.	0.	2.	0.	0.	0.	3.	2.	0.	1.
314.	0.	0.	1.	0.	1.	6.	9.	2.	2.	12.	2.	1.	3.	14.
297.	0.	0.	10.	0.	0.	2.	2.	10.	2.	10.	22.	7.	19.	1.
257.	2.	1.	7.	1.	0.	6.	2.	14.	13.	12.	6.	16.	12.	0.
237.	6.	2.	1.	1.	3.	10.	1.	14.	4.	1.	1.	8.	15.	5.
209.	0.	4.	5.	5.	29.	0.	27.	13.	4.	0.	0.	0.	2.	12.
142.	3.	4.	6.	5.	6.	7.	0.	4.	1.	0.	1.	1.	0.	0.
128.	14.	11.	0.	0.	0.	1.	0.	1.	3.	3.	3.	3.	1.	0.

TABLE LXV

CALCULATED INTERNAL COORDINATE DISTRIBUTIONS
ALPHA XYLOSE C1D,CH5,OH4

CONTRIBUTIONS FROM CH AND OH STR.

	CH15	CH16	CH17	CH18	CH19	CD20	OH11	OH12	OH13	OH14
3356.	0.	0.	0.	0.	0.	0.	1.	22.	73.	4.
3357.	0.	0.	0.	0.	0.	0.	99.	1.	0.	0.
3356.	0.	0.	0.	0.	0.	0.	0.	75.	24.	0.
3356.	0.	0.	0.	0.	0.	0.	0.	2.	2.	96.
3000.	48.	49.	1.	0.	0.	0.	0.	0.	0.	0.
2953.	0.	0.	23.	51.	24.	0.	0.	0.	0.	0.
2942.	0.	0.	48.	0.	51.	0.	0.	0.	0.	0.
2933.	0.	0.	27.	48.	24.	0.	0.	0.	0.	0.
2888.	51.	49.	0.	0.	0.	0.	0.	0.	0.	0.
2191.	0.	0.	0.	0.	0.	95.	0.	0.	0.	0.

CONTRIBUTIONS FROM TORSIONS

	TC12	TC23	TC34	TC45	TC50	TOC1	TC06	TC07	TC08	TC09
891.	0.	0.	0.	0.	0.	1.	5.	1.	0.	0.
886.	1.	0.	0.	0.	0.	1.	0.	0.	0.	0.
741.	0.	0.	0.	0.	0.	4.	1.	0.	0.	0.
619.	0.	0.	0.	2.	6.	0.	1.	0.	1.	0.
569.	0.	0.	1.	0.	0.	3.	0.	2.	2.	0.
534.	0.	0.	0.	0.	2.	0.	1.	0.	0.	1.
505.	0.	0.	0.	1.	1.	0.	0.	0.	0.	0.
435.	1.	0.	0.	0.	0.	0.	7.	2.	0.	6.
424.	0.	1.	0.	0.	12.	2.	2.	1.	1.	2.
389.	0.	0.	0.	0.	0.	2.	0.	0.	5.	14.
360.	1.	0.	0.	1.	0.	1.	43.	9.	5.	11.
359.	0.	0.	0.	1.	0.	1.	0.	16.	45.	3.
349.	0.	0.	0.	1.	1.	1.	20.	38.	13.	1.
331.	0.	1.	0.	0.	0.	1.	1.	10.	8.	45.
275.	1.	1.	0.	2.	0.	0.	0.	12.	0.	2.
270.	1.	0.	2.	3.	1.	4.	7.	0.	8.	4.
260.	0.	2.	3.	2.	0.	4.	2.	2.	4.	2.
232.	2.	0.	0.	5.	3.	0.	4.	0.	0.	0.
134.	24.	7.	3.	11.	1.	12.	1.	0.	0.	0.
127.	3.	24.	25.	3.	3.	4.	0.	0.	0.	0.

TABLE LXV (Continued)

CALCULATED INTERNAL COORDINATE DISTRIBUTIONS
ALPHA XYLOSE C1D,CH5,OH4

CONTRIBUTIONS FROM HCC,HCO,HCH BEND

	HO6C	HO7C	HO8C	HO9C	H15O	H16O	HC4O	HC3O	HC2O	DC1O	DCO*	DC1C	HC2C	HC2C	HC3C	HC3C	HC4C	HC4C	H15C	H16C	HC5H
1480.	0.	0.	2.	0.	0.	0.	0.	0.	0.	0.	0.	0.	0.	1.	0.	2.	4.	0.	18.	13.	42.
1447.	3.	38.	3.	0.	0.	0.	0.	0.	20.	0.	0.	0.	6.	0.	8.	2.	1.	0.	0.	0.	0.
1440.	0.	2.	16.	19.	0.	0.	1.	1.	3.	0.	0.	0.	2.	9.	1.	11.	2.	0.	0.	4.	7.
1393.	0.	6.	2.	25.	6.	5.	2.	1.	5.	0.	0.	0.	1.	7.	1.	2.	6.	16.	0.	3.	5.
1380.	8.	6.	1.	2.	23.	22.	2.	0.	4.	0.	0.	0.	0.	4.	3.	3.	0.	0.	10.	5.	8.
1367.	18.	1.	36.	10.	1.	1.	3.	6.	0.	0.	0.	0.	0.	1.	0.	3.	7.	1.	0.	0.	0.
1358.	59.	1.	4.	1.	4.	2.	3.	3.	0.	0.	1.	0.	1.	2.	1.	3.	7.	2.	2.	0.	1.
1340.	1.	4.	0.	5.	5.	5.	7.	2.	4.	0.	0.	0.	0.	2.	21.	13.	4.	16.	4.	3.	0.
1328.	0.	0.	3.	2.	0.	0.	2.	7.	1.	1.	0.	1.	32.	14.	7.	0.	11.	5.	1.	0.	0.
1259.	1.	0.	0.	10.	10.	14.	46.	0.	0.	0.	0.	0.	0.	0.	2.	2.	7.	9.	3.	3.	1.
1249.	1.	0.	19.	12.	1.	1.	1.	56.	0.	0.	0.	0.	0.	1.	8.	12.	0.	1.	2.	4.	0.
1223.	0.	1.	2.	7.	24.	21.	18.	10.	0.	0.	0.	0.	2.	0.	2.	0.	4.	3.	10.	8.	0.
1208.	1.	27.	6.	0.	1.	0.	3.	1.	35.	0.	0.	0.	8.	13.	0.	1.	1.	0.	0.	0.	0.
1156.	0.	2.	0.	1.	4.	1.	10.	10.	1.	0.	1.	1.	1.	1.	1.	3.	2.	0.	5.	13.	0.
1142.	0.	2.	0.	1.	0.	1.	4.	1.	2.	1.	0.	3.	0.	1.	4.	0.	0.	0.	0.	1.	1.
1120.	1.	2.	0.	0.	1.	1.	1.	2.	2.	0.	5.	1.	3.	1.	2.	0.	0.	0.	0.	0.	0.
1099.	0.	0.	0.	2.	2.	8.	0.	5.	0.	1.	0.	0.	5.	2.	0.	0.	0.	2.	0.	0.	3.
1088.	1.	3.	1.	1.	1.	0.	0.	0.	9.	1.	1.	0.	2.	0.	0.	0.	1.	1.	1.	3.	0.
1076.	1.	7.	1.	0.	0.	0.	1.	0.	14.	0.	1.	2.	0.	4.	1.	3.	3.	0.	0.	0.	1.
1057.	0.	0.	1.	2.	1.	3.	2.	0.	0.	0.	0.	0.	0.	0.	0.	2.	2.	2.	9.	4.	2.
1022.	1.	1.	0.	0.	1.	0.	1.	0.	0.	6.	2.	2.	1.	0.	4.	3.	3.	1.	2.	5.	1.
977.	1.	0.	0.	1.	0.	0.	0.	0.	1.	52.	4.	4.	0.	0.	1.	0.	2.	4.	3.	2.	0.
934.	1.	0.	0.	0.	1.	2.	0.	0.	0.	19.	36.	1.	0.	0.	1.	0.	2.	2.	5.	5.	0.
916.	1.	2.	3.	0.	0.	0.	0.	0.	4.	0.	8.	0.	0.	1.	1.	3.	1.	0.	1.	1.	0.
891.	1.	0.	0.	0.	0.	0.	0.	1.	0.	10.	34.	44.	7.	1.	0.	0.	1.	1.	0.	2.	0.
886.	0.	0.	0.	0.	0.	0.	0.	1.	0.	5.	12.	1.	0.	0.	0.	0.	1.	0.	0.	0.	1.
741.	2.	0.	0.	0.	0.	0.	0.	0.	0.	3.	1.	14.	0.	5.	0.	0.	0.	0.	1.	0.	0.
619.	0.	0.	0.	0.	0.	0.	0.	0.	0.	1.	0.	1.	3.	3.	1.	1.	2.	2.	0.	0.	0.
569.	0.	0.	1.	0.	0.	0.	0.	0.	0.	3.	0.	3.	0.	2.	6.	0.	2.	6.	6.	0.	0.
534.	1.	0.	0.	1.	0.	0.	0.	0.	0.	2.	0.	7.	0.	0.	0.	2.	2.	0.	2.	0.	2.
505.	0.	0.	0.	0.	0.	0.	0.	0.	1.	2.	0.	0.	0.	0.	0.	5.	0.	0.	0.	1.	0.
435.	0.	0.	0.	0.	0.	2.	0.	0.	0.	2.	0.	1.	0.	0.	3.	0.	0.	3.	1.	0.	0.
424.	0.	0.	0.	0.	0.	0.	0.	0.	0.	3.	0.	0.	0.	2.	1.	7.	2.	1.	0.	1.	0.
389.	0.	0.	1.	0.	0.	0.	0.	0.	0.	0.	0.	1.	0.	0.	0.	2.	0.	5.	2.	0.	1.
360.	0.	0.	0.	0.	0.	1.	0.	0.	0.	0.	1.	0.	0.	1.	1.	0.	1.	1.	1.	0.	0.
359.	0.	0.	0.	0.	0.	0.	0.	0.	0.	0.	1.	0.	0.	0.	3.	0.	0.	0.	0.	0.	0.
349.	0.	0.	0.	0.	0.	1.	0.	0.	0.	1.	1.	4.	3.	3.	1.	1.	1.	0.	1.	0.	0.
331.	0.	0.	0.	0.	0.	0.	0.	0.	0.	0.	0.	0.	1.	2.	0.	4.	5.	0.	0.	0.	0.
275.	0.	0.	0.	0.	0.	0.	0.	0.	0.	0.	0.	1.	0.	3.	1.	1.	1.	1.	0.	0.	0.
270.	1.	0.	0.	0.	0.	0.	0.	0.	0.	1.	1.	10.	5.	0.	6.	0.	4.	1.	0.	0.	0.
260.	0.	0.	0.	0.	0.	1.	0.	0.	0.	0.	0.	1.	1.	1.	0.	1.	2.	0.	1.	1.	0.
232.	0.	0.	0.	0.	0.	2.	0.	0.	0.	2.	25.	11.	3.	4.	2.	1.	1.	1.	2.	0.	0.
134.	0.	0.	0.	0.	0.	0.	0.	0.	0.	7.	2.	0.	0.	1.	1.	0.	0.	0.	0.	0.	0.
127.	0.	0.	0.	0.	0.	0.	0.	0.	0.	0.	1.	0.	0.	0.	0.	0.	0.	0.	1.	0.	0.

TABLE LXV (Continued)

CALCULATED INTERNAL COORDINATE DISTRIBUTIONS
ALPHA XYLOSE C1D,CH5,OH4

CONTRIBUTIONS FROM CC STRETCH

	C1C2	C2C3	C3C4	C4C5	C5O5	O5C1	C1O6	C2O7	C3O8	C4O9
1480.	0.	0.	0.	0.	0.	0.	0.	0.	1.	1.
1447.	0.	3.	0.	0.	0.	0.	0.	1.	0.	0.
1440.	0.	2.	2.	0.	0.	0.	0.	0.	0.	0.
1393.	0.	0.	1.	0.	0.	0.	0.	0.	0.	1.
1380.	1.	0.	0.	1.	1.	0.	0.	0.	0.	0.
1367.	2.	1.	4.	1.	0.	0.	0.	0.	1.	0.
1358.	3.	0.	1.	0.	0.	1.	1.	0.	0.	0.
1340.	0.	0.	0.	1.	1.	0.	0.	0.	0.	1.
1328.	0.	0.	0.	0.	0.	0.	5.	0.	0.	0.
1259.	0.	1.	2.	2.	2.	2.	0.	0.	1.	0.
1249.	1.	1.	1.	0.	0.	0.	1.	1.	0.	0.
1223.	0.	0.	0.	0.	1.	2.	1.	0.	0.	0.
1208.	5.	0.	0.	0.	0.	0.	6.	0.	0.	1.
1156.	0.	3.	12.	14.	8.	4.	0.	0.	1.	11.
1142.	1.	17.	1.	1.	1.	1.	1.	31.	17.	11.
1120.	15.	10.	2.	0.	10.	4.	4.	7.	13.	23.
1099.	3.	3.	3.	3.	38.	20.	2.	9.	2.	2.
1088.	16.	1.	4.	0.	0.	1.	14.	0.	42.	0.
1076.	1.	12.	7.	0.	0.	0.	6.	28.	5.	31.
1057.	3.	3.	9.	58.	0.	3.	1.	0.	1.	2.
1022.	2.	7.	0.	6.	0.	0.	16.	9.	3.	11.
977.	0.	1.	8.	5.	1.	7.	0.	0.	12.	1.
934.	3.	4.	22.	1.	2.	10.	16.	9.	1.	1.
916.	20.	17.	16.	0.	1.	9.	25.	1.	0.	3.
891.	18.	2.	2.	1.	0.	20.	18.	0.	0.	0.
886.	1.	0.	3.	0.	35.	27.	0.	1.	1.	1.
741.	8.	15.	1.	1.	3.	11.	3.	2.	4.	1.
619.	5.	2.	0.	1.	0.	5.	0.	1.	0.	0.
569.	4.	3.	3.	2.	1.	1.	0.	0.	2.	0.
534.	0.	7.	0.	3.	2.	0.	0.	1.	0.	5.
505.	2.	1.	14.	8.	2.	0.	0.	3.	1.	3.
435.	3.	3.	0.	4.	3.	1.	0.	3.	0.	0.
424.	2.	1.	1.	0.	1.	0.	0.	0.	2.	2.
389.	1.	0.	0.	1.	1.	0.	0.	0.	1.	0.
360.	0.	2.	1.	0.	2.	0.	0.	0.	0.	0.
359.	1.	0.	1.	0.	0.	0.	0.	0.	0.	0.
349.	3.	0.	0.	0.	0.	0.	0.	0.	0.	0.
331.	2.	0.	0.	0.	1.	0.	0.	0.	0.	0.
275.	0.	4.	3.	0.	1.	2.	0.	0.	1.	0.
270.	5.	0.	1.	0.	0.	1.	1.	0.	1.	0.
260.	0.	0.	0.	2.	2.	0.	1.	0.	0.	0.
232.	0.	0.	0.	0.	2.	15.	0.	0.	0.	1.
134.	1.	0.	0.	0.	0.	2.	0.	0.	0.	0.
127.	0.	0.	0.	0.	0.	1.	0.	1.	1.	1.

CALCULATED INTERNAL COORDINATE DISTRIBUTIONS
ALPHA XYLOSE C1D,CH5,OH4

CONTRIBUTIONS FROM CCC AND CCO BEND

	CC2C	CC3C	CC4C	CC5O	COC	OC1C	OC06	O6CC	CCO7	O7CC	CCO8	O8CC	CCO9	O9CC
1480.	0.	0.	0.	0.	0.	0.	0.	0.	0.	0.	0.	0.	0.	1.
1447.	2.	0.	0.	0.	0.	0.	0.	1.	0.	1.	1.	0.	0.	0.
1440.	0.	1.	0.	0.	0.	0.	0.	0.	0.	0.	1.	0.	3.	0.
1393.	0.	0.	0.	0.	0.	0.	0.	0.	0.	0.	0.	0.	1.	0.
1380.	0.	0.	0.	0.	0.	0.	0.	0.	0.	0.	0.	0.	0.	0.
1367.	0.	0.	0.	0.	0.	0.	0.	0.	0.	1.	1.	1.	0.	0.
1358.	0.	0.	0.	0.	0.	0.	0.	1.	0.	0.	0.	0.	0.	0.
1340.	0.	0.	0.	0.	0.	0.	0.	0.	0.	0.	0.	0.	0.	0.
1328.	0.	0.	0.	0.	0.	1.	0.	1.	0.	1.	0.	0.	0.	0.
1259.	0.	0.	0.	1.	0.	0.	0.	0.	0.	0.	0.	0.	0.	0.
1249.	0.	0.	1.	0.	0.	0.	0.	0.	0.	0.	0.	0.	0.	0.
1223.	0.	0.	0.	0.	0.	0.	0.	0.	0.	0.	0.	0.	0.	0.
1208.	1.	0.	0.	0.	0.	1.	1.	0.	1.	0.	1.	0.	0.	0.
1156.	0.	0.	6.	0.	0.	0.	0.	1.	0.	2.	0.	3.	0.	0.
1142.	0.	0.	1.	1.	0.	4.	0.	0.	5.	0.	0.	1.	0.	1.
1120.	3.	7.	4.	0.	1.	0.	2.	0.	0.	3.	1.	3.	2.	0.
1099.	0.	4.	0.	2.	1.	1.	2.	0.	1.	4.	0.	0.	1.	2.
1088.	0.	3.	2.	1.	1.	3.	0.	0.	3.	0.	0.	1.	1.	0.
1076.	8.	0.	0.	1.	1.	2.	1.	0.	2.	0.	3.	0.	1.	2.
1057.	0.	0.	0.	5.	2.	0.	0.	0.	1.	0.	0.	2.	2.	5.
1022.	2.	0.	0.	3.	1.	0.	2.	4.	0.	1.	1.	0.	0.	3.
977.	0.	0.	0.	0.	1.	2.	2.	0.	1.	1.	0.	1.	1.	0.
934.	0.	0.	0.	0.	3.	1.	0.	2.	1.	0.	0.	3.	0.	0.
916.	3.	0.	0.	0.	2.	0.	0.	1.	0.	0.	10.	3.	0.	1.
891.	0.	1.	0.	0.	1.	1.	2.	3.	1.	0.	0.	0.	1.	0.
886.	1.	0.	1.	3.	0.	1.	2.	0.	1.	0.	0.	0.	0.	5.
741.	3.	1.	0.	1.	15.	1.	1.	5.	6.	0.	0.	1.	3.	1.
619.	0.	0.	1.	0.	13.	0.	19.	14.	5.	3.	0.	0.	5.	0.
569.	0.	0.	5.	6.	0.	6.	15.	0.	1.	13.	8.	1.	4.	1.
534.	1.	0.	2.	19.	1.	2.	3.	6.	3.	6.	1.	9.	9.	2.
505.	0.	1.	0.	0.	1.	7.	4.	0.	0.	10.	2.	11.	9.	6.
435.	8.	6.	0.	0.	3.	3.	5.	0.	15.	0.	2.	1.	2.	15.
424.	0.	8.	27.	1.	3.	10.	0.	6.	4.	0.	0.	2.	1.	3.
389.	10.	14.	1.	8.	6.	0.	2.	0.	4.	3.	9.	9.	2.	8.
360.	0.	1.	1.	1.	7.	1.	1.	0.	4.	2.	1.	1.	2.	1.
359.	1.	0.	0.	0.	0.	2.	0.	6.	1.	0.	9.	0.	5.	0.
349.	0.	1.	1.	1.	4.	0.	0.	0.	3.	2.	2.	0.	1.	0.
331.	0.	0.	1.	0.	0.	0.	0.	1.	1.	1.	14.	1.	0.	5.
275.	0.	2.	0.	0.	0.	0.	0.	0.	9.	21.	1.	0.	25.	9.
270.	0.	0.	1.	1.	11.	11.	17.	2.	1.	13.	2.	20.	2.	3.
260.	3.	0.	1.	3.	8.	9.	6.	3.	4.	2.	21.	14.	6.	8.
232.	4.	3.	0.	1.	12.	6.	19.	42.	11.	0.	0.	1.	2.	2.
134.	12.	0.	5.	3.	6.	4.	0.	2.	2.	1.	0.	0.	1.	3.
127.	6.	11.	5.	0.	5.	0.	1.	2.	1.	2.	3.	3.	2.	2.

TABLE LXVI

CALCULATED INTERNAL COORDINATE DISTRIBUTIONS
BETA ARABINOSE CH6, OD4

CONTRIBUTIONS FROM CH AND OH STR.

	CH15	CH16	CH17	CH18	CH19	CH20	OD11	OD12	OD13	OD14
3002.	48.	50.	0.	0.	0.	0.	0.	0.	0.	0.
2949.	0.	0.	2.	40.	49.	7.	0.	0.	0.	0.
2942.	0.	0.	1.	6.	1.	90.	0.	0.	0.	0.
2939.	0.	0.	95.	0.	4.	1.	0.	0.	0.	0.
2935.	0.	0.	2.	53.	44.	1.	0.	0.	0.	0.
2885.	51.	50.	0.	0.	0.	0.	0.	0.	0.	0.
2447.	0.	0.	0.	0.	0.	0.	97.	2.	0.	0.
2447.	0.	0.	0.	0.	0.	0.	2.	82.	14.	1.
2446.	0.	0.	0.	0.	0.	0.	0.	0.	7.	93.
2447.	0.	0.	0.	0.	0.	0.	0.	15.	79.	6.

CONTRIBUTIONS FROM TORSIONS

	TC12	TC23	TC34	TC45	TC50	TOC1	TC06	TC07	TC08	TC09
847.	0.	0.	0.	0.	0.	0.	0.	0.	0.	0.
828.	0.	0.	0.	0.	0.	0.	0.	0.	0.	0.
766.	0.	0.	0.	0.	0.	2.	0.	0.	0.	0.
687.	0.	0.	0.	0.	1.	0.	0.	0.	0.	0.
599.	0.	0.	0.	2.	8.	3.	1.	0.	0.	0.
574.	0.	0.	0.	0.	0.	0.	0.	0.	1.	0.
478.	0.	0.	1.	1.	0.	0.	0.	2.	0.	0.
460.	0.	0.	0.	3.	11.	2.	0.	0.	0.	0.
396.	0.	0.	0.	0.	0.	1.	1.	1.	1.	1.
377.	0.	0.	0.	1.	1.	0.	6.	1.	0.	4.
313.	0.	0.	0.	0.	0.	1.	2.	3.	20.	2.
298.	1.	1.	1.	0.	4.	1.	24.	0.	0.	13.
272.	0.	4.	0.	1.	0.	4.	8.	9.	4.	9.
260.	0.	0.	1.	0.	0.	1.	0.	27.	28.	5.
245.	2.	0.	2.	1.	0.	0.	29.	0.	0.	41.
219.	0.	2.	0.	0.	0.	2.	0.	47.	1.	2.
212.	1.	0.	0.	1.	0.	1.	0.	2.	35.	2.
185.	1.	1.	1.	5.	2.	6.	19.	0.	0.	10.
138.	12.	0.	14.	14.	0.	13.	2.	0.	0.	2.
122.	14.	29.	13.	0.	4.	0.	0.	0.	1.	0.

TABLE LXVI (Continued)

CALCULATED INTERNAL COORDINATE DISTRIBUTIONS
BETA ARABINOSE CH6, OD4

CONTRIBUTIONS FROM HCC,HCO,HCH BEND

	DO6C	DO7C	HO8C	HO9C	H15O	H16O	HC4O	HC3O	HC2O	HC1O	HCO*	HC1C	HC2C	HC2C	HC3C	HC3C	HC4C	HC4C	H15C	H16C	HC5H
1476.	0.	0.	0.	0.	3.	1.	0.	0.	0.	0.	0.	0.	0.	0.	0.	0.	1.	2.	12.	13.	58.
1405.	0.	2.	0.	0.	1.	1.	3.	0.	5.	2.	0.	0.	8.	7.	21.	17.	1.	0.	1.	0.	0.
1414.	0.	0.	0.	0.	20.	22.	1.	0.	0.	0.	2.	2.	0.	1.	2.	2.	10.	14.	6.	10.	5.
1373.	0.	0.	2.	0.	6.	5.	4.	0.	1.	1.	1.	3.	19.	25.	3.	11.	4.	0.	6.	0.	1.
1351.	0.	0.	0.	0.	1.	1.	1.	2.	0.	0.	33.	26.	0.	0.	0.	1.	8.	4.	0.	0.	0.
1347.	0.	0.	0.	0.	1.	2.	0.	0.	0.	62.	21.	8.	0.	0.	0.	0.	0.	0.	0.	0.	0.
1313.	0.	6.	0.	0.	0.	1.	6.	11.	57.	0.	3.	0.	4.	13.	0.	4.	1.	0.	1.	3.	0.
1310.	0.	0.	1.	0.	1.	10.	7.	1.	0.	1.	6.	2.	3.	2.	2.	1.	17.	4.	0.	12.	0.
1296.	0.	0.	0.	0.	0.	3.	3.	43.	18.	0.	1.	0.	10.	2.	17.	5.	0.	2.	1.	4.	0.
1258.	0.	0.	0.	0.	9.	0.	52.	1.	0.	1.	1.	0.	1.	1.	1.	0.	0.	24.	8.	1.	0.
1234.	0.	0.	0.	0.	32.	22.	5.	16.	1.	3.	2.	0.	2.	0.	1.	5.	6.	0.	15.	6.	0.
1174.	2.	5.	4.	2.	4.	0.	4.	19.	0.	4.	2.	2.	5.	0.	2.	0.	0.	6.	0.	3.	1.
1152.	1.	1.	8.	2.	4.	3.	10.	2.	1.	2.	1.	1.	0.	1.	8.	15.	9.	2.	7.	6.	0.
1138.	7.	0.	0.	5.	2.	14.	2.	4.	1.	5.	2.	0.	2.	0.	3.	0.	1.	3.	1.	1.	0.
1130.	20.	6.	0.	1.	0.	0.	1.	0.	1.	3.	8.	4.	1.	0.	0.	0.	0.	0.	0.	0.	0.
1100.	3.	0.	4.	3.	1.	0.	0.	0.	0.	1.	2.	2.	0.	1.	1.	0.	0.	1.	3.	6.	0.
1089.	4.	0.	6.	2.	1.	3.	0.	3.	1.	1.	0.	1.	4.	2.	0.	1.	3.	0.	1.	0.	1.
1076.	7.	0.	1.	8.	0.	1.	0.	0.	1.	9.	1.	0.	0.	3.	0.	1.	1.	1.	1.	1.	2.
1029.	1.	1.	5.	3.	1.	0.	6.	0.	0.	0.	3.	9.	0.	3.	0.	0.	2.	3.	12.	8.	0.
994.	4.	0.	21.	18.	0.	0.	1.	4.	0.	4.	2.	6.	5.	4.	1.	0.	1.	0.	1.	0.	0.
955.	0.	44.	20.	0.	0.	0.	0.	0.	7.	1.	0.	1.	8.	2.	1.	3.	0.	0.	0.	0.	0.
934.	3.	1.	1.	1.	0.	0.	1.	0.	1.	3.	0.	9.	1.	1.	2.	1.	6.	0.	4.	5.	0.
912.	28.	7.	7.	6.	0.	0.	0.	0.	2.	0.	8.	0.	0.	1.	0.	1.	1.	0.	1.	0.	1.
867.	4.	0.	7.	24.	0.	0.	0.	0.	0.	1.	1.	1.	0.	0.	0.	1.	0.	3.	1.	0.	2.
847.	3.	16.	3.	5.	0.	0.	0.	0.	4.	0.	1.	0.	0.	0.	0.	4.	0.	1.	0.	0.	0.
828.	5.	12.	9.	11.	0.	0.	0.	0.	4.	0.	3.	1.	0.	1.	0.	1.	0.	3.	0.	0.	0.
766.	2.	0.	0.	0.	0.	0.	0.	0.	0.	0.	2.	1.	0.	2.	0.	0.	2.	2.	1.	0.	0.
687.	2.	0.	1.	5.	0.	0.	0.	0.	0.	0.	2.	5.	0.	1.	1.	0.	6.	7.	1.	2.	2.
599.	1.	0.	0.	2.	0.	0.	0.	0.	0.	2.	0.	4.	1.	0.	2.	2.	0.	0.	1.	0.	0.
574.	3.	1.	0.	3.	0.	0.	0.	0.	0.	0.	0.	0.	1.	3.	4.	2.	2.	0.	0.	0.	0.
478.	0.	0.	1.	0.	0.	0.	0.	0.	1.	3.	0.	2.	0.	4.	3.	0.	1.	1.	1.	1.	0.
460.	0.	0.	0.	0.	0.	0.	0.	0.	0.	4.	0.	0.	0.	0.	1.	0.	0.	0.	0.	0.	0.
396.	0.	0.	0.	0.	0.	0.	0.	0.	0.	0.	0.	0.	0.	0.	0.	0.	0.	0.	0.	0.	0.
377.	0.	0.	1.	0.	0.	0.	0.	0.	0.	0.	1.	5.	1.	1.	1.	0.	1.	1.	1.	0.	0.
313.	0.	0.	0.	0.	0.	0.	0.	0.	0.	0.	0.	2.	3.	1.	0.	0.	1.	0.	0.	0.	0.
298.	0.	0.	0.	1.	0.	0.	0.	0.	0.	2.	1.	0.	1.	0.	0.	2.	1.	0.	1.	1.	1.
272.	0.	0.	0.	1.	0.	1.	0.	0.	0.	0.	3.	0.	0.	1.	0.	2.	0.	2.	1.	1.	0.
260.	0.	0.	0.	0.	0.	0.	0.	0.	0.	0.	2.	0.	0.	7.	0.	6.	0.	1.	0.	0.	0.
245.	0.	0.	0.	0.	0.	0.	0.	0.	0.	1.	1.	5.	1.	0.	0.	1.	4.	1.	0.	0.	0.
219.	0.	0.	0.	0.	0.	0.	0.	0.	0.	0.	4.	1.	6.	0.	0.	0.	0.	0.	0.	0.	0.
212.	0.	0.	0.	0.	0.	0.	0.	0.	0.	0.	1.	0.	2.	2.	11.	0.	1.	2.	0.	0.	0.
185.	0.	0.	0.	0.	0.	2.	0.	0.	0.	1.	15.	13.	0.	1.	0.	0.	2.	0.	2.	0.	1.
138.	0.	0.	0.	0.	1.	0.	3.	0.	0.	7.	5.	0.	0.	1.	0.	0.	1.	0.	0.	0.	1.
122.	0.	0.	0.	0.	0.	0.	1.	0.	0.	1.	0.	0.	0.	0.	0.	0.	0.	0.	1.	0.	0.

TABLE LXVI (Continued)

CALCULATED INTERNAL COORDINATE DISTRIBUTIONS
BETA ARABINOSE CH6, OD4

CONTRIBUTIONS FROM CC STRETCH

	C1C2	C2C3	C3C4	C4C5	C5O*	O*C1	C1O6	C2O7	C3O8	C4O9
1476.	0.	0.	0.	0.	0.	0.	0.	0.	0.	1.
1405.	0.	2.	0.	0.	0.	0.	0.	0.	0.	2.
1414.	0.	0.	0.	1.	1.	0.	0.	0.	0.	0.
1373.	0.	0.	0.	0.	0.	0.	2.	0.	0.	3.
1351.	4.	7.	0.	0.	3.	1.	0.	0.	0.	0.
1347.	2.	1.	0.	0.	1.	0.	1.	1.	0.	0.
1313.	0.	0.	1.	0.	0.	0.	0.	3.	0.	1.
1310.	2.	1.	7.	0.	0.	0.	2.	1.	1.	3.
1296.	0.	0.	1.	0.	0.	0.	2.	1.	1.	1.
1258.	0.	0.	0.	0.	0.	0.	1.	0.	1.	2.
1234.	0.	1.	0.	1.	1.	2.	1.	0.	1.	0.
1174.	2.	9.	0.	12.	2.	3.	11.	5.	1.	14.
1152.	0.	5.	28.	0.	3.	1.	1.	2.	8.	6.
1138.	3.	5.	6.	23.	12.	2.	3.	5.	4.	2.
1130.	28.	4.	2.	6.	1.	1.	0.	18.	12.	0.
1100.	4.	7.	0.	5.	0.	0.	1.	3.	58.	4.
1089.	0.	2.	0.	4.	15.	9.	3.	36.	0.	3.
1076.	2.	1.	5.	11.	4.	18.	19.	15.	0.	7.
1029.	3.	4.	13.	3.	2.	23.	1.	1.	3.	1.
994.	12.	11.	2.	3.	8.	0.	17.	0.	0.	6.
955.	3.	1.	2.	0.	4.	0.	13.	2.	0.	6.
934.	8.	1.	10.	10.	2.	12.	18.	5.	6.	20.
912.	5.	7.	1.	10.	9.	6.	3.	0.	2.	0.
867.	5.	7.	6.	6.	26.	16.	3.	0.	2.	0.
847.	3.	1.	3.	2.	4.	0.	7.	2.	0.	23.
828.	12.	7.	8.	1.	12.	10.	8.	0.	0.	7.
766.	5.	3.	3.	0.	7.	18.	5.	4.	4.	2.
687.	0.	27.	0.	1.	0.	1.	0.	1.	0.	1.
599.	8.	7.	3.	1.	1.	3.	0.	2.	1.	0.
574.	0.	0.	2.	0.	0.	1.	0.	0.	0.	0.
478.	9.	1.	6.	2.	0.	0.	0.	2.	0.	0.
460.	9.	1.	2.	2.	0.	0.	0.	2.	3.	0.
396.	0.	0.	1.	5.	0.	1.	0.	1.	2.	0.
377.	0.	0.	2.	1.	0.	2.	1.	0.	0.	0.
313.	5.	1.	0.	0.	0.	0.	0.	0.	0.	0.
298.	1.	0.	3.	0.	1.	1.	0.	0.	0.	0.
272.	0.	0.	1.	1.	1.	0.	0.	0.	0.	0.
260.	0.	1.	1.	0.	0.	1.	0.	0.	1.	0.
245.	1.	0.	1.	0.	0.	0.	0.	0.	0.	0.
219.	1.	0.	1.	0.	0.	3.	1.	0.	0.	0.
212.	1.	0.	0.	1.	0.	0.	0.	1.	0.	0.
185.	1.	0.	1.	0.	2.	9.	0.	0.	0.	0.
138.	1.	0.	0.	0.	0.	2.	0.	0.	0.	0.
122.	0.	0.	0.	0.	0.	0.	0.	1.	1.	0.

CALCULATED INTERNAL COORDINATE DISTRIBUTIONS
BETA ARABINOSE CH6, OD4

CONTRIBUTIONS FROM CCC AND CCO BEND

	CC2C	CC3C	CC4C	CC5O	COC	OC1C	OC06	O6CC	CCO7	O7CC	CCO8	O8CC	CCO9	O9CC
1476.	0.	0.	0.	0.	0.	0.	0.	0.	0.	0.	0.	0.	0.	0.
1405.	1.	0.	0.	0.	0.	0.	0.	1.	0.	1.	1.	0.	0.	0.
1414.	0.	0.	0.	0.	0.	0.	0.	0.	0.	0.	0.	0.	0.	0.
1373.	0.	0.	0.	0.	0.	0.	0.	0.	0.	0.	2.	0.	1.	0.
1351.	0.	0.	0.	0.	0.	0.	0.	0.	1.	1.	0.	0.	0.	0.
1347.	0.	0.	0.	0.	0.	0.	0.	0.	1.	0.	0.	0.	0.	0.
1313.	1.	1.	1.	0.	0.	1.	0.	0.	0.	0.	0.	0.	0.	0.
1310.	1.	1.	0.	0.	0.	0.	0.	0.	0.	0.	1.	1.	0.	0.
1296.	0.	0.	0.	0.	0.	0.	0.	0.	0.	0.	0.	0.	0.	0.
1258.	0.	0.	0.	0.	0.	0.	0.	0.	0.	0.	0.	0.	0.	0.
1234.	0.	0.	0.	0.	0.	0.	0.	0.	0.	0.	0.	0.	0.	0.
1174.	3.	0.	2.	0.	0.	0.	0.	2.	0.	1.	3.	2.	4.	0.
1152.	2.	1.	3.	0.	0.	1.	0.	0.	0.	1.	3.	1.	1.	2.
1138.	1.	0.	0.	1.	6.	3.	1.	2.	2.	0.	0.	1.	2.	3.
1130.	0.	0.	2.	0.	1.	1.	0.	4.	0.	0.	0.	1.	0.	0.
1100.	2.	4.	3.	1.	0.	0.	0.	1.	0.	2.	2.	1.	0.	0.
1089.	0.	6.	0.	2.	0.	1.	0.	0.	0.	3.	0.	0.	1.	2.
1076.	0.	1.	0.	2.	0.	8.	1.	3.	8.	1.	0.	0.	2.	0.
1029.	1.	0.	3.	0.	0.	0.	3.	0.	0.	1.	0.	6.	0.	1.
994.	0.	0.	0.	1.	0.	1.	0.	0.	1.	2.	0.	0.	1.	1.
955.	0.	0.	0.	0.	0.	0.	1.	1.	1.	2.	0.	0.	0.	0.
934.	1.	0.	0.	0.	1.	0.	6.	0.	0.	0.	0.	0.	0.	2.
912.	1.	1.	0.	3.	2.	0.	1.	1.	1.	1.	0.	0.	0.	0.
867.	0.	0.	0.	6.	0.	1.	0.	1.	0.	0.	0.	0.	0.	0.
847.	1.	0.	0.	0.	0.	0.	1.	0.	0.	1.	1.	4.	1.	1.
828.	4.	0.	0.	0.	2.	0.	0.	0.	0.	2.	4.	2.	0.	1.
766.	2.	3.	1.	7.	16.	1.	0.	3.	7.	3.	2.	0.	0.	3.
687.	0.	3.	3.	13.	3.	0.	4.	2.	1.	0.	0.	0.	3.	7.
599.	0.	0.	0.	2.	3.	3.	19.	2.	3.	0.	1.	5.	8.	4.
574.	3.	2.	1.	3.	8.	0.	6.	18.	6.	0.	0.	8.	17.	2.
478.	0.	0.	2.	0.	0.	17.	11.	2.	0.	19.	12.	1.	0.	14.
460.	0.	2.	19.	0.	2.	10.	1.	1.	5.	3.	5.	1.	0.	6.
396.	15.	16.	0.	4.	6.	0.	1.	0.	23.	0.	0.	16.	0.	0.
377.	1.	1.	3.	6.	15.	1.	15.	1.	0.	17.	13.	1.	0.	22.
313.	0.	0.	0.	0.	1.	1.	1.	2.	12.	15.	21.	17.	0.	1.
298.	0.	0.	2.	1.	7.	1.	3.	10.	0.	3.	4.	0.	15.	4.
272.	1.	1.	12.	3.	6.	7.	0.	10.	1.	0.	0.	0.	19.	1.
260.	4.	2.	1.	0.	0.	2.	0.	7.	2.	0.	8.	1.	5.	0.
245.	0.	0.	4.	0.	0.	3.	4.	0.	0.	2.	4.	0.	1.	5.
219.	3.	0.	0.	0.	0.	6.	0.	13.	9.	3.	2.	1.	1.	1.
212.	1.	4.	1.	0.	0.	1.	0.	3.	0.	6.	1.	15.	13.	...
185.	0.	2.	2.	4.	21.	0.	26.	10.	3.	0.	0.	1.	0.	11.
138.	3.	4.	5.	5.	7.	7.	1.	5.	1.	0.	0.	1.	0.	0.
122.	13.	11.	0.	0.	0.	0.	0.	1.	3.	3.	3.	3.	1.	0.

TABLE LXVII

CALCULATED INTERNAL COORDINATE DISTRIBUTIONS
ALPHA XYLOSE CH6, OD4

CONTRIBUTIONS FROM CH AND OH STR.

	CH15	CH16	CH17	CH18	CH19	CH20	OD11	OD12	OD13	OD14
3000.	48.	49.	1.	0.	0.	0.	0.	0.	0.	0.
2953.	0.	0.	22.	50.	25.	2.	0.	0.	0.	0.
2943.	0.	0.	20.	1.	14.	63.	0.	0.	0.	0.
2941.	0.	0.	29.	0.	35.	34.	0.	0.	0.	0.
2933.	0.	0.	27.	48.	25.	0.	0.	0.	0.	0.
2888.	51.	50.	0.	0.	0.	0.	0.	0.	0.	0.
2447.	0.	0.	0.	0.	0.	0.	97.	2.	0.	0.
2447.	0.	0.	0.	0.	0.	0.	2.	82.	14.	2.
2447.	0.	0.	0.	0.	0.	0.	0.	10.	26.	64.
2447.	0.	0.	0.	0.	0.	0.	0.	5.	60.	34.

CONTRIBUTIONS FROM TORSIONS

	TC12	TC23	TC34	TC45	TC50	TOC1	TC06	TC07	TC08	TC09
878.	0.	0.	0.	0.	1.	0.	0.	0.	0.	0.
834.	0.	0.	0.	0.	0.	0.	0.	0.	0.	0.
752.	0.	0.	0.	0.	0.	2.	0.	0.	0.	0.
600.	0.	0.	0.	2.	7.	1.	1.	0.	0.	0.
562.	0.	0.	1.	0.	0.	2.	0.	1.	1.	0.
537.	0.	0.	0.	0.	1.	0.	0.	0.	0.	1.
492.	0.	0.	0.	1.	1.	0.	0.	0.	0.	0.
428.	1.	0.	0.	0.	2.	0.	1.	0.	0.	1.
416.	0.	1.	0.	0.	10.	2.	2.	1.	0.	2.
378.	0.	1.	0.	0.	0.	3.	0.	0.	1.	4.
319.	0.	0.	0.	3.	0.	3.	12.	1.	12.	1.
304.	0.	1.	0.	1.	0.	0.	2.	17.	4.	9.
298.	1.	1.	1.	4.	2.	4.	21.	4.	9.	1.
252.	0.	0.	3.	0.	0.	0.	2.	10.	23.	35.
244.	2.	2.	1.	0.	0.	2.	11.	0.	7.	12.
225.	0.	1.	1.	3.	0.	1.	11.	35.	3.	12.
217.	1.	0.	0.	0.	0.	0.	1.	22.	27.	8.
206.	0.	0.	1.	5.	2.	0.	23.	2.	3.	5.
129.	23.	7.	3.	10.	1.	12.	3.	0.	0.	1.
121.	2.	22.	25.	3.	3.	4.	0.	0.	2.	2.

TABLE LXVII (Continued)

CALCULATED INTERNAL COORDINATE DISTRIBUTIONS
ALPHA XYLOSE CH6, OD4

CONTRIBUTIONS FROM HCC,HCO,HCH BEND

	D06C	D07C	H08C	H09C	H15O	H16O	HC4O	HC3O	HC2O	HC1O	HCO'	HC1C	HC2C	HC2C	HC3C	HC3C	HC4C	HC4C	H15C	H16C	HC5H
1479.	0.	0.	0.	0.	0.	0.	0.	0.	0.	0.	0.	0.	0.	1.	0.	1.	3.	0.	18.	15.	46.
1408.	0.	1.	1.	0.	2.	1.	1.	0.	0.	2.	0.	0.	13.	20.	4.	0.	13.	4.	0.	0.	5.
1395.	0.	2.	0.	1.	8.	7.	1.	0.	7.	1.	0.	0.	0.	0.	21.	24.	1.	0.	3.	0.	7.
1383.	0.	0.	0.	1.	17.	19.	1.	0.	2.	2.	6.	10.	2.	6.	4.	6.	0.	2.	4.	11.	3.
1348.	0.	0.	0.	0.	7.	0.	2.	1.	1.	24.	47.	3.	5.	1.	0.	2.	3.	0.	1.	1.	0.
1347.	0.	0.	0.	0.	5.	8.	0.	1.	3.	32.	1.	15.	3.	1.	0.	0.	7.	9.	4.	2.	2.
1339.	0.	0.	0.	1.	0.	0.	0.	7.	2.	2.	4.	11.	4.	1.	0.	3.	11.	23.	3.	2.	0.
1307.	0.	2.	0.	0.	1.	1.	13.	5.	48.	2.	1.	0.	14.	6.	11.	1.	0.	7.	0.	1.	1.
1297.	0.	3.	0.	1.	1.	0.	1.	31.	13.	1.	9.	0.	4.	13.	6.	8.	4.	0.	1.	2.	0.
1272.	0.	0.	1.	0.	1.	3.	61.	10.	7.	2.	0.	0.	1.	2.	2.	1.	9.	12.	0.	1.	0.
1234.	0.	0.	1.	1.	29.	27.	0.	13.	1.	2.	1.	0.	2.	0.	0.	4.	0.	0.	16.	12.	0.
1182.	1.	6.	5.	1.	3.	2.	2.	29.	0.	3.	1.	3.	7.	1.	3.	0.	1.	2.	0.	1.	0.
1141.	2.	0.	9.	9.	7.	7.	12.	2.	0.	0.	0.	0.	0.	0.	4.	8.	6.	0.	1.	1.	0.
1135.	18.	3.	1.	2.	1.	5.	0.	0.	3.	9.	6.	2.	1.	0.	0.	0.	0.	0.	0.	0.	0.
1130.	6.	0.	0.	6.	0.	3.	1.	2.	0.	2.	1.	0.	2.	1.	3.	0.	0.	1.	1.	7.	1.
1125.	2.	2.	0.	0.	1.	0.	6.	0.	0.	3.	3.	1.	0.	0.	3.	0.	0.	0.	0.	5.	1.
1090.	13.	0.	4.	0.	2.	1.	0.	0.	0.	0.	6.	4.	0.	0.	1.	0.	0.	0.	0.	1.	0.
1078.	3.	0.	1.	5.	0.	0.	1.	2.	0.	0.	1.	0.	2.	2.	1.	1.	0.	0.	3.	2.	2.
1043.	2.	0.	4.	0.	0.	0.	0.	0.	0.	5.	0.	2.	0.	3.	0.	0.	6.	1.	2.	5.	2.
1019.	1.	3.	28.	0.	0.	1.	1.	2.	0.	2.	4.	11.	3.	7.	1.	1.	0.	0.	5.	2.	1.
980.	0.	4.	1.	39.	1.	2.	2.	0.	0.	3.	0.	2.	0.	2.	1.	1.	0.	0.	9.	8.	0.
951.	1.	36.	10.	0.	0.	0.	0.	0.	8.	2.	1.	2.	9.	1.	1.	1.	2.	0.	1.	2.	1.
931.	18.	9.	2.	0.	0.	0.	0.	0.	3.	1.	1.	7.	1.	0.	1.	0.	0.	0.	0.	0.	1.
895.	9.	7.	1.	23.	0.	0.	0.	0.	1.	0.	5.	3.	1.	1.	0.	1.	2.	5.	1.	1.	0.
878.	9.	1.	13.	7.	0.	0.	0.	1.	0.	2.	4.	1.	0.	0.	1.	1.	2.	2.	1.	1.	0.
834.	7.	23.	17.	0.	0.	0.	0.	0.	7.	0.	3.	0.	0.	1.	0.	3.	0.	0.	0.	0.	0.
752.	4.	1.	0.	1.	0.	0.	0.	0.	0.	0.	4.	4.	0.	3.	0.	0.	0.	0.	0.	0.	0.
600.	3.	1.	0.	1.	0.	0.	0.	0.	0.	1.	0.	1.	3.	3.	1.	1.	2.	2.	0.	0.	0.
562.	0.	0.	1.	0.	0.	0.	0.	0.	1.	2.	0.	5.	0.	2.	6.	0.	1.	7.	6.	0.	1.
537.	2.	0.	0.	1.	0.	0.	0.	0.	0.	1.	0.	4.	0.	0.	0.	1.	2.	0.	2.	0.	2.
492.	0.	0.	0.	2.	0.	0.	0.	0.	1.	2.	0.	0.	0.	1.	0.	4.	1.	0.	0.	1.	0.
428.	0.	0.	0.	0.	0.	2.	0.	0.	0.	3.	0.	0.	0.	0.	1.	0.	0.	1.	1.	0.	0.
416.	0.	0.	0.	0.	0.	0.	0.	0.	0.	2.	0.	0.	0.	2.	3.	7.	3.	1.	0.	1.	0.
378.	0.	0.	1.	0.	0.	0.	0.	0.	0.	0.	1.	1.	0.	0.	1.	3.	1.	5.	2.	0.	1.
319.	0.	0.	0.	0.	0.	1.	0.	0.	0.	0.	0.	3.	3.	1.	0.	0.	0.	0.	0.	0.	0.
304.	0.	0.	0.	1.	0.	0.	0.	0.	0.	0.	1.	0.	0.	0.	0.	0.	1.	0.	0.	0.	0.
298.	0.	0.	0.	0.	0.	2.	0.	0.	0.	1.	0.	0.	1.	1.	0.	0.	1.	1.	2.	0.	1.
252.	0.	0.	0.	0.	0.	0.	0.	0.	0.	0.	0.	0.	0.	3.	0.	5.	3.	0.	0.	0.	0.
244.	1.	0.	0.	0.	0.	0.	0.	0.	0.	2.	1.	2.	4.	4.	4.	1.	0.	1.	0.	1.	0.
225.	0.	0.	0.	0.	0.	0.	0.	0.	0.	0.	1.	3.	4.	3.	0.	0.	1.	1.	0.	0.	0.
217.	0.	0.	0.	0.	0.	0.	0.	0.	0.	0.	1.	1.	0.	0.	4.	1.	3.	1.	0.	0.	0.
206.	0.	0.	0.	0.	0.	2.	0.	0.	0.	1.	20.	13.	2.	1.	2.	0.	2.	0.	2.	0.	0.
129.	0.	0.	0.	0.	0.	0.	0.	0.	0.	7.	4.	1.	0.	1.	1.	0.	0.	0.	0.	0.	0.
121.	0.	0.	0.	0.	0.	0.	0.	0.	0.	0.	2.	0.	0.	0.	0.	0.	1.	0.	1.	0.	0.

TABLE LXVII (Continued)

CALCULATED INTERNAL COORDINATE DISTRIBUTIONS
ALPHA XYLOSE CH6, OD4

CONTRIBUTIONS FROM CC STRETCH

	C1C2	C2C3	C3C4	C4C5	C5O*	O*C1	C1O6	C2O7	C3O8	C4O9
1479.	0.	0.	0.	0.	0.	0.	0.	0.	0.	1.
1408.	0.	2.	1.	0.	0.	0.	1.	0.	0.	0.
1395.	0.	0.	1.	0.	0.	0.	0.	0.	0.	0.
1383.	0.	0.	0.	1.	0.	1.	0.	0.	0.	0.
1348.	0.	0.	0.	0.	5.	1.	0.	1.	0.	0.
1347.	3.	1.	0.	0.	1.	0.	0.	0.	1.	0.
1339.	3.	4.	0.	0.	0.	0.	2.	0.	0.	0.
1307.	0.	0.	0.	0.	0.	0.	1.	2.	0.	1.
1297.	0.	0.	2.	0.	0.	0.	2.	1.	1.	0.
1272.	0.	1.	0.	0.	0.	0.	1.	0.	0.	1.
1234.	0.	0.	4.	1.	2.	2.	0.	1.	1.	0.
1182.	4.	16.	0.	2.	1.	2.	11.	10.	0.	0.
1141.	0.	1.	38.	3.	1.	0.	1.	2.	18.	0.
1135.	20.	0.	1.	2.	2.	0.	1.	0.	1.	18.
1130.	5.	3.	2.	22.	11.	2.	2.	3.	0.	38.
1125.	4.	7.	0.	8.	6.	5.	0.	33.	17.	5.
1090.	2.	2.	0.	2.	14.	21.	11.	0.	36.	1.
1078.	1.	9.	1.	21.	10.	13.	3.	12.	12.	2.
1043.	4.	2.	7.	11.	2.	1.	12.	19.	2.	25.
1019.	10.	14.	1.	6.	4.	4.	12.	3.	2.	1.
980.	6.	0.	3.	6.	2.	0.	4.	3.	5.	1.
951.	6.	1.	1.	2.	10.	0.	18.	3.	0.	1.
931.	1.	2.	0.	0.	20.	12.	14.	3.	0.	0.
895.	9.	3.	12.	7.	1.	20.	0.	3.	3.	1.
878.	5.	9.	20.	1.	12.	21.	6.	2.	1.	3.
834.	14.	11.	5.	0.	0.	2.	13.	0.	0.	1.
752.	5.	14.	0.	1.	3.	17.	5.	2.	4.	1.
600.	4.	1.	0.	1.	0.	3.	0.	0.	0.	0.
562.	6.	2.	3.	2.	1.	1.	0.	0.	2.	0.
537.	0.	6.	0.	4.	2.	1.	0.	1.	0.	6.
492.	1.	1.	14.	6.	2.	0.	0.	4.	1.	3.
428.	4.	1.	0.	3.	5.	1.	0.	3.	0.	0.
416.	1.	2.	1.	1.	0.	0.	0.	0.	3.	2.
378.	2.	0.	0.	0.	1.	0.	0.	0.	0.	0.
319.	3.	1.	0.	0.	2.	1.	0.	0.	0.	0.
304.	0.	2.	3.	0.	1.	3.	0.	0.	0.	0.
298.	2.	0.	0.	0.	2.	0.	0.	0.	0.	1.
252.	0.	1.	0.	0.	0.	0.	0.	0.	1.	0.
244.	2.	0.	0.	0.	0.	0.	1.	1.	1.	0.
225.	2.	3.	0.	0.	0.	0.	0.	0.	0.	0.
217.	0.	0.	2.	1.	0.	1.	0.	0.	0.	0.
206.	0.	0.	0.	1.	2.	11.	0.	0.	0.	3.
129.	1.	0.	0.	0.	0.	2.	0.	0.	0.	0.
121.	0.	0.	0.	0.	0.	1.	0.	1.	1.	1.

CALCULATED INTERNAL COORDINATE DISTRIBUTIONS
ALPHA XYLOSE CH6, OD4

CONTRIBUTIONS FROM CCC AND CCO BEND

	CC2C	CC3C	CC4C	CC5O	C0C	0C1C	OCO6	O6CC	CCO7	O7CC	CCO8	O8CC	CCO9	O9CC
1479.	0.	0.	0.	0.	0.	0.	0.	0.	0.	0.	0.	0.	0.	1.
1408.	0.	1.	0.	0.	0.	0.	0.	0.	0.	1.	1.	0.	1.	0.
1395.	1.	0.	0.	0.	0.	0.	0.	1.	0.	0.	0.	0.	1.	0.
1383.	0.	0.	0.	0.	0.	0.	0.	0.	0.	0.	0.	0.	1.	0.
1348.	0.	0.	0.	0.	0.	0.	0.	0.	0.	0.	0.	0.	0.	0.
1347.	0.	0.	0.	0.	0.	0.	0.	0.	1.	0.	0.	0.	0.	0.
1339.	0.	0.	0.	0.	0.	1.	0.	0.	1.	0.	0.	0.	1.	0.
1307.	0.	0.	0.	0.	0.	1.	0.	0.	0.	0.	0.	0.	0.	0.
1297.	2.	0.	1.	0.	0.	0.	0.	1.	0.	0.	0.	0.	0.	0.
1272.	0.	0.	0.	0.	0.	0.	0.	0.	0.	0.	0.	0.	0.	0.
1234.	0.	1.	0.	0.	0.	0.	0.	0.	0.	0.	0.	0.	0.	0.
1182.	4.	0.	1.	0.	0.	0.	1.	1.	0.	0.	4.	0.	2.	0.
1141.	2.	2.	1.	0.	0.	0.	0.	0.	0.	2.	3.	0.	2.	1.
1135.	0.	1.	2.	1.	5.	4.	0.	3.	2.	0.	1.	1.	2.	0.
1130.	0.	3.	6.	1.	1.	0.	1.	2.	0.	0.	0.	3.	3.	0.
1125.	0.	0.	2.	1.	0.	2.	1.	1.	2.	1.	0.	3.	0.	1.
1090.	2.	2.	2.	0.	0.	1.	1.	3.	1.	0.	1.	1.	0.	0.
1078.	0.	3.	0.	5.	1.	0.	1.	0.	0.	3.	0.	0.	0.	4.
1043.	0.	0.	0.	3.	0.	4.	0.	1.	5.	0.	0.	0.	0.	4.
1019.	1.	1.	1.	3.	0.	0.	2.	0.	0.	0.	0.	5.	1.	2.
980.	0.	1.	1.	0.	1.	1.	1.	0.	2.	0.	0.	1.	0.	0.
951.	0.	0.	0.	2.	0.	0.	0.	1.	0.	3.	0.	0.	0.	3.
931.	3.	0.	0.	3.	1.	0.	8.	0.	2.	0.	0.	0.	0.	2.
895.	0.	2.	0.	0.	1.	0.	0.	1.	0.	2.	0.	1.	1.	0.
878.	0.	1.	0.	0.	2.	1.	0.	1.	1.	0.	0.	1.	0.	1.
834.	5.	0.	0.	0.	1.	0.	1.	0.	0.	1.	7.	0.	0.	0.
752.	2.	1.	0.	1.	18.	1.	2.	4.	6.	1.	1.	0.	2.	0.
600.	1.	0.	1.	0.	10.	0.	18.	13.	5.	3.	0.	0.	5.	0.
562.	0.	0.	6.	8.	0.	5.	14.	0.	1.	9.	6.	2.	3.	1.
537.	1.	0.	2.	19.	2.	1.	2.	6.	3.	7.	1.	8.	9.	2.
492.	0.	0.	0.	0.	0.	9.	4.	0.	0.	11.	2.	11.	11.	5.
428.	6.	2.	2.	0.	6.	8.	5.	0.	18.	0.	1.	2.	1.	21.
416.	3.	17.	26.	0.	0.	6.	1.	6.	0.	0.	1.	0.	3.	0.
378.	9.	10.	0.	9.	5.	0.	2.	3.	6.	3.	17.	9.	2.	12.
319.	0.	1.	0.	1.	13.	5.	9.	1.	9.	12.	10.	13.	0.	0.
304.	0.	0.	0.	0.	0.	2.	1.	7.	6.	6.	3.	1.	22.	9.
298.	0.	1.	2.	4.	16.	1.	4.	1.	2.	5.	10.	5.	0.	1.
252.	1.	0.	1.	0.	0.	2.	0.	3.	0.	0.	9.	0.	1.	0.
244.	3.	2.	0.	0.	1.	12.	2.	13.	1.	8.	4.	0.	9.	3.
225.	0.	1.	0.	1.	2.	4.	5.	0.	1.	0.	0.	2.	8.	4.
217.	1.	0.	1.	0.	0.	0.	1.	2.	3.	8.	6.	14.	2.	3.
206.	2.	2.	0.	1.	8.	1.	20.	24.	6.	0.	0.	2.	0.	5.
129.	11.	0.	5.	3.	7.	4.	1.	2.	3.	1.	0.	1.	1.	3.
121.	6.	11.	5.	0.	5.	0.	2.	2.	1.	2.	3.	3.	2.	2.

TABLE LXVIII

INFRARED SPECTRA REPORTED FOR THE C1-D ANALOGS OF ARABINOSE AND XYLOSE (29)

α-D-Xylopyranose		β-D-Arabinopyranose	
$C_{(1)}$-H	$C_{(1)}$-D	$C_{(1)}$-H	$C_{(1)}$-D
1480 s	1478 s	1472 m	1476 m
1465 w	1460 s	1450 vw	1450 m
1455 s	1450 m	1425 m	1425 m
1445 w	1425 s	1402 w	1397 w
1425 vw	1405 w	1375 s	1375 s
1398 m	1375 s	1357 s[a]	
1375 s	1360 s	1329 m	1332 s
1360 w	1340 m	1318 s[b]	
1340 s[a]		1260 s	1266 s
1315 m	1322 s	1247 w	1255 w
1305 s[b]		1234 s	1227 s
1255 vw	1275 w	1135 vs	1162 vs
1250 w?	1260 m		1115 s[a]
1240 m	1240 s	1103 s	1108 m
1205 m	1218 m	1093 s	1088 vs
1195 s	1200 s	1065 s	1076 s
1150 s	1188 s	1053 vs	1047 vs
1130 vs	1125 vs		1035 s[b]
1110 w	1110 w	1001 vs	985 s
1080 m	1095 w	998 s	974 s
1070 m	1082 m	943 m	920 s
	1065 sa	925 vw	893 vw
1055 s	1050 s	893 s	864 s
1035 vs	1033 vs	865 vw	858 vw
1020 s	1022 s	843 s	824 s
	975 s[a]	785 s	777 s
935 s	900 s 881 s	710 m	699 m
905 s	865 s	675 s	672 s 667 s
762 s	742 s		
675 w	675 w		

TABLE LXIX

CALCULATED INTERNAL COORDINATE DISTRIBUTIONS
ALPHA ARABINOSE

CONTRIBUTIONS FROM CH AND OH STR.

	CH15	CH16	CH17	CH18	CH19	CH20	OH11	OH12	OH13	OH14
3357.	0.	0.	0.	0.	0.	0.	97.	3.	0.	0.
3357.	0.	0.	0.	0.	0.	0.	0.	9.	59.	31.
3356.	0.	0.	0.	0.	0.	0.	0.	16.	18.	65.
3356.	0.	0.	0.	0.	0.	0.	2.	72.	23.	3.
3000.	48.	50.	0.	0.	0.	0.	0.	0.	0.	0.
2954.	0.	0.	0.	18.	53.	26.	0.	0.	0.	0.
2942.	0.	0.	9.	47.	0.	43.	0.	0.	0.	0.
2938.	0.	0.	89.	5.	1.	4.	0.	0.	0.	0.
2934.	0.	0.	0.	29.	44.	26.	0.	0.	0.	0.
2888.	51.	49.	0.	0.	0.	0.	0.	0.	0.	0.

CONTRIBUTIONS FROM TORSIONS

	TC12	TC23	TC34	TC45	TC50	TOC1	TC06	TC07	TC08	TC09
902.	0.	0.	0.	0.	1.	0.	0.	0.	0.	0.
859.	0.	0.	0.	0.	0.	1.	2.	0.	0.	0.
757.	0.	0.	0.	0.	0.	2.	0.	0.	0.	0.
677.	0.	1.	0.	0.	3.	0.	1.	2.	0.	0.
589.	0.	0.	0.	1.	0.	2.	2.	0.	0.	0.
520.	0.	0.	0.	0.	1.	1.	2.	2.	0.	0.
507.	0.	0.	0.	3.	6.	0.	1.	0.	1.	1.
444.	0.	0.	0.	2.	10.	3.	0.	0.	4.	0.
436.	0.	0.	1.	0.	0.	1.	11.	1.	2.	3.
390.	1.	0.	0.	3.	3.	1.	7.	0.	6.	0.
365.	0.	0.	0.	0.	1.	2.	8.	7.	24.	25.
358.	0.	0.	0.	0.	0.	0.	19.	18.	1.	29.
343.	0.	1.	0.	0.	0.	0.	0.	21.	38.	17.
331.	0.	1.	1.	1.	0.	3.	26.	34.	1.	1.
284.	0.	0.	1.	0.	2.	4.	3.	1.	4.	0.
276.	3.	1.	0.	1.	0.	10.	0.	0.	4.	13.
261.	0.	1.	0.	0.	0.	0.	12.	7.	0.	0.
245.	2.	2.	1.	0.	1.	0.	0.	1.	6.	0.
137.	2.	4.	25.	15.	0.	10.	0.	0.	0.	1.
127.	24.	26.	3.	2.	3.	3.	0.	0.	0.	0.

TABLE LXIX (Continued)

CALCULATED INTERNAL COORDINATE DISTRIBUTIONS
ALPHA ARABINOSE

CONTRIBUTIONS FROM HCC,HCO,HCH BEND

	HO6C	HO7C	HO8C	HO9C	HC5D	HC5D	HC4O	HC3O	HC2O	HC1O	HCO'	HC1C	HC2C	HC2C	HC3C	HC3C	HC4C	HC4C	HC5C	HC5C	HC5H
1476.	6.	11.	1.	3.	0.	0.	0.	1.	3.	1.	0.	4.	0.	0.	5.	0.	1.	2.	7.	9.	24.
1470.	5.	14.	1.	1.	0.	0.	1.	0.	5.	0.	0.	4.	0.	0.	4.	2.	0.	2.	9.	6.	23.
1428.	16.	5.	21.	2.	0.	0.	1.	0.	3.	1.	5.	0.	15.	7.	0.	2.	4.	1.	0.	0.	0.
1423.	11.	7.	17.	0.	4.	3.	0.	1.	11.	5.	7.	0.	2.	2.	1.	6.	8.	5.	1.	2.	1.
1397.	1.	7.	2.	15.	15.	14.	2.	0.	6.	2.	0.	0.	0.	5.	2.	0.	2.	10.	1.	3.	14.
1378.	1.	2.	3.	2.	8.	6.	7.	6.	2.	1.	3.	0.	3.	9.	8.	21.	1.	0.	6.	0.	2.
1365.	0.	0.	0.	45.	3.	1.	2.	0.	0.	11.	4.	0.	6.	9.	1.	0.	3.	0.	4.	0.	0.
1352.	2.	9.	5.	9.	0.	0.	2.	2.	6.	21.	23.	1.	8.	0.	8.	2.	1.	0.	0.	0.	0.
1306.	4.	1.	13.	0.	2.	0.	0.	14.	0.	0.	23.	11.	3.	5.	6.	0.	6.	7.	2.	0.	0.
1295.	6.	0.	0.	6.	0.	18.	0.	0.	0.	3.	4.	0.	2.	3.	1.	5.	9.	10.	0.	17.	0.
1286.	38.	0.	2.	2.	0.	2.	0.	5.	1.	25.	0.	22.	4.	0.	1.	2.	0.	0.	0.	2.	0.
1263.	0.	0.	18.	1.	0.	1.	39.	22.	0.	0.	0.	0.	1.	2.	10.	0.	14.	1.	1.	2.	0.
1245.	0.	1.	7.	7.	5.	1.	24.	13.	1.	2.	2.	4.	1.	0.	6.	1.	0.	14.	6.	0.	1.
1226.	2.	0.	3.	0.	36.	23.	0.	9.	0.	2.	4.	0.	2.	3.	0.	5.	3.	1.	14.	5.	0.
1201.	4.	27.	2.	1.	0.	1.	4.	9.	32.	3.	3.	3.	10.	8.	3.	0.	1.	2.	0.	0.	0.
1164.	0.	5.	1.	0.	4.	1.	15.	18.	6.	1.	0.	0.	0.	1.	1.	7.	3.	1.	3.	9.	0.
1134.	0.	0.	0.	1.	0.	0.	1.	0.	0.	0.	1.	0.	0.	1.	0.	0.	0.	0.	0.	0.	0.
1109.	1.	2.	0.	0.	0.	8.	1.	2.	3.	0.	1.	0.	0.	0.	1.	1.	5.	1.	1.	2.	0.
1090.	0.	0.	1.	2.	5.	8.	4.	0.	1.	4.	0.	0.	0.	1.	0.	3.	0.	2.	9.	7.	0.
1067.	0.	2.	0.	0.	0.	0.	0.	2.	4.	11.	1.	6.	3.	2.	3.	0.	0.	0.	0.	0.	0.
1052.	4.	7.	1.	0.	0.	0.	0.	0.	16.	4.	12.	0.	2.	2.	1.	2.	0.	0.	3.	4.	1.
1030.	0.	1.	1.	0.	0.	1.	3.	0.	4.	1.	0.	1.	0.	0.	5.	6.	1.	0.	0.	1.	2.
988.	0.	0.	1.	4.	0.	0.	0.	0.	0.	2.	1.	1.	3.	5.	1.	4.	0.	9.	1.	0.	2.
957.	0.	0.	0.	1.	0.	1.	1.	2.	0.	1.	2.	1.	4.	1.	1.	0.	5.	4.	10.	7.	1.
902.	0.	0.	0.	0.	0.	0.	1.	0.	0.	0.	1.	1.	0.	0.	1.	2.	2.	3.	1.	2.	0.
859.	0.	0.	0.	0.	0.	1.	0.	0.	2.	0.	3.	15.	1.	1.	0.	0.	0.	1.	0.	0.	1.
757.	1.	0.	0.	2.	0.	0.	0.	0.	0.	0.	1.	0.	0.	0.	3.	1.	7.	6.	2.	1.	2.
677.	1.	0.	2.	0.	0.	0.	0.	0.	0.	0.	1.	7.	4.	1.	4.	4.	0.	0.	2.	0.	0.
589.	0.	0.	0.	1.	0.	0.	0.	0.	0.	0.	0.	3.	0.	0.	0.	1.	2.	0.	0.	0.	0.
520.	0.	0.	0.	0.	0.	0.	0.	0.	0.	0.	1.	0.	2.	0.	0.	0.	1.	0.	0.	0.	0.
507.	1.	0.	0.	0.	0.	1.	0.	0.	0.	1.	0.	1.	1.	1.	0.	0.	3.	3.	0.	2.	0.
444.	0.	0.	0.	0.	0.	0.	0.	0.	0.	1.	0.	0.	1.	0.	1.	0.	0.	1.	0.	1.	0.
436.	0.	0.	0.	0.	0.	0.	0.	0.	0.	0.	0.	1.	6.	7.	2.	0.	0.	0.	0.	1.	0.
390.	0.	0.	0.	0.	0.	1.	0.	0.	0.	0.	2.	0.	0.	0.	0.	1.	0.	0.	0.	0.	0.
365.	0.	0.	0.	0.	0.	0.	0.	0.	0.	0.	0.	0.	1.	1.	1.	1.	0.	1.	1.	0.	1.
358.	0.	0.	0.	0.	0.	0.	0.	0.	0.	0.	0.	1.	2.	1.	0.	0.	1.	1.	0.	0.	0.
343.	0.	0.	0.	0.	0.	0.	0.	0.	0.	0.	1.	0.	4.	0.	3.	2.	0.	1.	0.	0.	0.
331.	0.	0.	0.	0.	0.	0.	0.	0.	0.	0.	1.	4.	0.	7.	2.	0.	0.	0.	0.	0.	0.
284.	0.	0.	0.	0.	0.	0.	0.	0.	0.	0.	3.	1.	0.	1.	0.	3.	1.	0.	0.	0.	0.
276.	0.	0.	0.	0.	0.	1.	0.	0.	0.	1.	1.	3.	0.	1.	1.	2.	6.	0.	4.	0.	1.
261.	0.	0.	0.	0.	0.	0.	0.	0.	0.	0.	11.	18.	0.	1.	0.	1.	0.	0.	0.	0.	0.
245.	0.	0.	0.	1.	0.	1.	0.	0.	0.	0.	0.	1.	1.	2.	8.	3.	0.	3.	1.	1.	0.
137.	0.	0.	0.	0.	1.	0.	3.	0.	0.	0.	0.	0.	0.	1.	0.	0.	0.	0.	0.	0.	1.
127.	0.	0.	0.	0.	0.	0.	0.	0.	0.	0.	0.	1.	0.	0.	0.	0.	0.	0.	2.	0.	1.

TABLE LXIX (Continued)

CALCULATED INTERNAL COORDINATE DISTRIBUTIONS
ALPHA ARABINOSE

CONTRIBUTIONS FROM CC STRETCH

	C1C2	C2C3	C3C4	C4C5	C5O'	O'C1	C1O6	C2O7	C3O8	C4O9
1476.	2.	1.	0.	0.	0.	0.	0.	0.	1.	0.
1470.	2.	2.	0.	0.	0.	0.	0.	0.	0.	1.
1428.	0.	3.	1.	0.	0.	0.	0.	1.	0.	0.
1423.	1.	1.	0.	0.	1.	0.	0.	0.	0.	0.
1397.	0.	0.	1.	0.	1.	0.	0.	1.	0.	0.
1378.	0.	0.	0.	0.	0.	0.	0.	1.	0.	3.
1365.	0.	1.	5.	2.	0.	0.	0.	0.	0.	0.
1352.	0.	1.	0.	0.	0.	0.	0.	0.	0.	1.
1306.	1.	0.	0.	0.	0.	0.	0.	0.	0.	0.
1295.	0.	0.	3.	1.	0.	2.	1.	0.	0.	6.
1286.	0.	2.	0.	1.	2.	1.	1.	2.	0.	1.
1263.	0.	0.	1.	1.	0.	1.	1.	0.	0.	0.
1245.	1.	0.	0.	1.	1.	0.	1.	0.	0.	6.
1226.	0.	0.	0.	1.	3.	3.	0.	0.	0.	0.
1201.	1.	2.	1.	0.	0.	0.	0.	0.	0.	1.
1164.	0.	1.	14.	8.	8.	6.	0.	1.	1.	15.
1134.	2.	9.	3.	1.	1.	3.	29.	9.	43.	1.
1107.	0.	0.	4.	22.	22.	4.	1.	27.	4.	0.
1090.	0.	0.	1.	18.	2.	1.	2.	19.	2.	0.
1067.	26.	6.	0.	1.	7.	3.	33.	2.	30.	0.
1052.	4.	8.	0.	1.	4.	8.	20.	33.	0.	2.
1030.	2.	13.	3.	12.	13.	35.	1.	0.	0.	13.
988.	17.	33.	28.	6.	9.	0.	3.	0.	5.	4.
952.	23.	2.	28.	8.	0.	1.	1.	1.	12.	4.
902.	0.	7.	2.	6.	0.	15.	5.	0.	0.	47.
859.	17.	2.	1.	7.	36.	35.	3.	0.	2.	3.
757.	0.	6.	4.	1.	0.	0.	3.	4.	1.	5.
677.	3.	0.	2.	0.	1.	1.	0.	1.	1.	0.
589.	8.	12.	4.	1.	4.	3.	5.	4.	1.	0.
520.	8.	1.	1.	0.	4.	4.	1.	0.	0.	0.
507.	1.	0.	2.	2.	1.	3.	1.	1.	0.	0.
444.	2.	0.	3.	6.	1.	0.	0.	1.	2.	0.
436.	3.	6.	2.	0.	0.	0.	2.	0.	3.	0.
390.	0.	0.	1.	1.	2.	0.	0.	1.	0.	0.
365.	0.	1.	0.	1.	1.	1.	0.	0.	0.	0.
358.	0.	1.	3.	0.	0.	0.	0.	0.	0.	0.
343.	0.	2.	1.	0.	0.	0.	0.	0.	0.	0.
331.	4.	0.	1.	1.	0.	0.	0.	0.	0.	0.
284.	1.	3.	2.	2.	0.	1.	0.	1.	0.	0.
276.	1.	0.	0.	0.	1.	2.	0.	0.	0.	0.
261.	1.	0.	2.	0.	0.	8.	0.	0.	0.	0.
245.	0.	0.	1.	1.	0.	0.	0.	1.	1.	1.
137.	1.	0.	1.	0.	0.	0.	0.	0.	0.	0.
127.	0.	0.	0.	0.	0.	0.	1.	1.	1.	0.

CALCULATED INTERNAL COORDINATE DISTRIBUTIONS
ALPHA ARABINOSE

CONTRIBUTIONS FROM CCC AND CCO BEND

	CC2C	CC3C	CC4C	CC5O	COC	OC1C	OCO6	O6CC	CCO7	O7CC	CCO8	O8CC	CCO9	O9CC
1476.	1.	0.	0.	0.	0.	0.	0.	1.	0.	0.	1.	0.	1.	0.
1470.	1.	0.	0.	0.	0.	0.	0.	1.	0.	0.	0.	0.	0.	0.
1428.	0.	0.	0.	0.	0.	0.	0.	1.	0.	0.	2.	0.	1.	0.
1423.	0.	0.	0.	0.	0.	0.	0.	0.	0.	0.	1.	0.	0.	0.
1397.	0.	0.	0.	0.	0.	0.	0.	0.	0.	0.	0.	0.	1.	0.
1378.	0.	0.	1.	0.	0.	0.	0.	0.	0.	0.	0.	0.	0.	0.
1365.	0.	0.	0.	0.	0.	0.	0.	0.	0.	0.	0.	0.	0.	1.
1352.	0.	0.	0.	0.	0.	0.	0.	0.	0.	0.	0.	0.	0.	0.
1306.	0.	0.	0.	0.	0.	0.	0.	0.	0.	0.	0.	0.	0.	0.
1295.	0.	0.	1.	0.	0.	0.	0.	0.	0.	0.	0.	1.	0.	0.
1286.	0.	0.	0.	0.	0.	0.	0.	1.	1.	0.	0.	0.	0.	0.
1263.	0.	0.	0.	0.	0.	0.	0.	0.	0.	0.	0.	0.	1.	0.
1245.	0.	0.	0.	0.	0.	0.	0.	0.	0.	1.	0.	0.	1.	0.
1226.	0.	0.	0.	0.	0.	0.	0.	0.	0.	0.	0.	0.	0.	0.
1201.	0.	1.	0.	0.	0.	1.	0.	1.	0.	0.	0.	0.	0.	0.
1164.	0.	1.	4.	0.	0.	0.	0.	0.	0.	2.	0.	2.	0.	1.
1134.	2.	2.	3.	0.	1.	0.	1.	0.	0.	0.	1.	2.	0.	0.
1109.	0.	6.	1.	0.	1.	1.	1.	0.	1.	3.	0.	1.	0.	3.
1090.	1.	1.	0.	1.	3.	4.	0.	0.	2.	1.	0.	0.	1.	3.
1067.	1.	2.	1.	0.	0.	4.	0.	0.	3.	2.	3.	1.	0.	0.
1052.	9.	1.	0.	0.	1.	4.	1.	6.	2.	0.	2.	0.	0.	0.
1030.	1.	0.	1.	2.	2.	0.	2.	0.	0.	0.	1.	2.	0.	0.
988.	0.	0.	0.	4.	0.	1.	0.	0.	3.	1.	1.	0.	5.	0.
952.	0.	1.	1.	1.	0.	1.	0.	0.	3.	5.	1.	3.	0.	0.
902.	0.	0.	1.	1.	1.	0.	2.	1.	2.	5.	0.	2.	0.	3.
859.	1.	1.	0.	0.	9.	0.	22.	3.	2.	0.	1.	1.	0.	1.
757.	0.	5.	3.	21.	5.	0.	1.	2.	0.	0.	0.	1.	4.	5.
677.	0.	0.	1.	7.	2.	5.	0.	6.	3.	1.	11.	3.	8.	3.
589.	1.	2.	0.	1.	3.	0.	9.	0.	0.	1.	3.	5.	11.	2.
520.	1.	0.	2.	0.	1.	0.	13.	13.	11.	7.	11.	7.	5.	6.
507.	1.	0.	2.	0.	32.	9.	2.	4.	8.	2.	0.	0.	1.	20.
444.	0.	4.	18.	1.	0.	13.	7.	0.	0.	2.	2.	9.	0.	2.
436.	13.	5.	0.	2.	0.	6.	2.	2.	0.	6.	0.	0.	5.	4.
390.	15.	10.	1.	3.	19.	3.	2.	2.	8.	7.	3.	5.	0.	1.
365.	1.	0.	0.	3.	2.	0.	0.	0.	8.	2.	4.	2.	1.	2.
358.	1.	0.	1.	2.	1.	1.	0.	6.	1.	8.	0.	0.	0.	2.
343.	0.	0.	1.	0.	1.	0.	1.	3.	0.	3.	0.	0.	4.	1.
331.	0.	0.	1.	0.	2.	0.	1.	0.	0.	5.	5.	1.	4.	0.
284.	2.	0.	0.	1.	1.	0.	7.	14.	1.	2.	30.	12.	3.	0.
276.	0.	0.	10.	5.	14.	0.	1.	1.	2.	0.	4.	7.	0.	34.
261.	0.	0.	0.	0.	0.	3.	24.	19.	27.	16.	2.	0.	1.	1.
245.	1.	4.	15.	1.	1.	0.	0.	1.	0.	6.	0.	15.	35.	0.
137.	0.	12.	4.	5.	2.	3.	1.	0.	0.	0.	1.	2.	0.	1.
127.	13.	5.	0.	3.	0.	4.	2.	1.	3.	3.	2.	1.	1.	1.

TABLE LXX

CALCULATED INTERNAL COORDINATE DISTRIBUTIONS
ALPHA LYXOSE (O6 AND O7 AXIAL)

CONTRIBUTIONS FROM CH AND OH STR.

	CH15	CH16	CH17	CH18	CH19	CH20	OH11	OH12	OH13	OH14
3356.	0.	0.	0.	0.	0.	0.	0.	1.	9.	90.
3357.	0.	0.	0.	0.	0.	0.	97.	2.	0.	0.
3356.	0.	0.	0.	0.	0.	0.	1.	10.	79.	10.
3356.	0.	0.	0.	0.	0.	0.	2.	86.	12.	0.
2999.	49.	49.	0.	0.	0.	0.	0.	0.	0.	0.
2948.	0.	0.	48.	48.	2.	0.	0.	0.	0.	0.
2939.	0.	0.	3.	0.	93.	3.	0.	0.	0.	0.
2943.	0.	0.	0.	0.	3.	95.	0.	0.	0.	0.
2935.	0.	0.	47.	51.	1.	0.	0.	0.	0.	0.
2888.	51.	50.	0.	0.	0.	0.	0.	0.	0.	0.

CONTRIBUTIONS FROM TORSIONS

	TC12	TC23	TC34	TC45	TC50	TOC1	TCO6	TCO7	TCO8	TCO9
896.	0.	0.	0.	1.	3.	0.	0.	0.	0.	1.
879.	0.	0.	0.	0.	0.	1.	2.	1.	0.	0.
757.	0.	0.	0.	0.	0.	1.	0.	0.	0.	0.
658.	0.	0.	0.	1.	0.	1.	0.	0.	0.	0.
596.	0.	0.	0.	0.	6.	3.	2.	0.	0.	0.
529.	0.	0.	0.	0.	0.	0.	0.	0.	0.	0.
514.	0.	0.	0.	1.	4.	0.	0.	0.	2.	2.
461.	0.	0.	0.	0.	0.	0.	5.	1.	0.	0.
423.	0.	2.	0.	0.	1.	0.	4.	3.	4.	2.
393.	0.	0.	0.	0.	1.	3.	0.	5.	1.	15.
368.	0.	0.	0.	2.	2.	4.	8.	21.	22.	4.
357.	0.	0.	0.	0.	1.	0.	43.	5.	18.	8.
346.	2.	0.	0.	1.	0.	0.	12.	44.	9.	0.
337.	0.	0.	0.	0.	0.	1.	0.	2.	26.	50.
283.	0.	1.	1.	3.	5.	1.	5.	5.	3.	4.
265.	0.	0.	1.	0.	0.	0.	0.	1.	6.	5.
241.	1.	1.	3.	6.	0.	8.	9.	1.	0.	0.
209.	3.	1.	3.	1.	1.	0.	0.	3.	1.	0.
136.	23.	13.	0.	10.	2.	7.	0.	0.	0.	0.
126.	0.	16.	28.	7.	3.	8.	0.	0.	0.	0.

TABLE LXX (Continued)

CALCULATED INTERNAL COORDINATE DISTRIBUTIONS
ALPHA LYXOSE (O6 AND O7 AXIAL)

CONTRIBUTIONS FROM HCC,HCO,HCH BEND

	HO6C	HO7C	HO8C	HO9C	HC5O	HC5O	HC4O	HC3O	HC2O	HC1O	HCO'	HC1C	HC2C	HC2C	HC3C	HC3C	HC4C	HC4C	HC5C	HC5C	HC5H
1474.	0.	0.	0.	0.	0.	0.	0.	0.	0.	0.	0.	0.	0.	0.	0.	1.	2.	0.	17.	18.	49.
1440.	13.	20.	5.	5.	0.	0.	0.	0.	5.	5.	0.	7.	0.	7.	5.	8.	0.	1.	0.	1.	0.
1433.	15.	3.	19.	10.	0.	0.	0.	3.	0.	1.	1.	1.	6.	3.	1.	10.	0.	1.	0.	1.	0.
1403.	4.	8.	6.	22.	0.	1.	2.	0.	0.	0.	5.	2.	6.	8.	3.	3.	4.	0.	1.	0.	0.
1389.	2.	0.	7.	7.	20.	22.	3.	0.	0.	0.	5.	1.	0.	0.	0.	0.	3.	8.	3.	7.	10.
1379.	13.	8.	12.	0.	5.	1.	1.	5.	1.	15.	17.	1.	0.	1.	10.	1.	0.	1.	1.	1.	1.
1361.	0.	0.	1.	9.	12.	8.	2.	2.	0.	0.	0.	0.	0.	0.	2.	1.	17.	26.	11.	3.	1.
1339.	2.	11.	2.	10.	1.	0.	6.	0.	1.	1.	6.	0.	1.	3.	19.	8.	13.	2.	0.	0.	0.
1335.	7.	4.	15.	2.	1.	1.	2.	5.	1.	20.	16.	0.	7.	8.	0.	3.	2.	0.	0.	0.	0.
1319.	2.	18.	3.	0.	2.	0.	0.	0.	14.	6.	14.	22.	15.	0.	0.	0.	1.	1.	0.	0.	1.
1283.	21.	3.	0.	2.	0.	3.	2.	16.	7.	21.	1.	4.	3.	11.	0.	9.	1.	0.	0.	0.	0.
1262.	7.	10.	5.	6.	0.	4.	27.	8.	20.	1.	1.	3.	6.	0.	1.	0.	2.	9.	0.	1.	1.
1257.	5.	5.	1.	5.	10.	9.	25.	7.	12.	8.	0.	1.	8.	0.	0.	2.	5.	3.	3.	2.	0.
1233.	1.	0.	11.	11.	11.	10.	10.	28.	10.	0.	0.	0.	0.	3.	3.	7.	4.	1.	4.	5.	0.
1223.	0.	4.	8.	3.	12.	14.	11.	19.	19.	2.	4.	0.	1.	5.	5.	1.	1.	2.	6.	6.	0.
1134.	1.	0.	2.	4.	2.	3.	4.	10.	3.	0.	1.	1.	0.	3.	0.	0.	0.	2.	2.	3.	1.
1106.	0.	0.	0.	1.	0.	5.	5.	0.	1.	5.	0.	0.	1.	0.	5.	0.	0.	0.	1.	5.	0.
1102.	0.	0.	0.	0.	2.	2.	2.	1.	2.	1.	0.	1.	1.	1.	2.	2.	2.	0.	0.	0.	3.
1094.	1.	0.	0.	0.	0.	0.	0.	0.	0.	1.	0.	4.	1.	2.	0.	0.	0.	0.	0.	0.	0.
1068.	0.	0.	1.	0.	2.	2.	3.	0.	8.	3.	0.	8.	0.	1.	9.	7.	1.	0.	11.	11.	0.
1047.	0.	0.	0.	2.	1.	1.	0.	0.	1.	10.	0.	4.	5.	0.	0.	0.	3.	3.	3.	2.	1.
1037.	1.	2.	0.	0.	1.	2.	0.	1.	1.	1.	10.	0.	1.	0.	0.	1.	0.	0.	3.	3.	1.
1019.	0.	0.	0.	0.	0.	0.	2.	0.	0.	0.	4.	2.	7.	0.	6.	1.	0.	1.	5.	3.	3.
948.	3.	2.	0.	0.	1.	0.	0.	1.	1.	1.	13.	5.	0.	5.	0.	0.	6.	5.	6.	10.	1.
896.	2.	0.	2.	2.	0.	1.	0.	1.	0.	0.	6.	0.	1.	1.	3.	0.	0.	5.	1.	2.	0.
879.	0.	0.	0.	0.	0.	0.	0.	0.	0.	0.	3.	11.	2.	6.	0.	2.	1.	0.	0.	0.	0.
757.	0.	2.	0.	0.	0.	0.	0.	0.	0.	0.	2.	1.	2.	5.	0.	0.	0.	0.	1.	0.	0.
658.	0.	1.	1.	0.	0.	0.	0.	0.	0.	1.	1.	0.	2.	7.	1.	6.	0.	0.	0.	0.	0.
596.	0.	0.	0.	0.	0.	0.	0.	0.	1.	3.	0.	6.	3.	0.	1.	1.	0.	1.	3.	0.	1.
529.	1.	0.	0.	1.	0.	0.	0.	0.	0.	0.	1.	2.	2.	0.	0.	0.	0.	0.	0.	1.	2.
514.	0.	0.	0.	0.	0.	0.	0.	0.	0.	0.	0.	0.	0.	2.	0.	1.	5.	8.	0.	0.	0.
461.	0.	0.	0.	0.	0.	1.	0.	0.	0.	0.	0.	0.	0.	0.	0.	1.	0.	0.	0.	1.	0.
423.	0.	0.	0.	0.	0.	0.	0.	0.	0.	0.	1.	2.	0.	0.	0.	10.	6.	2.	0.	0.	0.
393.	0.	0.	1.	0.	0.	0.	0.	0.	0.	2.	0.	0.	0.	0.	0.	0.	0.	5.	5.	0.	0.
368.	0.	0.	0.	0.	0.	0.	0.	0.	0.	1.	0.	1.	1.	1.	0.	0.	0.	0.	2.	0.	0.
357.	0.	0.	0.	0.	0.	1.	0.	0.	0.	0.	1.	2.	0.	0.	1.	0.	0.	1.	0.	0.	0.
346.	0.	0.	0.	0.	0.	0.	0.	0.	0.	0.	1.	1.	2.	2.	2.	0.	1.	0.	0.	0.	0.
337.	0.	0.	0.	0.	0.	0.	0.	0.	0.	0.	0.	0.	0.	0.	1.	3.	5.	0.	1.	0.	0.
283.	0.	0.	0.	0.	0.	0.	0.	0.	0.	2.	6.	1.	0.	0.	3.	0.	1.	1.	1.	1.	0.
265.	0.	0.	0.	0.	0.	1.	0.	0.	0.	1.	1.	0.	0.	3.	1.	3.	2.	1.	1.	1.	0.
241..	0.	0.	0.	0.	0.	2.	0.	0.	0.	1.	5.	19.	1.	3.	0.	0.	0.	0.	1.	0.	1.
209.	1.	1.	0.	0.	0.	1.	0.	0.	0.	3.	13.	2.	7.	0.	4.	1.	2.	0.	0.	0.	0.
136.	0.	0.	0.	0.	0.	0.	0.	0.	4.	7.	1.	0.	0.	0.	2.	0.	0.	0.	2.	0.	0.
126.	0.	0.	0.	0.	0.	0.	0.	0.	1.	1.	2.	0.	0.	0.	0.	0.	0.	0.	0.	0.	0.

TABLE LXX (Continued)

CALCULATED INTERNAL COORDINATE DISTRIBUTIONS
ALPHA LYXOSE (O6 AND O7 AXIAL)

CONTRIBUTIONS FROM CC STRETCH

	C1C2	C2C3	C3C4	C4C5	C5O'	O'C1	C1O6	C2O7	C3O8	C4O9
1474.	0.	0.	1.	0.	1.	0.	0.	0.	0.	1.
1440.	5.	1.	0.	0.	0.	0.	0.	1.	0.	0.
1433.	2.	5.	0.	0.	0.	1.	0.	1.	0.	0.
1403.	0.	0.	6.	0.	0.	0.	0.	0.	0.	0.
1389.	0.	1.	1.	0.	0.	1.	0.	0.	0.	0.
1379.	0.	2.	0.	0.	1.	0.	0.	5.	0.	0.
1361.	0.	0.	0.	3.	2.	0.	0.	0.	0.	1.
1339.	2.	0.	1.	1.	1.	1.	0.	2.	0.	0.
1335.	0.	0.	0.	0.	1.	2.	0.	1.	0.	0.
1319.	0.	0.	0.	0.	2.	0.	0.	1.	0.	0.
1283.	0.	2.	1.	0.	0.	0.	0.	0.	1.	1.
1262.	0.	0.	1.	1.	0.	0.	1.	0.	1.	0.
1257.	0.	1.	1.	1.	2.	3.	1.	1.	0.	0.
1233.	0.	0.	0.	0.	0.	1.	0.	1.	0.	1.
1223.	0.	0.	0.	0.	0.	0.	0.	1.	0.	0.
1134.	1.	15.	8.	7.	1.	2.	1.	23.	10.	4.
1106.	2.	4.	1.	20.	16.	5.	0.	2.	26.	7.
1102.	1.	2.	8.	11.	7.	8.	5.	1.	7.	49.
1094.	2.	0.	1.	2.	7.	9.	1.	0.	40.	25.
1068.	13.	9.	11.	2.	0.	1.	28.	8.	0.	0.
1047.	20.	8.	13.	32.	3.	2.	21.	7.	6.	1.
1037.	6.	3.	0.	1.	0.	2.	45.	21.	1.	2.
1019.	0.	14.	8.	2.	35.	3.	1.	1.	0.	1.
948.	30.	0.	15.	6.	5.	6.	1.	4.	1.	0.
896.	5.	12.	9.	5.	2.	3.	2.	24.	1.	0.
879.	7.	18.	5.	1.	18.	51.	0.	0.	4.	2.
757.	5.	6.	2.	0.	5.	36.	2.	1.	2.	4.
658.	1.	0.	26.	1.	0.	1.	0.	2.	1.	2.
596.	8.	0.	1.	0.	0.	0.	2.	0.	1.	1.
529.	0.	6.	0.	1.	2.	0.	0.	1.	0.	5.
514.	4.	3.	4.	12.	3.	0.	0.	2.	3.	1.
461.	1.	1.	0.	3.	2.	0.	2.	2.	1.	0.
423.	0.	0.	0.	1.	2.	1.	1.	0.	0.	2.
393.	5.	2.	0.	0.	3.	0.	1.	0.	1.	0.
368.	2.	1.	1.	0.	0.	0.	0.	0.	0.	0.
357.	1.	0.	1.	0.	1.	0.	0.	0.	0.	0.
346.	1.	2.	0.	0.	0.	0.	0.	0.	0.	1.
337.	0.	0.	0.	0.	1.	0.	0.	0.	0.	0.
283.	0.	4.	0.	0.	0.	2.	1.	0.	0.	0.
265.	1.	1.	0.	2.	2.	1.	0.	0.	0.	0.
241.	3.	0.	0.	0.	2.	4.	3.	0.	0.	1.
209.	2.	1.	0.	0.	0.	5.	1.	3.	1.	0.
136.	1.	0.	0.	0.	0.	1.	0.	0.	1.	0.
126.	0.	0.	0.	0.	0.	1.	0.	0.	1.	1.

CALCULATED INTERNAL COORDINATE DISTRIBUTIONS
ALPHA LYXOSE (O6 AND O7 AXIAL)

CONTRIBUTIONS FROM CCC AND CCO BEND

	CC2C	CC3C	CC4C	CC5O	COC	OC1C	OC06	O6CC	CCO7	O7CC	CCO8	O8CC	CCO9	O9CC
1474.	0.	0.	0.	0.	0.	0.	0.	0.	0.	0.	0.	0.	0.	1.
1440.	0.	0.	0.	0.	0.	0.	0.	1.	2.	0.	1.	0.	1.	0.
1433.	0.	0.	0.	0.	0.	0.	0.	1.	0.	0.	1.	0.	2.	0.
1403.	1.	1.	0.	0.	0.	0.	0.	0.	0.	0.	1.	1.	1.	0.
1389.	0.	0.	0.	0.	0.	0.	0.	0.	0.	0.	0.	0.	0.	1.
1379.	1.	0.	0.	0.	0.	0.	0.	0.	1.	0.	0.	0.	0.	0.
1361.	0.	0.	0.	0.	0.	0.	0.	0.	0.	0.	0.	1.	0.	0.
1339.	1.	0.	0.	0.	0.	0.	0.	0.	0.	1.	0.	0.	0.	0.
1335.	0.	0.	0.	0.	0.	0.	0.	1.	0.	0.	0.	0.	0.	0.
1319.	0.	0.	0.	0.	0.	0.	0.	0.	0.	0.	0.	0.	0.	0.
1283.	0.	1.	1.	0.	0.	0.	0.	0.	0.	0.	0.	1.	0.	0.
1262.	0.	0.	0.	1.	0.	0.	0.	0.	0.	0.	0.	0.	0.	0.
1257.	0.	0.	0.	0.	0.	0.	0.	0.	0.	0.	0.	0.	0.	0.
1233.	0.	0.	0.	0.	0.	0.	0.	0.	0.	0.	0.	0.	0.	0.
1223.	0.	0.	0.	0.	0.	0.	0.	0.	0.	0.	0.	0.	0.	0.
1134.	1.	2.	1.	0.	0.	0.	0.	1.	0.	1.	1.	1.	1.	1.
1106.	1.	0.	4.	1.	1.	2.	1.	0.	0.	3.	1.	5.	0.	2.
1102.	2.	1.	2.	2.	1.	2.	0.	0.	0.	0.	1.	1.	2.	2.
1094.	4.	6.	5.	1.	1.	4.	1.	0.	0.	0.	1.	3.	3.	0.
1068.	4.	0.	1.	0.	0.	1.	3.	1.	1.	0.	2.	1.	0.	0.
1047.	1.	0.	0.	3.	1.	3.	1.	0.	0.	4.	0.	0.	0.	4.
1037.	0.	0.	0.	0.	5.	0.	4.	2.	3.	3.	1.	0.	0.	1.
1019.	2.	1.	0.	6.	0.	1.	0.	0.	0.	2.	2.	3.	0.	5.
948.	0.	4.	0.	1.	0.	0.	0.	6.	4.	1.	1.	1.	1.	2.
896.	1.	1.	0.	0.	3.	0.	0.	5.	4.	0.	4.	0.	7.	1.
879.	0.	0.	1.	1.	0.	3.	4.	1.	2.	1.	1.	1.	0.	1.
757.	3.	3.	0.	0.	14.	5.	0.	0.	4.	0.	0.	1.	0.	1.
658.	0.	4.	0.	2.	8.	2.	2.	1.	1.	20.	8.	0.	0.	0.
596.	0.	0.	0.	5.	1.	10.	35.	1.	6.	2.	3.	2.	0.	0.
529.	3.	0.	8.	21.	6.	0.	1.	10.	2.	2.	4.	6.	5.	1.
514.	0.	1.	6.	0.	2.	0.	0.	3.	1.	4.	0.	0.	1.	9.
461.	7.	3.	2.	0.	5.	5.	2.	14.	17.	2.	1.	11.	11.	3.
423.	1.	1.	9.	3.	3.	1.	6.	8.	3.	1.	2.	23.	12.	3.
393.	2.	8.	6.	3.	0.	5.	2.	0.	0.	0.	12.	2.	0.	21.
368.	2.	1.	3.	1.	2.	0.	0.	0.	1.	5.	2.	0.	9.	0.
357.	0.	0.	1.	1.	7.	0.	0.	0.	0.	0.	3.	0.	3.	1.
346.	0.	5.	2.	0.	4.	1.	0.	3.	1.	0.	0.	0.	3.	1.
337.	0.	0.	0.	0.	0.	1.	0.	0.	0.	1.	4.	0.	0.	4.
283.	0.	0.	3.	0.	7.	2.	4.	13.	12.	10.	4.	3.	8.	2.
265.	1.	0.	0.	1.	1.	0.	1.	2.	3.	2.	28.	22.	17.	18.
241.	1.	2.	0.	2.	22.	11.	38.	0.	20.	5.	0.	0.	0.	1.
209.	18.	5.	0.	0.	4.	13.	2.	30.	9.	26.	1.	1.	1.	1.
136.	15.	2.	3.	4.	2.	6.	0.	0.	0.	3.	1.	3.	1.	2.
126.	1.	12.	7.	0.	6.	0.	2.	2.	0.	0.	2.	2.	2.	4.

TABLE LXXI

CALCULATED INTERNAL COORDINATE DISTRIBUTIONS
ALPHA LYXOSE (O8 AND O9 AXIAL)

CONTRIBUTIONS FROM CH AND OH STR.

	CH15	CH16	CH17	CH18	CH19	CH20	OH11	OH12	OH13	OH14
3357.	0.	0.	0.	0.	0.	0.	***	0.	0.	0.
3356.	0.	0.	0.	0.	0.	0.	0.	26.	58.	16.
3356.	0.	0.	0.	0.	0.	0.	0.	10.	7.	83.
3356.	0.	0.	0.	0.	0.	0.	0.	64.	35.	1.
3000.	50.	48.	0.	0.	0.	0.	0.	0.	0.	0.
2950.	0.	0.	0.	1.	45.	51.	0.	0.	0.	0.
2939.	0.	0.	56.	43.	0.	0.	0.	0.	0.	0.
2938.	0.	0.	43.	54.	0.	2.	0.	0.	0.	0.
2935.	0.	0.	0.	1.	53.	45.	0.	0.	0.	0.
2888.	49.	51.	0.	0.	0.	0.	0.	0.	0.	0.

CONTRIBUTIONS FROM TORSIONS

	TC12	TC23	TC34	TC45	TC50	TOC1	TCO6	TCO7	TCO8	TCO9
887.	0.	0.	0.	0.	0.	1.	1.	0.	0.	0.
850.	0.	0.	0.	0.	0.	0.	2.	0.	0.	0.
767.	0.	0.	0.	0.	0.	1.	0.	0.	0.	0.
640.	0.	0.	0.	0.	0.	1.	0.	0.	0.	0.
587.	0.	1.	0.	0.	1.	1.	6.	0.	0.	0.
547.	0.	0.	0.	3.	12.	1.	0.	0.	0.	1.
511.	0.	0.	0.	1.	0.	1.	0.	1.	0.	0.
480.	0.	1.	0.	0.	0.	0.	1.	1.	0.	0.
445.	0.	1.	0.	0.	0.	1.	0.	1.	7.	4.
404.	1.	0.	0.	4.	6.	2.	10.	3.	0.	0.
372.	0.	0.	0.	2.	3.	5.	14.	26.	13.	6.
358.	0.	0.	0.	0.	0.	0.	5.	11.	12.	44.
342.	0.	2.	0.	0.	0.	2.	6.	1.	45.	17.
337.	0.	0.	0.	0.	0.	0.	34.	41.	2.	3.
295.	3.	0.	0.	0.	2.	7.	4.	0.	7.	10.
257.	0.	0.	0.	0.	0.	1.	7.	4.	1.	0.
254.	0.	1.	3.	0.	0.	4.	3.	2.	2.	5.
211.	6.	1.	2.	1.	1.	0.	0.	1.	2.	0.
139.	0.	7.	23.	13.	1.	10.	0.	0.	0.	0.
125.	24.	22.	1.	5.	3.	4.	0.	0.	0.	0.

TABLE LXXI (Continued)

CALCULATED INTERNAL COORDINATE DISTRIBUTIONS
ALPHA LYXOSE (O8 AND O9 AXIAL)

CONTRIBUTIONS FROM HCC,HCO,HCH BEND

	H06C	H07C	H08C	H09C	H15O	H16O	HC4O	HC3O	HC2O	HC1O	HCO'	HC1C	HC2C	HC2C	HC3C	HC3C	HC4C	HC4C	H15C	H16C	HC5H
1479.	1.	1.	1.	5.	0.	0.	1.	0.	0.	0.	0.	0.	1.	0.	1.	4.	1.	4.	15.	12.	39.
1450.	24.	13.	0.	0.	0.	0.	0.	0.	1.	2.	2.	3.	18.	3.	2.	1.	0.	0.	1.	2.	3.
1418.	7.	6.	5.	6.	6.	8.	0.	2.	0.	4.	3.	0.	0.	0.	6.	12.	6.	7.	0.	0.	15.
1412.	4.	18.	19.	2.	3.	4.	0.	0.	3.	3.	0.	1.	0.	1.	2.	0.	6.	3.	0.	1.	2.
1386.	6.	4.	6.	35.	4.	2.	6.	1.	0.	7.	2.	1.	2.	3.	2.	0.	4.	1.	1.	0.	6.
1375.	0.	0.	18.	0.	5.	7.	4.	9.	3.	11.	18.	1.	3.	11.	0.	5.	0.	0.	3.	4.	0.
1366.	1.	10.	3.	14.	8.	10.	0.	0.	5.	7.	4.	0.	2.	11.	1.	2.	1.	1.	3.	8.	0.
1343.	0.	6.	15.	0.	0.	0.	0.	2.	0.	1.	28.	14.	1.	7.	9.	1.	6.	2.	0.	0.	0.
1314.	7.	7.	5.	3.	1.	1.	10.	0.	9.	0.	7.	6.	11.	2.	9.	9.	3.	0.	0.	0.	0.
1297.	7.	0.	5.	3.	6.	1.	0.	7.	3.	12.	4.	1.	0.	2.	7.	2.	11.	12.	1.	2.	0.
1286.	27.	2.	4.	3.	2.	2.	2.	3.	1.	24.	0.	19.	0.	0.	0.	1.	8.	3.	1.	2.	0.
1273.	3.	3.	6.	4.	5.	0.	10.	33.	10.	0.	1.	1.	4.	0.	4.	4.	0.	3.	10.	2.	0.
1243.	3.	8.	0.	1.	18.	24.	0.	0.	20.	1.	0.	0.	8.	0.	0.	1.	0.	0.	11.	15.	0.
1240.	0.	0.	1.	17.	5.	0.	56.	10.	1.	4.	0.	2.	0.	0.	0.	10.	6.	8.	3.	0.	0.
1216.	1.	17.	3.	1.	3.	7.	5.	18.	33.	0.	1.	0.	3.	11.	6.	0.	0.	3.	1.	4.	0.
1162.	1.	0.	3.	0.	4.	14.	3.	3.	1.	0.	2.	0.	0.	0.	0.	3.	1.	3.	13.	2.	0.
1125.	4.	2.	0.	0.	1.	0.	0.	10.	12.	1.	8.	2.	1.	2.	4.	0.	2.	0.	0.	1.	0.
1109.	0.	0.	1.	0.	7.	1.	0.	5.	0.	0.	1.	2.	1.	0.	0.	1.	3.	1.	0.	1.	0.
1087.	0.	0.	1.	2.	6.	2.	3.	1.	1.	6.	3.	2.	1.	5.	2.	0.	3.	5.	1.	4.	0.
1075.	1.	0.	0.	0.	0.	0.	1.	0.	1.	9.	4.	1.	0.	1.	3.	0.	4.	0.	0.	0.	0.
1060.	2.	2.	0.	0.	4.	0.	0.	1.	1.	0.	5.	1.	3.	1.	0.	1.	0.	1.	1.	0.	3.
1001.	0.	0.	0.	0.	0.	0.	4.	3.	0.	6.	1.	0.	2.	7.	1.	0.	1.	0.	7.	10.	0.
982.	0.	1.	3.	2.	0.	0.	0.	0.	0.	1.	1.	3.	2.	4.	6.	11.	1.	13.	0.	0.	1.
961.	0.	1.	0.	2.	0.	1.	1.	0.	0.	0.	0.	1.	1.	2.	4.	0.	5.	2.	7.	4.	1.
887.	1.	1.	1.	0.	0.	0.	0.	0.	1.	0.	4.	3.	0.	0.	0.	4.	1.	0.	1.	2.	0.
850.	0.	1.	0.	0.	1.	0.	0.	0.	1.	1.	1.	13.	2.	0.	0.	0.	1.	2.	0.	0.	1.
767.	0.	0.	0.	1.	0.	0.	0.	0.	0.	0.	0.	0.	0.	0.	3.	2.	4.	7.	1.	4.	2.
640.	0.	1.	3.	0.	0.	0.	0.	0.	0.	0.	0.	0.	4.	1.	6.	3.	1.	0.	0.	0.	0.
587.	0.	0.	0.	0.	0.	0.	0.	0.	0.	0.	0.	12.	3.	0.	2.	0.	0.	0.	0.	0.	0.
547.	0.	1.	0.	0.	0.	0.	0.	0.	0.	0.	0.	1.	4.	1.	0.	5.	0.	0.	0.	0.	0.
511.	0.	0.	0.	1.	1.	0.	0.	0.	0.	1.	0.	0.	0.	0.	0.	0.	4.	4.	1.	1.	0.
480.	1.	0.	0.	0.	0.	0.	0.	0.	0.	0.	1.	0.	5.	0.	0.	0.	0.	0.	0.	1.	0.
445.	0.	0.	0.	0.	0.	0.	0.	0.	0.	1.	0.	0.	2.	1.	0.	0.	0.	0.	2.	0.	0.
404.	0.	0.	0.	0.	1.	0.	1.	0.	0.	0.	2.	0.	1.	0.	0.	0.	0.	0.	0.	0.	0.
372.	0.	0.	0.	0.	0.	0.	0.	0.	0.	0.	0.	0.	1.	0.	1.	1.	0.	0.	0.	1.	0.
358.	0.	0.	0.	0.	0.	0.	0.	0.	0.	0.	0.	0.	0.	1.	0.	1.	2.	1.	0.	0.	0.
342.	0.	0.	0.	0.	0.	0.	0.	0.	0.	0.	0.	0.	0.	0.	2.	2.	1.	2.	0.	1.	0.
337.	0.	0.	0.	0.	0.	0.	0.	0.	0.	0.	2.	4.	2.	3.	1.	0.	0.	0.	0.	0.	0.
295.	0.	0.	0.	0.	0.	0.	0.	0.	0.	0.	2.	3.	1.	1.	1.	0.	0.	0.	0.	2.	1.
257.	0.	0.	0.	0.	0.	0.	0.	0.	0.	0.	11.	12.	3.	0.	2.	1.	1.	0.	0.	0.	0.
254.	0.	0.	0.	0.	0.	0.	0.	0.	0.	0.	2.	4.	0.	3.	0.	2.	5.	0.	0.	1.	1.
211.	0.	0.	1.	1.	1.	0.	1.	0.	0.	0.	0.	3.	0.	4.	3.	2.	1.	1.	0.	1.	0.
139.	0.	0.	0.	0.	0.	1.	4.	4.	0.	0.	0.	0.	0.	1.	0.	0.	0.	0.	0.	0.	1.
125.	0.	0.	0.	0.	0.	0.	0.	1.	0.	0.	0.	1.	0.	0.	0.	0.	0.	0.	0.	2.	1.

TABLE LXXI (Continued)

CALCULATED INTERNAL COORDINATE DISTRIBUTIONS
ALPHA LYXOSE (O8 AND O9 AXIAL)

CONTRIBUTIONS FROM CC STRETCH

	C1C2	C2C3	C3C4	C4C5	C5O'	O'C1	C1O6	C2O7	C3O8	C4O9
1479.	0.	0.	0.	0.	0.	0.	0.	0.	0.	1.
1450.	1.	1.	0.	0.	0.	0.	1.	0.	0.	0.
1418.	2.	0.	0.	0.	0.	0.	0.	0.	0.	0.
1412.	3.	8.	1.	1.	0.	0.	0.	0.	0.	0.
1386.	1.	1.	4.	0.	0.	0.	0.	0.	0.	0.
1375.	0.	1.	0.	1.	0.	0.	0.	1.	3.	0.
1366.	0.	0.	2.	5.	1.	0.	0.	1.	1.	0.
1343.	2.	1.	0.	0.	0.	0.	0.	0.	4.	0.
1314.	0.	1.	0.	0.	0.	1.	1.	1.	2.	0.
1297.	1.	0.	0.	1.	3.	2.	0.	0.	0.	1.
1286.	0.	1.	0.	0.	0.	0.	1.	2.	0.	0.
1273.	1.	0.	3.	0.	1.	1.	1.	0.	0.	3.
1243.	0.	0.	1.	0.	0.	2.	1.	0.	0.	5.
1240.	0.	1.	0.	0.	0.	0.	0.	0.	0.	1.
1216.	0.	0.	0.	0.	0.	0.	0.	0.	3.	1.
1162.	0.	1.	8.	10.	10.	6.	0.	0.	0.	29.
1125.	5.	17.	8.	5.	3.	3.	2.	9.	30.	0.
1109.	3.	0.	2.	3.	1.	5.	33.	39.	1.	0.
1087.	6.	1.	2.	28.	7.	2.	1.	4.	1.	2.
1075.	1.	3.	2.	0.	6.	1.	51.	31.	0.	3.
1060.	14.	1.	1.	1.	37.	24.	0.	6.	5.	13.
1001.	6.	1.	15.	5.	0.	14.	0.	0.	17.	11.
982.	17.	37.	28.	1.	1.	2.	0.	1.	1.	11.
961.	0.	0.	16.	10.	1.	4.	2.	2.	27.	12.
887.	5.	17.	0.	10.	6.	34.	3.	0.	8.	6.
850.	26.	1.	2.	18.	30.	14.	0.	0.	1.	4.
767.	1.	6.	1.	5.	1.	1.	7.	5.	0.	2.
640.	19.	0.	2.	2.	2.	3.	3.	1.	2.	0.
587.	11.	7.	2.	0.	4.	2.	3.	4.	1.	0.
547.	0.	2.	5.	0.	1.	1.	0.	1.	0.	2.
511.	1.	1.	2.	5.	0.	1.	1.	1.	1.	0.
480.	0.	4.	2.	0.	4.	3.	0.	0.	0.	1.
445.	0.	0.	1.	0.	0.	0.	1.	1.	2.	2.
404.	1.	1.	5.	0.	3.	0.	0.	1.	0.	0.
372.	1.	1.	1.	1.	0.	1.	0.	0.	0.	0.
358.	1.	0.	2.	1.	0.	0.	0.	0.	0.	0.
342.	0.	1.	0.	1.	0.	0.	0.	0.	0.	0.
337.	0.	2.	0.	0.	0.	0.	0.	0.	0.	0.
295.	0.	1.	1.	0.	0.	1.	0.	0.	0.	0.
257.	1.	1.	2.	0.	0.	8.	0.	0.	0.	0.
254.	0.	2.	1.	0.	1.	1.	1.	0.	0.	1.
211.	0.	2.	0.	0.	0.	1.	0.	1.	2.	2.
139.	0.	0.	1.	0.	0.	0.	0.	0.	0.	0.
125.	0.	0.	0.	0.	0.	0.	1.	1.	0.	0.

CALCULATED INTERNAL COORDINATE DISTRIBUTIONS
ALPHA LYXOSE (O8 AND O9 AXIAL)

CONTRIBUTIONS FROM CCC AND CCO BEND

	CC2C	CO3C	CC4C	CC5O	COC	OC1C	OCO6	O6CC	CCO7	O7CC	CCO8	O8CC	CCO9	O9CC
1479.	0.	0.	0.	0.	0.	0.	0.	0.	0.	0.	0.	0.	1.	0.
1450.	1.	0.	0.	0.	0.	1.	0.	3.	0.	1.	0.	0.	0.	0.
1418.	0.	0.	0.	0.	0.	0.	0.	0.	0.	1.	0.	0.	0.	0.
1412.	0.	1.	0.	0.	0.	0.	0.	0.	1.	1.	1.	1.	0.	0.
1386.	0.	0.	0.	0.	0.	0.	0.	0.	0.	0.	0.	1.	1.	0.
1375.	0.	1.	0.	0.	0.	0.	0.	0.	0.	0.	1.	0.	0.	0.
1366.	0.	1.	0.	0.	0.	0.	0.	0.	0.	0.	0.	0.	0.	0.
1343.	1.	0.	0.	0.	0.	0.	0.	0.	0.	0.	1.	0.	0.	0.
1314.	0.	0.	0.	0.	0.	0.	0.	0.	0.	0.	0.	0.	0.	0.
1297.	0.	0.	1.	0.	0.	0.	0.	0.	0.	0.	0.	0.	0.	0.
1286.	0.	0.	0.	0.	0.	0.	0.	0.	1.	0.	0.	0.	0.	0.
1273.	0.	0.	1.	0.	0.	0.	0.	0.	0.	0.	0.	0.	0.	0.
1243.	0.	0.	0.	0.	0.	0.	0.	0.	0.	0.	0.	0.	0.	0.
1240.	0.	0.	0.	0.	0.	0.	0.	0.	0.	0.	0.	0.	0.	0.
1216.	0.	0.	0.	0.	0.	0.	0.	0.	0.	0.	0.	0.	0.	0.
1162.	0.	0.	6.	0.	0.	0.	0.	0.	0.	0.	0.	0.	0.	2.
1125.	2.	3.	0.	0.	1.	1.	0.	2.	0.	1.	1.	1.	0.	1.
1109.	0.	4.	0.	0.	3.	0.	2.	1.	0.	3.	1.	0.	0.	1.
1087.	1.	0.	1.	0.	1.	3.	0.	0.	4.	0.	2.	1.	2.	3.
1075.	7.	2.	0.	1.	3.	9.	1.	3.	5.	1.	0.	0.	0.	1.
1060.	3.	2.	0.	4.	0.	1.	0.	1.	0.	2.	0.	1.	1.	1.
1001.	1.	1.	1.	0.	3.	2.	1.	0.	4.	1.	0.	0.	0.	0.
982.	0.	2.	2.	3.	0.	0.	0.	0.	1.	0.	5.	7.	4.	1.
961.	0.	1.	1.	1.	0.	0.	1.	1.	0.	1.	0.	3.	3.	1.
887.	0.	0.	0.	0.	4.	0.	7.	6.	2.	3.	1.	2.	1.	1.
850.	0.	0.	1.	0.	5.	0.	15.	1.	0.	2.	0.	2.	1.	2.
767.	2.	4.	8.	24.	3.	2.	0.	1.	1.	0.	0.	2.	0.	4.
640.	4.	0.	2.	4.	3.	0.	1.	0.	1.	7.	20.	1.	2.	3.
587.	2.	0.	0.	0.	1.	2.	13.	0.	1.	0.	3.	0.	0.	0.
547.	1.	5.	8.	2.	0.	1.	1.	1.	5.	6.	5.	7.	5.	17.
511.	0.	6.	0.	1.	30.	15.	6.	1.	2.	0.	0.	1.	10.	5.
480.	0.	2.	1.	1.	2.	0.	9.	25.	26.	5.	2.	7.	1.	2.
445.	8.	3.	2.	2.	1.	9.	2.	0.	0.	1.	1.	15.	20.	10.
404.	7.	2.	6.	1.	19.	4.	7.	1.	7.	4.	0.	0.	0.	3.
372.	0.	0.	1.	0.	4.	2.	0.	8.	1.	1.	3.	2.	0.	0.
358.	1.	0.	0.	2.	1.	1.	0.	2.	0.	5.	0.	0.	2.	1.
342.	1.	0.	2.	2.	3.	1.	0.	0.	0.	2.	0.	0.	7.	0.
337.	0.	0.	1.	0.	0.	0.	3.	0.	1.	1.	1.	0.	4.	0.
295.	1.	0.	0.	3.	6.	0.	2.	3.	0.	13.	3.	9.	7.	12.
257.	1.	2.	0.	0.	0.	1.	21.	23.	22.	24.	7.	2.	0.	1.
254.	4.	0.	4.	4.	3.	2.	5.	4.	3.	0.	21.	10.	0.	18.
211.	2.	16.	17.	0.	4.	0.	1.	0.	3.	0.	13.	20.	22.	3.
139.	1.	14.	6.	4.	3.	2.	0.	0.	1.	0.	3.	1.	0.	0.
125.	15.	1.	0.	4.	0.	4.	2.	1.	3.	3.	0.	0.	0.	2.

TABLE LXXII

CALCULATED INTERNAL COORDINATE DISTRIBUTIONS
BETA XYLOSE

CONTRIBUTIONS FROM CH AND OH STR.

	CH15	CH16	CH17	CH18	CH19	CH20	OH11	OH12	OH13	OH14
3357.	0.	0.	0.	0.	0.	0.	98.	2.	0.	0.
3356.	0.	0.	0.	0.	0.	0.	0.	21.	73.	5.
3356.	0.	0.	0.	0.	0.	0.	0.	2.	3.	94.
3356.	0.	0.	0.	0.	0.	0.	2.	74.	24.	0.
3000.	48.	49.	1.	0.	0.	0.	0.	0.	0.	0.
2955.	0.	0.	9.	31.	41.	16.	0.	0.	0.	0.
2938.	0.	0.	36.	12.	14.	37.	0.	0.	0.	0.
2947.	0.	0.	36.	20.	11.	30.	0.	0.	0.	0.
2933.	0.	0.	16.	36.	32.	15.	0.	0.	0.	0.
2888.	51.	50.	0.	0.	0.	0.	0.	0.	0.	0.

CONTRIBUTIONS FROM TORSIONS

	T1-2	T2-3	T3-4	T4-5	T510	T101	T1-6	T2-7	T3-8	T4-9
933.	0.	0.	0.	1.	5.	0.	0.	0.	1.	1.
883.	0.	0.	0.	0.	0.	1.	3.	0.	0.	0.
682.	0.	0.	0.	0.	0.	0.	1.	2.	0.	0.
634.	0.	0.	0.	0.	0.	2.	0.	0.	0.	1.
553.	0.	1.	0.	0.	3.	0.	6.	0.	1.	0.
543.	0.	1.	0.	1.	7.	1.	0.	1.	1.	1.
510.	0.	0.	0.	0.	0.	0.	0.	0.	1.	0.
416.	0.	0.	1.	0.	1.	3.	3.	0.	4.	4.
394.	0.	0.	0.	0.	0.	0.	0.	0.	9.	8.
386.	0.	0.	0.	1.	5.	2.	13.	1.	7.	2.
370.	2.	0.	1.	5.	5.	8.	1.	0.	0.	23.
362.	0.	0.	0.	0.	1.	1.	40.	5.	13.	5.
351.	0.	1.	0.	2.	1.	3.	6.	53.	4.	6.
339.	0.	1.	0.	1.	1.	3.	0.	18.	37.	19.
304.	1.	0.	2.	0.	0.	1.	2.	1.	1.	17.
281.	2.	0.	0.	1.	0.	1.	11.	4.	5.	0.
268.	0.	0.	1.	0.	0.	0.	2.	4.	3.	4.
256.	0.	1.	0.	0.	0.	0.	7.	5.	4.	2.
140.	13.	0.	17.	18.	0.	16.	0.	0.	0.	0.
128.	15.	31.	13.	0.	3.	0.	0.	0.	0.	0.

TABLE LXXII (Continued)

CALCULATED INTERNAL COORDINATE DISTRIBUTIONS
BETA XYLOSE

CONTRIBUTIONS FROM HCC,HCO,HCH BEND

	HO6C	HO7C	HO8C	HO9C	15C'	16C'	HC4O	HC3O	HC2O	HC1O	H1O'	HC1C	C2CH	HC2C	C3CH	HC3C	C4CH	HC4C	C5I5	C5I6	BHCH
1481.	1.	1.	2.	0.	0.	0.	0.	0.	0.	1.	0.	1.	0.	1.	1.	1.	4.	1.	16.	13.	40.
1472.	10.	24.	0.	1.	0.	0.	0.	0.	9.	1.	0.	7.	1.	2.	9.	4.	0.	0.	2.	0.	3.
1440.	1.	1.	20.	15.	1.	0.	1.	1.	0.	0.	1.	0.	5.	9.	0.	7.	3.	0.	0.	3.	7.
1424.	27.	12.	1.	3.	1.	1.	0.	1.	15.	7.	12.	0.	10.	0.	0.	2.	0.	1.	0.	1.	0.
1394.	0.	6.	2.	25.	4.	4.	2.	2.	5.	2.	0.	0.	1.	8.	2.	3.	6.	16.	0.	3.	4.
1379.	1.	0.	1.	2.	27.	24.	2.	0.	0.	1.	2.	0.	2.	5.	3.	3.	0.	0.	11.	6.	8.
1366.	0.	1.	36.	12.	0.	0.	5.	7.	1.	5.	4.	0.	3.	2.	0.	5.	10.	1.	0.	0.	0.
1350.	2.	7.	1.	3.	0.	0.	3.	0.	5.	26.	27.	1.	11.	0.	6.	3.	6.	1.	0.	0.	0.
1340.	1.	3.	0.	3.	5.	5.	4.	1.	2.	2.	0.	0.	1.	5.	13.	10.	10.	22.	5.	3.	0.
1297.	12.	1.	4.	0.	1.	6.	5.	9.	0.	1.	22.	7.	8.	9.	6.	0.	5.	0.	1.	2.	0.
1285.	34.	0.	2.	0.	0.	1.	0.	1.	1.	27.	2.	29.	2.	0.	0.	2.	0.	0.	0.	1.	0.
1254.	1.	0.	2.	7.	9.	11.	41.	8.	0.	1.	4.	1.	0.	0.	7.	0.	5.	9.	3.	4.	0.
1249.	1.	0.	16.	19.	0.	0.	7.	41.	0.	0.	0.	0.	0.	2.	4.	13.	2.	3.	1.	3.	0.
1220.	0.	0.	7.	3.	26.	20.	16.	11.	0.	1.	2.	0.	1.	2.	1.	1.	4.	2.	10.	6.	0.
1205.	4.	25.	3.	1.	0.	0.	1.	8.	30.	3.	5.	3.	10.	8.	2.	0.	1.	1.	0.	0.	1.
1155.	0.	7.	0.	1.	5.	1.	13.	7.	7.	0.	0.	0.	0.	1.	1.	2.	2.	0.	4.	12.	0.
1137.	0.	1.	0.	1.	0.	1.	1.	0.	1.	0.	0.	0.	0.	0.	0.	1.	0.	0.	1.	0.	2.
1115.	0.	2.	0.	1.	1.	0.	0.	1.	6.	4.	0.	0.	0.	1.	0.	1.	0.	1.	0.	1.	1.
1097.	2.	0.	0.	1.	1.	5.	0.	0.	0.	0.	2.	0.	0.	0.	0.	0.	2.	1.	1.	2.	0.
1072.	0.	1.	1.	1.	1.	4.	1.	6.	1.	8.	0.	5.	3.	2.	3.	1.	1.	1.	2.	0.	1.
1060.	0.	0.	0.	2.	2.	3.	1.	0.	1.	0.	0.	1.	0.	1.	0.	1.	0.	1.	8.	8.	0.
1049.	3.	8.	2.	0.	1.	0.	1.	0.	19.	4.	10.	0.	1.	4.	3.	4.	1.	0.	1.	2.	1.
1028.	0.	1.	0.	0.	2.	0.	2.	0.	2.	7.	1.	0.	1.	3.	1.	1.	4.	1.	0.	2.	4.
977.	0.	0.	1.	0.	0.	0.	0.	0.	0.	1.	2.	3.	6.	4.	3.	3.	0.	0.	0.	0.	0.
933.	0.	0.	1.	1.	0.	1.	1.	1.	0.	1.	1.	0.	1.	1.	2.	0.	6.	7.	9.	9.	0.
883.	0.	1.	0.	0.	0.	0.	0.	0.	2.	0.	4.	15.	0.	1.	0.	0.	0.	0.	0.	0.	1.
682.	2.	0.	1.	1.	0.	0.	0.	0.	0.	0.	2.	8.	1.	3.	4.	1.	1.	1.	1.	0.	0.
634.	0.	0.	0.	0.	0.	0.	0.	0.	0.	0.	0.	0.	2.	0.	1.	1.	0.	1.	5.	0.	1.
553.	0.	0.	0.	1.	0.	0.	0.	0.	0.	0.	0.	5.	0.	2.	2.	3.	2.	1.	0.	0.	0.
543.	1.	0.	0.	0.	0.	0.	0.	0.	0.	0.	0.	0.	7.	1.	0.	3.	4.	5.	1.	0.	0.
510.	0.	0.	0.	0.	0.	1.	0.	0.	0.	1.	0.	0.	0.	0.	0.	3.	0.	2.	1.	1.	0.
416.	0.	0.	0.	0.	0.	0.	0.	0.	0.	1.	0.	0.	2.	2.	1.	2.	1.	0.	0.	0.	1.
394.	0.	0.	0.	0.	0.	0.	0.	0.	0.	1.	0.	0.	1.	0.	0.	0.	0.	1.	0.	0.	0.
386.	0.	0.	0.	0.	0.	0.	0.	0.	0.	0.	3.	0.	0.	1.	0.	4.	0.	0.	0.	1.	0.
370.	0.	0.	0.	0.	0.	4.	0.	0.	0.	0.	0.	1.	0.	0.	0.	1.	0.	8.	6.	0.	2.
362.	0.	0.	0.	0.	0.	0.	0.	0.	0.	0.	0.	1.	1.	1.	0.	0.	0.	0.	0.	0.	0.
351.	0.	0.	0.	0.	0.	0.	0.	0.	0.	0.	0.	0.	4.	2.	0.	1.	2.	0.	1.	0.	0.
339.	0.	0.	0.	0.	0.	1.	0.	0.	0.	0.	1.	0.	3.	0.	3.	2.	2.	0.	1.	0.	0.
304.	0.	0.	1.	0.	0.	0.	0.	0.	0.	0.	0.	3.	3.	4.	6.	3.	5.	0.	0.	0.	0.
281.	0.	0.	0.	0.	0.	0.	0.	0.	0.	0.	4.	8.	0.	5.	3.	1.	3.	0.	0.	0.	0.
268.	0.	0.	0.	0.	0.	0.	0.	0.	0.	0.	3.	2.	0.	2.	0.	2.	0.	1.	0.	0.	0.
256.	0.	0.	0.	0.	0.	0.	0.	0.	0.	0.	8.	12.	0.	1.	4.	1.	2.	0.	0.	0.	0.
140.	0.	0.	0.	0.	1.	0.	0.	0.	0.	0.	0.	0.	0.	1.	1.	0.	0.	0.	0.	0.	1.
128.	0.	0.	0.	0.	0.	0.	0.	0.	0.	0.	0.	1.	0.	0.	0.	0.	0.	0.	1.	0.	0.

TABLE LXXII (Continued)

CALCULATED INTERNAL COORDINATE DISTRIBUTIONS
BETA XYLOSE

CONTRIBUTIONS FROM CC STRETCH

	C1C2	C2C3	C3C4	C4C5	C5O'	O'C1	C1O6	C2O7	C3O8	C4O9
1481.	0.	0.	0.	0.	0.	0.	0.	0.	1.	1.
1472.	4.	1.	0.	0.	0.	0.	1.	0.	0.	0.
1440.	0.	3.	1.	0.	0.	0.	0.	0.	0.	0.
1424.	1.	0.	0.	0.	0.	0.	1.	1.	0.	0.
1394.	0.	0.	1.	0.	0.	0.	0.	1.	0.	1.
1379.	0.	0.	0.	1.	1.	0.	0.	0.	0.	0.
1366.	0.	1.	4.	0.	0.	0.	0.	0.	1.	0.
1350.	0.	0.	0.	0.	0.	0.	0.	0.	0.	0.
1340.	0.	0.	0.	1.	1.	0.	0.	0.	0.	1.
1297.	1.	0.	0.	0.	0.	2.	0.	1.	0.	0.
1285.	0.	1.	0.	0.	2.	1.	1.	1.	0.	0.
1254.	1.	0.	2.	2.	1.	1.	1.	0.	0.	0.
1249.	1.	1.	0.	0.	0.	1.	2.	1.	0.	0.
1220.	0.	0.	0.	0.	1.	2.	0.	1.	0.	0.
1205.	1.	2.	0.	1.	0.	0.	0.	0.	0.	1.
1155.	0.	1.	12.	14.	5.	4.	0.	1.	0.	9.
1137.	1.	6.	5.	0.	1.	3.	14.	25.	22.	17.
1115.	1.	5.	0.	0.	2.	2.	17.	8.	25.	18.
1097.	4.	1.	10.	3.	48.	18.	0.	2.	1.	17.
1072.	18.	7.	2.	11.	2.	2.	29.	2.	29.	1.
1060.	3.	0.	1.	33.	4.	1.	5.	13.	6.	16.
1049.	1.	19.	5.	1.	1.	3.	19.	34.	0.	3.
1028.	4.	0.	2.	22.	7.	18.	0.	3.	1.	8.
977.	36.	43.	8.	1.	6.	3.	5.	3.	10.	5.
933.	8.	1.	44.	3.	1.	0.	0.	3.	5.	1.
883.	15.	7.	0.	1.	21.	57.	8.	1.	2.	0.
682.	6.	0.	2.	2.	0.	2.	3.	1.	0.	1.
634.	0.	0.	1.	1.	0.	0.	3.	2.	2.	4.
553.	7.	0.	0.	0.	2.	2.	1.	2.	0.	0.
543.	5.	1.	0.	1.	0.	5.	0.	1.	0.	0.
510.	3.	6.	15.	12.	4.	1.	2.	3.	2.	4.
416.	4.	1.	2.	1.	0.	0.	2.	1.	3.	0.
394.	0.	2.	0.	0.	0.	0.	0.	0.	0.	1.
386.	1.	0.	0.	1.	2.	0.	0.	0.	0.	1.
370.	1.	1.	2.	0.	8.	3.	0.	0.	0.	1.
362.	0.	3.	0.	0.	0.	0.	0.	0.	0.	0.
351.	2.	1.	1.	0.	0.	0.	0.	0.	0.	0.
339.	0.	2.	0.	0.	1.	0.	0.	0.	0.	0.
304.	3.	3.	0.	0.	1.	1.	0.	1.	0.	0.
281.	0.	4.	2.	1.	1.	1.	0.	0.	1.	0.
268.	0.	1.	1.	2.	0.	3.	0.	0.	0.	0.
256.	1.	2.	1.	0.	1.	5.	0.	0.	0.	0.
140.	0.	0.	0.	0.	0.	0.	1.	0.	0.	1.
128.	0.	0.	0.	0.	0.	0.	0.	1.	1.	0.

CALCULATED INTERNAL COORDINATE DISTRIBUTIONS
BETA XYLOSE

CONTRIBUTIONS FROM CCC AND CCO BEND

	8C2C	BC3C	BC4C	BC5O	BCOC	O'C2	O'C6	B612	B721	B723	B832	B834	B943	B945
1481.	0.	0.	0.	0.	0.	0.	0.	0.	0.	0.	1.	0.	0.	1.
1472.	2.	0.	0.	0.	0.	0.	0.	2.	0.	0.	0.	0.	0.	0.
1440.	0.	1.	0.	0.	0.	0.	0.	0.	0.	9.	2.	0.	2.	0.
1424.	0.	0.	0.	0.	0.	1.	0.	1.	0.	0.	0.	0.	0.	0.
1394.	0.	0.	0.	0.	0.	0.	0.	0.	0.	0.	0.	0.	1.	0.
1379.	0.	0.	0.	0.	0.	0.	0.	0.	0.	0.	0.	0.	0.	0.
1366.	0.	1.	0.	0.	0.	0.	0.	0.	0.	0.	1.	1.	0.	0.
1350.	0.	0.	0.	0.	0.	0.	0.	0.	0.	1.	0.	0.	0.	0.
1340.	0.	0.	0.	0.	0.	0.	0.	0.	0.	0.	0.	0.	0.	0.
1297.	0.	0.	0.	0.	0.	0.	0.	0.	0.	0.	0.	0.	0.	0.
1285.	0.	0.	0.	0.	0.	0.	0.	1.	1.	0.	0.	0.	0.	0.
1254.	0.	0.	0.	0.	0.	0.	0.	0.	0.	0.	0.	0.	0.	0.
1249.	0.	0.	1.	0.	0.	0.	0.	0.	0.	0.	0.	1.	0.	0.
1220.	0.	0.	0.	0.	0.	0.	0.	0.	0.	0.	0.	0.	0.	0.
1205.	0.	1.	0.	1.	0.	1.	0.	1.	0.	0.	0.	0.	1.	0.
1155.	0.	0.	7.	0.	1.	0.	0.	0.	0.	2.	0.	4.	0.	0.
1137.	0.	0.	0.	1.	1.	0.	1.	0.	1.	0.	0.	0.	0.	1.
1115.	2.	9.	4.	3.	1.	4.	0.	0.	2.	4.	0.	1.	3.	2.
1097.	0.	0.	0.	0.	1.	0.	0.	0.	0.	0.	0.	0.	0.	0.
1072.	0.	5.	2.	1.	2.	3.	0.	0.	2.	2.	2.	3.	2.	1.
1060.	0.	0.	0.	0.	2.	0.	0.	0.	0.	1.	0.	0.	2.	0.
1049.	10.	0.	0.	1.	1.	4.	1.	6.	3.	0.	3.	0.	0.	1.
1028.	0.	0.	0.	7.	1.	3.	1.	0.	4.	0.	1.	1.	0.	9.
977.	0.	0.	0.	0.	0.	1.	1.	0.	2.	3.	1.	0.	0.	0.
933.	0.	2.	1.	0.	1.	1.	0.	0.	2.	3.	2.	5.	2.	1.
883.	1.	0.	0.	1.	8.	0.	20.	4.	3.	0.	1.	0.	1.	4.
682.	0.	0.	0.	0.	1.	0.	4.	8.	3.	7.	15.	1.	6.	1.
634.	1.	0.	5.	19.	17.	10.	7.	1.	0.	0.	2.	4.	1.	1.
553.	1.	0.	2.	0.	0.	1.	16.	5.	2.	12.	1.	5.	15.	3.
543.	0.	1.	4.	1.	11.	0.	2.	9.	12.	3.	2.	0.	2.	5.
510.	0.	0.	1.	0.	0.	4.	2.	0.	0.	2.	0.	10.	4.	9.
416.	22.	13.	2.	7.	0.	5.	0.	1.	0.	1.	4.	2.	1.	0.
394.	1.	16.	11.	0.	16.	7.	2.	0.	0.	5.	2.	12.	3.	7.
386.	8.	0.	13.	4.	4.	9.	5.	3.	12.	1.	0.	4.	1.	1.
370.	0.	0.	0.	9.	23.	0.	0.	0.	5.	1.	2.	0.	0.	8.
362.	0.	1.	3.	1.	1.	2.	0.	8.	4.	4.	2.	0.	5.	0.
351.	0.	0.	0.	1.	3.	0.	0.	0.	1.	2.	1.	1.	6.	0.
339.	0.	0.	0.	0.	4.	0.	0.	4.	0.	2.	0.	0.	0.	3.
304.	2.	0.	1.	0.	0.	1.	0.	4.	9.	0.	22.	0.	0.	7.
281.	0.	2.	1.	1.	1.	0.	13.	8.	0.	12.	1.	10.	9.	1.
268.	1.	1.	0.	0.	0.	0.	5.	7.	4.	5.	16.	12.	20.	13.
256.	0.	0.	1.	0.	0.	1.	17.	14.	19.	17.	7.	13.	3.	6.
140.	3.	3.	8.	4.	3.	4.	1.	1.	0.	0.	0.	0.	3.	5.
128.	11.	10.	1.	1.	1.	1.	1.	0.	3.	3.	3.	3.	1.	0.

TABLE LXXIII

CALCULATED INTERNAL COORDINATE DISTRIBUTIONS
BETA RIBOSE 1C-D RING CONFORMATION 1-2-3-4 = E-E-A-E

C-H AND O-H STRETCH CONTRIBUTION

	CH15	CH16	CH17	CH18	CH19	CH20	OH11	OH12	OH13	OH14
3357.	0.	0.	0.	0.	0.	0.	95.	5.	0.	0.
3356.	0.	0.	0.	0.	0.	0.	3.	33.	59.	4.
3356.	0.	0.	0.	0.	0.	0.	0.	5.	1.	94.
3356.	0.	0.	0.	0.	0.	0.	2.	57.	40.	2.
3000.	49.	49.	0.	0.	0.	0.	0.	0.	0.	0.
2940.	0.	1.	75.	23.	0.	1.	0.	0.	0.	0.
2950.	0.	0.	0.	2.	45.	51.	0.	0.	0.	0.
2938.	0.	0.	24.	74.	0.	1.	0.	0.	0.	0.
2935.	0.	0.	0.	1.	54.	45.	0.	0.	0.	0.
2888.	51.	50.	0.	0.	0.	0.	0.	0.	0.	0.

TORSIONAL BENDING CONTRIBUTION

	T1-2	T2-3	T3-4	T4-5	T510	T101	T1-6	T2-7	T3-8	T4-9
897.	0.	0.	0.	0.	1.	0.	0.	0.	0.	0.
879.	0.	0.	0.	0.	1.	0.	2.	0.	0.	0.
689.	0.	0.	1.	0.	0.	0.	0.	1.	0.	0.
665.	0.	0.	0.	0.	5.	0.	0.	0.	0.	0.
606.	0.	0.	0.	0.	1.	3.	4.	1.	0.	0.
567.	0.	0.	0.	0.	1.	1.	2.	0.	0.	0.
510.	0.	1.	0.	0.	3.	0.	0.	1.	0.	2.
450.	0.	0.	0.	1.	0.	0.	0.	2.	0.	3.
405.	0.	0.	0.	0.	0.	2.	1.	1.	14.	2.
377.	2.	0.	1.	4.	9.	9.	9.	2.	8.	2.
371.	0.	0.	0.	2.	3.	4.	22.	33.	1.	5.
362.	0.	0.	0.	0.	1.	1.	13.	0.	5.	34.
346.	1.	1.	0.	2.	1.	5.	0.	11.	50.	5.
338.	0.	0.	0.	0.	0.	0.	23.	28.	1.	22.
290.	0.	0.	0.	0.	0.	0.	3.	4.	0.	15.
265.	0.	2.	2.	0.	0.	1.	7.	1.	6.	0.
258.	0.	0.	0.	0.	0.	0.	7.	7.	2.	0.
236.	6.	0.	0.	2.	0.	0.	0.	1.	3.	1.
140.	7.	1.	21.	18.	0.	15.	0.	0.	0.	0.
131.	19.	28.	8.	1.	3.	1.	0.	0.	0.	0.

TABLE LXXIII (Continued)

CALCULATED INTERNAL COORDINATE DISTRIBUTIONS
BETA RIBOSE 1C-D RING CONFORMATION 1-2-3-4 = E-E-A-E

C-H BENDING CONTRIBUTION

	HO6C	HO7C	HO8C	HO9C	15C'	16C'	HC4O	HC3O	HC2O	HC1O	H1O'	HC1C	C2CH	HC2C	C3CH	HC3C	C4CH	HC4C	C515	C516	BHCH
1450.	26.	11.	1.	0.	0.	0.	0.	0.	0.	5.	2.	6	9.	0.	0.	0.	0.	0.	0.	0.	0.
1478.	1.	0.	1.	2.	0.	0.	0.	0.	0.	0.	0.	0.	0.	0.	1.	2.	1.	1.	14.	17.	44.
1434.	0.	14.	0.	16.	0.	0.	2.	1.	3.	2.	0.	0.	5.	15.	11.	7.	1.	2.	2.	0.	3.
1406.	3.	9.	14.	9.	6.	5.	0.	7.	1.	0.	1.	0.	2.	7.	0.	7.	7.	10.	0.	1.	7.
1382.	5.	5.	0.	0.	11.	7.	3.	2.	2.	6.	16.	1.	0.	3.	2.	4.	11.	4.	7.	2.	1.
1374.	7.	2.	32.	0.	13.	12.	1.	2.	0.	2.	1.	0.	0.	1.	1.	1.	2.	4.	4.	5.	3.
1373.	1.	8.	17.	35.	5.	4.	4.	0.	2.	1.	1.	0.	1.	2.	1.	2.	2.	1.	4.	0.	1.
1357.	2.	4.	7.	1.	2.	5.	1.	0.	0.	21.	30.	3.	3.	0.	1.	0.	7.	4.	2.	1.	1.
1321.	5.	12.	4.	3.	0.	3.	4.	0.	17.	0.	8.	7.	10.	0.	9.	7.	0.	5.	0.	1.	1.
1291.	23.	0.	0.	2.	1.	1.	3.	5.	1.	7.	7.	0.	7.	11.	0.	6.	3.	12.	1.	0.	0.
1288.	10.	1.	0.	0.	0.	1.	1.	7.	9.	29.	0.	22.	4.	0.	12.	4.	1.	3.	0.	1.	0.
1270.	1.	3.	9.	1.	3.	6.	34.	22.	1.	1.	2.	3.	0.	1.	9.	0.	6.	3.	2.	5.	0.
1243.	4.	7.	2.	4.	11.	14.	9.	23.	12.	6.	0.	5.	4.	0.	2.	4.	2.	2.	3.	3.	0.
1233.	4.	15.	4.	12.	0.	0.	9.	10.	34.	0.	0.	2.	10.	4.	0.	7.	1.	4.	1.	0.	0.
1218.	0.	4.	1.	8.	23.	14.	23.	0.	7.	0.	3.	1.	0.	4.	0.	1.	6.	1.	10.	5.	0.
1150.	0.	0.	0.	1.	2.	0.	4.	7.	1.	0.	1.	0.	0.	1.	2.	3.	0.	0.	6.	12.	0.
1113.	1.	0.	0.	1.	0.	1.	3.	15.	9.	1.	3.	0.	1.	0.	5.	0.	0.	2.	1.	1.	1.
1110.	3.	0.	1.	0.	3.	1.	1.	0.	6.	1.	5.	3.	1.	0.	1.	0.	0.	1.	3.	6.	0.
1101.	2.	0.	1.	0.	1.	7.	1.	2.	0.	3.	3.	1.	0.	0.	0.	1.	4.	1.	1.	3.	0.
1082.	1.	0.	0.	2.	1.	1.	0.	1.	1.	1.	8.	0.	0.	0.	5.	0.	5.	2.	2.	1.	1.
1064.	0.	2.	1.	1.	0.	2.	3.	1.	2.	7.	1.	1.	0.	4.	0.	0.	1.	2.	1.	0.	1.
1047.	0.	0.	1.	0.	4.	2.	0.	1.	0.	0.	0.	1.	1.	0.	0.	1.	10.	1.	4.	12.	5.
993.	1.	5.	2.	0.	0.	0.	0.	1.	0.	10.	2.	1.	5.	17.	4.	3.	1.	0.	2.	1.	1.
958.	0.	0.	2.	0.	0.	1.	1.	1.	0.	0.	0.	1.	0.	0.	2.	5.	2.	2.	4.	4.	0.
897.	1.	0.	0.	0.	0.	0.	0.	0.	1.	0.	3.	1.	1.	0.	1.	4.	0.	0.	0.	0.	0.
879.	0.	0.	0.	0.	0.	0.	0.	0.	1.	1.	3.	15.	1.	0.	0.	0.	1.	0.	1.	1.	2.
689.	0.	0.	2.	0.	0.	0.	0.	0.	0.	0.	0.	0.	3.	1.	7.	5.	0.	2.	4.	0.	0.
665.	0.	0.	0.	2.	0.	1.	0.	0.	0.	0.	0.	1.	1.	1.	0.	6.	3.	10.	2.	0.	0.
606.	1.	0.	1.	0.	0.	1.	0.	0.	0.	0.	0.	8.	2.	2.	4.	0.	0.	0.	0.	0.	0.
567.	0.	0.	0.	0.	0.	0.	0.	0.	0.	1.	0.	4.	1.	0.	0.	0.	0.	0.	2.	0.	0.
510.	1.	1.	0.	0.	0.	0.	0.	0.	0.	0.	1.	1.	7.	1.	0.	0.	0.	0.	0.	1.	0.
450.	0.	0.	0.	0.	0.	0.	0.	0.	0.	0.	0.	0.	1.	0.	1.	2.	0.	4.	2.	0.	0.
405.	0.	0.	0.	0.	0.	0.	0.	0.	0.	2.	0.	0.	0.	0.	0.	1.	0.	0.	1.	1.	1.
377.	0.	0.	0.	0.	0.	2.	0.	0.	0.	0.	3.	0.	0.	0.	0.	0.	0.	1.	2.	0.	1.
371.	0.	0.	0.	0.	0.	1.	0.	0.	0.	0.	0.	0.	1.	1.	0.	0.	0.	2.	2.	0.	1.
362.	0.	0.	0.	0.	0.	0.	0.	0.	0.	0.	0.	1.	0.	0.	0.	0.	1.	2.	0.	1.	0.
346.	0.	0.	0.	0.	0.	1.	0.	0.	0.	0.	0.	0.	1.	0.	2.	2.	2.	0.	1.	0.	0.
338.	0.	0.	0.	0.	0.	0.	0.	0.	0.	0.	1.	2.	1.	3.	1.	0.	1.	0.	0.	0.	0.
290.	0.	0.	0.	0.	1.	1.	0.	0.	0.	0.	1.	0.	0.	0.	0.	2.	1.	1.	0.	1.	0.
265.	0.	0.	0.	0.	0.	0.	0.	0.	0.	0.	4.	8.	2.	2.	1.	2.	1.	1.	0.	0.	0.
258.	0.	0.	0.	0.	0.	0.	0.	0.	0.	0.	11.	11.	3.	1.	3.	1.	0.	0.	0.	0.	0.
236.	0.	0.	1.	0.	0.	1.	0.	0.	0.	0.	0.	2.	2.	4.	3.	1.	6.	1.	0.	0.	0.
140.	0.	0.	0.	0.	0.	0.	0.	2.	0.	0.	0.	0.	0.	1.	0.	0.	0.	0.	0.	0.	0.
131.	0.	0.	0.	0.	0.	0.	0.	3.	0.	0.	0.	1.	0.	0.	0.	0.	0.	1.	1.	0.	0.

TABLE LXXIII (Continued)

CALCULATED INTERNAL COORDINATE DISTRIBUTIONS
BETA RIBOSE 1C-D RING CONFORMATION 1-2-3-4 = E-E-A-E

HEAVY ATOM STRETCH CONTRIBUTION

	C1C2	C2C3	C3C4	C4C5	C5O'	O'C1	C1O6	C2O7	C3O8	C4O9
1450.	7.	0.	0.	0.	0.	0.	0.	0.	0.	0.
1478.	0.	0.	1.	0.	0.	0.	0.	0.	0.	0.
1434.	1.	0.	2.	2.	0.	0.	0.	1.	2.	1.
1406.	0.	1.	0.	0.	0.	0.	0.	0.	3.	0.
1382.	1.	1.	0.	0.	1.	0.	1.	0.	3.	0.
1374.	0.	4.	0.	1.	1.	0.	0.	0.	0.	0.
1373.	0.	0.	4.	1.	1.	0.	0.	0.	1.	1.
1357.	0.	3.	0.	0.	0.	0.	0.	0.	1.	0.
1321.	1.	0.	0.	0.	0.	0.	0.	2.	1.	1.
1291.	0.	1.	0.	1.	1.	2.	1.	1.	0.	0.
1288.	0.	0.	0.	1.	1.	0.	0.	0.	0.	0.
1270.	1.	0.	3.	0.	1.	1.	2.	0.	1.	0.
1243.	0.	0.	0.	0.	0.	1.	0.	0.	1.	0.
1233.	1.	0.	0.	0.	0.	0.	0.	0.	4.	0.
1218.	0.	1.	0.	1.	2.	2.	1.	1.	0.	0.
1150.	1.	5.	10.	9.	5.	5.	1.	11.	8.	27.
1113.	0.	10.	0.	0.	0.	1.	3.	13.	8.	17.
1110.	13.	11.	1.	1.	15.	0.	18.	20.	6.	0.
1101.	0.	0.	10.	5.	31.	20.	13.	2.	1.	20.
1082.	1.	0.	18.	18.	2.	3.	37.	4.	0.	0.
1064.	2.	9.	0.	29.	1.	0.	16.	30.	0.	9.
1047.	6.	4.	2.	2.	15.	9.	1.	6.	0.	14.
993.	25.	20.	3.	9.	1.	9.	0.	0.	9.	0.
958.	3.	20.	30.	1.	7.	6.	1.	4.	16.	6.
897.	5.	6.	7.	6.	4.	20.	0.	1.	39.	0.
879.	24.	1.	7.	4.	15.	36.	7.	3.	7.	0.
689.	16.	0.	3.	0.	1.	2.	9.	0.	1.	3.
665.	4.	1.	2.	13.	0.	1.	0.	0.	1.	1.
606.	0.	1.	0.	3.	0.	0.	1.	0.	0.	2.
567.	17.	3.	1.	6.	5.	5.	1.	6.	0.	4.
510.	0.	0.	0.	0.	1.	2.	0.	0.	0.	0.
450.	0.	3.	9.	1.	2.	0.	1.	2.	0.	2.
405.	0.	0.	0.	1.	0.	0.	1.	1.	0.	1.
377.	2.	0.	1.	0.	8.	1.	0.	0.	0.	0.
371.	2.	0.	1.	0.	2.	2.	0.	0.	0.	0.
362.	0.	7.	0.	0.	1.	0.	0.	0.	0.	1.
346.	0.	0.	2.	0.	0.	0.	0.	0.	0.	0.
338.	0.	2.	1.	0.	0.	0.	0.	0.	0.	0.
290.	0.	2.	0.	0.	4.	0.	0.	0.	0.	0.
265.	0.	1.	0.	0.	1.	2.	0.	0.	0.	0.
258.	1.	1.	1.	0.	0.	7.	0.	0.	0.	0.
236.	0.	4.	4.	0.	0.	0.	0.	1.	1.	1.
140.	0.	0.	0.	0.	0.	0.	0.	0.	0.	1.
131.	0.	1.	0.	0.	0.	0.	1.	1.	0.	0.

CALCULATED INTERNAL COORDINATE DISTRIBUTIONS
BETA RIBOSE 1C-D RING CONFORMATION 1-2-3-4 = E-E-A-E

HEAVY ATOM BEND CONTRIBUTION

	BC2C	BC3C	BC4C	BC5O	BCOC	O'C2	O'C6	B612	B721	B723	B832	B834	B943	B945
1450.	0.	0.	0.	0.	0.	0.	0.	0.	0.	0.	0.	0.	0.	0.
1478.	0.	0.	0.	0.	0.	0.	0.	0.	0.	0.	0.	0.	0.	1.
1434.	0.	1.	0.	0.	0.	0.	0.	0.	1.	0.	0.	0.	2.	0.
1406.	0.	0.	0.	0.	0.	0.	0.	0.	0.	0.	1.	0.	0.	0.
1382.	0.	1.	0.	0.	0.	0.	0.	0.	0.	1.	0.	0.	0.	0.
1374.	0.	0.	0.	0.	0.	0.	0.	0.	0.	0.	0.	1.	0.	0.
1373.	0.	0.	0.	0.	0.	0.	0.	0.	0.	1.	1.	0.	1.	0.
1357.	0.	0.	0.	0.	0.	0.	0.	0.	0.	0.	0.	0.	0.	0.
1321.	1.	0.	0.	0.	0.	0.	0.	0.	0.	0.	0.	0.	0.	0.
1291.	0.	0.	0.	1.	0.	0.	0.	0.	0.	0.	0.	0.	0.	0.
1288.	0.	0.	0.	0.	0.	0.	0.	0.	0.	0.	0.	0.	0.	0.
1270.	0.	0.	1.	0.	0.	0.	0.	0.	0.	0.	0.	0.	0.	0.
1243.	0.	0.	0.	0.	0.	0.	0.	0.	0.	0.	0.	0.	0.	0.
1233.	0.	1.	0.	0.	0.	0.	0.	0.	0.	0.	0.	0.	0.	0.
1218.	0.	0.	0.	0.	0.	0.	0.	0.	0.	0.	0.	0.	0.	0.
1150.	1.	0.	7.	1.	0.	0.	0.	0.	0.	0.	0.	0.	0.	1.
1113.	0.	8.	0.	2.	1.	2.	1.	1.	1.	5.	0.	2.	4.	1.
1110.	2.	0.	2.	1.	1.	0.	0.	1.	0.	0.	0.	0.	0.	1.
1101.	0.	0.	0.	0.	2.	1.	1.	1.	0.	1.	1.	1.	0.	0.
1082.	8.	3.	0.	0.	0.	1.	1.	3.	0.	2.	0.	3.	2.	1.
1064.	2.	0.	2.	2.	3.	7.	0.	1.	4.	0.	1.	0.	1.	1.
1047.	0.	0.	1.	4.	0.	0.	0.	0.	0.	2.	0.	2.	0.	6.
993.	0.	1.	0.	2.	1.	5.	1.	0.	6.	1.	3.	2.	0.	1.
958.	0.	1.	0.	0.	3.	0.	2.	0.	0.	0.	3.	1.	0.	0.
897.	0.	1.	0.	1.	4.	0.	4.	5.	2.	2.	1.	2.	1.	0.
879.	1.	0.	0.	4.	3.	0.	13.	2.	0.	0.	0.	1.	0.	4.
689.	6.	1.	12.	4.	1.	3.	1.	1.	2.	5.	10.	2.	1.	1.
665.	0.	0.	4.	0.	0.	0.	2.	0.	0.	7.	2.	19.	17.	0.
606.	2.	0.	1.	6.	16.	0.	20.	0.	0.	6.	13.	0.	1.	2.
567.	1.	0.	0.	7.	8.	12.	1.	0.	0.	0.	0.	0.	0.	0.
510.	0.	3.	0.	0.	3.	0.	9.	24.	26.	0.	1.	1.	7.	7.
450.	4.	11.	0.	4.	13.	0.	0.	1.	3.	6.	0.	0.	0.	17.
405.	13.	0.	5.	11.	4.	13.	5.	1.	2.	5.	2.	7.	4.	1.
377.	1.	0.	7.	1.	15.	5.	3.	2.	3.	0.	0.	3.	0.	10.
371.	0.	0.	0.	2.	6.	0.	0.	2.	5.	4.	0.	0.	0.	3.
362.	0.	2.	6.	3.	2.	4.	0.	7.	0.	0.	0.	2.	6.	0.
346.	0.	0.	0.	2.	7.	0.	0.	2.	1.	0.	0.	0.	1.	0.
338.	1.	3.	0.	1.	0.	0.	1.	0.	1.	1.	7.	0.	1.	3.
290.	1.	2.	1.	0.	0.	0.	3.	2.	2.	7.	6.	1.	29.	21.
265.	1.	0.	0.	1.	0.	2.	10.	7.	6.	1.	23.	17.	5.	0.
258.	0.	0.	0.	0.	0.	1.	20.	21.	23.	26.	4.	7.	1.	0.
236.	2.	24.	6.	0.	2.	0.	1.	0.	1.	4.	13.	21.	3.	0.
140.	1.	4.	10.	4.	4.	3.	0.	1.	0.	0.	1.	0.	3.	6.
131.	17.	3.	2.	1.	1.	2.	2.	0.	3.	4.	0.	0.	0.	0.

TABLE LXXIV

CALCULATED INTERNAL COORDINATE DISTRIBUTIONS
ALPHA RIBOSE 1C-D RING CONFORMATION 1-2-3-4 = A-E-A-E

C-H AND O-H STRETCH CONTRIBUTION

	CH15	CH16	CH17	CH18	CH19	CH20	OH11	OH12	OH13	OH14
3357.	0.	0.	0.	0.	0.	0.	97.	3.	0.	0.
3356.	0.	0.	0.	0.	0.	0.	0.	21.	76.	3.
3356.	0.	0.	0.	0.	0.	0.	0.	3.	1.	96.
3356.	0.	0.	0.	0.	0.	0.	3.	73.	23.	1.
3000.	48.	49.	0.	0.	0.	0.	0.	0.	0.	0.
2943.	0.	0.	0.	6.	12.	80.	0.	0.	0.	0.
2941.	0.	1.	65.	21.	5.	8.	0.	0.	0.	0.
2939.	0.	0.	20.	3.	65.	11.	0.	0.	0.	0.
2938.	0.	0.	13.	69.	17.	0.	0.	0.	0.	0.
2888.	51.	49.	0.	0.	0.	0.	0.	0.	0.	0.

TORSIONAL BENDING CONTRIBUTION

	TC12	TC23	TC34	TC45	TC50	TOC1	TC06	TC07	TC08	TC09
907.	0.	0.	0.	0.	1.	0.	0.	0.	0.	1.
874.	0.	0.	0.	0.	0.	1.	0.	0.	0.	0.
818.	0.	0.	0.	0.	0.	0.	0.	0.	0.	0.
668.	0.	0.	0.	1.	7.	0.	0.	0.	0.	0.
645.	0.	0.	0.	1.	1.	0.	2.	0.	0.	0.
531.	0.	0.	0.	0.	3.	2.	1.	0.	0.	1.
513.	0.	0.	1.	1.	2.	4.	0.	2.	2.	0.
449.	0.	0.	0.	1.	0.	1.	0.	1.	0.	0.
429.	0.	0.	0.	0.	2.	1.	3.	3.	0.	9.
385.	0.	0.	0.	1.	6.	2.	17.	15.	13.	10.
364.	0.	0.	0.	0.	0.	0.	1.	18.	38.	10.
357.	0.	0.	1.	0.	1.	0.	49.	1.	17.	10.
340.	1.	0.	0.	0.	1.	0.	0.	38.	0.	28.
310.	1.	2.	0.	0.	0.	1.	0.	1.	6.	18.
287.	0.	0.	1.	4.	3.	3.	7.	6.	9.	6.
263.	0.	1.	0.	0.	1.	0.	4.	1.	4.	0.
245.	0.	2.	4.	4.	0.	5.	4.	5.	2.	0.
212.	5.	1.	0.	5.	1.	0.	1.	0.	1.	1.
134.	23.	5.	4.	12.	0.	13.	1.	0.	0.	0.
129.	3.	23.	23.	2.	3.	3.	0.	0.	0.	0.

TABLE LXXIV (Continued)

CALCULATED INTERNAL COORDINATE DISTRIBUTIONS
ALPHA RIBOSE 1C-O RING CONFORMATION 1-2-3-4 = A-E-A-E

C-H BENDING CONTRIBUTION

	HO6C	HO7C	HO8C	HO9C	H15O	H16O	HC4O	HC3O	HC2O	HC1O	HCO'	HC1C	HC2C	HC2C	HC3C	HC3C	HC4C	HC4C	H15C	H16C	HC5H
1478.	0.	0.	1.	2.	0.	0.	0.	0.	0.	0.	0.	0.	0.	0.	1.	3.	2.	1.	15.	17.	44.
1452.	7.	24.	1.	2.	0.	0.	0.	1.	3.	3.	1.	8.	1.	7.	10.	3.	0.	1.	1.	0.	3.
1420.	8.	2.	9.	24.	1.	1.	2.	0.	0.	1.	1.	1.	4.	4.	2.	6.	0.	2.	2.	0.	4.
1400.	5.	4.	7.	1.	4.	2.	0.	7.	2.	1.	1.	0.	3.	12.	0.	6.	16.	11.	0.	0.	4.
1385.	25.	4.	1.	6.	8.	14.	0.	0.	0.	7.	23.	1.	0.	0.	0.	0.	1.	0.	5.	3.	3.
1374.	1.	4.	27.	10.	12.	8.	8.	2.	1.	3.	3.	0.	0.	1.	1.	5.	2.	1.	3.	4.	2.
1370.	8.	0.	21.	11.	12.	8.	0.	0.	0.	6.	3.	0.	1.	3.	0.	0.	4.	8.	8.	1.	2.
1345.	1.	19.	6.	6.	1.	0.	2.	1.	12.	2.	3.	6.	27.	3.	4.	1.	2.	0.	0.	0.	0.
1323.	21.	5.	1.	4.	1.	1.	0.	0.	1.	28.	29.	1.	2.	1.	1.	1.	3.	2.	0.	0.	0.
1302.	6.	1.	0.	1.	0.	0.	6.	8.	11.	5.	1.	4.	1.	9.	1.	6.	5.	19.	0.	0.	0.
1301.	1.	1.	4.	2.	2.	0.	2.	3.	2.	13.	7.	16.	1.	0.	18.	11.	0.	3.	1.	0.	2.
1272.	7.	7.	9.	1.	1.	9.	26.	21.	0.	1.	0.	3.	1.	1.	9.	0.	6.	1.	1.	7.	0.
1243.	3.	13.	0.	2.	8.	6.	15.	12.	31.	9.	0.	1.	7.	2.	1.	2.	3.	1.	3.	2.	0.
1232.	0.	10.	6.	11.	0.	2.	10.	28.	26.	0.	1.	1.	6.	4.	1.	8.	1.	4.	0.	0.	0.
1220.	0.	1.	1.	11.	25.	20.	23.	0.	3.	0.	1.	1.	0.	2.	1.	1.	5.	2.	13.	7.	0.
1154.	0.	0.	0.	1.	2.	1.	1.	5.	2.	0.	0.	1.	0.	0.	3.	2.	0.	0.	1.	4.	0.
1119.	0.	2.	1.	0.	0.	2.	3.	1.	2.	3.	0.	5.	0.	1.	2.	2.	1.	2.	3.	13.	0.
1110.	0.	0.	1.	1.	3.	8.	2.	1.	4.	3.	0.	1.	1.	0.	2.	1.	2.	0.	2.	1.	0.
1089.	1.	0.	0.	2.	2.	2.	2.	13.	5.	2.	4.	0.	3.	3.	2.	0.	0.	2.	3.	4.	2.
1056.	0.	0.	0.	0.	1.	1.	2.	2.	1.	3.	0.	0.	0.	1.	0.	0.	6.	1.	8.	10.	0.
1040.	0.	0.	0.	1.	0.	0.	1.	0.	0.	1.	2.	2.	1.	1.	9.	1.	11.	3.	1.	0.	5.
1007.	3.	1.	2.	0.	1.	0.	0.	0.	1.	3.	17.	8.	6.	3.	1.	5.	0.	0.	0.	1.	1.
980.	1.	0.	0.	0.	0.	1.	0.	1.	0.	10.	2.	13.	2.	8.	0.	0.	0.	0.	1.	2.	0.
913.	0.	0.	1.	0.	0.	0.	1.	0.	0.	1.	0.	2.	0.	0.	1.	0.	1.	0.	3.	3.	0.
907.	0.	0.	0.	1.	0.	0.	0.	1.	0.	0.	3.	2.	0.	0.	2.	3.	2.	0.	0.	0.	2.
874.	1.	0.	1.	0.	0.	0.	0.	0.	2.	0.	5.	0.	0.	0.	1.	4.	0.	0.	1.	0.	0.
818.	2.	3.	2.	0.	0.	0.	0.	0.	0.	0.	3.	0.	5.	8.	2.	1.	0.	0.	1.	0.	0.
668.	0.	0.	0.	2.	0.	0.	0.	0.	0.	0.	0.	0.	1.	1.	0.	7.	3.	11.	3.	0.	0.
645.	0.	0.	1.	0.	0.	1.	0.	0.	0.	1.	1.	5.	2.	0.	2.	3.	0.	0.	1.	0.	0.
531.	0.	0.	0.	0.	0.	0.	0.	0.	1.	4.	0.	4.	0.	0.	0.	0.	0.	0.	4.	0.	2.
513.	0.	0.	0.	1.	0.	0.	0.	0.	0.	1.	0.	0.	0.	0.	5.	0.	0.	0.	0.	1.	0.
449.	0.	1.	0.	0.	0.	0.	0.	0.	0.	0.	0.	1.	0.	1.	1.	1.	0.	2.	2.	0.	0.
429.	0.	0.	0.	0.	1.	1.	0.	0.	0.	3.	0.	2.	0.	0.	0.	1.	0.	4.	4.	0.	0.
385.	0.	0.	0.	0.	0.	0.	0.	0.	0.	1.	0.	0.	0.	1.	0.	1.	0.	0.	0.	0.	0.
364.	0.	0.	0.	0.	0.	0.	0.	0.	0.	0.	0.	0.	0.	0.	2.	1.	2.	0.	0.	0.	0.
357.	0.	0.	0.	0.	0.	1.	0.	0.	0.	0.	1.	2.	0.	0.	1.	0.	0.	2.	1.	0.	0.
340.	0.	0.	0.	0.	0.	0.	0.	0.	0.	1.	0.	1.	3.	5.	1.	0.	1.	0.	1.	0.	0.
310.	1.	0.	1.	0.	0.	1.	0.	0.	0.	0.	1.	0.	1.	0.	0.	3.	3.	1.	0.	2.	0.
287.	0.	0.	0.	0.	0.	0.	0.	0.	0.	0.	1.	2.	0.	0.	3.	0.	1.	0.	0.	0.	1.
263.	0.	0.	0.	0.	0.	0.	0.	0.	0.	0.	8.	8.	0.	0.	1.	0.	3.	1.	0.	0.	0.
245.	0.	0.	0.	0.	0.	1.	0.	0.	0.	1.	1.	7.	6.	0.	1.	2.	0.	1.	1.	0.	1.
212.	0.	0.	1.	0.	0.	2.	0.	0.	0.	2.	15.	5.	2.	5.	2.	1.	4.	1.	1.	0.	0.
134.	0.	0.	0.	0.	0.	0.	0.	0.	0.	7.	2.	0.	0.	1.	0.	0.	0.	0.	0.	0.	0.
129.	0.	0.	0.	0.	0.	0.	0.	4.	0.	0.	2.	0.	0.	0.	0.	0.	0.	0.	1.	0.	0.

TABLE LXXIV (Continued)

CALCULATED INTERNAL COORDINATE DISTRIBUTIONS
ALPHA RIBOSE 1C-D RING CONFORMATION 1-2-3-4 = A-E-A-E

HEAVY ATOM STRETCH CONTRIBUTION

	C1C2	C2C3	C3C4	C4C5	C5O*	O*C1	C1O6	C2O7	C3O8	C4O9
1478.	0.	0.	1.	0.	0.	0.	0.	0.	0.	0.
1452.	7.	3.	0.	0.	0.	0.	0.	1.	0.	0.
1420.	2.	4.	2.	2.	0.	0.	0.	0.	1.	1.
1400.	0.	0.	1.	0.	0.	0.	0.	0.	8.	0.
1385.	0.	0.	1.	1.	0.	0.	1.	0.	1.	0.
1374.	0.	0.	2.	0.	1.	0.	0.	0.	1.	0.
1370.	0.	2.	1.	1.	2.	0.	0.	0.	0.	0.
1345.	0.	0.	0.	0.	1.	1.	3.	1.	0.	0.
1323.	1.	0.	0.	0.	2.	1.	0.	1.	0.	0.
1302.	1.	0.	1.	1.	0.	0.	3.	0.	0.	0.
1301.	0.	0.	0.	1.	2.	1.	0.	0.	0.	0.
1272.	0.	0.	2.	0.	0.	1.	1.	0.	1.	0.
1243.	0.	0.	0.	0.	1.	1.	2.	0.	0.	0.
1232.	0.	0.	0.	0.	0.	0.	1.	0.	4.	0.
1220.	0.	0.	0.	1.	0.	1.	0.	0.	0.	0.
1154.	3.	9.	6.	6.	1.	1.	4.	28.	9.	25.
1119.	0.	11.	1.	19.	25.	13.	1.	9.	0.	2.
1110.	7.	5.	18.	4.	12.	7.	7.	15.	1.	17.
1089.	0.	10.	1.	0.	0.	1.	2.	4.	12.	28.
1056.	1.	1.	5.	1.	0.	0.	7.	19.	15.	14.
1040.	1.	2.	18.	40.	6.	17.	6.	3.	1.	0.
1007.	38.	17.	4.	0.	17.	6.	1.	5.	1.	3.
980.	3.	2.	2.	0.	0.	0.	59.	9.	11.	0.
913.	0.	10.	24.	7.	18.	22.	0.	2.	0.	5.
907.	14.	0.	5.	8.	15.	18.	8.	3.	15.	0.
874.	18.	22.	0.	1.	3.	15.	2.	0.	26.	2.
818.	0.	0.	3.	0.	1.	13.	12.	0.	6.	0.
668.	0.	1.	3.	10.	1.	1.	0.	0.	1.	0.
645.	21.	0.	0.	4.	3.	10.	1.	2.	0.	0.
531.	0.	3.	3.	7.	2.	0.	1.	3.	0.	9.
513.	2.	8.	0.	0.	1.	0.	0.	0.	0.	1.
449.	2.	2.	6.	0.	0.	0.	0.	4.	0.	0.
429.	1.	0.	1.	1.	5.	0.	0.	1.	0.	0.
385.	0.	2.	0.	0.	0.	0.	0.	0.	0.	0.
364.	0.	0.	3.	0.	1.	0.	0.	0.	0.	0.
357.	2.	2.	0.	0.	1.	0.	0.	0.	0.	0.
340.	1.	2.	1.	0.	1.	0.	0.	0.	0.	0.
310.	1.	0.	1.	0.	1.	0.	0.	0.	0.	0.
287.	0.	0.	0.	0.	0.	0.	0.	0.	0.	0.
263.	0.	2.	4.	0.	1.	8.	0.	0.	0.	0.
245.	3.	0.	0.	0.	1.	1.	1.	0.	0.	1.
212.	0.	2.	1.	0.	1.	7.	0.	1.	1.	1.
134.	1.	1.	0.	0.	0.	2.	0.	0.	0.	0.
129.	0.	0.	0.	0.	0.	1.	0.	1.	0.	1.

CALCULATED INTERNAL COORDINATE DISTRIBUTIONS
ALPHA RIBOSE 1C-D RING CONFORMATION 1-2-3-4 = A-E-A-E

HEAVY ATOM BEND CONTRIBUTION

	CC2C	CC3C	CC4C	CC5O	COC	OC1C	OCO6	O6CC	CCO7	O7CC	CCO8	O8CC	CCO9	O9CC
1478.	0.	0.	0.	0.	0.	0.	0.	0.	0.	0.	0.	0.	0.	1.
1452.	0.	0.	0.	0.	0.	1.	0.	0.	2.	1.	0.	0.	0.	0.
1420.	0.	1.	0.	0.	0.	0.	0.	0.	0.	0.	0.	0.	3.	0.
1400.	0.	1.	0.	0.	0.	0.	0.	0.	0.	1.	1.	0.	0.	0.
1385.	0.	0.	0.	0.	0.	0.	0.	1.	0.	0.	0.	0.	0.	0.
1374.	0.	0.	0.	0.	0.	0.	0.	0.	0.	1.	1.	0.	0.	0.
1370.	0.	0.	0.	0.	0.	0.	0.	0.	0.	0.	0.	0.	0.	0.
1345.	0.	0.	0.	0.	0.	1.	0.	0.	0.	0.	0.	0.	0.	0.
1323.	0.	0.	0.	0.	0.	0.	0.	1.	0.	0.	0.	0.	0.	0.
1302.	0.	0.	0.	1.	0.	0.	0.	1.	0.	0.	0.	0.	0.	0.
1301.	0.	0.	0.	1.	0.	0.	0.	0.	0.	0.	0.	0.	0.	1.
1272.	0.	0.	1.	0.	0.	0.	0.	0.	0.	0.	0.	0.	0.	0.
1243.	0.	0.	0.	0.	0.	0.	0.	0.	0.	0.	0.	0.	0.	0.
1232.	0.	0.	0.	0.	0.	0.	0.	0.	0.	0.	0.	0.	0.	0.
1220.	0.	0.	0.	0.	0.	0.	0.	0.	0.	0.	0.	0.	0.	0.
1154.	4.	1.	5.	1.	1.	1.	0.	0.	1.	0.	0.	0.	0.	1.
1119.	4.	0.	4.	0.	1.	3.	3.	0.	2.	0.	0.	0.	0.	0.
1110.	3.	0.	1.	1.	1.	1.	0.	0.	0.	1.	0.	3.	0.	1.
1089.	0.	9.	0.	2.	0.	1.	0.	1.	0.	4.	0.	2.	6.	2.
1056.	0.	2.	0.	0.	2.	5.	0.	0.	2.	4.	1.	0.	0.	0.
1040.	1.	1.	1.	5.	0.	1.	1.	0.	1.	0.	0.	6.	1.	7.
1007.	0.	0.	0.	3.	1.	2.	0.	4.	1.	1.	2.	0.	0.	2.
980.	2.	1.	0.	1.	4.	1.	5.	3.	1.	0.	0.	0.	1.	0.
913.	0.	0.	1.	0.	1.	2.	3.	0.	3.	0.	1.	2.	0.	0.
907.	5.	0.	0.	6.	0.	0.	1.	1.	0.	0.	2.	1.	0.	5.
874.	0.	1.	1.	0.	7.	1.	0.	1.	0.	1.	2.	0.	1.	0.
818.	5.	0.	0.	0.	2.	0.	0.	10.	6.	3.	11.	0.	0.	0.
668.	1.	0.	9.	1.	2.	0.	1.	2.	1.	5.	2.	19.	14.	0.
645.	0.	0.	2.	0.	19.	0.	19.	3.	0.	1.	3.	2.	0.	0.
531.	0.	0.	2.	19.	1.	10.	17.	0.	0.	0.	0.	0.	0.	2.
513.	0.	3.	6.	1.	0.	2.	5.	10.	16.	15.	4.	0.	11.	1.
449.	12.	8.	3.	13.	13.	3.	0.	0.	11.	6.	0.	1.	1.	2.
429.	0.	1.	1.	1.	0.	9.	6.	2.	12.	3.	1.	1.	2.	35.
385.	0.	3.	5.	0.	4.	2.	1.	3.	0.	4.	0.	9.	2.	0.
364.	0.	0.	0.	1.	3.	2.	1.	3.	0.	0.	4.	1.	6.	1.
357.	0.	0.	1.	2.	4.	0.	0.	1.	1.	0.	1.	1.	0.	1.
340.	0.	5.	0.	0.	0.	1.	0.	3.	2.	1.	10.	0.	0.	5.
310.	0.	5.	3.	1.	4.	8.	0.	12.	1.	0.	21.	0.	16.	9.
287.	0.	0.	2.	1.	7.	2.	7.	0.	5.	13.	1.	13.	6.	3.
263.	0.	4.	3.	0.	2.	1.	11.	14.	12.	8.	0.	12.	13.	3.
245.	2.	0.	0.	3.	9.	10.	16.	1.	1.	13.	14.	9.	2.	1.
212.	4.	19.	1.	0.	8.	5.	7.	24.	8.	0.	9.	13.	2.	2.
134.	12.	0.	5.	3.	6.	4.	0.	1.	2.	2.	1.	0.	1.	3.
129.	10.	6.	8.	0.	7.	0.	2.	3.	2.	2.	0.	0.	1.	3.

TABLE LXXV

CALCULATED INTERNAL COORDINATE DISTRIBUTIONS
ALPHA RIBOSE C1-D RING CONFORMATION 1-2-3-4 = E-A-E-A

C-H AND O-H STRETCH CONTRIBUTION

	CH15	CH16	CH17	CH18	CH19	CH20	OH11	OH12	OH13	OH14
3357.	0.	0.	0.	0.	0.	0.	98.	2.	0.	0.
3356.	0.	0.	0.	0.	0.	0.	0.	1.	42.	56.
3356.	0.	0.	0.	0.	0.	0.	1.	78.	8.	13.
2941.	0.	0.	12.	21.	28.	38.	0.	0.	0.	0.
3356.	0.	0.	0.	0.	0.	0.	1.	19.	49.	31.
3000.	50.	48.	0.	0.	0.	0.	0.	0.	0.	0.
2940.	0.	0.	20.	19.	4.	56.	0.	0.	0.	0.
2938.	0.	0.	0.	43.	53.	3.	0.	0.	0.	0.
2938.	0.	0.	67.	16.	14.	2.	0.	0.	0.	0.
2888.	49.	51.	0.	0.	0.	0.	0.	0.	0.	0.

TORSIONAL BENDING CONTRIBUTION

	T1-2	T2-3	T3-4	T4-5	T510	T101	T1-6	T2-7	T3-8	T4-9
882.	0.	0.	0.	0.	0.	0.	2.	0.	0.	0.
856.	0.	0.	0.	0.	0.	0.	0.	0.	0.	0.
823.	0.	0.	0.	0.	0.	1.	0.	0.	0.	0.
740.	0.	0.	0.	0.	1.	0.	0.	0.	0.	0.
672.	0.	0.	0.	0.	2.	2.	0.	0.	0.	1.
531.	0.	0.	0.	0.	1.	0.	2.	0.	1.	1.
485.	0.	0.	0.	2.	3.	2.	5.	1.	3.	0.
447.	0.	0.	0.	5.	6.	0.	8.	1.	0.	2.
445.	0.	0.	0.	1.	5.	3.	0.	1.	3.	0.
377.	0.	0.	0.	0.	1.	0.	13.	22.	15.	0.
367.	0.	0.	0.	1.	3.	2.	11.	22.	2.	26.
361.	1.	0.	0.	0.	0.	0.	7.	21.	12.	31.
338.	0.	0.	0.	0.	1.	0.	15.	0.	46.	12.
299.	1.	0.	0.	0.	0.	2.	0.	14.	1.	10.
294.	1.	1.	0.	0.	2.	1.	27.	3.	0.	3.
279.	0.	1.	1.	0.	0.	4.	0.	1.	4.	1.
260.	2.	2.	0.	0.	0.	11.	1.	2.	2.	4.
218.	1.	1.	6.	0.	0.	1.	1.	2.	2.	0.
135.	5.	1.	21.	17.	0.	11.	0.	0.	0.	1.
129.	19.	27.	5.	1.	4.	1.	0.	0.	0.	0.

TABLE LXXV (Continued)

CALCULATED INTERNAL COORDINATE DISTRIBUTIONS
ALPHA RIBOSE C1-D RING CONFORMATION 1-2-3-4 = E-A-E-A

C-H BENDING CONTRIBUTION

	HO6C	HO7C	HO8C	HO9C	15C'	16C'	HC4O	HC3O	HC2O	HC1O	H1O'	HC1C	C2CH	HC2C	C3CH	HC3C	C4CH	HC4C	C515	C516	BHCH
1474.	0.	0.	0.	3.	0.	0.	1.	0.	0.	0.	0.	0.	0.	0.	0.	0.	1.	4.	15.	15.	47.
1447.	7.	3.	17.	1.	0.	1.	1.	1.	1.	1.	2.	0.	7.	15.	5.	11.	8.	2.	0.	0.	1.
1435.	24.	2.	12.	1.	0.	0.	0.	1.	0.	7.	1.	7.	0.	0.	4.	0.	2.	1.	0.	1.	0.
1402.	4.	0.	2.	13.	13.	16.	2.	0.	1.	2.	10.	2.	2.	0.	4.	2.	2.	9.	4.	1.	11.
1389.	4.	41.	2.	0.	5.	5.	1.	1.	8.	3.	3.	0.	1.	3.	5.	2.	1.	2.	0.	1.	3.
1373.	5.	17.	8.	5.	5.	6.	3.	7.	1.	4.	4.	0.	0.	2.	2.	16.	0.	1.	0.	5.	2.
1364.	2.	5.	0.	48.	0.	2.	2.	2.	1.	3.	17.	4.	0.	0.	3.	0.	1.	0.	0.	3.	1.
1334.	1.	1.	3.	4.	1.	0.	2.	2.	4.	32.	8.	4.	23.	8.	0.	3.	0.	0.	2.	0.	0.
1313.	7.	3.	28.	2.	0.	1.	2.	1.	3.	1.	22.	10.	3.	0.	6.	2.	6.	2.	0.	1.	0.
1296.	12.	6.	0.	6.	10.	2.	1.	13.	10.	13.	0.	7.	0.	3.	2.	4.	2.	4.	12.	1.	0.
1286.	9.	2.	3.	1.	9.	0.	7.	5.	2.	3.	2.	0.	5.	8.	2.	0.	22.	10.	4.	0.	0.
1266.	7.	1.	5.	4.	0.	2.	30.	13.	1.	4.	1.	4.	5.	4.	4.	0.	1.	9.	0.	1.	0.
1240.	9.	8.	1.	1.	8.	6.	15.	1.	33.	6.	1.	2.	6.	2.	0.	0.	4.	2.	5.	3.	0.
1233.	0.	0.	10.	4.	0.	8.	17.	30.	4.	0.	3.	3.	0.	4.	14.	1.	0.	6.	1.	7.	0.
1226.	1.	4.	4.	0.	16.	26.	0.	10.	17.	0.	2.	2.	1.	3.	0.	5.	3.	1.	3.	11.	0.
1157.	0.	1.	0.	0.	1.	4.	11.	14.	1.	3.	0.	1.	2.	1.	2.	8.	3.	1.	10.	4.	0.
1136.	0.	0.	0.	1.	0.	1.	2.	0.	1.	2.	0.	1.	0.	2.	1.	1.	1.	0.	4.	0.	0.
1104.	1.	0.	0.	1.	18.	4.	3.	2.	2.	1.	4.	0.	0.	0.	1.	0.	2.	1.	0.	4.	0.
1079.	4.	0.	2.	2.	0.	1.	1.	1.	13.	1.	15.	3.	2.	0.	2.	5.	0.	2.	4.	4.	1.
1072.	0.	1.	0.	0.	0.	0.	0.	1.	0.	12.	0.	6.	4.	1.	3.	0.	1.	1.	1.	1.	0.
1018.	0.	1.	1.	0.	1.	0.	4.	0.	3.	2.	0.	0.	1.	3.	8.	6.	4.	1.	4.	2.	1.
1005.	0.	0.	1.	2.	1.	1.	0.	0.	0.	2.	0.	0.	6.	0.	0.	0.	2.	8.	1.	1.	2.
954.	0.	4.	0.	0.	0.	0.	2.	1.	0.	0.	2.	6.	1.	6.	1.	1.	6.	0.	6.	5.	0.
907.	1.	1.	0.	0.	1.	0.	0.	0.	0.	1.	1.	2.	0.	5.	0.	1.	1.	0.	1.	1.	1.
882.	0.	0.	0.	1.	1.	0.	0.	1.	0.	1.	0.	15.	1.	1.	0.	0.	0.	4.	0.	4.	2.
856.	2.	0.	0.	1.	0.	0.	0.	0.	1.	0.	1.	5.	0.	1.	0.	0.	1.	5.	1.	0.	0.
823.	0.	0.	1.	2.	0.	0.	0.	0.	0.	0.	0.	1.	1.	2.	4.	6.	3.	3.	0.	1.	0.
740.	1.	1.	1.	0.	0.	0.	0.	0.	0.	1.	3.	0.	4.	0.	2.	2.	0.	0.	0.	0.	0.
672.	0.	0.	0.	0.	0.	0.	0.	0.	0.	1.	0.	0.	1.	3.	0.	2.	0.	1.	2.	2.	1.
531.	0.	0.	0.	1.	0.	0.	0.	0.	0.	1.	0.	2.	2.	2.	0.	0.	4.	3.	2.	0.	0.
485.	0.	0.	0.	0.	0.	0.	0.	0.	0.	0.	2.	2.	1.	3.	0.	0.	2.	0.	0.	0.	0.
447.	0.	0.	0.	0.	1.	0.	0.	0.	0.	0.	0.	1.	2.	1.	0.	0.	0.	1.	0.	0.	0.
445.	0.	0.	0.	0.	0.	0.	0.	0.	0.	0.	0.	0.	0.	1.	0.	0.	0.	1.	0.	0.	0.
377.	0.	0.	0.	0.	0.	0.	0.	0.	0.	0.	0.	0.	0.	2.	0.	0.	1.	0.	0.	0.	0.
367.	0.	0.	0.	0.	1.	0.	0.	0.	0.	0.	0.	0.	1.	0.	0.	0.	1.	2.	0.	2.	1.
361.	0.	0.	0.	0.	0.	0.	0.	0.	0.	0.	0.	0.	1.	1.	1.	1.	2.	1.	0.	0.	0.
338.	0.	0.	0.	0.	0.	0.	0.	0.	0.	0.	1.	2.	0.	1.	3.	4.	0.	1.	1.	0.	0.
299.	0.	0.	0.	0.	1.	0.	0.	0.	0.	0.	0.	1.	1.	2.	0.	0.	3.	0.	0.	2.	0.
294.	0.	0.	0.	0.	0.	0.	0.	0.	0.	0.	13.	15.	4.	0.	1.	1.	0.	0.	1.	0.	0.
279.	0.	0.	0.	0.	0.	0.	0.	0.	0.	0.	1.	0.	0.	0.	0.	0.	1.	1.	1.	0.	0.
260.	0.	0.	0.	0.	1.	0.	0.	0.	0.	1.	0.	0.	1.	3.	1.	2.	3.	0.	0.	2.	1.
218.	0.	1.	0.	0.	0.	0.	0.	0.	0.	0.	1.	5.	5.	0.	7.	3.	0.	2.	0.	0.	0.
135.	0.	0.	0.	0.	0.	1.	3.	0.	0.	0.	0.	0.	0.	0.	1.	0.	0.	0.	0.	0.	1.
129.	0.	0.	0.	0.	0.	0.	0.	0.	4.	0.	0.	1.	0.	0.	0.	0.	0.	0.	0.	2.	0.

TABLE LXXV (Continued)

CALCULATED INTERNAL COORDINATE DISTRIBUTIONS
ALPHA RIBOSE C1-D RING CONFORMATION 1-2-3-4 = E-A-E-A

HEAVY ATOM STRETCH CONTRIBUTION

	C1C2	C2C3	C3C4	C4C5	C5O'	O'C1	C1C6	C2C7	C3C8	C4C9
1474.	0.	0.	0.	0.	0.	0.	0.	0.	0.	1.
1447.	0.	1.	2.	0.	0.	1.	0.	1.	0.	1.
1435.	6.	3.	2.	0.	0.	2.	1.	5.	0.	0.
1402.	0.	0.	1.	0.	1.	0.	0.	1.	0.	0.
1389.	2.	4.	0.	0.	0.	0.	0.	3.	0.	0.
1373.	0.	0.	2.	0.	0.	0.	0.	0.	0.	3.
1364.	1.	0.	2.	2.	0.	0.	0.	1.	0.	0.
1334.	0.	0.	0.	1.	0.	2.	0.	0.	0.	2.
1313.	0.	0.	0.	0.	0.	0.	0.	0.	0.	1.
1296.	0.	2.	1.	2.	0.	0.	0.	0.	0.	3.
1286.	0.	0.	0.	0.	1.	0.	0.	0.	0.	1.
1266.	0.	0.	0.	1.	2.	0.	1.	1.	0.	3.
1240.	0.	1.	1.	1.	1.	2.	0.	3.	0.	0.
1233.	0.	0.	0.	0.	0.	0.	1.	0.	0.	3.
1226.	0.	0.	0.	1.	2.	2.	1.	3.	0.	0.
1157.	0.	2.	14.	7.	6.	8.	1.	4.	6.	18.
1136.	3.	8.	2.	6.	7.	0.	24.	2.	42.	0.
1104.	0.	2.	2.	27.	21.	9.	12.	1.	0.	0.
1079.	10.	5.	2.	12.	2.	5.	6.	17.	0.	4.
1072.	20.	13.	0.	1.	7.	1.	37.	4.	33.	0.
1018.	0.	21.	13.	5.	12.	19.	1.	6.	3.	12.
1005.	2.	14.	20.	12.	7.	7.	9.	8.	1.	7.
954.	33.	8.	5.	5.	3.	9.	0.	0.	13.	13.
907.	21.	0.	1.	12.	11.	0.	0.	23.	0.	19.
882.	0.	5.	15.	1.	8.	20.	4.	4.	1.	1.
856.	0.	6.	9.	3.	6.	3.	1.	21.	0.	11.
823.	2.	1.	0.	0.	4.	6.	0.	6.	0.	10.
740.	1.	1.	0.	1.	11.	33.	4.	0.	1.	0.
672.	0.	0.	19.	2.	2.	2.	3.	0.	2.	2.
531.	6.	11.	1.	0.	1.	0.	5.	0.	1.	0.
485.	4.	4.	0.	0.	0.	0.	0.	0.	0.	0.
447.	2.	0.	0.	2.	5.	1.	0.	0.	0.	0.
445.	4.	1.	3.	8.	0.	0.	0.	0.	4.	0.
377.	4.	0.	0.	0.	0.	0.	1.	0.	1.	0.
367.	0.	0.	0.	1.	1.	1.	0.	0.	0.	0.
361.	0.	4.	2.	0.	1.	0.	0.	0.	0.	0.
338.	0.	0.	1.	0.	0.	0.	0.	0.	0.	0.
299.	0.	0.	1.	0.	1.	0.	0.	0.	0.	0.
294.	3.	2.	0.	0.	0.	4.	0.	0.	0.	0.
279.	4.	1.	0.	3.	0.	0.	0.	0.	0.	0.
260.	0.	0.	0.	0.	1.	0.	0.	0.	0.	0.
218.	3.	2.	1.	0.	0.	1.	0.	1.	2.	0.
135.	0.	0.	1.	0.	0.	0.	0.	0.	0.	0.
129.	0.	0.	0.	0.	0.	0.	1.	0.	1.	0.

CALCULATED INTERNAL COORDINATE DISTRIBUTIONS
ALPHA RIBOSE C1-D RING CONFORMATION 1-2-3-4 = E-A-E-A

HEAVY ATOM BEND CONTRIBUTION

	BC2C	BC3C	BC4C	BC5O	BCOC	O'C2	O'C6	B612	B721	B723	B832	B834	B943	B945
1474.	0.	0.	0.	0.	0.	0.	0.	0.	0.	0.	0.	0.	1.	0.
1447.	0.	0.	0.	0.	0.	0.	0.	1.	0.	0.	2.	1.	0.	0.
1435.	3.	0.	0.	0.	0.	0.	0.	3.	0.	0.	2.	0.	0.	0.
1402.	0.	0.	0.	0.	0.	0.	0.	0.	0.	0.	0.	0.	0.	0.
1389.	0.	0.	0.	0.	0.	0.	0.	0.	2.	0.	0.	0.	0.	0.
1373.	0.	0.	1.	0.	0.	0.	0.	0.	0.	0.	0.	0.	0.	0.
1364.	0.	0.	0.	0.	0.	0.	0.	0.	0.	0.	0.	0.	1.	0.
1334.	0.	0.	0.	0.	0.	0.	0.	1.	0.	0.	0.	0.	0.	0.
1313.	0.	0.	0.	0.	0.	0.	0.	0.	0.	0.	0.	0.	0.	0.
1296.	0.	0.	1.	0.	0.	0.	0.	0.	0.	0.	0.	1.	0.	0.
1286.	0.	0.	0.	0.	0.	0.	0.	0.	0.	0.	0.	0.	0.	0.
1266.	0.	1.	0.	0.	0.	0.	0.	0.	0.	0.	0.	0.	1.	0.
1240.	0.	1.	0.	0.	0.	0.	0.	0.	1.	0.	0.	0.	0.	0.
1233.	0.	0.	0.	0.	0.	0.	0.	0.	0.	0.	0.	0.	0.	0.
1226.	0.	0.	0.	0.	0.	1.	0.	0.	0.	0.	0.	0.	0.	0.
1157.	0.	2.	3.	0.	0.	1.	0.	0.	0.	0.	0.	1.	0.	1.
1136.	2.	4.	5.	0.	1.	2.	1.	0.	0.	0.	0.	4.	0.	0.
1104.	2.	1.	0.	0.	5.	2.	1.	2.	0.	0.	0.	1.	0.	6.
1079.	6.	0.	0.	1.	0.	0.	1.	5.	1.	0.	3.	0.	2.	1.
1072.	0.	1.	1.	0.	0.	5.	0.	1.	1.	4.	1.	2.	0.	0.
1018.	2.	0.	1.	1.	1.	0.	0.	1.	1.	1.	2.	2.	0.	0.
1005.	0.	1.	0.	4.	1.	3.	1.	0.	1.	5.	1.	0.	3.	0.
954.	0.	4.	0.	0.	0.	0.	2.	0.	5.	0.	0.	1.	1.	1.
907.	1.	0.	0.	1.	0.	0.	1.	2.	3.	1.	1.	1.	0.	2.
882.	1.	0.	2.	6.	3.	7.	9.	0.	3.	0.	1.	1.	1.	1.
856.	1.	1.	3.	2.	3.	0.	4.	3.	1.	1.	0.	2.	1.	2.
823.	0.	11.	1.	5.	4.	2.	3.	0.	0.	7.	2.	1.	8.	1.
740.	1.	0.	0.	0.	5.	5.	3.	5.	9.	4.	6.	2.	3.	0.
672.	0.	1.	1.	19.	5.	0.	2.	0.	1.	5.	1.	0.	6.	10.
531.	2.	0.	0.	1.	13.	11.	15.	1.	0.	1.	1.	2.	3.	8.
485.	0.	0.	3.	0.	1.	1.	11.	15.	1.	4.	18.	18.	10.	7.
447.	2.	2.	4.	2.	30.	0.	10.	3.	1.	0.	1.	1.	0.	14.
445.	2.	9.	13.	2.	1.	7.	6.	0.	0.	0.	2.	13.	0.	1.
377.	9.	1.	1.	2.	1.	2.	0.	7.	0.	12.	3.	1.	2.	0.
367.	1.	0.	0.	2.	6.	0.	0.	0.	9.	0.	4.	0.	0.	2.
361.	0.	1.	0.	1.	4.	0.	0.	0.	0.	1.	0.	2.	2.	1.
338.	1.	0.	3.	0.	0.	1.	3.	0.	1.	1.	3.	2.	9.	1.
299.	0.	1.	7.	2.	5.	0.	0.	3.	23.	12.	0.	1.	2.	12.
294.	1.	0.	1.	0.	1.	3.	21.	25.	3.	3.	4.	0.	9.	2.
279.	7.	0.	5.	1.	1.	1.	3.	6.	2.	3.	17.	18.	14.	1.
260.	3.	0.	7.	3.	9.	1.	0.	1.	22.	5.	8.	6.	0.	19.
218.	17.	4.	7.	0.	1.	1.	2.	1.	6.	21.	3.	5.	16.	0.
135.	1.	10.	3.	7.	1.	4.	1.	0.	0.	2.	1.	1.	0.	1.
129.	7.	11.	0.	3.	0.	5.	3.	0.	0.	0.	2.	3.	1.	1.

TABLE LXXVI

CALCULATED INTERNAL COORDINATE DISTRIBUTIONS
BETA RIBOSE C1-D RING CONFORMATION 1-2-3-4 = A-A-E-A

C-H AND O-H STRETCH CONTRIBUTION

	CH15	CH16	CH17	CH18	CH19	CH20	OH11	OH12	OH13	OH14
3357.	0.	0.	0.	0.	0.	0.	98.	2.	0.	0.
3356.	0.	0.	0.	0.	0.	0.	2.	84.	5.	9.
3356.	0.	0.	0.	0.	0.	0.	0.	1.	44.	55.
3356.	0.	0.	0.	0.	0.	0.	0.	13.	51.	36.
2942.	0.	0.	0.	0.	4.	94.	0.	0.	0.	0.
3000.	50.	48.	0.	0.	0.	0.	0.	0.	0.	0.
2941.	0.	0.	28.	42.	27.	1.	0.	0.	0.	0.
2938.	0.	0.	4.	51.	42.	3.	0.	0.	0.	0.
2938.	0.	0.	67.	6.	26.	0.	0.	0.	0.	0.
2888.	49.	51.	0.	0.	0.	0.	0.	0.	0.	0.

TORSIONAL BENDING CONTRIBUTION

	T1-2	T2-3	T3-4	T4-5	T510	T101	T1-6	T2-7	T3-8	T4-9
891.	0.	0.	0.	0.	2.	0.	0.	0.	0.	0.
832.	0.	0.	0.	0.	0.	1.	0.	0.	0.	0.
799.	0.	0.	0.	0.	0.	0.	0.	0.	0.	0.
720.	0.	0.	0.	0.	0.	2.	1.	0.	0.	0.
651.	0.	0.	0.	0.	5.	2.	0.	0.	0.	1.
591.	0.	0.	0.	1.	5.	1.	1.	0.	0.	0.
491.	0.	0.	0.	0.	0.	0.	2.	0.	3.	0.
453.	0.	0.	0.	4.	10.	2.	1.	1.	0.	1.
445.	0.	0.	0.	1.	0.	0.	1.	2.	5.	0.
396.	0.	0.	0.	0.	0.	0.	17.	1.	2.	13.
362.	1.	0.	0.	0.	0.	0.	1.	54.	5.	11.
359.	0.	0.	0.	0.	1.	1.	38.	14.	0.	26.
345.	0.	0.	0.	0.	0.	0.	1.	2.	63.	17.
310.	0.	1.	0.	0.	0.	0.	21.	4.	5.	17.
280.	0.	0.	1.	1.	1.	0.	0.	10.	3.	0.
273.	0.	4.	0.	0.	5.	0.	1.	0.	3.	3.
208.	1.	1.	3.	2.	0.	16.	4.	0.	1.	1.
202.	5.	0.	2.	1.	0.	0.	1.	3.	1.	0.
142.	13.	1.	11.	17.	0.	11.	0.	0.	0.	1.
127.	8.	27.	15.	0.	4.	1.	0.	0.	0.	0.

TABLE LXXVI (Continued)

CALCULATED INTERNAL COORDINATE DISTRIBUTIONS
BETA RIBOSE C1-D RING CONFORMATION 1-2-3-4 = A-A-E-A

C-H BENDING CONTRIBUTION

	HO6C	HO7C	HO8C	HO9C	15C'	16C'	HC4O	HC3O	HC2O	HC1O	H1O'	HC1C	C2CH	HC2C	C3CH	HC3C	C4CH	HC4C	C515	C516	BHCH
1473.	0.	0.	0.	3.	0.	0.	1.	0.	0.	0.	0.	0.	0.	0.	0.	0.	1.	4.	16.	16.	47.
1448.	1.	13.	17.	1.	1.	2.	1.	0.	3.	2.	0.	4.	3.	14.	3.	8.	8.	2.	0.	0.	1.
1437.	25.	12.	9.	1.	0.	0.	0.	2.	4.	4.	1.	4.	5.	0.	1.	0.	2.	0.	0.	0.	0.
1397.	1.	0.	5.	21.	17.	15.	4.	0.	0.	0.	2.	0.	0.	1.	2.	0.	1.	9.	4.	1.	13.
1385.	4.	1.	0.	5.	5.	10.	3.	0.	1.	7.	2.	0.	0.	1.	15.	17.	0.	1.	0.	7.	2.
1378.	18.	18.	6.	4.	0.	0.	0.	4.	0.	6.	24.	3.	1.	3.	0.	6.	2.	1.	0.	1.	0.
1353.	1.	5.	8.	42.	1.	4.	2.	4.	1.	1.	0.	0.	1.	0.	12.	2.	4.	0.	1.	3.	0.
1337.	4.	3.	13.	1.	2.	0.	1.	6.	3.	12.	25.	2.	5.	10.	1.	1.	0.	1.	1.	0.	0.
1325.	0.	13.	3.	0.	0.	0.	0.	0.	12.	16.	5.	21.	20.	2.	0.	1.	2.	2.	0.	0.	0.
1302.	18.	5.	0.	5.	4.	3.	1.	9.	0.	15.	6.	0.	3.	3.	1.	4.	5.	6.	10.	1.	0.
1284.	1.	4.	16.	0.	3.	0.	21.	17.	11.	2.	0.	0.	0.	3.	4.	0.	21.	3.	0.	1.	0.
1261.	16.	3.	4.	0.	9.	2.	10.	6.	0.	7.	1.	7.	7.	6.	1.	0.	1.	12.	6.	1.	1.
1245.	4.	10.	1.	8.	0.	1.	35.	5.	20.	2.	0.	1.	6.	1.	2.	1.	2.	8.	0.	2.	0.
1241.	0.	3.	4.	1.	15.	30.	0.	0.	11.	1.	0.	0.	2.	1.	2.	0.	3.	2.	8.	18.	0.
1219.	0.	6.	9.	0.	9.	5.	6.	36.	26.	2.	4.	0.	1.	8.	6.	6.	2.	0.	4.	3.	0.
1152.	1.	0.	0.	0.	5.	9.	11.	13.	0.	4.	3.	0.	1.	0.	2.	4.	2.	1.	6.	2.	0.
1125.	0.	0.	0.	1.	10.	1.	5.	2.	2.	2.	0.	0.	1.	3.	5.	1.	1.	0.	3.	0.	0.
1104.	0.	0.	0.	0.	5.	3.	1.	0.	1.	1.	0.	0.	1.	1.	0.	0.	0.	1.	6.	5.	0.
1080.	1.	0.	2.	1.	1.	0.	0.	1.	8.	1.	0.	10.	0.	1.	5.	11.	2.	2.	2.	6.	1.
1053.	0.	0.	0.	1.	0.	0.	1.	0.	2.	15.	1.	5.	4.	0.	0.	0.	1.	2.	0.	1.	1.
1041.	1.	1.	0.	0.	2.	0.	0.	1.	1.	0.	7.	1.	3.	0.	0.	1.	0.	1.	0.	0.	1.
989.	0.	0.	1.	0.	0.	0.	5.	0.	1.	0.	3.	1.	4.	1.	8.	3.	8.	1.	8.	6.	1.
962.	3.	1.	1.	2.	0.	0.	0.	1.	1.	1.	14.	3.	0.	3.	0.	0.	0.	8.	1.	2.	1.
926.	0.	1.	0.	1.	0.	0.	0.	0.	0.	0.	5.	10.	3.	7.	0.	2.	4.	4.	2.	1.	0.
891.	1.	2.	0.	1.	1.	0.	0.	1.	0.	1.	4.	2.	1.	6.	0.	1.	0.	1.	1.	6.	2.
832.	0.	0.	2.	1.	0.	0.	0.	0.	0.	0.	2.	0.	0.	1.	3.	5.	1.	0.	0.	0.	0.
799.	0.	1.	0.	1.	0.	0.	0.	0.	0.	0.	1.	1.	2.	1.	0.	0.	1.	3.	0.	0.	0.
720.	1.	0.	1.	1.	0.	0.	0.	0.	0.	0.	3.	3.	0.	0.	2.	2.	1.	1.	0.	0.	0.
651.	0.	0.	0.	0.	0.	0.	0.	0.	0.	0.	0.	5.	0.	3.	0.	2.	2.	3.	3.	2.	2.
591.	0.	1.	0.	0.	0.	0.	0.	0.	1.	4.	0.	2.	6.	2.	0.	0.	1.	1.	1.	1.	0.
491.	1.	0.	0.	0.	0.	0.	0.	0.	0.	0.	2.	0.	0.	2.	0.	0.	2.	0.	0.	0.	0.
453.	0.	0.	1.	0.	0.	0.	0.	0.	0.	1.	0.	1.	0.	0.	0.	0.	0.	0.	0.	0.	0.
445.	0.	0.	0.	0.	0.	0.	0.	0.	0.	0.	0.	0.	0.	4.	0.	1.	0.	0.	0.	0.	0.
396.	0.	0.	0.	0.	0.	0.	0.	0.	0.	1.	0.	2.	0.	0.	0.	0.	1.	2.	0.	2.	1.
362.	0.	0.	0.	0.	0.	0.	0.	0.	0.	0.	0.	0.	2.	2.	2.	1.	1.	0.	0.	0.	0.
359.	0.	0.	0.	0.	0.	0.	0.	0.	0.	0.	1.	2.	1.	0.	0.	0.	2.	1.	0.	1.	0.
345.	0.	0.	0.	0.	0.	0.	0.	0.	0.	0.	1.	0.	0.	0.	3.	4.	0.	1.	0.	0.	0.
310.	0.	0.	0.	1.	0.	0.	0.	0.	0.	1.	4.	12.	0.	0.	0.	2.	6.	0.	0.	1.	0.
280.	0.	0.	0.	0.	0.	0.	0.	0.	0.	1.	0.	1.	1.	3.	0.	1.	0.	1.	0.	1.	0.
273.	1.	0.	0.	0.	0.	0.	0.	0.	0.	2.	6.	0.	1.	1.	2.	2.	0.	1.	2.	0.	0.
208.	0.	0.	0.	0.	1.	0.	0.	0.	0.	0.	2.	7.	0.	2.	2.	0.	1.	0.	0.	1.	1.
202.	0.	1.	0.	0.	2.	0.	0.	0.	0.	2.	13.	5.	7.	0.	4.	3.	0.	1.	0.	1.	0.
142.	0.	0.	0.	0.	0.	1.	3.	0.	1.	8.	1.	0.	0.	0.	1.	0.	0.	0.	0.	0.	1.
127.	0.	0.	0.	0.	0.	0.	1.	0.	4.	1.	0.	0.	0.	0.	0.	0.	0.	0.	0.	1.	0.

TABLE LXXVI (Continued)

CALCULATED INTERNAL COORDINATE DISTRIBUTIONS
BETA RIBOSE C1-D RING CONFORMATION 1-2-3-4 = A-A-E-A

HEAVY ATOM STRETCH CONTRIBUTION

	C1C2	C2C3	C3C4	C4C5	C5O'	O'C1	C1C6	C2O7	C3O8	C4O9
1473.	0.	0.	0.	0.	0.	0.	0.	0.	0.	1.
1448.	2.	0.	2.	0.	0.	0.	0.	0.	0.	1.
1437.	4.	7.	1.	0.	0.	1.	1.	2.	0.	0.
1397.	0.	0.	2.	0.	1.	0.	0.	0.	0.	0.
1385.	1.	1.	2.	0.	0.	1.	0.	4.	0.	3.
1378.	0.	1.	1.	0.	1.	0.	0.	0.	0.	1.
1353.	1.	0.	1.	3.	1.	0.	0.	2.	0.	1.
1337.	1.	0.	0.	0.	2.	3.	0.	0.	1.	0.
1325.	0.	1.	0.	0.	1.	0.	0.	0.	0.	0.
1302.	0.	1.	2.	2.	0.	0.	1.	0.	0.	4.
1284.	0.	0.	0.	0.	0.	0.	0.	0.	0.	0.
1261.	0.	0.	0.	0.	0.	0.	1.	0.	1.	0.
1245.	0.	0.	0.	1.	2.	1.	1.	0.	0.	4.
1241.	0.	1.	1.	0.	1.	3.	0.	3.	0.	3.
1219.	0.	1.	1.	0.	0.	0.	1.	1.	0.	0.
1152.	2.	1.	13.	8.	4.	2.	0.	12.	2.	20.
1125.	0.	19.	2.	19.	22.	8.	2.	4.	25.	0.
1104.	3.	2.	1.	6.	4.	3.	8.	2.	41.	0.
1080.	6.	7.	7.	8.	1.	7.	1.	23.	13.	1.
1053.	21.	3.	4.	21.	0.	5.	59.	2.	2.	1.
1041.	9.	7.	0.	5.	1.	0.	30.	23.	2.	4.
989.	0.	16.	20.	0.	21.	7.	0.	2.	2.	16.
962.	23.	0.	16.	3.	8.	3.	0.	6.	0.	11.
926.	13.	13.	0.	10.	0.	26.	0.	0.	9.	15.
891.	10.	1.	9.	9.	24.	6.	3.	9.	0.	6.
832.	1.	11.	6.	2.	0.	3.	0.	10.	1.	21.
799.	0.	4.	4.	1.	26.	41.	0.	0.	0.	1.
720.	4.	14.	5.	0.	1.	14.	1.	1.	3.	0.
651.	1.	2.	14.	2.	0.	1.	0.	0.	1.	2.
591.	8.	5.	2.	0.	0.	0.	2.	0.	0.	0.
491.	0.	1.	0.	0.	0.	0.	1.	5.	0.	0.
453.	10.	0.	3.	1.	1.	0.	0.	0.	4.	0.
445.	0.	2.	0.	7.	0.	0.	0.	0.	1.	0.
396.	3.	0.	0.	2.	0.	0.	2.	0.	0.	0.
362.	0.	4.	2.	0.	0.	0.	0.	0.	0.	0.
359.	0.	0.	1.	1.	1.	0.	0.	0.	0.	0.
345.	0.	1.	1.	0.	0.	0.	0.	0.	0.	0.
310.	1.	0.	1.	0.	0.	2.	1.	0.	0.	0.
280.	2.	0.	0.	2.	0.	0.	1.	0.	0.	0.
273.	0.	0.	1.	1.	0.	2.	1.	1.	0.	0.
208.	1.	0.	0.	0.	2.	2.	1.	1.	0.	0.
202.	3.	1.	1.	0.	1.	6.	0.	2.	1.	1.
142.	1.	0.	0.	0.	0.	0.	1.	0.	0.	0.
127.	0.	0.	0.	0.	0.	0.	0.	0.	1.	0.

CALCULATED INTERNAL COORDINATE DISTRIBUTIONS
BETA RIBOSE C1-D RING CONFORMATION 1-2-3-4 = A-A-E-A

HEAVY ATOM BEND CONTRIBUTION

	BC2C	BC3C	BC4C	BC5O	BCOC	O'C2	O'C6	B612	B721	B723	B832	B834	B943	B945
1473.	0.	0.	0.	0.	0.	0.	0.	0.	0.	0.	0.	0.	1.	0.
1448.	0.	0.	0.	0.	0.	0.	0.	0.	1.	0.	2.	1.	0.	0.
1437.	0.	0.	0.	0.	0.	0.	0.	3.	2.	0.	0.	0.	0.	0.
1397.	0.	0.	0.	0.	0.	0.	0.	0.	0.	0.	0.	0.	1.	0.
1385.	1.	0.	1.	0.	0.	0.	0.	0.	0.	0.	0.	0.	0.	0.
1378.	0.	0.	0.	0.	0.	0.	0.	0.	0.	0.	0.	0.	0.	0.
1353.	1.	0.	0.	0.	0.	0.	0.	0.	0.	0.	0.	0.	1.	0.
1337.	0.	0.	0.	0.	0.	0.	0.	0.	0.	0.	0.	0.	0.	0.
1325.	0.	0.	0.	0.	0.	0.	0.	0.	0.	0.	0.	0.	0.	0.
1302.	0.	0.	1.	0.	0.	0.	0.	0.	0.	0.	0.	1.	0.	0.
1284.	1.	1.	0.	0.	0.	0.	0.	0.	0.	0.	0.	0.	1.	0.
1261.	0.	0.	0.	0.	0.	0.	0.	0.	0.	0.	0.	0.	0.	0.
1245.	0.	0.	0.	0.	0.	0.	0.	0.	0.	0.	0.	0.	1.	0.
1241.	0.	0.	0.	0.	0.	0.	0.	0.	0.	0.	0.	0.	0.	0.
1219.	0.	0.	0.	0.	0.	0.	0.	0.	0.	0.	0.	0.	0.	0.
1152.	0.	1.	4.	0.	0.	0.	0.	0.	0.	1.	0.	2.	0.	1.
1125.	0.	4.	4.	0.	1.	2.	1.	0.	0.	0.	0.	4.	0.	3.
1104.	1.	1.	2.	0.	3.	3.	0.	0.	0.	0.	1.	0.	0.	2.
1080.	11.	1.	1.	0.	0.	0.	2.	1.	1.	0.	5.	1.	2.	1.
1053.	1.	0.	0.	1.	1.	6.	2.	1.	1.	2.	0.	0.	1.	2.
1041.	0.	0.	0.	0.	4.	2.	5.	1.	2.	6.	1.	0.	0.	0.
989.	1.	0.	1.	1.	0.	0.	0.	0.	0.	2.	1.	4.	0.	0.
962.	0.	1.	0.	6.	2.	1.	0.	6.	4.	1.	1.	1.	2.	1.
926.	0.	4.	1.	1.	0.	1.	3.	1.	1.	0.	1.	0.	3.	3.
891.	2.	1.	1.	8.	0.	3.	0.	4.	5.	1.	1.	0.	1.	0.
832.	0.	5.	0.	1.	2.	0.	0.	1.	0.	3.	3.	4.	3.	0.
799.	0.	6.	1.	1.	3.	1.	1.	0.	1.	2.	0.	1.	2.	1.
720.	1.	1.	0.	0.	17.	1.	2.	1.	2.	10.	3.	1.	8.	0.
651.	1.	0.	2.	21.	0.	0.	6.	0.	0.	2.	1.	1.	3.	15.
591.	1.	0.	1.	1.	5.	17.	25.	1.	11.	0.	0.	1.	1.	0.
491.	5.	2.	0.	1.	5.	2.	7.	32.	4.	4.	8.	6.	7.	0.
453.	0.	4.	21.	0.	4.	1.	1.	0.	1.	1.	10.	0.	1.	18.
445.	5.	4.	0.	2.	6.	4.	1.	2.	6.	8.	3.	26.	5.	3.
396.	0.	1.	1.	6.	7.	2.	10.	1.	5.	3.	8.	1.	0.	12.
362.	2.	1.	0.	0.	2.	0.	0.	0.	0.	4.	1.	2.	3.	0.
359.	0.	0.	0.	1.	4.	0.	0.	0.	1.	0.	2.	0.	1.	1.
345.	0.	0.	1.	0.	0.	0.	1.	1.	0.	0.	0.	1.	5.	1.
310.	0.	0.	9.	2.	0.	1.	13.	2.	5.	3.	5.	3.	3.	15.
280.	0.	0.	1.	1.	2.	0.	0.	1.	16.	16.	26.	12.	6.	0.
273.	3.	0.	7.	0.	2.	7.	1.	19.	12.	0.	2.	6.	26.	3.
208.	8.	0.	2.	4.	20.	7.	22.	0.	14.	1.	0.	5.	0.	10.
202.	11.	8.	7.	0.	14.	2.	8.	18.	3.	24.	1.	1.	9.	2.
142.	6.	3.	4.	7.	3.	8.	0.	1.	0.	4.	0.	0.	0.	1.
127.	8.	17.	1.	0.	1.	1.	2.	1.	0.	0.	3.	4.	1.	0.

TABLE LXXVII

METHYL ALPHA XYLOPYRANOSIDE

C-H AND O-H STRETCH CONTRIBUTION

CM-1	CH15	CH16	CH17	CH18	CH19	CH20	CH21	CH22	CH23	OH12	OH13	OH14
3356.	0.	0.	0.	0.	0.	0.	0.	0.	0.	24.	71.	5.
3356.	0.	0.	0.	0.	0.	0.	0.	0.	0.	3.	2.	95.
3356.	0.	0.	0.	0.	0.	0.	0.	0.	0.	73.	27.	1.
3000.	48.	49.	1.	0.	0.	0.	0.	0.	0.	0.	0.	0.
2997.	0.	0.	0.	0.	0.	0.	66.	16.	17.	0.	0.	0.
2997.	0.	0.	0.	0.	0.	0.	0.	50.	49.	0.	0.	0.
2953.	0.	0.	22.	49.	24.	2.	0.	0.	0.	0.	0.	0.
2944.	0.	0.	17.	1.	10.	70.	0.	0.	0.	0.	0.	0.
2941.	0.	0.	33.	0.	39.	26.	0.	0.	0.	0.	0.	0.
2934.	0.	0.	26.	48.	25.	0.	0.	0.	0.	0.	0.	0.
2831.	0.	0.	0.	0.	0.	0.	34.	34.	34.	0.	0.	0.
2888.	51.	49.	0.	0.	0.	0.	0.	0.	0.	0.	0.	0.

METHYL ALPHA XYLOPYRANOSIDE

TORSIONAL BEND CONTRIBUTION

CM-1	TCO'	TCO'	TC45	TC34	TC23	TC12	TCO9	TCO8	TCO7	TCO6	TC'O
1098.	0.	1.	0.	0.	0.	0.	0.	0.	0.	0.	0.
1076.	0.	0.	0.	0.	0.	0.	0.	0.	0.	0.	0.
1050.	0.	0.	0.	0.	0.	0.	0.	0.	0.	0.	0.
1037.	0.	8.	2.	0.	0.	0.	0.	0.	0.	0.	0.
998.	1.	2.	0.	0.	0.	0.	0.	0.	0.	0.	0.
962.	1.	0.	0.	0.	0.	0.	0.	0.	0.	0.	1.
920.	0.	3.	1.	0.	0.	0.	0.	0.	0.	0.	1.
901.	1.	0.	0.	0.	0.	0.	0.	0.	1.	0.	2.
889.	1.	0.	0.	0.	0.	0.	0.	0.	1.	0.	1.
749.	2.	0.	0.	0.	0.	0.	0.	0.	0.	0.	3.
671.	1.	4.	0.	0.	0.	0.	0.	0.	0.	0.	8.
583.	1.	1.	1.	1.	0.	0.	0.	0.	1.	0.	1.
563.	0.	0.	0.	0.	0.	0.	0.	0.	0.	0.	52.
515.	1.	2.	0.	0.	0.	0.	0.	0.	0.	0.	15.
508.	0.	2.	0.	0.	0.	0.	0.	0.	0.	0.	8.
434.	0.	1.	0.	0.	0.	1.	2.	1.	1.	1.	0.
412.	2.	7.	0.	0.	1.	1.	1.	2.	1.	0.	2.
382.	1.	0.	0.	0.	1.	0.	20.	11.	1.	0.	0.
359.	0.	0.	0.	0.	0.	0.	31.	48.	9.	0.	0.
353.	0.	0.	0.	0.	0.	0.	3.	26.	45.	0.	0.
341.	1.	0.	0.	0.	0.	0.	39.	4.	14.	0.	0.
319.	2.	9.	0.	0.	0.	0.	0.	1.	6.	0.	0.
278.	0.	0.	0.	0.	0.	0.	1.	5.	1.	0.	0.
275.	0.	0.	0.	1.	0.	1.	1.	0.	9.	0.	0.
247.	11.	1.	0.	3.	3.	1.	0.	0.	2.	2.	1.
182.	1.	1.	0.	0.	5.	9.	0.	0.	0.	0.	1.
121.	6.	1.	2.	34.	12.	0.	0.	0.	0.	3.	0.
111.	3.	4.	1.	0.	13.	19.	0.	0.	0.	6.	0.
62.	2.	0.	0.	1.	0.	2.	0.	0.	0.	87.	0.

TABLE LXXVII (Continued)

METHYL ALPHA XYLOPYRANOSIDE

METHYL GROUP C-H BEND CONTRIBUTION

CM-1	H23O	H22O	H21O	2123	2223	2122
1480.	0.	0.	0.	0.	0.	0.
1457.	9.	5.	25.	26.	1.	14.
1448.	17.	1.	3.	10.	20.	41.
1447.	4.	32.	0.	13.	43.	10.
1443.	8.	1.	5.	15.	0.	0.
1437.	0.	0.	0.	0.	0.	0.
1385.	0.	0.	0.	0.	0.	0.
1373.	0.	0.	0.	0.	0.	0.
1356.	0.	0.	0.	0.	0.	0.
1333.	0.	0.	1.	0.	1.	1.
1313.	0.	0.	0.	0.	0.	0.
1318.	0.	0.	0.	0.	0.	0.
1278.	0.	0.	0.	1.	0.	0.
1263.	0.	0.	0.	0.	0.	0.
1245.	0.	0.	0.	0.	0.	0.
1220.	0.	0.	0.	0.	0.	0.
1192.	0.	0.	0.	0.	0.	0.
1168.	17.	34.	2.	10.	1.	5.
1150.	13.	4.	32.	1.	8.	3.
1138.	11.	2.	4.	0.	1.	3.
1128.	4.	7.	2.	1.	0.	1.
1111.	0.	1.	4.	0.	1.	0.
1098.	0.	0.	0.	0.	0.	0.
1076.	1.	0.	4.	0.	1.	0.
1050.	2.	0.	8.	0.	2.	0.
1037.	0.	0.	0.	0.	0.	0.
998.	0.	0.	0.	0.	0.	0.
962.	0.	0.	0.	0.	0.	0.
920.	0.	0.	0.	0.	0.	0.
901.	0.	0.	1.	0.	0.	0.
889.	0.	0.	0.	0.	0.	0.
749.	0.	0.	0.	0.	0.	0.
671.	0.	1.	0.	0.	0.	0.
583.	0.	0.	0.	0.	0.	0.
563.	0.	0.	0.	0.	0.	0.
515.	0.	0.	0.	0.	0.	0.
508.	0.	0.	0.	0.	0.	0.
434.	0.	0.	0.	0.	0.	0.
412.	0.	0.	0.	0.	0.	0.
382.	0.	0.	0.	0.	0.	0.
359.	0.	0.	0.	0.	0.	0.
353.	0.	0.	0.	0.	0.	0.
341.	0.	0.	0.	0.	0.	0.
319.	0.	0.	1.	0.	0.	0.
278.	0.	0.	0.	0.	0.	0.
275.	0.	0.	0.	0.	0.	0.
247.	0.	0.	0.	0.	0.	0.
182.	0.	0.	0.	0.	0.	0.
121.	0.	0.	0.	0.	0.	0.
111.	0.	0.	0.	0.	0.	0.
62.	0.	0.	0.	0.	0.	0.

METHYL ALPHA XYLOPYRANOSIDE

HEAVY ATOM STRETCH CONTRIBUTIONS

CM-1	C1C2	C2C3	C3C4	C4C5	C5O'	O'C1	C1O6	C2O7	C3O8	C4O9	O6C'
1480.	0.	0.	0.	0.	0.	0.	0.	0.	1.	0.	0.
1457.	0.	1.	0.	0.	0.	0.	0.	0.	0.	0.	1.
1448.	0.	0.	0.	0.	0.	0.	0.	0.	0.	0.	0.
1447.	0.	0.	0.	0.	0.	0.	0.	0.	0.	0.	1.
1443.	0.	3.	0.	0.	0.	0.	0.	1.	0.	0.	1.
1437.	0.	0.	2.	0.	0.	0.	0.	1.	0.	1.	0.
1385.	0.	0.	3.	1.	0.	0.	0.	0.	0.	0.	0.
1373.	0.	0.	0.	0.	1.	1.	0.	0.	0.	0.	0.
1356.	0.	1.	2.	0.	0.	0.	1.	1.	1.	0.	0.
1333.	0.	1.	0.	0.	1.	0.	4.	2.	0.	0.	0.
1313.	0.	0.	1.	0.	1.	1.	2.	0.	0.	0.	0.
1318.	0.	1.	0.	0.	0.	0.	0.	0.	0.	1.	0.
1278.	19.	3.	1.	0.	1.	1.	3.	0.	1.	0.	3.
1263.	2.	0.	2.	1.	4.	4.	2.	0.	0.	0.	0.
1245.	0.	3.	0.	0.	0.	2.	0.	0.	1.	0.	0.
1220.	2.	0.	0.	0.	0.	1.	0.	0.	0.	0.	0.
1192.	0.	6.	0.	0.	2.	1.	1.	1.	1.	0.	0.
1168.	1.	1.	0.	0.	3.	3.	1.	2.	0.	0.	2.
1150.	0.	3.	1.	0.	0.	0.	8.	9.	2.	5.	8.
1138.	1.	1.	11.	3.	2.	1.	0.	7.	0.	24.	1.
1128.	3.	1.	9.	3.	15.	14.	1.	4.	1.	3.	6.
1111.	2.	0.	0.	0.	4.	3.	0.	19.	14.	10.	0.
1098.	0.	10.	4.	0.	6.	2.	0.	5.	65.	3.	0.
1076.	1.	11.	5.	0.	2.	3.	8.	24.	0.	35.	5.
1050.	8.	0.	0.	0.	3.	1.	4.	4.	0.	3.	65.
1037.	0.	4.	3.	39.	4.	0.	3.	2.	4.	6.	1.
998.	14.	0.	7.	32.	16.	0.	8.	0.	6.	1.	0.
962.	0.	4.	0.	16.	17.	1.	11.	15.	1.	1.	2.
920.	2.	23.	48.	1.	10.	0.	0.	2.	0.	4.	0.
901.	37.	6.	3.	8.	4.	42.	7.	0.	2.	0.	0.
889.	3.	10.	0.	3.	11.	27.	53.	1.	2.	0.	7.
749.	6.	12.	1.	1.	2.	13.	11.	1.	4.	0.	3.
671.	0.	3.	0.	0.	1.	13.	0.	0.	1.	0.	1.
583.	0.	1.	1.	3.	0.	0.	0.	0.	1.	0.	0.
563.	0.	1.	0.	0.	1.	0.	1.	1.	0.	3.	0.
515.	3.	0.	6.	1.	0.	0.	0.	0.	0.	0.	0.
508.	3.	6.	9.	9.	3.	1.	0.	4.	2.	6.	0.
434.	6.	1.	0.	2.	4.	1.	1.	3.	0.	0.	0.
412.	1.	2.	1.	1.	0.	0.	0.	1.	3.	2.	0.
382.	1.	1.	0.	1.	0.	0.	0.	0.	0.	1.	0.
359.	0.	0.	1.	0.	0.	1.	0.	0.	0.	0.	0.
353.	0.	0.	0.	0.	0.	0.	0.	0.	0.	0.	0.
341.	3.	0.	0.	0.	1.	0.	0.	0.	0.	0.	0.
319.	5.	0.	0.	0.	2.	3.	2.	0.	0.	0.	1.
278.	6.	0.	0.	2.	0.	0.	1.	0.	0.	0.	0.
275.	0.	5.	3.	0.	2.	2.	0.	0.	1.	0.	0.
247.	5.	0.	0.	1.	2.	0.	3.	0.	0.	1.	0.
182.	1.	0.	0.	0.	2.	21.	0.	1.	0.	0.	1.
121.	0.	0.	0.	0.	0.	1.	0.	0.	1.	1.	0.
111.	0.	0.	0.	0.	0.	0.	1.	0.	0.	0.	1.
62.	0.	0.	0.	0.	0.	0.	0.	0.	0.	0.	0.

TABLE LXXVII (Continued)

METHYL ALPHA XYLOPYRANOSIDE

C-H BEND CONTRIBUTIONS

CM-1	HC1O	HCO*	HC2O	HC3O	HC4O	H15O	H16O	HC5H	H15C	H16C	HC4C	CC4H	HC3C	CC3H	HC2C	CC2H	HC1C
1480.	0.	0.	0.	0.	0.	0.	1.	45.	16.	12.	0.	3.	1.	0.	1.	0.	0.
1457.	1.	0.	3.	0.	0.	0.	0.	1.	0.	0.	0.	0.	0.	1.	0.	2.	0.
1448.	1.	0.	1.	0.	0.	0.	0.	0.	0.	0.	0.	0.	0.	0.	0.	0.	0.
1447.	0.	0.	0.	0.	0.	0.	0.	0.	0.	0.	0.	0.	0.	0.	0.	0.	0.
1443.	1.	0.	9.	1.	0.	0.	0.	1.	0.	1.	0.	1.	0.	3.	2.	6.	0.
1437.	0.	0.	14.	0.	1.	0.	0.	2.	0.	2.	1.	2.	9.	2.	9.	0.	0.
1385.	0.	0.	2.	0.	3.	10.	10.	8.	0.	5.	6.	1.	0.	1.	5.	1.	0.
1373.	0.	0.	4.	0.	0.	21.	19.	7.	12.	4.	1.	0.	3.	3.	5.	0.	0.
1356.	1.	0.	0.	13.	3.	1.	0.	0.	0.	0.	3.	11.	6.	0.	9.	7.	0.
1333.	46.	12.	2.	2.	4.	3.	1.	0.	0.	0.	1.	0.	1.	5.	0.	5.	4.
1313.	2.	0.	0.	0.	0.	0.	1.	0.	2.	0.	25.	24.	1.	0.	9.	15.	2.
1318.	15.	1.	2.	4.	14.	2.	1.	0.	0.	3.	4.	1.	11.	24.	0.	6.	7.
1278.	3.	14.	1.	9.	8.	0.	0.	0.	1.	2.	0.	2.	2.	0.	2.	0.	10.
1263.	1.	2.	2.	1.	26.	9.	21.	0.	6.	1.	5.	2.	2.	6.	1.	2.	1.
1245.	0.	3.	1.	36.	12.	1.	0.	1.	1.	3.	3.	3.	15.	2.	2.	0.	1.
1220.	1.	1.	3.	17.	19.	17.	17.	0.	8.	6.	2.	4.	2.	3.	5.	0.	0.
1192.	1.	4.	33.	10.	0.	1.	0.	0.	0.	2.	3.	1.	0.	3.	5.	12.	7.
1168.	0.	2.	1.	1.	0.	3.	0.	0.	0.	1.	0.	0.	0.	1.	0.	1.	0.
1150.	2.	1.	1.	0.	0.	1.	0.	0.	0.	0.	0.	0.	0.	0.	0.	1.	1.
1138.	1.	2.	1.	3.	3.	5.	4.	0.	1.	3.	0.	1.	1.	0.	1.	0.	0.
1128.	6.	0.	2.	0.	5.	1.	1.	0.	2.	11.	0.	2.	3.	5.	0.	0.	0.
1111.	2.	2.	0.	3.	4.	3.	6.	2.	0.	3.	1.	0.	0.	1.	1.	3.	1.
1098.	0.	0.	1.	4.	0.	0.	0.	0.	0.	2.	2.	0.	0.	1.	1.	1.	0.
1076.	0.	1.	14.	0.	1.	0.	0.	0.	0.	0.	0.	2.	2.	1.	3.	0.	0.
1050.	2.	0.	2.	0.	0.	0.	0.	0.	0.	1.	0.	0.	0.	0.	0.	0.	0.
1037.	2.	1.	2.	0.	2.	9.	0.	1.	23.	2.	0.	0.	5.	0.	0.	0.	1.
998.	4.	11.	4.	0.	1.	1.	2.	1.	0.	8.	7.	4.	1.	0.	1.	1.	17.
962.	2.	20.	0.	1.	2.	3.	1.	3.	2.	1.	1.	3.	1.	4.	0.	1.	0.
920.	0.	2.	2.	1.	0.	0.	0.	0.	4.	5.	5.	6.	5.	3.	1.	0.	0.
901.	2.	31.	1.	0.	0.	0.	0.	0.	0.	2.	2.	1.	0.	0.	2.	7.	45.
889.	10.	18.	1.	1.	0.	0.	1.	1.	0.	1.	1.	1.	1.	0.	3.	1.	0.
749.	0.	1.	0.	0.	0.	0.	0.	0.	0.	0.	0.	0.	1.	0.	4.	1.	4.
671.	0.	0.	0.	0.	0.	0.	0.	0.	1.	0.	0.	0.	1.	0.	0.	2.	0.
583.	0.	0.	0.	0.	0.	0.	0.	0.	2.	0.	7.	5.	2.	8.	5.	2.	0.
563.	2.	0.	0.	0.	0.	1.	0.	0.	1.	0.	1.	0.	0.	0.	0.	0.	1.
515.	0.	0.	0.	0.	0.	0.	0.	1.	3.	0.	1.	2.	5.	0.	0.	0.	7.
508.	1.	0.	0.	0.	0.	0.	0.	0.	0.	0.	0.	0.	0.	0.	1.	0.	1.
434.	1.	0.	0.	0.	0.	2.	1.	0.	0.	0.	0.	0.	0.	1.	0.	0.	0.
412.	2.	0.	0.	0.	0.	0.	0.	0.	0.	1.	0.	2.	4.	3.	1.	0.	0.
382.	0.	1.	0.	0.	0.	0.	0.	0.	2.	1.	3.	4.	4.	3.	1.	0.	1.
359.	0.	0.	0.	0.	0.	0.	0.	0.	0.	0.	0.	0.	0.	0.	1.	0.	0.
353.	0.	1.	0.	0.	0.	0.	0.	0.	0.	0.	0.	0.	0.	0.	1.	2.	1.
341.	0.	0.	0.	0.	0.	0.	0.	0.	0.	0.	1.	0.	2.	1.	3.	1.	0.
319.	13.	2.	0.	0.	0.	1.	0.	0.	2.	0.	1.	0.	0.	0.	0.	1.	1.
278.	2.	0.	0.	0.	0.	0.	0.	0.	2.	0.	0.	3.	0.	2.	0.	2.	5.
275.	1.	0.	0.	0.	0.	0.	0.	0.	0.	1.	1.	2.	2.	1.	4.	0.	3.
247.	2.	0.	0.	0.	0.	1.	0.	0.	1.	1.	0.	0.	0.	0.	0.	4.	8.
182.	2.	32.	1.	0.	0.	1.	0.	0.	1.	0.	0.	1.	1.	1.	3.	2.	18.
121.	2.	3.	0.	0.	0.	0.	0.	0.	0.	0.	0.	1.	0.	0.	0.	0.	0.
111.	8.	1.	0.	0.	0.	0.	0.	0.	1.	0.	0.	0.	0.	1.	2.	0.	5.
62.	0.	0.	0.	0.	0.	0.	0.	0.	0.	0.	0.	0.	0.	0.	0.	0.	0.

TABLE LXXVII (Continued)

METHYL ALPHA XYLOPYRANOSIDE

HEAVY ATOM BEND CONTRIBUTIONS

CM-1	CC2C	CC3C	CC4C	CC5O	COC	O'CC	COC'	O6CC	OCO'	CCO7	O7CC	CCO8	O8CC	CCO9	O9CC
1480.	0.	0.	0.	0.	0.	0.	0.	0.	0.	0.	0.	0.	0.	0.	1.
1457.	0.	0.	0.	0.	0.	0.	0.	0.	0.	0.	0.	0.	0.	0.	0.
1448.	0.	0.	0.	0.	0.	0.	0.	0.	0.	0.	0.	0.	0.	0.	0.
1447.	0.	0.	0.	0.	0.	0.	0.	0.	0.	0.	0.	0.	0.	0.	0.
1443.	1.	0.	0.	0.	0.	0.	0.	0.	0.	0.	0.	1.	0.	0.	0.
1437.	0.	1.	0.	0.	0.	0.	0.	0.	0.	0.	0.	0.	0.	2.	0.
1385.	0.	0.	0.	0.	0.	0.	0.	0.	0.	0.	0.	0.	0.	1.	1.
1373.	0.	0.	0.	0.	0.	0.	0.	0.	0.	0.	0.	0.	0.	0.	1.
1356.	0.	1.	0.	0.	0.	0.	0.	0.	0.	0.	1.	0.	1.	0.	0.
1333.	0.	0.	0.	0.	0.	0.	1.	1.	0.	0.	0.	0.	0.	0.	0.
1313.	0.	0.	0.	1.	0.	0.	0.	0.	0.	0.	1.	0.	0.	0.	0.
1318.	0.	0.	0.	0.	0.	0.	0.	0.	0.	0.	1.	0.	0.	0.	0.
1278.	0.	0.	0.	1.	1.	2.	1.	1.	1.	2.	1.	1.	0.	0.	0.
1263.	1.	0.	0.	0.	0.	0.	0.	0.	1.	0.	0.	0.	0.	0.	0.
1245.	0.	0.	0.	0.	0.	0.	0.	0.	0.	0.	0.	0.	0.	0.	0.
1220.	0.	0.	0.	0.	0.	0.	0.	0.	0.	0.	0.	0.	0.	0.	0.
1192.	0.	1.	0.	0.	0.	0.	0.	0.	0.	0.	1.	0.	0.	1.	0.
1168.	1.	0.	0.	0.	1.	2.	0.	0.	1.	1.	0.	0.	0.	0.	0.
1150.	0.	0.	0.	0.	0.	1.	1.	0.	0.	1.	0.	0.	0.	0.	0.
1138.	2.	1.	4.	0.	2.	1.	0.	0.	1.	1.	0.	0.	2.	0.	0.
1128.	1.	0.	2.	0.	1.	5.	2.	0.	1.	3.	0.	0.	1.	0.	1.
1111.	0.	2.	1.	1.	1.	0.	0.	1.	1.	0.	2.	0.	1.	1.	2.
1098.	2.	10.	4.	2.	0.	0.	0.	0.	0.	0.	4.	1.	2.	3.	1.
1076.	4.	0.	1.	1.	0.	0.	0.	0.	0.	0.	0.	2.	0.	2.	1.
1050.	0.	0.	0.	0.	1.	0.	1.	0.	1.	0.	0.	1.	0.	0.	0.
1037.	1.	0.	1.	1.	1.	0.	0.	2.	0.	0.	1.	1.	2.	1.	0.
998.	1.	0.	0.	1.	0.	2.	0.	0.	0.	1.	0.	1.	0.	1.	1.
962.	1.	1.	0.	8.	2.	0.	1.	5.	1.	0.	0.	0.	4.	0.	8.
920.	0.	1.	1.	0.	0.	1.	1.	0.	0.	1.	1.	6.	4.	0.	1.
901.	1.	1.	0.	0.	0.	0.	3.	4.	9.	0.	1.	0.	0.	1.	0.
889.	1.	0.	0.	1.	5.	1.	8.	9.	0.	3.	0.	2.	0.	1.	3.
749.	3.	1.	0.	1.	11.	1.	0.	2.	1.	8.	1.	2.	0.	2.	1.
671.	1.	0.	0.	0.	6.	2.	13.	4.	20.	5.	0.	2.	0.	0.	0.
583.	0.	0.	4.	1.	2.	2.	2.	2.	1.	0.	21.	7.	0.	13.	1.
563.	0.	0.	4.	11.	11.	2.	2.	1.	0.	3.	0.	0.	3.	1.	0.
515.	2.	0.	2.	14.	0.	0.	0.	2.	3.	1.	7.	1.	19.	11.	2.
508.	0.	0.	0.	4.	0.	7.	1.	2.	5.	1.	1.	0.	1.	0.	6.
434.	7.	2.	2.	2.	5.	5.	1.	0.	2.	20.	1.	1.	3.	2.	20.
412.	5.	23.	24.	0.	1.	6.	0.	5.	0.	0.	1.	0.	0.	3.	1.
382.	3.	1.	2.	7.	4.	0.	0.	2.	2.	5.	2.	11.	7.	0.	10.
359.	0.	0.	0.	0.	0.	0.	2.	0.	0.	4.	2.	0.	2.	0.	0.
353.	3.	2.	0.	1.	1.	0.	2.	1.	0.	0.	5.	1.	0.	6.	1.
341.	0.	1.	0.	1.	0.	0.	1.	1.	0.	6.	0.	19.	0.	0.	5.
319.	2.	1.	0.	1.	17.	5.	57.	0.	1.	1.	4.	0.	0.	3.	1.
278.	0.	0.	1.	1.	0.	2.	3.	1.	3.	4.	15.	21.	37.	6.	11.
275.	1.	2.	0.	0.	0.	1.	1.	0.	4.	7.	19.	4.	0.	28.	10.
247.	2.	1.	0.	4.	25.	21.	7.	6.	24.	2.	0.	3.	0.	0.	0.
182.	0.	5.	0.	0.	14.	8.	4.	56.	25.	11.	1.	0.	0.	1.	1.
121.	2.	12.	9.	1.	4.	2.	0.	6.	1.	0.	1.	2.	2.	6.	3.
111.	18.	0.	2.	4.	0.	5.	8.	2.	6.	0.	2.	1.	1.	2.	2.
62.	2.	0.	1.	0.	1.	0.	0.	0.	0.	1.	0.	0.	0.	0.	1.

TABLE LXXVIII

METHYL BETA XYLOPYRANOSIDE

C-H AND O-H STRETCH CONTRIBUTION

CM-1	CH15	CH16	CH17	CH18	CH19	CH20	CH21	CH22	CH23	OH12	OH13	OH14
3356.	0.	0.	0.	0.	0.	0.	0.	0.	0.	18.	64.	18.
3356.	0.	0.	0.	0.	0.	0.	0.	0.	0.	6.	13.	81.
3356.	0.	0.	0.	0.	0.	0.	0.	0.	0.	76.	23.	0.
3000.	48.	49.	1.	0.	0.	0.	0.	0.	0.	0.	0.	0.
2997.	0.	0.	0.	0.	0.	0.	66.	17.	16.	0.	0.	0.
2997.	0.	0.	0.	0.	0.	0.	0.	49.	50.	0.	0.	0.
2956.	0.	0.	9.	30.	41.	17.	0.	0.	0.	0.	0.	0.
2947.	0.	0.	36.	21.	10.	31.	0.	0.	0.	0.	0.	0.
2938.	0.	0.	37.	11.	15.	36.	0.	0.	0.	0.	0.	0.
2933.	0.	0.	16.	36.	33.	15.	0.	0.	0.	0.	0.	0.
2888.	51.	49.	0.	0.	0.	0.	0.	0.	0.	0.	0.	0.
2831.	0.	0.	0.	0.	0.	0.	34.	34.	34.	0.	0.	0.

METHYL BETA XYLOPYRANOSIDE

TORSIONAL BEND CONTRIBUTION

CM-1	TCO'	TCO'	TC45	TC34	TC23	TC12	TCO9	TCO8	TCO7	TCO6	TC'O
1097.	0.	1.	0.	0.	0.	0.	0.	0.	0.	0.	0.
1064.	0.	1.	0.	0.	0.	0.	0.	0.	0.	0.	0.
1051.	0.	4.	1.	0.	0.	0.	0.	0.	0.	0.	0.
1045.	1.	3.	1.	0.	0.	0.	0.	0.	0.	0.	1.
1019.	1.	0.	0.	0.	0.	0.	0.	0.	0.	0.	0.
995.	1.	0.	0.	0.	0.	0.	0.	0.	0.	0.	1.
955.	0.	0.	0.	0.	0.	0.	0.	0.	1.	0.	0.
924.	0.	5.	1.	0.	0.	0.	0.	0.	0.	0.	0.
879.	1.	0.	0.	0.	0.	0.	0.	0.	0.	0.	4.
685.	0.	0.	0.	0.	0.	0.	0.	0.	1.	0.	12.
657.	0.	0.	0.	0.	0.	0.	0.	0.	0.	0.	2.
596.	1.	0.	0.	0.	0.	0.	0.	0.	0.	0.	23.
556.	4.	3.	1.	1.	1.	0.	0.	1.	0.	0.	16.
514.	1.	4.	0.	0.	1.	0.	0.	0.	0.	0.	19.
507.	0.	4.	0.	0.	0.	0.	0.	0.	0.	0.	11.
436.	3.	0.	0.	1.	0.	0.	2.	0.	2.	0.	2.
403.	1.	1.	0.	0.	0.	0.	7.	5.	0.	0.	0.
369.	5.	5.	3.	1.	0.	0.	6.	45.	0.	0.	3.
363.	0.	0.	1.	0.	0.	1.	49.	7.	6.	0.	0.
352.	5.	3.	4.	0.	1.	1.	3.	17.	38.	0.	1.
344.	3.	2.	1.	0.	0.	0.	17.	10.	31.	0.	1.
324.	1.	1.	0.	0.	0.	0.	12.	5.	0.	0.	0.
310.	1.	0.	0.	1.	0.	2.	2.	7.	0.	0.	0.
273.	1.	0.	0.	2.	0.	0.	1.	2.	0.	0.	0.
266.	1.	0.	1.	0.	2.	1.	0.	0.	13.	0.	0.
190.	0.	1.	3.	2.	1.	4.	0.	0.	0.	2.	1.
131.	6.	1.	8.	29.	17.	0.	0.	0.	0.	0.	0.
125.	9.	1.	6.	0.	11.	21.	0.	0.	0.	8.	0.
67.	1.	0.	1.	0.	2.	3.	0.	0.	0.	88.	0.

TABLE LXXVIII (Continued)

METHYL BETA XYLOPYRANOSIDE

METHYL GROUP C-H BEND CONTRIBUTION

CM-1	H23O	H22O	H21O	2123	2223	2122
1480.	0.	0.	0.	0.	0.	0.
1458.	5.	8.	22.	13.	1.	22.
1449.	0.	0.	9.	7.	6.	7.
1448.	0.	24.	0.	32.	19.	19.
1447.	32.	4.	0.	12.	39.	13.
1439.	0.	1.	1.	0.	0.	2.
1388.	0.	0.	0.	0.	0.	0.
1377.	0.	0.	1.	0.	0.	1.
1372.	0.	0.	0.	0.	0.	0.
1348.	0.	0.	0.	0.	0.	0.
1325.	0.	0.	1.	0.	1.	0.
1313.	0.	0.	0.	0.	0.	0.
1251.	0.	0.	0.	0.	0.	0.
1263.	0.	0.	0.	0.	0.	0.
1233.	0.	0.	0.	0.	0.	0.
1220.	0.	0.	0.	0.	0.	0.
1175.	0.	11.	5.	4.	2.	0.
1165.	38.	6.	14.	2.	4.	11.
1156.	4.	18.	5.	5.	1.	1.
1143.	2.	1.	0.	0.	0.	0.
1127.	0.	8.	6.	2.	2.	0.
1108.	2.	2.	13.	0.	2.	0.
1097.	0.	0.	0.	0.	0.	0.
1064.	1.	0.	8.	0.	1.	0.
1051.	0.	1.	4.	0.	1.	0.
1045.	1.	1.	0.	0.	0.	0.
1019.	0.	0.	0.	0.	0.	0.
995.	0.	1.	0.	0.	0.	0.
955.	0.	0.	0.	0.	0.	0.
924.	0.	0.	0.	0.	0.	0.
879.	0.	0.	0.	0.	0.	0.
685.	0.	0.	0.	0.	0.	0.
657.	0.	0.	0.	0.	0.	0.
596.	0.	0.	0.	0.	0.	0.
556.	0.	0.	0.	0.	0.	0.
514.	0.	0.	0.	0.	0.	0.
507.	0.	0.	0.	0.	0.	0.
436.	0.	0.	0.	0.	0.	0.
403.	0.	0.	0.	0.	0.	0.
369.	0.	0.	0.	0.	0.	0.
363.	0.	0.	0.	0.	0.	0.
352.	0.	0.	0.	0.	0.	0.
344.	0.	0.	0.	0.	0.	0.
324.	0.	0.	0.	0.	0.	0.
310.	0.	0.	0.	0.	0.	0.
273.	0.	0.	0.	0.	0.	0.
266.	0.	0.	0.	0.	0.	0.
190.	0.	0.	1.	0.	0.	0.
131.	0.	0.	0.	0.	0.	0.
125.	0.	0.	0.	0.	0.	0.
67.	0.	0.	0.	0.	0.	0.

METHYL BETA XYLOPYRANOSIDE

HEAVY ATOM STRETCH CONTRIBUTIONS

CM-1	C1C2	C2C3	C3C4	C4C5	C5O'	O'C1	C1O6	C2O7	C3O8	C4O9	O6C'
1480.	0.	0.	0.	0.	0.	0.	0.	0.	1.	0.	0.
1458.	2.	1.	0.	0.	0.	0.	0.	0.	0.	0.	1.
1449.	1.	2.	0.	0.	0.	0.	0.	1.	0.	0.	0.
1448.	0.	0.	0.	0.	0.	0.	0.	0.	0.	0.	0.
1447.	0.	0.	0.	0.	0.	0.	0.	0.	0.	0.	1.
1439.	0.	2.	2.	0.	0.	0.	0.	0.	0.	1.	0.
1388.	0.	0.	2.	0.	0.	0.	0.	0.	0.	0.	0.
1377.	1.	1.	1.	0.	0.	0.	0.	1.	1.	0.	1.
1372.	0.	0.	0.	0.	1.	0.	0.	0.	0.	0.	0.
1348.	0.	0.	2.	0.	0.	0.	0.	2.	0.	0.	0.
1325.	0.	1.	1.	0.	0.	0.	1.	0.	0.	0.	1.
1313.	0.	0.	1.	0.	1.	0.	0.	0.	0.	1.	0.
1251.	3.	1.	1.	0.	0.	0.	2.	1.	0.	0.	0.
1263.	2.	0.	1.	1.	1.	2.	0.	0.	0.	0.	0.
1233.	4.	0.	0.	1.	0.	1.	0.	0.	0.	0.	0.
1220.	1.	0.	0.	0.	1.	2.	0.	1.	0.	0.	1.
1175.	3.	0.	0.	0.	0.	0.	11.	1.	0.	1.	6.
1165.	0.	1.	0.	0.	1.	1.	11.	0.	3.	0.	4.
1156.	1.	3.	0.	0.	0.	0.	4.	7.	5.	0.	1.
1143.	2.	5.	16.	6.	4.	7.	0.	0.	4.	14.	0.
1127.	2.	0.	1.	0.	2.	0.	0.	30.	2.	21.	2.
1108.	0.	8.	0.	0.	0.	3.	5.	1.	40.	9.	2.
1097.	3.	0.	8.	0.	43.	21.	1.	2.	9.	13.	6.
1064.	1.	10.	0.	0.	2.	2.	13.	8.	12.	17.	30.
1051.	0.	0.	0.	16.	23.	1.	6.	14.	3.	14.	4.
1045.	11.	1.	2.	4.	1.	5.	0.	21.	8.	0.	7.
1019.	20.	28.	6.	5.	2.	8.	15.	3.	0.	0.	19.
995.	0.	1.	1.	57.	1.	3.	14.	0.	1.	1.	1.
955.	18.	24.	4.	5.	3.	12.	16.	7.	5.	4.	16.
924.	5.	2.	51.	8.	2.	0.	0.	2.	4.	1.	0.
879.	18.	11.	0.	3.	13.	42.	5.	0.	3.	1.	0.
685.	8.	0.	2.	1.	1.	5.	3.	1.	0.	1.	2.
657.	0.	1.	0.	0.	1.	3.	9.	1.	2.	1.	0.
596.	0.	0.	0.	1.	3.	6.	0.	1.	0.	3.	1.
556.	1.	0.	0.	0.	0.	2.	0.	1.	0.	1.	0.
514.	0.	1.	8.	2.	1.	3.	0.	1.	0.	1.	0.
507.	6.	5.	8.	9.	3.	0.	4.	3.	3.	3.	0.
436.	5.	0.	0.	2.	1.	0.	1.	2.	0.	0.	0.
403.	3.	0.	1.	1.	0.	0.	0.	0.	2.	1.	0.
369.	0.	0.	0.	0.	3.	0.	0.	0.	0.	0.	0.
363.	0.	1.	0.	0.	2.	2.	0.	0.	0.	1.	0.
352.	0.	0.	0.	0.	2.	0.	0.	0.	0.	0.	0.
344.	1.	0.	0.	0.	3.	1.	0.	0.	0.	0.	0.
324.	8.	5.	0.	0.	1.	1.	0.	0.	0.	0.	0.
310.	2.	5.	0.	0.	0.	3.	0.	0.	1.	0.	0.
273.	3.	2.	0.	2.	2.	0.	0.	0.	0.	0.	0.
266.	0.	0.	3.	0.	0.	3.	0.	0.	0.	0.	0.
190.	3.	3.	0.	1.	1.	4.	1.	0.	0.	0.	2.
131.	1.	0.	0.	0.	0.	0.	0.	1.	1.	1.	0.
125.	1.	0.	0.	0.	0.	1.	0.	0.	0.	0.	1.
67.	0.	0.	0.	0.	0.	0.	0.	0.	0.	0.	0.

TABLE LXXVIII (Continued)

METHYL BETA XYLOPYRANOSIDE

C-H BEND CONTRIBUTIONS

CM-1	HC1O	HC0'	HC2O	HC3O	HC4O	H15O	H16O	HC5H	H15C	H16C	HC4C	CC4H	HC3C	CC3H	HC2C	CC2H	HC1C
1480.	0.	0.	0.	0.	0.	0.	1.	45.	16.	12.	1.	3.	1.	0.	1.	0.	0.
1458.	1.	0.	4.	0.	0.	0.	0.	0.	0.	0.	0.	0.	1.	2.	1.	1.	1.
1449.	0.	0.	13.	1.	0.	0.	0.	0.	0.	0.	0.	0.	1.	5.	0.	1.	3.
1448.	1.	0.	0.	0.	0.	0.	0.	0.	0.	0.	0.	0.	0.	0.	0.	0.	0.
1447.	0.	0.	0.	0.	0.	0.	0.	0.	0.	0.	0.	0.	0.	0.	0.	0.	0.
1439.	0.	0.	2.	1.	1.	0.	0.	4.	0.	2.	0.	3.	7.	0.	11.	3.	0.
1388.	2.	0.	0.	1.	3.	8.	8.	6.	0.	4.	6.	1.	1.	0.	8.	8.	0.
1377.	1.	0.	15.	4.	0.	0.	1.	0.	2.	0.	0.	0.	0.	4.	0.	20.	1.
1372.	3.	1.	0.	1.	0.	22.	21.	9.	10.	5.	1.	0.	4.	1.	7.	6.	0.
1348.	3.	1.	4.	4.	7.	2.	1.	1.	0.	2.	3.	16.	7.	6.	2.	2.	3.
1325.	53.	17.	0.	3.	0.	1.	0.	0.	0.	0.	10.	8.	0.	1.	0.	0.	5.
1313.	9.	3.	0.	0.	9.	1.	1.	0.	2.	1.	20.	5.	12.	12.	4.	3.	1.
1251.	0.	0.	0.	61.	0.	2.	2.	0.	2.	4.	0.	1.	9.	12.	0.	0.	0.
1263.	0.	1.	2.	2.	38.	11.	13.	0.	6.	4.	1.	12.	0.	0.	5.	0.	4.
1233.	0.	2.	4.	7.	18.	2.	0.	0.	0.	4.	14.	0.	6.	11.	6.	0.	2.
1220.	2.	1.	4.	4.	11.	19.	25.	0.	8.	4.	0.	5.	4.	0.	8.	0.	0.
1175.	0.	19.	16.	2.	0.	0.	1.	0.	0.	0.	0.	0.	0.	0.	1.	8.	7.
1165.	1.	1.	0.	0.	0.	0.	0.	0.	0.	0.	0.	0.	0.	0.	0.	0.	2.
1156.	1.	1.	17.	0.	2.	1.	2.	0.	0.	1.	0.	1.	0.	0.	0.	3.	7.
1143.	0.	3.	1.	10.	7.	0.	4.	0.	4.	15.	1.	2.	4.	1.	1.	2.	1.
1127.	4.	2.	1.	1.	1.	0.	0.	1.	0.	0.	1.	0.	0.	0.	0.	0.	2.
1108.	0.	0.	2.	0.	1.	2.	1.	0.	0.	2.	1.	0.	1.	2.	1.	0.	0.
1097.	0.	3.	0.	0.	1.	4.	0.	1.	1.	4.	0.	1.	0.	0.	0.	0.	0.
1064.	3.	1.	2.	2.	1.	1.	1.	0.	1.	0.	0.	0.	0.	1.	5.	1.	3.
1051.	0.	1.	0.	0.	0.	5.	1.	0.	8.	2.	1.	1.	1.	1.	2.	0.	1.
1045.	3.	12.	12.	1.	0.	3.	1.	1.	3.	0.	0.	1.	3.	0.	0.	2.	7.
1019.	15.	2.	2.	1.	0.	0.	0.	1.	4.	1.	0.	1.	4.	4.	5.	1.	4.
995.	0.	5.	2.	0.	5.	8.	4.	3.	5.	5.	3.	3.	0.	4.	1.	0.	0.
955.	1.	19.	0.	0.	0.	0.	0.	0.	0.	0.	0.	0.	2.	2.	1.	6.	5.
924.	0.	2.	0.	2.	0.	0.	1.	1.	6.	12.	11.	10.	1.	3.	0.	1.	0.
879.	0.	20.	4.	0.	0.	0.	0.	1.	0.	0.	0.	0.	1.	0.	1.	1.	32.
685.	0.	0.	0.	0.	0.	0.	0.	0.	1.	0.	1.	1.	1.	4.	1.	1.	10.
657.	1.	0.	0.	0.	0.	1.	0.	0.	2.	0.	1.	0.	0.	1.	0.	2.	1.
596.	0.	0.	0.	0.	0.	1.	0.	0.	1.	0.	0.	1.	1.	1.	2.	0.	0.
556.	1.	0.	0.	0.	0.	0.	0.	0.	2.	0.	6.	3.	2.	1.	3.	4.	1.
514.	0.	0.	0.	0.	0.	1.	0.	0.	1.	0.	0.	2.	9.	0.	0.	1.	5.
507.	3.	0.	0.	0.	0.	0.	0.	0.	0.	0.	2.	1.	0.	0.	0.	0.	2.
436.	0.	0.	0.	0.	0.	1.	0.	0.	0.	0.	0.	1.	0.	3.	0.	0.	3.
403.	0.	0.	0.	0.	0.	1.	0.	0.	0.	0.	0.	0.	0.	0.	0.	0.	0.
369.	0.	1.	0.	0.	0.	1.	0.	0.	1.	0.	1.	0.	0.	1.	0.	0.	0.
363.	0.	1.	0.	0.	0.	1.	0.	0.	2.	1.	1.	2.	1.	1.	2.	0.	2.
352.	0.	0.	0.	0.	0.	2.	0.	0.	2.	0.	2.	1.	0.	0.	1.	3.	0.
344.	0.	3.	0.	0.	0.	1.	0.	0.	0.	0.	0.	0.	0.	0.	1.	4.	0.
324.	2.	0.	0.	0.	0.	0.	0.	0.	1.	1.	1.	1.	2.	3.	2.	0.	5.
310.	2.	3.	0.	0.	0.	0.	0.	0.	1.	0.	0.	3.	3.	2.	5.	4.	3.
273.	0.	0.	0.	0.	0.	0.	1.	0.	1.	1.	1.	0.	3.	0.	5.	0.	2.
266.	2.	3.	0.	0.	0.	0.	0.	0.	0.	0.	0.	2.	0.	1.	0.	0.	2.
190.	2.	10.	0.	0.	0.	0.	0.	0.	0.	0.	0.	0.	0.	1.	0.	2.	16.
131.	0.	1.	0.	0.	0.	0.	0.	0.	0.	0.	0.	0.	0.	0.	0.	0.	3.
125.	1.	1.	0.	0.	0.	0.	0.	0.	1.	0.	0.	0.	0.	1.	0.	1.	1.
67.	0.	0.	0.	0.	0.	0.	0.	0.	0.	0.	0.	0.	0.	0.	0.	0.	0.

TABLE LXXVIII (Continued)

METHYL BETA XYLOPYRANOSIDE

HEAVY ATOM BEND CONTRIBUTIONS

CM-1	CC2C	CC3C	CC4C	CC5O	COC	O'CC	COC'	O6CC	OCO'	CCO7	O7CC	CCO8	O8CC	CCO9	O9CC
1480.	0.	0.	0.	0.	0.	0.	0.	0.	0.	0.	0.	0.	0.	0.	1.
1458.	1.	0.	0.	0.	0.	0.	1.	1.	0.	0.	0.	0.	0.	0.	0.
1449.	2.	0.	0.	0.	0.	0.	0.	1.	0.	0.	0.	1.	0.	0.	0.
1448.	0.	0.	0.	0.	0.	0.	0.	0.	0.	0.	0.	0.	0.	0.	0.
1447.	0.	0.	0.	0.	0.	0.	0.	0.	0.	0.	0.	0.	0.	0.	0.
1439.	0.	1.	0.	0.	0.	0.	0.	0.	0.	0.	0.	1.	0.	3.	0.
1388.	0.	0.	0.	0.	0.	0.	0.	0.	0.	0.	0.	0.	0.	1.	1.
1377.	0.	0.	0.	0.	0.	1.	1.	1.	0.	0.	0.	0.	0.	0.	0.
1372.	0.	0.	0.	0.	0.	0.	0.	0.	0.	0.	0.	0.	0.	0.	1.
1348.	0.	1.	0.	0.	0.	1.	0.	0.	0.	0.	1.	0.	1.	0.	0.
1325.	0.	0.	0.	0.	0.	0.	1.	0.	0.	0.	0.	0.	0.	0.	0.
1313.	0.	0.	0.	1.	0.	0.	0.	0.	0.	0.	0.	0.	0.	0.	0.
1251.	0.	0.	1.	0.	0.	0.	0.	0.	0.	0.	0.	1.	0.	0.	0.
1263.	0.	0.	0.	0.	0.	0.	0.	0.	0.	0.	0.	0.	0.	0.	0.
1233.	0.	0.	0.	1.	0.	0.	0.	0.	0.	1.	0.	1.	0.	0.	0.
1220.	0.	0.	0.	0.	0.	0.	0.	0.	0.	0.	0.	0.	0.	0.	0.
1175.	0.	0.	0.	0.	1.	0.	0.	0.	2.	0.	0.	0.	0.	0.	0.
1165.	0.	0.	0.	0.	0.	0.	1.	0.	0.	0.	0.	0.	0.	0.	0.
1156.	0.	0.	1.	0.	0.	0.	0.	0.	1.	1.	0.	0.	1.	0.	0.
1143.	0.	1.	4.	1.	1.	0.	0.	0.	0.	0.	3.	0.	1.	0.	0.
1127.	0.	4.	0.	3.	0.	2.	0.	0.	0.	1.	2.	0.	0.	1.	2.
1108.	2.	5.	5.	1.	1.	2.	1.	0.	0.	0.	1.	0.	3.	2.	0.
1097.	0.	0.	0.	1.	0.	0.	0.	0.	0.	0.	1.	0.	0.	0.	0.
1064.	1.	2.	1.	0.	0.	3.	2.	0.	0.	2.	0.	0.	1.	2.	0.
1051.	0.	0.	0.	0.	1.	1.	0.	0.	0.	1.	0.	0.	0.	1.	1.
1045.	4.	2.	0.	1.	0.	1.	0.	0.	2.	0.	1.	3.	1.	0.	1.
1019.	4.	0.	0.	1.	1.	8.	0.	5.	1.	7.	1.	0.	0.	0.	1.
995.	1.	0.	1.	6.	6.	0.	1.	2.	4.	0.	0.	0.	4.	1.	5.
955.	0.	0.	0.	0.	0.	0.	5.	5.	1.	0.	2.	1.	1.	0.	0.
924.	0.	2.	0.	0.	1.	0.	0.	0.	0.	1.	3.	1.	4.	2.	1.
879.	1.	0.	0.	1.	5.	0.	4.	5.	19.	4.	0.	2.	1.	1.	4.
685.	0.	0.	0.	0.	0.	1.	0.	3.	3.	4.	6.	13.	0.	3.	1.
657.	2.	0.	3.	9.	4.	5.	15.	3.	10.	2.	1.	4.	1.	0.	3.
596.	1.	1.	1.	8.	12.	2.	2.	5.	0.	2.	7.	3.	6.	12.	0.
556.	1.	0.	6.	5.	8.	1.	7.	2.	0.	8.	4.	0.	1.	2.	2.
514.	0.	1.	0.	1.	7.	0.	2.	0.	7.	0.	7.	0.	12.	10.	4.
507.	0.	0.	4.	0.	2.	7.	2.	0.	0.	0.	0.	0.	2.	0.	4.
436.	18.	4.	1.	9.	0.	4.	14.	3.	1.	12.	0.	0.	0.	1.	8.
403.	5.	22.	13.	0.	14.	2.	1.	0.	2.	0.	4.	5.	4.	3.	6.
369.	0.	0.	3.	1.	10.	0.	0.	0.	3.	0.	1.	1.	5.	2.	1.
363.	0.	3.	5.	3.	4.	0.	0.	0.	1.	6.	1.	0.	1.	3.	5.
352.	0.	1.	0.	2.	13.	0.	0.	0.	1.	0.	0.	0.	1.	2.	1.
344.	2.	0.	3.	0.	4.	2.	0.	5.	1.	0.	7.	2.	1.	0.	5.
324.	2.	0.	2.	4.	0.	2.	10.	4.	2.	13.	1.	16.	1.	2.	8.
310.	2.	0.	0.	0.	1.	11.	12.	7.	2.	4.	4.	0.	15.	6.	0.
273.	2.	1.	0.	0.	0.	0.	0.	0.	1.	1.	0.	29.	17.	26.	18.
266.	1.	1.	2.	2.	2.	5.	7.	4.	1.	17.	28.	2.	5.	3.	0.
190.	0.	0.	0.	2.	0.	1.	26.	28.	42.	2.	5.	1.	0.	1.	0.
131.	2.	12.	8.	0.	4.	0.	1.	1.	1.	0.	2.	2.	2.	3.	3.
125.	12.	1.	1.	3.	1.	3.	5.	11.	1.	4.	1.	1.	0.	0.	2.
67.	1.	0.	0.	1.	0.	1.	0.	0.	1.	0.	0.	0.	0.	0.	0.